

International Evaluation Co-operation

Volume 26

**Uncertainty and Target Accuracy
Assessment for Innovative Systems
Using Recent Covariance Data
Evaluations**

Nuclear Science
NEA/WPEC-26

ISBN 978-92-64-99053-1

International Evaluation Co-operation

VOLUME 26

**UNCERTAINTY AND TARGET ACCURACY
ASSESSMENT FOR INNOVATIVE SYSTEMS USING
RECENT COVARIANCE DATA EVALUATIONS**

*A report by the Working Party
on International Evaluation Co-operation
of the NEA Nuclear Science Committee*

CO-ORDINATOR

M. Salvatores

Argonne National Laboratory/Commissariat à l'Énergie Atomique
USA/France

MONITOR

R. Jacqmin

Commissariat à l'Énergie Atomique
France

©OECD 2008
NEA No. 6410

NUCLEAR ENERGY AGENCY
ORGANISATION FOR ECONOMIC CO-OPERATION AND DEVELOPMENT

ORGANISATION FOR ECONOMIC CO-OPERATION AND DEVELOPMENT

The OECD is a unique forum where the governments of 30 democracies work together to address the economic, social and environmental challenges of globalisation. The OECD is also at the forefront of efforts to understand and to help governments respond to new developments and concerns, such as corporate governance, the information economy and the challenges of an ageing population. The Organisation provides a setting where governments can compare policy experiences, seek answers to common problems, identify good practice and work to co-ordinate domestic and international policies.

The OECD member countries are: Australia, Austria, Belgium, Canada, the Czech Republic, Denmark, Finland, France, Germany, Greece, Hungary, Iceland, Ireland, Italy, Japan, Korea, Luxembourg, Mexico, the Netherlands, New Zealand, Norway, Poland, Portugal, the Slovak Republic, Spain, Sweden, Switzerland, Turkey, the United Kingdom and the United States. The Commission of the European Communities takes part in the work of the OECD.

OECD Publishing disseminates widely the results of the Organisation's statistics gathering and research on economic, social and environmental issues, as well as the conventions, guidelines and standards agreed by its members.

This work is published on the responsibility of the Secretary-General of the OECD. The opinions expressed and arguments employed herein do not necessarily reflect the official views of the Organisation or of the governments of its member countries.

NUCLEAR ENERGY AGENCY

The OECD Nuclear Energy Agency (NEA) was established on 1st February 1958 under the name of the OEEC European Nuclear Energy Agency. It received its present designation on 20th April 1972, when Japan became its first non-European full member. NEA membership today consists of 28 OECD member countries: Australia, Austria, Belgium, Canada, the Czech Republic, Denmark, Finland, France, Germany, Greece, Hungary, Iceland, Ireland, Italy, Japan, Luxembourg, Mexico, the Netherlands, Norway, Portugal, the Republic of Korea, the Slovak Republic, Spain, Sweden, Switzerland, Turkey, the United Kingdom and the United States. The Commission of the European Communities also takes part in the work of the Agency.

The mission of the NEA is:

- to assist its member countries in maintaining and further developing, through international co-operation, the scientific, technological and legal bases required for a safe, environmentally friendly and economical use of nuclear energy for peaceful purposes, as well as
- to provide authoritative assessments and to forge common understandings on key issues as input to government decisions on nuclear energy policy and to broader OECD policy analyses in areas such as energy and sustainable development.

Specific areas of competence of the NEA include safety and regulation of nuclear activities, radioactive waste management, radiological protection, nuclear science, economic and technical analyses of the nuclear fuel cycle, nuclear law and liability, and public information. The NEA Data Bank provides nuclear data and computer program services for participating countries.

In these and related tasks, the NEA works in close collaboration with the International Atomic Energy Agency in Vienna, with which it has a Co-operation Agreement, as well as with other international organisations in the nuclear field.

© OECD 2008

OECD freely authorises the use, including the photocopy, of this material for private, non-commercial purposes. Permission to photocopy portions of this material for any public use or commercial purpose may be obtained from the Copyright Clearance Center (CCC) at info@copyright.com or the Centre français d'exploitation du droit de copie (CFC) contact@cfcopies.com. All copies must retain the copyright and other proprietary notices in their original forms. All requests for other public or commercial uses of this material or for translation rights should be submitted to rights@oecd.org.

FOREWORD

A Working Party on International Evaluation Co-operation has been established by the OECD/NEA Nuclear Science Committee (NSC) to promote the exchange of information on nuclear data evaluations, validation and related topics. Another specific aim is to provide a framework for co-operative activities between the members of the major nuclear data evaluation projects. This initiative includes the possible exchange of scientists in order to encourage co-operation. Requirements for experimental data resulting from this activity are also compiled. The working party determines common criteria for evaluated nuclear data files in order to assess and improve the quality and completeness of evaluated data.

The parties to the project are: ENDF (United States of America), JEFF/EFF (member countries of the NEA Data Bank) and JENDL (Japan). Co-operation with evaluation projects of non-OECD countries, specifically the Russian BROND and Chinese CENDL projects, are organised through the Nuclear Data Section of the International Atomic Energy Agency (IAEA).

This publication reports the conclusions from the work undertaken by Subgroup 26, which focussed on the development of a systematic approach to define data needs for advanced reactor systems and to make a comprehensive study of such needs for Generation-IV (Gen-IV) reactors. A comprehensive sensitivity and uncertainty study has been performed to evaluate the impact of neutron cross-section uncertainty on the most significant integral parameters related to the core and fuel cycle of a wide range of innovative systems, even beyond the Gen-IV range of systems. A compilation of preliminary “Design Target Accuracies” has been put together and a target accuracy assessment has been performed to provide an indicative quantitative evaluation of nuclear data improvement requirements by isotope, nuclear reaction and energy range, in order to meet the Design target accuracies, as compiled in the present study. First priorities were formulated on the basis of common needs for fast reactors and, separately, thermal systems.

The opinions expressed in this report are those of the authors only, and do not necessarily represent the position of any member country or international organisation. This report is published under the auspices and responsibility of the Secretary-General of the OECD.

MEMBERS OF SUBGROUP 26

M. Salvatores (Co-ordinator)	Argonne National Laboratory, USA Commissariat à l'Énergie Atomique, France
G. Aliberti	Argonne National Laboratory, USA
M. Dunn	Oak Ridge National Laboratory
A. Hogenbirk	NRG, The Netherlands
A. Ignatyuk	CJD-IPPE, Russian Federation
M. Ishikawa	Japan Atomic Energy Agency, Japan
I. Kodeli	OECD Nuclear Energy Agency, France
A.J. Koning	NRG, The Netherlands
R. McKnight	Argonne National Laboratory, USA
R.W. Mills	Nexia Solutions, Ltd., United Kingdom
P. Oblozinsky	Brookhaven National Laboratory, USA
G. Palmiotti	Idaho National Laboratory, USA
A. Plompen	Joint Research Centre, Belgium
G. Rimpault	Commissariat à l'Énergie Atomique, France
Y. Rugama	OECD Nuclear Energy Agency, France
P. Talou	Los Alamos National Laboratory, USA
W.S. Yang	Argonne National Laboratory, USA

TABLE OF CONTENTS

Foreword	3
Executive summary	11
1. Introduction	15
2. Approach and theoretical background	17
2.1 Sensitivity coefficients	17
2.1.1 <i>Multiplication factor</i>	19
2.1.2 <i>Power peak</i>	19
2.1.3 <i>Reactivity coefficients</i>	21
2.1.4 <i>Nuclide transmutation</i>	22
2.1.5 <i>Reactivity loss during irradiation</i>	22
2.1.6 <i>Neutron source (e.g. at fuel fabrication)</i>	23
2.1.7 <i>Decay heat</i>	23
2.2 Uncertainties and target accuracies	25
2.3 Sensitivity/uncertainty analysis using Monte Carlo methods.....	25
3. Covariance data	27
3.1 ANL covariance matrix	27
3.2 BOLNA covariance matrix	28
4. Calculation tools	35
5. Systems and integral parameters analysed	35
6. Uncertainty analysis	50
6.1 Uncertainty evaluation	50
6.2 Summary of lessons drawn from the uncertainty analysis	57
7. Target accuracy	60
7.1 Data target accuracies	60
7.2 Computational strategy	62
7.3 Target accuracy results	64
7.3.1 <i>Analysis for separated systems</i>	66
7.3.2 <i>Analysis for groups of systems</i>	81
7.4 Summary of the target accuracy study	85
7.5 Complementary use of differential and integral experiments	86
8. General conclusions and recommendations	87
References	90

Appendix A	Accuracy of measurements	93
Appendix B	Evaluation of Doppler reactivity uncertainty	101
Appendix C	Evaluation of fission spectra uncertainty and their propagation	115
Appendix D	Comments on response parameter uncertainty due to fission spectrum uncertainties	127
Appendix E	Nuclear data for the handling, reprocessing and disposal of spent nuclear fuel	139
Appendix F	Resonance region importance for advanced fuel cycle applications	159
Appendix G	BNL methodology for cross-section covariances	165
Appendix H	Report to Subgroup 26 on the preliminary conclusions of the April 2007 meeting in Nice	173
Appendix I	Importance of ^{23}Na reaction cross-correlations in the uncertainty assessment of SFR characteristics	185
Appendix J	Subgroup 26 recommendations for future work	199

Appendices available on CD-ROM

Appendix K	Model description
Appendix L	Isotope contributions
Appendix M	Total isotope uncertainty breakdown
Appendix N	Δn , n_f , burn-up component due to Δn , decay, dose, neutron source uncertainty (%) breakdown
Appendix O	Uncertainty (%) breakdown by isotope, energy group, cross-section
Appendix P	Complete lists of target accuracy results
Appendix Q	ANL diagonal matrix
Appendix R	BOLNA diagonal matrix

List of figures

Figure 1. Energy correlations used in the ANL partial energy correlation (PEC) matrix	29
Figure 2. Covariance matrix in 15 groups for the $^{239}\text{Pu}(\text{n},\text{f})$ reaction.....	31
Figure 3. Covariance matrix in 187 (left) and 15 (right) groups for the $^{240}\text{Pu}(\text{n},\gamma)$ reaction.....	32
Figure 4. Covariance matrix in 187 (left) and 15 (right) groups for the $^{241}\text{Pu}(\text{n},\text{f})$ reaction	33
Figure 5. Covariance matrix in 187 (left) and 15 (right) groups for the $^{241}\text{Am}(\text{n},\text{f})$ reaction	34
Figure 6. ABTR direct flux distribution	37
Figure 7. ABTR adjoint flux distribution	37
Figure 8. SFR direct flux distribution.....	38
Figure 9. SFR adjoint flux distribution.....	38
Figure 10. EFR direct flux distribution.....	39
Figure 11. EFR adjoint flux distribution.....	39
Figure 12. GFR direct flux distribution	40
Figure 13. GFR adjoint flux distribution	40
Figure 14. LFR direct flux distribution.....	41
Figure 15. LFR adjoint flux distribution.....	41
Figure 16. ADMAB direct flux distribution	42
Figure 17. ADMAB adjoint flux distribution	42
Figure 18. VHTR direct flux distribution	43
Figure 19. VHTR adjoint flux distribution	43
Figure 20. PWR direct flux distribution	44
Figure 21. PWR adjoint flux distribution	44

List of tables

Table 1.	Features of investigated systems	8
Table 2.	ABTR, SFR, EFR nominal values	45
Table 3.	GFR nominal values.....	46
Table 4.	LFR nominal values	46
Table 5.	ADMAB nominal values.....	47
Table 6.	VHTR nominal values.....	47
Table 7.	PWR nominal values.....	48
Table 8.	Δn (units) and $\Delta n/n_f$ nominal values.....	49
Table 9.	Fast neutron systems: total uncertainties (%).....	51
Table 10.	High burn-up VHTR: uncertainties (%).....	52
Table 11.	High burn-up PWR: uncertainties (%).....	52
Table 12.	$\Delta \rho$ burn-up uncertainty breakdown into components (pcm).....	52
Table 13.	Fast reactor systems: uncertainties (%) due to Pu isotope cross-sections (BOLNA).....	54
Table 14.	Fast reactor systems: uncertainties (%) due to selected MA cross-sections (BOLNA).....	54
Table 15.	Fast reactor systems: uncertainties (%) due to inelastic and capture (BOLNA).....	55
Table 16.	Uncertainty (%) on Pu isotope density at end of cycle (EFR)	56
Table 17.	Uncertainty (%) on selected MA density at end of cycle (EFR)	56
Table 18.	Thermal systems: uncertainties (%) due to selected isotopes and reactions (BOLNA)	58
Table 19.	SFR k_{eff} uncertainties (%): energy breakdown (pcm) for selected isotopes/reactions.....	58
Table 20.	Fast reactor and ADMAB target accuracies (1σ).....	61
Table 21.	Target accuracy (1σ) for UO_2 - and PuO_2 -fuelled HTRs	61
Table 22.	PWR target accuracies (1σ)	61
Table 23.	Integral parameter uncertainties (%) using the BOLNA diagonal covariance matrix	63

Table 24.	λ_i sets used for the analysis	63
Table 25.	ABTR: uncertainty reduction requirements needed to meet integral parameter target accuracies	69
Table 26.	SFR: uncertainty reduction requirements needed to meet integral parameter target accuracies	70
Table 27.	EFR: uncertainty reduction requirements needed to meet integral parameter target accuracies	71
Table 28.	GFR: uncertainty reduction requirements needed to meet integral parameter target accuracies	72
Table 29.	LFR: uncertainty reduction requirements needed to meet integral parameter target accuracies	73
Table 30.	ADMAB: uncertainty reduction requirements needed to meet integral parameter target accuracies	74
Table 31.	Summary target accuracy requirements occurring for at least two fast reactors.....	75
Table 32.	Summary of Highest Priority Target Accuracies for Fast Reactors.....	76
Table 33.	VHTR: uncertainty reduction requirements needed to meet integral parameter target accuracies	77
Table 34.	PWR: uncertainty reduction requirements needed to meet integral parameter target accuracies	77
Table 35.	Integral parameter uncertainties (%) with initial and required cross-section uncertainties	78
Table 36.	Transmutation uncertainties (%) with initial and required cross-section uncertainties.....	79
Table 37.	Integral parameter uncertainties (%) with initial and required cross-section uncertainties	81
Table 38.	Transmutation uncertainties (%) with initial and required cross-section uncertainties.....	82
Table 39.	Integral parameter uncertainties (%) with initial and required cross-section uncertainties	83
Table 40.	Transmutation uncertainties (%) with initial and required cross-section uncertainties.....	84

EXECUTIVE SUMMARY

The Working Party on Evaluation Co-operation (WPEC) of the OECD Nuclear Energy Agency Nuclear Science Committee established Subgroup 26 to develop a systematic approach to define data needs for advanced reactor systems and to undertake a comprehensive study of such needs for Generation-IV (Gen-IV) reactors.

The subgroup was established at the end of 2005, and during its two-year mandate met three times. The active participation of most of the members allowed to expand the discussion well beyond the original subject matter, and allowed to gather material, often original, that has been summarised in the present report. More material related to the subgroup's activity was published at the ND2007 International Conference (Nice, April 2007) and at the NEMEA Workshop (Prague, October 2007). At that workshop, a full day was devoted to subgroup-related presentations.

A comprehensive sensitivity and uncertainty study was performed to evaluate the impact of neutron cross-section uncertainty on the most significant integral parameters related to the core and fuel cycle of a wide range of innovative systems, even beyond the Gen-IV range of systems. Results were obtained for the advanced breeder test reactor (ABTR), the sodium-cooled fast reactor (SFR), the European fast reactor (EFR), the gas-cooled fast reactor (GFR), the lead-cooled fast reactor (LFR), the accelerator-driven minor actinide burner (ADMAB), the very high-temperature reactor (VHTR) and a pressurised water reactor with extended burn-up (PWR). These systems correspond to current studies within the Generation-IV initiative, the Global Nuclear Energy Partnership (GNEP), the Advanced Fuel Cycle Initiative (AFCI), and advanced fuel cycle and partitioning/transmutation studies in Japan and Europe.

State-of-the-art sensitivity and uncertainty methods were used and they are briefly described in this report.

In the first phase, the analysis was performed with covariance matrices developed at ANL through an educated guess based on nuclear data performance in the analysis of selected clean integral experiments. Successively, the integral parameter uncertainties previously calculated using the ANL covariance matrices were revised using covariance data developed through the joint effort of several laboratories contributing to Subgroup 26. This new set of covariance matrices is

referred to as BOLNA (*Brookhaven, Oak Ridge, Los Alamos, NRG Petten, Argonne* – participating developmental laboratories). The BOLNA covariance matrices are unique in terms of completeness and applied methodology. However, it must be understood that the field of covariance generation for nuclear data is a relatively new one. Although BOLNA is the state of the art, it is often termed preliminary and conclusions about achieved accuracies are conditioned by the partly untested quality of this set of covariance matrices.

The results of the uncertainty analysis are fully documented in the present report. The analysis is mostly focused on integral parameter (k_{eff} , reactivity coefficients, power distributions, etc.) uncertainty due to neutron cross-section uncertainties. However, a few specific items were also examined in some detail, e.g. fission spectrum uncertainties, the effect of resonance parameter uncertainty on Doppler. The integral parameters considered are related to the reactor core performances but also to some important fuel-cycle-related parameters, like the transmutation potential, the doses in a waste repository or the neutron source at fuel fabrication. However, while a detailed uncertainty analysis of fuel cycle parameters (like the decay heat) can be carried out in the case of current LWRs (as documented in an appendix of this report), this analysis is still a challenge for the future in the case of fast reactors, in particular if their fuel is heavily loaded with minor actinides (MA).

A first significant result is the strong impact of correlation data (e.g. off-diagonal elements) on the uncertainty assessment. Any credible uncertainty analysis should include the best available covariance data accounting for energy correlations (as in the present study) and possibly for cross-correlations among reactions (a typical case would be the inter-relation among total, elastic and inelastic cross-sections) and even for cross-correlation among isotopes, if needed, e.g. to account for normalisation issues.

The calculated integral parameter uncertainties, resulting from the presently assessed uncertainties on nuclear data, are probably acceptable in the early phases of design feasibility studies. In fact, the uncertainty on k_{eff} is less than 2% for all systems [except for accelerator-driven systems (ADS)] and reactivity coefficient uncertainties are below 20%. Power distribution uncertainties are also relatively small, except, once again, in the case of the ADS.

However, later conceptual and design optimisation phases of selected reactor and fuel cycle concepts will require improved data and methods in order to reduce margins, both for economical and safety reasons. For this purpose, a compilation of preliminary “design target accuracies” has been compiled and a target accuracy assessment has been performed to provide an indicative quantitative evaluation of nuclear data improvement requirements by isotope,

nuclear reaction and energy range, in order to meet the design target accuracies as compiled in the present study. First priorities were formulated on the basis of common needs for fast reactors and, separately, thermal systems.

The present status of nuclear data uncertainties, and in particular the very low values for ^{235}U , ^{238}U and ^{239}Pu fission and capture uncertainties in the BOLNA covariance data compilation, tend to indicate, in the case of the wide range of fast reactors considered in this study, a priority requirement for a drastic uncertainty reduction for some σ_{inel} (in particular for ^{238}U , but also for Fe and Na), for the σ_{fiss} of higher Pu isotopes and in particular for ^{241}Pu (between $\sim 1\text{-}500$ keV) and for σ_{capt} of ^{239}Pu ($\sim 1\text{-}500$ keV). These indications are valid for all fast reactors considered in this work, and which are representative of the current priorities of the Gen-IV and GNEP initiatives. Other requirements are of course associated to specific systems (as Si data for the GFR or Pb in the case of LFR and ADMAB).

The present analysis also indicates some significant requirements in the case of the VHTR. For this system it is required to improve ^{241}Pu σ_{fiss} below ~ 400 eV. Very tight σ_{capt} requirements for ^{239}Pu and ^{241}Pu below ~ 0.5 eV are also identified, together with carbon data improvements (both capture and inelastic) with respect to current uncertainty estimates. Finally, for the PWR with extended burn-up, the necessity to improve ^{241}Pu and some O data has been pointed out.

Finally, in the case of ADS, where the fuel should in principle be heavily loaded with MA, tight requirements are found for some MA cross-sections, in particular for σ_{fiss} of ^{244}Cm , ^{241}Am , ^{245}Cm , ^{243}Am , ^{242}Cm , $^{242\text{m}}\text{Am}$, for σ_{inel} of ^{243}Am and for ν of ^{244}Cm . For these reactions, the required accuracies are an order of magnitude below the present uncertainties. Concerning the major actinides, improvements are required for σ_{fiss} of ^{241}Pu (again \sim factor 10), for σ_{fiss} of ^{238}Pu (\sim factor 5) and for ν of ^{238}Pu (\sim factor 3).

For both fast (critical and subcritical) and thermal neutron systems, detailed results are presented in this report.

The results of the nuclear data target accuracy assessment indicate that a careful analysis is needed in order to define the most appropriate and effective strategy for data uncertainty reduction.

In fact, some key requirements are very specific and would be difficult to establish within a reasonable time horizon, as discussed in Appendix A, where some comments are made concerning the accuracy of individual measurements of microscopic cross-sections in relation to the accuracy requirements that

emerged from the studies of this subgroup; it seems that a strategy of combined use of integral and differential measurements should be pursued in order to meet the requirements.

As indicated above, specific studies were also devoted to the resonance parameter uncertainty impact on the Doppler reactivity coefficient (Appendix B) and on fission spectrum uncertainty impact. In this last case, the activity of the subgroup allowed to clarify several basic issues, such as the theoretical basis for practical sensitivity coefficient expressions and the prescriptions to set up a fission spectrum covariance matrix. As for the actual uncertainty analysis, it was made clear that more work is needed in that field (Appendices C and D).

As for data needs related to fuel cycle parameters, the present study has addressed in a quantitative way the uncertainties of a number of parameters directly related to the nuclei density uncertainties. A more comprehensive study related, e.g. to the decay heat, is still to be undertaken. However, the subgroup preliminarily addressed several important issues. In particular, Appendix E deals with the case of nuclear data for the handling, reprocessing and disposal of spent nuclear fuel. Since it is recognised that for future facilities any nuclear data which dominates the uncertainties need to be identified as well as any biases so that improvements can be made to the basic nuclear data, an initial study is described in Appendix E, considering only thermal reactors and some conclusions made about how these could be extended for novel systems. As an example, the calculation of decay heat in the context of the current fuel reprocessing plants is discussed there.

Moreover, some specific requirements for resonance data important for advanced fuel cycle applications are discussed in Appendix F.

In order to render the present report as clear as possible, Appendix G was introduced to summarise the basic approaches used to prepare, e.g. the BNL covariance data. In turn, Appendix H summarises some preliminary comments concerning the performance of the covariance data generated at LANL for the three major actinides (^{235}U , ^{238}U and ^{239}Pu) at high energy.

Considerations related to the impact of reaction cross-correlations are given in Appendix I. The example considered is the cross-correlation of the Na elastic and inelastic cross-sections.

Finally, the subgroup members discussed further activities to be proposed to the WPEC for consideration. Two recommendations were formulated (Appendix J). In particular the need for a co-ordinated effort in the field of the use of integral experiments for data improvement has been strongly underlined.

1. Introduction

The Working Party on Evaluation Co-operation (WPEC) of the OECD Nuclear Energy Agency Nuclear Science Committee established an international subgroup (Subgroup 26) to perform an activity to develop a systematic approach to define data needs for Gen-IV and, in general, for advanced reactor systems.

The systems considered within the Subgroup 26 are taken from the list of preferred systems of Gen-IV, essentially a very high-temperature reactor (VHTR) with particle fuel and different types of fast reactors (FRs), all based on the uranium cycle.

A preliminary uncertainty analysis was carried out on these systems [1]. For the subgroup study, it was decided to add a pressurised water reactor (PWR) with extended burn-up (100 GWd/t), and for fast reactors it was decided to widen the scope to an ensemble of fast neutron systems, not only with different coolants (Na, gas, lead, lead-bismuth eutectic), but also with different fuel types (oxides, metals, carbides, nitrides) and different Pu/TRU compositions, in different core volumes. These fast reactor systems are a sodium-cooled fast reactor (SFR) in a TRU burning configuration, i.e. with a conversion ratio (CR) < 1 , the European fast reactor (EFR) with full recycling of MA and CR ~ 1 , a gas-cooled fast reactor (GFR) also with full recycling of MA, a lead-cooled fast reactor (LFR) as defined for an IAEA benchmark, an advanced burner test reactor (ABTR) Na-cooled core, recently studied within the GNEP initiative and an accelerator-driven minor actinides burner (ADMAB). The fast reactor specifications are defined in [1-4] and their characteristics are summarised in Table 1. Section 5 discusses these systems in greater detail.

In Ref. [1], the preliminary uncertainty study was carried out with an “educated” guess of uncertainties for all the isotopes of interest (actinides, structural and coolant materials), based as much as possible on the nuclear data performance in the analysis of selected, clean integral experiments (irradiated fuel and sample analysis, criticality and fission rates in zero-power critical facilities) [2,5]. For the correlations, a very crude hypothesis of partial energy correlations (PEC) “by energy band” was used as a first guess.

However, within Subgroup 26 a major step forward was made with the assessment of preliminary cross-section covariance data through the joint efforts of several laboratories and in particular BNL, LANL, ORNL and NRG. The new set of uncertainties is called BOLNA; they are further elaborated upon in Section 3.

Table 1. Features of investigated systems

System	Fuel	Coolant	TRU/(U+TRU)	MA^(a)/(U+TRU)	Power (MWth)
ABTR	Metal	Na	0.162	~0	250
SFR	Metal	Na	0.605	0.106	840
EFR	MOX	Na	0.237	0.012	3 600
GFR	Carbide	He	0.217	0.050	2 400
LFR	Metal	Pb	0.233	0.024	900
ADMAB	Nitride	Pb-Bi	1.0	0.680	380

^(a) Minor actinides.

The integral parameter objects of the uncertainty evaluation, characterising the reference systems and their associated fuel cycle are: criticality (k_{eff}), power peak in the core, Doppler and coolant void reactivity coefficients, reactivity swing during burn-up, isotope concentrations in the spent fuel, decay heat of the spent fuel in a repository, dose (radiotoxicity) of the spent fuel or of the wastes in a repository, at selected times after storage and neutron source associated to the spent fuel, e.g. at fuel fabrication.

A study was also carried out based both on the results of the uncertainty evaluation and on target accuracies for the various integral parameters that were defined within the subgroup, so as to provide guidelines concerning priority requirements for data improvements.

Part of the results and relative conclusions provided in the present document were published in Refs. [6] (uncertainty evaluation) and [7] (target accuracy study).

2. Approach and theoretical background

The approach used for the present work includes:

- sensitivity studies using Generalised Perturbation Theory (GPT) on the selected integral parameters of representative models of systems;
- uncertainty assessment using covariance data.

In order to undertake a comprehensive assessment, the tools of sensitivity and uncertainty analysis are thus required. They have been widely developed in the past, in particular for the assessment of fast reactor performances in the 70s and 80s. A brief description is given below (Section 2.1) of the sensitivity formulations, based on deterministic methods as used for the study. Moreover, Monte Carlo methods have been shown to be useful for the treatment of full three-dimensional geometries and have been applied in some preliminary studies related to some linear functionals of the neutron flux (such as the heat deposited in the structures of a fusion device) and to the multiplication factor of a standard fission reactor. These methods will be briefly described in Section 2.2.

2.1 Sensitivity coefficients

Sensitivity coefficients can be used for different objectives like uncertainty estimates, design optimisation, determination of target accuracy requirements, adjustment of input parameters, and evaluations of the representativity of an

experiment with respect to a reference design configuration. In this section (based on Ref. [8]) the theory, based on the adjoint approach, that is implemented in the ERANOS fast reactor code system [9] is presented along with some features related to specific types of problems as is the case for nuclide transmutation, reactivity loss during the cycle, decay heat, neutron source associated to fuel fabrication, and experiment representativity.

It should first be recalled that, by definition, the sensitivity coefficients, $S_R = \frac{\partial R}{\partial \sigma} \cdot \frac{\sigma}{R}$, give the subsequent change in the integral parameter R due to a constant variation (generally 1%) of the cross-sections.

Sensitivity coefficients are calculated using GPT methods. In the following, the formulae used to obtain sensitivity coefficients for the integral parameters under study will be provided. Depending on the specific case, the classical Boltzmann equations have to be solved in order to establish the direct and adjoint fluxes:

$$M\Phi = \left(A - \frac{1}{k}F \right) \Phi = 0 \quad \text{Eq. (1)}$$

for the homogeneous (source free) direct flux (actual neutron flux of critical cores and first order harmonic of subcritical systems):

$$M\Phi_s = \left(A - \frac{1}{k}F \right) \Phi_s = S \quad \text{Eq. (2)}$$

for the inhomogeneous (source-driven) direct flux (actual neutron flux of subcritical systems) and:

$$M^* \Phi^* = \left(A^* - \frac{1}{k}F^* \right) \Phi^* = 0 \quad \text{Eq. (3)}$$

for the adjoint flux.

In Eqs. (1) to (3), A is the loss (leakage + absorption) operator, F is the fission production operator, M is the Boltzmann operator and S is the external neutron source driving the subcritical system.

Only for the power peak do the relative equations to obtain the sensitivity coefficients for critical and subcritical (source-driven) cores require different

approaches and they will therefore be discussed separately. For all other parameters, the equations are the same for both critical and subcritical systems.

2.1.1 Multiplication factor

In the present study, the sensitivity coefficients were obtained according to the equation:

$$S_{k,calc} = \frac{1}{k} S_k = \frac{1}{k} \left(\frac{\partial k}{\partial \sigma} \cdot \frac{\sigma}{k} \right) = - \frac{1}{I_f} \left\langle \Phi^*, \left(\frac{\partial A}{\partial \sigma} - \frac{1}{k} \frac{\partial F}{\partial \sigma} \right) \Phi \right\rangle \quad \text{Eq. (4)}$$

where $I_f = \langle \Phi^*, F\Phi \rangle$ and $\langle \cdot \rangle$ denote the integration over space, angle and energy.

2.1.2 Power peak

As mentioned earlier, for the power peak the case of critical and subcritical (source-driven) systems are separately discussed.

The power peak is defined as the ratio between the maximum and the core power density:

$$P_{max} = \frac{V_{core}}{V_{max}} \frac{\langle \Sigma_p \Phi \rangle_{max}}{\langle \Sigma_p \Phi \rangle} \quad \text{Eq. (5)}$$

for critical systems and:

$$P_{max} = \frac{V_{core}}{V_{max}} \frac{\langle \Sigma_p \Phi_s \rangle_{max}}{\langle \Sigma_p \Phi_s \rangle} \quad \text{Eq. (6)}$$

for source-driven systems, where Σ_p is the macroscopic power cross-section (essentially represented by $E_f \times \Sigma_f$, E_f being the average energy released per fission and Σ_f the macroscopic fission cross-section), V_{max} is the mesh volume associated to the point where the maximum power occurs and V_{core} is the core volume.

Sensitivity coefficients are obtained by solving the equations:

$$S_{P_{\max}} = \frac{\sigma}{P_{\max}} \frac{dP_{\max}}{d\sigma} = \frac{\sigma}{P_{\max}} \left\{ \frac{\partial P_{\max}}{\partial \sigma} - \left\langle \Psi^*, \left(\frac{\partial A}{\partial \sigma} - \frac{1}{k} \frac{\partial F}{\partial \sigma} \right) \Phi \right\rangle \right\} \quad \text{Eq. (7)}$$

$$= \{S_{P_{\max},D} - S_{P_{\max},I}\}$$

for critical systems and:

$$S_{P_{\max}} = \frac{\sigma}{P_{\max}} \frac{dP_{\max}}{d\sigma} = \frac{\sigma}{P_{\max}} \left\{ \frac{\partial P_{\max}}{\partial \sigma} - \left\langle \Psi^*, \left(\frac{\partial A}{\partial \sigma} - \frac{1}{k} \frac{\partial F}{\partial \sigma} \right) \Phi \right\rangle \right\} \quad \text{Eq. (8)}$$

$$= \{S_{P_{\max},D} - S_{P_{\max},I}\}$$

for source-driven systems.

In Eqs. (7) and (8):

$$S_{P_{\max},D} = \frac{\sigma}{P_{\max}} \cdot \frac{\partial P_{\max}}{\partial \sigma} = (S_{P_{\max},D})_{i,g,d}$$

$$\bullet \quad = \frac{\sigma}{P_{\max}} \left(\frac{\left(\langle \Sigma_p \Phi \rangle_{\max} \right)_{i,g}}{\langle \Sigma_p \Phi \rangle_{\max}} - \frac{\left(\langle \Sigma_p \Phi \rangle \right)_{i,g,d}}{\langle \Sigma_p \Phi \rangle} \right) \quad \text{Eq. (9)}$$

$\begin{matrix} i=\text{isotope} \\ g=\text{energy group} \\ d=\text{reactor domain} \end{matrix}$

is the direct term of the sensitivity coefficients accounting for the variations in the power peak directly due to variations of Σ_p . Eq. (9) is for critical cores: simply replace Φ by Φ_s to get the appropriate formulation for subcritical systems. In the present study, the direct term $S_{P_{\max},D}$ has been neglected since it is obtained from the difference of comparable quantities.

- $S_{P_{\max},I}$ is the indirect term of the sensitivity coefficients, accounting for the variations in the power peak due to the change in the flux spectrum determined by the cross-section variations.
- $\frac{\partial S}{\partial \sigma}$ accounts for possible variation of the external source due to the cross-section variations. This term is neglected in the present study, based on the assumption that cross-section variations leave the external neutron source unchanged.

- ψ^* is the generalised importance function, solution of the following equations:

$$\left(A^* - \frac{1}{k} F^*\right) \tilde{\Psi}^* = \frac{1}{P_{\max}} \frac{\partial P_{\max}}{\partial \Phi} = \frac{\Sigma_p(\vec{r}_{\max}, E)}{\langle \Sigma_p \Phi \rangle_{\max}} - \frac{\Sigma_p(\vec{r}, E)}{\langle \Sigma_p \Phi \rangle} \quad \text{Eq. (10)}$$

for critical systems and:

$$(A^* - F^*) \tilde{\Psi}^* = \frac{1}{P_{\max}} \frac{\partial P_{\max}}{\partial \Phi_s} = \frac{\Sigma_p(\vec{r}_{\max}, E)}{\langle \Sigma_p \Phi_s \rangle_{\max}} - \frac{\Sigma_p(\vec{r}, E)}{\langle \Sigma_p \Phi_s \rangle} \quad \text{Eq. (11)}$$

for source-driven systems, with \vec{r}_{\max} the mesh point where maximum power occurs and $\tilde{\Psi}^* = \frac{\Psi^*}{P_{\max}}$.

2.1.3 Reactivity coefficients

A reactivity coefficient (like the Doppler effect) can be expressed as the reactivity variation, $\Delta\rho$, of the unperturbed system (characterised by a value k of the multiplication factor, a Boltzmann operator M , a flux Φ and an adjoint flux Φ^*):

$$\Delta\rho = \left(1 - \frac{1}{k_p}\right) - \left(1 - \frac{1}{k}\right) = \frac{1}{k} - \frac{1}{k_p} \quad \text{Eq. (12)}$$

where k_p corresponds to a variation of the Boltzmann operator such that:

$$\begin{aligned} M &\rightarrow M_p (= M + \delta M), \quad \Phi \rightarrow \Phi_p (= \Phi + \delta\Phi_p) \\ \Phi^* &\rightarrow \Phi_p^* (= \Phi^* + \delta\Phi_p^*), \quad k \rightarrow k_p (= k + \delta k_p) \end{aligned} \quad \text{Eq. (13)}$$

The sensitivity coefficients for $\Delta\rho$ to variations (1%) of σ are given as:

$$S_{\Delta\rho} = \frac{\partial(\Delta\rho)}{\partial\sigma} \cdot \frac{\sigma}{\Delta\rho} = \frac{1}{\Delta\rho} \left\{ \begin{aligned} &\frac{1}{I_f^p} \left\langle \Phi^*, \left(\frac{\partial A_p}{\partial\sigma_p} - \frac{1}{k_p} \frac{\partial F_p}{\partial\sigma_p} \right) \Phi_p \right\rangle \\ &- \frac{1}{I_f} \left\langle \Phi^*, \left(\frac{\partial A}{\partial\sigma} - \frac{1}{k} \frac{\partial F}{\partial\sigma} \right) \Phi \right\rangle \end{aligned} \right\} \quad \text{Eq. (14)}$$

where $I_f = \langle \Phi^*, F\Phi \rangle$ and $I_f^p = \langle \Phi_p^*, F_p \Phi_p \rangle$.

2.1.4 Nuclide transmutation

In the case of nuclide transmutation (i.e. nuclide densities at the end of irradiation), the transmutation of the generic nuclide, i , during irradiation can be represented as the nuclide density variation between the time t_0 and t_F .

Denoting n_F^i the “final” density for the isotope i , the appropriate sensitivity coefficients are given by:

$$S_n^i = \frac{\partial n_F^i}{\partial\sigma} \cdot \frac{\sigma}{n_F^i} = \frac{1}{n_F^i} \int_{t_0}^{t_F} n^* \sigma n \, dt \quad \text{Eq. (15)}$$

where the time-dependent equations to obtain n^* and n are the classical Bateman equation and its adjoint equation, with appropriate boundary conditions.

2.1.5 Reactivity loss during irradiation

In the case of the reactivity loss during irradiation, $\Delta\rho^{\text{cycle}}$, at the first order:

$$\Delta\rho^{\text{cycle}} = \sum_i \Delta n^i \rho_i \quad \text{Eq. (16)}$$

with $\Delta n^i = n_F^i - n_0^i$ and ρ_i is the reactivity per unit mass associated to the isotope i .

The related sensitivity coefficients associated to the variation of σ , are given by:

$$\begin{aligned}
S_{\Delta\rho^{\text{cycle}}} &= \frac{\sigma}{\Delta\rho^{\text{cycle}}} \cdot \frac{\partial(\Delta\rho^{\text{cycle}})}{\partial\sigma} \\
&= \frac{\sigma}{\Delta\rho^{\text{cycle}}} \left(\sum_i \frac{\partial n^i}{\partial\sigma} \cdot \rho_i + \sum_i \Delta n^i \frac{\partial \rho_i}{\partial\sigma} \right)
\end{aligned}
\tag{Eq. (17)}$$

or:

$$\begin{aligned}
S_{\Delta\rho^{\text{cycle}}} &= \sum_i \frac{\rho_i}{\Delta\rho^{\text{cycle}}} \int_{t_0}^{t_F} n^* \sigma n dt + \\
&\quad \frac{1}{\Delta\rho^{\text{cycle}}} \left\{ \frac{1}{I_f^p} \left\langle \Phi^*, \left(\frac{\partial A_p}{\partial\sigma_p} - \frac{1}{k_p} \frac{\partial F_p}{\partial\sigma_p} \right) \Phi_p \right\rangle \right. \\
&\quad \left. - \frac{1}{I_f} \left\langle \Phi^*, \left(\frac{\partial A}{\partial\sigma} - \frac{1}{k} \frac{\partial F}{\partial\sigma} \right) \Phi \right\rangle \right\}
\end{aligned}
\tag{Eq. (18)}$$

2.1.6 Neutron source (e.g. at fuel fabrication)

A neutron source $NS_{t=t_F}$ at $t = t_F$ can be defined as:

$$NS_{t=t_F} = \sum_i P_i n_{t=t_F}^i \tag{Eq. (19)}$$

where P_i is the neutron production cross-section (e.g. by spontaneous fissions).

The sensitivity coefficients are:

$$S_{NF}^i = P_i \cdot \frac{\partial n_F^i}{\partial\sigma} \cdot \frac{\sigma}{n_F^i} = \frac{P_i}{n_F^i} \int_{t_0}^{t_F} n^* \sigma n dt \tag{Eq. (20)}$$

where effects due to P_i cross-section variations are assumed to be negligible.

2.1.7 Decay heat

The decay heat is defined as:

$$H(t) = \sum_i \lambda_i Q_i n^i(t) \quad \text{Eq. (21)}$$

where for each isotope i , λ_i are the decay constants, Q_i the heat released in decay reaction and $n^i(t)$ are the nuclide densities at the time t .

The equations for $n^i(t)$ are the classical ones:

$$\begin{aligned} \frac{dn^i(t)}{dt} = & \sum_F \gamma_{i,f} \tau_f + \sum_j n^j(t) \tau_j b_{j \rightarrow i} \\ & + \sum_l n^l(t) \lambda_l b_{l \rightarrow i} - \tau_i n^i(t) - \lambda_i n^i(t) \end{aligned} \quad \text{Eq. (22)}$$

Or in a more compact form:

$$\frac{dn^i(t)}{dt} = b_i + \sum_{j=1}^{I-1} C_{ij} n^j(t) - C_{ii} n^i(t) \quad \text{Eq. (23)}$$

where $\gamma_{i,f}$ are fission yields for fissionable isotope f , τ are microscopic reaction rates and $b_{j \rightarrow i}$ are branching ratios. Eqs. (22) and (23) are the inhomogeneous Bateman-type equations that define the appropriate nuclide field.

The uncertainty on $H(t)$ is obtained by combining the appropriate derivatives of H with respect to λ , Q and n , and accounting for possible correlations. As for the variations of the n^i terms, they can be evaluated using the perturbation techniques indicated in Section 2.1.4. A specific feature is represented by the variation of the fission yields γ , i.e. by the variation of the “source” term b_i in Eq. (23).

The relative sensitivity coefficients corresponding to the decay heat at $t = t_x$ are given by:

$$S_{H_{i,f}}^\gamma = \tau_f \frac{\partial n_{t=t_x}^i}{\partial \gamma_{i,f}} \cdot \frac{\gamma_{i,f}}{n_{t=t_x}^i} = \frac{\tau_f}{n_{t=t_x}^i} \int_0^{t_x} n^* \gamma_{i,f} dt \quad \text{Eq. (24)}$$

2.2 Uncertainties and target accuracies

Once the sensitivity coefficient matrix S_R for each integral parameter R and the covariance matrix D are available, the uncertainty on the integral parameter can be evaluated as follows:

$$\Delta R_0^2 = S_R^+ D S_R \quad \text{Eq. (25)}$$

A successive step is the assessment of target accuracy requirements. To establish priorities and target accuracies on data uncertainty reduction, a formal approach can be adopted by defining target accuracies on the design parameters and determining required accuracies on the data. In fact, the unknown uncertainty data requirements d_i can be obtained (e.g. for parameters i not correlated among themselves), by solving the following minimisation problem:

$$\sum_i \lambda_i / d_i^2 = \min \quad i = 1 \dots I \quad (I: \text{total no. of parameters}) \quad \text{Eq. (26)}$$

with the following constraints:

$$\sum_i S_{ni}^2 d_i^2 < (R_n^T)^2 \quad n = 1 \dots N \quad \text{Eq. (27)}$$

where N is the total number of integral design parameters, S_{ni} are the sensitivity coefficients for the integral parameter R_n and R_n^T are the target accuracies on the N integral parameters; λ_i are “cost” parameters related to each σ_i and should give a relative figure of merit of the difficulty of improving that parameter (e.g. reducing uncertainties with an appropriate experiment).

2.3 Sensitivity/uncertainty analysis using Monte Carlo methods

Uncertainty calculations in arbitrary three-dimensional radiation transport problems can be performed in an easy and straightforward manner. Although 3-D uncertainty tools do exist, their use has been rather limited up to now because they are tied to 3-D deterministic radiation transport codes, which are not commonly used because of their complexity. The method described in Ref. [10] makes use of the 3-D Monte Carlo code MCNP, which is the most commonly used radiation transport code world wide.

It has been shown that, using standard options of MCNP, a sensitivity profile may be calculated in an arbitrary three-dimensional geometry. The

preparation of the MCNP input for such an analysis may easily be taken care of by a simple piece of coding or a shell-script. Several uncertainty codes offer the possibility to start the uncertainty calculation from such a sensitivity profile instead of starting from forward and adjoint fluxes.

The sensitivity profile P_g (or sensitivity vector) is defined as the relative change in a response parameter R due to a relative change in a cross-section in energy group g : $P_g = (\delta R/R)/(\delta \sigma_g/\sigma_g)$.

In this case the response parameter is a scalar quantity, which is a linear function of the neutron and/or γ - flux. Examples are energy-integrated fluxes, the value of k_{eff} , radiation damage and radiation heating. The method may easily be extended to non-scalar response parameters, such as (energy-dependent) flux spectra. In this case the sensitivity vector will become a sensitivity matrix.

Using the perturbation option of MCNP (invoked with the PERT-card with the default option (i.e. method = 1)) the sensitivity profile is generated as follows:

- The cross-section is selected for which the profile is to be generated [e.g. the fission cross-section for ^{238}U , $\sigma_{\text{fiss}}(^{238}\text{U})$].
- A material card is created in which the atomic density for the relevant isotope (i.e. ^{238}U) is increased by 1%.
- A PERT-card is created specifying that the relevant material is replaced by the perturbed material in each of the cells in which the material is present. Perturbation cards should be given for all energy groups (the group structure is defined by the group structure of the covariance data used in the uncertainty calculation). Of course, care should be taken only to perturb the relevant cross-section [in this case $\sigma_{\text{fiss}}(^{238}\text{U})$]. This is implemented by using the rxn-keyword of the PERT-card. One should take care to specify the correct density for the perturbed material (i.e. $\rho' = 1.01 \times \rho$).
- Finally, MCNP is run with these modifications in the input. In the MCNP output a table is given with the result of the perturbations. For response parameters other than k_{eff} the results are also generated on the MCTAL output of MCNP.

The sensitivity profile thus produced by MCNP and the relevant covariance matrices are then used to carry out an uncertainty calculation with the SUSI modular code.

In order to validate the new approach, some comparisons have been carried out with existing sensitivity codes.

In the case of the heat deposited by neutrons and gammas in the superconducting coils of a fusion device, sensitivity profiles were calculated for the total cross-section of Fe. The sensitivity profile obtained from the MCNP/SUSD calculation was successfully compared to those obtained with the deterministic ANISN/SENSIT code system.

The Monte Carlo method was also used for a GCFR benchmark design. The uncertainty in the value of k_{eff} due to cross-section uncertainties was calculated. Calculated sensitivities were compared with those obtained with the ERANOS sensitivity/uncertainty modules, described previously. A good agreement is observed for nearly all isotopes and reactions.

3. Covariance data

As discussed in the introduction, in the present document the uncertainty assessment is made using the new cross-section evaluations – BOLNA – that were produced for the needs of the subgroup. Further, a comparison is provided with the results of the preliminary analysis performed in Ref. [1] with the use of a “homemade” ANL covariance matrix. Consequently, in the present section, after a short recall of the main features characterising the ANL covariance matrix, the details of the BOLNA covariance data will be discussed.

3.1 ANL covariance matrix

The “homemade” ANL covariance matrix [11] was obtained by updating the covariance matrix used in an initial ADS study [2] by taking into account the results of clean integral experiment analysis – in particular, irradiated sample/fuel analysis, which provided valuable information on capture and some (n,2n) cross-sections, and fission rate measurements in critical assemblies [5].

The uncertainty values were given by “energy bands” consistent with multi-group energy structures used for deterministic calculations of both thermal and fast reactors. Fifteen energy groups were selected between 20 MeV and thermal energy. Two extra groups were added between 150 MeV and 20 MeV for ADS applications. The uncertainty values are given only for neutron cross-section data of actinides and structural materials. Fission-product-related uncertainties were not considered.

In the compilation of the covariance matrix there was an attempt to account for the work done, in particular for major actinides, within the framework of the JEF project, in order to produce “adjusted” cross-sections. For minor actinides, the analysis and recommendations of a WPEC working group (updated, once again, for selected isotopes and reactions, on the basis of integral experiment analysis) were used. For most structural materials, data were often derived from the graphical intercomparison of different data files.

The covariance matrix diagonal values were estimated on the performance of the most recent JEF files in the analysis of a large set of integral experiments in different spectra. However, it was observed that the performance obtained using ENDF/B files was not substantially different. Therefore, the covariance matrix can be applied to both files.

At first, only “diagonal” values of the full covariance matrices were used. Their use implies neglect of all types of correlation (in energy, between different isotopes, among reactions, etc.) and, consequently, to underestimating uncertainties. The ANL diagonal matrix is presented in Appendix Q (available on CD-ROM).

In a second step, partial energy correlations (PEC) were introduced. As a first guess, the same correlations were used for all isotopes and reactions, under the form of full energy correlation in five energy bands. The thought was to single out:

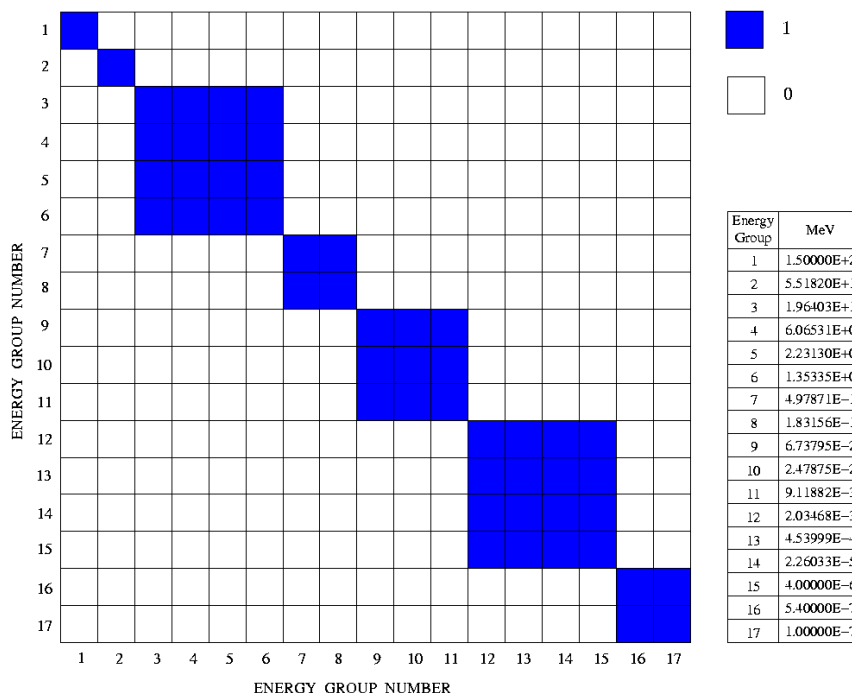
- the region above the threshold of fertile isotope fission cross-sections, and of many inelastic cross-sections, up to 20 MeV;
- the region of the continuum down to the upper unresolved resonance energy limit;
- the unresolved resonance energy region;
- the resolved resonance region;
- the thermal range.

The correlations used are shown in Figure 1.

3.2 *BOLNA covariance matrix*

Preliminary cross-section covariances were recently developed within the WPEC subgroup through the joint efforts of several laboratories. The new set of uncertainties is called BOLNA (standing for BNL, ORNL, LANL, NRG, ANL, from the laboratories wherein the covariances were produced).

Figure 1. Energy correlations used in the ANL partial energy correlation (PEC) matrix



Cross-section covariances for 45 out of 52 requested materials [12,13] were developed at BNL. The cross-section covariances were produced in 15- and 187-group representations as follows:

- Thirty-six (36) isotopes (^{16}O ; ^{19}F ; ^{23}Na ; ^{27}Al ; ^{28}Si ; ^{52}Cr ; $^{56,57}\text{Fe}$; ^{58}Ni ; $^{90,91,92,94}\text{Zr}$; $^{166,167,168,170}\text{Er}$; $^{206,207,208}\text{Pb}$; ^{209}Bi ; $^{233,234,236}\text{U}$; ^{237}Np , $^{238,240,241,242}\text{Pu}$; $^{241,242\text{m},243}\text{Am}$; $^{242,243,244,245}\text{Cm}$) were evaluated using the BNL-LANL methodology, based on the ENDF/B-VII.0 library [14], the Atlas of Neutron Resonances [15], the nuclear model code EMPIRE [16] and the Bayesian code Kalman [17].
- Six (6) isotopes ($^{155,156,157,158,160}\text{Gd}$ and ^{232}Th) were taken from ENDF/BVII.0.
- Three (3) isotopes (^1H , ^{238}U and ^{239}Pu) were taken from JENDL-3.3.

Covariances for the average number of neutrons per fission, total nu-bar, were provided for 16 actinides identified as priority by the subgroup.

LANL has evaluated the covariance matrices for ^{235}U , ^{238}U and ^{239}Pu in the fast energy region using only differential measurements and nuclear model calculations. A generalised-least-squares technique is used to evaluate a global covariance matrix based solely on experimental differential information. Since nuclear model calculations are used to complement experimental data, a Kalman filter is then used to combine experimental data and model calculation covariance matrices. This procedure was used for the three isotopes ^{235}U , ^{238}U and ^{239}Pu , for the reaction cross-sections of (n,fission), (n,capture), (n,total), (n,elastic), (n,inelastic) and (n,xn). The covariance matrices related to the average number of neutrons per fission were obtained from experimental data only.

To complete these data, resonance-parameter covariance evaluations were performed at ORNL for ^{235}U , ^{238}U and ^{239}Pu with the SAMMY [18] computer code. The covariance evaluations were made in the resolved and unresolved energy regions for ^{235}U , while only the resolved resonance covariance evaluations were undertaken for ^{238}U and ^{239}Pu . Experimental uncertainties are incorporated directly into the evaluation process in order to propagate them into the resonance parameter results [19].

Finally, covariance data files for the Pb isotopes were produced at NRG by a purely stochastic approach [20]. This is accomplished by subjecting the nuclear model code TALYS [21] to a Monte Carlo scheme for perturbing the input parameters of the various nuclear models, such as level densities, gamma-ray strength functions and the optical model.

In summary, for the BOLNA covariance matrix, all the available BNL data were used, except the ^{235}U , ^{238}U and ^{239}Pu data that were taken from the combined LANL/ORNL evaluation and the Pb isotope data, which were taken from the NRG evaluation. Missing data were taken from the ANL estimated covariance data [11].

The BOLNA diagonal matrix (no correlations among isotopes, reactions and energy groups) is presented in Appendix R (available on CD-ROM). As examples, some BOLNA covariance matrices for selected isotopes and reactions are given in Figures 2 through 5.

Further details concerning the methods used to produce the BNL covariance matrices are described in Appendix G.

Figure 2. Covariance matrix in 15 groups for the $^{239}\text{Pu}(n,f)$ reaction

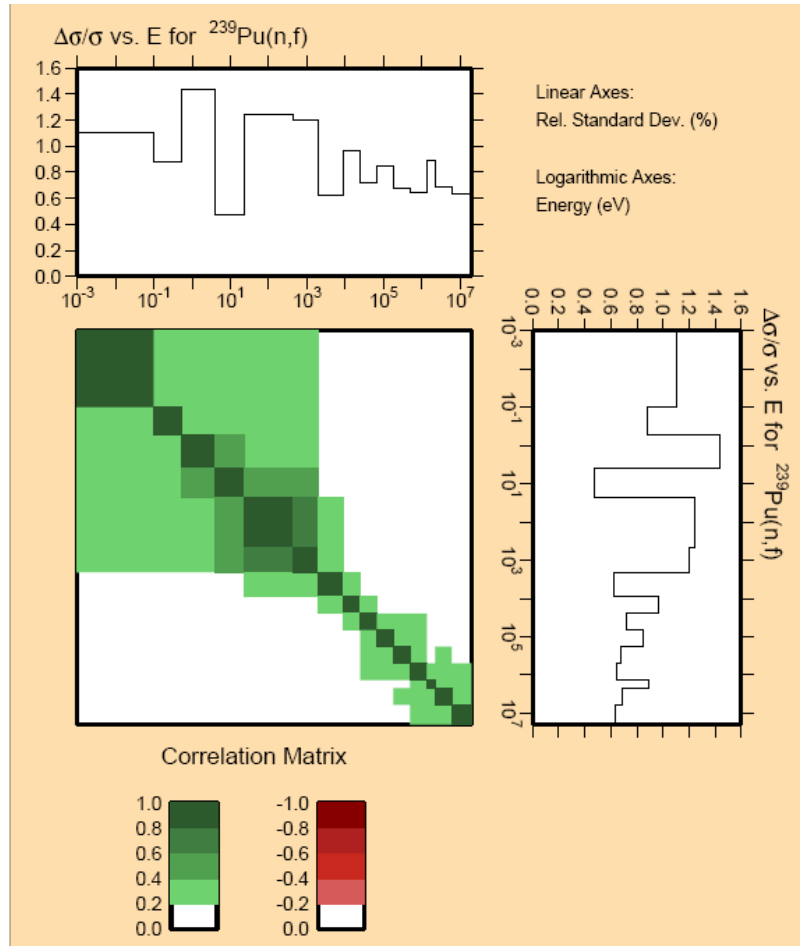


Figure 3. Covariance matrix in 187 (left) and 15 (right) groups for the $^{240}\text{Pu}(n,\gamma)$ reaction

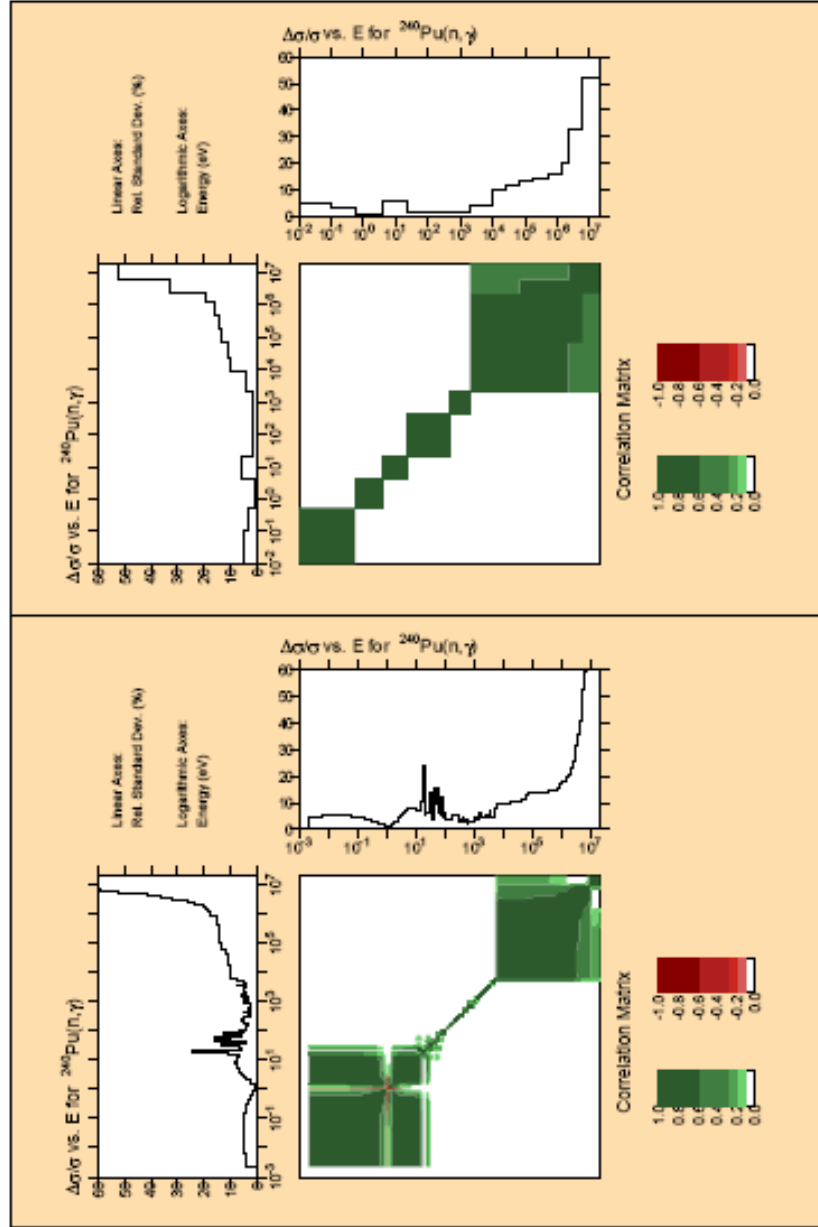


Figure 4. Covariance matrix in 187 (left) and 15 (right) groups for the $^{241}\text{Pu}(n,f)$ reaction

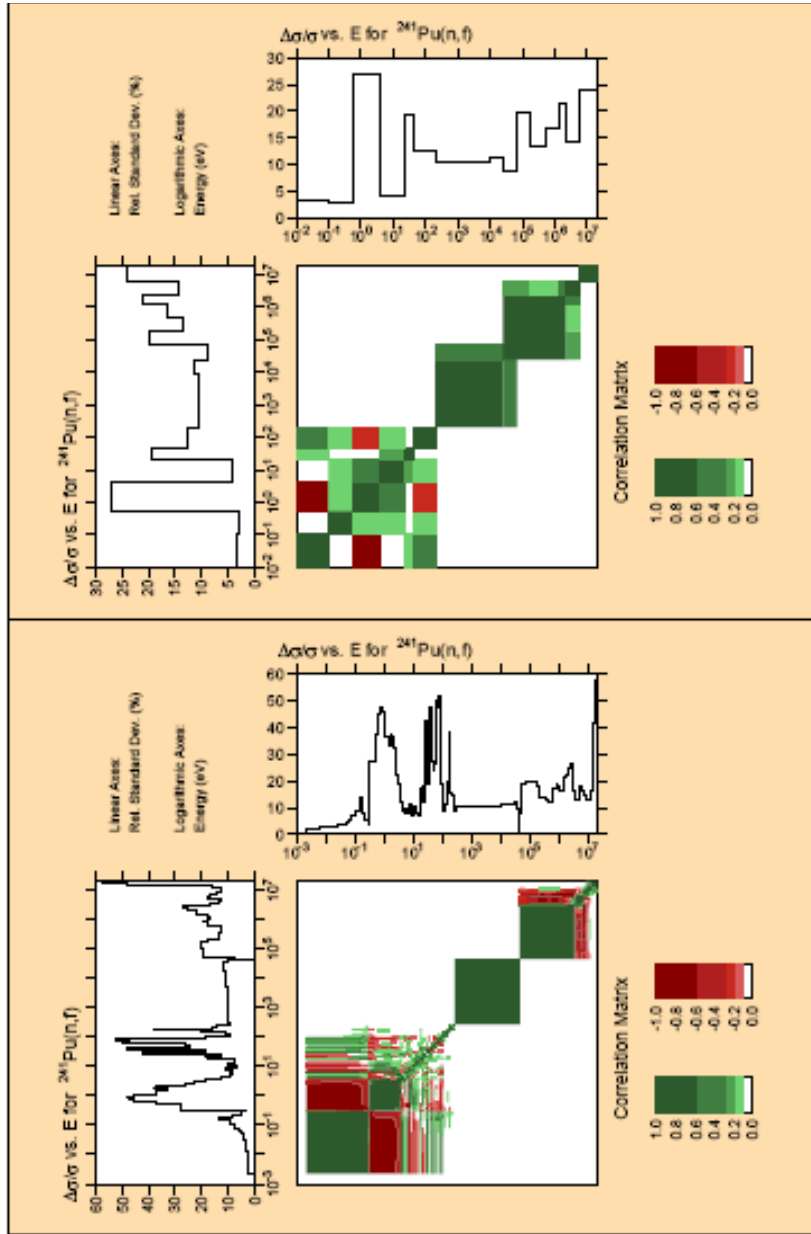
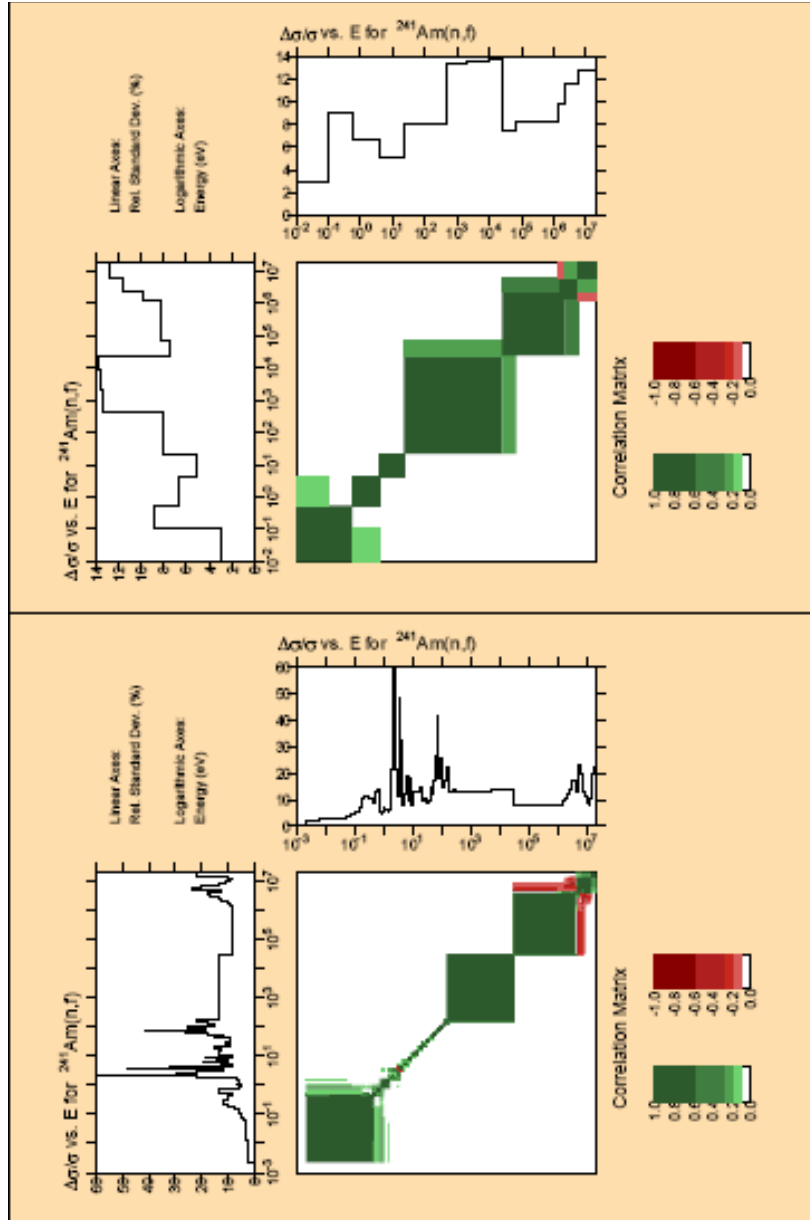


Figure 5. Covariance matrix in 187 (left) and 15 (right) groups for the $^{241}\text{Am}(n,f)$ reaction



4. Calculation tools

All the sensitivity calculations were performed with the ERANOS code system, which allows, as indicated previously, calculating homogeneous and inhomogeneous solutions of the Boltzmann equations, generalised importance functions and performing perturbation and uncertainty analysis. The discrete ordinate module BISTRO [22] was used to perform flux and generalised importance function calculations. An S_4P_1 approximation in RZ geometry proved sufficiently accurate for this type of calculation. Decay heat calculations were performed with the ORIGENRA code [23].

Cross-section data were processed with the ECCO code [24] for all the systems investigated, except for the thermal reactors for which the WIMS code [25] was used. The nuclear data are from the JEF libraries, in particular from JEF-3.0 [26] for the fast reactors (FRs) and from JEF-2.2 [27] for the ADMAD and the two thermal reactors VHTR and PWR. For most of the reactors investigated (except the ABTR, VHTR and PWR), homogenised cross-sections were calculated, since heterogeneity effects on the cross-sections are rather small in the systems under study. The target accuracy analysis was performed with the SNOPT code [28].

Note that for the present study the covariance data were produced rather independently from the cross-section data used to assess the nominal parameter values (JEFF-2.2 data). If this approach was justified in order to give, as required by the subgroup charter, trends and major indications on priority issues (e.g. issues that would require priority actions, such as new differential measurements with very low associated uncertainty), in the future (and for specific design applications) a consistent library for both is clearly to be preferred (i.e. cross-section library used in design and associated covariance data library).

5. Systems and integral parameters analysed

As mentioned previously, eight systems related to Gen-IV, AFCI and GNEP were considered. Geometry and compositions are presented in Appendix K (available on CD-ROM) and their main features are:

- ABTR: 250 MW_{th} – Na-cooled; U-TRU-10Zr fuel; HT9(75%)-Na(15%) reflector; enrichment: 17%, MA: <1%; irradiation cycle: 109.8 days (4 months at 90% capacity);
- SFR: (burner: CR = 0.25) 840 MW_{th} – Na-cooled; U-TRU-Zr metallic alloy fuel; SS reflector; enrichment: 56%, MA: 10%; irradiation cycle: 155 days;

- EFR: 3 600 MW_{th} – Na-cooled; U-TRU oxide fuel; U blanket; enrichment: 22%, MA: 1%; irradiation cycle: 1 700 days;
- GFR: 2 400 MW_{th} – He-cooled; SiC-(U-TRU)C fuel; Zr₃Si₂ reflector; enrichment: 17%, MA: 5%; irradiation cycle: 415 days;
- LFR: 900 MW_{th} – Pb-cooled; U-TRU-Zr metallic alloy fuel; Pb reflector; enrichment: 21%, MA: 2%; irradiation cycle: 310 days;
- ADMAB: 377 MW_{th} – Pb-Bi-cooled; TRU fuel; HT9(70%) Pb-Bi(30%) reflector; enrichment: 32%, MA: 67%; irradiation cycle: 366 days;
- VHTR: TRISO fuel; enrichment: 14%; burn-up: 90 GWd/tHM;
- Extended BU PWR: enrichment: 8.5%; burn-up: 100 GWd/tHM.

The neutron spectra and adjoint fluxes at core centre are shown in Figures 6 to 21. For the ADMAB, the flux spectra presented in Figures 16 and 17 correspond to the solution of the homogeneous (“source-free”) transport equation; however, the sensitivity analysis was carried by solving the equations with the source term (spallation source) in place.

The parameters considered are:

- criticality (multiplication factor);
- power peak value;
- Doppler reactivity coefficient;
- coolant void reactivity coefficient;
- reactivity loss during irradiation;
- transmutation potential (i.e. nuclide concentrations at end of irradiation, n_f , or density variation during burn-up, $\Delta n = n_f - n_i$);
- decay heat in a repository (at 100 years after disposal);
- radiotoxicity at $t = 100\,000$ years after disposal;
- radiation source at fuel discharge.

Nominal values calculated for each reactor are summarised in Tables 2 to 8. The isotope contribution to decay heat, radiotoxicity and radiation source can be found in Appendix L (available on CD-ROM) for each investigated system.

Figure 6. ABTR direct flux distribution

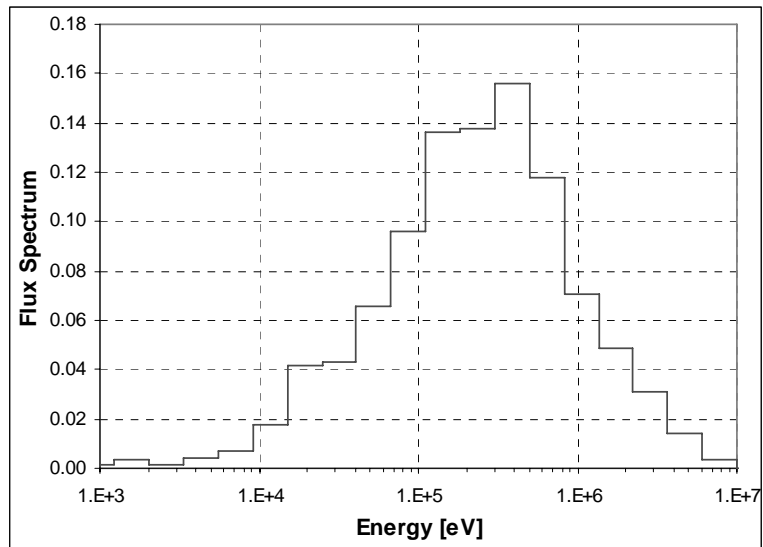


Figure 7. ABTR adjoint flux distribution

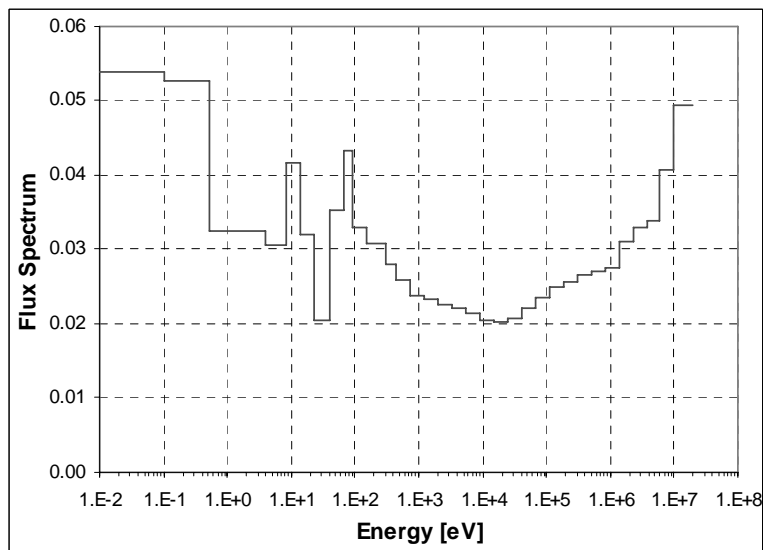


Figure 8. SFR direct flux distribution

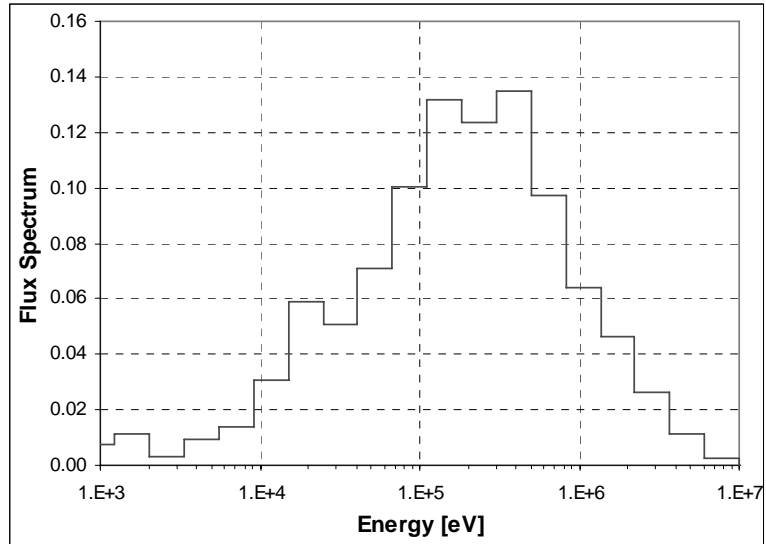


Figure 9. SFR adjoint flux distribution

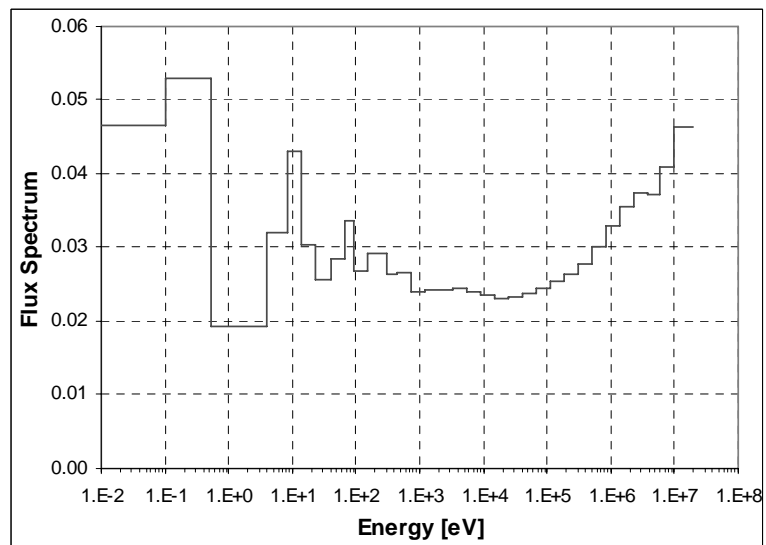


Figure 10. EFR direct flux distribution

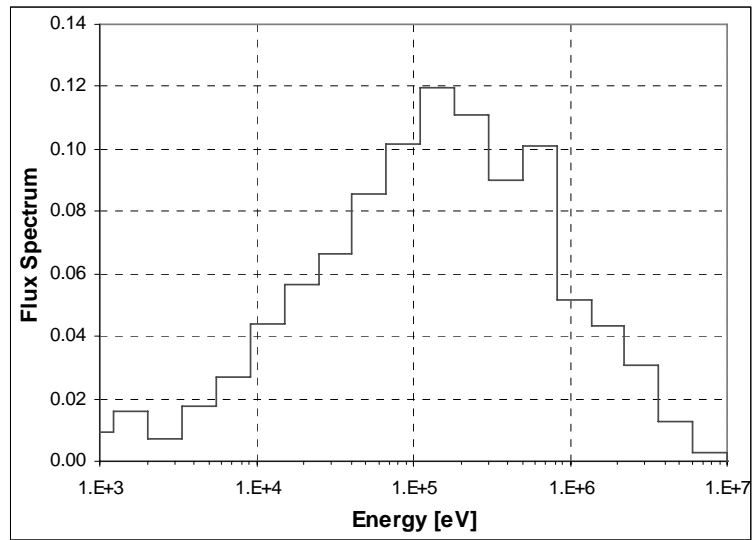


Figure 11. EFR adjoint flux distribution

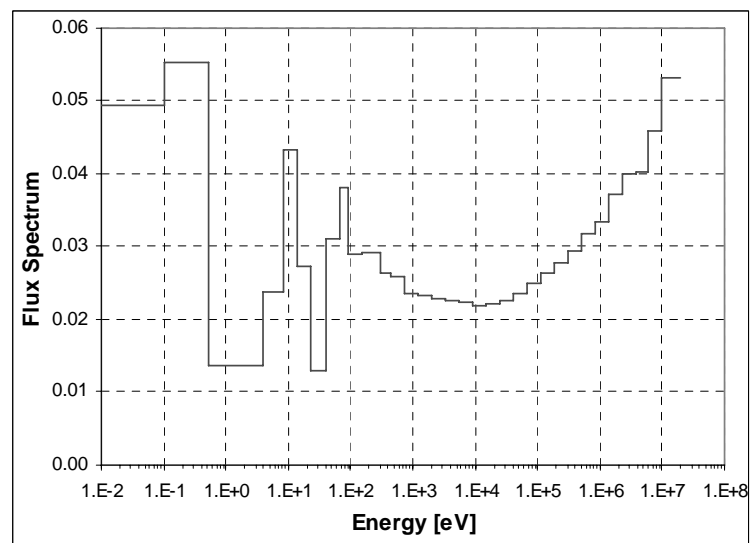


Figure 12. GFR direct flux distribution

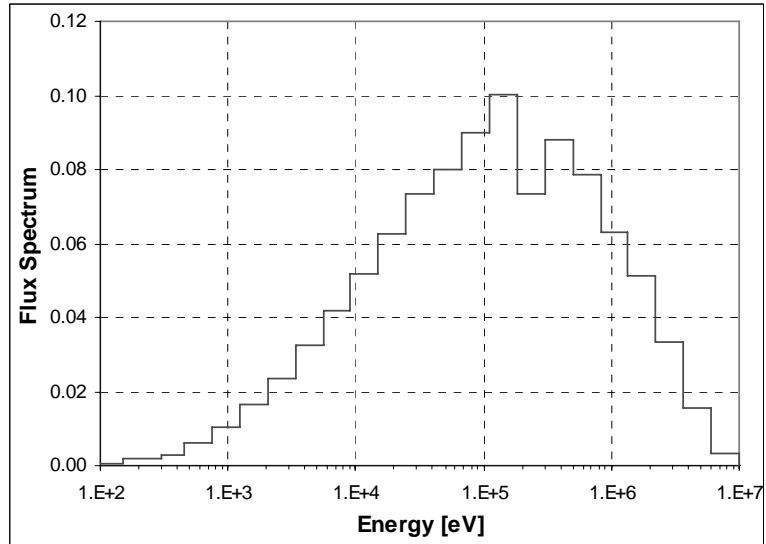


Figure 13. GFR adjoint flux distribution

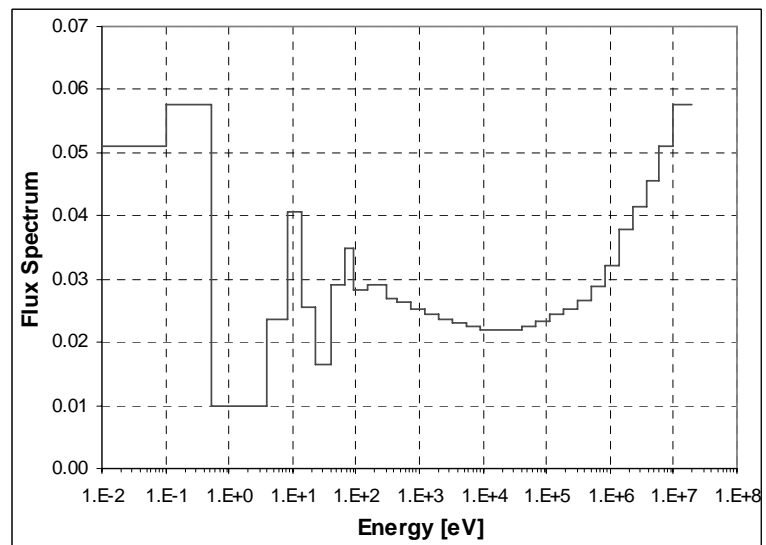


Figure 14. LFR direct flux distribution

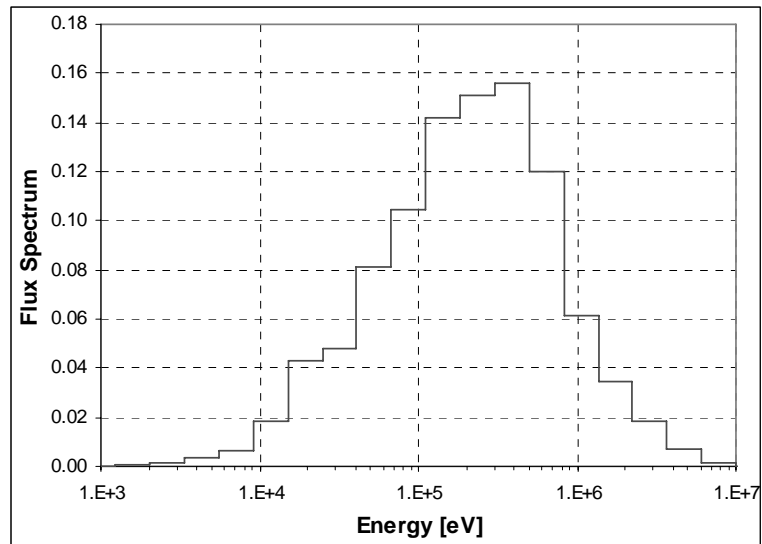


Figure 15. LFR adjoint flux distribution

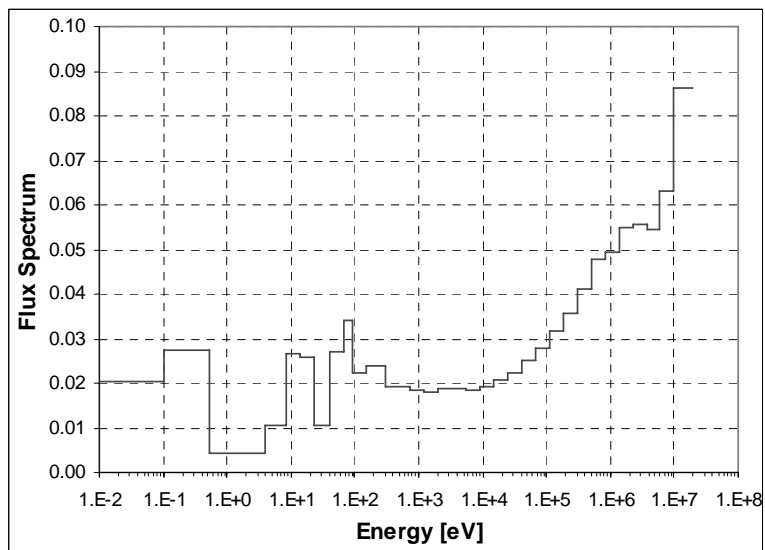


Figure 16. ADMAB direct flux distribution

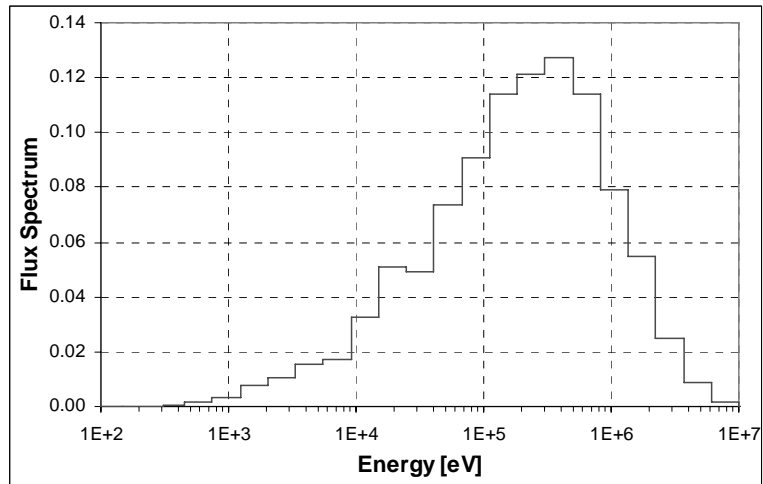


Figure 17. ADMAB adjoint flux distribution

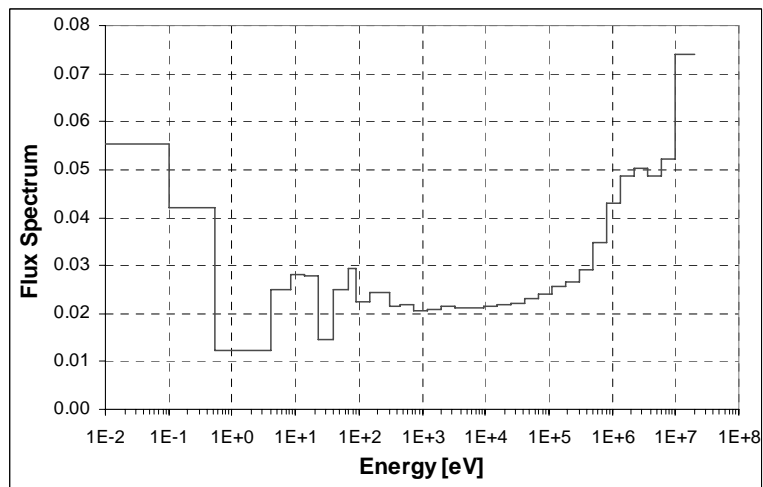


Figure 18. VHTR direct flux distribution

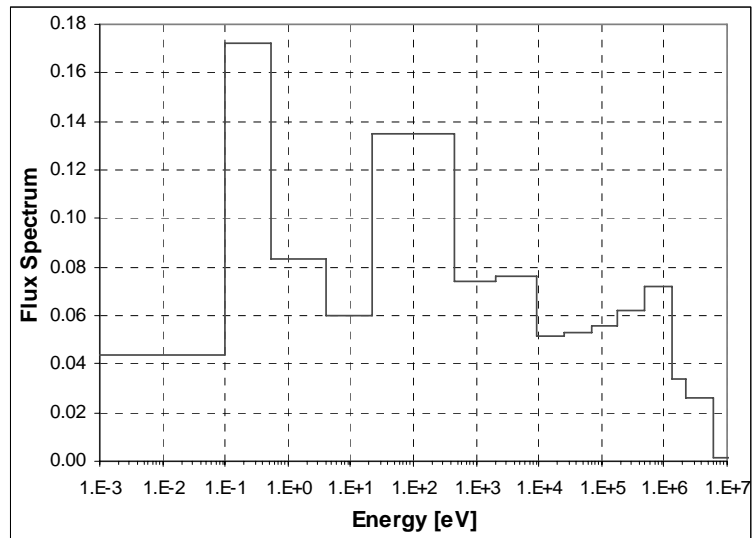


Figure 19. VHTR adjoint flux distribution

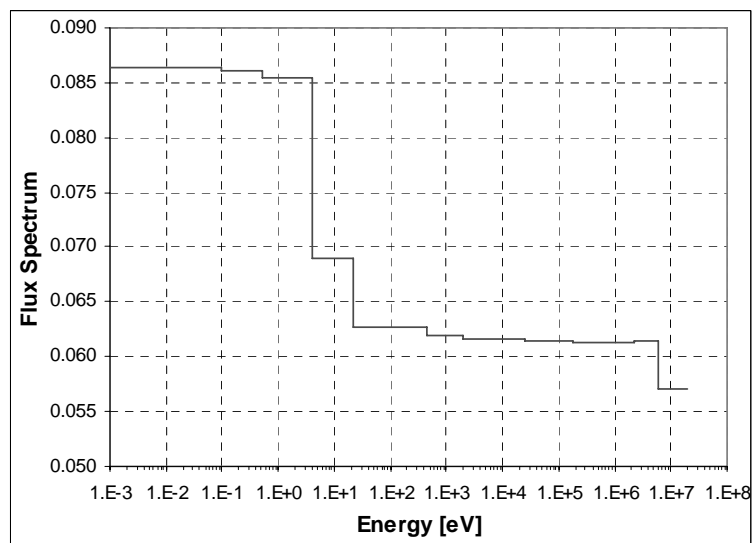


Figure 20. PWR direct flux distribution

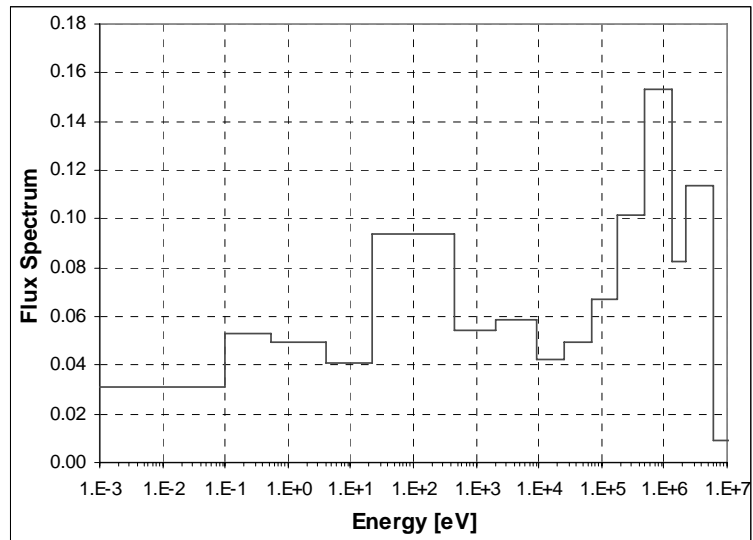


Figure 21. PWR adjoint flux distribution

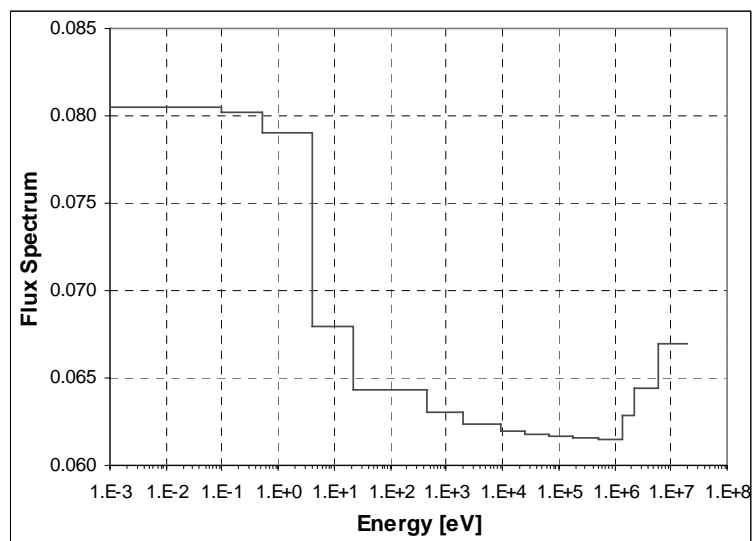


Table 2. ABTR, SFR, EFR nominal values

Reactor	Reactivity [pcm]	Power peak	Doppler [pcm]	Void [pcm]	Burn-up [pcm]	Decay heat ^(o) [W]	Dose ^(p) [Sv]	Neutron source ^(q) [n/s]
ABTR	3 319.8	1.73 ^(a)	368.3 ^(b)	277 ^(c)	-1 325.8 ^(d)	1.402E+03	1.687E+01	7.005E+09
SFR	5 015.4	1.53 ^(e)	231 ^(f)	1 831 ^(g)	-3 981.1 ^(h)	1.400E+4	2.319E+1	8.537E+11
EFR	9 786.5	1.63 ⁽ⁱ⁾	1 289 ^(l)	1 934.5 ^(m)	-9 123.9 ⁽ⁿ⁾	4.324E+3	1.235E+1	1.996E+11

^(a) (R,Z) = (10.6,151.3)cm

^(b) $T_{\text{fuel}} = 300 \text{ K} - T_{\text{fuel}} = 856 \text{ K}$

^(c) Na loss at the core centre

^(d) 109.8 days (4 months at 90% capacity)

^(e) (R,Z) = (66.59,143.03)cm

^(f) $T_{\text{fuel}} = 300 \text{ K} - T_{\text{fuel}} = 850 \text{ K}$

^(g) Na loss in core

^(h) 155 days

⁽ⁱ⁾ (R,Z) = (153.24,125)cm

^(l) $T_{\text{fuel}} = 300 \text{ K} - T_{\text{fuel}} = 1 520 \text{ K}$

^(m) Na loss in core and blanket

⁽ⁿ⁾ 1 700 days

^(o) 100 y after discharge

^(p) 100 000 y after discharge

^(q) 2 y after discharge

Table 3. GFR nominal values

Reactivity [pcm]	Power peak	Doppler [pcm]	Void [pcm]	Burn-up [pcm]	Decay heat [W]	Dose [Sv]	Neutron source [n/s]
1 038.0	1.45 ^(a)	1 549 ^(b)	350.1 ^(c)	1 081.3 ^(d)	6.246E+3	1.028E+1	2.183E+11

^(a) Centre core radially and axially

^(b) $T_{\text{fuel}} = 300 \text{ K} - T_{\text{fuel}} = 1 \text{ 263 K}$

^(c) He loss in core and reflector

^(d) 415 days

Table 4. LFR nominal values

Reactivity [pcm]	Power peak	Doppler [pcm]	Void [pcm]	Burn-up [pcm]	Decay heat [W]	Dose [Sv]	Neutron source [n/s]
22.9	1.29 ^(a)	228.1 ^(b)	6 575.5 ^(c)	-1 464 ^(d)	4.616E+3	1.140E+1	2.275E+11

^(a) $(R,Z) = (100.96, 117.90)_{\text{cm}}$

^(b) $T_{\text{fuel}} = 300 \text{ K} - T_{\text{fuel}} = 900 \text{ K}$

^(c) Pb loss in core

^(d) 310 days

Table 5. ADMAB nominal values

Reactivity [pcm]	Power peak	Doppler [pcm]	Void [pcm]	Burn-up [pcm]	Decay heat [W]	Dose [Sv]	Neutron source [n/s]
-5 466.9	2.67 ^(a)	28.3 ^(b)	3 138.4 ^(c)	-1 347.6 ^(d)	1.545E+5	2.653E+1	3.122E+12

- (a) $(R,Z) = (20,102.5)_{\text{cm}}$
(b) $T_{\text{fuel}} = 1\,773\text{ K} - T_{\text{fuel}} = 980\text{ K}$
(c) Pb-Bi loss in core
(d) 366 days

Table 6. VHTR nominal values

k_{eff} ^(a)	k_{eff} ^(b)	Power peak ^(c)	Power peak ^(d)	Doppler ^(e) [pcm]	Doppler ^(f) [pcm]	Burn-up ^(g) [pcm]	Decay heat ^(h) [W]	Dose ⁽ⁱ⁾ [Sv]	Neutron source ^(j) [n/s]
1.37767	1.01610	1.96	2.25	2 095.3	3 416.3	-25 829.4	1.670E+1	2.979E-2	2.227E+8

- (a) BOC
(b) EOC
(c) BOC at $(R,Z) = (147.6,556.5)_{\text{cm}}$
(d) EOC at $(R,Z) = (147.6,556.5)_{\text{cm}}$
(e) $T_{\text{fuel}} = 773\text{ K} - (T_{\text{fuel}} = 1\,373\text{ K}; T_{\text{moderator}} = 1\,200\text{ K})$ at BOC
(f) $T_{\text{fuel}} = 773\text{ K} - (T_{\text{fuel}} = 1\,373\text{ K}; T_{\text{moderator}} = 1\,200\text{ K})$ at EOC
(g) 845.63 days
(h) 100 y after discharge
(i) 100 000 y after discharge
(j) 2 y after discharge

Table 7. PWR nominal values

$k_{\text{eff}}^{(a)}$	$k_{\text{eff}}^{(b)}$	Doppler ^(c) [pcm]	Doppler ^(d) [pcm]	Burn-up ^(e) [pcm]	Decay heat ^(f) [W]	Dose ^(g) [Sv]	Neutron source ^(h) [n/s]
1.49802	0.87231	695.2	1 054.6	-47 883.6	6.000E+2	1.128E+0	2.486E+10

^(a) BOC

^(b) EOC

^(c) $T_{\text{fuel}} = 550 \text{ K} - T_{\text{fuel}} = 900 \text{ K}$ at BOC

^(d) $T_{\text{fuel}} = 550 \text{ K} - T_{\text{fuel}} = 900 \text{ K}$ at EOC

^(e) 2 773.5 days

^(f) 100 y after discharge

^(g) 100 000 y after discharge

^(h) 2 y after discharge

Table 8. Δn (units) and $\Delta n/n_f$ nominal values

		^{235}U	^{238}U	^{237}Np	^{238}Pu	^{239}Pu	^{240}Pu	^{241}Pu	^{242}Pu	^{241}Am	^{242m}Am	^{243}Am	^{242}Cm	^{243}Cm	^{244}Cm	^{245}Cm	^{246}Cm
		$\Delta n = n_f - n_i$	$\Delta n/n_f$	$\Delta n = n_f - n_i$	$\Delta n/n_f$	$\Delta n = n_f - n_i$	$\Delta n/n_f$	$\Delta n = n_f - n_i$	$\Delta n/n_f$	$\Delta n = n_f - n_i$	$\Delta n/n_f$	$\Delta n = n_f - n_i$	$\Delta n/n_f$	$\Delta n = n_f - n_i$	$\Delta n/n_f$	$\Delta n = n_f - n_i$	$\Delta n/n_f$
ABTR	$\Delta n = n_f - n_i$	-5.2E-7	-4.3E-5	1.9E-7	2.1E-7	-3.5E-5	4.3E-6	-1.4E-7	4.6E-8	-9.4E-9	2.3E-8	5.1E-9	1.9E-8	9.6E-10	2.6E-8	1.6E-9	1.8E-10
	$\Delta n/n_f$	-0.04	0.00	0.02	0.05	-0.02	0.02	-0.01	0.00	0.00	0.08	0.00	0.05	0.08	0.05	0.03	0.06
SFR	$\Delta n = n_f - n_i$	-1.4E-7	-2.0E-5	-5.0E-6	-3.2E-6	-4.6E-5	-2.3E-5	-7.7E-6	-5.2E-6	-4.9E-6	-8.5E-6	-1.3E-6	3.1E-7	-7.5E-9	4.9E-7	-7.5E-7	-1.2E-7
	$\Delta n/n_f$	-0.03	-0.01	-0.06	-0.02	-0.07	-0.03	-0.05	-0.02	-0.05	-0.13	-0.01	0.05	-0.01	0.01	-0.05	-0.01
EFR	$\Delta n = n_f - n_i$	-2.6E-6	-9.1E-4	-4.8E-7	-3.4E-6	-2.5E-4	-6.2E-5	1.7E-5	-3.9E-6	-2.6E-5	9.8E-8	6.0E-7	2.8E-6	-3.8E-8	3.4E-6	-2.4E-7	-2.3E-7
	$\Delta n/n_f$	-0.78	-0.16	-0.05	-0.10	-0.29	-0.10	0.20	-0.06	-0.79	0.03	0.03	1.00	-0.10	0.22	-0.09	-0.15
GFR	$\Delta n = n_f - n_i$	-4.9E-6	-1.0E-4	-5.1E-6	8.3E-6	1.4E-5	5.0E-7	-9.3E-6	3.0E-8	-2.1E-5	2.8E-6	-2.2E-6	7.0E-6	9.8E-8	3.2E-6	6.3E-8	6.3E-8
	$\Delta n/n_f$	-0.17	-0.02	-0.11	0.18	0.03	0.00	-0.13	0.00	-0.13	0.80	-0.05	0.99	0.32	0.18	0.18	0.18
LFR	$\Delta n = n_f - n_i$	-5.7E-7	-6.3E-5	-1.9E-6	-5.3E-7	-1.5E-5	-9.0E-6	-4.7E-7	-1.4E-6	-3.2E-6	-7.3E-10	-4.4E-7	4.8E-7	6.0E-9	3.2E-7	-3.0E-7	-2.8E-8
	$\Delta n/n_f$	-0.08	-0.01	-0.06	-0.01	-0.02	-0.02	-0.01	-0.02	-0.06	0.00	-0.02	0.22	0.04	0.02	-0.06	-0.01
ADMAB	$\Delta n = n_f - n_i$	-	-	-4.1E-5	5.2E-5	-6.0E-5	7.8E-6	-1.8E-5	9.6E-6	-8.6E-5	8.3E-6	-5.2E-5	2.7E-5	-1.9E-7	2.3E-5	1.5E-6	5.0E-7
	$\Delta n/n_f$	-	-	-0.10	0.55	-0.13	0.03	-0.17	0.10	-0.12	0.43	-0.10	1.00	-0.06	0.09	0.05	0.48
VHTR	$\Delta n = n_f - n_i$	-1.4E-5	-9.8E-6	1.5E-7	4.9E-8	2.5E-6	7.6E-7	8.9E-7	2.4E-7	2.1E-8	4.2E-10	3.4E-8	7.6E-9	1.3E-10	8.1E-9	4.3E-10	-
	$\Delta n/n_f$	-1.29	-0.07	1.00	1.00	1.00	1.00	1.00	1.00	1.00	1.00	1.00	1.00	1.00	1.00	1.00	-
PWR	$\Delta n = n_f - n_i$	-5.1E-4	-3.9E-4	9.6E-6	6.9E-6	5.1E-5	2.5E-5	1.7E-5	1.0E-5	8.7E-7	2.0E-8	3.1E-6	3.3E-7	1.4E-8	2.1E-6	2.1E-7	-
	$\Delta n/n_f$	-7.58	-0.07	1.00	1.00	1.00	1.00	1.00	1.00	1.00	1.00	1.00	1.00	1.00	1.00	1.00	-

6. Uncertainty analysis

6.1 Uncertainty evaluation

A selection of the results obtained with the full BOLNA covariance matrix is shown in this section. The uncertainty values calculated both with the full and diagonal (no correlations among isotopes, reactions and energy groups) BOLNA covariance matrix are presented with more details for each system and selected parameter in Appendix M (total uncertainty by isotope, available on CD-ROM), Appendix N (uncertainty breakdown by isotope and reaction for Δn , n_f , burn-up component due to the Δn uncertainties, decay, dose and neutron source, available on CD-ROM) and in Appendix O (uncertainty breakdown by isotope and reaction for k_{eff} , power peak, Doppler and void reactivity coefficient, burn-up component due to cross-section uncertainties, available on CD-ROM). Uncertainty evaluations and target accuracy assessment were not carried out for the Doppler coefficient of the ADMAB due to its small calculated value.

Table 9 provides a summary of the integral parameter uncertainties in fast reactors (FRs), including the ADMAB, and Tables 10 and 11 for the VHTR and the high burn-up PWR respectively. Uncertainties obtained with the BOLNA covariance data are compared to the ones obtained with the PEC matrix used in Ref. [1]. Uncertainties on the FR k_{eff} are still very relevant and generally beyond design target accuracies, even if a general reduction with respect to the data obtained in Ref. [1] is observed.

The uncertainties shown for the reactivity loss due to burn-up account only for the heavy element component, since individual fission product uncertainties are not generally available. In Ref. [1], an “integral” estimation of the uncertainty on the capture and scattering components of a “lumped” fission product was used, i.e. 10% on the capture cross-section and 20% on the total scattering cross-section of a “lumped” fission product in a fast spectrum, and 2% on the capture cross-section of a “lumped” fission product in a thermal spectrum. The contribution of the fission product uncertainty to the overall burn-up reactivity is significant only in the case of fast reactors with an extended burn-up (as for the EFR, see Table 12). For that case, it would be valuable, to improve the uncertainty assessment, to have available the covariance data of the ~20 most important fission products, in particular in the fast energy range.

As for the other integral parameters, the results presented in Tables 9 to 11 confirm a relatively small impact of data uncertainties on the power peak values (except for the ADMAB) and on the Doppler coefficient. However, further analysis has been suggested to investigate in more detail possible effects due to resonance parameter uncertainties. As for the void reactivity coefficients, the

Table 9. Fast neutron systems: total uncertainties (%)

Reactor	k_{eff}	Power peak	Doppler	Void	Burn-up [pcm]	Decay heat	Dose	Neutron source
ABTR	PEC ^(a)	1.96	6.4	12.5	97	0.1	0.1	0.5
	BOLNA ^(b)	0.92	4.4	6.0	52	0.2	0.1	0.5
SFR	PEC	1.66	6.0	23.4	234	0.3	0.2	0.9
	BOLNA	1.82	5.6	17.1	272	0.4	0.3	1.0
EFR	PEC	1.57	5.1	12.1	989	2.3	1.7	6.0
	BOLNA	1.18	3.8	7.8	871	2.4	1.2	6.6
GFR	PEC	1.90	5.5	7.1	384	0.5	0.6	1.8
	BOLNA	1.88	5.5	7.7	381	0.4	0.5	1.4
LFR	PEC	2.26	7.8	20.6	258	0.5	0.5	1.1
	BOLNA	1.43	4.3	7.2	198	0.6	0.4	1.1
ABMAB	PEC	3.25	–	56.6	962	0.9	1.4	2.7
	BOLNA	2.94	–	15.5	1 044	0.7	1.0	2.5

^(a) Partial energy correlation as used in Ref. [1]

^(b) BNL_ORNL_LANL_NRG_ANL

Table 10. High burn-up VHTR: uncertainties (%)

	k_{eff} BOC	k_{eff} EOC	Power peak BOC	Power peak EOC	Doppler BOC	Doppler EOC	Burn-up [pcm]	Decay heat	Dose	Neutron source
PEC^(a)	0.58	1.07	1.9	2.1	3.4	5.6	1 574	3.1	2.6	14.3
BOLNA^(b)	0.53	0.46	1.0	1.1	1.7	2.0	530	1.4	1.0	5.9

^(a) Partial energy correlation as used in Ref. [1]

^(b) BNL_ORNL_LANL_NRG_ANL

Table 11. High burn-up PWR: uncertainties (%)

	k_{eff} BOC	k_{eff} EOC	Doppler BOC	Doppler EOC	Burn-up [pcm]	Decay heat	Dose	Neutron source
PEC^(a)	0.52	1.27	3.1	4.6	2 206	3.8	3.1	13.2
BOLNA^(b)	0.51	0.74	1.4	1.9	851	1.5	1.0	5.2

^(a) Partial energy correlation as used in Ref. [1]

^(b) BNL_ORNL_LANL_NRG_ANL

Table 12. $\Delta\rho$ burn-up uncertainty breakdown into components (pcm)^(a)

$\downarrow \Delta\rho$ component	System \rightarrow	SFR	EFR	GFR	LFR	VHTR	PWR
Actinides		± 272	± 871	± 381	± 198	± 530	± 851
Fission products		± 73	± 755	± 130	± 76	± 215	± 244
Total		± 282	$\pm 1\,153$	± 402	± 212	± 572	± 885

^(a) Partial energy correlation as used in Ref. [1]

impact of nuclear data uncertainty is not negligible in Na-cooled systems and could have some impact on current Na-void coefficient minimisation studies.

In summary, most of the uncertainty values shown in Table 9, although sometimes significant, would not in principle affect the early phases of study on the different FR concepts that were investigated here. However, the conservatism which could be suggested by the results shown in the table could probably have an economic impact in later phases of the design and also an impact on the safety assessment. If such is the case, new evaluations/experiments (differential or integral) could well be justified in order to reduce uncertainties and associated cost. This point will be discussed later on.

Potential high-priority domains of investigation are highlighted in Tables 13 to 15, wherein the major features of the uncertainty impact for FRs are summarised.

Three major data sources for the overall uncertainties can be pinpointed:

- 1) Pu isotopes (other than ^{239}Pu) major reactions (fission, capture and nu-bar), see Table 13. In the case of ^{239}Pu , the major impact is due to the capture cross-section, since the uncertainties associated to this isotope, and in particular to its fission cross-section, are in the present covariance data (BOLNA) extremely reduced, i.e. most often well below 1%.
- 2) Selected MA fission cross-sections (see Table 14), but only in TRU burner fast reactors like the SFR, which has a 15% MA content in the fuel, or obviously in the ADMAB.
- 3) Inelastic cross-section data (see Table 15), and most notably of ^{238}U , ^{56}Fe and ^{23}Na (in Na-cooled FRs).

In addition to these three wide “categories” of uncertainty contributions, there is still some impact of the ^{238}U capture uncertainty, despite the very small uncertainty values of the present covariance data evaluation.

As for the uncertainties on the nuclide density variation between beginning and end of cycle, the most relevant results are once more related to cases where the irradiation time is significant. Since the case of the EFR is that with the highest burn-up for fast reactors, results are shown for Pu isotopes (Table 16) and for selected minor actinides (Table 17). These tables give the uncertainty on the nuclide density at end of cycle. In all cases, as expected, the uncertainties are due to the capture and fission cross-sections of the very same isotopes. The impact of such uncertainties can have some relevance on mass flows and inventories in the fuel cycle.

Table 13. Fast reactor systems: uncertainties (%) due to Pu isotope cross-sections (BOLNA)

Isotope	Cross-section	ABTR		SFR		GFR		LFR	ADMAD	
		k_{eff}		k_{eff}	Void	k_{eff}	Power peak	k_{eff}	k_{eff}	Power peak
^{238}Pu	v	0.01		0.34	0.44	0.15	0.03	0.23	0.13	0.94
	Fission	0.01		0.53	2.90	0.20	0.06	0.34	0.21	1.52
^{239}Pu	Fission	0.24		0.12	0.87	0.15	0.03	0.21	0.12	0.90
	Capture	0.23		0.12	1.16	0.23	0.06	0.17	0.10	0.77
^{240}Pu	v	0.08		0.39	2.18	0.20	0.06	0.33	0.14	1.02
	Fission	0.09		0.44	2.60	0.23	0.08	0.35	0.16	1.15
^{241}Pu	Capture	0.06		0.31	1.80	0.17	0.06	0.27	0.08	0.63
	Fission	0.12		0.96	4.09	0.82	0.16	0.61	1.04	7.61
^{242}Pu	Fission	0.01		0.36	2.46	0.21	0.08	0.17	0.15	1.08
	Capture	0.01		0.17	2.21	0.17	0.05	0.08	0.06	0.45

Table 14. Fast reactor systems: uncertainties (%) due to selected MA cross-sections (BOLNA)

Isotope	Cross-section	ABTR		SFR		GFR		LFR	ADMAD	
		k_{eff}		k_{eff}	Void	k_{eff}	Power peak	k_{eff}	k_{eff}	Power peak
^{241}Am	Fission	0.01		0.08	0.43	0.24	0.13	0.06	0.83	5.81
^{242m}Am	Fission	–		0.73	3.70	0.01	0.01	0.07	0.14	1.05
^{243}Am	Fission	–		0.04	0.25	0.04	0.02	0.02	0.35	2.43
^{244}Cm	Fission	–		0.39	2.95	0.13	0.08	0.16	1.90	13.43
^{245}Cm	Fission	–		0.39	0.95	0.12	0.10	0.22	1.04	7.56

Table 15. Fast reactor systems: uncertainties (%) due to inelastic and capture (BOLNA)

Isotope	Cross-section	ABTR		SFR		GFR		LFR		ADMAD	
		k_{eff}	k_{eff}	k_{eff}	Void	k_{eff}	Power peak	k_{eff}	k_{eff}	Power peak	Void
^{238}U	Inelastic	0.69	0.23	0.23	1.96	1.41	1.54	0.73	—	—	—
	Capture	0.26	0.07	0.07	1.24	0.41	0.30	0.25	—	—	—
^{56}Fe	Inelastic	0.24	0.53	0.53	4.14	—	—	0.24	0.93	7.22	5.43
Na	Inelastic	0.07	0.25	0.25	13.43	—	—	—	—	—	—
^{28}Si	Inelastic	—	—	—	—	0.22	0.25	—	—	—	—
C	Elastic	—	—	—	—	0.31	0.28	—	—	—	—
^{206}Pb	Inelastic	—	—	—	—	—	—	0.18	—	—	—
^{207}Pb	Inelastic	—	—	—	—	—	—	0.16	—	—	—
^{208}Pb	Elastic	—	—	—	—	—	—	0.13	—	—	—
$\text{Pb}^{(a)}$	Inelastic	—	—	—	—	—	—	—	0.04	0.28	2.28
	Elastic	—	—	—	—	—	—	—	0.05	0.09	2.84
	Capture	—	—	—	—	—	—	—	0.07	0.46	1.53
^{209}Bi	Inelastic	—	—	—	—	—	—	—	0.31	2.23	12.01

^(a) For the ADMAB calculations have been performed with the JEF-2.2 library (see Section 4) that do not distinguish the Pb isotopes

Table 16. Uncertainty (%) on Pu isotope density at end of cycle (EFR)

Uncertainty on →		²³⁸ Pu	²³⁹ Pu	²⁴⁰ Pu	²⁴¹ Pu	²⁴² Pu
Due to ↓						
²³⁸ U	Capture	—	1.1	0.2	0.1	—
²³⁸ Pu	Capture	1.7	0.1	—	—	—
	Fission	4.6	—	—	—	—
²³⁹ Pu	Capture	—	0.8	1.3	0.7	0.1
	Fission	—	0.2	—	—	—
²⁴⁰ Pu	Capture	0.2	—	1.5	6.0	1.0
	Fission	—	—	0.8	0.4	—
²⁴¹ Pu	Capture	—	—	—	0.8	1.5
	Fission	0.2	—	—	5.0	0.7
²⁴² Pu	Capture	—	—	—	—	3.9
	Fission	—	—	—	—	2.2
²⁴¹ Am	Capture	1.3	—	—	—	0.2
	Fission	0.2	—	—	—	—
Total		5.1	1.3	2.1	7.9	4.9

Table 17. Uncertainty (%) on selected MA density at end of cycle (EFR)

Uncertainty on →		²⁴¹ Am	^{242m} Am	²⁴³ Am	²⁴⁴ Cm	²⁴⁵ Cm
Due to ↓						
²⁴⁰ Pu	Capture	1.6	0.6	0.2	—	—
	Fission	0.1	—	—	—	—
²⁴¹ Pu	Capture	0.2	0.1	0.4	0.1	—
	Fission	1.2	0.4	0.1	—	—
²⁴² Pu	Capture	—	—	9.3	4.1	1.5
	Fission	—	—	0.6	0.2	—
²⁴¹ Am	Capture	3.1	2.0	0.1	—	—
	Fission	0.9	0.5	—	—	—
^{242m} Am	Capture	—	1.6	0.3	0.2	0.1
	Fission	—	7.4	0.1	—	—
²⁴³ Am	Capture	—	—	1.9	1.9	1.0
	Fission	—	—	0.5	0.2	0.1
²⁴⁴ Cm	Capture	—	—	—	1.8	7.2
	Fission	—	—	—	6.0	2.8
²⁴⁵ Cm	Capture	—	—	—	—	0.9
	Fission	—	—	—	—	15.6
Total		3.8	7.8	9.5	7.8	17.6

As for thermal neutron systems, relatively small uncertainties on integral parameters are observed (Table 18) since very small uncertainties are assumed on the low-energy data of ^{235}U , ^{238}U and ^{239}Pu and also of the ^{240}Pu capture close to the first resonance. There are however a few significant contributions, e.g. the ^{241}Pu fission cross-section uncertainty to the PWR end-of-cycle reactivity.

As for the energy breakdown of the uncertainties, Table 19 gives, as a typical example, the energy breakdown in the case of the SFR k_{eff} of a few fission and capture contributions. The wide energy range ($\sim 5 \text{ MeV}$ - 1 keV) of relevance is due to the variety of fast spectra considered.

Finally, from the results presented in Appendices M, N and O (available on CD-ROM), it is concluded that the impact of the correlation (of diagonal) terms is significant, and of the same order of magnitude of the impact observed in Ref. [1].

6.2 *Summary of lessons drawn from the uncertainty analysis*

The present results are of high relevance for future reactor system feasibility studies, as for the first time a scientifically-based set of variance-covariance data is available to reactor system designers. Despite the preliminary nature of the data, it allows to establish uncertainties on the most important reactor core and fuel cycle design parameters.

A significant result is the strong impact of correlation data (i.e. off-diagonal elements) on the uncertainty assessment. Any credible uncertainty analysis should include the best available covariance data accounting for energy correlations (as in the present study) and possibly for cross-correlations among reactions (a typical case would be the inter-relation among total, elastic and inelastic cross-sections) and even for cross-correlation among isotopes, if needed, e.g. to account for normalisation issues.

In this respect, as for the numerical results so far obtained, it has been noted that the present BOLNA database provides correlations in energy but not cross-correlations, e.g. between different reactions. This is an area for future investigation, even if the general validity of the present conclusions will not be dramatically affected. An example is given in Appendix I.

One other important point seems to be the shift of priority from the three major actinide fission data to their inelastic (in particular for ^{238}U) and capture data (for ^{239}Pu , and, to a lesser extent, for ^{238}U ; the case of ^{235}U capture data in

Table 18. Thermal systems: uncertainties (%) due to selected isotopes and reactions (BOLNA)

Isotope	Cross-section	PWR	VHTR
		k_{eff} EOC	k_{eff} EOC
^{235}U	ν	0.17	0.27
^{238}U	Inelastic	0.17	0.00
	Capture	0.26	0.19
^{239}Pu	Fission	0.18	0.10
	Capture	0.07	0.11
^{240}Pu	Capture	0.12	0.06
^{241}Pu	Fission	0.34	0.18
	Capture	0.13	0.13
O	Capture	0.43	0.01

Table 19. SFR k_{eff} uncertainties (%): energy breakdown (pcm) for selected isotopes/reactions

Group	Energy ^(a)	^{238}Pu σ_{fission}	^{240}Pu σ_{capture}	^{241}Pu σ_{fission}	$^{242\text{m}}\text{Am}$ σ_{fission}
1	19.6 MeV	0.01	0.00	0.02	0.02
2	6.07 MeV	0.18	0.03	0.10	0.12
3	2.23 MeV	0.23	0.05	0.26	0.15
4	1.35 MeV	0.31	0.11	0.40	0.28
5	498 keV	0.28	0.14	0.47	0.39
6	183 keV	0.12	0.16	0.58	0.39
7	67.4 keV	0.07	0.13	0.29	0.28
8	24.8 keV	0.06	0.13	0.16	0.12
9	9.12 keV	0.03	0.05	0.10	0.08
10	2.03 keV	0.03	0.01	0.08	0.10
11	454 eV	0.00	0.00	0.03	0.02
12-15	22.6 eV	0.00	0.00	0.00	0.00
Total		0.53	0.31	0.96	0.73

^(a) Upper energy boundary

the keV region is presently under investigation). The shift in priority is obviously related to the relatively small uncertainty values associated with the fission cross-sections of ^{239}Pu . Some preliminary considerations on this issue are given in Appendix H. Higher priority should also be given to higher Pu isotopes (and in particular to their fission data) and to selected coolant/structural material

inelastic cross-sections (e.g. ^{56}Fe and ^{23}Na). Minor actinide data play a significant role only for dedicated burner reactors (ADMAB or SFR) with conversion ratio $\text{CR} = 0$ and a content of MA in the fuel of 50% or higher. For more conventional burners ($\text{Pu/MA} \sim 5$) and down to $\text{CR} \sim 0.25$, only selected MA data require significant improvements.

As for fission product data, it would be important to have covariance data for the most important of them, both in terms of reactivity or in terms of impact on specific aspects of the fuel cycle.

Some specific data uncertainties, not included in the present study, have also been investigated separately, e.g. fission spectra uncertainties and resonance parameters uncertainties impact on Doppler reactivity coefficient. In the first case, the activity of the subgroup allowed to clarify several basic issues, such as the theoretical basis for practical sensitivity coefficient expressions and the prescriptions to set up a fission spectrum covariance matrix. As for the actual uncertainty analysis, it was made clear that more work is needed in that field in order to assess significant covariances that should be represented accounting carefully numerical precision issues (see Appendices C and D).

As for the resonance parameter uncertainty impact on the Doppler reactivity coefficient (Appendix B), the results obtained in the specific case described in the appendix tend to confirm the relatively low impact of the resonance parameter uncertainties on the self-shielding variation with temperature and, consequently, on the Doppler reactivity coefficient. However, the problem of propagating resonance parameter uncertainties can have significant applications, e.g. in resonance parameter adjustment studies.

As for data needs related to fuel cycle parameters, the present study has quantitatively addressed the uncertainties of a number of parameters directly related to the nuclei density uncertainties. A more comprehensive study related, e.g. to the decay heat, is still to be done. However, the subgroup has preliminarily addressed several important issues. In particular Appendix E deals with the case of nuclear data for the handling, reprocessing and disposal of spent nuclear fuel. As it is recognised that for future facilities any nuclear data which dominate the uncertainties must be identified – as must any biases – such that improvements can be made to the basic nuclear data, an initial study is described in Appendix E, considering only thermal reactors and some conclusions made about how these could be extended for novel systems. As an example, the calculation of decay heat in the context of the current fuel reprocessing plants is discussed there. Additionally, some specific requirements for resonance data important for advanced fuel cycle applications are discussed in Appendix F.

7. Target accuracy

As general features, the integral parameter uncertainties resulting from the assumed uncertainties on nuclear data, as summarised in Tables 9 to 11, are generally acceptable both in the early phase of design feasibility studies. In fact, the uncertainties shown in Tables 9 to 11 will not prevent performance of meaningful parametric and preliminary optimisation studies and evaluation, on a comparative basis, of the impact of technological choices. This consideration is valid both for the reactor design and for the assessment of the major physics parameters of the associated fuel cycles.

However, later design phases of selected reactor and fuel cycle concepts will definitely require improved data and methods in order to reduce margins, both for economical and safety reasons. At that stage, it will be relevant to define priority issues, i.e. which are the nuclear data (isotope, reaction type, energy range) that need improvement, to quantify target accuracies and to select a strategy to meet the requirements needed, for example through new differential measurements or by the use of integral experiments. In this respect one should account for the wide range of high-accuracy integral experiments already performed and available in national or, better, international databases.

A first indicative target accuracy assessment was made within the subgroup as an extension of the study documented in Ref. [1]. In the present work, the combined information of the recent covariance evaluations and of the new resulting uncertainties on advanced reactor systems has been used to assess the nuclear data uncertainty reductions needed in order to meet the design parameter target accuracies established within the subgroup itself.

7.1 Data target accuracies

Within Subgroup 26, a preliminary list of design target accuracies was established for fast reactor systems (at first, independently of the coolant or the fuel type, see Table 20), for (V)HTRs (see Table 21) and for high burn-up PWRs (see Table 22). These target accuracies reflect the perceived state of the art from an R&D point of view, even if they are not the result of a systematic analysis, which should necessarily involve industrial partners, only marginally involved in the present assessment, with the noticeable exception of the VHTR target uncertainties, derived by values provided by AREVA for HTRs.

Further, it should be kept in mind that no fully defined “images” for any of the Gen-IV systems presently exist. This means that the target accuracies shown in particular in Table 20 reflect the current thinking of systems with innovative

Table 20. Fast reactor and ADMAB target accuracies (1σ)

Multiplication factor (BOL)	300 pcm
Power peak (BOL)	2%
Burn-up reactivity swing	300 pcm
Reactivity coefficients (coolant void and Doppler – BOL)	7%
Major nuclide density at end of irradiation cycle	2%
Other nuclide density at end of irradiation cycle	10%

Table 21. Target accuracy (1σ) for UO_2 - and PuO_2 -fuelled HTRs

Criticality	300 pcm (operation); 500 pcm (safety)
Local power (in fuel compact)	6% (2% in pin-wise fission rate of fresh fuel; 4% in main fissile isotope concentration of irradiated fuel)
Burn-up (cycle length)	1% ($\Rightarrow \sim 500 \text{ MWd/t}$)
Doppler coefficient	20%
Moderator temperature coefficient	1 pcm/ $^{\circ}\text{C}$
Nuclide inventories at EOL	
Main fissile isotopes	4%
Fertile isotopes	5%
MAs and FPs	20%

Source: AREVA-NP, reproduced with permission for WPEC/SG26.

Table 22. PWR target accuracies (1σ)

k_{eff}	Doppler reactivity coefficient	Burn-up $\Delta\rho$	Transmutation
0.5%	10%	500 pcm	5%

fuels and core configurations described in Refs. [1] and [3], i.e. Na-cooled systems (burners with different fuel types such as the SFR and ABTR, or self-sustaining as the EFR), the gas-cooled GFR and the lead-cooled LFR. The case of the (V)HTR is somewhat different, since the target accuracies shown in Table 21 were suggested by a major industry (AREVA). In the absence of specific information, the same target accuracies of the FRs have been selected for the ADMAB, while the accuracy requirements for the PWR have been taken from Ref. [1].

7.2 Computational strategy

Once the design target accuracies have been defined, the approach described in Section 2.2 [see Eq. (27)] is used to obtain the unknown uncertainty nuclear data requirements.

The cross-sections uncertainties required for satisfying the target accuracies have been calculated by a minimisation process that satisfies the non-linear constraints with bounded parameters. Several optimisation codes (including OPTIMA, KNITRO, SNOPT, etc.) were tested for this minimisation process in order to verify that consistent answers were obtained and not local minima. The SNOPT code [28] was finally selected due to the ease of using the FORTRAN interface.

At the first stage it was decided not to account for correlations between the data. This assumption is of course rather arbitrary, but it is consistent with standard requirements for reactor design in early phases of development. The “BOLNA diagonal” uncertainties are provided in Table 23 (the uncertainties which exceed the required accuracies are shaded). As a general view, it can be observed that the power peak, the Doppler and void reactivity coefficients meet the accuracy requirements in all cases with the only exceptions being the ADMAB for the three parameters and the SFR for the void coefficient. The worst situation is represented by the ADMAB, for which all integral parameter uncertainties (with the exception of the nuclide densities at end of irradiation due to the short burn-up) do not meet the accuracy requirements.

Additionally, to avoid the introduction of meaningless parameters, as unknown “d” parameters (i.e. as cross-sections for which target accuracies are required), only those which globally account at least for 98% of the overall uncertainty for each integral parameter have been chosen.

Concerning the cost parameters, and following the practice of previous work [1], a constant value of one for all λ_i is initially taken. However, to provide an initial indication of the impact of the choice of the λ_i parameters, related to achievable experimental uncertainties for σ_{fiss} , σ_{capt} , σ_{inel} measurements for actinide and structural materials, different sets of λ_i values were also used (Table 24), with the purpose of first distinguishing between major and minor actinides (set $\lambda \neq 1$ case A) and then emphasising, as an example, the difficulty of improving σ_{inel} with respect to σ_{fiss} (set $\lambda \neq 1$, Case B).

**Table 23. Integral parameter uncertainties (%)
using the BOLNA diagonal covariance matrix**

	ABTR	SFR	EFR	GFR	LFR	ADMAB	VHTR	PWR
k_{eff} BOC	0.62	1.04	0.79	1.24	0.88	1.95	0.37	0.36
k_{eff} EOC	–	–	–	–	–	–	0.41	0.64
Power peak BOC	0.32	0.31	0.81	1.18	0.45	14.22	0.85	–
Power peak EOC	–	–	–	–	–	–	0.90	–
Doppler BOC	2.86	3.62	2.46	3.62	2.85	–	4.27	1.53
Doppler EOC	–	–	–	–	–	–	2.77	2.01
Void	5.11	15.66	6.68	5.46	4.97	13.11	–	–
Burn-up (pcm)	37.4	152.1	584.9	254.2	127.7	602.9	487.0	684.6
N_{f,U235}	0.07	0.31	2.57	0.42	0.36	–	0.25	0.46
N_{f,U238}	0.01	0.02	0.24	0.04	0.03	–	0.05	0.04
N_{f,Np237}	0.25	0.11	2.51	0.25	0.18	0.20	1.03	1.05
N_{f,Pu238}	0.21	0.42	2.71	0.64	0.56	1.13	1.28	1.05
N_{f,Pu239}	0.04	0.06	1.13	0.37	0.20	0.12	0.96	0.88
N_{f,Pu240}	0.13	0.10	1.25	0.31	0.16	0.26	1.25	1.11
N_{f,Pu241}	0.35	0.62	3.99	0.83	1.19	0.90	2.04	2.02
N_{f,Pu242}	0.13	0.25	2.75	0.51	0.35	0.54	4.75	3.87
N_{f,Am241}	0.08	0.18	2.12	0.35	0.27	0.31	2.13	2.50
N_{f,Am242m}	0.47	0.70	4.26	2.17	1.17	1.72	5.63	5.41
N_{f,Am243}	0.35	0.47	6.41	1.07	0.91	0.27	5.58	4.48
N_{f,Cm242}	1.13	1.38	1.58	2.43	2.49	2.78	1.88	1.87
N_{f,Cm243}	1.30	1.90	10.59	3.91	3.29	3.04	8.37	5.50
N_{f,Cm244}	0.38	0.73	4.83	0.91	0.88	1.07	6.01	4.77
N_{f,Cm245}	0.90	1.47	9.37	1.83	2.35	2.48	8.02	6.84
N_{f,Cm246}	0.51	0.47	4.48	1.35	0.57	3.12	–	–

Table 24. λ_i sets used for the analysis

	$\lambda = 1$	$\lambda \neq 1$, Case A	$\lambda \neq 1$, Case B
$\lambda_{\text{capt,fiss,v}} (^{235}\text{U}, ^{238}\text{U}, ^{239}\text{Pu})$	1	1	1
$\lambda_{\text{capt,fiss,v}}$ (other fissiles)	1	2	2
λ_{capt} (structurals)	1	1	1
λ_{el} (fissiles and structurals)	1	1	1
λ_{inel} (fissiles and structurals)	1	3	10

7.3 Target accuracy results

As indicated previously, the target accuracy approach has been used in this work in order to point out as far as possible meaningful and general enough trends that can help to shape priorities for nuclear data improvement.

In order to make the most effective use of the results of the mathematical procedure outlined in Section 2, the following points should be made:

- a) Design target accuracies as defined in Section 7.1, are preliminary in nature and could evolve when specific innovative system features will be available. This is true for the fast reactor range explored in this study, but it is even more significant for thermal neutron systems, in view of the relatively restricted range of features considered.
- b) The characteristics of the systems considered are representative in a broad sense of potential features of innovative reactors. In particular, the range of systems considered is rather representative in the case of “critical” fast reactors, even if no single system is today a generally recognized as a “reference”. The case of thermal neutron systems is certainly not as representative, and the results/trends obtained have to be taken as indications of potential outstanding problems, recognizing however that more studies are definitely needed in that area. Finally, the ADMAB system (U-free TRU fuel on inert matrix) was added to the list of Gen-IV type fast reactors, to explore if there were some very outstanding issues related to minor actinides and of high importance for potential burner systems not pointed out by the other fast systems, despite to the fact that all of them “recycle” MA. Note that the SFR system is also in a sense a “burner” concept (it was studied at ANL with that purpose) but with a U-TRU fuel and a different MA/Pu ratio. Also in this case (burner reactors) one should recognize that more images of burner systems (critical fast reactors with very low conversion ratios, different ADS configurations, and different MA/Pu ratios in the fuel) would probably be needed for future assessments.
- c) The covariance data in BOLNA are definitely a major breakthrough, but we should recognize their “preliminary” label according to the recommendations of the authors. For this reason by the way, one should not stress the requirements on nubar, since probably the uncertainties for some Pu isotopes were somewhat pessimistic. In general only requirements for reduction of the uncertainty as given in BOLNA by more than a factor ~2 should be accounted for.

- d) Moreover, one should also use as far as possible the indications coming from high precision integral experiment analysis. In fact in some cases they give information very focussed on specific data and the performance of recent evaluated data should be compared to announced uncertainties. This can be the case of the capture of ^{240}Pu , ^{241}Pu and ^{242}Pu above ~ 1 keV: in all cases the analysis of high accuracy irradiation experiments seems to indicate that the required accuracy (see later) is probably more or less achieved
- e) It has been indicated above that the mathematical procedure, outlined in Section 2, did not consider explicitly correlation effects and is restricted to the most important data (in terms both of sensitivity and current uncertainty).

The target accuracy study has been performed first for each system separately. Then, the analysis has been carried out for the three Na-cooled (ABTR, SFR, EFR) and successively for the fast reactors (ABTR, SFR, EFR, GFR, LFR, and ADMAB) together. In this section, the most relevant target accuracy results are presented.

For fast reactors, the uncertainty reduction requirements are summarised in Tables 25-30. Uncertainty reduction requirements that occur for more than one fast system as result of the mathematical procedure are schematically summarised in Table 31. One can further focus on major, unequivocal data requirements, using the criteria and considerations made above (in particular, point b, c and d). The result is given in Table 32 that underlines both the energy range of interest and the range of uncertainty reduction required with respect to the present BOLNA data.

For the thermal neutron systems, uncertainty reduction requirements for the VHTR (Table 33) and PWR (Table 34) are given as well. As indicated above, these results should be taken as preliminary.

A complete list of accuracy requirements per energy group is provided in Appendix P (available on CD-ROM). The list, that represents the outcome of the mathematical procedure outlined above, includes those isotopes, quantities and energy groups that contribute 98% of the total uncertainty to the integral parameter uncertainties. Also, entries are shown for which the current BOLNA estimates indicate that the target uncertainties are met.

For a proper discussion of the results, as indicated above, the focus should therefore be on the main lines emerging from the tables.

7.3.1 Analysis for separated systems

Cost parameters

The cost parameters λ of Eq. 26 on page 25 may be varied according to the difficulty of achieving particular target accuracy. In principle, difficult to achieve target accuracies should get a higher weight factor than the easy cases. Thus, tighter requirements for easier cases may relax requirements for more difficult cases. By this method the analysis should provide the most achievable set of target accuracies. Two cases of cost parameters were tested (see Table 24).

As shown for all fast reactor systems, case (a), which somewhat emphasises the difficulty of improving data for minor actinides and inelastic scattering in general, has practically no impact on the target accuracies compared to the case where all cost parameters are equal. Only, for case (b - examples are given for ABTR and SFR), which emphasises the difficulty with inelastic scattering compared to other channels, do we see a significant impact with a substantial reduction of target uncertainties for inelastic scattering. Although, the discussion below primarily concerns the results for equal cost parameters, it is important to bear this in mind for follow-up activities.

Data requirements

An inspection of Tables 25-34 shows that the number of tight target accuracy requirements (<10%) is less than 15 for the systems which are more conventional (ABTR, EFR, VHTR, PWR), while the list has 20 entries or more for the more advanced SFR, GFR, LFR and ADMAB. The extended lists for the latter four are primarily accounted for by the minor actinides and even Pu isotopes: ^{237}Np , $^{238,240-242}\text{Pu}$, $^{241,242\text{m},243}\text{Am}$, $^{242-246}\text{Cm}$. The higher the minor actinide content, the larger the number of requirements. Also, the full list for the EFR (lower content of MA in the fuel and longer cycle) has 22 entries on account of less tight requirements for minor actinide data.

Due to the minor actinides and the fact that some of the systems differ in non-actinide content, the overall list of requirements is rather long:

- fission cross sections of ^{234}U , ^{237}Np , $^{238,240-242}\text{Pu}$, $^{241,242\text{m},243}\text{Am}$, $^{242-246}\text{Cm}$,
- fission nu-bar of $^{238,240}\text{Pu}$, ^{241}Am and ^{244}Cm ,
- capture of $^{235,238}\text{U}$, ^{237}Np , $^{238-242}\text{Pu}$, $^{241,242\text{m},243}\text{Am}$, ^{244}Cm ,

- inelastic scattering of ^{238}U , $^{239,240,242}\text{Pu}$, $^{241,243}\text{Am}$, C, O, Na, ^{56}Fe , Pb, Bi, ^{90}Zr ,
- neutron removal of ^{10}B , C, O, Na, Si, Fe, Ni, Pb,
- elastic scattering of ^{238}U , C, ^{15}N , O, ^{52}Cr , ^{56}Fe , Pb.

However, the above mentioned limitations of the methodology must be considered. For instance, the occurrence of requirements for $^{234,235}\text{U}$ for EFR and ^{235}U for GFR is odd given the very low number densities of these nuclides for these systems. Similarly, ^{242}Pu inelastic scattering occurs only for the SFR and not for other systems with large minor actinide content such as ADMAB and LFR. Fission of ^{242}Cm is a borderline requirement for EFR and ADMAB. Currently, no emphasis can be placed on limit cases like these.

Therefore, for fast systems, Table 31 is only a first guide to the important uncertainty reduction requirements whereas results given in Table 32 are more appropriate since they underline both the energy range of interest and the range of uncertainty reduction required with respect to the present BOLNA data.

Several general features can be pointed out. As expected from the results of the uncertainty analysis (see Section 6), very tight requirements are shown for the σ_{inel} of ^{238}U (2-3%), ^{239}Pu (6-15%), ^{56}Fe (3-6%), ^{23}Na (4-10%) and ^{90}Zr (4-10%) and even for Pb isotopes. In system specific cases Si, ^{209}Bi , $^{241,243}\text{Am}$ and even $^{240,242}\text{Pu}$ inelastic scattering show up. Some of the required accuracies are probably beyond achievable limits with current experimental techniques. As previously discussed, there are little margins to relax the requirements on σ_{inel} if one does not want to produce comparably difficult requirements on some Pu isotope σ_{fiss} and σ_{capt} . On the other hand, these margins need to be exploited to eliminate the requirements of Pu and Am inelastic scattering for which only improved theoretical estimates may be expected and the accuracy will thus not be significantly below 10%.

Further major actinide requirements are few. The main other requirement concerns neutron capture by ^{239}Pu (3-6%), a case which could be aggravated by putting a large cost parameter for inelastic scattering. An uncertainty reduction by an important factor of at least 2 is called for. Capture of ^{238}U (2%) is listed in Table 31, however, this concerns only the energy range from ~2 to ~25 keV for which the present status in BOLNA is 3 to 9%. This is not to say that capture by ^{238}U is not important: 2% accuracy is needed throughout the energy range! However, the recent standards evaluation concluded that this accuracy is met for all but a relatively limited energy range and this finding is incorporated in the BOLNA estimates.

Accuracy requirements for other Pu isotopes predominantly concern the fission cross section (2-4%) and for $^{238,240}\text{Pu}$ also ν -bar (1-3%). The high content of Pu in the fuel and the relatively clean Pu vector are at the origin of the observations made. The requirement for improved accuracy of the higher Pu isotopes, and in particular the fission of ^{241}Pu , is more stringent for the EFR, GFR and LFR cases.

For MA, uncertainty improvements for selected isotopes and reactions in some cases are very significant. However, this is the case when MA play an important role in the critical balance, as for MA dedicated burner with a fuel heavily loaded with MA (SFR and ADMAB, but to a lesser degree LFR). For these very specific cases, the accuracy requirement for σ_{fiss} of selected MA isotopes can range from 3-7%. Also for ADMAB some capture requirements emerge.

It may be noted, finally, that a few requirements concern elastic scattering (^{238}U , C, ^{15}N , O, ^{52}Cr , ^{56}Fe , Pb). Except for ^{52}Cr and ^{56}Fe these are system specific. Some of these are only important if a high value is adopted for the cost parameter of inelastic scattering. A notable exception is the stringent requirement for ^{15}N (1%) in the case of ADMAB (with ^{15}N fuel).

Table 25. ABTR: uncertainty reduction requirements needed to meet integral parameter target accuracies

Isotope	Cross-Section	Energy range	Uncertainty (%)			
			Initial	Required		
				$\lambda=1$	$\lambda \neq 1^{(a)}$	$\lambda \neq 1^{(b)}$
U238	σ_{capt}	24.8 - 9.12 keV	9	3	2	2
	σ_{el}	2.23 - 1.35 MeV	19	15	11	8
	σ_{inel}	6.07 - 1.35 MeV	20	3	4	6
Pu239	σ_{capt}	498 - 2.03 keV	12	5	4	3
	σ_{inel}	6.07 - 0.498 MeV	25	12	15	20
Pu241	σ_{fiss}	1.35 - 0.0674 MeV	15	9	9	7
Fe56	σ_{capt}	183 - 2.03 keV	12	8	6	5
	σ_{el}	6.07 - 2.23 MeV	8	7	5	4
	σ_{inel}	2.23 - 0.498 MeV	20	6	7	10
Cr52	σ_{el}	183 - 67.4 keV	11	8	6	4
Zr90	σ_{inel}	6.07 - 2.23 MeV	18	11	13	18
Na23	σ_{inel}	1.35 - 0.498 MeV	25	10	12	18
B10	σ_{capt}	498 - 183 keV	15	14	11	9

^{(a),(b)} See Table 24 for $\lambda \neq 1$, cases A and B

Table 26. SFR: uncertainty reduction requirements needed to meet integral parameter target accuracies

Isotope	Cross-Section	Energy range	Uncertainty (%)			
			Initial	Required		
				$\lambda=1$	$\lambda \neq 1$ ^(a)	$\lambda \neq 1$ ^(b)
U238	σ_{capt}	24.8 - 9.12 keV	9	4	3	3
	σ_{inel}	6.07 - 0.498 MeV	20	5	6	10
Pu238	σ_{capt}	183 - 24.8 keV	20	12	12	10
	σ_{fiss}	6.07 - 0.09 MeV	20	3	3	3
	ν	1.35 - 0.067 MeV	7	3	3	2
Pu239	σ_{capt}	498 - 2.03 keV	12	6	4	4
	σ_{inel}	6.07 - 0.498 MeV	25	12	15	22
Pu240	σ_{capt}	498 - 9 keV	12	5	5	4
	σ_{fiss}	6.07 - 0.0045 MeV	10	2	2	2
	ν	2.23 - 0.183 MeV	4	2	2	1
Pu241	σ_{capt}	1.35 - 0.183 MeV	20	11	11	10
	σ_{fiss}	6.07 MeV-22.6 eV	15	3	3	2
Pu242	σ_{capt}	498 - 2.03 keV	35	8	8	8
	σ_{fiss}	6.07 - 0.183 MeV	20	4	4	3
	σ_{inel}	1.35 - 0.498 MeV	60	26	27	38
Am241	σ_{fiss}	6.07 - 0.498 MeV	10	6	6	5
Am242m	σ_{capt}	498 - 67.4 keV	25	12	12	11
	σ_{fiss}	6.07 MeV-0.454 keV	17	3	3	3
Am243	σ_{fiss}	6.07 - 0.498 MeV	10	7	7	6
Cm244	σ_{fiss}	6.07 - 0.183 MeV	45	5	5	5
	ν	6.07 - 0.498 MeV	10	4	4	4
Cm245	σ_{fiss}	2.23 MeV-9.12 keV	45	7	7	6
Cm246	σ_{fiss}	1.35 - 0.498 MeV	40	16	17	15
Fe56	σ_{capt}	183 - 0.454 keV	12	5	4	3
	σ_{el}	6.07 - 1.35 MeV	8	5	4	3
	σ_{inel}	6.07 - 0.498 MeV	20	3	4	6
Cr52	σ_{el}	183 - 67.4 keV	11	6	5	4
Zr90	σ_{inel}	6.07 - 2.23 MeV	18	9	11	18
Na23	σ_{inel}	2.23 - 1.35 MeV	25	4	5	8
B10	σ_{capt}	1.35 MeV - 9.12 keV	15	4	3	3

^{(a),(b)} See Table 24 for $\lambda \neq 1$, cases A and B

Table 27. EFR: uncertainty reduction requirements needed to meet integral parameter target accuracies

Isotope	Cross-Section	Energy range	Uncertainty (%)		
			Initial	Required	
				$\lambda=1$	$\lambda \neq 1^{(a)}$
U234	σ_{fiss}	1.35 - 0.498 MeV	38	30	32
U235	σ_{capt}	183 - 2.03 keV	33	23	19
U238	σ_{capt}	24.8 - 9.12 keV	9	3	2
	σ_{inel}	6.07 MeV- 67.4 keV	20	4	4
Pu238	σ_{fiss}	1.35 - 0.183 MeV	20	10	9
Pu239	σ_{capt}	498 - 2.03 keV	12	6	3
	σ_{inel}	6.07 - 2.23 MeV	25	14	14
Pu240	σ_{capt}	498 - 9.12 keV	12	6	6
	σ_{fiss}	1.35 - 0.498 MeV	6	4	3
	ν	1.35 - 0.498 MeV	4	3	2
Pu241	σ_{fiss}	1.35 MeV-0.454 keV	15	6	5
Pu242	σ_{capt}	67.4 - 2.03 keV	35	25	26
	σ_{fiss}	1.35 - 0.498 MeV	20	11	9
Cm242	σ_{fiss}	6.07 - 2.23 MeV	55	44	42
Cm244	σ_{fiss}	1.35 - 0.498 MeV	45	20	17
Cm245	σ_{fiss}	1.35 - 0.498 MeV	45	42	40
Fe56	σ_{capt}	2.03 - 0.454 keV	12	8	5
	σ_{inel}	2.23 - 0.498 MeV	20	7	7
Ni58	σ_{capt}	6.07 - 2.23 MeV	15	9	5
Na23	σ_{inel}	1.35 - 0.498 MeV	25	8	8
O16	σ_{capt}	6.07 - 2.23 MeV	100	11	6
	σ_{el}	6.07 - 1.35 MeV	50	9	9

^(a) See Table 24 for $\lambda \neq 1$, case A

Table 28. GFR: uncertainty reduction requirements needed to meet integral parameter target accuracies

Isotope	Cross-Section	Energy range	Uncertainty (%)		
			Initial	Required $\lambda=1$	Required $\lambda \neq 1^{(a)}$
U235	σ_{capt}	9.12 - 2.03 keV	34	13	11
U238	σ_{capt}	24.8 - 9.12 keV	9	2	1
	σ_{inel}	6.07 MeV- 67.4 keV	20	2	2
Pu238	σ_{fiss}	6.07 MeV- 9.12 keV	20	5	5
	ν	1.35 - 0. 183 MeV	7	4	4
Pu239	σ_{capt}	183 - 2.03 keV	12	3	2
	σ_{inel}	6.07 - 0.498 MeV	25	8	10
Pu240	σ_{capt}	183 - 9.12 keV	12	5	6
	σ_{fiss}	6.07 MeV- 0.454 keV	10	3	3
	ν	1.35 - 0.498 MeV	4	2	2
Pu241	σ_{fiss}	6.07 MeV- 0.454 keV	15	2	2
Pu242	σ_{capt}	183 - 2.03 keV	33	7	8
	σ_{fiss}	6.07 - 0.498 MeV	20	4	4
Am241	σ_{capt}	183 - 2.03 keV	8	3	3
	σ_{fiss}	6.07 - 0.498 MeV	10	3	3
Cm244	σ_{fiss}	6.07 - 0.498 MeV	45	8	9
Cm245	σ_{fiss}	1.35 MeV- 24.8 keV	45	11	11
C	σ_{el}	6.07 MeV- 67.4 keV	5	2	1
	σ_{inel}	6.07 - 2.23 MeV	35	9	13
Si28	σ_{inel}	6.07 - 1.35 MeV	30	3	4

^(a) See Table 24 for $\lambda \neq 1$, case A

Table 29. LFR: uncertainty reduction requirements needed to meet integral parameter target accuracies

Isotope	Cross-Section	Energy range	Uncertainty (%)		
			Initial	Required	
				$\lambda=1$	$\lambda \neq 1^{(a)}$
U238	σ_{capt}	24.8 - 9.12 keV	9	2	2
	σ_{inel}	6.07 MeV- 67.4 keV	20	2	3
Pu238	σ_{fiss}	6.07 MeV- 9.12 keV	20	3	4
	ν	1.35 MeV- 67.4 keV	7	3	3
Pu239	σ_{capt}	498 - 2.03 keV	12	4	3
	σ_{inel}	1.35 - 0.498 MeV	25	7	10
Pu240	σ_{capt}	1.35 MeV- 9.12 keV	12	4	4
	σ_{fiss}	6.07 - 0.498 MeV	5	2	2
	ν	1.35 - 0.183MeV	5	1	1
	σ_{inel}	183 - 67.4 keV	43	13	16
Pu241	σ_{fiss}	2.23 MeV- 9.12 keV	15	3	3
Pu242	σ_{capt}	183 - 9.12 keV	35	11	12
	σ_{fiss}	6.07 - 0.498 MeV	20	4	4
Am241	σ_{fiss}	1.35 - 0.498 MeV	10	5	6
Am242m	σ_{fiss}	498 - 183 keV	17	8	8
Cm244	σ_{fiss}	2.23 - 0.498 MeV	45	6	7
Cm245	σ_{fiss}	1.35 MeV- 24.8 keV	45	7	8
Fe56	σ_{capt}	183 - 24.8 keV	12	6	4
	σ_{inel}	2.23 - 0.498 MeV	20	4	5
Zr90	σ_{inel}	6.07 - 2.23 MeV	18	6	9
Pb206	σ_{capt}	183 - 67.4 keV	20	7	5
	σ_{inel}	6.07 - 0.498 MeV	10	3	4
Pb207	σ_{inel}	2.23 - 0.498 MeV	12	3	4
Pb208	σ_{el}	1.35 - 0.183 MeV	5	3	2
B10	σ_{capt}	1.35 MeV- 2.03 keV	15	2	2

^(a) See Table 24 for $\lambda \neq 1$, case A

Table 30. ADMAB: uncertainty reduction requirements needed to meet integral parameter target accuracies

Isotope	Cross-Section	Energy range	Uncertainty (%)		
			Initial	Required	
				$\lambda=1$	$\lambda \neq 1^{(a)}$
Pu238	σ_{fiss}	6.07 - 0.498 MeV	20	3	3
	ν	1.35 - 0.183 MeV	7	3	3
Pu239	σ_{capt}	498 - 2.03 keV	12	4	3
	σ_{inel}	6.07 - 0.498 MeV	25	5	6
Pu240	σ_{capt}	183 - 67.4 keV	14	6	6
	σ_{fiss}	2.23 - 0.498 MeV	6	2	2
	ν	1.35 - 0.498 MeV	4	2	2
Pu241	σ_{capt}	1.35 - 0.183 MeV	20	7	7
	σ_{fiss}	6.07 MeV-22.6 eV	15	2	2
Pu242	σ_{capt}	24.8 - 9.12 keV	35	10	10
	σ_{fiss}	6.07 - 0.498 MeV	20	4	4
Np237	σ_{capt}	498 - 0.454 keV	6	3	3
	σ_{fiss}	6.07 - 0.183 MeV	8	2	2
	σ_{inel}	2.23 - 0.183 MeV	25	5	6
Am241	σ_{capt}	1.35 MeV- 0.454 keV	8	2	2
	σ_{fiss}	6.07 - 0.183 MeV	10	1	1
	ν	6.07 - 1.35 MeV	2	1	1
	σ_{inel}	6.07 - 0.183 MeV	25	4	5
Am242m	σ_{fiss}	1.35 MeV- 9.12 keV	17	5	5
Am243	σ_{capt}	1.35 MeV- 0.454 keV	10	2	2
	σ_{fiss}	6.07 - 0.498 MeV	10	2	2
	σ_{inel}	6.07 MeV- 24.8 keV	40	2	3
Cm242	σ_{fiss}	6.07 MeV- 67.4 keV	55	26	26
Cm243	σ_{fiss}	1.35 MeV- 67.4 keV	50	8	8
Cm244	σ_{capt}	498 -9.12 keV	20	6	6
	σ_{fiss}	6.07 MeV- 67.4 keV	45	2	2
	ν	6.07 - 0.183 MeV	10	1	1
Cm245	σ_{fiss}	6.07 MeV- 0.454 keV	45	3	3
Fe56	σ_{capt}	183 - 0.454 keV	12	5	3
	σ_{inel}	6.07 - 0.498 MeV	20	2	2
Zr90	σ_{inel}	6.07 - 2.23 MeV	18	3	4
N15	σ_{el}	2.23 MeV - 67.4 keV	5	1	1
Pb	σ_{capt}	9.12 - 2.03 keV	20	20	14
	σ_{inel}	6.07 - 2.23 MeV	12	3	4
Bi209	σ_{inel}	2.23 - 0.498 MeV	34	3	3

^(a) See Table 24 for $\lambda \neq 1$, case A

Table 31. Summary target accuracy requirements occurring for at least two fast reactors

Isotope	Quantity	ABTR	SFR	EFR	GFR	LFR	ADMAB
U238	σ_{capt}	3	4	3	2	2	
	σ_{inel}	3	5	4	2	2	
Pu238	ν		3		4	3	3
	σ_{fiss}		3	10	5	3	3
Pu239	σ_{capt}	5	6	6	3	4	3
	σ_{inel}	12	12	14	8	7	6
Pu240	ν		2	3	2	1	2
	σ_{capt}		5	6	5	4	6
	σ_{fiss}		2	4	3	2	2
	σ_{capt}		11				7
Pu241	σ_{fiss}	9	3	6	2	3	2
	σ_{capt}		8	25			10
Pu242	σ_{fiss}		4	11	4	4	4
	σ_{capt}				3		2
Am241	σ_{fiss}		6		3	5	1
	σ_{fiss}		3			8	5
Am242m	σ_{fiss}		3				
Am243	σ_{fiss}		7				2
Cm242	σ_{fiss}			44			26
Cm244	ν		4				1
	σ_{fiss}		5	20	8	6	2
Cm245	σ_{fiss}		7	42	11	7	3
B10	σ_{capt}	14	4				
Na23	σ_{inel}	10	4	8			
Cr52	σ_{el}	8	6				
Fe56	σ_{capt}	8	5	8		6	3
	σ_{el}	7	5				
	σ_{inel}	6	3	7		4	2
Pb	σ_{capt}					7	5
	σ_{inel}					3	3
Zr90	σ_{inel}	11	9			6	4

Table 32. Summary of Highest Priority Target Accuracies for Fast Reactors

		Energy Range	Current Accuracy (%)	Target Accuracy (%)
U238	σ_{inel}	6.07 \div 0.498 MeV	10 \div 20	2 \div 3
	σ_{capt}	24.8 \div 2.04 keV	3 \div 9	1.5 \div 2
Pu241	σ_{fiss}	1.35MeV \div 454 eV	8 \div 20	2 \div 3 (SFR,GFR, LFR) 5 \div 8 (ABTR, EFR)
Pu239	σ_{capt}	498 \div 2.04 keV	7 \div 15	4 \div 7
Pu240	σ_{fiss}	1.35 \div 0.498 MeV	6	1.5 \div 2
	ν	1.35 \div 0.498 MeV	4	1 \div 3
Pu242	σ_{fiss}	2.23 \div 0.498 MeV	19 \div 21	3 \div 5
Pu238	σ_{fiss}	1.35 \div 0.183 MeV	17	3 \div 5
Am242m	σ_{fiss}	1.35MeV \div 67.4keV	17	3 \div 4
Am241	σ_{fiss}	6.07 \div 2.23 MeV	12	3
Cm244	σ_{fiss}	1.35 \div 0.498 MeV	50	5
Cm245	σ_{fiss}	183 \div 67.4 keV	47	7
Fe56	σ_{inel}	2.23 \div 0.498 MeV	16 \div 25	3 \div 6
Na23	σ_{inel}	1.35 \div 0.498 MeV	28	4 \div 10
Pb206	σ_{inel}	2.23 \div 1.35 MeV	14	3
Pb207	σ_{inel}	1.35 \div 0.498 MeV	11	3
Si28	σ_{inel}	6.07 \div 1.35 MeV	14 \div 50	3 \div 6
	σ_{capt}	19.6 \div 6.07 MeV	53	6

Tables 33 and 34 provide a summary of the main data requirements related to thermal neutron systems, i.e. the VHTR (Table 33) and the extended burn-up PWR (Table 34). The present analysis indicates some relevant requirements. In the case of the VHTR, it is required to improve ^{241}Pu σ_{fiss} below ~ 400 eV. Very tight σ_{capt} requirements for ^{239}Pu and ^{241}Pu below ~ 0.5 eV are also identified, together with C data improvements (both capture and inelastic) with respect to current uncertainty estimates. For the PWR with extended burn-up, the requirements to improve ^{241}Pu and some O data can be stressed.

Table 33. VHTR: uncertainty reduction requirements needed to meet integral parameter target accuracies

Isotope	Cross-Section	Energy range	Uncertainty (%)		
			Initial	Required	
				$\lambda=1$	$\lambda \neq 1^{(a)}$
U235	σ_{capt}	24.8 - 2.03 keV	34	14	17
U238	σ_{capt}	454 - 22.6 eV	2	1	1
Pu241	σ_{capt}	0.54 - 0.10 eV	7	2	3
	σ_{fiss}	454 - 0.54 eV	20	6	8
C	σ_{capt}	19.6 - 6.07 MeV	20	7	7
		4.00 - 0.54 eV	20	5	5
	σ_{inel}	6.07 - 2.23 MeV	35	14	25

Table 34. PWR: uncertainty reduction requirements needed to meet integral parameter target accuracies

Isotope	Cross-Section	Energy range	Uncertainty (%)		
			Initial	Required	
				$\lambda=1$	$\lambda \neq 1^{(a)}$
U235	σ_{capt}	67.4 - 2.03 keV	33	12	10
U238	σ_{capt}	24.8 - 9.12 keV	9	5	4
		454 - 22.6 eV	2	1	1
	σ_{scatt}	6.07 - 1.35 MeV	20	5	5
Pu240	σ_{capt}	0.10 eV-thermal	5	3	4
Pu241	σ_{capt}	0.54 - 0.10 eV	7	3	4
	σ_{fiss}	454 - 0.54 eV	20	5	6
O	σ_{capt}	6.07 - 2.23 MeV	100	10	9
	σ_{scatt}	6.07 - 2.23 MeV	50	13	11
		2.23 - 1.35 MeV	12	8	8

The required cross-section accuracies obtained from the optimisation procedures are such that the design target accuracies are fulfilled in most cases. Tables 35 and 36 provide a summary of the uncertainties of the selected design parameters both with the original and with the required cross-section uncertainties (see Appendix P for a complete list), as obtained with the minimisation procedure indicated in Section 2.2. Note that the required parameter accuracies are not exactly met because of the cross-sections not accounted for in the minimisation procedures which give as consequence a residual uncertainty needed to be added to the specified accuracy (see Section 7.2).

Table 35. Integral parameter uncertainties (%) with initial and required cross-section uncertainties

		ABTR	SFR	EFR	GFR	LFR	ADMAB	VHTR	PWR
k_{eff} BOC	Initial	0.62	1.04	0.79	1.24	0.88	1.95	0.37	0.36
	Final	0.31	0.32	0.37	0.33	0.33	0.30	0.31	0.27
k_{eff} EOC	Initial	–	–	–	–	–	–	0.41	0.64
	Final	–	–	–	–	–	–	0.31	0.37
Power peak BOC	Initial	0.32	0.31	0.81	1.18	0.45	14.22	0.85	–
	Final	0.24	0.16	0.33	0.25	0.16	2.21	0.49	–
Power peak EOC	Initial	–	–	–	–	–	–	0.90	–
	Final	–	–	–	–	–	–	0.53	–
Doppler BOC	Initial	2.86	3.62	2.46	3.62	2.85	–	4.27	1.53
	Final	1.69	1.70	1.40	1.36	1.54	–	3.72	1.40
Doppler EOC	Initial	–	–	–	–	–	–	2.77	2.01
	Final	–	–	–	–	–	–	2.25	1.58
Void	Initial	5.11	15.66	6.68	5.46	4.97	13.11	–	–
	Final	3.07	4.06	3.26	3.12	1.88	3.49	–	–
Burn-up [pcm]	Initial	37.4	152.1	584.9	254.2	127.7	602.9	487.0	684.6
	Final	19.1	47.0	297.9	105.8	49.8	216.4	366.3	504.2

Table 36. Transmutation uncertainties (%) with initial and required cross-section uncertainties

		ABTR	SFR	EFR	GFR	LFR	ADMAB	VHTR	PWR
^{235}U	Initial	0.07	0.31	2.57	0.42	0.36	–	0.25	0.46
	Final	0.07	0.31	2.07	0.33	0.36	–	0.24	0.40
^{238}U	Initial	0.01	0.02	0.24	0.04	0.03	–	0.05	0.04
	Final	0.00	0.01	0.11	0.01	0.01	–	0.04	0.04
^{237}Np	Initial	0.25	0.11	2.51	0.25	0.18	0.20	1.03	1.05
	Final	0.25	0.11	2.51	0.25	0.18	0.10	0.99	0.96
^{238}Pu	Initial	0.21	0.42	2.71	0.64	0.56	1.13	1.28	1.05
	Final	0.21	0.13	2.09	0.37	0.22	0.46	1.25	0.97
^{239}Pu	Initial	0.04	0.06	1.13	0.37	0.20	0.12	0.96	0.88
	Final	0.02	0.04	0.56	0.12	0.08	0.06	0.77	0.77
^{240}Pu	Initial	0.13	0.10	1.25	0.31	0.16	0.26	1.25	1.11
	Final	0.08	0.04	0.74	0.10	0.06	0.14	0.99	0.95
^{241}Pu	Initial	0.35	0.62	3.99	0.83	1.19	0.90	2.04	2.02
	Final	0.28	0.18	2.17	0.29	0.38	0.26	1.21	1.25
^{242}Pu	Initial	0.13	0.25	2.75	0.51	0.35	0.54	4.75	3.87
	Final	0.13	0.07	2.06	0.14	0.16	0.31	2.10	2.34
^{241}Am	Initial	0.08	0.18	2.12	0.35	0.27	0.31	2.13	2.50
	Final	0.08	0.16	1.95	0.17	0.27	0.08	1.50	2.02
$^{242\text{m}}\text{Am}$	Initial	0.47	0.70	4.26	2.17	1.17	1.72	5.63	5.41
	Final	0.47	0.20	4.25	1.18	1.02	0.57	5.43	5.21
^{243}Am	Initial	0.35	0.47	6.41	1.07	0.91	0.27	5.58	4.48
	Final	0.35	0.20	4.76	0.36	0.46	0.10	3.53	3.14

Table 36. Transmutation uncertainties (%) with initial and required cross-section uncertainties (*cont.*)

		ABTR	SFR	EFR	GFR	LFR	ADMAB	VHTR	PWR
^{242}Cm	Initial	1.13	1.38	1.58	2.43	2.49	2.78	1.88	1.87
	Final	1.13	1.32	1.41	1.20	2.49	0.77	1.25	1.22
^{243}Cm	Initial	1.30	1.90	10.59	3.91	3.29	3.04	8.37	5.50
	Final	1.30	1.90	10.00	3.76	3.29	1.82	8.27	5.34
^{244}Cm	Initial	0.38	0.73	4.83	0.91	0.88	1.07	6.01	4.77
	Final	0.38	0.23	3.14	0.67	0.41	0.19	4.10	3.49
^{245}Cm	Initial	0.90	1.47	9.37	1.83	2.35	2.48	8.02	6.84
	Final	0.90	0.56	8.72	1.18	0.91	0.59	6.68	5.99
^{246}Cm	Initial	0.51	0.47	4.48	1.35	0.57	3.12	–	–
	Final	0.51	0.37	4.46	1.34	0.57	3.06	–	–

7.3.2 Analysis for groups of systems

A target accuracy study was performed for the three Na-cooled systems together (ABTR, SFR, EFR). The complete list of the required data uncertainties to meet the integral parameter accuracy requirements is presented in Appendix P, Tables 264 and 265. Tables 36 and 37 give the total uncertainties of the selected design parameters with both original and required cross-section uncertainties, as obtained from the target accuracy study.

A target accuracy study was performed for all fast systems taken together (ABTR, SFR, EFR, GFR, LFR and ADMAB). The complete list of the required data uncertainties to meet the integral parameter accuracy requirements is presented in Appendix P, Tables 266 and 267. Tables 38 and 39 give the total uncertainties of the selected design parameters both with original and required cross-section uncertainties, as obtained from the target accuracy study.

By and large, the analysis by group of systems does confirm the analysis by separated systems and confirms the interest to summarize the results as shown in Table 32. In fact, at the present stage it is more meaningful to stress requirements that are common to a large range of reference systems.

**Table 37. Integral parameter uncertainties (%)
with initial and required cross-section uncertainties**

		ABTR	SFR	EFR
k_{eff} BOC	Initial	0.62	1.04	0.79
	Final	0.31	0.34	0.35
Power peak BOC	Initial	0.32	0.31	0.81
	Final	0.22	0.16	0.41
Doppler BOC	Initial	2.86	3.62	2.46
	Final	1.74	1.74	1.29
Void	Initial	5.11	15.66	6.68
	Final	2.97	4.23	2.73
Burn-up [pcm]	Initial	-37.4	-152.1	-584.9
	Final	-17.9	-46.6	-269.5

**Table 38. Transmutation uncertainties (%)
with initial and required cross-section uncertainties**

		ABTR	SFR	EFR
^{235}U	Initial	0.07	0.31	2.57
	Final	0.06	0.27	2.07
^{238}U	Initial	0.01	0.02	0.24
	Final	0.00	0.01	0.13
^{237}Np	Initial	0.25	0.11	2.51
	Final	0.25	0.11	2.51
^{238}Pu	Initial	0.21	0.42	2.71
	Final	0.10	0.13	1.23
^{239}Pu	Initial	0.04	0.06	1.13
	Final	0.02	0.04	0.61
^{240}Pu	Initial	0.13	0.10	1.25
	Final	0.08	0.04	0.61
^{241}Pu	Initial	0.35	0.62	3.99
	Final	0.11	0.18	1.45
^{242}Pu	Initial	0.13	0.25	2.75
	Final	0.06	0.07	0.92
^{241}Am	Initial	0.08	0.18	2.12
	Final	0.07	0.16	1.78
$^{242\text{m}}\text{Am}$	Initial	0.47	0.70	4.26
	Final	0.35	0.20	1.82
^{243}Am	Initial	0.35	0.47	6.41
	Final	0.11	0.20	2.12
^{242}Cm	Initial	1.13	1.38	1.58
	Final	1.06	1.30	1.26
^{243}Cm	Initial	1.30	1.90	10.59
	Final	1.21	1.61	9.20
^{244}Cm	Initial	0.38	0.73	4.83
	Final	0.22	0.23	1.72
^{245}Cm	Initial	0.90	1.47	9.37
	Final	0.63	0.56	4.95
^{246}Cm	Initial	0.51	0.47	4.48
	Final	0.49	0.37	3.88

**Table 39. Integral parameter uncertainties (%)
with initial and required cross-section uncertainties**

		ABTR	SFR	EFR	GFR	LFR	ADMAB
k_{eff} BOC	Initial	0.62	1.04	0.79	1.24	0.88	1.95
	Final	0.28	0.33	0.29	0.32	0.32	0.29
Power peak BOC	Initial	0.32	0.31	0.81	1.18	0.45	14.22
	Final	0.20	0.13	0.34	0.26	0.18	2.17
Doppler BOC	Initial	2.86	3.62	2.46	3.62	2.85	–
	Final	1.41	1.66	1.12	1.38	1.43	–
Void	Initial	5.11	15.66	6.68	5.46	4.97	13.11
	Final	2.84	6.05	3.26	3.14	1.92	3.50
Burn-up [pcm]	Initial	-37.4	-152.1	-584.9	254.2	-127.7	-602.9
	Final	-14.5	-45.2	-201.2	91.9	-45.4	-207.1

Table 40. Transmutation uncertainties (%) with initial and required cross-section uncertainties

		ABTR	SFR	EFR	GFR	LFR	ADMAB
^{235}U	Initial	0.07	0.31	2.57	0.42	0.36	0.00
	Final	0.06	0.28	2.07	0.26	0.29	0.00
^{238}U	Initial	0.01	0.02	0.24	0.04	0.03	0.00
	Final	0.00	0.01	0.09	0.01	0.01	0.00
^{237}Np	Initial	0.25	0.11	2.51	0.25	0.18	0.20
	Final	0.24	0.05	2.34	0.14	0.11	0.10
^{238}Pu	Initial	0.21	0.42	2.71	0.64	0.56	1.13
	Final	0.08	0.13	1.13	0.26	0.20	0.46
^{239}Pu	Initial	0.04	0.06	1.13	0.37	0.20	0.12
	Final	0.02	0.03	0.42	0.13	0.08	0.06
^{240}Pu	Initial	0.13	0.10	1.25	0.31	0.16	0.26
	Final	0.05	0.04	0.47	0.09	0.06	0.09
^{241}Pu	Initial	0.35	0.62	3.99	0.83	1.19	0.90
	Final	0.10	0.16	1.31	0.25	0.37	0.19
^{242}Pu	Initial	0.13	0.25	2.75	0.51	0.35	0.54
	Final	0.05	0.07	0.90	0.14	0.11	0.18
^{241}Am	Initial	0.08	0.18	2.12	0.35	0.27	0.31
	Final	0.02	0.04	0.61	0.10	0.07	0.08
$^{242\text{m}}\text{Am}$	Initial	0.47	0.70	4.26	2.17	1.17	1.72
	Final	0.16	0.32	2.26	0.74	0.45	0.58
^{243}Am	Initial	0.35	0.47	6.41	1.07	0.91	0.27
	Final	0.12	0.19	1.82	0.28	0.31	0.09
^{242}Cm	Initial	1.13	1.38	1.58	2.43	2.49	2.78
	Final	0.33	0.47	0.66	0.75	0.69	0.78
^{243}Cm	Initial	1.30	1.90	10.59	3.91	3.29	3.04
	Final	1.06	1.03	6.75	3.51	2.20	1.82
^{244}Cm	Initial	0.38	0.73	4.83	0.91	0.88	1.07
	Final	0.08	0.08	0.90	0.26	0.13	0.19
^{245}Cm	Initial	0.90	1.47	9.37	1.83	2.35	2.48
	Final	0.23	0.22	1.93	0.44	0.34	0.60
^{246}Cm	Initial	0.51	0.47	4.48	1.35	0.57	3.12
	Final	0.50	0.42	4.08	1.32	0.52	3.05

7.4 Summary of the target accuracy study

When reliable design target accuracies and nuclear data uncertainties are available, quantitative indications can be defined on priority needs for data uncertainty reductions. Requirements can obviously differ between fast and thermal neutron systems. The present status of nuclear data uncertainties, and in particular the very low values for ^{235}U , ^{238}U and ^{239}Pu fission and ^{238}U capture uncertainties (see Appendix O) in a covariance data compilation like BOLNA, tend to indicate, in the case of the wide range of fast reactors considered in this assessment study, a priority requirement for a drastic uncertainty reduction for some σ_{inel} (in particular for ^{238}U), for the σ_{fiss} of higher Pu isotopes and in particular for ^{241}Pu (between ~1-500 keV) and for σ_{capt} of ^{239}Pu (~1-500 keV). These indications are valid for all the fast reactors considered in this work, and which are representative of the current priorities of the Gen-IV and GNEP initiatives. Other requirements are of course associated with specific systems, such as Si data for the GFR, Na for SFR and to a lesser extent ABTR and EFR, Pb in the case of LFR and ADMAB. As concerns ADMAB, tight requirements are found for some MA cross-sections, in particular for σ_{fiss} of ^{244}Cm , ^{241}Am , ^{245}Cm , ^{243}Am , ^{242}Cm , $^{242\text{m}}\text{Am}$, for σ_{inel} of ^{243}Am and for ν of ^{244}Cm . For these reactions, the required accuracies are an order of magnitude below the present uncertainties. Regarding the major actinides, improvements are required for the σ_{fiss} of ^{241}Pu (again ~factor 10), for σ_{fiss} of ^{238}Pu (~factor 5) and for ν of ^{238}Pu (~factor 3). Finally, important requirements are also found for structural materials, particularly for σ_{inel} of ^{56}Fe , ^{209}Bi , Pb and ^{90}Zr .

The present analysis also indicates some important requirements in the case of the VHTR. For this system it is required to improve ^{241}Pu σ_{fiss} below ~400 eV. Very tight σ_{capt} requirements for ^{239}Pu and ^{241}Pu below ~0.5 eV are also identified, along with C data improvements (both capture and inelastic) with respect to current uncertainty estimates. Finally, for PWR with extended burn-up, the requirements to improve ^{241}Pu and some O data can be stressed.

A method was also briefly investigated with the goal to tune the accuracy requirements on different cross-section types (e.g. inelastic and fission), according to the relative difficulty to achieve high accuracies in different types of measurement. Some preliminary results were made available using different values of the so-called cost parameters. It was shown for ABTR and SFR that certain inelastic scattering requirements are significantly relaxed by increasing the emphasis on other requirements (^{239}Pu capture, elastic scattering). More investigation in this important matter is required. In that regard, the discussion in Appendix A concerning quantified achievable experimental accuracies is a valuable starting point. Follow-up activities should provide better guidelines

and in that respect any attempt that significantly bridges the gap between the current and target uncertainties should be greatly encouraged.

Since some key requirements are very tight and difficult to be met within a reasonable time horizon, as discussed in Appendix A, where some comments are given concerning the accuracy of individual measurements of microscopic cross-sections in relation to the accuracy requirements that emerged from the studies of this subgroup, it seems that a strategy of combined use of integral and differential measurements should be pursued (see below).

Finally, the essential role played by the recent efforts in several laboratories to assess credible uncertainty data should be emphasised. Such undertakings are essential in defining a sound strategy for nuclear data improvements to meet the needs of future reactors and their associated fuel cycles.

7.5 Complementary use of differential and integral experiments

The very tight uncertainty requirements, discussed in the previous section, suggest the complementary use of differential and integral experiments in order to meet design target accuracies.

Initially, a realistic assessment of the potential role of experimental techniques at existing experimental facilities could help to streamline and prioritise new differential measurements. The added value of improved evaluations should also be assessed in particular when it comes to data uncertainties and scattering cross sections. These efforts should be as far as possible co-ordinated at an international level. Follow-up activities should provide better guidelines for cost parameters and any attempt that significantly bridges the gap between the current and target uncertainties should be greatly encouraged. In parallel, the use of integral experiments should be envisaged to provide complementary information. In fact, a powerful strategy has been developed and recently generalised and applied to Na-cooled fast reactors [29]. This strategy allows reducing current uncertainties on design parameters using integral experiments as “representative” as possible of the corresponding integral parameters for the “reference” design.

In particular, in Ref. [29] it is shown that in the case of the ABTR, the use of appropriate integral experiments reduces the uncertainty on the k_{eff} from 2.02 to 0.36%. In the case of the SFR the reduction is significant but smaller (from 1.77 to 1.13%), due to the fact that the chosen integral experiments are not sufficiently sensitive to MA data.

8. General conclusions and recommendations

Sensitivity and uncertainty analysis were performed on significant future systems (all based on the uranium cycle) presently under investigation within different international frameworks (Gen-IV, GNEP, AFCI, P/T studies in Japan and Europe) to provide information with regard to the Subgroup 26 mandate.

The results obtained on a wide range of integral parameters show that the assumed uncertainty impact is, in some cases, significant. However, the performance of early feasibility or pre-conceptual design studies is possible and meaningful with current data. Design target accuracies which will be relevant in successive design phases have been considered and nuclear data improvement requirements have been evaluated and quantified.

The results obtained thus far provide general indications and some well-defined, if preliminary, guidelines. The results should be employed with caution, as they indicate trends and general priority needs, and the quantitative values were obtained considering only diagonal (variance) uncertainty values that somewhat represent an underestimation of the real uncertainty. Moreover, and certainly more important, the accuracy requirements and priorities are strongly dependent on the assumed initial uncertainty variance-covariance data, and in particular on the very low initial uncertainty values on some key data of the three major actinides (^{238}U , ^{239}Pu , ^{235}U) and in particular on the fission cross-section of ^{239}Pu .

At the current stage, the work of the subgroup has focused on the most important neutron cross-section uncertainties and their impact on the core and fuel cycle's most significant design parameters. However, there are potential uncertainties in specific areas due to specific data, e.g. thermal scattering matrices for possible high-temperature effects under irradiation in graphite, or angular distribution (e.g. μ -bar) uncertainty effects on the criticality of, e.g. very hard spectrum systems or on the Na void reactivity coefficient in high-leakage configurations, or photon production data uncertainties effects on gamma-heating in structures or control systems. These data and their uncertainties should be considered for future investigations, along with their impact on specific parameters

The subgroup results provide further indications for future work:

- Improvement of the present covariance data, and confirmation of the very low values presently assessed for the major actinides.

- Covariance data assessment for the major fission products, for some selected structural materials, for fission spectra (where current uncertainty data seem to have an impact far beyond what is expected).
- Introduction of cross-correlations among different reactions of the same isotope and, possibly, among different isotopes, to account for potential normalisation effects.
- Evaluation of uncertainty on some fast reactor fuel cycle parameters, like decay heat, following the approach used successfully for present LWRs.
- Selection of a few priority differential measurements, where the expected experimental uncertainties can match the data required uncertainty. This can be the case of some Pu higher isotope fission cross-sections.
- Delayed neutron data uncertainty treatment and relation with reactivity scale should be investigated. The impact can vary according to specific design policies on how to account for the reactivity scale uncertainty.

The results obtained in the subgroup study did underline the need for the definition of a strategy of combined use of high-quality integral experiments, sophisticated analysis tools and scientifically-based covariance data within a statistical data adjustment, in order to fully validate calculation tools for the design of future innovative systems. In fact, in some cases very stringent requirements have been obtained that will be difficult to achieve even with very sophisticated measurement techniques or/and evaluations. These requirements indicate that a careful analysis is needed in order to define the most appropriate and effective strategy for data uncertainty reduction.

In this respect, it should be stressed that integral experiments and statistical data adjustments remain a powerful tool, since they provide a global validation of data, and allow developing improved evaluations for selected isotopes, reaction types and energy domains. In fact, statistical data adjustments can be used not only in design calculations, but also as indications of “trends” to be translated by evaluators in new evaluations.

However, a number of conditions should be satisfied:

- The integral experiments used in the adjustment procedure should be “clean”, in the sense that the associated experimental uncertainties are small and well understood.

- The integral experiment calculated values should not be affected by any significant modelling uncertainty (e.g. geometrical description, number of energy groups used in the analysis, etc.), in order to avoid the introduction of systematic errors.
- The covariance data should be reliable, complete and consistent.

In perspective, data adjustments should as much as possible relate to the physics parameters which describe the cross-sections, to make adjustments independent from the energy collapsing procedures (multi-group approximation). This will open the path towards direct “data file” adjustments.

Finally, the work of the subgroup addressed a wide range of potential innovative systems, in particular fast reactors with very different characteristics. The design parameters that were investigated are the “classical” ones that are expected to play a major role in the design of the next generation of prototypes. However, specific innovative features for reactor systems beyond the prototype phase can induce new needs that are difficult to quantify at the present stage.

In terms of specific recommendations to WPEC for future activities, on the basis of the previous discussion, the subgroup members indicated the potential interest of setting up two new subgroups:

- A new specific subgroup on “Methods and issues for the combined use of integral experiments and covariance data”. Participation of evaluators (to account for feedbacks to files) and a close link to related activities like the ones co-ordinated at the Uncertainty Analysis of Criticality Safety Assessment Expert Group (WPNCS) should be clearly established (a first draft is provided in Appendix J).
- A subgroup that should organise the work needed to meet the requirements as they have been pointed out: sharing work on different installations and different projects, evaluations, etc. (a first draft is provided in Appendix J).

REFERENCES

- [1] Aliberti, G., G. Palmiotti, M. Salvatores, T.K. Kim, T.A. Taiwo, M. Animescu, I. Kodeli, E. Sartori, J.C. Bosq, J. Tommasi, “Nuclear Data Sensitivity, Uncertainty and Target Accuracy Assessment for Future Nuclear Systems”, *Annals of Nucl. Energy*, 33, 700-733 (2006).
- [2] Aliberti, G., G. Palmiotti, M. Salvatores, C.G. Stenberg, “Transmutation Dedicated Systems: an Assessment of Nuclear Data Uncertainty Impact”, *Nucl. Sci. and Eng.*, 146, 13-50 (2004).
- [3] Chang, Y.I., P.J. Finck, C. Grandy, *Advanced Burner Reactor Preconceptual Design Report*, ANL-ABR-1, Argonne National Laboratory, September 2006.
- [4] Aliberti, G., G. Palmiotti, M. Salvatores, “New Covariance Data and Their Impact on ADS Designs”, *AccApp2007*, Pocatello, ID, USA, July-August 2007.
- [5] Palmiotti, G., G. Aliberti, M. Salvatores, J. Tommasi, “Integral Experiment Analysis for Validation and Improvement of Minor Actinide Data for Transmutation Needs”, *Proc. Int. Conf. ND-2004*, Santa Fe, NM, USA, September 2004.
- [6] Salvatores, M., G. Aliberti, G. Palmiotti, D. Rochman, P. Oblozinsky, M. Hermann, P. Talou, T. Kawano, L. Leal, A. Koning, I. Kodeli, “Nuclear Data Needs for Advanced Reactor Systems. A NEA Nuclear Science Committee Initiative”, *ND2007*, Nice, France, April 2007.
- [7] Salvatores, M., G. Aliberti, G. Palmiotti, “The Role of Differential and Integral Experiments to Meet Requirements for Improved Nuclear Data”, *ND2007*, Nice, France, April 2007.
- [8] Palmiotti, G., M. Salvatores, G. Aliberti, “Methods in Use for Sensitivity Analysis, Uncertainty Evaluations and Target Accuracy Assessment”, *Proc. International Workshop NEMEA-4*, Prague, October 2007.

- [9] Rimpault, G., *et al.*, “The ERANOS Code and Data System for Fast Reactor Neutronics Analyses”, *Proc. PHYSOR 2002 Conference*, Seoul, Korea, October 2002. See also Palmiotti, G., R.F. Burstall, E. Kiefhaber, W. Gebhardt, J.M. Rieunier, “New Methods Developments and Rationalization of Tools for LMFBR Design in the Frame of the European Collaboration”, *FR’91 International Conference on Fast Reactors and Related Fuel Cycles*, Kyoto, Japan, 28 October-1 November 1991.
- [10] Hogenbirk, A., “An Easy Way to Carry Out Sensitivity Analyses”, *Proc. Int. Topical Meeting M&C+SNA 2007*, Monterey, April 2007.
- [11] Palmiotti, G., M. Salvatores, *Proposal for Nuclear Data Covariance Matrix*, JEFDOC 1063 Rev.1, January 2005.
- [12] Rochman, D., M. Herman, P. Oblozinsky, S.F. Mughabghab, *Preliminary Cross-section Covariances for WPEC Subgroup 26*, Technical Report BNL-77407-2007-IR, Brookhaven National Laboratory (2007).
- [13] Rochman, D., M. Herman, P. Oblozinsky, S.F. Mughabghab, *Preliminary Nu-bar Covariances for $^{238,242}\text{Pu}$ and $^{242,243,244,245}\text{Cm}$* , Technical Report BNL-77407-2007-IR-Suppl. 1, Brookhaven National Laboratory (2007).
- [14] Chadwick, M., P. Oblozinsky, *et al.*, “ENDF/B-VII.0: Next Generation Evaluated Nuclear Data Library for Nuclear Science and Technology”, *Nuclear Data Sheets*, 107, pp. 2931 (December 2006).
- [15] Mughabghab, S.F., “Atlas of Neutron Resonances: Resonance Parameters and Thermal Cross-sections”, Amsterdam, Elsevier (2006).
- [16] Herman, M., R. Capote, B. Carlson, P. Oblozinsky, M. Sin, A. Trkov, V. Zerkin, “EMPIRE Nuclear Reaction Model Code”, version 2.19 (Lodi). www.nndc.bnl.gov/empire219/ (March 2005).
- [17] Kawano, T., Technical Report JAERI-Research 99-009, JAERI (1999).
- [18] Larson, N.M., *Updated Users’ Guide for SAMMY: Multilevel R-matrix Fits to Neutron Data Using Bayes’ Equations*, ORNL/TM-9179/R7 (2007).
- [19] Leal, L., H. Derrien, N. Larson, G. Arbanas, Royce Sayer, “ORNL Methodology for Covariance Generation for Sensitivity/Uncertainty Analysis”, *International Conference on Nuclear Criticality Safety*, St. Petersburg, Russia, May 2007.

- [20] Koning, A.J., “Generating Covariance Data with Nuclear Models”, *Proceedings of the International Workshop on Nuclear Data Needs for Generation IV Nuclear Energy Systems*, Antwerpen, 5-7 April 2005, P. Rullhusen (Ed.), World Scientific (2006), p. 153.
- [21] Koning, A.J., S. Hilaire, M.C. Duijvestijn, “TALYS: Comprehensive Nuclear Reaction Modeling”, *Proceedings of the International Conference on Nuclear Data for Science and Technology – ND2004*, AIP, Vol. 769, R.C. Haight, M.B. Chadwick, T. Kawano, P. Talou (Eds.), Santa Fe, NM, USA, 26 September-1 October 2004, p. 1154 (2005).
- [22] Palmiotti, G., J.M. Rieunier, C. Gho, M. Salvatores, “BISTRO Optimized Two Dimensional Sn Transport Code”, *Nucl. Sc. Eng.*, 104, 26 (1990).
- [23] Bell, M.J., “The ORNL Isotope Generation and Depletion Code”, Oak Ridge National Laboratory, May 1973.
- [24] Rimpault, G., “Algorithmic Features of the ECCO Cell Code for Treating Heterogeneous Fast Reactor Assemblies”, *International Topical Meeting on Reactor Physics and Computation*, Portland, Oregon, 1-5 May 1995.
- [25] “WIMS – A Modular Scheme for Neutronics Calculations”, User’s Guide for Version 8, ANSWER/WIMS(99)9, ANSWERS Software Package, AEA Technology.
- [26] *The JEFF-3.0 Nuclear Data Library*, OECD/NEA Data Bank, JEFF Report 19 (2005).
- [27] *The JEF-2.2 Nuclear Data Library*, OECD/NEA Data Bank, JEFF Report 17, April 2000.
- [28] Gill, P.E., W. Murray, M.A. Saunders, *SNOPT: An SQP Algorithm for Large-scale Constrained Programming*, Technical Report SOL 97-3, Systems Optimization Laboratory, Department of Operations Research, Stanford University, Stanford, California 94305-4022 (1997).
- [29] Salvatores, M., G. Aliberti, G. Palmiotti, “Nuclear Data Validation and Design Performances Uncertainty Reduction”, ANS Meeting, Boston, MA, USA, June 2007.

Appendix A
ACCURACY OF MEASUREMENTS

Arjan Plompen

Here, some comments are given regarding the accuracy of individual measurements of microscopic cross-sections in relation to the accuracy requirements that emerged from the studies of this subgroup. The main point to be answered is whether state-of-the-art individual measurements could meet the requested accuracies or whether they could make a significant contribution in another manner. These comments are geared towards the items identified as priority one or two by the report and will concentrate on inelastic, capture and fission cross-sections.

A limited number of recent measurement examples are quoted for illustration and no attempt at completeness or generality is made. Several efforts are ongoing or planned that will make important contributions to understanding first the status of nuclear data of interest and second the potential of present techniques with regard to improving our current knowledge. First, there is the MANREAD¹ (Minor actinide nuclear reaction data) co-ordinated research project of the IAEA-Nuclear Data Section that started in September 2007. Also of relevance are the European CANDIDE² co-ordination action and various ongoing measurement programmes in the USA, Japan, Russia and Europe.

For a discussion of measurement uncertainties versus the target accuracies as for instance stated in Table 31 of the report, it must be emphasised that the latter concern group-averaged cross-sections while data uncertainties are typically stated for one energy. In the case of a large number of measurements within one energy group, the accuracy of the average over these measurements must be considered. Thus, when such a large number of measurements may be made, the statistical component of the uncertainty of the group average may be significantly better than that of one individual measurement. The systematic component of

¹ www-nds.iaea.org

² candide.nri.cz

the uncertainty, on the other hand, may only be reduced by combining several independent measurements. It is therefore of interest to consider the systematic uncertainty in case the statistical uncertainty may be reduced by a group average.

No consideration will be given to resolved resonance data since the nature of the systems, the isotopes and energy ranges for which target accuracies were stated almost exclusively concern the unresolved resonance region, or in the case of VHTR and PWR the energy range below 0.5 eV.

It should be made clear that, with few exceptions, the target accuracies for priorities one and two identified in the report have not as yet been met by individual measurements. Thus, the comments below reflect only the accuracy that may potentially be met based on current experience.

1. Inelastic scattering cross-sections

Essentially, two measurement methods can be applied to determine inelastic scattering cross-sections.

The (n,n')-method uses mono-energetic incident neutrons and detects scattered neutrons using hydrogenous scintillators determining their energy with the time-of-flight technique. Differential cross-sections are determined for single levels and groups of levels or ultimately double-differential cross-sections, when resolution is insufficient to resolve groups of levels. These data can be used to extract the level inelastic and total inelastic cross-sections by corrections for the angular distribution, the emitted neutron energy distribution and in important cases the interference of the elastic neutron scattering response. The best achieved systematic uncertainty for a double-differential data point is about 3% (consisting of detection efficiency, multiple scattering and normalisation contributions) with a corresponding uncertainty for the angle integrated result of about 2%. For the integral over the emitted neutron's energy the number of contributing bins in the spectrum, their correlation matrix and, most importantly, the contribution of emitted neutrons with energies below the detection threshold are important. Typically a model-dependent estimate is required for the latter. In summary, an overall systematic accuracy of 3-4% may be feasible for the angle and secondary neutron energy integrated cross-section in particular for non-actinides.

The (n,n'γ)-method may be used with mono-energetic or continuous energy incident neutrons at a time-of-flight facility. By detecting the gamma-ray one measures level population cross-sections and for the first few MeV above the threshold the total inelastic cross-section and the level cross-sections may be determined. This technique is applicable when for every level up to a certain

excitation energy a gamma-ray may be detected which has a well-known emission probability with a magnitude over 10% and an energy that is easily detectable (100 keV to several MeV). It was recently shown that accurate results may be obtained using Ge detectors at time-of-flight facilities. For ^{52}Cr , ^{56}Fe , $^{206,207,208}\text{Pb}$ and ^{209}Bi accuracies of the order of 4-5% were reported [1-4]. The systematic component of the uncertainties was about 3%. Therefore, the inelastic scattering cross-sections for non-actinide target nuclides may be improved using data obtained with this technique to the level of the target uncertainties stated in this report.

1.1 Inelastic scattering on actinides

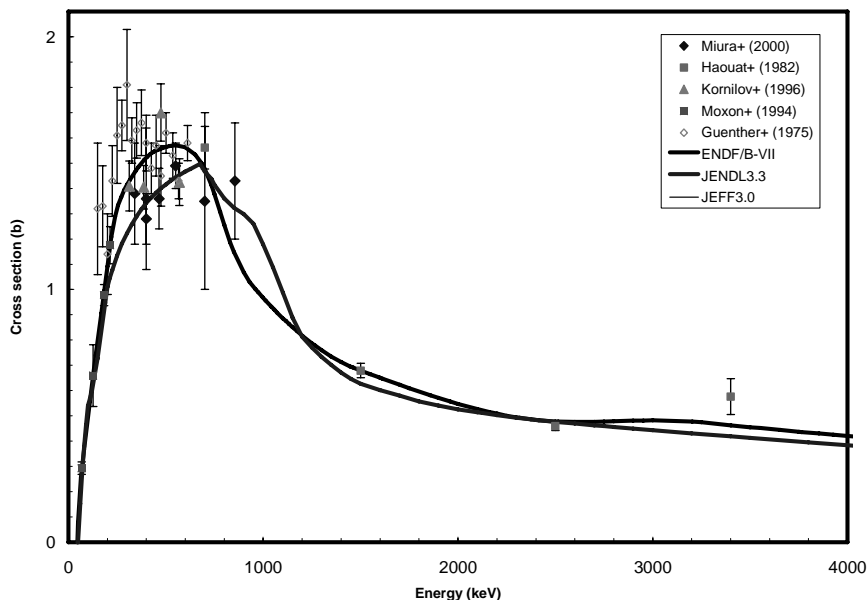
When it comes to inelastic scattering on actinides the main technique to be applied is the (n,n') technique. However, in that case great care is required to subtract the contribution from elastic scattering due to the very small level spacing. Similarly, it is difficult to measure resolved levels. In addition, with the current pulsed quasi mono-energetic neutron sources quite a large sample mass is required to obtain sufficient statistics in a reasonable measurement time (at least several tens of grammes). It is therefore unlikely that the status of the inelastic data on ^{238}U may be improved dramatically with new measurements. For the case of ^{238}U the more recent measurements for the cross-section of the excitation of the first level are shown in Figure 1 [5-9]. The best individual measurement for this level states an accuracy of about 4% in line with the above. It is seen that the data are reasonably consistent and the larger scatter is due to the earliest measurement shown in the graph. Nevertheless, agreement is such that this cross-section seems to be known to about 10% as is mostly confirmed by the differences between the evaluations. EXFOR [10] contains no experimental results for the total inelastic cross-section of ^{238}U that are more recent than 1978. The total inelastic cross-section consists of many contributions from additional levels and must therefore be considered less accurate than 10%.

In view of the sample requirements it is unlikely that any experimental data for inelastic scattering will be determined for isotopes like ^{243}Am . EXFOR has no data for either ^{241}Am or ^{243}Am .

2. Capture cross-sections

What is understood with capture cross-section in this report is probably best termed "neutron-removal" cross-section in the strict sense, i.e. it is for reactions in which one neutron is absorbed and none are emitted. For a discussion it is necessary to distinguish the radiative capture cross-sections on

Figure 1. The most recent experimental results for the inelastic scattering cross-section of the first level in ^{238}U compared with the ENDF/B-VII, JENDL-3.3 and JEFF-3.0 evaluations



^{238}U and $^{239,240,241}\text{Pu}$ from the (n,chnp) reactions that dominate the neutron removal cross-section for C, O and ^{28}Si . In this section capture will be identified with radiative capture and the (n,chnp)-cross-sections will be used for the latter.

Considerable improvement has been made regarding capture measurements in recent years owing to the development of new set-ups and an improved understanding of measurement equipment and techniques through extensive Monte Carlo modelling [11-16].

2.1 $^{238}\text{U}(n,\gamma)$

The difficulty of $^{238}\text{U}(n,\gamma)$ cross-section measurements in the URR may be compared with those for the $^{232}\text{Th}(n,\gamma)$ reaction. Careful ^{232}Th capture measurements in the unresolved resonance range (URR, 4-140 keV) were recently made in Geel [17] and by the n_TOF collaboration at CERN up to 1 MeV [18]. A systematic uncertainty of better than 2% was achieved, which dominates the total uncertainty. All available data were subsequently evaluated within the Th/U CRP of IAEA-NDS and a consistent result could be obtained with similar final accuracy [19]. As already indicated in the contribution by

P. Talou to this report, the Standards CRP of the IAEA established that the uncertainty for the $^{238}\text{U}(n,\gamma)$ evaluated cross-section in the URR already meets the requirements that result from the sensitivity studies in this report [19]. So, here we have an example where both a state-of-the-art measurement may meet and the current evaluation has met the requested target accuracy.

2.2 Fissile isotopes

Capture cross-section measurements for fissile nuclei such as ^{235}U and $^{239,241}\text{Pu}$ are considerably more complicated. Capture cross-section measurements rely on detection of the emitted gamma-rays and in the case of fissile isotopes gamma-rays are also contributed by the fission process. Because of this it is necessary to separate the two contributions. Further, the natural activity may contribute a significant gamma-ray component or an alpha component. The latter complicates measurements with a fission anti-coincidence arrangement.

EXFOR reports only one measurement for ^{241}Pu that covers other energies than thermal (Weston & Todd 1978, 10 meV-30 keV, samples 2 and 4.2 g, ~90% enr.) [20]. Since then no new work was done for this isotope. For ^{239}Pu considerably more work was done. Above 1 keV, eight works are reported in EXFOR. These were obtained in the period from 1956 to 1975.

The ideal measurement detects the gamma-rays in anti-coincidence with the fission events. This leads to conflicting demands on sample mass which should be low enough for an efficient detection of fission fragments and high enough for efficient capture measurements. For ^{235}U the most recent and most accurate work for this type of nuclide is reported in EXFOR. Here, Corvi, *et al.* report uncertainties from 5-12% in the energy range from 2-80 keV using a fission chamber with 21 deposits of $(^{235}\text{U})_3\text{O}_8$ 99.5% enriched for a total of 2.5 g of material [21].

Current efforts involve the DANCE array at Los Alamos where a high capture gamma-ray efficiency helps to reduce the sample mass [22]. A fission deposit is used to characterise the gamma-ray response due to fission in order to develop the sorting criteria for the data. The fission detector is not sufficiently efficient for an anti-coincidence set-up. For ^{239}Pu the high alpha activity poses an additional challenge for such an anti-coincidence arrangement. For ^{241}Pu the acquisition of good sample material and the high background gamma-rate pose additional problems. However for the thermal capture cross-section existing data suggest that 3% accuracy may be achieved. At IRMM there are plans to study the capture cross-section with a fission anti-coincidence arrangement for ^{233}U . It is at present unclear how accurate such measurements will be.

In summary, existing experimental data for fissile isotopes (^{235}U , $^{239,241}\text{Pu}$) in EXFOR predate 1982. Therefore, little is known about what may be achieved in terms of accuracy using modern experimental techniques. In comparison with earlier work the author believes that for ^{239}Pu above 1 keV a 4-15% accuracy is challenging but perhaps not out of reach. Also, below 1 eV, required target uncertainties for $^{239,241}\text{Pu}$ may be achieved with the current status of technology but with considerable effort.

2.3 (*n,chn*)

For C, O, Si, but also B the neutron removal cross-section is due to (*n,chn*) reactions. In most cases, the target accuracies (for energies above 10 keV) are probably achievable by single measurements. As an example, the work at Geel for the $^{16}\text{O}(\text{n},\alpha)$ reaction below 6 MeV may be taken. Here an accuracy of about 6.5% was obtained [23].

3. Fission cross-sections

Fission cross-section measurements for isotopes $^{238,240,241,242}\text{Pu}$, $^{241,242\text{m},243}\text{Am}$ and $^{244,245}\text{Cm}$ are considerable in number and therefore cannot be covered in detail. In fact, a review of available fission cross-section measurements, their accuracies, their discrepancies and what may be achieved with current day techniques is the subject of the MANREAD CRP of IAEA-NDS [19]. The results of this CRP cannot be anticipated here. Suffice it to say that for instance for $^{240,241}\text{Pu}$ and ^{243}Am in the range above 1 keV and below a few MeV, individual results were obtained, covering important parts of the energy range, which meet the target uncertainties of this report (e.g. for ^{241}Pu [24]). Much depends on the quality of the available fission deposits, the alpha activity of the sample, the knowledge of the detection efficiency and the intensity of the neutron source. Therefore, it seems feasible to achieve the target accuracies, in principle, but the effort will have to be considerable both in case new measurements are needed and for the evaluation of the different results. It is at present not clear if new experiments are always necessary or whether an improved evaluation can do the job. The MANREAD CRP should bring clarity in this domain, also because it will gather the experience from ongoing efforts in the various nuclear data communities (USA, Japan, and Europe).

REFERENCES

- [1] Mihailescu, L.C., *et al.*, *Nucl. Phys. A*, 786, 1 (2007).
- [2] Mihailescu, L.C., *et al.*, *Nucl. Phys. A*, forthcoming.
- [3] Nelson, R.O., *et al.*, *Proc. Int. Conf. on Nucl. Data for Sci. and Techn.*, Santa Fe, NM, USA, 1, 838 (2005).
- [4] Negret, *et al.*, *Proc. Int. Workshop NEMEA-4*, forthcoming.
- [5] Miura, T., *et al.*, *Ann. Nucl. Energy*, 27, 625 (2000).
- [6] Haouat, G., *et al.*, *Nucl. Sci. Eng.*, 81, 491 (1982).
- [7] Kornilov, N.V., A.B. Kagalenko, *Rept. JINR*, Dubna, Russia, 336, 245 (1996).
- [8] Moxon, M., *et al.*, *Proc. Int. Conf. on Nucl. Data for Sci. and Techn.*, Gatlinburg, TN, USA, 981 (1994).
- [9] Guenther, P., *et al.*, *ANL Reports*, Argonne, IL, USA, 16 (1975).
- [10] Consulted online at: <http://www.nea.fr/html/dbdata/x4/x4ret.html>;
<http://www-nds.iaea.org/exfor/exfor00.htm>;
<http://www.nndc.bnl.gov/exfor/exfor00.htm>.
- [11] Borella, *et al.*, *Nucl. Instrum. Meth. A*, 577, 626 (2007).
- [12] Reifarh, R., *et al.*, *Nucl. Instrum. Meth. A*, 531, 530 (2004).
- [13] Igashira, M., *et al.*, *Proc. Int. Conf. on Nucl. Data for Sci. and Techn.*, Santa Fe, NM, USA, 1, 601 (2005); Goto, J., *et al.*, *ibid.*, p. 788; Kimura, A., *et al.*, *ibid.*, p. 792.
- [14] Wisshak, K., *et al.*, *Nucl. Instrum. Meth. A*, 292, 595 (1990).

- [15] Cano Ott, D., *et al.*, *Proc. Int. Conf. on Nucl. Data for Sci. and Techn.*, Santa Fe, NM, USA, 1, 1442 (2005).
- [16] Belgia, T., *Phys. Rev. C*, 74, 024603 (2006).
- [17] Borella, *et al.*, *Nucl. Sci. Eng.*, 152, 1 (2006).
- [18] Aerts, G., *et al.*, *Phys. Rev. C*, 73, 054610 (2006).
- [19] www-nds.iaea.org (CRPs)
- [20] Weston, L.W., J.H. Todd, *Nucl. Sci. Eng.*, 65, 454 (1978); *ibid.*, 68, 125 (1978).
- [21] Corvi, F., P. Giacobbe, *Proc. Int. Conf. Nucl. Cross-sect. and Techn.*, Washington, USA, 599 (1975).
- [22] Ullmann, J., *Proc. Int. Conf. on Nucl. Data for Sci. and Techn.*, Nice (2008), forthcoming.
- [23] Khriatchkov, V., *et al.*, *Proc. Int. Conf. on Nucl. Data for Sci. and Techn.*, Nice (2008), forthcoming.
- [24] Wagemans, A.J. Deruytter, *Proc. Int. Conf. on Nucl. Data for Sci. and Techn.*, Antwerpen, 69 (1982).

Appendix B

EVALUATION OF DOPPLER REACTIVITY UNCERTAINTY (INCLUDING THE EFFECT FROM TEMPERATURE GRADIENT COVARIANCE OF ^{238}U SELF-SHIELDING FACTORS)

M. Ishikawa

1. Introduction

In reactor analysis, nuclear data sensitivity analysis is very important from several viewpoints: a) to understand quantitatively the physical mechanism, by tracing the components of nuclides, reactions and energy ranges; b) to evaluate the prediction error of reactor core parameters; c) to improve design accuracy. In order to fulfil such roles, the sensitivity of various core parameters must be calculated, not only for general characteristics such as criticality, reaction rate and control rod worth, etc., but also for burn-up-related core parameters such as fuel composition changes by power operation, and for Doppler reactivity.

As regards the sensitivity of general core parameters, Usachev first proposed the generalised perturbation theory on reaction rate in 1964 [1], and Gandini and Salvatores, *et al.* extended the theory to reactivity in 1966-1967 [2,3]. To solve the generalised perturbation equation, a numerical methodology to use the Neumann series expansion was equipped by Stacey in 1972 [4].

As for with the burn-up related core parameters, Gandini first established the theoretical basis in 1975 [5], it was developed by Salvatores, *et al.* [6], and finally completed by Williams in 1979 [7].

For the Doppler reactivity, which is necessary to take into account the self-shielding effect of effective cross-sections, Ishikawa, *et al.* established the methodology to calculate the sensitivity coefficient related to the temperature gradient of self-shielding factors (f-factors, hereafter) in the framework of the ABBN group constant system in 2001 [8]. However, no fixed methodology existed as yet to generate the covariance of the temperature gradient of self-shielding factors, which is needed to evaluate the accuracy of the Doppler

reactivity prediction. Recently, Otuka, *et al.* created the methodology and the analytical code, ERRORF, to generate the covariance, and applied it to the JENDL-3.3 library in 2007 [9].

In this appendix, we first review the equation to calculate the sensitivity of Doppler reactivity related to self-shielding effect, and second, we summarise the methodology to evaluate the covariance of the temperature gradient of f-factors, and finally demonstrate the evaluation results of Doppler reactivity accuracy for a typical 600-MWe-class FBR core.

2. Equation to calculate the sensitivity coefficient of Doppler reactivity

Since the Doppler reactivity is also a kind of reactivity, the sensitivity related to infinitely-diluted cross-sections must be considered, as well as the self-shielding factors.

2.1 Sensitivity coefficients related to infinitely-diluted cross-sections

The definition of reactivity, R , with use of the operators H_1 and H_2 , is as follows:

$$R \equiv \frac{[\Phi^* H_1 \Phi]}{[\Phi^* H_2 \Phi]} = \frac{\iiint d\vec{r} dE \Phi^*(\vec{r}, E) H_1(\vec{r}, E) \Phi(\vec{r}, E)}{\iiint d\vec{r} dE \Phi^*(\vec{r}, E) H_2(\vec{r}, E) \Phi(\vec{r}, E)} \quad \text{Eq. (1)}$$

The sensitivity, S , of the reactivity R is calculated by the generalised flux as below:

$$S \equiv \frac{\frac{dR}{d\sigma}}{\frac{R}{\sigma}} = \sigma \frac{d(\ln R)}{d\sigma} = \left\{ \frac{\left[\Phi^* \frac{dH_1}{d\sigma} \Phi \right]}{[\Phi^* H_1 \Phi]} - \frac{\left[\Phi^* \frac{dH_2}{d\sigma} \Phi \right]}{[\Phi^* H_2 \Phi]} - \left[\Gamma^* \frac{dB}{d\sigma} \Phi \right] - \left[\Gamma \frac{dB^*}{d\sigma} \Phi^* \right] \right\} \sigma \quad \text{Eq. (2)}$$

where:

$$B^* \Gamma^* = \frac{H_1^* \Phi^*}{[\Phi H_1^* \Phi^*]} - \frac{H_2^* \Phi^*}{[\Phi H_2^* \Phi^*]} \quad \leftarrow (A - \lambda F) \Phi(\vec{r}, E) \equiv B \Phi = 0 \quad \text{Eq. (3)}$$

$$B \Gamma = \frac{H_1 \Phi}{[\Phi^* H_1 \Phi]} - \frac{H_2 \Phi}{[\Phi^* H_2 \Phi]} \quad \leftarrow (A^* - \lambda F^*) \Phi^*(\vec{r}, E) \equiv B^* \Phi^* = 0 \quad \text{Eq. (4)}$$

In the right side of Eq. (2), the first and second terms are so-called “direct effect”, and the third and fourth terms are “indirect effect” through the change of normal flux or adjoint.

2.2 Sensitivity coefficients related to self-shielding factors

The Doppler reactivity, R , can be expressed using the k_{eff} values of low and high temperature:

$$R = \frac{1}{k_{\text{eff,low}}} - \frac{1}{k_{\text{eff,high}}} \quad \text{Eq. (5)}$$

The effective cross-section of high temperature is related to that of low temperature:

$$\sigma_{\text{eff,high}} \approx \left[f_{\text{low}} + \left(\frac{df}{dT} \right) \Delta T \right] \sigma_{\infty, \text{low}} = (1 + f' \Delta T) \sigma_{\text{eff,low}} \quad \text{Eq. (6)}$$

where f is the f -factor of the ABBN-type group constant, and here, a pseudo-cross-section, f' , that is, the temperature gradient of the f -factor, is newly introduced:

$$f' \equiv \frac{1}{f_{\text{low}}} \left(\frac{df}{dT} \right) \equiv \alpha \quad \text{Eq. (7)}$$

Finally, the sensitivity of Doppler reactivity related to f' is obtained by:

$$S_{f'} \equiv \frac{dR/R}{df'/f'} = \left(\frac{\sigma_{\text{eff,high}} - \sigma_{\text{eff,low}}}{\sigma_{\text{eff,high}}} \right) \times \frac{1}{R} \times \frac{S_{k_{\text{eff,high}}}}{k_{\text{eff,high}}} \quad \text{Eq. (8)}$$

where:

$$S_{k_{\text{eff,high}}} = \frac{dk_{\text{eff,high}}/k_{\text{eff,high}}}{d\sigma_{\infty,\text{high}}/\sigma_{\infty,\text{high}}} \quad \text{Eq. (9)}$$

The advances of Eq. (8) are: 1) easily calculated from the sensitivity of criticality, $S_{k_{\text{eff}}}$; 2) no influence to the f-factors at room temperature after some modification such as adjustment procedure.

3. Methodology to evaluate covariance of f-factor temperature gradient

The covariance of the f-factor temperature gradient is obtained to multiply the sensitivity coefficients of f-factor temperature gradient related to resonance parameters with the covariance of the resonance parameters.

3.1 Sensitivity coefficients of f-factors related to resonance parameters

As an example, consider the single-level Breit-Wigner equation below:

$$\sigma_{\gamma}(E, T) = \sigma_0 \left(\frac{\Gamma_{\gamma}}{\Gamma} \right) \left(\frac{E_0}{E} \right)^{1/2} \left(\frac{M}{2\pi kT} \right)^{1/2} \int_{-\infty}^{\infty} \frac{\exp\left(-\frac{MV_z^2}{2kT}\right)}{1 + \left(\frac{2(E_c - E_0)}{\Gamma}\right)} dV_z \quad \text{Eq. (10)}$$

where Γ_n is neutron width, Γ_{γ} is radiative width, $\Gamma = \Gamma_n + \Gamma_{\gamma} + \dots$ is total width, E_0 is resonance peak energy, E is neutron energy, E_c is neutron energy of relative velocity, T is temperature, M is mass of nuclei, V_z is velocity of nuclei to neutron direction and $\sigma_0 = \frac{4\pi\lambda^2 g_J \Gamma_n}{\Gamma}$ is total resonance cross-section at $E = E_0$.

The sensitivity coefficients of f-factor temperature gradient related to resonance parameters are:

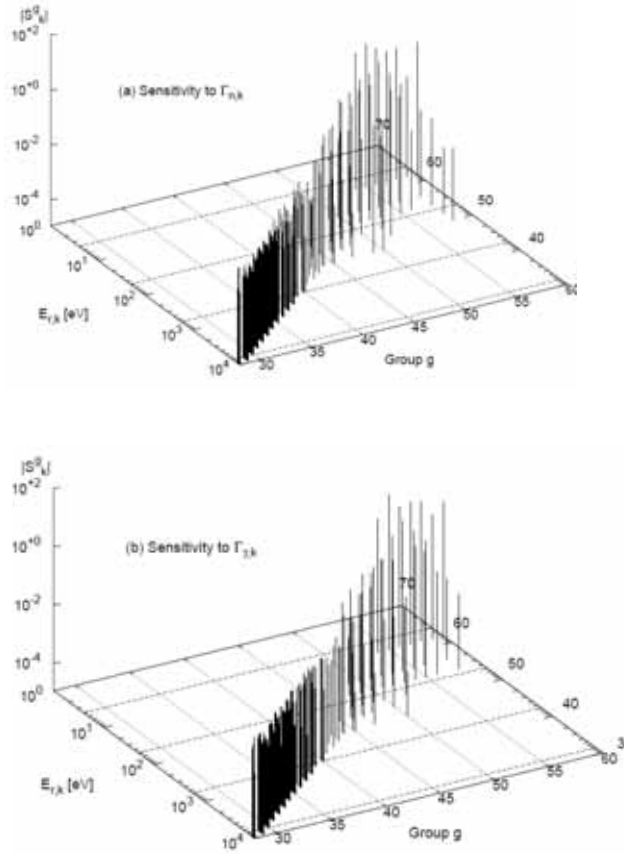
$$S_i^g(\vec{x}, T) = \frac{x_i}{\alpha^g(\vec{x}, T)} \frac{\partial \alpha^g(\vec{x}, T)}{\partial x_i} \quad \text{Eq. (11)}$$

where x_i is the resonance parameter, $\vec{x} = \{x_i\} = \{E_\gamma, \Gamma_n, \Gamma_\gamma, \dots\}$ and

$$\alpha \equiv f' \equiv \frac{1}{f_{\text{low}}} \left(\frac{df}{dT} \right).$$

Eq. (11) is calculated numerically by the ERRORF code, which has been newly developed by JAEA [9].

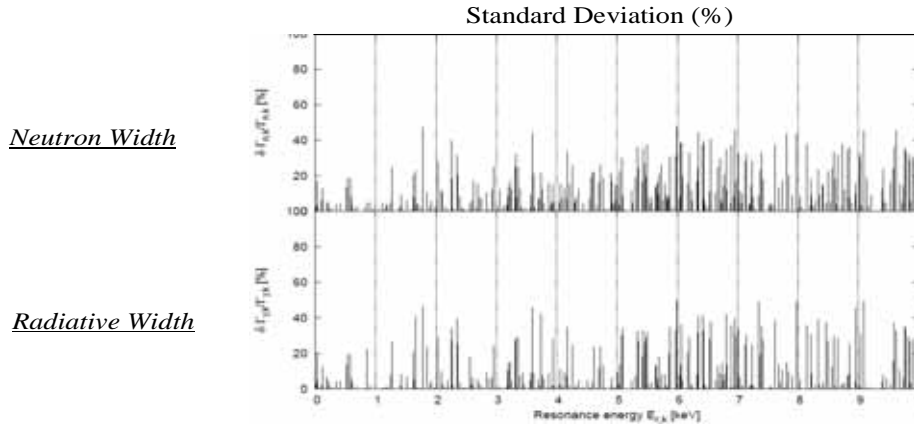
Figure 1. Sensitivity coefficients of f-factor temperature gradient related to resonance parameters (^{238}U capture reaction, $T = 800$ K, and $\text{Sigma-0} = 37$ barns)



3.2 Covariance of resonance parameters

In JENDL-3.3, the covariance of resonance parameters is evaluated for important nuclides as indicated in Figure 2.

Figure 2. Covariance of resonance parameters (correlation factors are also included in JENDL-3.3, but not depicted here) (^{238}U , JENDL-3.3)



3.3 Covariance of f-factor temperature gradient

The covariance of the f-factor temperature gradient is obtained as below:

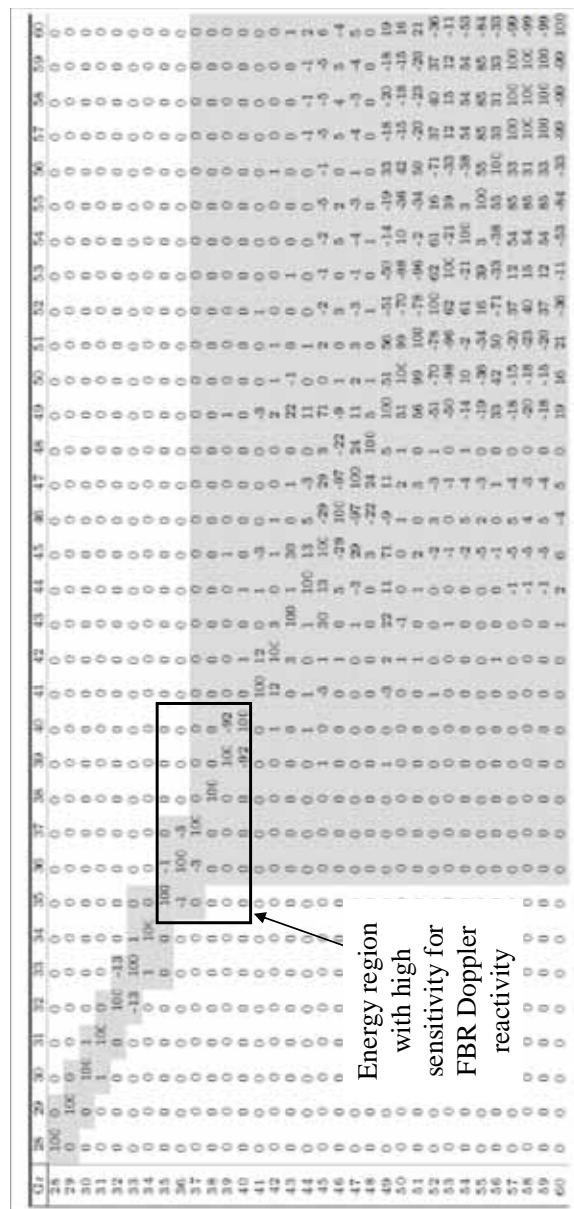
$$\begin{aligned} \text{Cov}[\alpha(\vec{x}, T)] &= S(\vec{x}, T) \times \text{Cov}[\vec{x}] \times S(\vec{x}, T)^t = \\ &= \begin{bmatrix} S_1^1 & S_1^2 & \cdots & S_1^n \\ \vdots & \vdots & \vdots & \vdots \\ S_n^1 & S_n^2 & \cdots & S_n^n \end{bmatrix} \begin{pmatrix} \delta x_{11} & \delta x_{12} & \cdots & \delta x_{1n} \\ \delta x_{21} & \delta x_{22} & \cdots & \delta x_{2n} \\ \vdots & \vdots & \vdots & \vdots \\ \delta x_{n1} & \delta x_{n2} & \cdots & \delta x_{nn} \end{pmatrix} \begin{bmatrix} S_1^1 & \cdots & S_1^G \\ S_2^1 & \cdots & S_2^G \\ \vdots & \cdots & \vdots \\ S_n^1 & \cdots & S_n^G \end{bmatrix} \quad \text{Eq. (12)} \end{aligned}$$

Figure 3. Standard deviation of f-factor temperature gradient in 70-group structure
 $(^{238}\text{U}$ capture reaction, $T = 800$ K, and $\text{Sigma-0} = 37$ barns)

Gr	E_{max} [eV]	$(\delta\sigma^2/\sigma^2)_{\text{tot}}$ [%]	0-1keV	1-2keV	2-3keV	3-4keV	4-5keV	5-6keV	6-7keV	7-8keV	8-9keV	9-10keV
...	0	0	0	0	0	0	0	0	0	0
27	1.5E+4	1.0054	0	0	0	0	0	0	0	0	0	1.0054
28	1.2E+4	1.4260	0	0	0	0	0	0	0	0	0	0.0955
29	9.1E+3	1.2854	0	0	0	0	0	0	0	0	0	0
30	7.1E+3	1.0125	0	0	0	0	0	0	0	0	0	0
31	5.3E+3	1.0125	0	0	0	0	0	0	0	0	0	0
32	4.3E+3	1.0387	0	0	0	0	0	0	0	0	0	0
33	3.4E+3	1.0435	0	0	0	0	0	0	0	0	0	0
34	2.6E+3	1.5242	0	0	0	0	0	0	0	0	0	0
35	2.0E+3	1.6642	0	0	0	0	0	0	0	0	0	0
36	1.6E+3	0.9159	0	0	0	0	0	0	0	0	0	0
37	1.2E+3	0.2855	0	0	0	0	0	0	0	0	0	0
38	9.6E+2	0.1997	0	0	0	0	0	0	0	0	0	0
39	7.5E+2	0.6442	0	0	0	0	0	0	0	0	0	0
40	5.8E+2	0.4129	0	0	0	0	0	0	0	0	0	0
41	4.5E+2	0.2084	0	0	0	0	0	0	0	0	0	0
42	3.5E+2	0.6127	0	0	0	0	0	0	0	0	0	0
43	2.8E+2	0.1280	0	0	0	0	0	0	0	0	0	0
44	2.1E+2	3.2950	0	0	0	0	0	0	0	0	0	0
45	1.7E+2	0.0758	0	0	0	0	0	0	0	0	0	0
46	1.3E+2	3.4535	0	0	0	0	0	0	0	0	0	0
47	1.0E+2	0.7534	0	0	0	0	0	0	0	0	0	0
48	7.9E+1	0.3075	0	0	0	0	0	0	0	0	0	0
49	6.1E+1	0.9149	0	0	0	0	0	0	0	0	0	0
50	4.8E+1	2.5131	0	0	0	0	0	0	0	0	0	0
51	3.8E+1	5.0272	0	0	0	0	0	0	0	0	0	0
52	3.0E+1	5.5672	0	0	0	0	0	0	0	0	0	0
53	2.3E+1	5.8284	0	0	0	0	0	0	0	0	0	0
54	1.8E+1	7.7558	0	0	0	0	0	0	0	0	0	0
55	1.4E+1	3.6872	0	0	0	0	0	0	0	0	0	0
56	1.1E+1	0.7534	0	0	0	0	0	0	0	0	0	0
57	8.3E+0	2.7591	0	0	0	0	0	0	0	0	0	0
58	6.5E+0	3.3961	0	0	0	0	0	0	0	0	0	0
59	5.0E+0	0.5157	0	0	0	0	0	0	0	0	0	0
60	3.9E+0	1.5629	0	0	0	0	0	0	0	0	0	0
61	3.1E+0	...	0	0	0	0	0	0	0	0	0	0
...	0	0	0	0	0	0	0	0	0	0

Energy region
with high
sensitivity for
FBR Doppler
reactivity

Figure 4. Correlation matrix of f-factor temperature gradient in 70-group structure
 $(^{238}\text{U}$ capture reaction, $T = 800$ K, and $\text{Sigma-0} = 37$ barns)



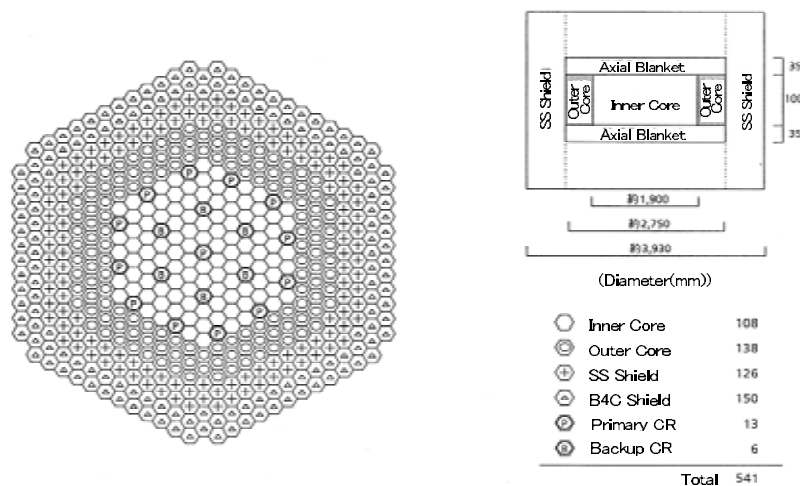
4. Evaluation of Doppler reactivity uncertainty for a 600-MWe-class sodium-cooled fast reactor

The covariance of the f-factor temperature-gradient evaluated above is applied to the Doppler reactivity of a typical FBR core.

4.1 Specification of a 600-MWe-class sodium-cooled fast reactor

The outline of the target FBR core is provided in Figure 5.

Figure 5. Specification of a 600-MWe-class sodium-cooled fast reactor



- Thermal power: 1 600 MWth
- Operating cycle: 365 days
- Pu ratio (inner/outer core): 16.5/20.5%
- Pu composition (238/239/240/241/242): 3/53/25/12/7
- Burn-up reactivity loss: 2.5%dk/kk' cycle
- Doppler coefficient (BOEC): -8.0E-3 Tdk/dT
- Sodium void reactivity (whole core, BOEC): 4.6 \$
- Prompt neutron lifetime (BOEC): 0.41 micro-sec
- Beta effective (BOEC): 3.8E-3

4.2 Doppler reactivity and its sensitivity coefficients

Figure 6 shows the energy breakdown of the whole-core Doppler reactivity for the 600-MWe-class FBR core, which was obtained with ordinary exact perturbation theory. It is found that the most of the Doppler reactivity occurs in the energy range from 500 eV to 2 keV.

The sensitivity coefficients of the Doppler reactivity related to temperature gradient of ^{238}U capture f-table and infinitely-diluted cross-sections of major nuclides and reactions are depicted in Figure 7, which was calculated by the

Figure 6. Energy breakdown of the whole-core Doppler reactivity for the 600-MWe-class FBR core

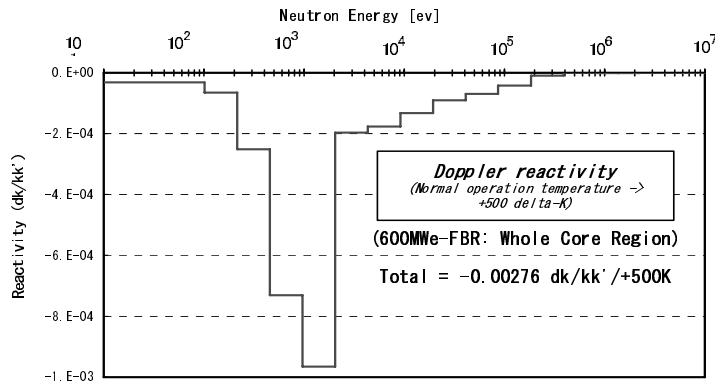
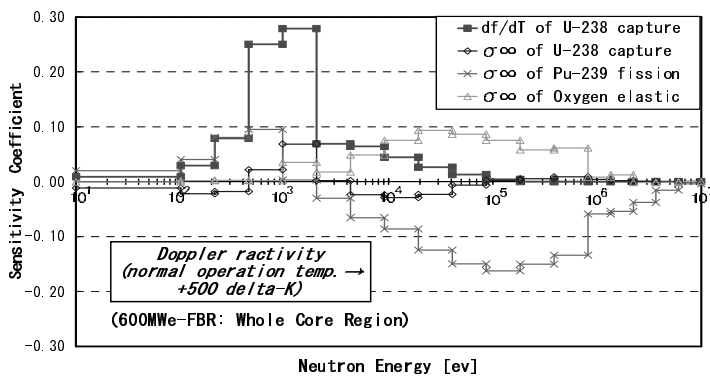


Figure 7. Sensitivity coefficients of the Doppler reactivity for the 600-MWe-class FBR core



generalised perturbation theory summarised in Section 2. The energy shape of the sensitivity of f-table temperature gradient corresponds to the energy breakdown of the Doppler reactivity, since it is the direct effect. On the other hand, those of the infinitely-diluted cross-sections are quite different, as these are the indirect effect through flux and adjoint changes.

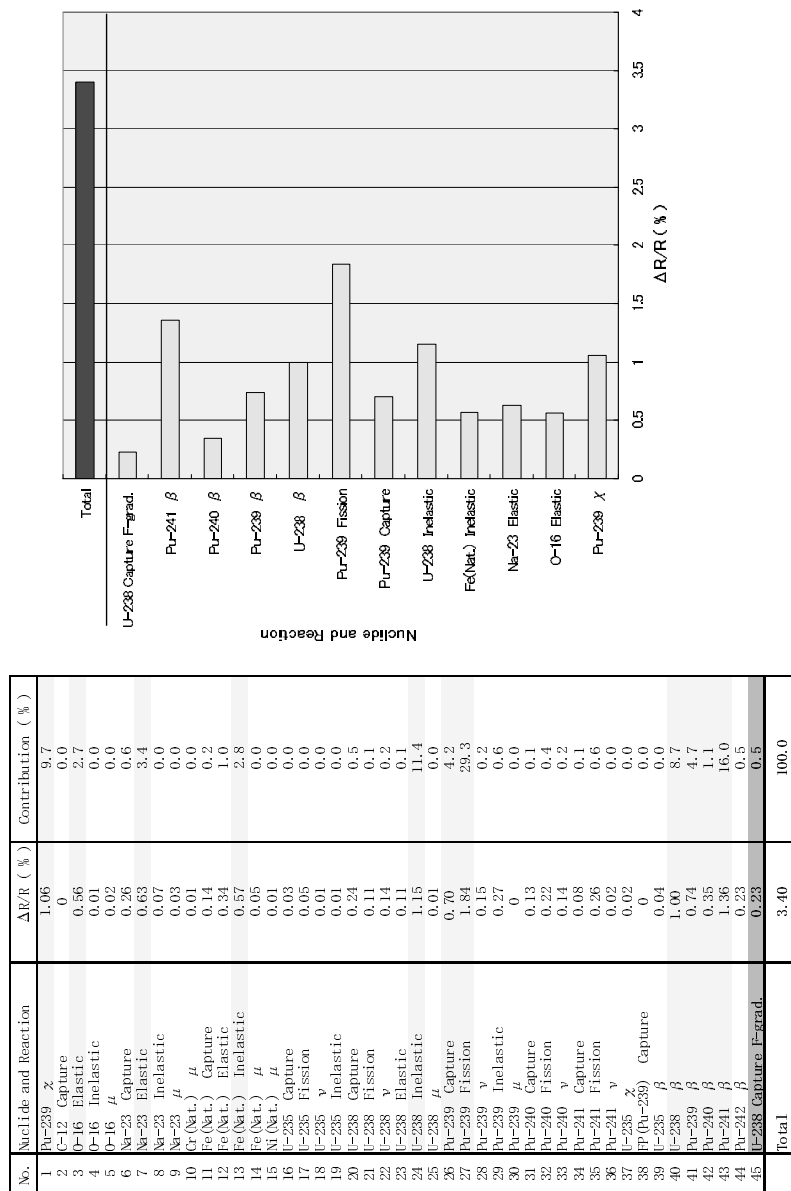
3.3 Doppler reactivity uncertainty

Figure 8 shows the nuclide- and reaction-wise contribution to the whole-core Doppler reactivity for the 600-MWe-class FBR core, which was obtained by multiplying the sensitivity coefficients, some of which are depicted in Figure 7, with the covariance described in Section 3. The total uncertainty of the Doppler reactivity is 3.4% in one-sigma, where the major contributions come from ^{239}Pu fission and ^{238}U inelastic reaction, ^{239}Pu fission spectrum, and delayed neutron fractions of ^{241}Pu and ^{238}U , etc. The temperature gradient of ^{238}U capture f-table contributes to the total Doppler reactivity uncertainty only by 0.5% in this FBR case.

5. Conclusions

The methodology to evaluate the uncertainty of Doppler reactivity has been developed, taking into account both infinitely-diluted cross-sections and self-shielding factors, and the related ERRORF code will be opened to public through OECD/NEA Databank. The temperature gradient covariance of ^{238}U f-factors was generated in 70-group structure from the covariance data of resonance parameters in the latest JENDL library. In conclusion, the uncertainty evaluation of Doppler reactivity for a 600-MWe-class FBR resulted in rather small contribution induced from ^{238}U self-shielding effect, compared with those from other nuclear data such as delayed neutron fraction, fission spectrum and some infinitely-diluted cross-sections.

Figure 8. Uncertainty evaluation of the whole-core Doppler reactivity for a 600-MWe-class FBR core



REFERENCES

- [1] Usachev, L.N., "Perturbation Theory for the Breeding Ratio and for Other Number Ratios Pertaining to Various Reactor Processes", *Journal of Nuclear Energy A/B*, Vol. 18, p. 571 (1964).
- [2] Gandini, A., M. Salvatores, G. Sena, "Analysis of Fast Reactors by the CIAP and GLOPERT Codes Using Improved Perturbation Methods", *Proc. Int. Conf. on Fast Critical Experiments and Their Analysis*, Illinois, ANL-7320, p. 304 (1966).
- [3] Gandini, A., "A Generalized Perturbation Method for Bi-linear Functionals of the Real and Adjoint Neutron Fluxes", *Journal of Nuclear Energy*, Vol. 21, p. 755 (1967).
- [4] Stacey, W.M., Jr., "Variational Estimates and Generalized Perturbation Theory for the Ratios of Linear and Bilinear Functionals", *J. Math. Phys.*, Vol. 13, No. 8, p. 1119 (1972).
- [5] Gandini, A., *Time-dependent Generalized Perturbation Methods for Burn-up Analysis*, RT/FI(75)4, Comitato Nazionale Energia Nucleare (CNEN) (1975).
- [6] Gandini, A., M. Salvatores, L. Tondinelli, "New Developments in Generalized Perturbation Methods in the Nuclide Field", *Nuclear Science and Engineering*, 62, p. 339 (1977).
- [7] Williams, M.L., "Development of Depletion Perturbation Theory for Coupled Neutron/Nuclide Fields", *Nuclear Science and Engineering*, 70, p. 20 (1979).
- [8] Ishikawa, M., K. Sugino, W. Sato, K. Numata, "Development of a Unified Cross-section Set ADJ2000 Based on Adjustment Technique for Fast Reactor Analysis", *Proc. Int. Conf. on Nuclear Data for Science and Technology (ND2001)*, Vol. 2, pp. 1073-1076 (2002).
- [9] Otuka, N., A. Zukeran, H. Takano, G. Chiba, M. Ishikawa, "Covariance Analyses of Self-shielding Factor and its Temperature Gradient for Uranium-238 Neutron Capture Reaction", *Journal of Nuclear Science and Technology*, Vol. 45, No. 3 (Mar. 2008).

Appendix C

**EVALUATION OF FISSION SPECTRA
UNCERTAINTY AND THEIR PROPAGATION**

I. Kodeli, M. Ishikawa, G. Aliberti

1. Introduction

The uncertainties in the fission spectra have important implications on the precision of the criticality and transport calculations involving fissile materials. In spite of this evident importance of the fission spectra uncertainties in the nuclear reactor analysis, available covariance data are still relatively scarce. Among the recent evaluations only the JENDL-3.3 library [1] includes complete covariance matrices for most frequent fissile materials, such as ^{233}U , ^{235}U , ^{238}U , ^{239}Pu and ^{240}Pu . ENDF/B-VII evaluation [2] includes the covariances of ^{252}Cf , taken from ENDF/B-VI. Some older evaluations (ENDF/B-V, see [3]) also include these data. The code ERRORJ [4], which is able to process the File 35 data, was developed only rather recently.

The impact of the fission spectra uncertainty in the case of a Gen-IV system (ABTR) and the KRITZ thermal benchmark experiment was studied in Ref. [5] presented at the NEMEA-4 Workshop in Prague in October 2007. High uncertainties of the order of several per cent were observed. Such uncertainties exceed the uncertainties linked to the cross-sections, and would impose important restrictions on the reactor design.

Inconsistencies in the sensitivity calculation methods and/or the covariance matrix evaluation and processing were suggested as a possible explanation for the high uncertainties. This study was therefore initiated to clarify the differences in the sensitivity methodologies used by different laboratories and recommend the method(s) to be used in the evaluation of the sensitivity and uncertainty of the effective multiplication factor with respect to the fission spectra.

As part of this effort, a computational exercise was proposed [6] to compare the different approaches. Differences among the results obtained by the codes

participating in this exercise (ERANOS [7], SAGEP [8] and SUS3D [9]) were put in evidence and are studied in detail in this appendix. In addition to providing a thorough comparison of the different methods used to calculate the sensitivity and the uncertainty of the effective multiplication factor with respect to the fission spectra, we review the rules which apply to the construction of the File 35 covariance matrices. The present status and recommendations on the methods as well as on the future activities in this area are presented.

Finally, the intention of this work is to stimulate both fission spectra covariance data evaluation and their use.

2. Error propagation equation

The uncertainty in a particular response (k_{eff} , reaction rate) is calculated using the standard error propagation equation from the sensitivity vector and the corresponding covariance matrix:

$$\left(\frac{\delta R}{R} \right)^2 \equiv \bar{S}_\chi M_\chi \bar{S}_\chi^t \quad \text{Eq. (1)}$$

The following two terms are therefore needed to evaluate the uncertainties:

- $\bar{S}_\chi \equiv \frac{\partial(\ln k_{\text{eff}})}{\partial(\ln \chi)} = \frac{\partial k_{\text{eff}} / k_{\text{eff}}}{\partial \chi / \chi}$ being the relative sensitivity coefficient vector;
- M_χ being the relative covariance matrix with elements
$$M_{i,j} = \frac{\langle \delta \chi_i \cdot \delta \chi_j \rangle}{\chi_i \cdot \chi_j} = \frac{V_{i,j}}{\chi_i \cdot \chi_j}$$

where V_χ is the absolute covariance matrix, χ_i is the fission spectrum (total number of fission neutrons in a group i) and $\langle \rangle$ denotes the expectation value.

For reasons which will be explained below, the fission spectra covariance matrices are stored in the evaluated files in the terms of the absolute matrix V_χ , instead of in the relative form.

For simplicity we omit in the following text the index χ and use S and V to represent the sensitivities related to the fission spectrum and the associated covariances.

3. Covariance matrices – rules for evaluation and availability

Because probability distributions must remain normalised to unity, the ENDF-6 Format Manual [10] prescribes a constraint which the covariance matrices in File 35 must satisfy in addition to being symmetric. This constraint is that the sums of the elements in any row of the matrix, therefore also of any column, must be zero. In practice this constraint states that the sum of each row or column should be below 10^{-5} on the evaluator's energy grid. Naturally, this condition must also be met with processed data on the user's energy grid. It is important to note that the above implies that the matrix elements must be provided in absolute and not relative terms.

Furthermore, if the above constraint has not been applied in the covariance matrix defined above for the normalised spectral yields on the evaluator's grid, a correction procedure is suggested in the ENDF-6 manual.

In practice the above constraint, which applies both to the matrix in the evaluator's as well as in the user's group structure, may be difficult to meet rigorously in some cases due to limitations of the ENDF-6 format concerning the number representation, and due to the use of single precision in the computation.

Among the recent evaluations only the JENDL-3.3 library includes complete covariance matrices for the most frequent fissile materials, such as ^{233}U , ^{235}U , ^{238}U , ^{239}Pu and ^{240}Pu [1]. The ENDF/B-VII evaluation [2] includes the covariances of ^{252}Cf . On the other hand, the two evaluations were found not to follow the same format standards. The first evaluations include the data in the form of probability per energy bin and the second as integrated probability in the bin. This ambiguity contained in the ENDF-6 format specifications was pointed out by Trkov [11], suggesting that the term "probability density distribution" (Section 35.2) is not consistent with the constraint that the sum of rows and columns of the matrix must be zero (Section 35.3), implying the use of "probability distributions". Clarification was requested at the CSEWG Meeting, indicating further that the code ERRORJ [3] can at present process the format of JENDL-3.3 data, but not that of the ^{252}Cf evaluation in ENDF/B-VII.

It is therefore of relevance to consider the advantages and inconveniences of the two representations in view of the File 35 constraint. Intuitively, the second option seems preferable for two reasons:

1. In the case of storing the probability density distributions (per energy bin, as in JENDL-3.3), the number of available digits is often additionally reduced, since the division of the probability distributions in the energy bins by the bin width in most cases results in small values requiring two exponential digits.

2. If stored in absolute terms (ENDF/B-VII) the probability distributions can be summed up directly and the File 35 zero-constraint can be fulfilled exactly [11]. For the data stored as probabilities per energy bin, the division with the energy bin width involves rounding errors and consequently a possible loss of numerical accuracy.

Additional ambiguity is in the application of the above zero-sum rule. At present it is interpreted as:

$$\sum_i \langle \delta\chi_i \cdot \delta\chi_j \rangle < 10^{-5} \quad \text{Eq. (2)}$$

This condition should be satisfied for each group j . In practice, a more restrictive definition would be appropriate:

$$\frac{1}{\chi_j} \sum_i \langle \delta\chi_i \cdot \delta\chi_j \rangle < 10^{-5} \quad \text{Eq. (3)}$$

Note that in case of storing the probability density distributions, χ_i^{jendl33} , these must be scaled by the energy width to obtain the total number of fission neutrons in a group i : $\chi_i = \chi_i^{\text{jendl33}} \Delta E_i$.

Processing of the fission spectra covariance data into the user's group structure is expected to have some impact on matrix normalisation due to the weighting and the numerical precision involved in the processing. An analysis made by Go Chiba indicates that using Eq. (2) the constraint condition of 10^{-5} for chi-covariance row-sum value is not sufficient for the target precision of k_{eff} error evaluation, if the un-normalised sensitivity coefficients are used. In this case, the limit of less than 10^{-8} is needed, which requires the use of the double precision calculation, not only in the ERRORJ code, but throughout the entire uncertainty evaluation procedure.

Recommendations include further study of the general validity of the above conclusions and the extension of investigations to other computational examples.

4. Equations to calculate the sensitivity of k_{eff} with respect to the fission spectrum

The relative sensitivity coefficients, S , of the effective multiplication factor k_{eff} represent a fractional change of a response (k_{eff}) with respect to the fractional change of the underlying nuclear data parameters (fission spectra in this case).

Using the generalised perturbation method based on the direct and adjoint flux approach the sensitivity coefficients are calculated from Eq. (4) in Section 2.1.1 of the main text, which, restraining the variation to the fission spectra only takes the following form:

$$S = \frac{\left\langle \Phi^*, \frac{1}{k} \frac{\partial F}{\partial \sigma} \Phi \right\rangle}{\left\langle \Phi^*, F\Phi \right\rangle} \quad \text{Eq. (4)}$$

where \langle, \rangle denotes the integration over space, angle and energy, and as before, the direct and adjoint fluxes Φ, Φ^* are the solutions of the homogeneous Boltzmann transport equation in the direct and adjoint mode, respectively:

$$\begin{aligned} M\Phi &= \left(A - \frac{1}{k} F \right) \Phi = 0 \\ M^* \Phi^* &= \left(A^* - \frac{1}{k} F^* \right) \Phi^* = 0 \end{aligned}$$

In the multi-group approximation the term $F\Phi_g$ is expressed as:

$$F\Phi_g(\vec{r}) = \sum_k \chi_g^k \sum_{g'} \bar{v}_g^k N^k(\vec{r}) \sigma_{g'}^{f,k} \Phi_{g'}(\vec{r}) \quad \text{Eq. (5)}$$

where χ_g^k is the fission spectrum for material k in group g (total number of neutrons in group g), $\sigma_{g'}^{f,k}$ is the fission cross-section for material k in group g , $N_i^k(\vec{r})$ is the material number density for material k at position r and $\Phi_g(\vec{r}), \Phi_g^*(\vec{r})$ is the direct/adjoint flux in the energy group g at position r .

And finally we obtain for the sensitivity coefficients:

$$S_i^j = \frac{1}{R} \cdot \chi_i^j \int_v d\vec{r} \sum_{g,k} N^k(\vec{r}) \Phi_g^*(\vec{r}) \frac{\partial \chi_g^k}{\partial \chi_i^j} \sum_{g'} \bar{v}_g^k \sigma_{g'}^{f,k} \Phi_{g'}(\vec{r}) \quad \text{Eq. (6)}$$

where v is the space volume of integration and:

$$R = \int_v d\vec{r} \sum_{g,k} N^k(\vec{r}) \Phi_g^*(\vec{r}) \chi_g^k \sum_{g'} \bar{v}_g^k \sigma_{g'}^{f,k} \Phi_{g'}(\vec{r})$$

4.1 Unconstrained sensitivity coefficients (codes *ERANOS* [7], *SUSD3D* [9])

Without applying the normalisation condition on the fission spectra variations, the derivatives can be expressed in terms of the Kronecker delta function:

$$\frac{d\chi_g^k}{d\chi_i^j} = \delta_{g,i} \cdot \delta_{k,j}$$

Inserting in the Eq. (6), the sensitivity coefficients are expressed by:

$$S_g^k = \frac{1}{R} \chi_g^k \int_v d\bar{r} N^k(\bar{r}) \Phi_g^*(\bar{r}) \sum_{g'} \bar{v}_g^k \cdot \sigma_{g'}^{f,k} \Phi_{g'}(\bar{r}) \quad \text{Eq. (7)}$$

Note that the sensitivity coefficients are in this case normalised to 1:

$$\sum_{g,k} S_g^k = 1$$

The corresponding uncertainties are calculated using Eq. (1).

From the evaluation it is evident that this method implicitly assumes that the normalisation was applied in the evaluation of the fission spectra covariance matrices. In order to obtain meaningful results it is essential that the input covariance were prepared according to the File 35 format constraints defined in the ENDF format manual, i.e. strictly respecting the zero-sum rule. If this is not the case in practice, the covariance matrix should be corrected to satisfy the zero-sum rule using the procedure proposed in the ENDF-6 Format Manual.

4.2 Constrained (normalised) sensitivity coefficients (*SAGEP* [8] code method)

The *SAGEP* code applies the normalisation condition to constrain the sensitivity coefficients. The corresponding derivations are demonstrated by Y. Nagaya [12]. Additional clarifications are presented in another report [13].

The correlations between fission spectra at different energy groups are taken into account explicitly (but not between different materials):

$$\frac{d\chi_g^k}{d\chi_i^j} = \frac{d\chi_g^k}{d\chi_i^j} \cdot \delta_{k,j}$$

The derivations are evaluated numerically using the finite difference approximation, with the perturbations $\Delta\chi_g^k$. In the evaluation of the sensitivity coefficients an additional term appears:

$$\begin{aligned}\tilde{S}_g^k &= -\frac{\chi_g^k \cdot \sum_{g''} S_{g''}^k}{1 + \Delta\chi_g^k} + \frac{\chi_g^k}{(1 + \Delta\chi_g^k)} \frac{\int dr \cdot N^k(r) \cdot \Phi_g^*(r) \cdot \sum_{g'} \bar{v}_{g'}^k \cdot \sigma_{g',k}^{f,k} \cdot \Phi_{g'}}{R} \\ &= \frac{S_g^k - \chi_g^k \cdot \sum_{g'} S_{g'}^k}{1 + \Delta\chi_g^k}\end{aligned}\quad \text{Eq. (8)}$$

where \tilde{S}_g^k and S_g^k represent respectively the constrained and the unconstrained sensitivity coefficients.

This equation is evaluated in the finite difference approximation, which in the limit $\Delta\chi_g^k \ll 1$ reduces to the following expression:

$$\tilde{S}_g^k = S_g^k - \chi_g^k \cdot \sum_{g'} S_{g'}^k \quad \text{Eq. (9)}$$

Further, the current version of SAGEP assumes a unique average fission spectrum for all fissile materials, namely: $\chi_g^k = \chi_g$ and $\Delta\chi_g^k = \Delta\chi_g$ for all k .

The variance in k_{eff} due to the fission spectra uncertainties is calculated from Eq. (8) which then takes the following form:

$$\tilde{\tilde{S}}^k M^k \tilde{\tilde{S}}^{t,k} = \frac{\bar{S}^k M^k \bar{S}^{t,k} - \sum_l S_l^k \sum_i \frac{S_i^k}{\chi_i^k} \sum_j v_{i,j}^k - \sum_l S_l^k \sum_j \frac{S_j^k}{\chi_j^k} \sum_i v_{i,j}^k + \left(\sum_l S_l^k \right)^2 \sum_i \sum_j v_{i,j}^k}{(1 + \Delta\chi_g^k)^2} \quad \text{Eq. (10)}$$

where $\tilde{\tilde{S}}$ is the normalised sensitivity vector with the elements defined by Eq. (8); as defined in Eq. (1), M^k and V^k are respectively the relative and absolute covariance matrices of the fission spectrum for the material k , with elements M_{ij} and V_{ij} .

Note that as above, the denominator term can be neglected in the limit of small perturbation of the fission spectrum.

If the absolute covariance matrix used satisfies the zero-sum constraint ($\sum_i V_{i,j}^k = 0$), it can immediately be seen from Eq. (10) that, although the constrained and unconstrained sensitivity coefficients are different, they both yield identical uncertainties for small perturbations of the fission spectra.

4.3 Consistency between the constrained sensitivity approach and the ENDF-102 formalism for the correction of fission spectrum covariance matrix

If the zero-sum constraint were not applied in the derivation of the File 35 matrix, the ENDF-6 Formats Manual [10] suggests correcting the matrix using the following relation:

$$\tilde{V}_{i,j} = V_{i,j} - \chi_i \sum_k V_{k,j} - \chi_j \sum_k V_{k,i} + \chi_i \chi_j \sum_{k,k'} V_{k,k'}, \quad \text{Eq. (11)}$$

Introducing this into Eq. (1) we obtain the following result for a given fissile material:

$$\begin{aligned} \bar{S} \tilde{M} \bar{S}^t &= \bar{S} M \bar{S}^t - \sum_j S_j \sum_i \frac{S_i}{\chi_i} \sum_k V_{i,k} - \sum_i S_i \sum_j \frac{S_j}{\chi_j} \sum_k V_{k,j} \\ &\quad + \sum_i S_i \sum_j S_j \sum_k \sum_{k'} V_{k,k'} \end{aligned} \quad \text{Eq. (12)}$$

which is identical to Eq. (10) in the case of small perturbations of the fission spectrum ($\Delta \chi_g^k \ll 1$).

In the limit of the finite difference approximation, and for the case of a single fissile material, the method used in SAGEP is therefore identical to the correction procedure proposed in the ENDF-6 Format Manual.

Additional details and demonstrations are presented in [14].

5. Conclusions

5.1 Conclusions concerning the sensitivity coefficients

Sensitivity coefficients of the response parameters with respect to the fission spectrum can be calculated with or without considering the constraint on the

fission spectrum normalisation. As demonstrated mathematically in [13], the constrained sensitivity coefficient vector is a transformation of the unconstrained sensitivity coefficient vector under an oblique projection operator, whose transpose maps the fission spectrum variation onto itself.

From the present study the following conclusions are drawn concerning the methods used in the sensitivity calculations:

- 1) Although different in magnitude, the unconstrained and constrained sensitivity coefficients yield, within the limits of the finite difference approximation, the same variation of the response. They also result in the same uncertainty under the condition that the fission spectra covariance matrices used in the uncertainty evaluation rigorously comply with the zero-sum constraint as specified for File 35 in the ENDF-6 Format Manual.
- 2) If the File 35 rule were not respected strictly in the evaluation of the fission spectra covariance matrix the constrained sensitivity method corrects for the deviation of the matrix from the zero-sum rule. In the case of small perturbations of the fission spectrum this correction is identical to applying the procedure proposed in the ENDF-6 Format Manual for the correction of the File 35 covariance matrices deviating from the zero-sum constraint. Both sensitivity methods would therefore also result in the same uncertainties if the covariance matrix used with the unconstrained sensitivity method is corrected by the ENDF-6 Format Manual formula. For the unconstrained sensitivity method the ENDF-6 correction procedure is not needed, but if applied it would not alter the results.
- 3) The constrained sensitivity coefficients calculated with the SAGEP code introduce an error in response uncertainty because of the finite difference approximation of derivatives. However, the upper bound of this error is proportional to the fission spectrum perturbation and thus can be reduced to a sufficiently small value for practical purposes. This error can be eliminated by using the small perturbation limit, i.e. if the sensitivity coefficients are calculated from Eq. (9) instead of Eq. (8). Note also that the assumption of a unique average fission spectrum for all fissile materials is made in the present version of SAGEP, which is usually reasonable, particularly in cases of materials with similar fission spectra or one preponderant material.
- 4) The corrective action (either through the sensitivity coefficients or the matrix) is in general appropriate only for small deviations of the matrix from the File 35 rule. Larger deviation from zero-sum rule indicates an inconsistency in the evaluation process and the correction may not

be suitable. Verification whether the matrix complies with the File 35 constraint before its use in the sensitivity analysis is therefore strongly recommended, whatever sensitivity method is being used.

Consequently, the following step approach is recommended:

- 1) The absolute covariance matrices should be tested before and after the multi-group processing in order to verify if they comply with the File 35 rule as specified in the ENDF-6 Format Manual. In case of “too-high” deviations from the MF35 rule, the matrix should be discarded. (A reasonable limit defining how high is “too high” deviation should be set.)
- 2) In case of a small inconsistency of the matrix with the File 35 constraint, either the normalised sensitivity method or the procedure proposed in the ENDF-6 Format Manual can be used, the two methods being equivalent.

5.2 Conclusions concerning the covariance matrices

The numerical precision is an important issue in assuring the compliance of the matrix with the File 35 rule, in particular taking into account the limits in number presentations of the ENDF format.

Two different interpretations of the File 35 format are in use today, either storing the bin probabilities or bin probability densities. Intuitively we expect that using the first option the File 35 zero-sum constraint may be easier to assure from the numerical point. The following two arguments can be found in support of the above:

- *Rounding error*: the elements of the rows or columns can be summed up directly without requiring any division, which permits the sum to be identically zero. Storing the probabilities per energy bin involves the multiplication/division by the energy bin in the computation in order to satisfy the File 35 constraint, potentially leading to a loss of accuracy.
- *Storage precision loss*: at some relevant energies the division by the energy bin width results in very small numbers requiring two-digit exponents (e.g. in the MeV range the matrix components are divided by factor of $\sim 10^{12}$), and consequently often in a loss of one precision digit.

Recommendation: a study should be performed to select which of the two formats is more suitable with respect to fulfilling the File 35 rule constraint.

Additional ambiguity is in the application of the above zero-sum rule. At present it is interpreted as:

$$\sum_i \langle \delta\chi_i \cdot \delta\chi_j \rangle < 10^{-5}$$

This condition was found to be insufficient to assure accurate results, if the un-normalised sensitivity coefficients are used.

In practice, a more restrictive definition would be appropriate in view of the ENDF-6 correction procedure [see Eqs. (11) and (12)]:

$$\frac{1}{\chi_j} \sum_i \langle \delta\chi_i \cdot \delta\chi_j \rangle < 10^{-5} \quad \text{for all groups } j.$$

Processing of the fission spectra covariance data into the user's group structure may have some impact on matrix normalisation due to the weighting and the numerical precision.

We recommend further studies to determine the magnitude of these effects. Verification tools to check, and if required, "repair" the matrices are needed.

REFERENCES

- [1] Shibata, K., *et al.*, "JENDL-3.2 Covariance File", *Proc. Nuclear Data Covariance Workshop*, BNL, 22-23 April 1999, ORNL/TM-2000/19.
- [2] Obložinský, P., "New ENDF/B-VII Library", *Proceeding of PHYSOR 2006 Conference* (2006).
- [3] Maerker, R.E., J.J. Wagschal, B.L. Broadhead, *Development and Demonstration of an Advanced Methodology for LWR Dosimetry Applications. (Section 7)*, EPRI NP-2188 (December 1981), report available in "ZZ DOSCOV, 24-Group Covariance Data Library from ENDF/B-V for Dosimetry Calculation", DLC-0090 package of NEA Data Bank collection (<http://www.nea.fr/abs/html/dlc-0090.html>).

- [4] Chiba, G., *ERRORJ Manual*, JNC TN9520 2003-008, September 2003.
- [5] Aliberti, G., I. Kodeli, G. Palmiotti, M. Salvatores, “Fission Spectrum Related Uncertainties”, *NEMEA-4 Conference*, Prague, Czech Republic, 16-18 October 2007.
- [6] Aliberti, G., *Sensitivity Coefficients for the Multiplication Factor Related to Fission Spectrum Variations*, Exercise specifications, Argonne National Laboratory, 26 October 2007
- [7] Rimpault, G., *et al.*, “The ERANOS Code and Data System for Fast Reactor Neutronic Analyses”, *Proc. of PHYSOR 2002 Conference*, Seoul, South Korea (October 2002).
- [8] Hara, A., T. Takeda, Y. Kikuchi, *SAGEP: Two-dimensional Sensitivity Analysis Code Based on Generalized Perturbation Theory*, JAERI-M 84-027 (1984) [in Japanese].
- [9] Kodeli, I., “Multidimensional Deterministic Nuclear Data Sensitivity and Uncertainty Code System, Method and Application”, *Nucl. Sci. Eng.*, 138, 45-66 (2001).
- [10] Cross-Section Evaluation Working Group, *ENDF-6 Format Manual; Data Formats and Procedures for the Evaluated Nuclear Data File ENDF/B-VI and ENDF/B-VII*, Document ENDF-102, Report BNL-NCS-44945-05-Rev., M. Herman (Ed.), (June 2005)
- [11] Trkov, A., Ambiguity in Coding the Covariances of Emission Spectra in MF35 of ENDF-6 Files, request addressed at CSEWG Meeting (Oct. 2007) <http://www.nndc.bnl.gov/proceedings/2007csewgusndp/>.
- [12] Nagaya, Y., *On Uncertainty of Effective Multiplication Factor with Respect to Fission Spectrum*, Japan Atomic Energy Agency, 19 November 2007.
- [13] Yang, W.S., Comments on Response Parameter Uncertainty Due to Fission Spectrum Uncertainties, Argonne National Laboratory, 4 December 2007.
- [14] Kodeli, I., *On the Equivalence Between the SAGEP Sensitivity Method and the ENDF-102 Formalism for the “Correction” of Fission Spectra Covariance Matrix*, IAEA/NEA, 30 November 2007.

Appendix D

COMMENTS ON RESPONSE PARAMETER UNCERTAINTY DUE TO FISSION SPECTRUM UNCERTAINTIES

Won Sik Yang

1. Introduction

At the Subgroup 26 Meeting of WPEC held 15-16 October 2007 in Prague, it was noted that the uncertainties of effective multiplication factor due to fission spectrum uncertainties reported by Dr. Aliberti of ANL were significantly larger than the previous values of the Reactor Physics Analysis and Evaluation Group at JAEA. Dr. Ishikawa of JAEA suggested that this deviation might be caused by the different treatment of the normalisation condition of fission spectrum in calculating the sensitivity coefficients; the condition that the fission spectrum must remain normalised to unity was directly considered in JAEA calculations, but not in Aliberti's analysis. In a follow-up analysis [1], Dr. Nagaya of JAEA mathematically showed that Aliberti's method is equivalent to the JAEA method as far as the covariance matrix of fission spectrum satisfies the constraint that the sum of the elements in each row (therefore also in each column) is zero; both methods result in the same variation and uncertainty of multiplication factor, although the sensitivity coefficients are different.

The purpose of this appendix is to provide additional clarification on the use of the fission spectrum normalisation condition in the sensitivity coefficient calculation and fission spectrum covariance matrix generation.

2. Covariance matrix of fission spectrum

In the multi-group formulation of the neutron transport or diffusion equation, the fission spectrum of a fissionable isotope can be represented as a vector:

$$\bar{\chi} = (\chi_1, \chi_2, \dots, \chi_n)^T \quad \text{Eq. (1)}$$

where n is the number of energy groups and the superscript T denotes the matrix transpose. By definition, the fission spectrum vector must satisfy the normalisation condition:

$$\sum_{i=1}^n \chi_i = 1 \quad \text{Eq. (2)}$$

Thus $\bar{\chi}$ is a vector on a $(n-1)$ -dimensional plane of a n -dimensional real space \mathcal{R}^n , and the components of $\bar{\chi}$ can generally be represented as a function of $n-1$ independent variables as:

$$\chi_i = \chi_i(\bar{t}), \quad i = 1, 2, \dots, n \quad \text{Eq. (3)}$$

where:

$$\bar{t} = (t_1, t_2, \dots, t_{n-1})^T \quad \text{Eq. (4)}$$

The independent variable vector \bar{t} would be a function of the underlying parameters involved in the evaluation of the fission spectrum.

Denoting the reference mean value of $\bar{\chi}$ and the corresponding value of \bar{t} by $\bar{\chi}_0$ and \bar{t}_0 , respectively, the (absolute) variation of $\bar{\chi}$ from its mean value can be represented in the first order approximation as:

$$\delta\bar{\chi} = \bar{\chi} - \bar{\chi}_0 = \bar{J}^T (\bar{t} - \bar{t}_0) = \bar{J}^T \delta\bar{t} \quad \text{Eq. (5)}$$

where \bar{J} is the Jacobian matrix defined as:

$$\bar{J} = \left[\frac{\partial \chi_j}{\partial t_i} \right], \quad i = 1, 2, \dots, n-1; \quad j = 1, 2, \dots, n \quad \text{Eq. (6)}$$

with the derivatives evaluated at $\bar{t} = \bar{t}_0$. Here the subscripts i and j are the row and column indices, respectively. The normalisation condition in Eq. (2) requires that the sum of the elements in each row of \bar{J} should be zero as:

$$\sum_{j=1}^n \frac{\partial \chi_j}{\partial t_i} = 0, \quad i = 1, 2, \dots, n-1 \quad \text{Eq. (7)}$$

Using Eq. (5), the (absolute) covariance matrix of the fission spectrum can be determined as:

$$\bar{V}_\chi = \langle (\delta\bar{\chi})(\delta\bar{\chi})^T \rangle = \bar{J}^T \langle (\delta\bar{t})(\delta\bar{t})^T \rangle \bar{J} = \bar{J}^T \bar{V}_t \bar{J} \quad \text{Eq. (8)}$$

where the symbol $\langle . \rangle$ denotes the expectation value. Since t_i are independent, the covariance matrix of \bar{t} can be represented by a diagonal matrix as:

$$\bar{V}_t = \langle (\delta\bar{t})(\delta\bar{t})^T \rangle = \text{diag}(\tau_1^2, \tau_2^2, \dots, \tau_{n-1}^2) \quad \text{Eq. (9)}$$

As a result, the elements of the covariance matrix \bar{V}_χ of fission spectrum can be determined as:

$$\sigma_{ij} = (\bar{V}_\chi)_{ij} = \langle \delta\chi_i \delta\chi_j \rangle = \sum_{k=1}^{n-1} \tau_k^2 \frac{\partial \chi_i}{\partial t_k} \frac{\partial \chi_j}{\partial t_k} \quad \text{Eq. (10)}$$

This covariance matrix is symmetric. It also satisfies the column and row sum conditions specified for File 35 of the ENDF/B file [2] as:

$$\sum_{i=1}^n \sigma_{ij} = \sum_{k=1}^{n-1} \tau_k^2 \frac{\partial \chi_j}{\partial t_k} \left(\sum_{i=1}^n \frac{\partial \chi_i}{\partial t_k} \right) = 0 \quad \text{Eq. 11(a)}$$

$$\sum_{j=1}^n \sigma_{ij} = \sum_{k=1}^{n-1} \tau_k^2 \frac{\partial \chi_i}{\partial t_k} \left(\sum_{j=1}^n \frac{\partial \chi_j}{\partial t_k} \right) = 0 \quad \text{Eq. 11(b)}$$

The relative covariance matrix \bar{M}_χ of fission spectrum can easily be obtained by pre- and post-multiplying the (absolute) covariance matrix by a diagonal matrix of fission spectrum as:

$$\bar{M}_\chi = \left[\frac{\langle \delta\chi_i \delta\chi_j \rangle}{\chi_i \chi_j} \right] = \bar{X}^{-1} \bar{V}_\chi \bar{X}^{-1} \quad \text{Eq. (12)}$$

$$\bar{X} = \text{diag}(\chi_1, \chi_2, \dots, \chi_n) \quad \text{Eq. (13)}$$

3. Variation and uncertainty of response parameter

Suppressing the dependency on the other parameters for notational simplicity, a response functional (e.g. effective multiplication factor) can be represented as a function of the fission spectrum vector as:

$$R = R(\bar{\chi}) \quad \text{Eq. (14)}$$

Limiting the discussion on the variation of the fission spectrum, the variation of the response R from its reference value R_0 can be written in the first order approximation as:

$$\delta R = R(\bar{\chi}) - R(\bar{\chi}_0) = \nabla R(\bar{\chi}_0) \cdot (\bar{\chi} - \bar{\chi}_0) = \bar{s}_\chi^T \delta \bar{\chi} \quad \text{Eq. (15)}$$

where \bar{s}_χ is the absolute sensitivity coefficient vector defined by the gradient of R at $\bar{\chi}_0$ as:

$$\bar{s}_\chi = \nabla R(\bar{\chi}_0) = \left(\frac{\partial R}{\partial \chi_1}, \frac{\partial R}{\partial \chi_2}, \dots, \frac{\partial R}{\partial \chi_n} \right)^T \quad \text{Eq. (16)}$$

Eq. (15) can be rewritten for the relative variation of the response R as:

$$\frac{\delta R}{R} = \frac{1}{R} \left(\bar{s}_\chi^T \bar{X} \right) \left(\bar{X}^{-1} \delta \bar{\chi} \right) = \frac{1}{R} \left(\bar{X} \bar{s}_\chi \right)^T \left(\bar{X}^{-1} \delta \bar{\chi} \right) = \bar{\bar{s}}_\chi^T \delta \bar{\bar{\chi}} \quad \text{Eq. (17)}$$

where $\bar{\bar{s}}_\chi$ and $\delta \bar{\bar{\chi}}$ are respectively the relative sensitivity coefficient vector and the relative variation of fission spectrum defined by:

$$\bar{\bar{s}}_\chi = \frac{1}{R} \left(\bar{X} \bar{s}_\chi \right)^T = \left(\frac{\chi_1}{R} \frac{\partial R}{\partial \chi_1}, \frac{\chi_2}{R} \frac{\partial R}{\partial \chi_2}, \dots, \frac{\chi_n}{R} \frac{\partial R}{\partial \chi_n} \right)^T \quad \text{Eq. (18)}$$

$$\delta \bar{\bar{\chi}} = \bar{X}^{-1} \delta \bar{\chi} = \left(\frac{\delta \chi_1}{\chi_1}, \frac{\delta \chi_2}{\chi_2}, \dots, \frac{\delta \chi_n}{\chi_n} \right)^T \quad \text{Eq. (19)}$$

Using the sensitivity coefficient vector and the covariance matrix of fission spectrum, the uncertainty of the response R due to the fission spectrum uncertainties can be determined as:

$$\sigma_R^2 = \langle (\delta R)^2 \rangle = \bar{s}_\chi^T \langle (\delta \bar{\chi})(\delta \bar{\chi})^T \rangle \bar{s}_\chi = \bar{s}_\chi^T \bar{V}_\chi \bar{s}_\chi \quad \text{Eq. (20)}$$

$$\frac{\sigma_R^2}{R^2} = \left(\frac{1}{R} \bar{s}_\chi^T \bar{X} \right) (\bar{X}^{-1} \bar{V}_\chi \bar{X}^{-1}) \left(\frac{1}{R} \bar{X} \bar{s}_\chi \right) = \bar{s}_\chi^T \bar{M}_\chi \bar{s}_\chi \quad \text{Eq. (21)}$$

Note that the sensitivity coefficient vector in Eq. (16) or (18) is calculated by treating the components of the fission spectrum vector independently. That is, the normalisation condition of fission spectrum is not used in calculating the sensitivity coefficients. This condition is taken into account by imposing the column and row sum conditions in Eq. (11) to the covariance matrix of fission spectrum.

Using Eqs. (5) and (8), the variation and uncertainty of the response can be represented in terms of the variance of the independent variable vector \bar{t} as:

$$\delta R = \bar{s}_\chi^T \delta \bar{\chi} = \bar{s}_\chi^T \bar{J}^T \delta \bar{t} = (\bar{J} \bar{s}_\chi)^T \delta \bar{t} = \bar{s}_t^T \delta \bar{t} \quad \text{Eq. (22)}$$

$$\sigma_R^2 = \bar{s}_\chi^T \bar{V}_\chi \bar{s}_\chi = \bar{s}_\chi^T \bar{J}^T \bar{V}_t \bar{J} \bar{s}_\chi = (\bar{J} \bar{s}_\chi)^T \bar{V}_t (\bar{J} \bar{s}_\chi) = \bar{s}_t^T \bar{V}_t \bar{s}_t \quad \text{Eq. (23)}$$

It can be easily seen that the vector $\bar{s}_t = \bar{J} \bar{s}_\chi$ is the sensitivity coefficient vector of the response R with respect to \bar{t} as:

$$(\bar{J} \bar{s}_\chi)_i = \sum_{k=1}^n \frac{\partial R}{\partial \chi_k} \frac{\partial \chi_k}{\partial t_i} = \frac{\partial R}{\partial t_i}, \quad i = 1, 2, \dots, n-1 \quad \text{Eq. (24)}$$

Eqs. (15), (20), (22) and (23) show that the variation and uncertainty of the response are independent of the specific representation of fission spectrum vector as far as the sensitivity coefficients and the covariance matrix are determined consistently. However, when the sensitivity coefficients with respect to the fission spectrum vector are used, the covariance matrix should satisfy the column and row sum conditions specified for File 35 of the ENDF/B file.

4. JAEA method

In the JAEA method described in Ref. [1], the normalisation condition of fission spectrum is used in computing the sensitivity coefficients of response R with respect to the fission spectrum. The constrained sensitivity coefficients discussed in Section 2.3 of Ref. [1] are obtained by pre-multiplying the

unconstrained sensitivity coefficient vector \bar{s}_χ in Eq. (16) by the following matrix:

$$\bar{P} = \left[(\delta_{ij} - \chi_{0j}) \right], \quad i, j = 1, 2, \dots, n \quad \text{Eq. (25)}$$

where δ_{ij} is the Kronecker delta and χ_{0j} is the j -th component of $\bar{\chi}_0$. That is, the constrained sensitivity coefficient vector is determined as:

$$\tilde{s}_\chi = \bar{P} \bar{s}_\chi \quad \text{Eq. (26)}$$

Using this constrained sensitivity coefficient vector, the variation of the response R is determined as:

$$\delta R = \tilde{s}_\chi^T \delta \bar{\chi} \quad \text{Eq. (27)}$$

By defining a n -dimensional vector with all elements of unity, $\bar{u} = (1, 1, \dots, 1)^T$, the matrix \bar{P} and the normalisation condition in Eq. (2) can be rewritten as:

$$\bar{P} = \bar{I} - \bar{u} \bar{\chi}_0^T \quad \text{Eq. (28)}$$

$$\sum_{i=1}^n \chi_{0i} = \bar{u}^T \bar{\chi}_0 = \bar{\chi}_0^T \bar{u} = 1 \quad \text{Eq. (29)}$$

where \bar{I} is the $n \times n$ identity matrix. Since $\bar{\chi}_0$ is on the surface $X = \{\bar{x} \in \mathfrak{R}^n \mid \bar{u}^T \bar{x} = 1\}$, we have:

$$\bar{\chi}_0^T (\bar{P} \bar{x}) = \bar{\chi}_0^T (\bar{I} - \bar{u} \bar{\chi}_0^T) \bar{x} = \bar{\chi}_0^T \bar{x} - (\bar{\chi}_0^T \bar{u}) \bar{\chi}_0^T \bar{x} = \bar{\chi}_0^T \bar{x} - \bar{\chi}_0^T \bar{x} = 0 \quad \text{Eq. (30)}$$

$$(\bar{I} - \bar{P}) \bar{x} = \bar{u} \bar{\chi}_0^T \bar{x} = (\bar{\chi}_0^T \bar{x}) \bar{u} \quad \text{Eq. (31)}$$

Thus the range L and null space U of \bar{P} can be represented as:

$$L = \{\bar{x} \in \mathfrak{R}^n \mid \bar{\chi}_0^T \bar{x} = 0\} \quad \text{Eq. (32)}$$

$$U = \{\bar{x} \in \mathfrak{R}^n \mid \bar{x} = \alpha \bar{u}, \alpha \in \mathfrak{R}\} \quad \text{Eq. (33)}$$

It can also be shown that the matrix $\bar{\mathbf{P}}$ is idempotent, i.e.:

$$\bar{\mathbf{P}}^2 = (\bar{\mathbf{I}} - \bar{\mathbf{u}}\bar{\chi}_0^T)(\bar{\mathbf{I}} - \bar{\mathbf{u}}\bar{\chi}_0^T) = \bar{\mathbf{I}} - 2\bar{\mathbf{u}}\bar{\chi}_0^T + \bar{\mathbf{u}}(\bar{\chi}_0^T\bar{\mathbf{u}})\bar{\chi}_0^T = \bar{\mathbf{I}} - \bar{\mathbf{u}}\bar{\chi}_0^T = \bar{\mathbf{P}} \quad \text{Eq. (34)}$$

Accordingly, $\bar{\mathbf{P}}$ is an oblique projection operator that projects a vector $\bar{\mathbf{x}}$ onto the subspace L and parallel to the subspace U (i.e. orthogonal to the subspace $U^\perp = X - \bar{\chi}_0$).

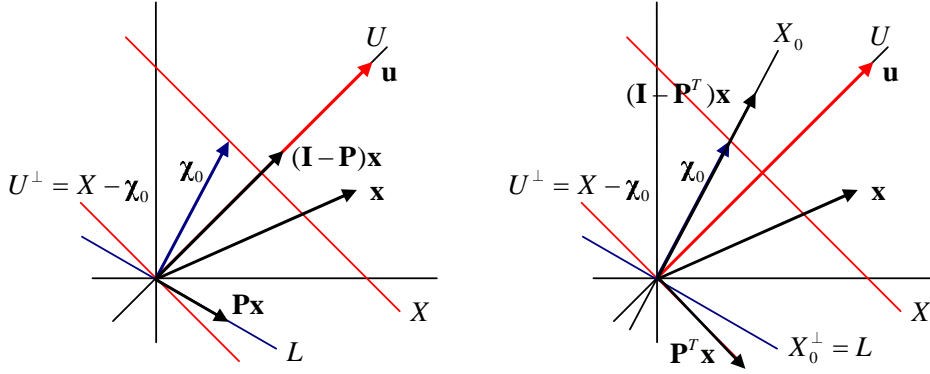
Similarly, $\bar{\mathbf{P}}^T$ is an oblique projection operator that projects a vector $\bar{\mathbf{x}}$ onto the subspace $U^\perp = X - \bar{\chi}_0$ and parallel to the subspace $X_0 = \{\bar{\mathbf{x}} \in \Re^n | \bar{\mathbf{x}} = \alpha\bar{\chi}_0, \alpha \in \Re\}$ (i.e. orthogonal to the subspace $X_0^\perp = L$) as:

$$\bar{\mathbf{u}}^T(\bar{\mathbf{P}}^T\bar{\mathbf{x}}) = \bar{\mathbf{u}}^T(\bar{\mathbf{I}} - \bar{\chi}_0\bar{\mathbf{u}}^T)\bar{\mathbf{x}} = \bar{\mathbf{u}}^T\bar{\mathbf{x}} - (\bar{\mathbf{u}}^T\bar{\chi}_0)\bar{\mathbf{u}}^T\bar{\mathbf{x}} = \bar{\mathbf{u}}^T\bar{\mathbf{x}} - \bar{\mathbf{u}}^T\bar{\mathbf{x}} = 0 \quad \text{Eq. (35)}$$

$$(\bar{\mathbf{I}} - \bar{\mathbf{P}}^T)\bar{\mathbf{x}} = \bar{\chi}_0\bar{\mathbf{u}}^T\bar{\mathbf{x}} = (\bar{\mathbf{u}}^T\bar{\mathbf{x}})\bar{\chi}_0 \quad \text{Eq. (36)}$$

The range and null space of $\bar{\mathbf{P}}$ and $\bar{\mathbf{P}}^T$ are illustrated in Figure 1.

Figure 1. Range and null space of projection operators $\bar{\mathbf{P}}$ and $\bar{\mathbf{P}}^T$



Since the range of $\bar{\mathbf{P}}^T$ is $U^\perp = X - \bar{\chi}_0$, $\bar{\mathbf{P}}^T$ projects the variation $\delta\bar{\chi} \in X - \bar{\chi}_0$ onto itself. This can be shown explicitly as:

$$\begin{aligned} \bar{\mathbf{P}}^T\delta\bar{\chi} &= (\bar{\mathbf{I}} - \bar{\chi}_0\bar{\mathbf{u}}^T)(\bar{\chi} - \bar{\chi}_0) = \bar{\chi} - \bar{\chi}_0 - \bar{\chi}_0(\bar{\mathbf{u}}^T\bar{\chi}) + \bar{\chi}_0(\bar{\mathbf{u}}^T\bar{\chi}_0) \\ &= \bar{\chi} - \bar{\chi}_0 = \delta\bar{\chi} \end{aligned} \quad \text{Eq. (37)}$$

As a result, the variation of the response R computed with the constrained sensitivity coefficient vector in Eq. (27) is equal to that obtained with the unconstrained sensitivity coefficient vector in Eq. (15) since:

$$\delta R = \tilde{s}_\chi^T \delta \bar{\chi} = (\bar{P} \bar{s}_\chi)^T \delta \bar{\chi} = \bar{s}_\chi^T \bar{P}^T \delta \bar{\chi} = \bar{s}_\chi^T \delta \bar{\chi} \quad \text{Eq. (38)}$$

It is noted that the projection operator \bar{P} employed in calculating the constrained sensitivity coefficients does not affect the variation $\delta \bar{\chi}$ and thus the covariance matrix should still satisfy the column and row sum conditions specified for File 35 of the ENDF/B file.

According to the formulae in Section 2.4 of Ref. [1], the SAGEP code [3] calculates the constrained sensitivity coefficients by pre-multiplying the unconstrained sensitivity coefficient vector \bar{s}_χ in Eq. (16) by the following matrix:

$$\bar{Q} = \bar{D} \bar{P} \quad \text{Eq. (39)}$$

where \bar{P} is the projection matrix defined in Eq. (25) and \bar{D} is a diagonal matrix defined as:

$$\bar{D} = \text{diag} \left(\frac{1}{1 + a_1 \chi_1}, \frac{1}{1 + a_2 \chi_2}, \dots, \frac{1}{1 + a_n \chi_n} \right) \quad \text{Eq. (40)}$$

with the fractional change a_i of χ_i . That is, the constrained sensitivity coefficient vector is determined as:

$$\tilde{s}_\chi = \bar{Q} \bar{s}_\chi = \bar{D} \bar{P} \bar{s}_\chi \quad \text{Eq. (41)}$$

With this constrained sensitivity coefficient vector, the variation of the response R is determined as:

$$\delta R = \tilde{s}_\chi^T \delta \bar{\chi} = \bar{s}_\chi^T \bar{P}^T \bar{D} \delta \bar{\chi} \quad \text{Eq. 42}$$

The only difference from Eq. (27) is that the variation $\delta \bar{\chi}$ is contracted by the diagonal matrix \bar{D} .

The matrix \bar{Q} is not a projection operator because of the diagonal matrix \bar{D} which arises from the finite difference approximation of derivatives. For small values of a_i , however, it becomes a good approximation to the projection matrix \bar{P} ; if $a_i \chi_i \ll 1$, $\bar{D} \approx \bar{I}$ and thus $\bar{Q} \approx \bar{P}$. In addition, since the variation $\delta\bar{\chi}$ is contracted by the diagonal matrix \bar{D} , the component sum of the resulting variation $\bar{D}\delta\bar{\chi}$ is not necessarily zero unless a_i are selected such that $a_i \chi_i$ be the same for all groups. As a simple example, suppose that a_i are selected such that $a_i \chi_i = 0.01$ for $i = 1, 2, \dots, n$. Then, the response variation δR computed with Eq. (42) is reduced by a factor of 1.01 relative to that computed with Eq. (27), although the constrained sensitivity coefficients are used for both cases.

5. Corrected covariance matrix of fission spectrum

As discussed in Ref. [4], the ENDF-6 Formats Manual [2] suggests that if the zero-sum constraint has not been applied in the derivation of the covariance matrix for normalised fission spectrum, the following correction to the covariance matrix is to be made:

$$\tilde{\sigma}_{ij} = \sigma_{ij} - \chi_i \sum_k \sigma_{kj} - \chi_j \sum_k \sigma_{ki} + \chi_i \chi_j \sum_{k,k'} \sigma_{kk'}, \quad \text{Eq. (43)}$$

It can be easily seen that the corrected covariance matrix is symmetric and satisfies the zero-sum constraint.

The suggested correction of covariance matrix is equivalent to transforming the original covariance matrix \bar{V}_χ as:

$$\tilde{V}_\chi = \bar{P}^T \bar{V}_\chi \bar{P} \quad \text{Eq. (44)}$$

where \bar{P} is projection matrix defined in Eq. (28). Using this corrected covariance matrix and unconstrained sensitivity coefficient vector \bar{s}_χ in Eq. (16), the uncertainty of the response R can be determined as:

$$\sigma_R^2 = \bar{s}_\chi^T \tilde{V}_\chi \bar{s}_\chi = \bar{s}_\chi^T \bar{P}^T \bar{V}_\chi \bar{P} \bar{s}_\chi = (\bar{P} \bar{s}_\chi)^T \bar{V}_\chi (\bar{P} \bar{s}_\chi) = \tilde{s}_\chi^T \bar{V}_\chi \tilde{s}_\chi \quad \text{Eq. (45)}$$

where \tilde{s}_χ is the constrained sensitivity coefficient vector defined in Eq. (26). Accordingly, as discussed in Ref. [4], the imposition of the fission spectrum

normalisation condition on the sensitivity coefficient calculation is equivalent to correcting the covariance matrix of fission spectrum as proposed in Ref. [2]. Thus, if the covariance matrix does not satisfy the zero-sum constraint, it is desirable to use the constrained sensitivity coefficients.

When the zero-sum constraint has already been applied to the covariance matrix, the transformation in Eq. (44) yields the same covariance matrix as:

$$\bar{\mathbf{P}}^T \tilde{\mathbf{V}}_\chi \bar{\mathbf{P}} = (\bar{\mathbf{P}}^T)^2 \bar{\mathbf{V}}_\chi \bar{\mathbf{P}}^2 = \bar{\mathbf{P}}^T \bar{\mathbf{V}}_\chi \bar{\mathbf{P}} = \tilde{\mathbf{V}}_\chi \quad \text{Eq. (46)}$$

since $\bar{\mathbf{P}}$ and $\bar{\mathbf{P}}^T$ are projection operators. In this case, both the unconstrained and constrained sensitivity coefficients result in the same uncertainty as:

$$\sigma_R^2 = \tilde{\mathbf{s}}_\chi^T \tilde{\mathbf{V}}_\chi \tilde{\mathbf{s}}_\chi = \bar{\mathbf{s}}_\chi^T (\bar{\mathbf{P}}^T)^2 \bar{\mathbf{V}}_\chi \bar{\mathbf{P}}^2 \bar{\mathbf{s}}_\chi = \bar{\mathbf{s}}_\chi^T \bar{\mathbf{P}}^T \bar{\mathbf{V}}_\chi \bar{\mathbf{P}} \bar{\mathbf{s}}_\chi = \bar{\mathbf{s}}_\chi^T \tilde{\mathbf{V}}_\chi \bar{\mathbf{s}}_\chi \quad \text{Eq. (47)}$$

In other words, the duplicated use of the fission spectrum normalisation condition in sensitivity calculation and covariance matrix generation does not cause any problem. However, the use of the constrained sensitivity coefficient vector $\tilde{\mathbf{s}}_\chi$ in Eq. (41) calculated with the SAGEP code introduces an error in response uncertainty because of the finite difference approximation of derivatives as:

$$\begin{aligned} \tilde{\mathbf{s}}_\chi^T \tilde{\mathbf{V}}_\chi \tilde{\mathbf{s}}_\chi &= \bar{\mathbf{s}}_\chi^T \bar{\mathbf{P}}^T \bar{\mathbf{D}} \tilde{\mathbf{V}}_\chi \bar{\mathbf{D}} \bar{\mathbf{P}} \bar{\mathbf{s}}_\chi \approx \bar{\mathbf{s}}_\chi^T \bar{\mathbf{P}}^T (\bar{\mathbf{I}} - \bar{\Delta}) \tilde{\mathbf{V}}_\chi (\bar{\mathbf{I}} - \bar{\Delta}) \bar{\mathbf{P}} \bar{\mathbf{s}}_\chi \\ &\approx \bar{\mathbf{s}}_\chi^T \tilde{\mathbf{V}}_\chi \bar{\mathbf{s}}_\chi - \bar{\mathbf{s}}_\chi^T \bar{\mathbf{P}}^T (\bar{\Delta} \tilde{\mathbf{V}}_\chi + \tilde{\mathbf{V}}_\chi \bar{\Delta}) \bar{\mathbf{P}} \bar{\mathbf{s}}_\chi = \sigma_R^2 - \tilde{\mathbf{s}}_\chi^T (\bar{\Delta} \tilde{\mathbf{V}}_\chi + \tilde{\mathbf{V}}_\chi \bar{\Delta}) \tilde{\mathbf{s}}_\chi \end{aligned} \quad \text{Eq. (48)}$$

where $\bar{\Delta}$ is a diagonal matrix defined as:

$$\bar{\Delta} = \text{diag}(a_1 \chi_1, a_2 \chi_2, \dots, a_n \chi_n) \quad \text{Eq. (49)}$$

The error in response uncertainty due to the finite difference approximation is bounded as:

$$\left\| \tilde{\mathbf{s}}_\chi^T (\bar{\Delta} \tilde{\mathbf{V}}_\chi + \tilde{\mathbf{V}}_\chi \bar{\Delta}) \tilde{\mathbf{s}}_\chi \right\| \leq 2 \left\| \tilde{\mathbf{s}}_\chi^T \tilde{\mathbf{V}}_\chi \bar{\Delta} \tilde{\mathbf{s}}_\chi \right\| \leq 2 \left\| \bar{\Delta} \right\| \cdot \left\| \tilde{\mathbf{s}}_\chi \right\|^2 \cdot \left\| \tilde{\mathbf{V}}_\chi \right\| \quad \text{Eq. (50)}$$

For practical purposes, this error can be made sufficiently small by reducing the fission spectrum perturbation used in calculating the sensitivity coefficients.

6. Concluding remarks

The sensitivity coefficients of a response parameter with respect to the fission spectrum can be computed with and without the constraint on the fission spectrum normalisation. The constrained sensitivity coefficient vector is a transformation of the unconstrained sensitivity coefficient vector under an oblique projection operator, whose transpose maps the fission spectrum variation onto itself. Both unconstrained and constrained sensitivity coefficients yield the same variation of the response. They also results in the same response uncertainty, if the covariance matrix of fission spectrum used in estimating the response uncertainty should satisfy the constraint that the sum of the elements in each row (therefore also in each column) is zero, which is specified for File 35 of the ENDF/B file.

As concerns computing the response uncertainty, the transformation of sensitivity coefficients is equivalent to correcting the covariance matrix of fission spectrum to satisfy the zero-sum constraint as proposed in the ENDF-6 Formats Manual. Thus, if the covariance matrix does not satisfy the zero-sum constraint, it is desirable to use the constrained sensitivity coefficients. When the zero-sum constraint has already been applied to the covariance matrix, this transformation yields the same covariance matrix. As a result, the duplicated use of the fission spectrum normalisation condition in sensitivity calculation and covariance matrix generation does not cause any problem. The constrained sensitivity coefficients calculated with the SAGEP code introduce an error in response uncertainty because of the finite difference approximation of derivatives. However, the upper bound of this error is proportional to the fission spectrum perturbation and thus can be reduced to a sufficiently small value for practical use.

REFERENCES

- [1] Nagaya, Yasunobu, *On Uncertainty of Effective Multiplication Factor with Respect to Fission Spectrum*, Japan Atomic Energy Agency, 19 November 2007.
- [2] Cross-Section Evaluation Working Group, *ENDF-6 Format Manual; Data Formats and Procedures for the Evaluated Nuclear Data File ENDF/B-VI and ENDF/B-VII*, ENDF-102, National Nuclear Data Center, Brookhaven National Laboratory (2005).

- [3] Hara, A., T. Takeda, Y. Kikuchi, *SAGEP: Two-dimensional Sensitivity Analysis Code Based on Generalized Perturbation Theory*, JAERI-M 84-027 (1984) [in Japanese].
- [4] Kodeli, Ivo, *On the Equivalence between the SAGEP Sensitivity Method and the ENDF-102 Formalism for the “Correction” of Fission Spectra Covariance Matrix*, IAEA, 30 November 2007.

Appendix E
**NUCLEAR DATA FOR THE HANDLING, REPROCESSING
AND DISPOSAL OF SPENT NUCLEAR FUEL**

Dr. Robert W. Mills

Abstract

The nuclear industry utilises nuclear data in many ways in the handling, reprocessing and disposal of spent nuclear fuel. These range from dose rate calculations for irradiated fuel transport to inventory calculations for waste consignment. In all situations the important nuclear safety parameters are criticality, radiation shielding and heat production which depend on the spent fuel inventory. The calculation uncertainties are highly dependent on the nuclear data used in calculating the spent fuel inventory.

Currently used fuel and reactor systems have sufficient measurements of irradiated fuel to justify safety cases by comparison between experiment and calculation. However until such measurements are available for novel systems these must be studied based upon the accuracy to which important nuclides can be determined from the basic nuclear data. Both the individual nuclide concentrations calculated and their uncertainties must be considered with the subsequent effect on operational parameters and costs.

Future facilities will need to be designed for both the calculated quantities and, typically, twice the uncertainty on the important operational parameters to giving bounding safety cases. Any nuclear data which dominates the uncertainties need to be identified as well as any biases so that improvements can be made to the basic nuclear data. An initial study is described considering only thermal reactors and some conclusions made about how these could be extended for novel systems. It must be stressed that not only is it important to predict engineering parameters, but the uncertainties on these parameters as well.

As an example, the calculation of decay heat in the context of the current fuel reprocessing plants is discussed. The radiogenic heating is calculated using the atoms present, half-lives and energy released per decay for each

nuclide. There are thus two sources of error in the resultant decay heat: the error on the nuclide number densities and the uncertainties on the nuclear data. Nexia Solutions has developed a validation database over a number of years which can be used to indicate uncertainty in the calculation of radionuclide number density. These data are being contributed to the NEA Expert Group on Assay Data of Spent Nuclear Fuel. This database includes PWR, BWR and the UK's Advanced Gas-cooled and Magnox Reactor fuel measurements of important nuclides and some direct decay heat measurements of PWR fuel. It should be noted that decay heat after a few days of cooling is dominated by only a few nuclides (less than 20 contribute greater than 99%) many of which have been measured in spent fuels. At shorter times over 100 nuclides contribute significantly and thus an alternative method is demonstrated to calculate the uncertainty on the decay heat on the time scale of seconds to days. A series of current and possible fuel cycle scenarios are considered and using the decay heat results an analysis is attempted to determine which nuclear data contributes most to the uncertainty on the final result and where future measurements are required.

This paper considers the decay heat and radiation source terms from a perspective based upon recent validation results for JEFF-3.1.

1. Introduction

Currently the majority of commercial nuclear power production uses two industrially applied fuel cycles that are well quantified for safety and licensed within the nations concerned: the once-through and the U/UOX/MOX recycling options in thermal reactors. These require the handling, transport and storage of the spent nuclear fuel; and for reprocessing the chemical separation of uranium and plutonium, and storage of the arising wastes in suitable material matrices for disposal.

Fuels and wastes from prototype reactors and chemical processing plants, and possible future reactor systems (e.g. Gen-IV, ADS, advanced reprocessing and transmutation technologies) will have to be dealt with by those responsible (e.g. private utilities or governments) in current and future regulatory frameworks. These fuels may be considerably different from those currently handled; composed of different materials, be irradiated in different reactors, have different burn-up and cooling; and so will have different requirements for operations and safety. Higher decay heat requires either greater cooling for the fuel, or requires less fuel to be transported, stored or processed at one time in existing facilities leading to greater costs. Similarly, larger or significantly different radiation source

terms (gamma-ray and neutron) would lead to similar issues with required shielding, again increasing costs. In addition, these fuels and wastes may be outside of currently accepted parameters for existing facilities and require new facilities to be built to accept them.

This paper considers the decay heat and radiation source terms from a theoretical perspective based upon recent validation results for JEFF-3.1 [1]. Currently used fuel and reactor systems have sufficient measurements of irradiated fuel to justify safety cases, however until such measurements are available for new systems they must be studied based upon the accuracy to which important nuclides can be determined. Both the individual nuclide concentration calculated and its uncertainty must be considered and the subsequent effect on costs estimated. It should be noted that facilities will need to be designed for both the calculated quantity and, typically, twice the uncertainty on the important parameters. Any nuclear data which dominates the uncertainties need to be identified as must any biases so that improvements can be made.

2. Safety and operational parameters

2.1 Situations to be considered

After nuclear fuel is irradiated it is necessary to consider it in a range of situations through the fuel cycle. For direct disposal this would include:

- storage at the reactor site, 30 days to 50 years;
- transport to disposal or reprocessing sites, 3 to 50 years;
- subsequent storage in water, 3 to 100 years;
- dry storage, 50 to 300 years;
- complete or dismantled irradiated fuel assembly in geological repository, 100 years onwards.

If reprocessing is included it is also necessary to consider:

- fuel being mechanically and chemically processed;
- separated product and waste streams;
- separated products being stored, transported and processed prior to fabrication of fuel;
- waste products being encapsulated stored and subsequently placed in a geological repository.

2.2 Fuel cycles

Nuclear data is important in the design and operation of nuclear fuel cycles. While accurate nuclear data is clearly required, what is much more important is an accurate estimate of the systematic and random uncertainties of nuclear data and its effects on engineering parameters required to develop bounding cases for the design and safe operation of plants. Current reprocessing operations carried out, for example, in France or the UK use the PUREX fuel cycle. This fuel cycle is well understood and involves operations associated with the transport of irradiated nuclear fuel, chemical processing of dissolved fuel, storage or use of uranium and plutonium and the disposal of the various waste streams from the cycle. In general, each of these stages has design requirements or operational safety case requirements which require the use of nuclear data in their specification. For example, the transport of irradiated nuclear fuel requires a safety case which specifies the radiation shielding to be used and sets a limit on the heat capacity of the transport cask. It is clear that uncertainty in the raw nuclear data which contributes to the calculated limits of these safety cases needs to be determined. As an example of this, the specific case of determining the uncertainties in the heat produced by the irradiation of nuclear fuel in LWRs will be discussed in this appendix.

The PUREX-based thermal reactor fuel cycle can be regarded as a subset of some advanced cycles. For example, the “double strata” fuel cycle proposed by the Japanese and French [11] comprises thermal reactor systems using UOX with single recycle MOX fuel, plutonium burning fast reactors (FR) which recycle plutonium and multiple recycling accelerator-driven systems (ADS) which burn minor actinides, plutonium and uranium. The same arguments concerning the accuracy of nuclear data hold for these advanced systems as they do for the current PUREX-based thermal reactors systems. A representation of the “double strata” fuel concept is shown in Figure 1. The difficulty here is that much less validation data are available for fast neutron systems in FR or ADS than for thermal systems and consequently the determination of systematic and random uncertainties is much more difficult.

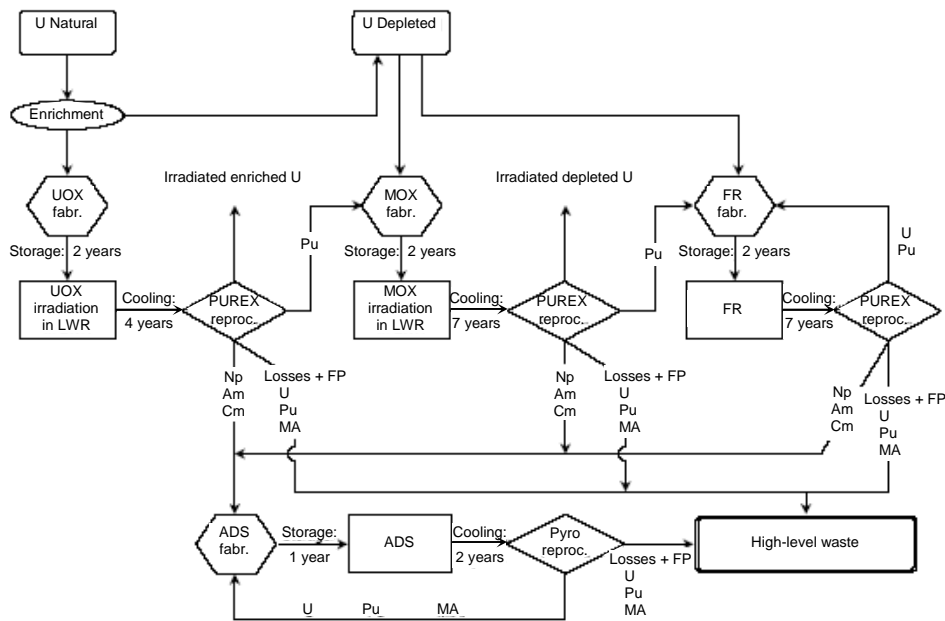
2.3 Calculated parameters

The properties of spent nuclear fuel are all dependent upon the composition of the fuel; the number densities of the nuclides present. Several important applied nuclear physics parameters for operation and safety calculations exist:

- decay heat for calculation of heat generation and material temperatures;
- radiation dose from gamma-rays and neutrons through shielding;
- neutron multiplication for criticality safety.

In addition, the spent fuel inventory affects many other considerations associated with process chemistry, engineering design and decommissioning such as process effluents, waste forms, leaching from repositories, etc., which are beyond the scope of this paper.

Figure 1. Diagram of a “double strata” fuel cycle



2.4 Important nuclides

Many hundreds of nuclides are formed in nuclear fuel during irradiation and it is thus necessary to concentrate on the much smaller number of nuclides that contribute to the heating, radiation dose and criticality so that an analysis can be made of the effects of uncertainties on the nuclide inventories. The analysis below considers only thermal reactors but could perhaps be applied to other systems.

2.4.1 Decay heat

Using FISPIN [2], decay heat following a single fission was calculated for ^{235}U , ^{239}Pu and ^{238}U from 0.1 second to 30 years using JEFF-3.1 fission yield and decay data only. These nuclides were chosen as they dominate the number of fissions in typical thermal reactor fuels. The decay heat contributions of each nuclide greater than 0.5% were then listed for each cooling time and an error analysis carried out. It was assumed that the half-life, fission yield and recoverable energy per decay for each nuclide were independent in this analysis. It was necessary to assume that the uncertainty on the nuclide number density was the same as that on the cumulative yield; the cumulative yield uncertainties in JEFF-3.1 being calculated from the measured uncertainty on the chain yield and the estimated uncertainties on the independent yields decaying to the nuclide. It would be beneficial to carry out inventory calculations using a full error analysis considering all of the correlations in the data. Tables 1, 2 and 3 show the results of this analysis for 90 days, 3 and 30 years. At these times fission product decay heat dominates spent fuel decay heat; at longer cooling times the actinide decay becomes more important and a full inventory calculation would be necessary.

For most nuclides the fission yield uncertainties dominate the uncertainty on the decay heat, except for ^{103}Ru , $^{129,129\text{m}}\text{Te}$, ^{144}Pr , ^{140}Ba , $^{103\text{m}}\text{Rh}$ and ^{144}Ce , where the energy release per decay contributes significantly to the uncertainties.

It can be seen from the results in the tables that a good approximation of decay heat can be determined using a small number of nuclides for practical fuel transport and storage calculations. When reprocessing fuel, it should be noted that dissolved fuel, and insoluble species sent for waste disposal, will contain a different spectra of nuclides and more nuclides may need to be explicitly tracked to accurately calculate decay heat.

2.4.2 Radiation dose

A ranking of nuclides important for spent LWR fuel shielding was published in 2000 [3]. Tables 4 and 5 show major contributors (>1% of total dose) for two specifications of spent LWR fuel assemblies and three cask types (27-cm steel, 12.7-cm lead and 50-cm concrete). It should be noted that ^{60}Co in the fuel assembly dominates at five years cooling and this is produced by activation of steel components. As the ^{59}Co content of steels is often not known, to determine this introduces a significant bias to such calculations.

Table 1. Percentage contribution of nuclides to the fission product decay heat for a set of target materials at 90 days

Nuclide*	²³⁵ U (thermal fission)	²³⁹ Pu (thermal fission)	²³⁸ U (fast fission)
¹⁰⁶ Rh	0.94 ± 0.03	16.74 ± 0.41	6.31 ± 0.28
⁹⁵ Nb	23.65 ± 0.26	17.41 ± 0.35	20.55 ± 0.35
⁹⁵ Zr	20.03 ± 0.23	14.75 ± 0.3	17.41 ± 0.3
¹⁰³ Ru	5.46 ± 0.16	14.09 ± 0.23	11.56 ± 0.23
^{129m} Te	<0.5	0.51 ± 0.21	<0.5
¹⁴⁴ Pr	11.93 ± 0.15	11 ± 0.12	11.08 ± 0.28
¹²⁹ Te	<0.5	0.65 ± 0.09	<0.5
¹⁴⁰ La	6.7 ± 0.1	7.47 ± 0.08	6.9 ± 0.1
⁹¹ Y	12.9 ± 0.12	5.01 ± 0.06	9.99 ± 0.33
¹⁴¹ Ce	3.88 ± 0.1	3.97 ± 0.06	4.28 ± 0.33
⁸⁹ Sr	9.61 ± 0.12	3.05 ± 0.06	6.77 ± 0.18
¹⁴⁰ Ba	1 ± 0.05	1.12 ± 0.06	1.03 ± 0.05
^{103m} Rh	<0.5	0.93 ± 0.06	0.76 ± 0.05
¹⁴⁴ Ce	1.07 ± 0.01	0.98 ± 0.01	0.99 ± 0.03
¹⁴³ Pr	0.85 ± 0.01	0.77 ± 0.01	0.73 ± 0.02
Total	98.02 ± 1.53	98.46 ± 2.18	98.35 ± 2.7

* Please note that nuclides in secular equilibrium are given separately (e.g. ¹³⁷Cs/^{137m}Ba, ¹⁰⁶Ru/¹⁰⁶Rh and ⁹⁰Sr/⁹⁰Y).

Table 2. Percentage contribution of nuclides to the fission product decay heat for a set of target materials at 3 years

Nuclide	²³⁵ U (thermal fission)	²³⁹ Pu (thermal fission)	²³⁸ U (fast fission)
¹⁰⁶ Rh	7.56 ± 0.21	61.68 ± 1.5	37.79 ± 1.67
¹⁴⁴ Pr	55.54 ± 0.68	23.55 ± 0.25	38.57 ± 0.99
¹²⁵ Sb	<0.5	1.08 ± 0.14	<0.5
^{137m} Ba	9.53 ± 0.14	5.54 ± 0.08	7.68 ± 0.21
⁹⁰ Y	14.02 ± 0.32	2.08 ± 0.06	6.2 ± 0.27
¹⁴⁴ Ce	4.96 ± 0.07	2.1 ± 0.03	3.45 ± 0.09
¹⁴⁷ Pm	2.03 ± 0.04	1.15 ± 0.02	1.98 ± 0.03
¹³⁷ Cs	2.88 ± 0.04	1.67 ± 0.02	2.32 ± 0.06
⁹⁰ Sr	2.61 ± 0.06	<0.5	1.15 ± 0.05
Total	99.1 ± 1.6	98.9 ± 2.2	99.2 ± 3.5

* Please note that nuclides in secular equilibrium are given separately (e.g. ¹³⁷Cs/^{137m}Ba, ¹⁰⁶Ru/¹⁰⁶Rh and ⁹⁰Sr/⁹⁰Y).

Table 3. Percentage contribution of nuclide to the fission product decay heat for a set of target materials at 30 years

Nuclide	²³⁵ U (thermal fission)	²³⁹ Pu (thermal fission)	²³⁸ U (fast fission)
⁹⁰ Y	47.4 ± 1.1	20.9 ± 0.6	34.9 ± 1.6
^{137m} Ba	33.2 ± 0.5	57.4 ± 0.9	44.6 ± 1.2
¹³⁷ Cs	10.0 ± 0.1	17.3 ± 0.2	13.5 ± 0.4
⁹⁰ Sr	8.8 ± 0.2	3.9 ± 0.1	6.5 ± 0.3
Total	99.5 ± 2.0	99.5 ± 1.8	99.5 ± 3.5

* Please note that nuclides in secular equilibrium are given separately (e.g. ¹³⁷Cs/^{137m}Ba, ¹⁰⁶Ru/¹⁰⁶Rh and ⁹⁰Sr/⁹⁰Y).

Table 4. Percentage contribution of nuclides to dose at 5 years cooling

Burn-up (GWd/t) Initial ²³⁵ U(wt.%)	Iron cask		Lead cask		Concrete cask	
	20	50	20	50	20	50
	3.0	4.5	3.0	4.5	3.0	4.5
⁶⁰ Co	49	33	56	40	50	39
¹⁴⁴ Pr	19	8	17	8	12	6
¹³⁴ Cs	11	15	10	16	14	23
¹⁰⁶ Rh	9	6	8	6	7	6
¹⁵⁴ Eu	4	7	4	8	5	10
^{137m} Ba	3	3	<1	<1	9	9
²⁴⁴ Cm	1	19	1	20	<1	4
⁹⁰ Y	1	<1	1	<1	1	1

Table 5. Percentage contribution of nuclides to dose at 10 000 years cooling

Burn-up (GWd/t) Initial ²³⁵ U(wt.%)	Iron cask		Lead cask		Concrete cask	
	20	50	20	50	20	50
	3.0	4.5	3.0	4.5	3.0	4.5
²⁴⁰ Pu	54	40	53	40	44	34
²⁴² Pu	25	47	25	46	21	41
²³⁹ Pu	15	7	16	8	12	5
²¹⁴ Bi	4	4	5	4	16	11

2.3.3 Criticality calculations

The selection of a range of important nuclides for criticality calculations is more difficult, however an OECD/NEA study [5] on burn-up credit was published that considered different sets of nuclides for criticality studies. They considered the contribution of major actinides and fission products to the calculation of k_{inf} for PWR fuel in an infinite lattice. The major actinides were $^{234,235,236,238}\text{U}$ and $^{239,240,241}\text{Pu}$, and the major fission products were ^{95}Mo , ^{99}Tc , ^{101}Ru , ^{103}Rh , ^{109}Ag , ^{133}Cs , $^{147,149,150,151,152}\text{Sm}$, $^{143,145}\text{Nd}$, ^{153}Eu and ^{155}Gd .

Table 6. Calculation of k_{inf} in a PWR infinite lattice considering different sets of nuclides

Nuclide sets	30 GWd/t 1 yr cooled
All actinides and fission products	1.1080
All actinides and no fission products	1.2456
Major actinides and no fission products	1.2635
All actinides and major fission products	1.1402

Although these results displayed here cannot indicate the individual importance of these nuclides for criticality calculations, they do show that this reduced set of 7 actinides and 15 fission products represent a significant part of the reactivity worth.

3. Results of JEFF-3.1 validation

Traditional validation exercises compare measured parameters (e.g. decay heat, gamma-dose, k_{eff}) against experiments and then set envelopes of operation so that problems cannot arise. An example of validating decay heat of PWR assemblies is given below. However to consider completely novel systems without expensive and time consuming experimentation it is necessary to consider the effects of the underlying uncertainties on nuclear data and spent fuel compositions. An example of validating spent fuel composition and its effect on the decay heat is shown below.

3.1 PWR assembly heat decay

For the transport, storage and geological disposal of spent fuel, it is important to have validation of the decay heat from complete assemblies.

Schmittroth reported measurements of the decay heat from irradiated PWR assemblies together with comparisons against ORIGEN2 [4]. This work considered 20 measurements with cooling times between 2.4 and 8.2 years for irradiations between 25 and 40 GWd/t; note that four measurements reported as suspect in this report were ignored. The assemblies came from the San Onofre, Point Beach and Turkey Point reactors. The stainless steel fuel from San Onofre gave a calculated over experiment decay heat ratio (C/E) of 1.06 when assuming 1 000 ppm of cobalt as in Ref. [4]. This type of stainless steel typically has between 120 and 1 200 ppm of cobalt; using these figures it is possible to calculate mean decay heat C/E values of 0.93 and 1.09 respectively. Unless the pre-irradiation cobalt content of the stainless steel can be discovered, it is thus not possible to draw any useful conclusions from the San Onofre results. Thus, only the Point Beach and Turkey Point data are considered in this work.

Decay heat calculations were carried out using the FISPIN code [2] and JEFF-3.1 based decay data and fission yield libraries. In this work, JEFF-3.1 cross-section libraries were generated using the reactor physics code WIMS9A and its associated cross-section processing code TRAIL1A [6]. The WIMS reactor physics models were based on design data reported in World Nuclear Industry Handbook, Ref. [7]. Minor uranium isotopes and fuel impurities were approximated by standard FISPIN methods. The structural materials for the assemblies were taken from Ref. [4]. It should be noted that, to accurately model the activation of the end-fittings, a full 3-D model would be necessary. In this work, a 2-D approximation of the assembly was modelled.

The experimental decay heats and the FISPIN results are compared in Table 7. These results show good agreement between experiment and calculations for the JEFF-3.1 data, with all results within 5%. The mean calculated over experiment decay heat ratio (C/E) for all assemblies was 1.00 ± 0.03 . It should be noted that the uncertainty on the heat measurements are given as $\pm 2\%$ and from the study above the calculated uncertainties on the decay heat are expected to be of a similar magnitude.

3.2 Irradiated fuel composition

As part of the “Actinide Research in a Nuclear Element” (ARIANE) programme, three UOX fuel samples were irradiated in the Goesgen PWR and then analysed at the Institute for Transuranium Elements Karlsruhe (ITU) and the Belgian Nuclear Research Centre (SCK•CEN) during the late 1990s [8,9]. The results from the two laboratories could be compared to ensure the reliability of the measurements. The samples are referred to as GU1 (analysed at SCK•CEN), GU3 and GU4 (ITU). The liquor solution derived from sample

Table 7. Comparison of PWR assembly decay heat measurements with calculations using the JEFF-3.1 library

Reactor	Initial ²³⁵ U (wt.%)	Burn-up (GWd/t)	Cooling (d)	Measured heat* (W)	JEFF-3.1 C/E
Point Beach	3.397	31.914	1 635	724	0.97
Point Beach	3.397	31.914	1 635	723	0.97
Point Beach	3.397	38.917	1 634	921	1.00
Point Beach	3.397	39.384	1 633	931	1.00
Point Beach	3.397	35.433	1 630	846	0.96
Point Beach	3.397	38.946	1 629	934	0.99
Point Beach	3.397	37.057	1 630	874	0.99
Turkey Point	2.556	28.430	962	1 423	1.04
Turkey Point	2.556	28.430	2 077	625	1.01
Turkey Point	2.556	26.485	963	1 284	1.05
Turkey Point	2.556	27.863	864	1 550	1.05
Turkey Point	2.559	25.595	1 782	637	0.98
Mean and standard			Point Beach		0.98 ± 0.02
Deviation of C/E values			Turkey Point		1.02 ± 0.03
All					1.00 ± 0.03

* The quoted experimental error is 2%.

GU3 was divided and analysed at both laboratories. These results are identified as GU3' (SCK•CEN) and GU3 (ITU). Enrichments were 3.5% and 4.1%, and sample irradiations ranged from 29 GWd/t and 60 GWd/t.

JEFF-3.1 WIMS, TRAIL and FISPIN cases were run to model the samples. The measured ¹⁴⁸Nd/fuel mass ratio was used to normalise the burn-up and thus the fuel ratings in the calculations. The ratios of the FISPIN predictions to the experimental results are presented in Table 8. The experimental values cannot yet be reported outside of the programme's participants and thus only over C/E values are reported. From the mean and scatter of C/E values for nuclides in the samples it is possible to estimate biases and uncertainties on the inventory and thus using the sensitivities above determine uncertainties on integral parameters. These biases can also be used to determine where nuclear data may be deficient.

From this single set of data it is clear that obtaining estimates of the accuracy of the prediction of individual nuclides will give rise to large uncertainties on nuclides important for shielding and criticality. For example, the ²⁴⁴Cm is 22% under predicted with a 14% uncertainty, thus from the sensitivities above, the calculated total dose from this fuel would be ~4.4% low with a ~2.8% uncertainty.

Table 8. Goesgen nuclide inventory C/E ratios using JEFF-3.1 data

Nuclide	Sample				JEFF-3.1 Mean ; SD
	GU1	GU3'	GU3	GU4	
⁹⁰ Sr	0.77	1.03	0.98	0.99	0.94 ; 0.12
⁹⁵ Mo	1.00	0.88	0.94	0.97	0.95 ; 0.05
⁹⁹ Tc	1.03	0.91	1.03	1.27	1.06 ; 0.15
¹⁰¹ Ru	1.06	0.87	0.95	0.97	0.96 ; 0.08
¹⁰⁶ Ru	1.08	0.87	0.47	0.85	0.82 ; 0.25
¹⁰³ Rh	1.14	1.16	1.19	0.96	1.11 ; 0.10
¹⁰⁹ Ag	2.18	1.09			1.64 ; 0.77
¹²⁵ Sb	1.90	1.98			1.94 ; 0.05
¹²⁹ I		0.99	0.97	0.90	0.96 ; 0.05
¹³³ Cs	1.02	1.04	0.95	0.99	1.00 ; 0.04
¹³⁴ Cs	1.05	1.03	0.84	1.01	0.98 ; 0.10
¹³⁵ Cs	1.05	1.07	1.01	1.14	1.07 ; 0.05
¹³⁷ Cs	0.97	0.99	0.95	1.06	0.99 ; 0.05
¹⁴⁴ Ce	1.06	1.07	1.06	1.08	1.07 ; 0.01
¹⁴² Nd	0.93	0.97	1.02	1.11	1.01 ; 0.08
¹⁴³ Nd	1.14	1.05	1.11	0.98	1.07 ; 0.07
¹⁴⁴ Nd	0.95	0.97	0.97	0.94	0.95 ; 0.02
¹⁴⁵ Nd	1.01	1.00	1.03	0.98	1.00 ; 0.02
¹⁴⁶ Nd	1.00	0.99	0.99	0.98	0.990 ; 0.008
¹⁴⁸ Nd	1.00	1.00	1.00	1.00	1.000 ; 0.000
¹⁵⁰ Nd	0.98	0.98	0.93	1.01	0.97 ; 0.03
¹⁴⁷ Pm	1.46	1.16	0.85	0.94	1.10 ; 0.27
¹⁴⁷ Sm	0.94	1.02	0.98	1.05	1.00 ; 0.05
¹⁴⁸ Sm	0.91	0.90	0.82	1.00	0.91 ; 0.07
¹⁴⁹ Sm	1.16	1.37	0.97	1.14	1.16 ; 0.16
¹⁵⁰ Sm	1.03	1.06	1.01	1.07	1.04 ; 0.03
¹⁵¹ Sm	1.34	1.30	1.25	1.26	1.29 ; 0.04
¹⁵² Sm	1.02	1.15	1.14	1.12	1.11 ; 0.06
¹⁵⁴ Sm	0.97	1.08	1.09	1.12	1.07 ; 0.07
¹⁵¹ Eu	0.57	0.76			0.67 ; 0.14
¹⁵³ Eu	1.13	1.11	1.03	1.10	1.09 ; 0.04
¹⁵⁴ Eu	2.27	1.80	1.57	1.60	1.81 ; 0.32
¹⁵⁵ Eu	1.05	0.99	0.86	0.96	0.96 ; 0.08
¹⁵⁵ Gd	1.12	1.23	1.00	0.68	1.01 ; 0.24
²³⁴ U	1.17	1.39	1.43	1.39	1.35 ; 0.12
²³⁵ U	1.41	1.14	1.26	1.06	1.21 ; 0.15
²³⁶ U	1.02	1.01	0.99	1.01	1.01 ; 0.01
²³⁸ U	1.00	1.00	1.00	0.99	0.996 ; 0.001

Table 8. Goesgen nuclide inventory C/E ratios using JEFF-3.1 data (cont.)

Nuclide	Sample				JEFF-3.1 Mean ; SD
	GU1	GU3'	GU3	GU4	
²³⁷ Np		0.90	0.84	0.74	0.82 ; 0.08
²³⁸ Pu	1.03	0.97	0.90	1.04	0.98 ; 0.06
²³⁹ Pu	1.18	1.04	1.04	1.07	1.08 ; 0.07
²⁴⁰ Pu	1.02	0.98	0.96	0.99	0.99 ; 0.03
²⁴¹ Pu	1.15	1.09	1.06	1.09	1.10 ; 0.03
²⁴² Pu	0.92	1.00	0.91	1.02	0.96 ; 0.06
²⁴⁴ Pu	0.69	0.55			0.62 ; 0.10
Pu	1.09	1.03	1.01	1.05	1.05 ; 0.04
²⁴¹ Am	1.23	1.28	1.25	1.06	1.20 ; 0.10
^{242m} Am	1.24	0.93			1.08 ; 0.22
²⁴³ Am	1.01	1.08	0.83	1.08	1.00 ; 0.12
²⁴² Cm	0.98	0.93			0.96 ; 0.03
²⁴³ Cm	3.13	1.18			2.16 ; 1.38
²⁴⁴ Cm	0.89	0.84	0.57	0.81	0.78 ; 0.14
²⁴⁵ Cm	1.05	0.87	0.57	0.87	0.84 ; 0.20
²⁴⁶ Cm	0.68	0.73			0.71 ; 0.03

4. The calculation of spent fuel inventories

All engineering quantities, such as decay heat and radiation emission, depend on the composition of the spent fuel. The general form of the differential equation governing the number density of a nuclide with time is given by:

$$\frac{dN_i}{dt} = -\lambda_i N_i + \sum_j \lambda_j N_j B_{j,i} + \sum_k N_k \sigma_{f,k} \Phi Y_{k,i} - \sum_l N_i \sigma_{i,l} \Phi + \sum_m N_m \sigma_{m,i} \Phi$$

The first two terms of this equation are those developed by Bateman [10] to describe a chain of radioactive decays. Here the first term is the decay of the nuclide i and the second term is the decay of direct precursor nuclides (given as the set of nuclides j) to i . N_x is the number density of a nuclide x , λ_x is the decay constant of x , $B_{x,y}$ is the branching fraction of decays of x that lead to y . The following three terms describe the general form of neutron reactions. The third term is the production of fission product nuclides i from the neutron-induced fission of nuclides, k , where $\sigma_{f,k}$ is the fission cross-section of nuclide k , Φ is the scalar neutron flux and $Y_{k,i}$ is the independent yield of nuclide i from the fission of nuclide k . The fourth term is the destruction of nuclide i by all possible

neutron reactions to a set of nuclides l , where $\sigma_{i,l}$ is the cross-section of i leading to l . The fifth term describes the product of nuclide i by neutron reactions on all nuclides that lead to i by one reaction step given as the set of nuclides m .

To carry out a full error analysis of such a calculation would require a complete set of covariances for the cross-sections and other parameters. As these are not available, an alternative is to estimate the accuracy of the FISPIN inventory through comparison with experimental measurements. Within Nexia Solutions a large database of measurements has been collected over the last 30 years for UK nuclear fuels (most Magnox and advanced gas-cooled reactors), and also including some BWR and PWR data. The database has comparisons with calculations using JEF-2.2-based libraries using the WIMS, TRAIL and FISPIN10 code route [6,2]. These data are being contributed to the NEA Expert Group on Assay Data of Spent Nuclear Fuel.

5. Calculation of decay heat using the C/E from assay predictions

An alternative method to calculate the biases and uncertainties on decay heat for more general cases is to use the nuclide concentration biases and uncertainties given in Table 8. In the following work, we consider a FISPIN calculation for a 4% UOX assembly irradiated in a PWR to 40 GWd/t and cooled in steps to 1×10^6 years. It was necessary to assume that shorter-lived daughters in equilibrium with parents had the same C/E values as their parents, that ^{239}U and ^{239}Np have a C/E the same as ^{239}Pu and that the $^{140}\text{Ba}/^{140}\text{La}$ had the same C/E as ^{137}Cs . Nuclides not in Table 8 were assumed to have no bias but 100% uncertainty. If no errors were quoted for nuclear data then a 50% value was assumed.

This technique leads to large uncertainties where the measured components make up little of the heat due to the 100% uncertainty assumed for the unmeasured component. However, after five years the decay heat is dominated by nuclides for which assay data exists, or where reasonable assumptions can be made. Here the uncertainties are around 5% which is only slightly larger than the comparison shown for the measured assemblies above. A large positive bias exists on decay heat between 100 and 50 000 years from the biases for ^{241}Am (+20%) and ^{239}Pu (+8%) and their daughters. At one million years the under prediction of ^{237}Np (-18%) and its daughters lead to a -9% under prediction of the heat.

If short decay times are considered, when fission products dominate decay heat and the large number of important unmeasured fission yields dominate the heat production, a similar approach to calculate decay heat by approximating

Table 9. Expected decay heat calculated from FISPIN and C/E of assay data

Cooling time (years unless stated)	FISPIN heat (kW/tUi)	Expected bias (%)	Expected uncertainty (%)	Fraction of heat from measured nuclides (%)	Expected heat (kW/tUi)	Expected heat uncertainty (kW/tUi)	Bounding heat (bias + 2*uncertainty)
Shutdown	2.45E+03	0.26	93.49	7.83	2.45E+03	2.29E+03	7.02E+03
3 days	1.58E+02	0.74	49.43	52.43	1.56E+02	7.73E+01	3.11E+02
5	2.18E+00	-0.31	4.76	99.35	2.19E+00	1.04E-01	2.40E+00
10	1.38E+00	0.50	4.79	99.31	1.37E+00	6.58E-02	1.51E+00
15	1.19E+00	0.27	4.74	99.42	1.18E+00	5.61E-02	1.30E+00
20	1.07E+00	0.23	4.58	99.54	1.07E+00	4.89E-02	1.16E+00
25	9.74E-01	0.35	4.43	99.63	9.71E-01	4.30E-02	1.06E+00
30	8.93E-01	0.62	4.31	99.71	8.87E-01	3.82E-02	9.64E-01
100	3.50E-01	7.32	4.79	100.00	3.27E-01	1.56E-02	3.58E-01
1 000	6.48E-02	12.35	5.82	100.00	5.77E-02	3.36E-03	6.44E-02
50 000	3.39E-03	7.05	6.31	99.56	3.17E-03	2.00E-04	3.57E-03
100 000	1.26E-03	5.07	5.06	98.78	1.20E-03	6.08E-05	1.32E-03
1 000 000	4.58E-04	-8.59	4.90	97.87	5.02E-04	2.46E-05	5.51E-04

the uncertainties of number densities as the uncertainties of cumulative fission product yields can be used. Then by combining the errors with those of half-lives and energy per decay it is possible to estimate the uncertainty of decay heat following a fission pulse. Table 10 shows the estimated percentage uncertainties on the decay heat.

It can be seen that the uncertainties after about 1 second are about 10%, these fall to under 5% after a few hours and continue in the region of 2-5% up to 30 years. However, this ignores any bias in the results. Comparisons with experiments [12] show that using JEFF-3.1.1 fission yields and decay data the total decay heat has a bias typical around 10% between 1 and 10 seconds and around 5% after this. A WPEC review of fission product decay data for decay heat assessments [13] suggested that this is due to incomplete decay schemes of several short-lived fission products. The review suggests that the historic available gamma-ray measurements on many of the short-lived fission products using small detectors missed high-energy gamma-rays and thus lead to incorrect decay schemes resulting in the incorrect estimation of total decay heat. Although this can be improved using modern large volume detectors or techniques such as total gamma-ray absorption spectrometry, the many contributing nuclides and limited number of measurers working in this area suggests that these biases will not be much further improved in the near future. It is thus probable that the decay heat of a PWR assembly would have an uncertainty around 5% very soon after reactor shutdown.

It can be concluded that decay heat from LWR spent fuel can be adequately determined using existing codes and data. Although nuclides can be identified where improvements may be possible, this will have little benefit to existing operations, although it may assist future technology development.

However, as no such measurements are published for spent fuels from fast reactors and ADS systems, this analysis cannot be repeated for these systems. Thus biases and uncertainties on their decay heat cannot be determined by this method.

The validation of nuclide concentrations shows many important nuclides poorly predicted but the quality of the measurements is difficult to determine. It thus appears that the best way to further this study would be to use an inventory calculation tool that includes a full error analysis, including errors on all input nuclear data and operational parameters and that considered all the correlations in the data and their errors. This would require comprehensive errors and covariances to be included for all parameters in nuclear data libraries.

Table 10. Percentage fission product heat uncertainties following a fission pulse assuming number density uncertainties are approximated by the cumulative yield uncertainties for fast neutron-induced fission of ^{232}Th and ^{238}U , and the thermal neutron-induced fission of ^{235}U and ^{239}Pu

Cooling time		^{232}Th F	^{235}U T	^{238}U F	^{239}Pu T
0.10	SECS	23.17%	18.60%	19.84%	23.99%
0.50	SECS	20.58%	17.09%	17.02%	22.84%
1.00	SECS	18.66%	15.78%	15.21%	21.64%
5.00	SECS	14.06%	11.82%	11.81%	17.30%
10.00	SECS	13.19%	9.84%	10.54%	14.92%
1.00	MINS	11.25%	6.18%	7.77%	9.53%
5.00	MINS	10.53%	6.54%	8.94%	9.43%
10.00	MINS	10.33%	6.28%	9.54%	8.75%
16.67	MINS	10.61%	5.86%	9.69%	7.94%
33.33	MINS	10.47%	5.04%	9.14%	6.83%
1.11	HOURS	9.12%	3.73%	7.90%	5.58%
1.39	HOURS	8.46%	3.30%	7.49%	5.20%
1.67	HOURS	7.92%	3.02%	7.20%	4.93%
1.94	HOURS	7.51%	2.84%	6.99%	4.73%
2.22	HOURS	7.20%	2.72%	6.82%	4.58%
2.50	HOURS	6.99%	2.65%	6.68%	4.45%
2.78	HOURS	6.84%	2.61%	6.54%	4.35%
5.56	HOURS	6.75%	2.56%	5.39%	3.76%
8.33	HOURS	7.05%	2.64%	4.85%	3.68%
11.11	HOURS	7.30%	2.70%	4.64%	3.71%
1.04	DAYS	7.59%	2.76%	4.13%	3.63%
4.63	DAYS	4.79%	2.16%	3.16%	2.53%
10.42	DAYS	4.68%	1.94%	2.74%	2.16%
23.15	DAYS	5.13%	1.94%	2.48%	2.09%
57.87	DAYS	6.66%	1.74%	2.65%	2.17%
115.70	DAYS	7.51%	1.44%	2.67%	2.14%
1.27	YEARS	6.94%	1.39%	3.17%	2.02%
3.17	YEARS	6.52%	1.65%	3.51%	2.20%
6.34	YEARS	5.37%	1.96%	3.63%	2.39%
15.84	YEARS	5.01%	1.97%	3.52%	1.94%
25.35	YEARS	4.96%	1.96%	3.48%	1.83%
31.69	YEARS	4.94%	1.95%	3.46%	1.81%

Acknowledgements

The author gratefully acknowledges support from the UK Nuclear Decommissioning Authority and the European Commission's EURATOM FP6 CANDIDE project. It should be noted that the opinions expressed in this document are those of the author and do not necessarily reflect those of these organisations or Nexia Solutions Ltd.

REFERENCES

- [1] *The JEFF-3.1 Nuclear Data Library*, JEFF Report 20, ISBN 92-64-02314-3 (2006).
- [2] FISPIN is developed by Nexia Solutions Ltd. with funding from the UK Nuclear Decommissioning Authority, and distributed by Serco Assurance. The code is described by R.F. Burstall in *FISPIN-A Computer Code for Nuclide Inventory Calculations*, ND-R-328I (1979).
- [3] Broadhead, B.L., I.C. Gauld, "Rankings of Nuclide Importance in Spent Fuel Shielding Applications", *Proc. of ANS2000 Radiation Protection and Shielding Division Topical Conference*, Spokane, Washington, USA, 17-20 September 2000.
- [4] Schmittroth, F., *ORIGEN2 Calculations of PWR Spent Fuel Decay Heat Compare with Calorimeter Data*, HEDL-TME 83-32 UC-85 (1984).
- [5] Brady, M.C., M. Takano, H. Okuno, A. Nouri, E. Sartori, M.D. DeHart, "Findings of an International Study on Burn-up Credit", *PHYSOR '96 in Proc. International Conf. on Physics of Reactors*, Vol. 4, Mito, Japan, 16-20 September 1996.
- [6] Details of WIMS and TRAIL can be obtained from Serco Assurance, contact details are available on their web site:
"www.sercoassurance.com/answers/".
- [7] *Nuclear Engineering International World Nuclear Industry Handbook 1987*, ISSN 0029-5507

- [8] Boulanger, D., M. Lippens, *ARIANE International Program, Final Report*, AR 2000/15, Belgonucléaire, December 2000.
- [9] Aoust, T., *ARIANE International Program, Irradiation Data Report Parts 1, 2 and 3*, AR 99/13, Belgonucléaire, July 1999.
- [10] Bateman, H., “The Solution of a System of Differential Equations Occurring in the Theory of Radioactive Transformations”, *Proc. Cambridge Phil. Soc.*, 15, p. 423 (1910).
- [11] *Accelerator-driven Systems (ADS) and Fast Reactors (FR) in Advanced Nuclear Fuel Cycles: A Comparative Study*, NEA report 3109, OECD Nuclear Energy Agency, Paris, ISBN 92-64-18482-1 (2002).
- [12] Mills, R.W., C. Shearer, *Testing of the JEFF-3.1.1 Radioactive Decay Data File for Consistency and Comparison with JEFF-3.1 Results*, JEF/DOC-1220 (2007).
- [13] *Assessment of Fission Product Decay Data for Decay Heat Calculations*, International Evaluation Co-operation, Volume 25, NEA report NEA/WPEC-25, OECD Nuclear Energy Agency, Paris, ISBN 978-92-64-99.

Appendix F

RESONANCE REGION IMPORTANCE FOR ADVANCED FUEL CYCLE APPLICATIONS

M. Dunn

1. Introduction

Although significant research has been performed to identify reactor nuclear data needs for fast reactor systems, the nuclear data needs (i.e. including accuracy requirements) for the rest of the fuel cycle (e.g. reprocessing, transportation, safeguards, etc.) have not been clearly defined. Although a detailed data needs study for the entire advanced fuel cycle (AFC) has not been performed, R&D recommendations can be made based on knowledge of existing measurement capabilities and the current state of nuclear data in the evaluated databases.

The AFC data needs will span energies from thermal to high energies. As part of the AFC plan, the fuel cycle will be closed thereby requiring that spent nuclear fuel (SNF) be reprocessed to produce new fuel for nuclear reactors. During reprocessing, two situations develop:

- Higher mass number isotopes of plutonium, americium and curium build-up.
- The transition from fluid to solid form in the fuel reprocessing involves systems, which establish intermediate- and thermal-energy neutron spectra.

The nuclear data for many of the actinides anticipated in the fuel reprocessing streams are not well known at intermediate energies that encompass the resonance region. Moreover, the safety basis for efficiently sized equipment, in terms of inventory and throughput, will require the demonstration of acceptable margins of subcriticality.

With regard to safeguards and material accountability, the novel process streams in SNF processing facilities and fuel fabrication plants may challenge the accuracy limits of existing detection techniques needed to monitor the proliferant material. As noted above, the safeguards and material accountability applications may drive the need for improved nuclear data for the following:

- (γ, f) , (γ, n) ;
- neutron multiplicity and associated energy distributions;
- delayed neutron fraction and associated energy distributions.

In addition to the reprocessing component of the advanced fuel cycle, additional operations will involve material handling and SNF transportation in approved shipping casks. The following are possible issues that should be investigated to assess differential data needs for advanced fuel cycle applications:

- improved fuel exposure prediction of spent fuel isotopes (actinides and fission products);
- improved prediction of spent fuel reactivity worth for criticality safety burn-up credit (BUC) that is needed for transportation in addition to efficient sizing of reprocessing equipment;
- improved prediction of neutron radiation source terms, required neutron shielding and subsequent neutron reflection in criticality evaluations;
- improved cross-section data for isotopes acting as chemical reagents (important for neutron moderation and absorption).

In the above list of AFC issues, BUC will be a significant issue that will be important for the transportation and handling of SNF. BUC consists of taking credit for the reactivity decrease associated with the presence of fission products in the SNF. Modelling SNF as fresh fuel is very conservative and limiting in terms of material throughput in transportation and handling operations. Efforts by the US Department of Energy (DOE), Electric Power Research Institute (EPRI), and the US Nuclear Regulatory Commission (NRC) have provided sufficient technical information to enable the NRC to issue regulatory guidance for implementation of pressurised water reactor (PWR) burn-up credit; however, consideration of only the reactivity change due to the major actinides is recommended in the guidance. If BUC can be implemented in the licensing process, the cost savings for shipping SNF could be several hundred million US dollars. The fission products that are the major contributors for BUC in SNF transportation applications are ^{103}Rh , ^{133}Cs , ^{143}Nd , ^{149}Sm , ^{151}Sm and ^{155}Gd , and a detailed data assessment [1] of these fission products has shown that improved resonance data with covariance information are needed to improve confidence

in reactivity predictions for BUC. In general, the anticipated AFC applications will have neutron spectra that span energies from thermal to high energies, and resonance region neutron cross-section data with covariance data will be needed to support advanced fuel cycle R&D.

2. Status of improved uranium and plutonium covariance data for SG26

SG26 identified the need for actinide cross-section covariance data to support the analyses of fast reactor systems. Moreover, full ENDF/B File 32 resonance parameter covariance matrices (RPCM) were produced by ORNL for ^{235}U , ^{238}U , and ^{239}Pu . The RPCMs were combined with high-energy cross-section covariance data (File 33) provided by LANL. To support the SG26 effort, ORNL processed the full energy-range covariance matrices into 15-group and 44-group covariance matrices for use in SG26 sensitivity/uncertainty (S/U) analyses. Although the RPCMs can be processed by standard cross-section processing software, the National Nuclear Data Center (NNDC) at BNL has expressed concern about the size of the RPCMs and the impact on distribution of the data files by NNDC. In particular, the memory required to store and process the complete or full covariance matrices can be several gigabytes for a single isotope. In contrast, other SG26 participants have noted the importance of preserving the File 32 RPCM data to support fuel cycle R&D analyses. The File 32 RPCM provides both short and long-range correlations between resonances, and it is not possible to specify covariance data for select resonances to reduce the size of the File 32 matrices. Therefore, a more rigorous approach is needed to reduce the size of the covariance matrices while preserving the important correlations.

ORNL has preserved the complete File 32 RPCM data for ^{235}U , ^{238}U and ^{239}Pu ; however, ORNL has performed work to address the concerns with the large File 32 matrices. In an effort to develop reduced (i.e. in memory storage requirements) covariance matrices that preserve the covariance information, ORNL has investigated three different options for preparing smaller matrices: 1) ENDF/B Compact Covariance Format (CCF); 2) eigenvalue/eigenvector method to preserve important covariance information in the reduced matrices; 3) produce ENDF/B File 33 cross-section covariance matrices (CSCM) from the File 32 RPCM. The methodology for producing File 33 CSCM from File 32 RPCM was presented by M.E. Dunn at the NEMEA-4 Workshop in Prague, Czech Republic, 26-18 October 2007 [2]. At this point, the File 33 CSCM approach appears to be the most promising to produce meaningful covariance matrices in a reduced memory format while preserving much of the resonance parameter covariance information. Additional work is needed to investigate and test the File 33 CSCM produced from the File 32 covariance matrices.

3. Resonance covariance improvement needs and recommendations

Based on the results in Ref. [2], different File 33 group structures have been investigated (i.e. 44 groups to 240 groups); however, producing groupwise covariance matrices from File 33 data that were generated from the File 32 RPCM does not always preserve the covariance information when compared with groupwise covariance matrices that are produced directly from File 32 data. The work in Ref. [2] demonstrates the feasibility of determining an optimum group structure to preserve the requisite resonance parameter covariance information. Currently, ORNL is investigating File 33 group structures that are on the order of the number of resonances and the corresponding level spacing. Once the optimum group structures are identified for ^{235}U , ^{238}U and ^{239}Pu , additional S/U testing will be needed by SG26 with the covariance data.

With regard to additional recommendations, SG26 has identified the following key materials for advanced reactor systems:

- 19 actinides (cross-section covariances, nubar covariances) in priority order:
 - $^{235,238}\text{U}$, ^{239}Pu ;
 - ^{237}Np , $^{240,241}\text{Pu}$, $^{241,242\text{m},243}\text{Am}$;
 - ^{232}Th , $^{233,234,236}\text{U}$, $^{238,242}\text{Pu}$, $^{242,243,244,245}\text{Cm}$.
- 34 structural, moderator and coolant materials (cross-section covariances) in priority order:
 - ^{16}O , ^{23}Na , ^{52}Cr , ^{58}Ni ;
 - ^1H , ^{12}C , ^{28}Si , $^{90,91,92,94}\text{Zr}$, $^{206,207,208}\text{Pb}$, ^{209}Bi ;
 - ^4He , $^{6,7}\text{Li}$, ^9Be , ^{10}B , ^{15}N , ^{19}F , ^{27}Al , $^{56,57}\text{Fe}$, $^{155,156,157,158,160}\text{Gd}$, $^{166,167,168,170}\text{Er}$.

As noted, significant progress has been made in providing covariance data for ^{235}U , ^{238}U and ^{239}Pu . In addition, improved resonance parameter covariance data have been produced for ^{233}U , ^{232}Th and the gadolinium isotopes. However, resonance region covariance data for the remaining resonance materials in the above list have not been addressed. Additional work will be needed to supply resonance region covariance data for the remaining actinides and structural materials identified by SG26. Covariance data for these key materials will greatly facilitate S/U analyses for advanced fuel cycle development.

REFERENCES

- [1] Leal, L.C., H. Derrien, M.E. Dunn, D.E. Mueller, *Assessment of Fission Product Cross-section Data for Burnup Credit Applications*, ORNL/TM-2005/65, Oak Ridge National Laboratory, December 2007.
- [2] Dunn, M.E., G. Arbanas, L.C. Leal, D. Wiarda, “Approximating Large Resonance Parameter Covariance Matrices with Group-wise Covariance Matrices for Advanced Nuclear Fuel Cycle Applications”, *4th Workshop on Neutron Measurements, Evaluations and Applications – Nuclear Data Needs for Generation IV and Accelerator Driven Systems (NEMEA-4)*, Prague, Czech Republic, 16-18 October 2007.

Appendix G

BNL METHODOLOGY FOR CROSS-SECTION COVARIANCES

M.W. Hermann, S.F. Mughabghab, P. Oblozinsky, D. Rochman

1. Basic components

The National Nuclear Data Center, BNL in collaboration with T-16, LANL is developing a methodology for evaluation of cross-section covariance data that covers the thermal energy, resolved and unresolved resonance regions as well as the fast neutron region. This approach is built on three major components:

- 1) Atlas of Neutron Resonances [1] contains recommended parameters of neutron resonances evaluated on the basis of virtually all pertinent experimental data available in 2005. The Atlas contains data for 486 ground and isomeric states of 476 isotopes along with their uncertainties. The most important quantities for the present project are:
 - thermal cross-sections (capture, elastic, fission), with uncertainties;
 - scattering radius, with uncertainties;
 - resonance integrals (capture, fission), calculated or measured, with uncertainties;
 - resonance parameters (radiative, neutron and fission widths), with uncertainties.
- 2) Nuclear reaction model code EMPIRE [2]. EMPIRE is a modular system of codes capable of producing model-based covariances. A suite of nuclear reaction models includes the spherical optical model, coupled channels, distorted wave born approximation, multi-step compound, multi-step direct, the exciton model with pre-equilibrium emission of clusters and gamma rays, and the full featured Hauser-Feshbach (HF) model with multi-particle emission and detailed-cascade.
- 3) Bayesian code KALMAN [3]. This code, based on the theory of the Kalman filter, allows estimating covariances by combining experimental uncertainties and correlations with theory predictions. KALMAN

calculates cross-section covariances P in two steps: (i) the model parameter covariance matrix X is calculated taking into account constraints imposed by the experimental covariances V , and (ii) the error propagation is used to calculate cross-section covariances P from the model parameter covariances X :

$$P = (X^{-1} + C^T V^{-1} C)^{-1} = X - X C^T (C X C^T + V)^{-1} C X$$

where C is the sensitivity matrix describing response of the model to the perturbation of its parameters.

2. Evaluation methods

The above three basic components are combined into two methods, Atlas-KALMAN for thermal and resonance region, and EMPIRE-KALMAN for the fast neutron region. The unresolved resonance region can, in principle, be treated by both methods. This overlap constitutes a link between the two approaches, which can be exploited for determining correlations between the resonance and fast neutron regions. The relatively simple considerations have been used to estimate covariances for the average number of fission neutrons (ν -bars).

2.1 *Atlas-KALMAN method*

One starts with the resonance parameters given in the Atlas. Cross-sections are calculated using the multi-level Breit-Wigner (or Reich-Moore) formalism and converted into a suitable multi-group representation. Uncertainties of resonance parameters and thermal-energy values from the Atlas are propagated with KALMAN to obtain uncertainties and correlations for cross-sections. Missing uncertainties of resonance parameters are estimated by extrapolating and/or interpolating available information on resonances in the same nucleus or in the neighbouring nuclei. When fitting the uncertainty for the thermal capture, the adequate uncertainties are assigned to the parameters of the negative-energy resonance.

2.2 *EMPIRE-KALMAN method*

This method employs a sensitivity matrix produced with the nuclear reaction theory code EMPIRE, and uses it in the Bayesian KALMAN code to propagate model parameter uncertainties onto cross-section covariances. To obtain the sensitivity matrix with EMPIRE, about 10-15 of the most relevant model

parameters (optical model, level densities, pre-equilibrium strength) are varied independently, typically by 3-5% around the optimal value, to determine their effect on total, elastic, inelastic, capture, fission, (n,2n), (n,p) and (n,f) cross-sections in the full energy range of the evaluation. Sensitivity matrix elements are calculated as a change of a given reaction cross-section in response to the change of the particular model parameter. Although the KALMAN filter can treat experimental data explicitly it was decided not to exploit this option in the current exercise. Instead, uncertainties of model parameters were adjusted to reproduce experimental cross-section uncertainties. Only the covariances that were taken over from the ENDF/B-VII.0 library were evaluated consistently by feeding experimental data to the KALMAN code.

2.3 Nu-bars

The covariances for the average number of neutrons per fission (total $\bar{\nu}$) were produced for 16 priority actinides:

- For $^{233,235,238}\text{U}$ and $^{239,240,241}\text{Pu}$ the data from the JENDL-3.3 library released in 2002 were adopted. These data were processed into the 15-energy group representation with the constant flux.
- For ^{237}Np , $^{238,242}\text{Pu}$, $^{241,242\text{m},243}\text{Am}$ and $^{242,243,244,245}\text{Cm}$, simple estimates were made. In doing so, it was ensured that the uncertainties embrace reasonably well the experimental data, while the correlations were assumed to be the same as those of the appropriately selected neighbouring nuclei. The applied procedure consists of three steps:
 - Taking into account the odd-even effects it was assumed that the uncertainties for the corresponding nuclei have the similar shape, while the correlations are identical:
 - $^{240}\text{Pu} \Leftrightarrow ^{237}\text{Np}$, $^{238,242}\text{Pu}$, $^{241,243}\text{Am}$ and $^{242,244}\text{Cm}$;
 - $^{241}\text{Pu} \Leftrightarrow ^{242\text{m}}\text{Am}$ and $^{243,245}\text{Cm}$.
- In the thermal region, the actual $\bar{\nu}$ uncertainties given in the Atlas of Neutron Resonances were adopted and the above uncertainties were renormalised for ^{237}Np and $^{241,242\text{m},243}\text{Am}$. For $^{238,242}\text{Pu}$ and $^{242,243,244,245}\text{Cm}$, simple averages of available evaluated data from libraries and the Atlas were calculated at thermal energy. Uncertainties correspond to the spread of the evaluated thermal values.
- Renormalised uncertainties were checked against the available data at higher energies and the $\bar{\nu}$ uncertainties were adjusted as necessary. The correlation matrices in the original ENDF-6 files were preserved.

3. Results and discussion

3.1 Thermal and resolved resonance region

In the case of thermal cross-section uncertainty, both the positive and negative energy resonances were considered. The missing uncertainties of the resonance parameters in the Atlas of Neutron Resonance were estimated to be 20% for radiative width and 50% for the neutron width. The uncertainties of the bound resonance parameters were adjusted to reproduce the calculated thermal cross-section uncertainty given in the Atlas.

In Table 1 we compare present results for the five selected thermal-energy capture cross-section uncertainties with the values given in the Atlas. Good agreement is found for ^{90}Zr and ^{167}Er while for the remaining isotopes thermal cross-section uncertainties could not be matched with the Atlas values due to the strong contribution to the uncertainty coming from the positive-energy resonances. In these cases, the uncertainties of the positive resonance parameters would have to be decreased to restore consistency with the uncertainties claimed for thermal cross-sections. We adopted a more conservative approach and about one-third of our thermal cross-sections uncertainties are higher than in Atlas.

Table 1. Thermal-energy capture cross-section uncertainties of the present work compared to the values of the Atlas of Neutron Resonances

Nuclide	Present work	Atlas 2006
^{23}Na	2.2%	1.0%
^{90}Zr	23%	21%
^{167}Er	1.3%	1.2%
^{208}Pb	27%	8.7%
^{242}Pu	7.1%	2.7%

In Table 2 we compare selected results for capture resonance integrals and their uncertainties with the values from the Atlas of Neutron Resonances. The resonance integrals are calculated from 0.5 eV up to the end of the resolved resonance region. In all cases, including those not shown in Table 2, our resonance integrals agree well with those in the Atlas. In most cases, however, our uncertainties are smaller by a factor of 2 or more. We note, however, that for many of the resonance integrals considered in this exercise Atlas provides experimental rather than calculated uncertainties. These measurements are independent from those used to derive resonance parameters and, in general, their uncertainties are not compatible. Therefore, our uncertainties obtained by propagating evaluated uncertainties of thermal cross-sections (generally pretty

Table 2. Capture resonance integrals and their uncertainties of the present work compared with the Atlas of Neutron Resonances

Nuclide	Present work		Atlas 2006	
²³ Na*	0.32b	2.0%	0.311b	3.2%
⁹⁰ Zr	0.17b	5.3%	0.17b	12%
¹⁶⁷ Er*	2971b	4.9%	2970b	2.0%
²⁰⁸ Pb	0.0012b	10%	0.0011b	18%
²⁴² Pu	1100b	3.6%	1115b	3.6%

* Denotes that Atlas Reports measured values rather than calculated

accurate) and of resonance parameters are often lower than the results of integral measurements reported in Atlas. In addition, we neglected certain sources of correlations (e.g. correlation between radiative and neutron widths for each resonance), which would tend to increase our calculated uncertainties of the resonance integrals.

3.2 Unresolved resonance region

Cross-section uncertainties in the unresolved resonance region can be calculated with both the EMPIRE-KALMAN and Atlas-KALMAN methods. Traditionally there is a sharp distinction between the fast neutron energy region and the resonance region as concerns evaluation methodology. Nevertheless, the unresolved resonance region can be estimated by two methods: either by extending Hauser-Feshbach calculations to the low energy region, or by using the single-level Breit-Wigner formalism with average resonance parameters (average neutron and radiative widths).

In the first case, sensitivities depend only on optical model parameters and on the a -parameter for the level density in the compound nucleus. It is well known that sensitivity to the optical model parameters increases as neutron energy decreases. This directly affects the calculated cross-section uncertainties, which smoothly decrease when moving from the lower boundary to the upper boundary of the unresolved region.

If the resonance formalism is used, the average resonance parameters, as deduced from the resonance region, and the scattering radius are considered. In the case of capture cross-section, sensitivity to both radiative and neutron widths is a smooth, slightly increasing function of the incident neutron energy. The resulting cross-section uncertainty follows this trend. In conclusion, the two methods predict somewhat different energy dependence for cross-section

uncertainties, and dramatically different correlations. Obviously, the former approach correlates unresolved region with the fast neutron range, while the latter with the resolved neutron range.

3.3 Fast neutron region

A total of 15 parameters, including real and imaginary surface depths of the optical potential for the compound nuclei, particle- and γ -emission widths, level densities and the mean free path in the exciton model were considered in the sensitivity calculations.

Figure 1 shows ENDF/B-VII.0 results for the uncertainties of total, elastic and capture cross-sections on ^{157}Gd . The results were obtained employing the EMPIRE-KALMAN method combining experimental uncertainties with model-based covariances. The (n, γ) cross-section uncertainties are relatively low between 10 and 100 keV due to the precise measurement by Wisshak. Above 1 MeV uncertainty increases dramatically due to the lack of experimental constraints and to the high sensitivity of the capture cross-section to model parameters. The uncertainties for the total cross-sections are driven by the experimental data while those for the elastic channel are determined nearly entirely by the model calculations. We note distinct minima in the elastic uncertainties which are due to the fundamental features of the optical model.

Generally, model calculations predict strong correlations in the whole energy range since individual model parameters tend to affect broad energy ranges. Correlation matrices accounting for experimental data are characterised by a more complicated structure with strong correlations aligned within a relatively narrow band along the diagonal (Figure 2). The positive long-range correlations, typical for model predictions, are annihilated or turned into anti-correlations leaving only short- and medium-range positive correlations. This is because measurements are believed to be quite independent from one other, i.e. long-range correlations (systematic errors) are assumed to be relatively weak.

Figure 1. Relative uncertainties in the unresolved resonance and fast neutron range for the total, elastic and capture reactions on ^{157}Gd obtained with the EMPIRE-KALMAN method

The experimental uncertainties for capture do not include 1.5% uncertainty from the normalisation to the Au standards cross-sections

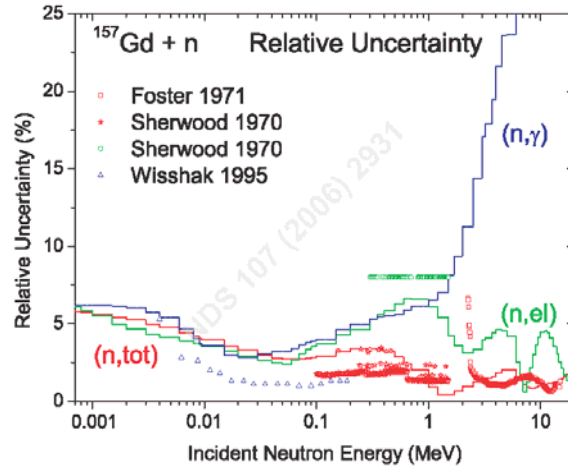
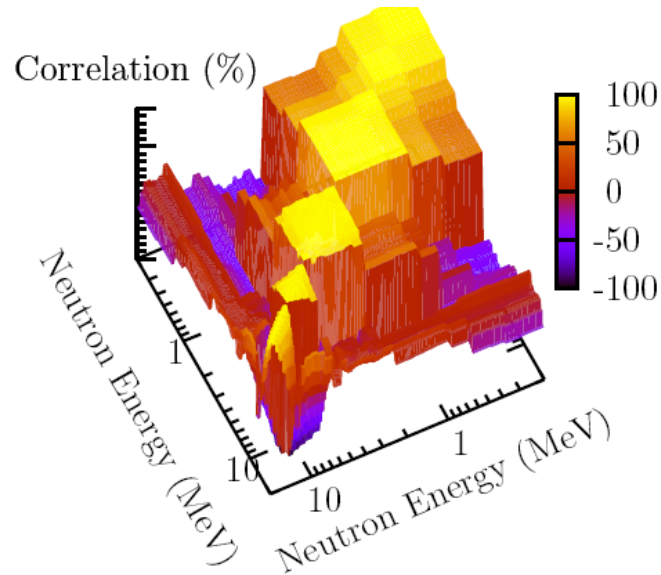


Figure 2. Correlation matrix for the ^{90}Zr neutron capture cross-sections in the fast neutron region obtained by combining model-based and experimental covariances



REFERENCES

- [1] Mughabghab, S.F., “Atlas of Neutron Resonances: Resonance Parameters and Thermal Cross-sections”, Elsevier Publisher, Amsterdam (2006).
- [2] Herman, M., *et al.*, “EMPIRE Nuclear Reaction Model Code System for Data Evaluation”, *Nucl. Data Sheets*, 108, 2655 (2007), www.nndc.bnl.gov/empire219/.
- [3] Kawano, T., Tech. Report JAERI-Research 99-009, JAERI (1999) (in Japanese).

Appendix H

REPORT TO OECD/WPEC SUBGROUP 26 ON THE PRELIMINARY CONCLUSIONS OF THE APRIL 2007 MEETING IN NICE

P. Talou, T. Kawano, P.G. Young, M.B. Chadwick

1. Evaluation

The evaluation of uncertainties carried out for neutron-induced reactions on $^{235,238}\text{U}$ and ^{239}Pu is based on similar input ingredients as those used for the ENDF/B-VII evaluation [1]. For more details on the specific evaluations for uranium and plutonium isotopes, see P.G. Young, *et al.* [2].

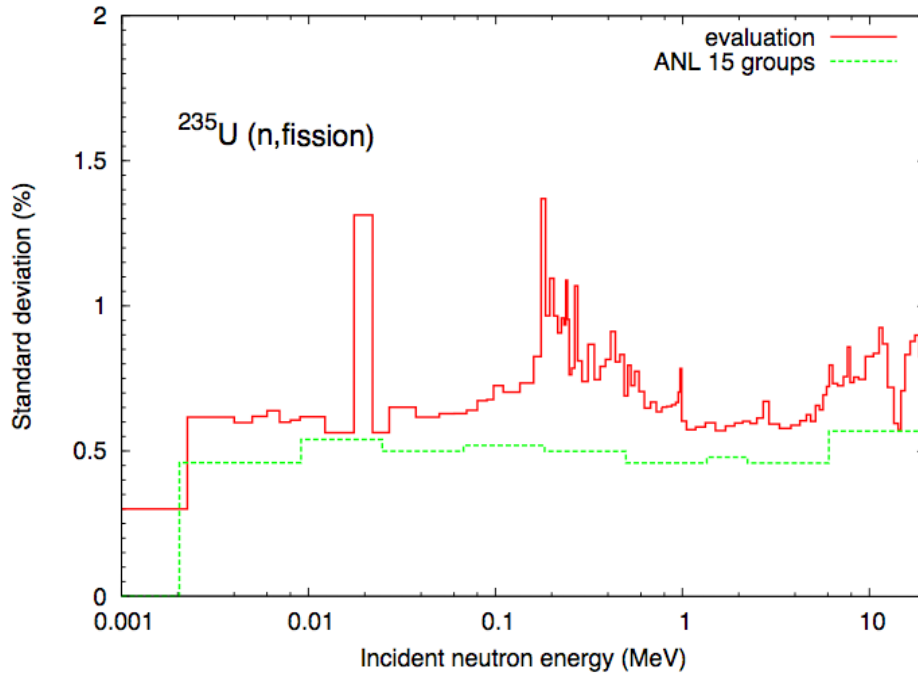
It should be noted however that a more correct and rigorous approach would have been to evaluate the uncertainties while performing the evaluation work. In addition, some differences may appear as the evaluation procedure does not necessarily follow nuclear reaction calculations and differential experimental data alone, but also depends on integral benchmarking that was not considered in the present work.

This appendix was extracted from a longer publication in preparation [3].

2. Processing

The evaluated covariance matrices were processed with the ERRORJ code in a 15-group energy structure, as used at ANL for reactor sensitivity calculations [4]. Using only 15 energy groups means that many fine details of the correlation matrix are washed out. Another consequence is that energy-group uncertainties are reduced compared to their energy pointwise counterparts, due to the accumulation of energy points in one bin, and therefore a reduction of the statistical error bars. Figure 1 illustrates this effect on the evaluated standard deviations (diagonal elements of the full covariance matrix) for the neutron-induced fission cross-section of ^{235}U . The reduction of uncertainties is

Figure 1. Standard deviations (in %) for the neutron-induced fission cross-section of ^{235}U

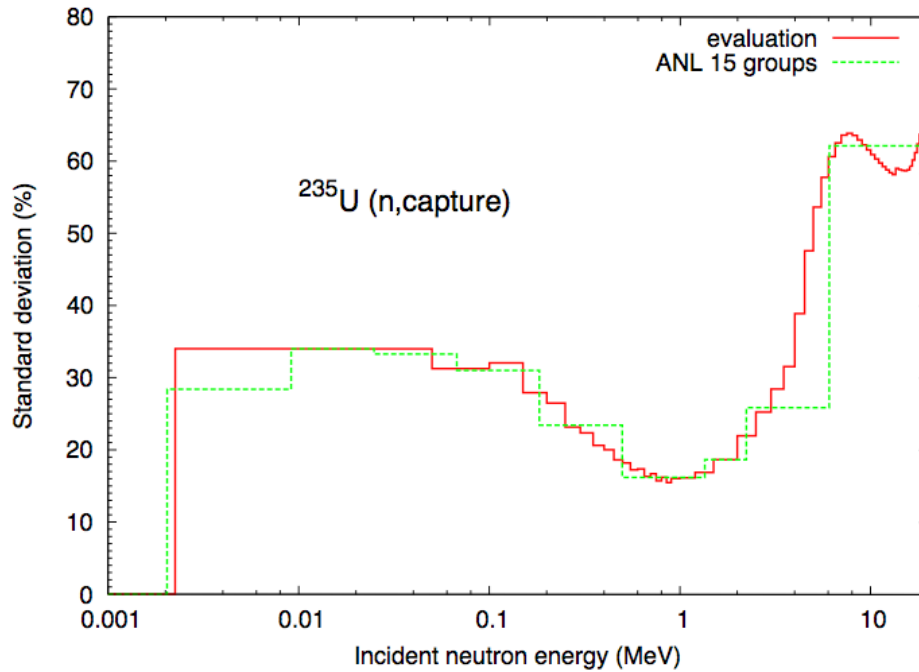


quite strong there as most of the evaluated uncertainties are of statistical nature, whereas only systematic uncertainties would be resilient to the multi-grouping procedure.

Although expected, the reduction of the uncertainties owing to the multi-grouping procedure should be checked properly to ensure that the results of sensitivity calculations do not depend on the number of groups used. Obviously, this conclusion would also depend on the particular neutron spectrum used in the calculations. If the spectrum behaves very smoothly over a wide energy range, the fine details of the covariance matrix are not needed. But the question of the influence of the number of groups on the final result remains.

Another example is given in Figure 2 for the uncertainties on the capture cross-section of ^{235}U . In this case, the systematic component of the total uncertainties is large, whereas the effect of the multi-grouping procedure is relatively small.

Figure 2. Standard deviations (in %) for the capture cross-section of ^{235}U



3. Discussion

The OECD/NEA Working Party on Evaluation and Co-operation (WPEC) Subgroup 26 chaired by M. Salvatores (ANL and CEA) was proposed to identify nuclear data needs, and in particular evaluated covariance matrices, for the safe and efficient deployment of the next generation (Generation-IV) of nuclear power plants. A set of target accuracies for key integral parameters such as the neutron multiplicative factor k_{eff} has been established by the reactor physics community, and sensitivity calculations to nuclear data were performed [4]. Of course, the result of such calculations depends strongly on the input itself, i.e. the uncertainties on the nuclear data present in the evaluated data libraries. While the subgroup activities were aimed at exploring the needs for covariance matrices only, it exceeded its mission by obtaining a large portion of all covariance matrices needed to run the sensitivity calculations. The present work contributed to this effort by providing the covariance matrices for $^{235,238}\text{U}$ and ^{239}Pu as described in Ref. [3].

Preliminary results of sensitivity calculations performed with this set of covariance matrices were obtained and are discussed below. Among the most important preliminary conclusions were:

- Very small uncertainties on ^{235}U and ^{239}Pu (n,f) cross-sections are shifting the focus of future data evaluation needs.
- Now, plutonium isotopes (other than ^{239}Pu) major reactions (fission, capture and $\langle n \rangle$) are large sources of uncertainties.
- In the case of ^{239}Pu , the major impact arises from the capture cross-section uncertainty.
- The ^{238}U inelastic and capture cross-section uncertainties remain important.
- Selected minor actinides (MA) fission cross-section uncertainties play an important role, but only in dedicated MA burners.

Also, several target accuracies for those isotopes, reactions and energy groups were obtained for fast reactor designs by performing inverse problem calculations, starting from fixed target accuracies for integral parameters and working backwards toward uncertainties on evaluated nuclear data. In particular, the following target accuracies were obtained: 2-3% for ^{238}U inelastic cross-section uncertainty in the 0.498-6.07 MeV energy range, 1.5-2% for ^{238}U capture cross-section uncertainty in the 2.04-24.8 keV region, and 4-7% for the ^{239}Pu capture cross-section uncertainty in the 2.04-498 keV range.

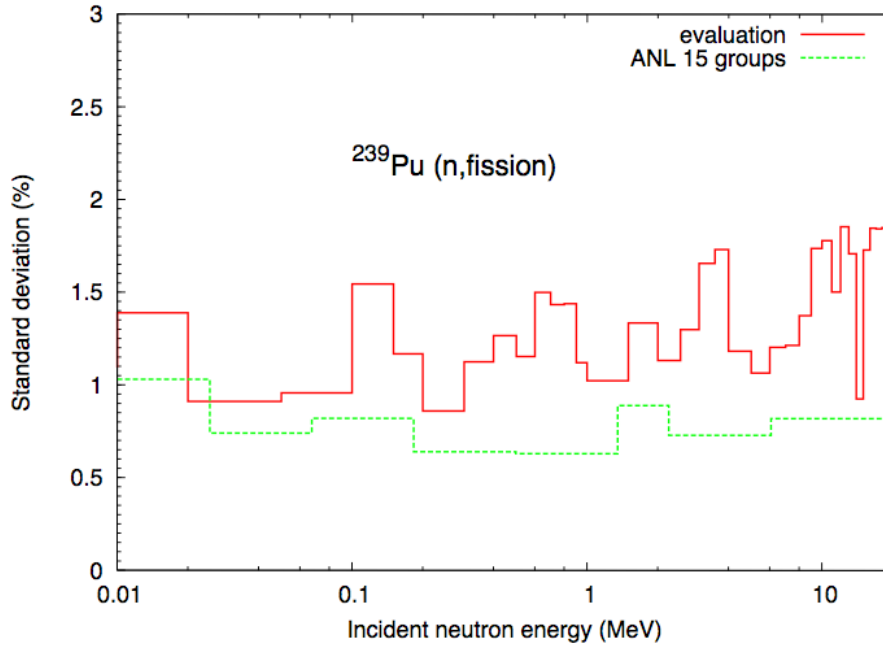
Let us now discuss briefly these preliminary results.

3.1 ^{235}U and ^{239}Pu fission cross-section uncertainties

Uranium-235 neutron-induced fission cross-section uncertainties were thoroughly investigated by a group of experts at the IAEA led by V. Pronyaev [5], and were adopted as such in the ENDF/B-VII library and in the present work. This is certainly the most thorough job on this question performed to date. The resulting uncertainties are of the order of 0.5-1.5% in the keV up to the 20 MeV region. Once processed in a 15 energy group structure, the uncertainties were further reduced to about 0.5% everywhere.

As for ^{239}Pu , the evaluated pointwise uncertainties are of the order of 1-2% while the processed ones lie between 0.5 and 1% (Figure 3). Note that many experimental data for ^{239}Pu were obtained as ratio data to the “standard” ^{235}U (n,f) cross-section. Therefore strong correlations between the two isotopes and reactions exist.

Figure 3. Standard deviations (in %) for the neutron-induced fission cross-section of ^{239}Pu

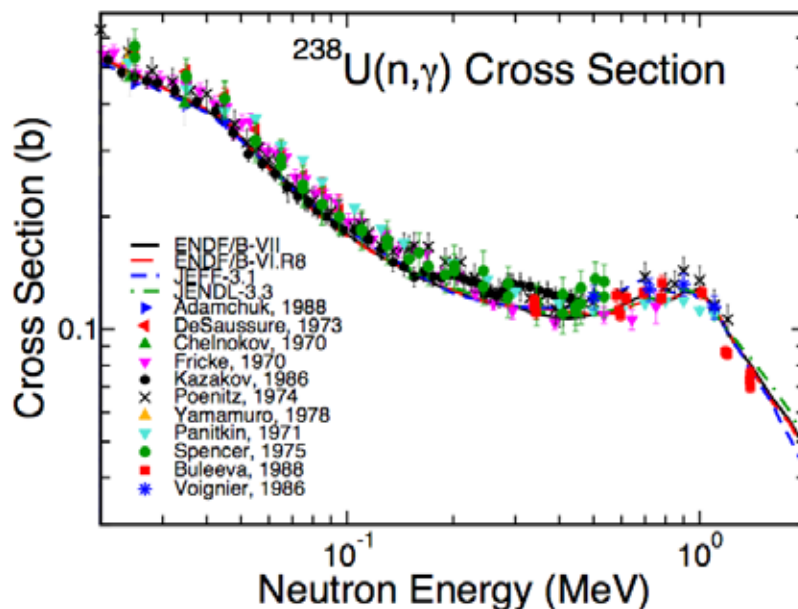


Although these uncertainties can seem very low, they are backed by a large number of data sets. When combined in a generalised-least-squares approach, the individual systematic errors tend to disappear. However, it is well known that such systematic uncertainties are very difficult to estimate. In addition, the smoothing numerical procedure used by Pronyaev, *et al.* [5] introduced some uncertainty in the final result, which led to adding a 0.3% fully correlated component to the evaluated uncertainties. This number of 0.3% was not obtained from very rigorous arguments, but instead represents an “expert” assessment for reasonable final uncertainties.

3.2 ^{238}U inelastic and capture cross-section uncertainties

The evaluated capture cross-section of ^{238}U is very close to the standard cross-section evaluated by Pronyaev, *et al.* [5]. The ENDF/B-VII evaluation [2] along with other evaluated libraries and experimental data points is shown in Figure 4. The evaluated capture cross-section follows the lowest values of the measurements, in agreement with the conclusions of NEA WPEC Subgroup 4 and with critical assemblies benchmark calculations [1].

Figure 4. Measured and evaluated cross-sections for the $^{238}\text{U}(n,\gamma)$ reaction from 0.02 to 2 MeV



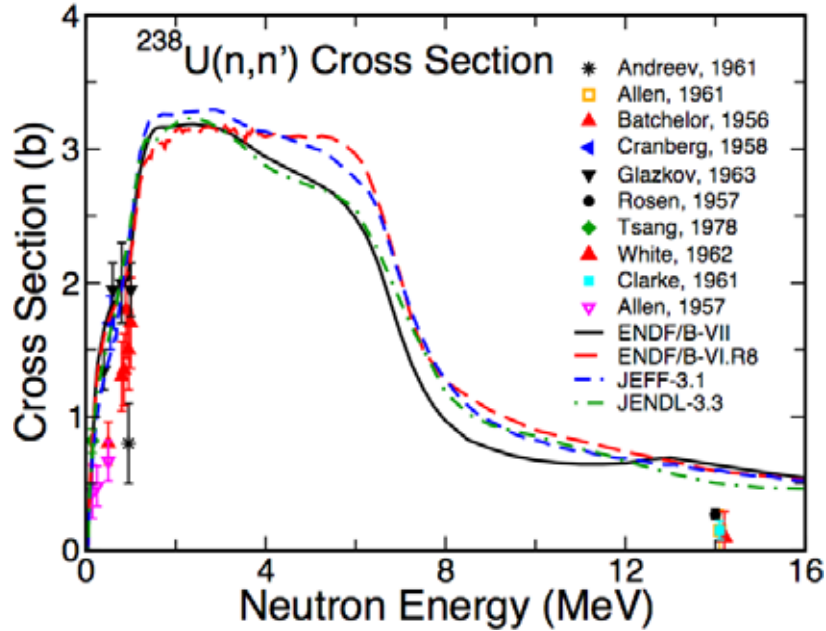
The target accuracy of WPEC Subgroup 26 of 1.5-2% in the 2.04-24.8 keV energy range is within the uncertainties obtained in the IAEA evaluation.

Concerning the inelastic cross-section uncertainties, in the 0.498-6.07 MeV energy range, they are currently evaluated at 10-20% while a target of 2-3% was established. Figure 5 shows the current status of the evaluated libraries along with experimental data. The target accuracy for the $^{238}\text{U}(n,n')$ reaction appears unreachable from differential data alone. This conclusion supports the arguments of WPEC Subgroup 26 in favour of integral measurements to constrain evaluated differential data.

3.3 ^{239}Pu capture cross-section uncertainties

Since the evaluated uncertainty on the $^{239}\text{Pu}(n,f)$ cross-section is small, the next major source of uncertainty for this isotope comes from the capture channel. A target accuracy of 4-7% in the 2.04-498 keV region was estimated by SG26, while the current evaluation lies in the 7-15% range. It is unclear if such a precision measurement could be made in a relatively short term. Experimentalists should be able to answer this question.

Figure 5. Experimental and evaluated inelastic cross-section of ^{238}U



3.4 Prompt neutrons multiplicities

The prompt neutron multiplicity for $n+^{235}\text{U}$ is shown in Figure 6 for incident neutron energies from 0 to 4 MeV. The scatter of data points is rather large, but combining all data sets in a generalised-least-square code leads to a strong reduction in the final evaluated uncertainties. In the 0.1 to 10 MeV region, the evaluated uncertainties on $\langle n \rangle$ for ^{235}U and ^{239}Pu are of the order of 0.2-0.3% (see Figure 7). This is to compare with the evaluated uncertainty of the standard $^{252}\text{Cf} (sf) \langle n \rangle = 3.7692 \pm 0.12\%$.

Again, unknown systematic errors could lead to higher final evaluated uncertainties. However, integral information from critical assemblies such as Godiva (for ^{235}U) and Jezebel (for ^{239}Pu) also constrain $\langle n \rangle$ values.

Figure 6. $n+^{235}\text{U}$ prompt fission neutron multiplicity from 0 to 4 MeV

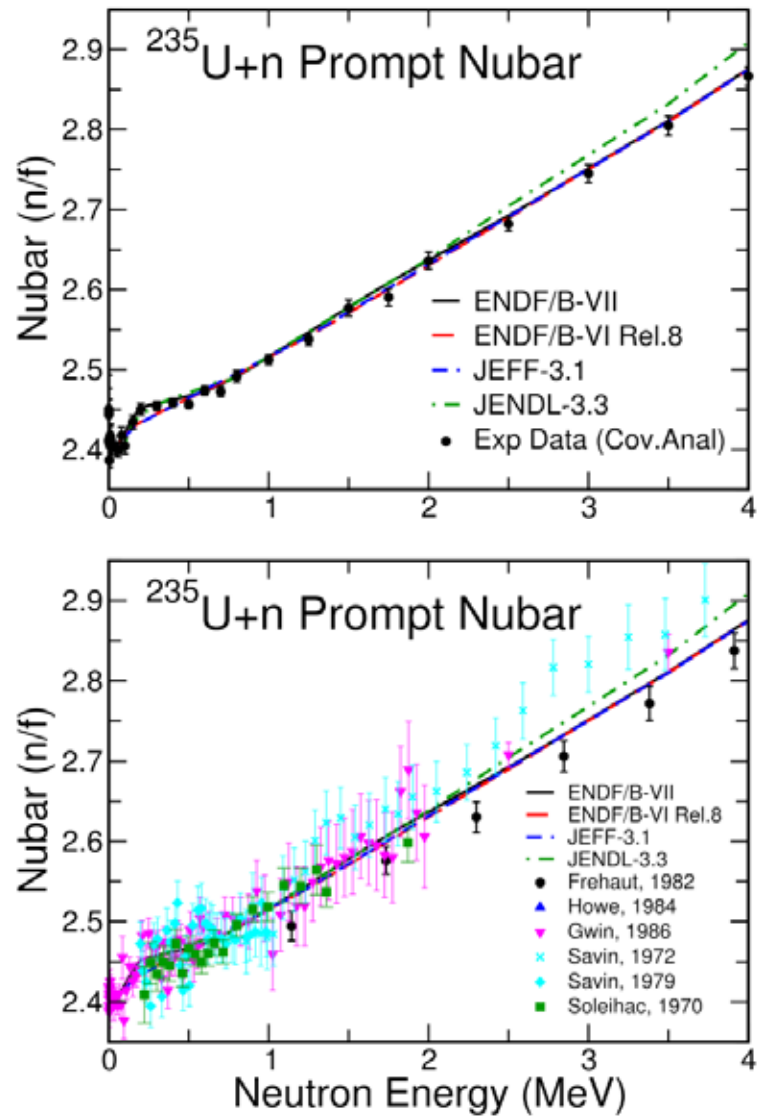
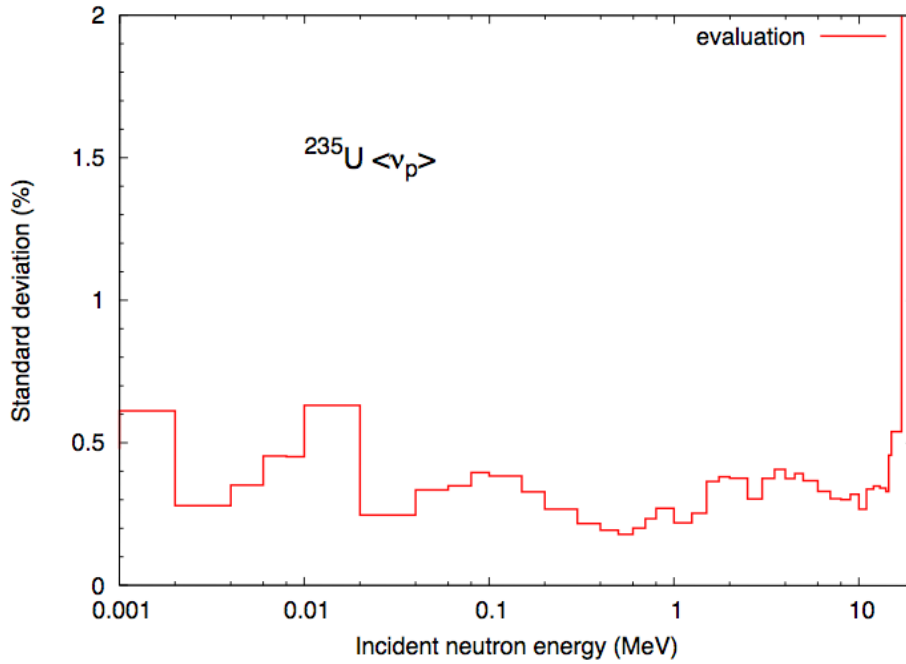


Figure 7. Standard deviations (in %) for the prompt neutron multiplicity of $n+^{235}\text{U}$



3.5 Other uncertainties?

It is important to note that nuclear reactor sensitivity calculations are first-order calculations, use multi-groups instead of pointwise energy covariance matrices, and take into account a subset of physical quantities uncertainties only. For instance, no uncertainty on the neutron fission spectra is included. Those approximations may lead to wrong assignments of uncertainties to particular isotopes, reactions or even energy regions.

On the other hand, uncertainties stemming from the present work may be flawed in several ways. In the analysis of experimental data, systematic uncertainties are very difficult to estimate properly. In addition, cross-correlations among isotopes and reactions are often neglected, at least in the presentation of the final results (e.g. standard cross-section uncertainties). Finally, the assumption that all model uncertainties come from the model input parameters and not the adequacy of the models themselves should be kept in mind.

4. Summary

Here is a brief summary of the most important features of this UQ evaluation:

- *^{235}U and ^{239}Pu (n,f) cross-sections.* The evaluated uncertainties are very small, and further reduced by the multi-grouping procedure. To be conservative, and to take into account the potential impact of the group processing on the evaluated uncertainties, the mean value of the 15-group uncertainties could be shifted upward to be consistent with the energy pointwise values. This shift would be about 0.2% in the case of ^{235}U and 0.4% in the case of ^{239}Pu .
- *^{238}U inelastic cross-section.* The target accuracy of 2-3% in the 0.498-6.07 MeV energy group seems unreachable from analysis of differential data alone. Integral information may help reduce the current status (10-20%).
- *^{238}U capture cross-section.* The target accuracy of 1.5-2% in the 2.04-24.8 keV energy range is within the uncertainties obtained in the latest standard IAEA evaluation.
- *^{239}Pu capture cross-section.* The target accuracy of 4-7% in the 2.04-498 keV range cannot be achieved at this stage without a new high-precision measurement. “Is such a measurement possible?” would have to be answered by expert experimentalists.
- *Prompt neutron multiplicities.* The accuracy of prompt neutron multiplicities for ^{235}U and ^{239}Pu is of the order of 0.2-0.3% in the 0.1-10 MeV region. There are a lot of experimental data sets but their scatter is rather large. Unknown systematic errors could lead to slightly larger errors; however, integral data place strong constraints on the product $s_f \times \langle n_p \rangle$.
- *Other uncertainties?* Other sources of uncertainties (model errors, unknown systematic errors, correlations among isotopes and reactions, use of different energy groups, ...) could lead to increased evaluated uncertainties. More work remains to be done in this arena. It is worth remembering that this work only represents a first (but big) step toward the production of covariance matrices as part of the nuclear data evaluation process.

REFERENCES

- [1] Chadwick, M.B., P. Oblozinsky, M. Herman, *et al.*, “ENDF/B-VII: Next Generation Evaluated Nuclear Data Library for Nuclear Science and Technology”, *Nuclear Data Sheets*, 107, 12, 2931-3060 (2006).
- [2] Young, P.G., M.B. Chadwick, R.E. MacFarlane, P. Talou, T. Kawano, D.G. Madland, W.B. Wilson, M.R. MacInnes, D.W. Barr, H.R. Trellue, C.W. Wilkerson, “Evaluation of Neutron Reactions for ENDF/B-VII: $^{232-241}\text{U}$ and ^{239}Pu ”, forthcoming in *Nuclear Data Sheets* (2007).
- [3] Talou, P., T. Kawano, P.G. Young, M.B. Chadwick, “Uncertainty Quantification of Neutron-induced Reactions on $^{235,238}\text{U}$ and ^{239}Pu in the Fast Energy Range”, in preparation.
- [4] Aliberti, G., G. Palmiotti, M. Salvatores, T.K. Kim, T.A. Taiwo, M. Anitescu, I. Kodeli, E. Sartori, J.C. Bosq, J. Tommasi, “Nuclear Data Sensitivity, Uncertainty and Target Accuracy Assessment for Future Nuclear Systems”, *Annals of Nuclear Energy*, 33, 700-733 (2006).
- [5] Pronyaev, V.G., S.A. Badikov, A.D. Carlson, Z. Chen, E.V. Gai, G.M. Hale, F.J. Hambsch, H.M. Hofmann, N.M. Larson, D.L. Smith, S.Y. Oh, S. Tagesen, H. Vonach, *An International Evaluation of the Neutron Cross-section Standards*, International Atomic Energy Agency, technical report, forthcoming.

Appendix I

IMPORTANCE OF ^{23}Na REACTION CROSS-CORRELATIONS IN THE UNCERTAINTY ASSESSMENT OF SFR CHARACTERISTICS

G. Rimpault, W. Khamakhem

1. Introduction

The design criteria of Gen-IV reactors tend to improve both their fuel management and reactor safety. Those design criteria require an improvement of the accuracy of results and a good knowledge of the associated uncertainties. This is particularly important for the safety parameters, in particular the Na void effect, and focus is being directed on the study of its associated uncertainties. The study of these uncertainties was performed on several core designs, but only the results obtained for a 3 600 MWth SFR using oxide fuel are presented here.

The results show a great sensibility of the uncertainties to the covariance data. The k_{eff} and Na void uncertainties are above the Gen-IV uncertainties targets what is a motivation for further studies. In order to decrease the safety margins, the nuclear data should be significantly improved and the cross-section uncertainties and variance-covariance data estimated with greater accuracy.

2. Covariance data

In order to study the impact of the variance-covariance matrix for the Na void effect uncertainties, we used the variance-covariance matrix developed for the WPEC Subgroup S26 and called BOLNA and a covariance matrix associated to an old evaluation for Na cross-sections.

3. BOLNA

Tables 1 and 2 display the description of the Na variance-covariance data from BOLNA. We note that there is no covariance data for the correlation between the inelastic and the elastic Na cross-section. Hence, the covariance

data do not reflect the way ^{23}Na evaluations have been done based on total and inelastic cross-sections measurements while elastic cross-sections are deduced from the other reactions.

4. Na variance-covariance matrix associated with an old evaluation

Na variance-covariance data associated to an old evaluation which exhibits Na elastic-inelastic cross-correlation data and which has also larger variances are displayed in Tables 3-5.

5. Results

In Table 6, results on uncertainty assessment on k_{eff} and Na void effect are presented. The uncertainties obtained with BOLNA for the k_{eff} and the Na void effect are respectively 1.80% and 12.4%, larger than the target uncertainties for Gen-IV. Moreover, the results of uncertainties calculation show, as expected, a major role of the Na to the Na void effect and to the uncertainty associated.

To illustrate the potential impact of the correlations between different reactions, we use the case of the elastic and the inelastic Na cross-sections comparing different calculations with different uncertainty data:

- the BOLNA covariance set;
- the BOLNA covariance set with elastic and inelastic cross-correlation from the old evaluation assuming that they are missing;
- the BOLNA covariance set with the exception of Na for which the variance-covariance data from the old Na evaluation without its own correlations between elastic and inelastic cross-sections;
- the BOLNA covariance set with the exception of Na for which the variance-covariance data from the old Na evaluation with its own correlations between elastic and inelastic cross-sections are being used (refer to Table 3).

The results are given by Table 7; they show that the use of the elastic and the inelastic cross-correlations associated with BOLNA covariance set (column 2 compared to column 1 in Table 7) decreases the uncertainty due to the Na by only 0.3%, which decreases the Na void uncertainty by only 0.2%. The decrease of the uncertainty takes place in the fourth macro group of energy for the inelastic contribution and in the third to the fifth macro group for the elastic contribution, according to Tables 8 and 9.

Now when we used the BOLNA and the variance-covariance data corresponding to an old ^{23}Na evaluation, data including the elastic and inelastic cross-correlations, we note that the Na void uncertainty obtained with BOLNA and the variance-covariance data from the old evaluation, without elastic and inelastic cross-correlation, is 1.4% bigger than the uncertainty calculated with BOLNA. Then, we find that the Na void uncertainty decreases by 0.5% when the overall uncertainty decreases by 0.7%. Here, the decrease of the uncertainty takes place in the first to the third macro group of energy for the inelastic contribution (i.e. just at the inelastic threshold) and in the first to the fourth macro group for the elastic contribution, according to Tables 10 and 11 (i.e. just below the inelastic threshold). The decrease of uncertainty due to the presence of cross-correlation is in this case more important than with the BOLNA covariance set.

It can thus be concluded that cross-correlations are important only when associated to large variances (i.e. when evaluated cross-sections are badly known).

6. Conclusions

The use of correlations between different cross-sections should reflect the way the evaluation has been done and this is particularly true for ^{23}Na . The use of ^{23}Na cross-correlations between elastic and inelastic cross-sections decreases the induced uncertainties and should not be neglected. However, the importance of these correlations is less important when using more recent ^{23}Na evaluations with reduced variances.

Table 1. Variance covariance matrix for the Na inelastic cross-section correlated to the Na inelastic cross-section

Energy group	1	2	3	4	5	6	7	8	9	10	11	12	13	14	15
Variance	0.1879	0.0887	0.1256	0.28	0.5	0	0	0	0	0	0	0	0	0	0
Variance-covariance	1	0.299	0.234	0.16	0	0	0	0	0	0	0	0	0	0	0
	0.299	1	0.596	0.315	0	0	0	0	0	0	0	0	0	0	0
	0.234	0.596	1	0.941	0	0	0	0	0	0	0	0	0	0	0
	0.16	0.315	0.941	1	0.147	0	0	0	0	0	0	0	0	0	0
	0	0	0	0.147	1	0	0	0	0	0	0	0	0	0	0
	0	0	0	0	0	0	0	0	0	0	0	0	0	0	0
	0	0	0	0	0	0	0	0	0	0	0	0	0	0	0
	0	0	0	0	0	0	0	0	0	0	0	0	0	0	0
	0	0	0	0	0	0	0	0	0	0	0	0	0	0	0
	0	0	0	0	0	0	0	0	0	0	0	0	0	0	0
	0	0	0	0	0	0	0	0	0	0	0	0	0	0	0
	0	0	0	0	0	0	0	0	0	0	0	0	0	0	0
	0	0	0	0	0	0	0	0	0	0	0	0	0	0	0
	0	0	0	0	0	0	0	0	0	0	0	0	0	0	0

Table 2. Variance covariance matrix for the Na elastic cross-section correlated to the Na elastic cross-section

Energy group	1	2	3	4	5	6	7	8	9	10	11	12	13	14	15
Variance	0.018	0.0462	0.0372	0.0301	0.0331	0.0325	0.0238	0.0287	0.0323	0.0493	0.0476	0.0473	0.0471	0.047	0.0459
Variance-covariance	1	-0.786	-0.612	-0.57	0	0	0	0	0	0	0	0	0	0	0
	-0.786	1	0.97	0.932	0	0	0	0	0	0	0	0	0	0	0
	-0.612	0.97	1	0.968	0	0	0	0	0	0	0	0	0	0	0
	-0.57	0.932	0.968	1	0.006	0.012	0.014	0.004	0	0.102	0.104	0.104	0.104	0.105	0.104
	0	0	0	0.006	1	0.962	0.932	0.948	0.129	0.53	0.567	0.575	0.58	0.581	0.581
	0	0	0	0.012	0.962	1	0.972	0.976	0.14	0.548	0.586	0.594	0.599	0.6	0.6
	0	0	0	0.014	0.932	0.972	1	0.935	0.161	0.538	0.573	0.581	0.586	0.587	0.587
	0	0	0	0.004	0.948	0.976	0.935	1	0.282	0.627	0.659	0.666	0.671	0.672	0.672
	0	0	0	0	0.129	0.14	0.161	0.282	1	0.774	0.744	0.737	0.733	0.733	0.732
	0	0	0	0.102	0.53	0.548	0.538	0.627	0.774	1	0.999	0.998	0.997	0.997	0.997
	0	0	0	0.104	0.567	0.586	0.573	0.659	0.744	0.999	1	1	1	1	1
	0	0	0	0.104	0.575	0.594	0.581	0.666	0.737	0.998	1	1	1	1	1
	0	0	0	0.104	0.58	0.599	0.586	0.671	0.733	0.997	1	1	1	1	1
	0	0	0	0.105	0.581	0.6	0.587	0.672	0.733	0.997	1	1	1	1	1
	0	0	0	0.104	0.581	0.6	0.587	0.672	0.732	0.997	1	1	1	1	1

Table 3. Variance covariance matrix for the Na elastic cross-section correlated to the Na inelastic cross-section

Energy group	1	2	3	4	5	6	7	8	9	10	11	12	13	14	15
Variance-covariance	-0.911	-0.899	-0.696	0	0	0	0	0	0	0	0	0	0	0	0
	-0.914	-0.975	-0.771	0	0	0	0	0	0	0	0	0	0	0	0
	-0.811	-0.885	-0.85	-0.193	-0.072	-0.008	0	0	0	0	0	0	0	0	0
	0	0	-0.273	-0.599	-0.196	-0.02	0	0	0	0	0	0	0	0	0
	0	0	-0.272	-0.526	-0.224	-0.023	0	0	0	0	0	0	0	0	0
	0	0	-0.227	-0.392	-0.162	-0.031	0	0	0	0	0	0	0	0	0
	0	0	0	0	0	0	-0.001	-0.002	-0.001	0	0	0	0	0	0
	0	0	0	0	0	0	-0.001	-0.002	-0.001	0	0	0	0	0	0
	0	0	0	0	0	0	-0.001	-0.002	-0.001	0	0	0	0	0	0
	0	0	0	0	0	0	0	0	0	0	0	0	0	0	0
	0	0	0	0	0	0	0	0	0	0	0	0	0	0	0
	0	0	0	0	0	0	0	0	0	0	0	0	0	0	0
	0	0	0	0	0	0	0	0	0	0	0	0	0	0	0
	0	0	0	0	0	0	0	0	0	0	0	0	0	0	0
	0	0	0	0	0	0	0	0	0	0	0	0	-0.001	-0.002	-0.002
	0	0	0	0	0	0	0	0	0	0	0	0	-0.001	-0.001	-0.002

Table 4. Variance covariance matrix for the Na inelastic cross-section correlated to the Na inelastic cross-section

Energy group	1	2	3	4	5	6	7	8	9	10	11	12	13	14	15
Variance	0.426	0.412	0.218	0.169	0.17	0.2003	0.5	0.5	0.202	0.138	0.145	0.121	0.074	0.01	0.01
Variance-covariance	1	0.922	0.819	0	0	0	0	0	0	0	0	0	0	0	0
	0.922	1	0.908	0	0	0	0	0	0	0	0	0	0	0	0
	0.819	0.908	1	0.322	0.32	0.266	0	0	0	0	0	0	0	0	0
	0	0	0.322	1	0.877	0.653	0	0	0	0	0	0	0	0	0
	0	0	0.32	0.877	1	0.725	0	0	0	0	0	0	0	0	0
	0	0	0.266	0.653	0.725	1	0.007	0.007	0.006	0	0	0	0	0	0
	0	0	0	0	0	0.007	1	1	0.774	0	0	0	0	0	0
	0	0	0	0	0	0.007	1	1	0.774	0	0	0	0	0	0
	0	0	0	0	0	0.006	0.774	0.774	1	0.16	0.115	0.137	0.136	0	0
	0	0	0	0	0	0	0	0	0.16	1	0.442	0.293	0.29	0	0
	0	0	0	0	0	0	0	0	0.115	0.442	1	0.297	0.276	0	0
	0	0	0	0	0	0	0	0	0.137	0.293	0.297	1	0.998	0	0
	0	0	0	0	0	0	0	0	0.136	0.29	0.276	0.998	1	0.054	0.054
	0	0	0	0	0	0	0	0	0	0	0	0	0.054	1	1
	0	0	0	0	0	0	0	0	0	0	0	0	0.054	1	1

Table 5. Variance covariance matrix for the Na elastic cross-section correlated to the Na elastic cross-section

Energy group	1	2	3	4	5	6	7	8	9	10	11	12	13	14	15
Variance	0.525	0.226	0.065	0.037	0.037	0.037	0.05	0.046	0.039	0.06	0.06	0.06	0.042	0.07	0.071
Variance-covariance	1	0.907	0.722	0.051	0.048	0.046	0.003	0	0	0	0	0	0	0	0
	0.907	1	0.847	0.082	0.076	0.074	0.006	0	0	0	0	0	0	0	0
	0.722	0.847	1	0.409	0.278	0.218	0.016	0	0	0	0	0	0	0	0
	0.051	0.082	0.409	1	0.658	0.343	0.025	0	0	0	0	0	0	0	0
	0.048	0.076	0.278	0.658	1	0.556	0.023	0	0	0	0	0	0	0	0
	0.046	0.074	0.218	0.343	0.556	1	0.088	0	0	0	0	0	0	0	0
	0.003	0.006	0.016	0.025	0.023	0.088	1	0.159	0.077	0	0	0	0	0	0
	0	0	0	0	0	0	0.159	1	0.167	0	0	0	0	0	0
	0	0	0	0	0	0	0.077	0.167	1	0.882	0.882	0.882	0.674	0	0
	0	0	0	0	0	0	0	0	0.882	1	1	1	0.765	0	0
	0	0	0	0	0	0	0	0	0.882	1	1	1	0.765	0	0
	0	0	0	0	0	0	0	0	0.882	1	1	1	0.765	0	0
	0	0	0	0	0	0	0	0	0.674	0.765	0.765	0.765	1	0.634	0.634
	0	0	0	0	0	0	0	0	0	0	0	0	0.634	1	1
	0	0	0	0	0	0	0	0	0	0	0	0	0.634	1	1

Table 6. k_{eff} – Na void effect: results of the calculation and uncertainties associated

In BOL	SFR 3 600 MWth	
	(pcm)	Uncertainties given at 1 σ (in %)
k_{eff}	1.008776	1.80
Na contribution for k_{eff}	–	0.10
$\Delta\rho_{Na Void}$	1 092	12.4
Na contribution for $\Delta\rho_{Na Void}$	700	7.3

Table 7. Impact of the correlations of the Na inelastic and elastic cross-sections

Parameters at BOL	Uncertainties given at 1 σ (in %)			
	With BOLNA (no cross-correlations)	With BOLNA and inelastic-elastic Na cross-correlations	With BOLNA except for Na: Na covariances without inelastic-elastic cross-correlation	With BOLNA except for Na: Na covariances with inelastic-elastic cross-correlation
k_{eff}	1.8	1.8	1.8	1.8
Na contribution for k_{eff}	0.10	0.10	0.12	0.13
$\Delta\rho_{Na Void}$	12.4	12.2	13.8	13.3
Na contribution for $\Delta\rho_{Na Void}$	7.3	7.0	9.5	8.8

Table 8. Contribution of Na to the Na void uncertainty calculated with BOLNA

Energy group	Na contribution for the Na void uncertainties (in %)					
	Capture	Fission	Nu	Elastic	Inelastic	Total
1	0.86	0	0	4.2E-02i	0.91	1.25
2	0.21	0	0	0.08	2.12	2.13
3	0.02	0	0	0.34	2.82	2.84
4	6.8E-02i	0	0	0.30	6.20	6.21
5	0.04	0	0	0.65	0.22	0.69
6	0.07	0	0	0.57	0	0.58
7	0.08	0	0	0.17	0	0.18
8	0.01	0	0	3.7E-02i	0	3.7E-02i
9	0.05	0	0	0.71	0	0.71
10	0.05	0	0	0.29	0	0.30
11	0.02	0	0	5.7E-02i	0	5.3E-02i
12	0.01	0	0	4.0E-02i	0	3.9E-02i
13	4.7E-03i	0	0	8.1E-03i	0	9.4E-03i
14	0.00	0	0	1.7E-02i	0	1.7E-02i
15	0.00	0	0	4.7E-03i	0	4.6E-03i
Total	0.90	0	0	1.20	7.20	7.35

Table 9. Contribution of Na to the Na void uncertainty calculated with BOLNA and elastic-inelastic correlations

Energy group	Na contribution for the Na void uncertainties (in %)					
	Capture	Fission	Nu	Elastic	Inelastic	Total
1	0.86	0	0	1.3E-01i	0.86	1.21
2	0.21	0	0	1.6E-01i	2.06	2.06
3	0.02	0	0	9.0E-01i	2.75	2.60
4	6.8E-02i	0	0	8.0E-01i	6.06	6.00
5	0.04	0	0	5.6E-01i	0.17	5.3E-01i
6	0.07	0	0	0.52	0	0.52
7	0.08	0	0	0.17	0	0.18
8	0.01	0	0	3.7E-01i	0	3.7E-01i
9	0.05	0	0	0.71	0	0.71
10	0.05	0	0	0.29	0	0.30
11	0.02	0	0	5.7E-02i	0	5.3E-02i
12	0.01	0	0	4.0E-02i	0	3.9E-02i
13	4.7E-03i	0	0	8.1E-03i	0	9.4E-03i
14	0.00	0	0	1.7E-02i	0	1.7E-02i
15	0.00	0	0	4.7E-03i	0	4.5E-03i
Total	0.90	0	0	1.03i	7.02	7.00

Table 10. Contribution of Na to the Na void uncertainty calculated with BOLNA and Na variance-covariance data associated to an old evaluation and without elastic-inelastic correlations

Energy group	Na contribution for the Na void uncertainties (in %)					
	Capture	Fission	Nu	Elastic	Inelastic	Total
1	1.00	0	0	0.35	2.74	2.94
2	0.45	0	0	0.21	6.79	6.80
3	0.11	0	0	0.68	4.15	4.21
4	0.16	0	0	0.53	3.62	3.66
5	0.36	0	0	0.96	0.26	1.06
6	0.35	0	0	0.82	0	0.89
7	0.83	0	0	0.06	0	0.84
8	0.13	0	0	0.49	0	0.50
9	0.88	0	0	0.95	0	1.29
10	0.28	0	0	0.60	0	0.67
11	0.10	0	0	1.3E-01i	0	9.30E-02i
12	0.03	0	0	9.7E-02i	0	9.30E-02i
13	1.3E-02i	0	0	1.46E-02i	0	1.99E-02i
14	2.0E-05i	0	0	0.00	0	0.00
15	1.3E-05i	0	0	0.00	0	0.00
Total	1.75	0	0	2.00	9.16	9.54

Table 11. Contribution of Na to the Na void uncertainty calculated with BOLNA and Na variance-covariance data associated to an old evaluation and elastic-inelastic correlations

Energy group	Na contribution for the Na void uncertainties (in %)					
	Capture	Fission	Nu	Elastic	Inelastic	n,xn
1	1.00	0	0	1.14i	2.64	0
2	0.45	0	0	6.7E-01i	6.55	0
3	0.11	0	0	1.69i	3.99	0
4	0.16	0	0	5.7E-01i	3.42	0
5	0.36	0	0	0.61	0.24	0
6	0.35	0	0	0.79	0	0
7	0.83	0	0	0.06	0	0
8	0.13	0	0	0.49	0	0
9	0.88	0	0	0.95	0	0
10	0.28	0	0	0.60	0	0
11	0.10	0	0	1.3E-01i	0	0
12	0.03	0	0	9.7E-02i	0	0
13	1.3E-02i	0	0	1.46E-02i	0	0
14	2.0E-05i	0	0	0.00	0	0
15	1.3E-05i	0	0	0.00	0	0
Total	1.75	0	0	1.57i	8.81	0
						8.84

Appendix J
SUBGROUP RECOMMENDATIONS FOR FUTURE WORK

1. WPEC subgroup proposal [G. Palmiotti, INL (ENDF)]

Title

“Methods and Issues for the Combined Use of Integral Experiments and Covariance Data”.

Justification for a subgroup

As a result of the work performed in the WPEC Subgroup 26 on “Nuclear Data Needs for Advanced Reactor Systems” many target accuracies for different reactions, isotopes and energy ranges were defined in order to satisfy design requirement uncertainty for many integral neutronic parameters. Many of these target accuracies are very tight and not likely to be achieved with current experimental measurement techniques. It has been suggested that a combined use of integral experiments and differential information (e.g. measurements, evaluation, uncertainty data) would make it possible to provide designers with improved nuclear data that would be able to meet design target accuracies.

Definition of the project and proposed activities

It is proposed as a mandate for this new subgroup to study methods and issues of the combined use of integral experiments and covariance data. Indications should be provided as to how best exploit existing integral experiments, define new ones if needed, provide trends and feedbacks to nuclear data evaluators and measurers. Participation of evaluators (to account for feedback to files) and a close link to related activities like those co-ordinated at the Uncertainty Analysis of Criticality Safety Assessment Expert Group (WPNCs) should be clearly established.

A two-year work plan should be envisaged.

2. WPEC subgroup proposal

[R.D. McKnight, ANL (ENDF), A. Plompen, IRMM (JEFF)]

Title

“Meeting Nuclear Data Needs for Advanced Reactor Systems”.

Justification for a subgroup

The activities of WPEC Subgroup 26 have identified the nuclear data needs for advanced reactor systems. The most important of the data needs identified by SG26 will be entered into the NEA High Priority Request List (HPRL). Furthermore, because the SG26 efforts have quantified these data needs and their impact on the selected nuclear systems, the identified primary nuclear data needs will be introduced into the HPRL as High Priority data needs. The identification of these priority data needs for advanced reactor systems creates an important opportunity to utilise the collective knowledge of the international nuclear data measurement and evaluation community to consider the appropriate resources to address and meet these priority needs.

Definition of the project and proposed activities

It is proposed to create a new WPEC subgroup on “Meeting Nuclear Data Needs for Advanced Reactor Systems.” This group will be comprised primarily of nuclear data measurement and evaluation experts from each of the international data projects. The mandate for this new SG will be to:

- 1) consider the scope of the priority nuclear data needs identified by SG26;
- 2) consider the practicality of meeting those data needs;
- 3) identify the correct path: evaluation of existing measurement data vs. requirement of new measurement data;
- 4) identify the optimal use of existing world-wide capabilities to meet these needs;
- 5) identify gaps in existing world-wide capabilities to meet these needs;
- 6) recommend a collaborative path forward to meet these needs and to address gaps.

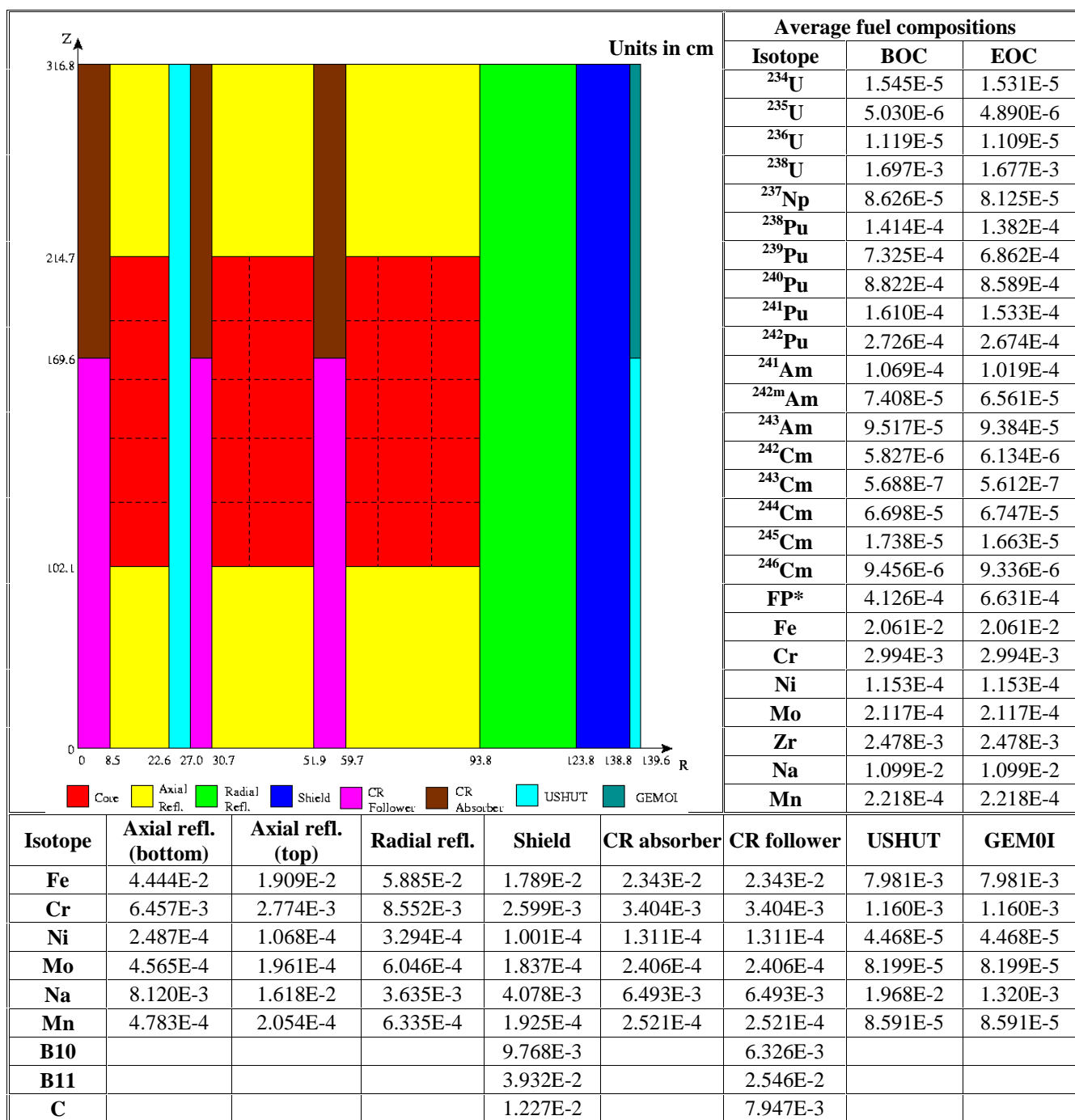
A two-year work plan should be envisaged.

Appendix K
MODEL DESCRIPTION

Table 1. ABTR geometry and homogenised compositions [10^{24} at/cm³]

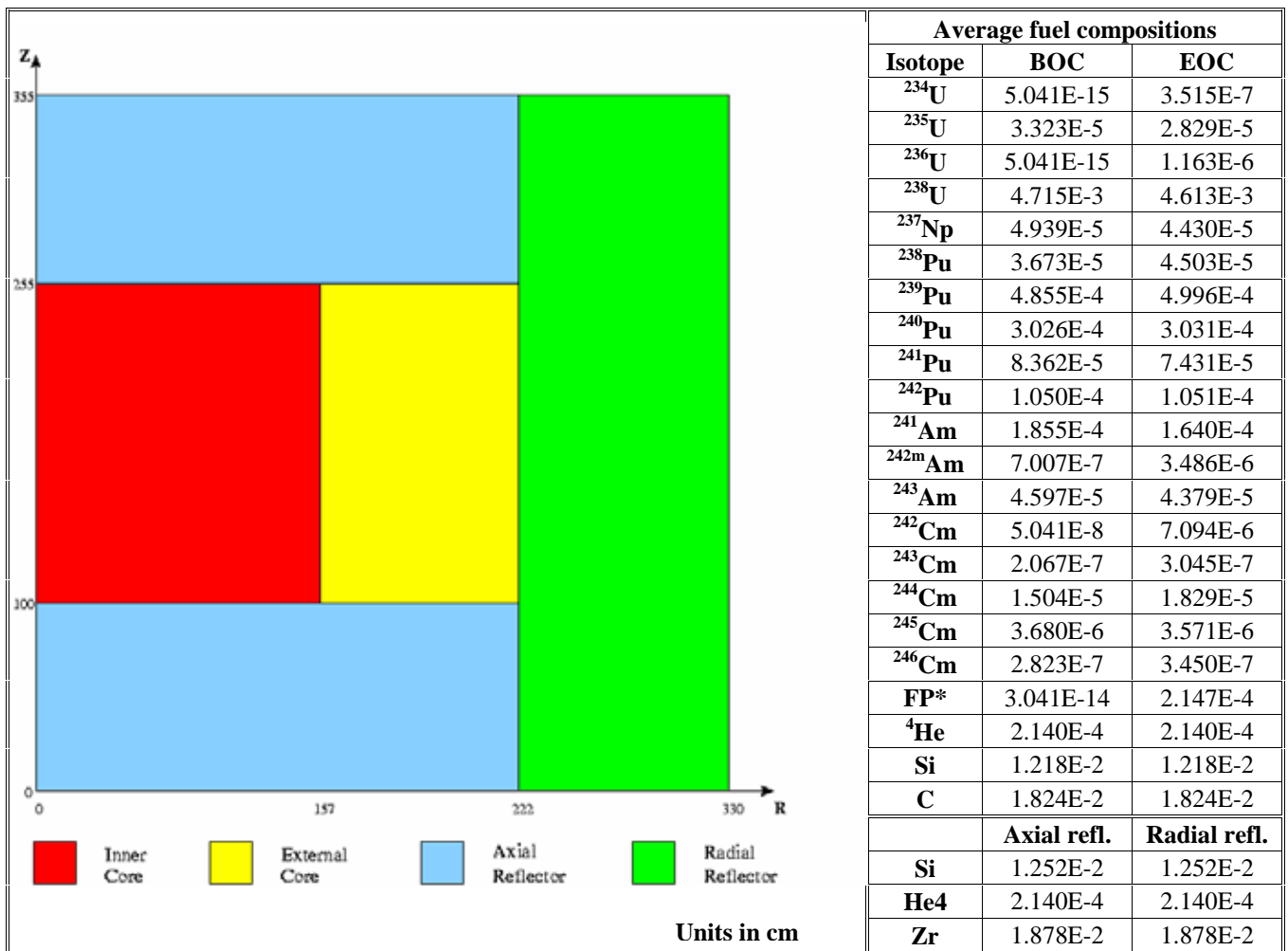
	Inner fuel	Middle fuel	Outer fuel	Lower structure	Lower reflector	Gas plenum with Na bond	Gas plenum	Empty control rod	Control rod follower	Control rod absorber	Gas plenum (control rod)	Reflector	Shield	Barrel
Na	7.148E-3	7.148E-3	7.148E-3	1.559E-2	7.148E-3	1.711E-2	7.148E-3	2.053E-2	1.105E-2	8.170E-3	8.170E-3	3.497E-3	3.857E-3	1.815E-2
Fe	1.618E-2	1.618E-2	1.618E-2	1.588E-2	4.743E-2	1.618E-2	1.618E-2	5.467E-3	2.762E-2	1.875E-2	1.875E-2	5.888E-2	2.124E-2	9.641E-3
Ni	9.976E-5	9.976E-5	9.976E-5	3.260E-3	2.924E-4	9.976E-5	9.976E-5	3.370E-5	4.582E-3	1.156E-4	1.156E-4	3.630E-4	1.309E-4	1.980E-3
Cr	2.406E-3	2.406E-3	2.406E-3	3.235E-3	7.052E-3	2.406E-3	2.406E-3	8.127E-4	5.326E-3	2.788E-3	2.788E-3	8.754E-3	3.158E-3	1.964E-3
Mn	1.066E-4	1.066E-4	1.066E-4	5.085E-4	3.124E-4	1.066E-4	1.066E-4	3.601E-5	7.453E-4	1.235E-4	1.235E-4	3.878E-4	1.399E-4	3.087E-4
Mo	5.505E-4	4.880E-4	5.530E-4	4.352E-4	3.334E-4	1.137E-4	1.137E-4	3.843E-5	6.456E-4	1.318E-4	1.318E-4	4.139E-4	1.493E-4	2.643E-4
C	–	–	–	–	–	–	–	–	–	1.422E-3	–	–	1.942E-3	–
¹⁰B	–	–	–	–	–	–	–	–	–	5.996E-3	–	–	8.191E-3	–
¹¹B	–	–	–	–	–	–	–	–	–	2.414E-2	–	–	3.297E-2	–
Zr	3.263E-3	3.263E-3	3.263E-3											
²³⁴U	5.470E-9	4.486E-7	6.710E-9											
²³⁵U	1.443E-5	1.433E-5	1.421E-5											
²³⁶U	9.199E-7	8.718E-7	8.319E-7											
²³⁸U	9.048E-3	8.834E-3	8.643E-3											
²³⁷Np	1.718E-6	8.095E-5	1.399E-6											
²³⁶Pu	6.227E-12	4.061E-10	4.075E-12											
²³⁸Pu	4.289E-7	4.050E-5	4.418E-7											
²³⁹Pu	1.566E-3	1.053E-3	1.927E-3											
²⁴⁰Pu	1.673E-4	4.868E-4	2.041E-4											
²⁴¹Pu	1.098E-5	1.317E-4	1.322E-5											
²⁴²Pu	7.849E-7	9.807E-5	9.224E-7											
²⁴¹Am	6.357E-7	9.533E-5	9.966E-7											
^{242m}Am	1.274E-8	2.610E-6	1.824E-8											
²⁴³Am	2.744E-8	1.952E-5	3.382E-8											
²⁴²Cm	2.107E-8	3.291E-6	2.519E-8											
²⁴³Cm	3.317E-10	1.093E-7	4.051E-10											
²⁴⁴Cm	2.161E-9	4.915E-6	2.474E-9											
²⁴⁵Cm	8.530E-11	4.372E-7	8.936E-11											
²⁴⁶Cm	1.168E-12	3.028E-8	1.077E-12											

Table 2. SFR geometry and homogenised compositions [10^{24} at/cm³]



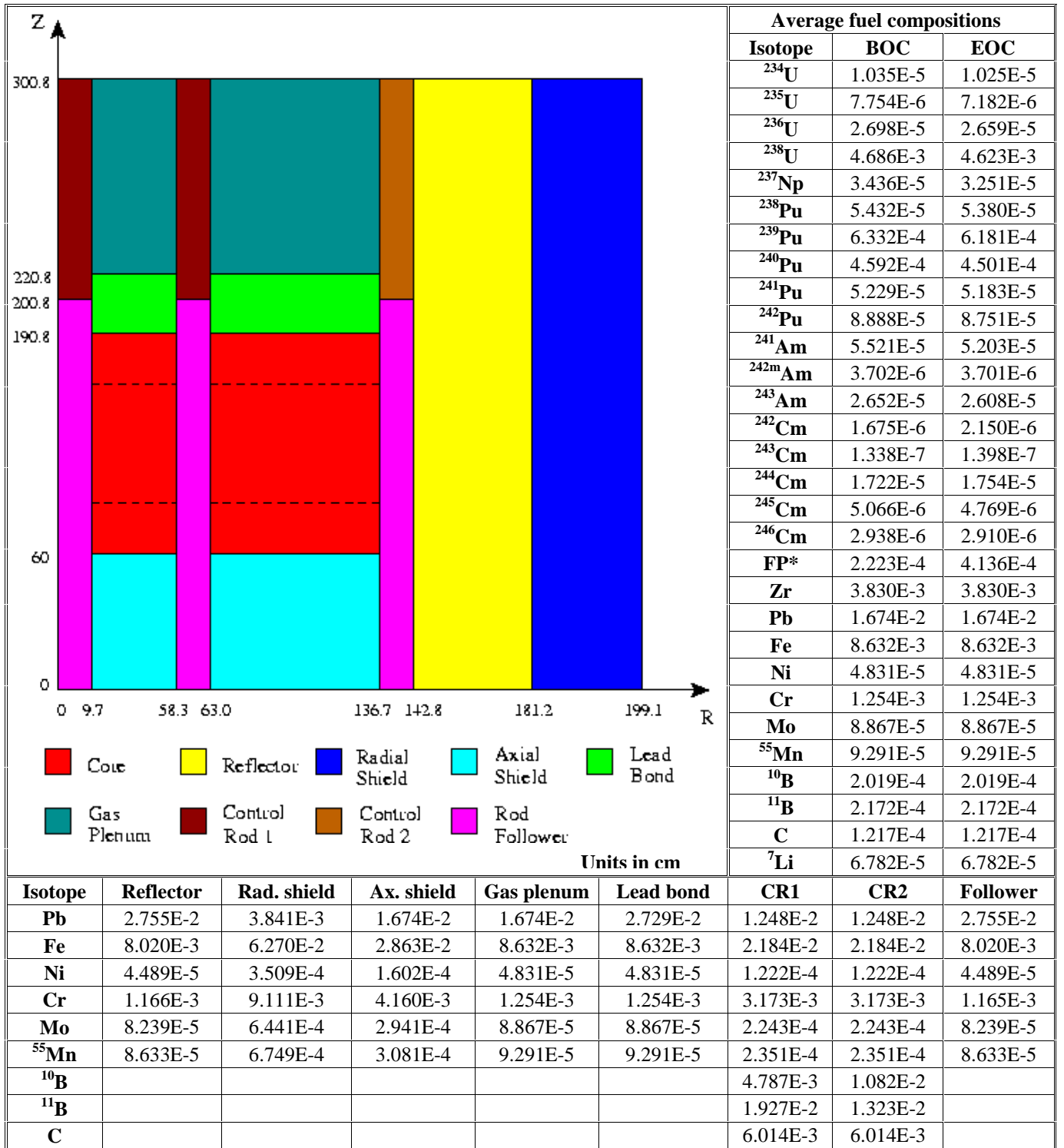
* Fission products

Table 4. GFR geometry and homogenised compositions [10^{24} at/cm³]



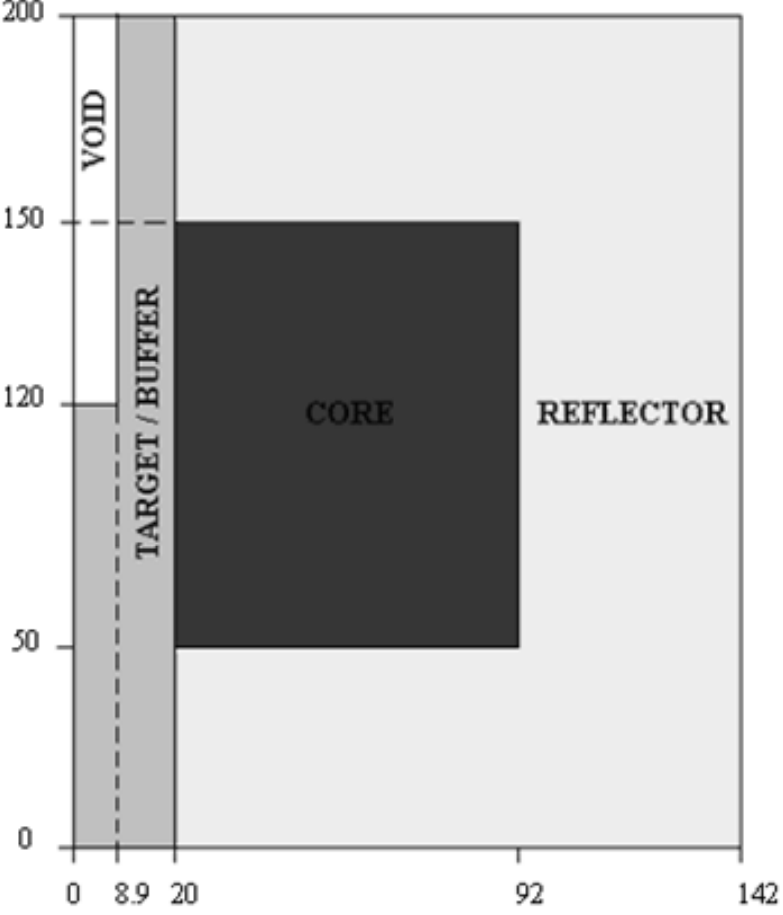
* Fission products

Table 5. LFR geometry and homogenised compositions [10^{24} at/cm³]



* Fission products

Table 6. ADMAB geometry and homogenised compositions [10^{24} at/cm³]

	Fuel		Reflector		Reflector		Reflector	
	BOC	EOC						
²³⁷ Np	4.377E-4	3.971E-4	⁵⁴ Fe	2.990E-3	⁵⁸ Ni	1.977E-4	Bi	5.039E-3
²³⁸ Pu	4.226E-5	9.415E-5	⁵⁶ Fe	4.560E-2	⁶⁰ Ni	7.305E-5	¹⁸² W	2.140E-5
²³⁹ Pu	5.051E-4	4.451E-4	⁵⁷ Fe	1.075E-3	⁶¹ Ni	3.111E-6	¹⁸³ W	1.155E-5
²⁴⁰ Pu	2.321E-4	2.399E-4	⁵⁸ Fe	1.344E-4	⁶² Ni	9.724E-6	¹⁸⁴ W	2.465E-5
²⁴¹ Pu	1.232E-4	1.051E-4	⁵⁰ Cr	3.458E-4	⁶⁴ Ni	2.388E-6	¹⁸⁶ W	2.280E-5
²⁴² Pu	9.102E-5	1.006E-4	⁵² Cr	6.422E-3	Mo	3.565E-4	Target/buffer	
²⁴¹ Am	8.084E-4	7.220E-4	⁵³ Cr	7.134E-4	Mn	3.412E-4	Pb	1.320E-2
^{242m} Am	1.089E-5	1.923E-5	⁵⁴ Cr	1.741E-4	Pb	4.075E-3	Bi	1.632E-2
²⁴³ Am	5.827E-4	5.303E-4						
²⁴² Cm	4.079E-8	2.686E-5						
²⁴³ Cm	3.326E-6	3.141E-6						
²⁴⁴ Cm	2.371E-4	2.599E-4						
²⁴⁵ Cm	3.164E-5	3.314E-5						
²⁴⁶ Cm	5.355E-7	1.032E-6						
Zr	7.477E-3	7.477E-3						
¹⁵ N	1.058E-2	1.058E-2						
⁵⁴ Fe	9.759E-4	9.759E-4						
⁵⁶ Fe	1.488E-2	1.488E-2						
⁵⁷ Fe	3.507E-4	3.507E-4						
⁵⁸ Fe	4.386E-5	4.386E-5						
⁵⁰ Cr	1.128E-4	1.128E-4						
⁵² Cr	2.096E-3	2.096E-3						
⁵³ Cr	2.328E-4	2.328E-4						
⁵⁴ Cr	5.682E-5	5.682E-5						
⁵⁸ Ni	6.451E-5	6.451E-5						
⁶⁰ Ni	2.384E-5	2.384E-5						
⁶¹ Ni	1.015E-6	1.015E-6						
⁶² Ni	3.173E-6	3.173E-6						
⁶⁴ Ni	7.792E-7	7.792E-7						
Mo	1.163E-4	1.163E-4						
Mn	1.114E-4	1.114E-4						
Pb	6.360E-3	6.360E-3						
Bi	7.865E-3	7.865E-3						
¹⁸² W	6.984E-6	6.984E-6						
¹⁸³ W	3.770E-6	3.770E-6						
¹⁸⁴ W	8.045E-6	8.045E-6						
¹⁸⁶ W	7.439E-6	7.439E-6						
FP*	—	2.636E-4						

* Fission products

Table 7. VHTR geometry and homogenised compositions [10^{24} at/cm³]

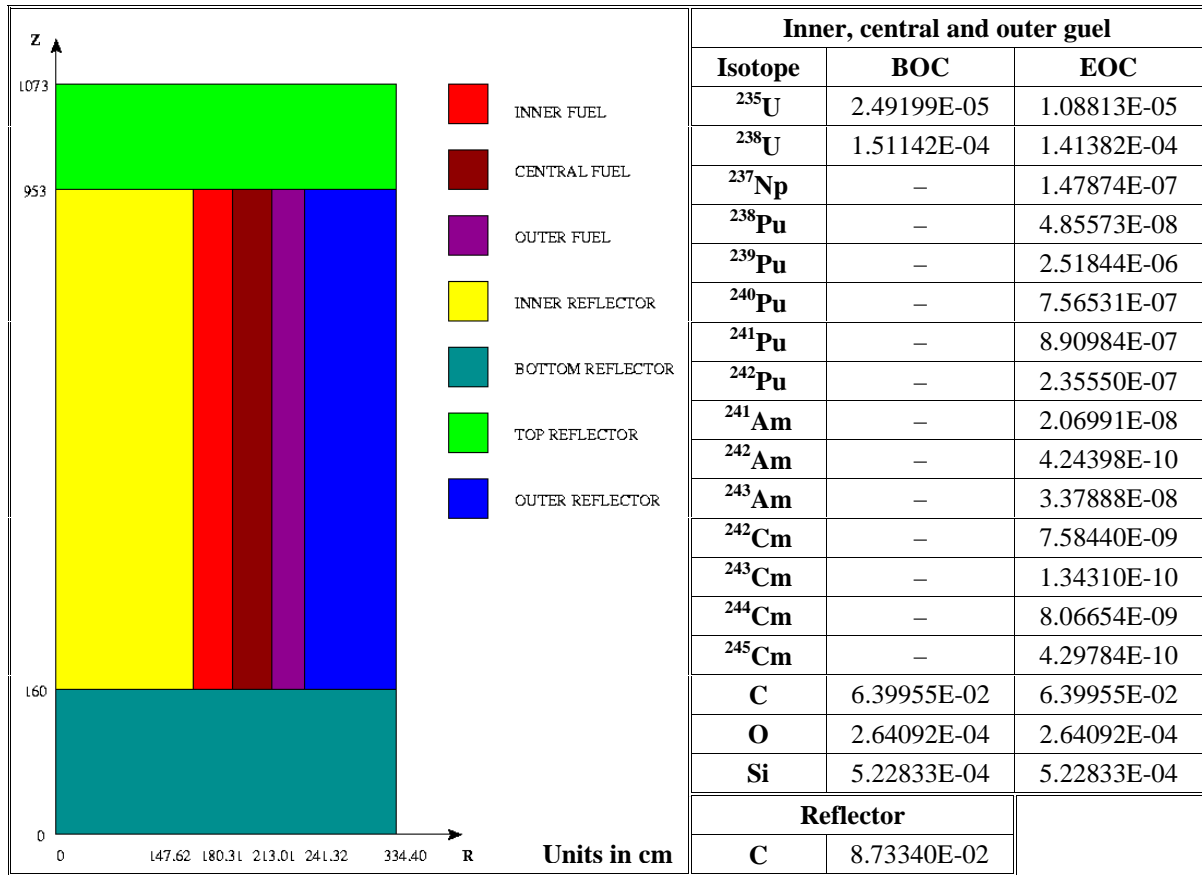
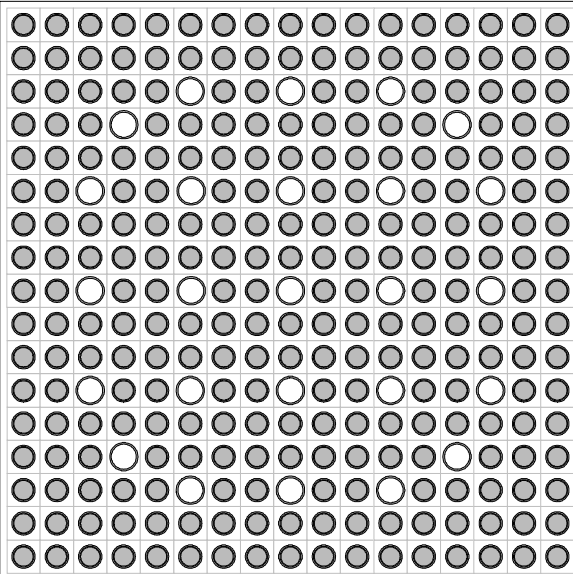
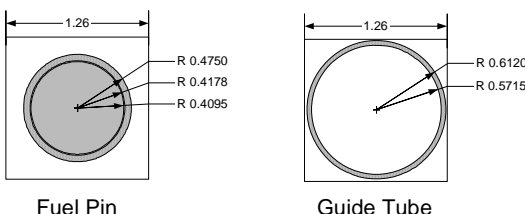


Table 8. PWR homogenised compositions [10^{-24} at/cm³] and fuel cell configuration

	BOC	EOC	21.50 cm															
²³³ U	3.00874E-20	1.11230E-12																
²³⁴ U	3.00874E-20	1.33133E-07																
²³⁵ U	5.72117E-04	6.39785E-05																
²³⁶ U	3.00874E-20	8.30524E-05																
²³⁷ U	3.00874E-20	1.13755E-07																
²³⁸ U	6.15867E-03	5.75867E-03																
²³⁷ Np	3.00874E-20	9.53439E-06																
²³⁹ Np	3.00874E-20	5.80481E-07																
²³⁸ Pu	3.00874E-20	7.04225E-06																
²³⁹ Pu	3.00874E-20	5.06995E-05																
²⁴⁰ Pu	3.00874E-20	2.52296E-05																
²⁴¹ Pu	3.00874E-20	1.70583E-05																
²⁴² Pu	3.00874E-20	1.04317E-05																
O	2.74355E-02	2.74355E-02																
H	2.79357E-02	2.79357E-02																
Zr	4.28183E-03	4.28183E-03																
FP*	2.70787E-18	2.34418E-03																

* Fission products

Appendix L
ISOTOPE CONTRIBUTIONS

Table 1. ABTR: isotope contribution (%)

Isotope	Decay heat	Dose	Neutron source
²¹⁰ Pb	—	0.97	—
²²⁶ Ra	—	0.37	—
²²⁷ Ac	—	0.18	—
²²⁹ Th	—	0.48	—
²³⁰ Th	—	0.28	—
²³¹ Pa	—	0.14	—
²³³ U	—	0.05	—
²³⁴ U	0.01	0.11	—
²³⁵ U	—	0.01	—
²³⁶ U	—	0.06	—
²³⁸ U	—	0.01	—
²³⁷ Np	—	0.24	—
²³⁸ Pu	13.64	—	2.51
²³⁹ Pu	33.09	96.53	2.29
²⁴⁰ Pu	16.37	0.02	4.13
²⁴¹ Pu	0.01	—	—
²⁴² Pu	0.01	0.54	0.31
²⁴¹ Am	35.76	—	1.25
^{242m} Am	0.01	—	—
²⁴³ Am	0.14	—	0.02
²⁴² Cm	0.59	—	7.30
²⁴³ Cm	0.02	—	0.02
²⁴⁴ Cm	0.35	—	81.74
²⁴⁶ Cm	—	—	0.44
Total	100.00	100.00	100.00

Table 2. SFR: isotope contribution (%)

Isotope	Decay heat	Dose	Neutron source
²¹⁰ Pb	—	28.01	—
²²⁶ Ra	—	10.76	—
²²⁷ Ac	—	0.06	—
²²⁹ Th	—	2.78	—
²³⁰ Th	—	7.95	—
²³¹ Pa	—	0.05	—
²³³ U	—	0.28	—
²³⁴ U	0.02	3.20	—
²³⁶ U	—	0.18	—
²³⁷ Np	—	1.38	—
²³⁸ Pu	46.51	—	0.59
²³⁹ Pu	1.37	34.71	0.01
²⁴⁰ Pu	6.82	0.07	0.13
²⁴² Pu	0.03	10.52	0.06
²⁴¹ Am	26.61	0.01	0.10
^{242m} Am	0.17	—	—
²⁴³ Am	0.65	0.02	0.01
²⁴² Cm	12.91	—	1.53
²⁴³ Cm	0.10	—	0.01
²⁴⁴ Cm	4.59	—	87.12
²⁴⁵ Cm	0.10	0.01	—
²⁴⁶ Cm	0.10	—	10.44
²⁴⁸ Cm	—	—	0.01
Total	100.00	100.00	100.00

Table 3. EFR: isotope contribution (%)

Isotope	Decay heat	Dose	Neutron source
²¹⁰ Pb	—	11.83	—
²²⁶ Ra	—	4.54	—
²²⁷ Ac	—	0.13	—
²²⁹ Th	—	1.90	—
²³⁰ Th	—	3.36	—
²³¹ Pa	—	0.10	—
²³³ U	—	0.19	—
²³⁴ U	0.02	1.35	—
²³⁵ U	—	0.01	—
²³⁶ U	—	0.23	—
²³⁸ U	—	0.01	—
²³⁷ Np	—	0.94	—
²³⁸ Pu	34.15	—	0.67
²³⁹ Pu	5.58	70.45	0.04
²⁴⁰ Pu	14.72	0.08	0.39
²⁴¹ Pu	0.01	—	—
²⁴² Pu	0.03	4.87	0.07
²⁴¹ Am	39.38	—	0.14
^{242m} Am	0.03	—	—
²⁴³ Am	0.39	0.01	—
²⁴² Cm	1.96	—	1.95
²⁴³ Cm	0.21	—	0.02
²⁴⁴ Cm	3.42	—	85.82
²⁴⁵ Cm	0.05	—	—
²⁴⁶ Cm	0.06	—	7.38
Total	100.00	100.00	100.00

Table 4. GFR: isotope contribution (%)

Isotope	Decay heat	Dose	Neutron source
²¹⁰ Pb	—	16.31	—
²²⁶ Ra	—	6.27	—
²²⁷ Ac	—	0.10	—
²²⁹ Th	—	5.11	—
²³⁰ Th	—	4.63	—
²³¹ Pa	—	0.08	—
²³³ U	—	0.51	—
²³⁴ U	0.01	1.87	—
²³⁵ U	—	0.01	—
²³⁶ U	—	0.14	—
²³⁸ U	—	0.01	—
²³⁷ Np	—	2.52	—
²³⁸ Pu	31.93	—	0.83
²³⁹ Pu	2.24	53.61	0.02
²⁴⁰ Pu	5.30	0.05	0.18
²⁴² Pu	0.03	8.75	0.10
²⁴¹ Am	55.27	—	0.55
^{242m} Am	0.02	—	—
²⁴³ Am	0.68	0.02	0.01
²⁴² Cm	1.54	—	4.42
²⁴³ Cm	0.12	—	0.02
²⁴⁴ Cm	2.79	—	92.35
²⁴⁵ Cm	0.05	—	—
²⁴⁶ Cm	0.01	—	1.51
Total	100.00	100.00	100.00

Table 5. LFR: isotope contribution (%)

Isotope	Decay heat	Dose	Neutron source
²¹⁰ Pb	—	18.40	—
²²⁶ Ra	—	7.07	—
²²⁷ Ac	—	0.11	—
²²⁹ Th	—	2.27	—
²³⁰ Th	—	5.22	—
²³¹ Pa	—	0.08	—
²³³ U	—	0.23	—
²³⁴ U	0.02	2.10	—
²³⁵ U	—	0.01	—
²³⁶ U	—	0.19	—
²³⁸ U	—	0.01	—
²³⁷ Np	—	1.12	—
²³⁸ Pu	46.33	—	0.86
²³⁹ Pu	3.75	56.32	0.03
²⁴⁰ Pu	10.45	0.07	0.26
²⁴² Pu	0.03	6.78	0.08
²⁴¹ Am	32.75	0.01	0.18
^{242m} Am	0.03	—	—
²⁴³ Am	0.55	0.01	0.01
²⁴² Cm	2.21	—	1.37
²⁴³ Cm	0.07	—	0.01
²⁴⁴ Cm	3.62	—	84.99
²⁴⁵ Cm	0.09	—	—
²⁴⁶ Cm	0.10	—	12.21
²⁴⁸ Cm	—	—	0.01
Total	100.00	100.00	100.00

Table 6. ADMAB: isotope contribution (%)

Isotope	Decay heat	Dose	Neutron source
²¹⁰ Pb	—	23.41	—
²²⁶ Ra	—	8.99	—
²²⁷ Ac	—	0.06	—
²²⁹ Th	—	7.71	—
²³⁰ Th	—	6.64	—
²³¹ Pa	—	0.04	—
²³³ U	—	0.78	—
²³⁴ U	0.01	2.70	—
²³⁶ U	—	0.09	—
²³⁷ Np	0.01	3.86	—
²³⁸ Pu	32.29	—	0.21
²³⁹ Pu	0.50	41.90	—
²⁴⁰ Pu	2.30	0.04	0.01
²⁴² Pu	0.01	3.66	0.01
²⁴¹ Am	47.16	0.02	0.15
^{242m} Am	0.03	—	—
²⁴³ Am	2.22	0.08	0.01
²⁴² Cm	3.27	—	1.33
²⁴³ Cm	0.36	—	0.01
²⁴⁴ Cm	11.34	—	97.81
²⁴⁵ Cm	0.13	0.02	—
²⁴⁶ Cm	0.01	—	0.47
PF	0.36	—	—
Total	100.00	100.00	100.00

Table 7. VHTR: isotope contribution (%)

Isotope	Decay heat	Dose	Neutron source
²¹⁰ Pb	—	8.80	—
²²⁶ Ra	—	3.38	—
²²⁷ Ac	—	0.74	—
²²⁹ Th	—	6.17	—
²³⁰ Th	—	2.50	—
²³¹ Pa	—	0.58	—
²³³ U	—	0.62	—
²³⁴ U	0.01	1.02	—
²³⁵ U	—	0.05	—
²³⁶ U	—	0.54	—
²³⁸ U	—	0.11	—
²³⁷ Np	0.01	3.04	—
²³⁸ Pu	18.77	—	1.32
²³⁹ Pu	3.06	63.00	0.08
²⁴⁰ Pu	4.11	0.04	0.38
²⁴¹ Pu	0.02	—	—
²⁴² Pu	0.03	9.42	0.30
²⁴¹ Am	72.45	—	0.29
²⁴³ Am	0.35	0.01	0.01
²⁴² Cm	0.09	—	5.23
²⁴³ Cm	0.03	—	0.01
²⁴⁴ Cm	1.06	—	92.14
²⁴⁵ Cm	0.01	—	—
²⁴⁶ Cm	—	—	0.23
Total	100.00	100.00	100.00

Table 8. PWR: isotope contribution (%)

Isotope	Decay heat	Dose	Neutron source
²¹⁰ Pb	—	20.03	—
²²⁶ Ra	—	7.70	—
²²⁷ Ac	—	0.23	—
²²⁹ Th	—	4.51	—
²³⁰ Th	—	5.69	—
²³¹ Pa	—	0.18	—
²³³ U	—	0.45	—
²³⁴ U	0.02	2.31	—
²³⁵ U	—	0.02	—
²³⁶ U	—	0.44	—
²³⁸ U	—	0.12	—
²³⁷ Np	0.01	2.22	—
²³⁸ Pu	44.92	—	1.02
²³⁹ Pu	2.39	48.39	0.02
²⁴⁰ Pu	4.65	0.04	0.13
²⁴¹ Pu	0.01	—	—
²⁴² Pu	0.03	7.68	0.08
²⁴¹ Am	43.87	—	0.07
²⁴³ Am	0.50	0.01	0.01
²⁴² Cm	0.09	—	1.78
²⁴³ Cm	0.06	—	0.01
²⁴⁴ Cm	3.41	—	95.31
²⁴⁵ Cm	0.03	—	—
²⁴⁶ Cm	0.01	—	1.56
Total	100.00	100.00	100.00

Appendix M

TOTAL ISOTOPE UNCERTAINTY BREAKDOWN

Table 1. ABTR BOLNA diagonal uncertainties (%) – breakdown by isotope

	k_{eff}	Power peak	Doppler	Void	Burn-up XS [pcm]	Burn-up Δn [pcm]	Burn-up total [pcm]
²³⁵ U	0.01	–	0.02	0.04	0.2	0.2	0.4
²³⁸ U	0.52	0.24	2.12	3.64	12.9	0.5	13.4
²³⁸ Pu	0.01	0.01	0.02	0.03	1.0	0.2	1.2
²³⁹ Pu	0.25	0.08	1.14	1.81	3.3	20.7	24.0
²⁴⁰ Pu	0.08	0.01	0.20	0.49	5.4	1.6	7.0
²⁴¹ Pu	0.07	0.04	0.21	0.27	3.2	3.6	6.8
²⁴² Pu	0.01	0.01	0.03	0.03	0.3	0.1	0.4
²³⁷ Np	–	–	0.03	0.01	0.2	–	0.2
²⁴¹ Am	0.01	0.01	0.03	0.01	0.1	–	0.2
^{242m} Am	–	–	–	–	0.2	0.1	0.3
²⁴³ Am	–	–	0.01	–	–	–	0.1
²⁴² Cm	–	–	–	–	0.3	0.1	0.3
²⁴³ Cm	–	–	–	–	–	–	–
²⁴⁴ Cm	–	–	–	–	0.2	–	0.2
²⁴⁵ Cm	–	–	–	–	–	–	0.1
²⁴⁶ Cm	–	–	–	–	–	–	–
⁵⁶ Fe	0.18	0.13	1.17	0.69	6.3	–	6.3
⁵² Cr	0.04	0.06	0.34	0.16	0.7	–	0.7
⁵⁸ Ni	–	0.01	0.11	0.03	0.1	–	0.1
⁹⁰ Zr	0.03	0.03	0.11	0.17	0.9	–	0.9
²³ Na	0.07	0.10	0.87	2.97	2.5	–	2.5
¹⁶ O	–	–	–	–	–	–	–
C	–	–	–	–	–	–	–
¹⁰ B	0.02	0.07	0.15	0.01	0.5	–	0.5
Total	0.62	0.32	2.86	5.11	16.3	21.1	37.4

Table 2. ABTR BOLNA full uncertainties (%) – breakdown by isotope

	k_{eff}	Power peak	Doppler	Void	Burn-up XS [pcm]	Burn-up Δn [pcm]	Burn-up total [pcm]
²³⁵ U	0.01	0.04	–	0.06	0.3	0.5	0.8
²³⁸ U	0.77	3.40	0.16	3.74	19.5	0.6	20.1
²³⁸ Pu	0.02	0.03	0.02	0.04	1.8	0.4	2.1
²³⁹ Pu	0.36	1.62	0.11	2.14	4.5	25.6	30.2
²⁴⁰ Pu	0.13	0.32	0.03	0.44	9.4	2.7	12.1
²⁴¹ Pu	0.12	0.34	0.07	0.27	6.0	7.3	13.3
²⁴² Pu	0.01	0.05	0.01	0.03	0.5	0.1	0.6
²³⁷ Np	0.01	0.04	0.01	0.01	0.3	0.1	0.3
²⁴¹ Am	0.01	0.05	0.01	0.02	0.2	0.1	0.3
^{242m} Am	–	0.01	–	–	0.4	0.2	0.5
²⁴³ Am	–	0.01	–	–	–	–	0.1
²⁴² Cm	–	–	–	–	0.5	0.1	0.6
²⁴³ Cm	–	–	–	–	0.1	–	0.1
²⁴⁴ Cm	–	0.01	–	0.01	0.3	–	0.3
²⁴⁵ Cm	–	–	–	–	0.1	–	0.1
²⁴⁶ Cm	–	–	–	–	–	–	–
⁵⁶ Fe	0.27	1.60	0.18	0.78	9.2	–	9.2
⁵² Cr	0.06	0.45	0.08	0.17	1.0	–	1.0
⁵⁸ Ni	–	0.12	0.01	0.03	0.1	–	0.1
⁹⁰ Zr	0.04	0.13	0.05	0.22	1.0	–	1.0
²³ Na	0.08	1.51	0.13	4.10	3.1	–	3.1
¹⁶ O	–	–	–	–	–	–	–
C	–	–	–	–	–	–	–
¹⁰ B	0.04	0.23	0.11	0.02	0.8	–	0.8
Total	0.92	4.42	0.34	6.03	25.0	26.8	51.8

Table 3. SFR BOLNA diagonal uncertainties (%) – breakdown by isotope

	k_{eff}	Power peak	Doppler	Void	Burn-up XS [pcm]	Burn-up Δn [pcm]	Burn-up total [pcm]
²³⁵ U	–	–	0.01	0.03	0.1	0.4	0.5
²³⁸ U	0.16	0.05	0.60	1.65	10.0	0.5	10.5
²³⁸ Pu	0.34	0.01	0.86	2.72	30.1	15.5	45.6
²³⁹ Pu	0.13	0.02	0.49	1.39	5.1	15.5	20.6
²⁴⁰ Pu	0.38	0.03	0.96	3.83	26.8	5.4	32.2
²⁴¹ Pu	0.52	0.02	1.70	4.34	41.2	48.6	89.8
²⁴² Pu	0.26	0.02	0.74	2.65	21.1	3.3	24.4
²³⁷ Np	0.03	0.01	0.23	0.40	1.0	0.2	1.2
²⁴¹ Am	0.07	0.01	0.34	0.62	2.6	0.8	3.4
^{242m} Am	0.37	0.02	1.08	3.06	14.7	35.7	50.4
²⁴³ Am	0.05	0.01	0.31	0.53	3.5	2.3	5.8
²⁴² Cm	0.02	–	0.06	0.14	7.0	1.7	8.6
²⁴³ Cm	0.01	–	0.02	0.05	1.3	1.0	2.3
²⁴⁴ Cm	0.27	0.01	0.66	2.84	37.4	5.2	42.6
²⁴⁵ Cm	0.19	0.01	0.49	1.28	13.6	17.9	31.5
²⁴⁶ Cm	0.02	–	0.09	0.22	2.2	0.3	2.5
⁵⁶ Fe	0.37	0.13	1.89	4.44	31.4	–	31.4
⁵² Cr	0.04	0.01	0.27	0.47	2.2	–	2.2
⁵⁸ Ni	–	–	0.09	0.03	0.2	–	0.2
⁹⁰ Zr	0.03	0.02	0.10	0.24	2.3	–	2.3
²³ Na	0.23	0.10	1.25	12.29	19.6	–	19.6
¹⁰ B	0.12	0.24	0.22	1.16	8.7	–	8.7
Total	1.04	0.31	3.62	15.66	85.0	67.2	152.1

Table 4. SFR BOLNA full uncertainties (%) – breakdown by isotope

	k_{eff}	Power peak	Doppler	Void	Burn-up XS [pcm]	Burn-up Δn [pcm]	Burn-up total [pcm]
²³⁵ U	–	–	0.01	0.04	0.2	0.8	1.0
²³⁸ U	0.24	0.07	0.94	2.43	15.5	0.5	16.0
²³⁸ Pu	0.64	0.02	1.50	3.00	55.9	27.3	83.2
²³⁹ Pu	0.19	0.04	0.71	1.75	7.0	22.3	29.3
²⁴⁰ Pu	0.66	0.05	1.60	3.86	46.5	10.4	56.9
²⁴¹ Pu	0.96	0.02	2.77	4.12	73.8	96.4	170.2
²⁴² Pu	0.41	0.03	1.15	3.37	32.3	5.2	37.5
²³⁷ Np	0.06	0.01	0.31	0.51	1.7	0.4	2.1
²⁴¹ Am	0.11	0.01	0.55	0.91	4.2	1.3	5.6
^{242m} Am	0.73	0.02	1.84	3.73	29.6	71.1	100.7
²⁴³ Am	0.07	0.01	0.49	0.78	5.1	3.7	8.8
²⁴² Cm	0.04	–	0.10	0.13	12.7	2.8	15.5
²⁴³ Cm	0.02	–	0.04	0.03	2.6	1.9	4.5
²⁴⁴ Cm	0.40	0.02	1.00	3.01	56.6	7.9	64.5
²⁴⁵ Cm	0.39	0.01	0.95	1.00	26.9	35.3	62.2
²⁴⁶ Cm	0.04	–	0.14	0.28	3.6	0.5	4.1
⁵⁶ Fe	0.55	0.20	2.48	4.47	47.0	–	47.0
⁵² Cr	0.06	0.01	0.38	0.51	2.9	–	2.9
⁵⁸ Ni	–	–	0.10	0.04	0.2	–	0.2
⁹⁰ Zr	0.03	0.03	0.12	0.29	2.5	–	2.5
²³ Na	0.25	0.13	1.85	13.53	21.6	–	21.6
¹⁰ B	0.17	0.36	0.35	1.53	12.8	–	12.8
Total	1.82	0.45	5.57	17.11	141.2	130.7	271.9

Table 5. EFR BOLNA diagonal uncertainties (%) – breakdown by isotope

	k_{eff}	Power peak	Doppler	Void	Burn-up XS [pcm]	Burn-up Δn [pcm]	Burn-up total [pcm]
²³⁵ U	–	–	0.01	0.02	1.2	2.5	3.7
²³⁸ U	0.59	0.66	1.75	2.12	39.2	30.5	69.7
²³⁸ Pu	0.07	0.03	0.22	0.29	13.2	23.1	36.3
²³⁹ Pu	0.23	0.07	0.88	1.47	20.1	350.5	370.6
²⁴⁰ Pu	0.23	0.09	0.61	0.98	32.9	28.2	61.1
²⁴¹ Pu	0.20	0.06	0.72	1.40	157.8	178.3	336.1
²⁴² Pu	0.06	0.02	0.18	0.20	5.8	4.1	10.0
²³⁷ Np	–	–	0.02	0.03	0.2	1.5	1.7
²⁴¹ Am	0.04	0.02	0.19	0.23	12.1	6.0	18.1
^{242m} Am	0.01	0.01	0.04	0.09	5.1	10.6	15.7
²⁴³ Am	0.01	0.01	0.05	0.06	1.6	9.8	11.3
²⁴² Cm	–	–	–	–	11.6	0.6	12.3
²⁴³ Cm	–	–	0.01	0.02	2.3	3.6	5.9
²⁴⁴ Cm	0.04	0.01	0.09	0.18	28.1	5.3	33.4
²⁴⁵ Cm	0.03	0.02	0.07	0.10	8.5	18.3	26.9
²⁴⁶ Cm	–	–	0.02	0.02	0.3	0.3	0.6
⁵⁶ Fe	0.17	0.17	0.56	0.92	43.3	–	43.3
⁵² Cr	0.01	0.04	0.07	0.07	3.7	–	3.7
⁵⁸ Ni	0.06	0.04	0.40	0.17	10.3	–	10.3
²³ Na	0.12	0.17	0.62	5.73	31.9	–	31.9
¹⁶ O	0.27	0.39	0.60	1.03	54.9	–	54.9
Total	0.79	0.81	2.46	6.68	188.0	396.9	584.9

Table 6. EFR BOLNA full uncertainties (%) – breakdown by isotope

	k_{eff}	Power peak	Doppler	Void	Burn-up XS [pcm]	Burn-up Δn [pcm]	Burn-up total [pcm]
²³⁵ U	0.01	–	0.02	0.01	2.5	5.0	7.5
²³⁸ U	0.88	0.90	2.79	3.10	50.0	32.9	82.8
²³⁸ Pu	0.15	0.04	0.36	0.22	26.2	41.9	68.1
²³⁹ Pu	0.32	0.09	1.08	1.49	28.2	411.5	439.7
²⁴⁰ Pu	0.43	0.13	1.02	0.79	59.8	49.7	109.5
²⁴¹ Pu	0.36	0.07	1.13	1.34	276.0	358.1	634.0
²⁴² Pu	0.09	0.03	0.28	0.13	8.9	7.0	15.9
²³⁷ Np	0.01	–	0.03	0.03	0.4	1.8	2.2
²⁴¹ Am	0.06	0.03	0.31	0.24	20.0	10.7	30.8
^{242m} Am	0.03	0.02	0.06	0.08	9.9	20.8	30.8
²⁴³ Am	0.01	0.01	0.08	0.07	2.4	16.6	19.0
²⁴² Cm	–	–	–	–	22.0	1.2	23.2
²⁴³ Cm	0.01	0.01	0.02	0.02	4.6	7.0	11.6
²⁴⁴ Cm	0.06	0.02	0.14	0.18	43.0	8.5	51.5
²⁴⁵ Cm	0.06	0.04	0.13	0.10	16.9	35.5	52.5
²⁴⁶ Cm	0.01	–	0.02	0.02	0.6	0.5	1.1
⁵⁶ Fe	0.26	0.27	0.86	0.95	64.0	–	64.0
⁵² Cr	0.01	0.06	0.12	0.07	4.9	–	4.9
⁵⁸ Ni	0.08	0.05	0.48	0.22	12.1	–	12.1
²³ Na	0.14	0.25	0.88	6.72	39.8	–	39.8
¹⁶ O	0.27	0.65	1.05	0.88	93.3	–	93.3
Total	1.18	1.18	3.80	7.83	318.6	552.4	871.0

Table 7. GFR BOLNA diagonal uncertainties (%) – breakdown by isotope

	k_{eff}	Power peak	Doppler	Void	Burn-up XS [pcm]	Burn-up Δn [pcm]	Burn-up total [pcm]
²³⁵ U	0.03	0.03	0.11	0.11	6.0	7.3	13.3
²³⁸ U	1.01	1.12	2.70	3.83	46.6	7.3	53.9
²³⁸ Pu	0.13	0.04	0.31	0.31	30.9	13.4	44.3
²³⁹ Pu	0.23	0.05	0.76	0.80	5.5	129.4	134.9
²⁴⁰ Pu	0.19	0.07	0.42	0.57	3.8	6.8	10.6
²⁴¹ Pu	0.47	0.09	1.47	1.43	64.6	67.7	132.3
²⁴² Pu	0.17	0.06	0.47	0.53	9.2	2.3	11.5
²³⁷ Np	0.04	0.03	0.16	0.12	4.7	1.3	6.0
²⁴¹ Am	0.21	0.13	0.79	0.57	27.2	7.4	34.6
^{242m} Am	0.01	0.01	0.02	0.02	27.2	12.6	39.8
²⁴³ Am	0.04	0.03	0.18	0.13	2.9	7.0	9.8
²⁴² Cm	–	–	–	–	41.0	4.8	45.8
²⁴³ Cm	–	–	0.01	0.01	2.8	2.2	5.0
²⁴⁴ Cm	0.09	0.06	0.21	0.28	20.6	2.4	23.0
²⁴⁵ Cm	0.06	0.05	0.14	0.15	2.6	10.1	12.7
²⁴⁶ Cm	–	–	–	–	0.3	–	0.3
C	0.21	0.17	1.20	1.59	5.5	–	5.5
⁴ He	0.01	0.01	0.03	2.89	0.2	–	0.2
²⁸ Si	0.24	0.23	0.61	0.63	5.5	–	5.5
⁹⁰ Zr	0.01	0.12	0.05	0.06	1.0	–	1.0
Total	1.24	1.18	3.62	5.46	105.6	148.6	254.2

Table 8. GFR BOLNA full uncertainties (%) – breakdown by isotope

	k_{eff}	Power peak	Doppler	Void	Burn-up XS [pcm]	Burn-up Δn [pcm]	Burn-up total [pcm]
²³⁵ U	0.07	0.05	0.14	0.17	11.5	14.7	26.2
²³⁸ U	1.48	1.57	4.13	5.56	66.1	7.8	73.9
²³⁸ Pu	0.25	0.07	0.53	0.32	61.5	24.1	85.6
²³⁹ Pu	0.30	0.07	0.86	0.92	7.1	143.7	150.7
²⁴⁰ Pu	0.35	0.12	0.73	0.53	6.5	9.8	16.3
²⁴¹ Pu	0.82	0.16	2.21	1.66	113.6	127.0	240.6
²⁴² Pu	0.27	0.09	0.68	0.68	14.4	3.8	18.2
²³⁷ Np	0.06	0.04	0.24	0.16	8.3	2.3	10.6
²⁴¹ Am	0.34	0.22	1.37	0.90	44.9	12.9	57.8
^{242m} Am	0.01	0.01	0.03	0.03	53.1	22.4	75.4
²⁴³ Am	0.07	0.05	0.30	0.21	4.6	11.7	16.4
²⁴² Cm	–	–	–	–	77.1	8.4	85.6
²⁴³ Cm	0.01	0.01	0.02	0.01	5.8	3.7	9.5
²⁴⁴ Cm	0.13	0.09	0.32	0.27	31.6	4.1	35.7
²⁴⁵ Cm	0.12	0.10	0.28	0.17	5.4	19.9	25.2
²⁴⁶ Cm	–	–	0.01	–	0.4	0.1	0.5
C	0.31	0.29	1.91	1.65	8.3	–	8.3
⁴ He	0.02	0.01	0.05	4.38	0.3	–	0.3
²⁸ Si	0.27	0.27	0.75	0.65	6.3	–	6.3
⁹⁰ Zr	0.02	0.20	0.07	0.07	1.7	–	1.7
Total	1.88	1.68	5.51	7.67	183.1	197.6	380.7

Table 9. LFR BOLNA diagonal uncertainties (%) – breakdown by isotope

	k_{eff}	Power peak	Doppler	Void	Burn-up XS [pcm]	Burn-up Δn [pcm]	Burn-up total [pcm]
²³⁵ U	0.01	–	0.03	0.02	0.3	1.3	1.6
²³⁸ U	0.50	0.11	1.58	3.29	3.4	3.7	7.1
²³⁸ Pu	0.23	0.01	0.53	0.43	6.9	14.0	20.9
²³⁹ Pu	0.21	0.03	1.07	0.65	3.1	86.6	89.7
²⁴⁰ Pu	0.32	0.02	0.74	0.50	4.8	7.1	11.9
²⁴¹ Pu	0.33	0.02	0.85	0.86	13.8	58.4	72.3
²⁴² Pu	0.13	0.01	0.45	0.24	1.6	2.0	3.6
²³⁷ Np	0.02	–	0.10	0.05	0.7	0.2	0.9
²⁴¹ Am	0.05	0.01	0.18	0.13	1.4	1.2	2.6
^{242m} Am	0.04	–	0.09	0.10	1.6	6.0	7.6
²⁴³ Am	0.02	–	0.09	0.05	0.3	2.1	2.4
²⁴² Cm	0.01	–	0.03	0.02	4.9	1.6	6.5
²⁴³ Cm	–	–	0.01	0.01	0.5	0.7	1.2
²⁴⁴ Cm	0.11	0.01	0.26	0.11	7.4	2.4	9.8
²⁴⁵ Cm	0.11	0.01	0.25	0.26	2.7	14.6	17.3
²⁴⁶ Cm	0.01	–	0.03	0.02	0.3	0.2	0.4
⁵⁶ Fe	0.17	0.06	0.81	0.93	3.7	–	3.7
⁵² Cr	0.01	0.01	0.14	0.05	0.2	–	0.2
⁵⁸ Ni	–	–	0.05	0.01	–	–	–
⁹⁰ Zr	0.04	0.02	0.13	0.58	0.7	–	0.7
²⁰⁴ Pb	0.01	0.01	0.16	0.21	0.3	–	0.3
²⁰⁶ Pb	0.14	0.05	0.56	2.07	2.9	–	2.9
²⁰⁷ Pb	0.12	0.06	0.62	1.89	2.5	–	2.5
²⁰⁸ Pb	0.10	0.14	0.81	1.57	1.7	–	1.7
¹⁰ B	0.31	0.40	0.71	0.73	4.5	–	4.5
Total	0.88	0.45	2.85	4.97	20.7	107.0	127.7

Table 10. LFR BOLNA full uncertainties (%) – breakdown by isotope

	k_{eff}	Power peak	Doppler	Void	Burn-up XS [pcm]	Burn-up Δn [pcm]	Burn-up total [pcm]
²³⁵ U	0.01	–	0.04	0.03	0.6	2.6	3.2
²³⁸ U	0.78	0.08	2.59	4.73	4.5	4.0	8.5
²³⁸ Pu	0.42	0.02	0.85	0.60	12.5	23.9	36.4
²³⁹ Pu	0.31	0.05	1.35	0.87	4.2	102.0	106.1
²⁴⁰ Pu	0.56	0.03	1.18	0.70	8.3	13.6	21.9
²⁴¹ Pu	0.61	0.02	1.44	1.37	25.2	119.9	145.1
²⁴² Pu	0.19	0.02	0.68	0.37	2.4	3.2	5.5
²³⁷ Np	0.04	0.01	0.17	0.07	1.3	0.4	1.7
²⁴¹ Am	0.08	0.01	0.31	0.18	2.2	2.0	4.3
^{242m} Am	0.07	–	0.16	0.16	3.1	11.3	14.4
²⁴³ Am	0.03	0.01	0.17	0.06	0.3	3.4	3.7
²⁴² Cm	0.02	–	0.04	0.03	8.7	2.7	11.4
²⁴³ Cm	0.01	–	0.02	0.01	0.9	1.4	2.3
²⁴⁴ Cm	0.16	0.01	0.38	0.12	10.8	3.5	14.3
²⁴⁵ Cm	0.22	0.01	0.49	0.44	5.3	28.2	33.5
²⁴⁶ Cm	0.02	–	0.05	0.03	0.4	0.3	0.7
⁵⁶ Fe	0.25	0.08	1.09	1.51	5.4	–	5.4
⁵² Cr	0.01	0.01	0.20	0.07	0.2	–	0.2
⁵⁸ Ni	–	–	0.05	0.01	–	–	–
⁹⁰ Zr	0.04	0.04	0.16	0.62	0.9	–	0.9
²⁰⁴ Pb	0.03	0.02	0.26	0.46	0.6	–	0.6
²⁰⁶ Pb	0.20	0.08	0.88	3.10	4.3	–	4.3
²⁰⁷ Pb	0.17	0.08	0.86	2.61	3.4	–	3.4
²⁰⁸ Pb	0.14	0.22	1.15	2.17	2.3	–	2.3
¹⁰ B	0.44	0.57	1.02	1.14	6.6	–	6.6
Total	1.43	0.64	4.35	7.18	35.4	162.9	198.2

Table 11. ADMAB BOLNA diagonal uncertainties (%) – breakdown by isotope

	k_{eff}	Power peak	Void	Burn-up XS [pcm]	Burn-up Δn [pcm]	Burn-up total [pcm]
²³⁸ Pu	0.14	1.00	0.36	264.7	40.3	305.0
²³⁹ Pu	0.14	1.07	0.59	16.9	32.1	49.0
²⁴⁰ Pu	0.14	0.99	0.38	10.9	6.4	17.4
²⁴¹ Pu	0.56	4.08	1.45	73.8	75.8	149.6
²⁴² Pu	0.11	0.80	0.35	23.2	3.7	26.9
²³⁷ Np	0.21	1.54	0.85	21.8	–	21.8
²⁴¹ Am	0.61	4.37	3.13	75.2	2.6	77.8
^{242m} Am	0.07	0.53	0.21	86.6	37.8	124.5
²⁴³ Am	0.64	4.93	2.14	61.5	6.3	67.8
²⁴² Cm	–	–	–	174.6	16.8	191.4
²⁴³ Cm	0.06	0.43	0.12	6.1	12.5	18.6
²⁴⁴ Cm	1.35	9.53	2.83	270.7	45.1	315.8
²⁴⁵ Cm	0.50	3.69	1.13	79.4	101.3	180.8
²⁴⁶ Cm	–	0.01	0.01	2.8	0.4	3.2
⁵⁶ Fe	0.63	4.88	3.89	21.7	–	21.7
⁵⁷ Fe	0.02	0.17	0.09	1.2	–	1.2
⁵² Cr	0.01	0.09	0.23	0.5	–	0.5
⁵⁸ Ni	–	0.03	0.03	0.1	–	0.1
⁹⁰ Zr	0.09	0.69	1.49	2.7	–	2.7
¹⁵ N	0.19	1.62	0.56	7.5	–	7.5
Pb	0.06	0.39	2.92	4.5	–	4.5
²⁰⁹ Bi	0.28	2.02	10.88	7.5	–	7.5
Total	1.95	14.22	13.11	452.3	150.6	602.9

Table 12. ADMAB BOLNA full uncertainties (%) – breakdown by isotope

	k_{eff}	Power peak	Void	Burn-up XS [pcm]	Burn-up Δn [pcm]	Burn-up total [pcm]
²³⁸ Pu	0.25	1.79	0.47	477.3	74.0	551.3
²³⁹ Pu	0.20	1.54	0.76	24.9	47.6	72.5
²⁴⁰ Pu	0.23	1.68	0.48	20.2	10.8	31.0
²⁴¹ Pu	1.05	7.63	2.04	143.0	145.9	288.9
²⁴² Pu	0.17	1.20	0.49	35.3	6.2	41.6
²³⁷ Np	0.37	2.73	1.18	36.8	–	36.9
²⁴¹ Am	0.97	7.03	4.08	118.5	4.4	122.9
^{242m} Am	0.14	1.05	0.32	173.2	67.4	240.7
²⁴³ Am	0.63	4.88	2.22	67.8	10.5	78.3
²⁴² Cm	–	–	–	318.6	28.6	347.2
²⁴³ Cm	0.12	0.87	0.18	12.1	23.6	35.7
²⁴⁴ Cm	1.94	13.71	3.51	391.7	67.5	459.2
²⁴⁵ Cm	1.05	7.63	1.58	162.4	198.4	360.7
²⁴⁶ Cm	–	0.02	0.01	4.6	0.8	5.3
⁵⁶ Fe	0.93	7.23	5.53	15.8	–	15.8
⁵⁷ Fe	0.03	0.22	0.13	1.1	–	1.1
⁵² Cr	0.01	0.10	0.31	0.5	–	0.5
⁵⁸ Ni	–	0.03	0.03	0.1	–	0.1
⁹⁰ Zr	0.10	0.79	1.57	2.8	–	2.8
¹⁵ N	0.22	1.94	0.77	6.6	–	6.6
Pb	0.09	0.54	3.96	5.5	–	5.5
²⁰⁹ Bi	0.31	2.23	12.13	7.4	–	7.4
Total	2.94	21.42	15.49	763.1	281.3	1044.4

Table 13. VHTR BOLNA diagonal uncertainties (%) – breakdown by isotope

	k_{eff} BOC	Power peak BOC
²³⁵ U	0.34	0.09
²³⁸ U	0.12	0.02
O	–	–
Si	0.01	0.01
C	0.09	0.84
Total	0.37	0.85

Table 14. VHTR BOLNA diagonal uncertainties (%) – breakdown by isotope

	k_{eff} EOC	Power peak EOC	Doppler BOC	Doppler EOC	Burn-up XS [pcm]	Burn-up Δn pcm]	Burn-up total [pcm]
²³⁵ U	0.18	0.03	3.96	1.48	158.3	7.0	165.2
²³⁸ U	0.16	0.02	0.81	0.66	35.2	7.9	43.1
²³⁷ Np	0.01	–	–	0.04	5.3	3.5	8.8
²³⁸ Pu	–	–	–	0.01	0.7	0.8	1.5
²³⁹ Pu	0.24	0.10	–	1.60	236.8	18.7	255.5
²⁴⁰ Pu	0.05	0.01	–	0.35	49.0	127.7	176.8
²⁴¹ Pu	0.19	0.09	–	1.02	194.1	29.5	223.5
²⁴² Pu	0.01	–	–	0.05	14.7	15.6	30.3
²⁴¹ Am	–	–	–	0.02	3.0	4.3	7.3
^{242m} Am	–	–	–	0.01	1.2	0.4	1.7
²⁴³ Am	–	–	–	0.01	2.9	4.9	7.8
²⁴² Cm	–	–	–	–	0.1	–	0.2
²⁴³ Cm	–	–	–	–	–	–	0.1
²⁴⁴ Cm	–	–	–	–	0.4	0.3	0.7
²⁴⁵ Cm	–	–	–	–	0.2	0.2	0.3
O	0.01	–	0.01	0.01	1.5	–	1.5
Si	0.01	0.01	0.09	0.06	1.3	–	1.3
C	0.11	0.89	1.35	1.15	43.5	–	43.5
Total	0.41	0.90	4.27	2.77	353.0	134.0	487.0

Table 15. VHTR BOLNA full uncertainties (%) – breakdown by isotope

	k_{eff} BOC	Power peak BOC
²³⁵ U	0.49	0.15
²³⁸ U	0.15	0.02
O	–	–
Si	0.01	0.01
C	0.12	0.99
Total	0.53	1.00

Table 16. VHTR BOLNA full uncertainties (%) – breakdown by isotope

	k_{eff} EOC	Power peak EOC	Doppler BOC	Doppler EOC	Burn-up XS [pcm]	Burn-up Δn [pcm]	Burn-up total [pcm]
²³⁵ U	0.27	0.06	0.74	0.73	223.4	12.3	235.8
²³⁸ U	0.19	0.02	0.87	0.67	38.7	9.6	48.3
²³⁷ Np	0.01	–	–	0.04	5.5	4.7	10.2
²³⁸ Pu	–	–	–	0.01	1.0	1.0	2.0
²³⁹ Pu	0.17	0.13	–	0.98	167.1	23.7	190.8
²⁴⁰ Pu	0.06	0.01	–	0.26	56.3	159.6	215.9
²⁴¹ Pu	0.22	0.10	–	0.93	218.8	33.7	252.5
²⁴² Pu	0.02	–	–	0.05	15.6	16.5	32.0
²⁴¹ Am	–	–	–	0.02	3.2	4.9	8.0
^{242m} Am	–	–	–	–	1.6	0.6	2.2
²⁴³ Am	–	–	–	0.01	3.2	5.2	8.5
²⁴² Cm	–	–	–	–	0.2	–	0.2
²⁴³ Cm	–	–	–	–	0.1	–	0.1
²⁴⁴ Cm	–	–	–	–	0.4	0.3	0.7
²⁴⁵ Cm	–	–	–	–	0.3	0.2	0.5
O	0.01	–	0.01	0.01	1.6	–	1.6
Si	0.01	0.01	0.02	0.03	1.3	–	1.3
C	0.13	1.04	1.26	1.09	38.1	–	38.1
Total	0.46	1.06	1.70	2.01	363.5	166.6	530.1

Table 17. PWR BOLNA diagonal uncertainties (%) – breakdown by isotope

	k_{eff} BOC	k_{eff} EOC	Doppler BOC	Doppler EOC	Burn-up XS [pcm]	Burn-up Δn [pcm]	Burn-up total [pcm]
²³⁵ U	0.25	0.11	1.12	0.44	150.5	2.5	153.0
²³⁸ U	0.12	0.24	0.95	1.09	134.0	5.6	139.6
²³⁷ Np	–	0.02	–	0.04	17.1	3.8	20.8
²³⁸ Pu	–	0.01	–	0.04	14.8	6.1	20.9
²³⁹ Pu	–	0.25	–	1.08	245.5	189.7	435.2
²⁴⁰ Pu	–	0.09	–	0.34	90.9	19.6	110.5
²⁴¹ Pu	–	0.29	–	1.06	291.0	36.8	327.8
²⁴² Pu	–	0.04	–	0.03	44.8	8.9	53.8
²⁴¹ Am	–	0.01	–	0.01	7.2	6.1	13.4
^{242m} Am	–	–	–	0.01	3.5	0.6	4.1
²⁴³ Am	–	0.02	–	0.01	20.1	21.8	41.9
²⁴² Cm	–	–	–	–	1.0	–	1.0
²⁴³ Cm	–	–	–	–	0.5	0.1	0.6
²⁴⁴ Cm	–	0.01	–	0.01	10.9	4.5	15.4
²⁴⁵ Cm	–	0.01	–	0.05	10.8	3.2	13.9
O	0.24	0.43	0.41	0.49	202.2	–	202.2
H	0.01	0.04	0.08	0.11	25.7	–	25.7
Zr	0.01	0.02	0.02	0.03	10.4	–	10.4
Total	0.36	0.64	1.53	2.01	488.6	196.0	684.6

Table 18. PWR BOLNA full uncertainties (%) – breakdown by isotope

	k_{eff} BOC	k_{eff} EOC	Doppler BOC	Doppler EOC	Burn-up XS [pcm]	Burn-up Δn [pcm]	Burn-up total [pcm]
²³⁵ U	0.42	0.17	0.57	0.18	256.1	4.7	260.8
²³⁸ U	0.16	0.33	1.16	1.27	186.5	7.5	194.0
²³⁷ Np	–	0.02	–	0.04	19.1	5.2	24.2
²³⁸ Pu	–	0.02	–	0.04	22.6	8.4	31.0
²³⁹ Pu	–	0.21	–	0.69	205.3	254.9	460.1
²⁴⁰ Pu	–	0.12	–	0.17	121.3	24.8	146.1
²⁴¹ Pu	–	0.37	–	0.99	366.5	42.5	409.0
²⁴² Pu	–	0.05	–	0.03	48.6	12.7	61.3
²⁴¹ Am	–	0.01	–	0.01	7.7	7.2	14.9
^{242m} Am	–	–	–	–	5.0	0.9	5.8
²⁴³ Am	–	0.02	–	0.01	22.5	24.5	47.0
²⁴² Cm	–	–	–	–	1.4	0.1	1.5
²⁴³ Cm	–	–	–	–	0.7	0.1	0.9
²⁴⁴ Cm	–	0.01	–	0.02	13.4	5.1	18.5
²⁴⁵ Cm	–	0.02	–	0.03	16.0	3.5	19.5
O	0.24	0.46	0.44	0.54	224.5	–	224.5
H	0.02	0.06	0.12	0.17	39.5	–	39.5
Zr	0.02	0.04	0.02	0.02	16.4	–	16.4
Total	0.51	0.74	1.37	1.86	589.9	261.6	851.5

Appendix N

ΔN , N_F , BURN-UP COMPONENT DUE TO ΔN , DECAY, DOSE, NEUTRON SOURCE UNCERTAINTY (%) BREAKDOWN

Table 1. ABTR: $\Delta n^{(a)}$, decay, dose, neutron source BOLNA diagonal uncertainty (%)

		²³⁵ U	²³⁸ U	²³⁷ Np	²³⁸ Pu	²³⁹ Pu	²⁴⁰ Pu	²⁴¹ Pu	²⁴² Pu	²⁴¹ Am	^{242m} Am	²⁴³ Am	²⁴² Cm	²⁴³ Cm	²⁴⁴ Cm	²⁴⁵ Cm	²⁴⁶ Cm	Decay	Dose	N. Sr
	Capture	—	—	—	—	—	—	—	—	—	—	—	—	—	—	—	—	—	—	—
²³⁴ U	Fission	—	—	—	—	—	—	—	—	—	—	—	—	—	—	—	—	—	—	—
	n,2n	—	—	—	—	—	—	—	—	—	—	—	—	—	—	—	—	—	—	—
	Capture	1.95	—	—	—	—	—	—	—	—	—	—	—	—	—	—	—	—	—	—
²³⁵ U	Fission	0.20	—	—	—	—	—	—	—	—	—	—	—	—	—	—	—	—	—	—
	n,2n	0.02	—	—	—	—	—	—	—	—	—	—	—	—	—	—	—	—	—	—
	Capture	—	—	—	—	—	—	—	—	—	—	—	—	—	—	—	—	—	—	—
²³⁶ U	Fission	—	—	—	—	—	—	—	—	—	—	—	—	—	—	—	—	—	—	—
	n,2n	—	—	—	—	—	—	—	—	—	—	—	—	—	—	—	—	—	—	—
	Capture	—	1.37	0.01	—	1.65	—	—	—	—	—	—	—	—	—	—	—	0.01	0.03	—
²³⁸ U	Fission	—	0.10	—	—	—	—	—	—	—	—	—	—	—	—	—	—	—	—	—
	n,2n	—	0.05	12.61	—	—	—	—	—	—	—	—	—	—	—	—	—	—	—	—
	Capture	—	—	1.86	1.62	—	—	—	—	—	—	—	—	—	—	—	—	0.01	—	—
²³⁷ Np	Fission	—	—	1.77	0.01	—	—	—	—	—	—	—	—	—	—	—	—	—	—	—
	n,2n	—	—	—	—	—	—	—	—	—	—	—	—	—	—	—	—	—	—	—
	Capture	—	—	—	0.81	—	—	—	—	—	—	—	—	—	—	—	—	—	—	—
²³⁸ Pu	Fission	—	—	—	4.03	—	—	—	—	—	—	—	—	—	—	—	—	0.02	—	—
	n,2n	—	—	—	0.02	—	—	—	—	—	—	—	—	—	—	—	—	—	—	—
	Capture	—	—	—	—	0.76	6.37	0.59	—	—	—	—	—	—	—	—	—	0.02	0.02	—
²³⁹ Pu	Fission	—	—	—	—	0.49	0.01	—	—	—	—	—	—	—	—	—	—	—	0.01	—
	n,2n	—	—	—	1.05	0.01	—	—	—	—	—	—	—	—	—	—	—	0.01	—	—
	Capture	—	—	—	—	—	1.44	41.94	—	—	—	—	—	—	—	—	—	0.06	—	—
²⁴⁰ Pu	Fission	—	—	—	—	—	1.56	0.14	—	—	—	—	—	—	—	—	—	0.01	—	—
	n,2n	—	—	—	—	—	0.03	—	—	—	—	—	—	—	—	—	—	—	—	—

^(a) Multiply by the ratio between the total uncertainty on the n_f and the total uncertainty on the Δn of each isotope to get the uncertainty breakdown on n_f (see Table 17 for total uncertainty on the n_f of the isotopes of each system). Multiply by the ratio between the total uncertainty on the burn-up component due to the Δn and the total uncertainty on the Δn of each isotope to get the uncertainty breakdown on the burn-up component due to the Δn (see Table 18 for total uncertainty on the burn-up component due to the Δn of the isotopes of each system).

Table 1. ABTR: $\Delta n^{(a)}$, decay, dose, neutron source BOLNA diagonal uncertainty (%) (*cont.*)

		²³⁵ U	²³⁸ U	²³⁷ Np	²³⁸ Pu	²³⁹ Pu	²⁴⁰ Pu	²⁴¹ Pu	²⁴² Pu	²⁴¹ Am	^{242m} Am	²⁴³ Am	²⁴² Cm	²⁴³ Cm	²⁴⁴ Cm	²⁴⁵ Cm	²⁴⁶ Cm	Decay	Dose	N. Sr
²⁴¹ Pu	Capture	—	—	—	—	—	—	5.69	18.11	0.62	—	—	—	—	—	—	—	0.01	—	—
	Fission	—	—	—	—	—	—	41.50	0.41	4.55	—	—	0.01	—	—	—	—	0.06	—	—
	n,2n	—	—	—	—	—	—	0.36	—	0.04	—	—	—	—	—	—	—	—	—	—
²⁴² Pu	Capture	—	—	—	—	—	—	—	14.88	—	—	132.36	—	—	0.27	—	—	—	—	—
	Fission	—	—	—	—	—	—	—	20.11	—	—	0.48	—	—	—	—	—	—	—	—
	n,2n	—	—	—	—	—	—	—	0.29	—	—	0.01	—	—	—	—	—	—	—	—
²⁴¹ Am	Capture	—	—	—	0.49	—	—	—	2.14	76.88	4.56	—	21.36	1.09	—	—	—	0.01	—	0.08
	Fission	—	—	—	—	—	—	—	0.02	42.93	0.03	—	0.17	0.01	—	—	—	—	—	—
	n,2n	—	—	—	—	—	—	—	—	—	—	—	—	—	—	—	—	—	—	—
^{242m} Am	Capture	—	—	—	—	—	—	—	—	—	0.90	4.16	—	—	—	—	—	—	—	—
	Fission	—	—	—	—	—	—	—	—	—	3.92	0.07	—	—	—	—	—	—	—	—
	n,2n	—	—	—	—	—	—	—	—	—	—	—	—	—	—	—	—	—	—	—
²⁴³ Am	Capture	—	—	—	—	—	—	—	—	—	—	21.58	—	—	4.21	0.26	—	—	—	0.17
	Fission	—	—	—	—	—	—	—	—	—	—	11.66	—	—	0.02	—	—	—	—	—
	n,2n	—	—	—	—	—	—	—	—	—	—	—	—	—	—	—	—	—	—	—
²⁴² Cm	Capture	—	—	—	0.01	—	—	—	—	—	—	—	0.54	13.02	—	—	—	—	—	—
	Fission	—	—	—	0.09	—	—	—	—	—	—	—	4.19	0.21	—	—	—	—	—	0.02
	n,2n	—	—	—	—	—	—	—	—	—	—	—	—	—	—	—	—	—	—	—
²⁴³ Cm	Capture	—	—	—	—	—	—	—	—	—	—	—	—	0.24	—	—	—	—	—	—
	Fission	—	—	—	—	—	—	—	—	—	—	—	—	10.10	—	—	—	—	—	—
	n,2n	—	—	—	—	—	—	—	—	—	—	—	—	0.01	—	—	—	—	—	—
²⁴⁴ Cm	Capture	—	—	—	—	—	—	—	—	—	—	—	—	—	1.09	17.62	0.39	—	—	0.04
	Fission	—	—	—	—	—	—	—	—	—	—	—	—	—	6.36	0.38	0.01	—	—	0.26
	n,2n	—	—	—	—	—	—	—	—	—	—	—	—	—	0.01	—	—	—	—	—
²⁴⁵ Cm	Capture	—	—	—	—	—	—	—	—	—	—	—	—	—	—	0.94	8.44	—	—	—
	Fission	—	—	—	—	—	—	—	—	—	—	—	—	—	—	18.87	0.42	—	—	—
	n,2n	—	—	—	—	—	—	—	—	—	—	—	—	—	—	0.04	—	—	—	—
²⁴⁶ Cm	Capture	—	—	—	—	—	—	—	—	—	—	—	—	—	—	—	1.58	—	—	—
	Fission	—	—	—	—	—	—	—	—	—	—	—	—	—	—	—	3.09	—	—	—
	n,2n	—	—	—	—	—	—	—	—	—	—	—	—	—	—	—	—	—	—	—
Total		1.96	1.38	12.87	4.57	1.88	6.72	59.28	30.96	88.18	6.08	134.68	21.77	16.52	7.71	25.84	9.14	0.09	0.04	0.32

^(a) Multiply by the ratio between the total uncertainty on the n_f and the total uncertainty on the Δn of each isotope to get the uncertainty breakdown on n_f (see Table 17 for total uncertainty on the n_f of the isotopes of each system). Multiply by the ratio between the total uncertainty on the burn-up component due to the Δn and the total uncertainty on the Δn of each isotope to get the uncertainty breakdown on the burn-up component due to the Δn (see Table 18 for total uncertainty on the burn-up component due to the Δn of the isotopes of each system).

Table 2. ABTR: $\Delta n^{(a)}$, decay, dose, neutron source BOLNA full uncertainty (%)

		²³⁵ U	²³⁸ U	²³⁷ Np	²³⁸ Pu	²³⁹ Pu	²⁴⁰ Pu	²⁴¹ Pu	²⁴² Pu	²⁴¹ Am	^{242m} Am	²⁴³ Am	²⁴² Cm	²⁴³ Cm	²⁴⁴ Cm	²⁴⁵ Cm	²⁴⁶ Cm	Decay	Dose	N. Sr
²³⁴ U	Capture	–	–	–	–	–	–	–	–	–	–	–	–	–	–	–	–	–	–	–
	Fission	–	–	–	–	–	–	–	–	–	–	–	–	–	–	–	–	–	–	–
	n,2n	–	–	–	–	–	–	–	–	–	–	–	–	–	–	–	–	–	–	–
²³⁵ U	Capture	4.18	–	–	–	–	–	–	–	–	–	–	–	–	–	–	–	–	–	–
	Fission	0.35	–	–	–	–	–	–	–	–	–	–	–	–	–	–	–	–	–	–
	n,2n	0.02	–	–	–	–	–	–	–	–	–	–	–	–	–	–	–	–	–	–
²³⁶ U	Capture	–	–	–	–	–	–	–	–	–	–	–	–	–	–	–	–	–	–	–
	Fission	–	–	–	–	–	–	–	–	–	–	–	–	–	–	–	–	–	–	–
	n,2n	–	–	–	–	–	–	–	–	–	–	–	–	–	–	–	–	–	–	–
²³⁸ U	Capture	–	1.51	0.01	–	1.81	–	–	–	–	–	–	–	–	–	–	–	0.01	0.04	–
	Fission	–	0.14	–	–	–	–	–	–	–	–	–	–	–	–	–	–	–	–	–
	n,2n	–	0.05	12.61	–	–	–	–	–	–	–	–	–	–	–	–	–	–	–	–
²³⁷ Np	Capture	–	–	3.76	3.28	–	–	–	–	–	–	–	–	–	–	–	–	0.02	–	–
	Fission	–	–	3.08	0.02	–	–	–	–	–	–	–	–	–	–	–	–	–	–	–
	n,2n	–	–	–	–	–	–	–	–	–	–	–	–	–	–	–	–	–	–	–
²³⁸ Pu	Capture	–	–	–	1.47	–	–	–	–	–	–	–	–	–	–	–	–	0.01	–	–
	Fission	–	–	–	7.06	–	–	–	–	–	–	–	–	–	–	–	–	0.04	–	–
	n,2n	–	–	–	0.02	–	–	–	–	–	–	–	–	–	–	–	–	–	–	–
²³⁹ Pu	Capture	–	–	–	–	1.29	10.75	1.00	–	–	–	–	–	–	–	–	–	0.03	0.03	0.01
	Fission	–	–	–	–	0.70	0.03	–	–	–	–	–	–	–	–	–	–	0.01	0.01	–
	n,2n	–	–	–	1.05	0.01	–	–	–	–	–	–	–	–	–	–	–	0.01	–	–
²⁴⁰ Pu	Capture	–	–	–	–	–	3.17	92.69	–	–	–	–	–	–	–	–	–	0.13	–	–
	Fission	–	–	–	–	–	2.64	0.24	–	–	–	–	–	–	–	–	–	0.01	–	–
	n,2n	–	–	–	–	–	0.03	–	–	–	–	–	–	–	–	–	–	–	–	–
²⁴¹ Pu	Capture	–	–	–	–	–	–	10.64	33.85	1.17	–	–	–	–	–	–	–	0.02	–	–
	Fission	–	–	–	–	–	–	77.08	0.77	8.45	–	–	0.02	–	–	–	–	0.12	–	–
	n,2n	–	–	–	–	–	–	0.43	–	0.05	–	–	–	–	–	–	–	–	–	–
²⁴² Pu	Capture	–	–	–	–	–	–	–	23.64	–	–	210.27	–	–	0.43	–	–	–	–	–
	Fission	–	–	–	–	–	–	–	30.50	–	–	0.73	–	–	–	–	–	–	–	–
	n,2n	–	–	–	–	–	–	–	0.29	–	–	0.01	–	–	–	–	–	–	–	–
²⁴¹ Am	Capture	–	–	–	0.83	–	–	–	3.60	129.47	7.67	–	35.96	1.83	–	–	–	0.02	–	0.14
	Fission	–	–	–	–	–	–	–	0.03	68.67	0.05	–	0.28	0.01	–	–	–	0.01	–	–
	n,2n	–	–	–	–	–	–	–	–	–	–	–	–	–	–	–	–	–	–	–

- ^(a) Multiply by the ratio between the total uncertainty on the n_f and the total uncertainty on the Δn of each isotope to get the uncertainty breakdown on n_f (see Table 17 for total uncertainty on the n_f of the isotopes of each system). Multiply by the ratio between the total uncertainty on the burn-up component due to the Δn and the total uncertainty on the Δn of each isotope to get the uncertainty breakdown on the burn-up component due to the Δn (see Table 18 for total uncertainty on the burn-up component due to the Δn of the isotopes of each system).

Table 2. ABTR: $\Delta n^{(a)}$, decay, dose, neutron source BOLNA full uncertainty (%) (*cont.*)

		²³⁵ U	²³⁸ U	²³⁷ Np	²³⁸ Pu	²³⁹ Pu	²⁴⁰ Pu	²⁴¹ Pu	²⁴² Pu	²⁴¹ Am	^{242m} Am	²⁴³ Am	²⁴² Cm	²⁴³ Cm	²⁴⁴ Cm	²⁴⁵ Cm	²⁴⁶ Cm	Decay	Dose	N. Sr
	Capture	—	—	—	—	—	—	—	—	—	1.58	7.28	—	—	—	—	—	—	—	—
^{242m} Am	Fission	—	—	—	—	—	—	—	—	—	7.77	0.13	—	—	—	—	—	0.01	—	—
	n,2n	—	—	—	—	—	—	—	—	—	—	—	—	—	—	—	—	—	—	—
	Capture	—	—	—	—	—	—	—	—	—	—	34.69	—	—	6.77	0.41	—	—	—	0.27
²⁴³ Am	Fission	—	—	—	—	—	—	—	—	—	—	15.87	—	—	0.03	—	—	—	—	—
	n,2n	—	—	—	—	—	—	—	—	—	—	—	—	—	—	—	—	—	—	—
	Capture	—	—	—	0.02	—	—	—	—	—	—	—	1.03	25.00	—	—	—	—	—	—
²⁴² Cm	Fission	—	—	—	0.17	—	—	—	—	—	—	—	7.54	0.38	—	—	—	—	—	0.03
	n,2n	—	—	—	—	—	—	—	—	—	—	—	—	—	—	—	—	—	—	—
	Capture	—	—	—	—	—	—	—	—	—	—	—	—	0.44	—	—	—	—	—	—
²⁴³ Cm	Fission	—	—	—	—	—	—	—	—	—	—	—	—	20.00	—	—	—	—	—	—
	n,2n	—	—	—	—	—	—	—	—	—	—	—	—	0.01	—	—	—	—	—	—
	Capture	—	—	—	—	—	—	—	—	—	—	—	—	—	1.92	31.03	0.69	—	—	0.08
²⁴⁴ Cm	Fission	—	—	—	—	—	—	—	—	—	—	—	—	—	9.50	0.57	0.01	—	—	0.39
	n,2n	—	—	—	—	—	—	—	—	—	—	—	—	—	0.01	—	—	—	—	—
	Capture	—	—	—	—	—	—	—	—	—	—	—	—	—	—	1.66	14.89	—	—	—
²⁴⁵ Cm	Fission	—	—	—	—	—	—	—	—	—	—	—	—	—	—	37.29	0.83	—	—	—
	n,2n	—	—	—	—	—	—	—	—	—	—	—	—	—	—	0.04	—	—	—	—
	Capture	—	—	—	—	—	—	—	—	—	—	—	—	—	—	—	2.38	—	—	—
²⁴⁶ Cm	Fission	—	—	—	—	—	—	—	—	—	—	—	—	—	—	—	5.07	—	—	—
	n,2n	—	—	—	—	—	—	—	—	—	—	—	—	—	—	—	—	—	—	—
Total		4.19	1.51	13.51	8.03	2.33	11.52	121.03	51.46	146.80	11.03	213.82	36.76	32.07	11.83	48.54	15.94	0.18	0.05	0.50

^(a) Multiply by the ratio between the total uncertainty on the n_f and the total uncertainty on the Δn of each isotope to get the uncertainty breakdown on n_f (see Table 17 for total uncertainty on the n_f of the isotopes of each system). Multiply by the ratio between the total uncertainty on the burn-up component due to the Δn and the total uncertainty on the Δn of each isotope to get the uncertainty breakdown on the burn-up component due to the Δn (see Table 18 for total uncertainty on the burn-up component due to the Δn of the isotopes of each system).

Table 3. SFR: $\Delta n^{(a)}$, decay, dose, neutron source BOLNA diagonal uncertainty (%)

		²³⁵ U	²³⁸ U	²³⁷ Np	²³⁸ Pu	²³⁹ Pu	²⁴⁰ Pu	²⁴¹ Pu	²⁴² Pu	²⁴¹ Am	^{242m} Am	²⁴³ Am	²⁴² Cm	²⁴³ Cm	²⁴⁴ Cm	²⁴⁵ Cm	²⁴⁶ Cm	Decay	Dose	N. Sr
²³⁴ U	Capture	9.46	–	–	–	–	–	–	–	–	–	–	–	–	–	–	–	–	–	–
	Fission	0.39	–	–	–	–	–	–	–	–	–	–	–	–	–	–	–	–	0.01	–
	n,2n	–	–	–	–	–	–	–	–	–	–	–	–	–	–	–	–	–	–	–
²³⁵ U	Capture	5.50	–	–	–	–	–	–	–	–	–	–	–	–	–	–	–	–	–	–
	Fission	0.60	–	–	–	–	–	–	–	–	–	–	–	–	–	–	–	–	–	–
	n,2n	0.05	–	–	–	–	–	–	–	–	–	–	–	–	–	–	–	–	–	–
²³⁶ U	Capture	–	–	0.09	–	–	–	–	–	–	–	–	–	–	–	–	–	–	–	–
	Fission	–	–	–	–	–	–	–	–	–	–	–	–	–	–	–	–	–	–	–
	n,2n	–	–	–	–	–	–	–	–	–	–	–	–	–	–	–	–	–	–	–
²³⁸ U	Capture	–	1.41	–	–	0.57	–	–	–	–	–	–	–	–	–	–	–	–	0.01	–
	Fission	–	0.10	–	–	–	–	–	–	–	–	–	–	–	–	–	–	–	–	–
	n,2n	–	0.05	0.18	–	–	–	–	–	–	–	–	–	–	–	–	–	–	–	–
²³⁷ Np	Capture	–	–	1.36	2.06	–	–	–	–	–	–	–	–	–	–	–	–	0.02	0.01	–
	Fission	–	–	1.25	0.04	–	–	–	–	–	–	–	–	–	–	–	–	–	–	–
	n,2n	–	–	–	–	–	–	–	–	–	–	–	–	–	–	–	–	–	–	–
²³⁸ Pu	Capture	–	–	–	3.55	0.24	–	–	–	–	–	–	–	–	–	–	–	0.03	0.02	–
	Fission	–	–	–	17.48	0.01	–	–	–	–	–	–	–	–	–	–	–	0.15	0.13	–
	n,2n	–	–	–	0.06	–	–	–	–	–	–	–	–	–	–	–	–	–	–	–
²³⁹ Pu	Capture	–	–	–	–	0.56	1.13	–	–	–	–	–	–	–	–	–	–	–	0.01	–
	Fission	–	–	–	–	0.33	–	–	–	–	–	–	–	–	–	–	–	–	0.01	–
	n,2n	–	–	–	–	–	–	–	–	–	–	–	–	–	–	–	–	–	–	–
²⁴⁰ Pu	Capture	–	–	–	–	–	2.30	6.66	–	0.11	–	–	–	–	–	–	–	0.05	0.01	–
	Fission	–	–	–	–	–	2.48	0.05	–	–	–	–	–	–	–	–	–	–	–	–
	n,2n	–	–	–	–	–	0.05	–	–	–	–	–	–	–	–	–	–	–	–	–
²⁴¹ Pu	Capture	–	–	–	–	–	–	1.46	2.23	0.02	–	–	–	–	–	–	–	0.01	–	–
	Fission	–	–	–	–	–	–	10.37	0.11	0.16	–	–	0.03	–	–	–	–	0.08	0.01	–
	n,2n	–	–	–	–	–	–	0.08	–	–	–	–	–	–	–	–	–	–	–	–
²⁴² Pu	Capture	–	–	–	–	–	–	–	7.98	–	–	30.72	–	–	2.01	–	–	–	0.01	0.01
	Fission	–	–	–	–	–	–	–	9.98	–	–	0.24	–	–	0.01	–	–	–	0.02	–
	n,2n	–	–	–	–	–	–	–	0.13	–	–	–	–	–	–	–	–	–	–	–
²⁴¹ Am	Capture	–	–	–	0.92	–	–	–	0.41	3.19	0.26	–	26.33	6.72	–	–	–	0.02	0.03	0.01
	Fission	–	–	–	0.01	–	–	–	0.01	1.88	–	–	0.53	0.08	–	–	–	0.01	–	–
	n,2n	–	–	–	–	–	–	–	–	–	–	–	–	–	–	–	–	–	–	–

^(a) Multiply by the ratio between the total uncertainty on the n_f and the total uncertainty on the Δn of each isotope to get the uncertainty breakdown on n_f (see Table 17 for total uncertainty on the n_f of the isotopes of each system). Multiply by the ratio between the total uncertainty on the burn-up component due to the Δn and the total uncertainty on the Δn of each isotope to get the uncertainty breakdown on the burn-up component due to the Δn (see Table 18 for total uncertainty on the burn-up component due to the Δn of the isotopes of each system).

Table 3. SFR: $\Delta n^{(a)}$, decay, dose, neutron source BOLNA diagonal uncertainty (%) (*cont.*)

		²³⁵ U	²³⁸ U	²³⁷ Np	²³⁸ Pu	²³⁹ Pu	²⁴⁰ Pu	²⁴¹ Pu	²⁴² Pu	²⁴¹ Am	^{242m} Am	²⁴³ Am	²⁴² Cm	²⁴³ Cm	²⁴⁴ Cm	²⁴⁵ Cm	²⁴⁶ Cm	Decay	Dose	N. Sr
	Capture	—	—	—	—	—	—	—	—	—	1.22	8.00	0.02	—	—	—	—	0.03	0.01	—
^{242m} Am	Fission	—	—	—	—	—	—	—	—	—	5.31	0.29	0.11	—	—	—	—	0.15	0.09	—
	n,2n	—	—	—	—	—	—	—	—	—	—	—	—	—	—	—	—	—	—	—
	Capture	—	—	—	—	—	—	—	—	—	—	8.79	—	—	23.50	0.13	—	0.01	0.01	0.15
²⁴³ Am	Fission	—	—	—	—	—	—	—	—	—	—	4.77	—	—	0.31	—	—	—	—	—
	n,2n	—	—	—	—	—	—	—	—	—	—	—	—	—	—	—	—	—	—	—
	Capture	—	—	—	0.04	—	—	—	—	—	—	—	1.19	62.45	—	—	—	—	—	—
²⁴² Cm	Fission	—	—	—	0.28	—	—	—	—	—	—	—	8.25	2.04	—	—	—	0.01	—	—
	n,2n	—	—	—	—	—	—	—	—	—	—	—	—	—	—	—	—	—	—	—
	Capture	—	—	—	—	—	—	—	—	—	—	—	—	3.51	—	—	—	—	—	—
²⁴³ Cm	Fission	—	—	—	—	—	—	—	—	—	—	—	—	126.35	—	—	—	—	—	—
	n,2n	—	—	—	—	—	—	—	—	—	—	—	—	0.09	—	—	—	—	—	—
	Capture	—	—	—	—	—	—	—	—	—	—	—	—	0.02	16.57	10.37	—	0.01	—	0.10
²⁴⁴ Cm	Fission	—	—	—	—	—	0.02	—	—	—	—	—	—	0.10	97.04	0.51	—	0.04	—	0.61
	n,2n	—	—	—	—	—	—	—	—	—	—	—	—	11.39	0.18	—	—	—	—	—
	Capture	—	—	—	—	—	—	—	—	—	—	—	—	—	—	1.57	10.11	—	—	0.01
²⁴⁵ Cm	Fission	—	—	—	—	—	—	—	—	—	—	—	—	—	—	30.90	1.09	—	—	—
	n,2n	—	—	—	—	—	—	—	—	—	—	—	—	—	—	0.06	—	—	—	—
	Capture	—	—	—	—	—	—	—	—	—	—	—	—	—	—	—	16.17	—	—	0.02
²⁴⁶ Cm	Fission	—	—	—	—	—	—	—	—	—	—	—	—	—	—	—	30.74	—	—	0.04
	n,2n	—	—	—	—	—	—	—	—	—	—	—	—	—	—	—	—	—	—	—
Total		10.97	1.42	1.86	17.98	0.90	3.57	12.41	12.98	3.71	5.46	33.28	27.62	141.62	101.23	32.64	36.20	0.24	0.17	0.64

^(a) Multiply by the ratio between the total uncertainty on the n_f and the total uncertainty on the Δn of each isotope to get the uncertainty breakdown on n_f (see Table 17 for total uncertainty on the n_f of the isotopes of each system). Multiply by the ratio between the total uncertainty on the burn-up component due to the Δn and the total uncertainty on the Δn of each isotope to get the uncertainty breakdown on the burn-up component due to the Δn (see Table 18 for total uncertainty on the burn-up component due to the Δn of the isotopes of each system).

Table 4. SFR: BOLNA $\Delta n^{(a)}$, decay, dose, neutron source full uncertainty (%)

		²³⁵ U	²³⁸ U	²³⁷ Np	²³⁸ Pu	²³⁹ Pu	²⁴⁰ Pu	²⁴¹ Pu	²⁴² Pu	²⁴¹ Am	^{242m} Am	²⁴³ Am	²⁴² Cm	²⁴³ Cm	²⁴⁴ Cm	²⁴⁵ Cm	²⁴⁶ Cm	Decay	Dose	N. Sr
²³⁴ U	Capture	16.88	—	—	—	—	—	—	—	—	—	—	—	—	—	—	—	—	0.01	—
	Fission	0.61	—	—	—	—	—	—	—	—	—	—	—	—	—	—	—	—	0.02	—
	n,2n	—	—	—	—	—	—	—	—	—	—	—	—	—	—	—	—	—	—	—
²³⁵ U	Capture	11.96	—	—	—	—	—	—	—	—	—	—	—	—	—	—	—	—	—	—
	Fission	1.03	—	—	—	—	—	—	—	—	—	—	—	—	—	—	—	—	—	—
	n,2n	0.05	—	—	—	—	—	—	—	—	—	—	—	—	—	—	—	—	—	—
²³⁶ U	Capture	—	—	0.15	—	—	—	—	—	—	—	—	—	—	—	—	—	—	—	—
	Fission	—	—	—	—	—	—	—	—	—	—	—	—	—	—	—	—	—	—	—
	n,2n	—	—	—	—	—	—	—	—	—	—	—	—	—	—	—	—	—	—	—
²³⁸ U	Capture	—	1.53	—	—	0.62	—	—	—	—	—	—	—	—	—	—	—	—	0.01	—
	Fission	—	0.13	—	—	—	—	—	—	—	—	—	—	—	—	—	—	—	—	—
	n,2n	—	0.05	0.18	—	—	—	—	—	—	—	—	—	—	—	—	—	—	—	—
²³⁷ Np	Capture	—	—	2.75	4.16	—	—	—	—	—	—	—	—	—	—	—	—	0.04	0.03	—
	Fission	—	—	2.18	0.07	—	—	—	—	—	—	—	—	—	—	—	—	—	—	—
	n,2n	—	—	—	—	—	—	—	—	—	—	—	—	—	—	—	—	—	—	—
²³⁸ Pu	Capture	—	—	—	6.61	0.45	—	—	—	—	—	—	—	—	—	—	—	0.06	0.04	—
	Fission	—	—	—	30.72	0.02	—	—	—	—	—	—	—	—	—	—	—	0.26	0.23	—
	n,2n	—	—	—	0.06	—	—	—	—	—	—	—	—	—	—	—	—	—	—	—
²³⁹ Pu	Capture	—	—	—	—	0.92	1.87	—	—	—	—	—	—	—	—	—	—	—	0.02	—
	Fission	—	—	—	—	0.47	0.01	—	—	—	—	—	—	—	—	—	—	—	0.01	—
	n,2n	—	—	—	—	—	—	—	—	—	—	—	—	—	—	—	—	—	—	—
²⁴⁰ Pu	Capture	—	—	—	—	—	5.16	14.92	—	0.24	—	—	—	—	—	—	—	0.11	0.01	—
	Fission	—	—	—	—	—	4.20	0.09	—	—	—	—	—	—	—	—	—	0.01	—	—
	n,2n	—	—	—	—	—	0.05	—	—	—	—	—	—	—	—	—	—	—	—	—
²⁴¹ Pu	Capture	—	—	—	—	—	—	2.77	4.23	0.04	—	—	0.01	—	—	—	—	0.02	0.01	—
	Fission	—	—	—	—	—	—	19.38	0.21	0.31	—	—	0.06	—	—	—	—	0.16	0.02	—
	n,2n	—	—	—	—	—	—	0.10	—	—	—	—	—	—	—	—	—	—	—	—
²⁴² Pu	Capture	—	—	—	—	—	—	—	12.83	—	—	49.38	—	—	3.23	—	—	—	0.02	0.02
	Fission	—	—	—	—	—	—	—	15.25	—	—	0.37	—	—	0.02	—	—	—	0.03	—
	n,2n	—	—	—	—	—	—	—	0.13	—	—	—	—	—	—	—	—	—	—	—
²⁴¹ Am	Capture	—	—	—	1.56	—	—	—	0.69	5.41	0.44	—	44.66	11.39	—	—	—	0.03	0.05	0.02
	Fission	—	—	—	0.02	—	—	—	0.01	2.99	0.01	—	0.84	0.13	—	—	—	0.02	—	—
	n,2n	—	—	—	—	—	—	—	—	—	—	—	—	—	—	—	—	—	—	—

^(a) Multiply by the ratio between the total uncertainty on the n_f and the total uncertainty on the Δn of each isotope to get the uncertainty breakdown on n_f (see Table 17 for total uncertainty on the n_f of the isotopes of each system). Multiply by the ratio between the total uncertainty on the burn-up component due to the Δn and the total uncertainty on the Δn of each isotope to get the uncertainty breakdown on the burn-up component due to the Δn (see Table 18 for total uncertainty on the burn-up component due to the Δn of the isotopes of each system).

Table 4. SFR: BOLNA $\Delta n^{(a)}$, decay, dose, neutron source full uncertainty (%) (*cont.*)

		²³⁵ U	²³⁸ U	²³⁷ Np	²³⁸ Pu	²³⁹ Pu	²⁴⁰ Pu	²⁴¹ Pu	²⁴² Pu	²⁴¹ Am	^{242m} Am	²⁴³ Am	²⁴² Cm	²⁴³ Cm	²⁴⁴ Cm	²⁴⁵ Cm	²⁴⁶ Cm	Decay	Dose	N. Sr
	Capture	–	–	–	–	–	–	–	–	–	2.15	14.13	0.04	–	–	–	–	0.06	0.03	–
^{242m} Am	Fission	–	–	–	–	–	–	–	–	–	10.65	0.58	0.22	–	–	–	–	0.29	0.18	0.01
	n,2n	–	–	–	–	–	–	–	–	–	–	–	–	–	–	–	–	–	–	–
	Capture	–	–	–	–	–	–	–	–	–	–	14.46	–	–	38.66	0.21	–	0.01	0.01	0.24
²⁴³ Am	Fission	–	–	–	–	–	–	–	–	–	–	6.52	–	–	0.43	–	–	–	0.01	–
	n,2n	–	–	–	–	–	–	–	–	–	–	–	–	–	–	–	–	–	–	–
	Capture	–	–	–	0.08	–	–	–	–	–	–	–	2.26	118.61	–	–	–	–	–	–
²⁴² Cm	Fission	–	–	–	0.51	–	–	–	–	–	–	–	15.02	3.71	–	–	–	0.02	–	0.01
	n,2n	–	–	–	–	–	–	–	–	–	–	–	–	–	–	–	–	–	–	–
	Capture	–	–	–	–	–	–	–	–	–	–	–	–	6.50	–	–	–	–	–	–
²⁴³ Cm	Fission	–	–	–	–	–	–	–	–	–	–	–	–	253.15	–	–	–	–	–	–
	n,2n	–	–	–	–	–	–	–	–	–	–	–	–	0.09	–	–	–	–	–	–
	Capture	–	–	–	–	–	–	–	–	–	–	–	–	0.03	28.94	18.11	–	0.01	–	0.18
²⁴⁴ Cm	Fission	–	–	–	–	–	0.02	–	–	–	–	–	–	0.15	145.34	0.77	–	0.05	–	0.91
	n,2n	–	–	–	–	–	–	–	–	–	–	–	–	11.39	0.18	–	–	–	–	–
	Capture	–	–	–	–	–	–	–	–	–	–	–	–	–	–	2.81	18.13	–	–	0.02
²⁴⁵ Cm	Fission	–	–	–	–	–	–	–	–	–	–	–	–	–	–	61.89	2.19	–	0.01	–
	n,2n	–	–	–	–	–	–	–	–	–	–	–	–	–	–	0.06	–	–	–	–
	Capture	–	–	–	–	–	–	–	–	–	–	–	–	–	–	–	24.45	–	–	0.03
²⁴⁶ Cm	Fission	–	–	–	–	–	–	–	–	–	–	–	–	–	–	–	51.16	–	–	0.07
	n,2n	–	–	–	–	–	–	–	–	–	–	–	–	–	–	–	–	–	–	–
Total		20.72	1.54	3.52	31.74	1.29	6.91	24.61	20.39	6.20	10.88	53.76	47.18	280.12	153.19	64.55	59.57	0.45	0.31	0.96

^(a) Multiply by the ratio between the total uncertainty on the n_f and the total uncertainty on the Δn of each isotope to get the uncertainty breakdown on n_f (see Table 17 for total uncertainty on the n_f of the isotopes of each system). Multiply by the ratio between the total uncertainty on the burn-up component due to the Δn and the total uncertainty on the Δn of each isotope to get the uncertainty breakdown on the burn-up component due to the Δn (see Table 18 for total uncertainty on the burn-up component due to the Δn of the isotopes of each system).

Table 5. EFR: $\Delta n^{(a)}$, decay, dose, neutron source BOLNA diagonal uncertainty (%)

		²³⁵ U	²³⁸ U	²³⁷ Np	²³⁸ Pu	²³⁹ Pu	²⁴⁰ Pu	²⁴¹ Pu	²⁴² Pu	²⁴¹ Am	^{242m} Am	²⁴³ Am	²⁴² Cm	²⁴³ Cm	²⁴⁴ Cm	²⁴⁵ Cm	²⁴⁶ Cm	Decay	Dose	N. Sr
²³⁴ U	Capture	2.10	–	0.10	–	–	–	–	–	–	–	–	–	–	–	–	–	–	0.04	–
	Fission	0.87	–	0.02	–	–	–	–	–	–	–	–	–	–	–	–	–	–	0.10	–
	n,2n	–	–	–	–	–	–	–	–	–	–	–	–	–	–	–	–	–	–	–
²³⁵ U	Capture	2.37	–	1.50	–	–	–	–	–	–	–	–	–	–	–	–	–	–	–	–
	Fission	0.32	–	0.02	–	–	–	–	–	–	–	–	–	–	–	–	–	–	–	–
	n,2n	0.01	–	–	–	–	–	–	–	–	–	–	–	–	–	–	–	–	–	–
²³⁶ U	Capture	–	–	4.14	0.17	–	–	–	–	–	–	–	–	–	–	–	–	–	–	–
	Fission	–	–	0.82	0.02	–	–	–	–	–	–	–	–	–	–	–	–	–	–	–
	n,2n	–	–	–	–	–	–	–	–	–	–	–	–	–	–	–	–	–	–	–
²³⁸ U	Capture	0.02	1.53	1.07	0.01	3.48	1.53	0.32	0.08	0.01	0.06	–	0.01	–	–	–	–	0.10	0.69	–
	Fission	–	0.06	0.04	–	0.01	–	–	–	–	–	–	–	–	–	–	–	–	–	–
	n,2n	–	0.03	42.09	1.71	–	–	–	–	–	–	–	–	–	–	–	–	0.05	0.03	–
²³⁷ Np	Capture	–	–	17.95	1.77	–	–	–	–	–	–	–	–	–	–	–	–	0.05	0.03	–
	Fission	–	–	8.30	0.33	–	–	–	–	–	–	–	–	–	–	–	–	0.01	0.01	–
	n,2n	–	–	0.02	–	–	–	–	–	–	–	–	–	–	–	–	–	–	–	–
²³⁸ Pu	Capture	0.01	–	–	8.75	0.10	–	–	–	–	–	–	–	–	–	–	–	0.25	0.11	0.01
	Fission	0.04	–	–	25.53	0.03	–	–	–	–	–	–	–	–	–	–	–	0.75	0.39	0.02
	n,2n	–	–	–	0.07	–	–	–	–	–	–	–	–	–	–	–	–	–	–	–
²³⁹ Pu	Capture	0.01	–	–	0.06	1.81	8.84	2.48	0.82	0.11	0.79	0.27	0.06	0.17	–	–	–	0.26	0.34	0.01
	Fission	–	–	–	0.01	0.57	0.25	0.05	0.01	–	0.01	–	–	–	–	–	–	0.02	0.11	–
	n,2n	–	–	–	0.46	0.01	–	–	–	–	–	–	–	–	–	–	–	0.01	0.01	–
²⁴⁰ Pu	Capture	–	–	0.11	0.99	–	6.75	13.32	7.18	0.91	8.46	3.11	0.57	2.04	0.10	0.06	–	0.80	0.10	0.03
	Fission	–	–	0.01	0.04	–	4.68	1.26	0.40	0.05	0.38	0.13	0.03	0.08	–	–	–	0.15	0.01	–
	n,2n	–	–	–	–	–	0.09	0.03	0.01	–	0.01	–	–	–	–	–	–	–	–	–
²⁴¹ Pu	Capture	–	–	0.02	0.12	–	–	1.98	12.91	0.12	1.07	6.86	0.07	0.25	0.27	0.18	–	–	–	0.05
	Fission	–	–	0.11	0.86	–	–	13.93	6.66	0.85	7.53	2.73	0.52	1.78	0.08	0.05	–	–	0.01	0.03
	n,2n	–	–	–	0.01	–	–	0.09	0.04	0.01	0.05	0.02	–	0.01	–	–	–	–	–	–
²⁴² Pu	Capture	–	–	–	–	–	–	–	38.43	–	–	183.03	–	–	11.09	10.08	0.42	0.12	0.02	2.07
	Fission	–	–	–	–	–	–	–	23.47	–	–	12.79	–	–	0.51	0.35	0.01	0.01	0.07	0.10
	n,2n	–	–	–	–	–	–	–	0.32	–	–	0.18	–	–	0.01	–	–	–	–	–
²⁴¹ Am	Capture	0.02	–	–	7.68	0.01	–	–	1.82	2.25	39.04	2.17	1.07	12.85	0.11	0.09	–	0.10	0.14	0.05
	Fission	–	–	–	1.37	–	–	–	0.34	0.78	9.97	0.27	0.55	2.67	0.01	0.01	–	0.13	0.04	0.01
	n,2n	–	–	–	–	–	–	–	–	–	–	–	–	–	–	–	–	–	–	–

^(a) Multiply by the ratio between the total uncertainty on the n_f and the total uncertainty on the Δn of each isotope to get the uncertainty breakdown on n_f (see Table 17 for total uncertainty on the n_f of the isotopes of each system). Multiply by the ratio between the total uncertainty on the burn-up component due to the Δn and the total uncertainty on the Δn of each isotope to get the uncertainty breakdown on the burn-up component due to the Δn (see Table 18 for total uncertainty on the burn-up component due to the Δn of the isotopes of each system).

Table 5. EFR: $\Delta n^{(a)}$, decay, dose, neutron source BOLNA diagonal uncertainty (%) (*cont.*)

		²³⁵ U	²³⁸ U	²³⁷ Np	²³⁸ Pu	²³⁹ Pu	²⁴⁰ Pu	²⁴¹ Pu	²⁴² Pu	²⁴¹ Am	^{242m} Am	²⁴³ Am	²⁴² Cm	²⁴³ Cm	²⁴⁴ Cm	²⁴⁵ Cm	²⁴⁶ Cm	Decay	Dose	N. Sr
	Capture	–	–	–	0.01	–	–	–	–	–	29.37	6.25	–	0.01	0.37	0.33	–	0.03	0.01	0.07
^{242m} Am	Fission	–	–	–	0.02	–	–	–	–	–	122.97	2.07	0.01	0.05	0.09	0.06	–	0.13	0.05	0.02
	n,2n	–	–	–	–	–	–	–	–	–	–	–	–	–	–	–	–	–	–	–
	Capture	–	–	–	–	–	0.02	–	–	–	–	35.37	–	0.05	4.76	6.26	0.36	0.04	0.02	0.89
²⁴³ Am	Fission	–	–	–	–	–	–	–	–	–	–	11.25	–	–	0.65	0.57	0.02	0.01	0.01	0.12
	n,2n	–	–	–	–	–	–	–	–	–	–	–	–	–	–	–	–	–	–	–
	Capture	–	–	–	0.72	–	–	–	–	–	–	–	0.19	53.30	0.04	–	–	0.01	0.01	–
²⁴² Cm	Fission	–	–	–	2.44	–	–	–	–	–	–	–	0.65	4.50	–	–	–	0.09	0.05	0.01
	n,2n	–	–	–	–	–	–	–	–	–	–	–	–	–	–	–	–	–	–	–
	Capture	–	–	–	–	–	–	–	–	–	–	–	–	4.62	0.08	0.09	–	–	–	0.01
²⁴³ Cm	Fission	–	–	–	–	–	–	–	–	–	–	–	–	87.12	0.06	0.06	–	0.02	–	0.01
	n,2n	–	–	–	–	–	–	–	–	–	–	–	–	0.06	–	–	–	–	–	–
	Capture	–	–	–	–	–	0.02	–	–	–	–	–	–	0.04	4.91	46.63	3.78	0.04	–	0.87
²⁴⁴ Cm	Fission	–	–	–	–	–	0.08	0.02	–	–	–	–	–	0.15	18.01	20.67	1.09	0.15	–	3.37
	n,2n	–	–	–	–	–	–	–	–	–	–	–	–	2.20	0.04	0.04	–	–	–	0.01
	Capture	–	–	–	–	–	–	–	–	–	–	–	–	–	–	5.12	7.59	–	–	0.09
²⁴⁵ Cm	Fission	–	–	–	–	–	–	–	–	–	–	–	–	–	–	86.00	7.19	–	–	0.08
	n,2n	–	–	–	–	–	–	–	–	–	–	–	–	–	–	0.13	0.01	–	–	–
	Capture	–	–	–	–	–	–	–	–	–	–	–	–	–	–	–	19.99	–	–	0.14
²⁴⁶ Cm	Fission	–	–	–	–	–	–	–	–	–	–	–	–	–	–	–	18.98	–	–	0.22
	n,2n	–	–	–	–	–	–	–	–	–	–	–	–	–	–	–	–	–	–	–
Total		3.30	1.53	46.73	28.35	3.96	12.16	19.57	47.90	2.70	133.19	187.49	1.58	103.24	22.25	100.83	29.75	1.21	0.91	4.16

^(a) Multiply by the ratio between the total uncertainty on the n_f and the total uncertainty on the Δn of each isotope to get the uncertainty breakdown on n_f (see Table 17 for total uncertainty on the n_f of the isotopes of each system). Multiply by the ratio between the total uncertainty on the burn-up component due to the Δn and the total uncertainty on the Δn of each isotope to get the uncertainty breakdown on the burn-up component due to the Δn (see Table 18 for total uncertainty on the burn-up component due to the Δn of the isotopes of each system).

Table 6. EFR: BOLNA $\Delta n^{(a)}$, decay, dose, neutron source full uncertainty (%)

		²³⁵ U	²³⁸ U	²³⁷ Np	²³⁸ Pu	²³⁹ Pu	²⁴⁰ Pu	²⁴¹ Pu	²⁴² Pu	²⁴¹ Am	^{242m} Am	²⁴³ Am	²⁴² Cm	²⁴³ Cm	²⁴⁴ Cm	²⁴⁵ Cm	²⁴⁶ Cm	Decay	Dose	N. Sr
²³⁴ U	Capture	3.90	–	0.18	–	–	–	–	–	–	–	–	–	–	–	–	–	–	0.07	–
	Fission	1.36	–	0.03	–	–	–	–	–	–	–	–	–	–	–	–	–	–	0.15	–
	n,2n	–	–	–	–	–	–	–	–	–	–	–	–	–	–	–	–	–	–	–
²³⁵ U	Capture	5.12	–	3.25	–	–	–	–	–	–	–	–	–	–	–	–	–	–	–	–
	Fission	0.47	–	0.04	–	–	–	–	–	–	–	–	–	–	–	–	–	–	–	–
	n,2n	0.01	–	–	–	–	–	–	–	–	–	–	–	–	–	–	–	–	–	–
²³⁶ U	Capture	–	–	7.23	0.30	–	–	–	–	–	–	–	–	–	–	–	–	0.01	0.01	–
	Fission	–	–	1.43	0.04	–	–	–	–	–	–	–	–	–	–	–	–	–	–	–
	n,2n	–	–	–	–	–	–	–	–	–	–	–	–	–	–	–	–	–	–	–
²³⁸ U	Capture	0.02	1.65	1.16	0.01	3.75	1.65	0.35	0.08	0.01	0.07	–	0.01	–	–	–	–	0.11	0.74	–
	Fission	–	0.09	0.06	–	0.02	0.01	–	–	–	–	–	–	–	–	–	–	–	–	–
	n,2n	–	0.03	42.09	1.71	–	–	–	–	–	–	–	–	–	–	–	–	0.05	0.03	–
²³⁷ Np	Capture	0.01	–	33.94	3.34	–	–	–	–	–	–	–	–	–	–	–	–	0.10	0.05	–
	Fission	–	–	14.48	0.58	–	–	–	–	–	–	–	–	–	–	–	–	0.02	0.01	–
	n,2n	–	–	0.02	–	–	–	–	–	–	–	–	–	–	–	–	–	–	–	–
²³⁸ Pu	Capture	0.03	–	–	17.35	0.20	–	–	–	–	–	–	–	–	–	–	–	0.50	0.22	0.01
	Fission	0.08	–	–	45.91	0.06	–	–	–	–	–	–	–	–	–	–	–	1.34	0.71	0.03
	n,2n	–	–	–	0.07	–	–	–	–	–	–	–	–	–	–	–	–	–	–	–
²³⁹ Pu	Capture	0.01	–	–	0.09	2.62	12.75	3.58	1.19	0.16	1.14	0.39	0.09	0.25	–	–	–	0.37	0.49	0.01
	Fission	–	–	–	0.01	0.83	0.45	0.10	0.03	–	0.02	0.01	–	–	–	–	–	0.03	0.16	–
	n,2n	–	–	–	0.46	0.01	–	–	–	–	–	–	–	–	–	–	–	0.01	0.01	–
²⁴⁰ Pu	Capture	–	–	0.26	2.22	–	15.07	29.76	16.05	2.02	18.91	6.96	1.27	4.56	0.22	0.13	–	1.79	0.23	0.07
	Fission	–	–	0.02	0.07	–	8.11	2.18	0.70	0.09	0.66	0.22	0.05	0.14	0.01	–	–	0.26	0.02	0.01
	n,2n	–	–	–	–	–	0.09	0.03	0.01	–	0.01	–	–	–	–	–	–	–	–	–
²⁴¹ Pu	Capture	–	–	0.03	0.24	–	–	3.89	25.41	0.24	2.10	13.50	0.15	0.50	0.52	0.36	–	–	–	0.10
	Fission	–	–	0.20	1.55	–	–	25.03	11.96	1.53	13.54	4.91	0.93	3.21	0.15	0.09	–	–	0.02	0.05
	n,2n	–	–	–	0.01	–	–	0.10	0.05	0.01	0.06	0.02	–	0.01	–	–	–	–	–	–
²⁴² Pu	Capture	–	–	–	–	–	–	–	65.08	–	–	309.96	–	–	18.78	17.08	0.71	0.20	0.04	3.51
	Fission	–	–	–	–	–	–	–	36.11	–	–	19.68	–	–	0.78	0.54	0.02	0.01	0.11	0.15
	n,2n	–	–	–	–	–	–	–	0.32	–	–	0.18	–	–	0.01	–	–	–	–	–
²⁴¹ Am	Capture	0.03	–	–	13.22	0.02	–	–	3.14	3.88	67.19	3.73	1.84	22.11	0.19	0.15	–	0.17	0.24	0.08
	Fission	–	–	–	2.15	–	–	–	0.54	1.23	15.68	0.42	0.87	4.20	0.02	0.01	–	0.21	0.06	0.02
	n,2n	–	–	–	–	–	–	–	–	–	–	–	–	–	–	–	–	–	–	–

^(a) Multiply by the ratio between the total uncertainty on the n_f and the total uncertainty on the Δn of each isotope to get the uncertainty breakdown on n_f (see Table 17 for total uncertainty on the n_f of the isotopes of each system). Multiply by the ratio between the total uncertainty on the burn-up component due to the Δn and the total uncertainty on the Δn of each isotope to get the uncertainty breakdown on the burn-up component due to the Δn (see Table 18 for total uncertainty on the burn-up component due to the Δn of the isotopes of each system).

Table 6. EFR: BOLNA $\Delta n^{(a)}$, decay, dose, neutron source full uncertainty (%) (cont.)

		²³⁵ U	²³⁸ U	²³⁷ Np	²³⁸ Pu	²³⁹ Pu	²⁴⁰ Pu	²⁴¹ Pu	²⁴² Pu	²⁴¹ Am	^{242m} Am	²⁴³ Am	²⁴² Cm	²⁴³ Cm	²⁴⁴ Cm	²⁴⁵ Cm	²⁴⁶ Cm	Decay	Dose	N. Sr
	Capture	—	—	—	0.01	—	—	—	—	—	52.61	11.19	—	0.02	0.67	0.60	—	0.05	0.01	0.12
^{242m} Am	Fission	—	—	—	0.05	—	—	—	—	—	245.27	4.13	0.02	0.10	0.18	0.13	—	0.26	0.09	0.04
	n,2n	—	—	—	—	—	—	—	—	—	—	—	—	—	—	—	—	—	—	—
	Capture	—	—	—	—	—	0.04	—	—	—	—	63.32	—	0.08	8.52	11.21	0.65	0.06	0.04	1.60
²⁴³ Am	Fission	—	—	—	—	—	—	—	—	—	—	15.30	—	0.01	0.88	0.78	0.03	0.01	0.01	0.16
	n,2n	—	—	—	—	—	—	—	—	—	—	—	—	—	—	—	—	—	—	—
	Capture	—	—	—	1.27	—	—	—	—	—	—	—	0.34	93.73	0.06	—	—	0.02	0.02	0.01
²⁴² Cm	Fission	0.01	—	—	4.62	—	—	—	—	—	—	—	1.23	8.50	—	—	—	0.17	0.09	0.03
	n,2n	—	—	—	—	—	—	—	—	—	—	—	—	—	—	—	—	—	—	—
	Capture	—	—	—	—	—	—	—	—	—	—	—	—	8.65	0.14	0.17	—	—	—	0.03
²⁴³ Cm	Fission	—	—	—	—	—	—	—	—	—	—	—	—	176.01	0.12	0.11	—	0.04	—	0.03
	n,2n	—	—	—	—	—	—	—	—	—	—	—	—	0.06	—	—	—	—	—	—
	Capture	—	—	—	—	—	0.04	0.01	—	—	—	—	—	0.07	8.45	80.23	6.50	0.07	—	1.50
²⁴⁴ Cm	Fission	—	—	—	—	—	0.12	0.02	—	—	—	—	—	0.23	27.35	31.38	1.66	0.23	—	5.11
	n,2n	—	—	—	—	—	—	—	—	—	—	—	—	2.20	0.04	0.04	—	—	—	0.01
	Capture	—	—	—	—	—	—	—	—	—	—	—	—	—	—	9.56	14.18	—	—	0.16
²⁴⁵ Cm	Fission	—	—	—	—	—	—	—	—	—	—	—	—	—	—	173.84	14.54	—	—	0.17
	n,2n	—	—	—	—	—	—	—	—	—	—	—	—	—	—	0.14	0.01	—	—	—
	Capture	—	—	—	—	—	—	—	—	—	—	—	—	—	—	—	30.67	—	—	0.22
²⁴⁶ Cm	Fission	—	—	—	—	—	—	—	—	—	—	—	—	—	—	—	32.32	—	—	0.37
	n,2n	—	—	—	—	—	—	—	—	—	—	—	—	—	—	—	—	—	—	—
Total		6.59	1.65	56.56	51.32	4.65	21.41	39.30	81.23	4.80	261.21	317.99	2.88	201.14	35.32	195.32	49.43	2.40	1.24	6.60

^(a) Multiply by the ratio between the total uncertainty on the n_f and the total uncertainty on the Δn of each isotope to get the uncertainty breakdown on n_f (see Table 17 for total uncertainty on the n_f of the isotopes of each system). Multiply by the ratio between the total uncertainty on the burn-up component due to the Δn and the total uncertainty on the Δn of each isotope to get the uncertainty breakdown on the burn-up component due to the Δn (see Table 18 for total uncertainty on the burn-up component due to the Δn of the isotopes of each system).

Table 7. GFR: $\Delta n^{(a)}$, decay, dose, neutron source BOLNA diagonal uncertainty (%)

		²³⁵ U	²³⁸ U	²³⁷ Np	²³⁸ Pu	²³⁹ Pu	²⁴⁰ Pu	²⁴¹ Pu	²⁴² Pu	²⁴¹ Am	^{242m} Am	²⁴³ Am	²⁴² Cm	²⁴³ Cm	²⁴⁴ Cm	²⁴⁵ Cm	²⁴⁶ Cm	Decay	Dose	N. Sr
²³⁵ U	Capture	2.35	—	—	—	—	—	—	—	—	—	—	—	—	—	—	—	—	—	—
	Fission	0.44	—	—	—	—	—	—	—	—	—	—	—	—	—	—	—	—	—	—
	n,2n	0.01	—	—	—	—	—	—	—	—	—	—	—	—	—	—	—	—	—	—
²³⁸ U	Capture	—	1.76	—	—	11.79	6.16	—	—	—	—	—	—	—	—	—	—	0.01	0.16	—
	Fission	—	0.06	—	—	—	—	—	—	—	—	—	—	—	—	—	—	—	—	—
	n,2n	—	0.03	0.56	—	—	—	—	—	—	—	—	—	—	—	—	—	—	—	—
²³⁷ Np	Capture	—	—	1.96	1.14	—	—	—	—	—	—	—	—	—	—	—	—	0.06	0.05	—
	Fission	—	—	0.68	0.02	—	—	—	—	—	—	—	—	—	—	—	—	—	—	—
	n,2n	—	—	—	—	—	—	—	—	—	—	—	—	—	—	—	—	—	—	—
²³⁸ Pu	Capture	—	—	—	0.83	0.47	—	—	—	—	—	—	—	—	—	—	—	0.04	0.03	—
	Fission	—	—	—	2.01	0.02	—	—	—	—	—	—	—	—	—	—	—	0.10	0.09	—
	n,2n	—	—	—	0.01	—	—	—	—	—	—	—	—	—	—	—	—	—	—	—
²³⁹ Pu	Capture	—	—	—	—	5.81	169.94	0.15	—	—	—	—	—	—	—	—	—	0.01	0.08	—
	Fission	—	—	—	—	0.99	0.51	—	—	—	—	—	—	—	—	—	—	—	0.01	—
	n,2n	—	—	—	—	0.01	0.01	—	—	—	—	—	—	—	—	—	—	—	—	—
²⁴⁰ Pu	Capture	—	—	—	—	—	65.11	3.10	16.08	0.04	—	—	—	—	—	—	—	0.06	0.01	—
	Fission	—	—	—	—	—	41.28	0.04	0.12	—	—	—	—	—	—	—	—	—	—	—
	n,2n	—	—	—	—	—	0.95	—	—	—	—	—	—	—	—	—	—	—	—	—
²⁴¹ Pu	Capture	—	—	—	—	—	—	0.85	286.92	0.01	—	—	—	—	—	—	—	0.02	—	—
	Fission	—	—	—	—	—	—	5.75	30.23	0.07	—	—	—	—	—	—	—	0.13	0.02	—
	n,2n	—	—	—	—	—	—	0.04	0.21	—	—	—	—	—	—	—	—	—	—	—
²⁴² Pu	Capture	—	—	—	—	—	—	—	1595.98	—	—	20.81	—	—	0.78	—	—	—	0.02	0.13
	Fission	—	—	—	—	—	—	—	674.45	—	—	0.15	—	—	—	—	—	—	0.02	—
	n,2n	—	—	—	—	—	—	—	10.34	—	—	—	—	—	—	—	—	—	—	—
²⁴¹ Am	Capture	—	—	0.01	2.43	—	—	—	242.23	2.53	2.61	0.11	2.43	3.72	—	—	—	0.15	0.22	0.11
	Fission	—	—	—	0.04	—	—	—	4.83	0.76	0.05	—	0.06	0.06	—	—	—	0.04	0.01	—
	n,2n	—	—	—	—	—	—	—	—	—	—	—	—	—	—	—	—	—	—	—
^{242m} Am	Capture	—	—	—	—	—	—	—	—	—	0.17	0.22	—	—	—	—	—	—	—	—
	Fission	—	—	—	—	—	—	—	—	—	0.72	0.01	—	—	—	—	—	0.01	0.01	—
	n,2n	—	—	—	—	—	—	—	—	—	—	—	—	—	—	—	—	—	—	—
²⁴³ Am	Capture	—	—	—	—	—	—	—	—	—	—	5.47	—	—	3.50	1.81	0.02	0.02	0.02	0.57
	Fission	—	—	—	—	—	—	—	—	—	—	1.46	—	—	0.05	0.02	—	—	—	0.01
	n,2n	—	—	—	—	—	—	—	—	—	—	—	—	—	—	—	—	—	—	—

^(a) Multiply by the ratio between the total uncertainty on the n_f and the total uncertainty on the Δn of each isotope to get the uncertainty breakdown on n_f (see Table 17 for total uncertainty on the n_f of the isotopes of each system). Multiply by the ratio between the total uncertainty on the burn-up component due to the Δn and the total uncertainty on the Δn of each isotope to get the uncertainty breakdown on the burn-up component due to the Δn (see Table 18 for total uncertainty on the burn-up component due to the Δn of the isotopes of each system).

Table 7. GFR: $\Delta n^{(a)}$, decay, dose, neutron source BOLNA diagonal uncertainty (%) (cont.)

		²³⁵ U	²³⁸ U	²³⁷ Np	²³⁸ Pu	²³⁹ Pu	²⁴⁰ Pu	²⁴¹ Pu	²⁴² Pu	²⁴¹ Am	^{242m} Am	²⁴³ Am	²⁴² Cm	²⁴³ Cm	²⁴⁴ Cm	²⁴⁵ Cm	²⁴⁶ Cm	Decay	Dose	N. Sr
	Capture	—	—	—	0.06	—	—	—	—	—	—	—	0.09	10.60	—	—	—	—	—	—
²⁴² Cm	Fission	—	—	—	0.14	—	—	—	—	—	—	—	0.20	0.21	—	—	—	0.02	0.02	0.01
	n,2n	—	—	—	—	—	—	—	—	—	—	—	—	—	—	—	—	—	—	—
	Capture	—	—	—	—	—	—	—	—	—	—	—	—	0.37	—	—	—	—	—	—
²⁴³ Cm	Fission	—	—	—	—	—	—	—	—	—	—	—	—	4.63	—	—	—	—	—	—
	n,2n	—	—	—	—	—	—	—	—	—	—	—	—	—	—	—	—	—	—	—
	Capture	—	—	—	—	—	0.15	—	—	—	—	—	—	—	1.07	30.06	0.57	0.01	—	0.17
²⁴⁴ Cm	Fission	—	—	—	—	—	0.48	—	—	—	—	—	—	—	3.48	1.69	0.02	0.02	—	0.57
	n,2n	—	—	—	—	—	—	—	—	—	—	—	—	0.24	0.01	—	—	—	—	—
	Capture	—	—	—	—	—	—	—	—	—	—	—	—	—	—	3.51	6.46	—	—	0.02
²⁴⁵ Cm	Fission	—	—	—	—	—	—	—	—	—	—	—	—	—	—	51.62	1.02	—	—	—
	n,2n	—	—	—	—	—	—	—	—	—	—	—	—	—	—	0.10	—	—	—	—
	Capture	—	—	—	—	—	—	—	—	—	—	—	—	—	—	—	2.80	—	—	—
²⁴⁶ Cm	Fission	—	—	—	—	—	—	—	—	—	—	—	—	—	—	—	2.00	—	—	—
	n,2n	—	—	—	—	—	—	—	—	—	—	—	—	—	—	—	—	—	—	—
Total		2.39	1.76	2.15	3.45	13.19	186.72	6.59	1773.23	2.64	2.72	21.57	2.44	12.16	5.11	59.89	7.41	0.25	0.30	0.85

^(a) Multiply by the ratio between the total uncertainty on the n_f and the total uncertainty on the Δn of each isotope to get the uncertainty breakdown on n_f (see Table 17 for total uncertainty on the n_f of the isotopes of each system). Multiply by the ratio between the total uncertainty on the burn-up component due to the Δn and the total uncertainty on the Δn of each isotope to get the uncertainty breakdown on the burn-up component due to the Δn (see Table 18 for total uncertainty on the burn-up component due to the Δn of the isotopes of each system).

Table 8. GFR: $\Delta n^{(a)}$, decay, dose, neutron source BOLNA full uncertainty (%)

		²³⁵ U	²³⁸ U	²³⁷ Np	²³⁸ Pu	²³⁹ Pu	²⁴⁰ Pu	²⁴¹ Pu	²⁴² Pu	²⁴¹ Am	^{242m} Am	²⁴³ Am	²⁴² Cm	²⁴³ Cm	²⁴⁴ Cm	²⁴⁵ Cm	²⁴⁶ Cm	Decay	Dose	N. Sr
²³⁵ U	Capture	4.78	—	—	—	—	—	—	—	—	—	—	—	—	—	—	—	—	—	—
	Fission	0.59	—	—	—	—	—	—	—	—	—	—	—	—	—	—	—	—	—	—
	n,2n	0.01	—	—	—	—	—	—	—	—	—	—	—	—	—	—	—	—	—	—
²³⁸ U	Capture	—	1.88	—	—	12.61	6.58	—	—	—	—	—	—	—	—	—	—	0.01	0.17	—
	Fission	—	0.08	—	—	0.02	0.01	—	—	—	—	—	—	—	—	—	—	—	—	—
	n,2n	—	0.03	0.56	—	—	—	—	—	—	—	—	—	—	—	—	—	—	—	—
²³⁷ Np	Capture	—	—	3.58	2.08	—	—	—	—	—	—	—	—	—	—	—	—	0.10	0.09	—
	Fission	—	—	1.20	0.04	—	—	—	—	—	—	—	—	—	—	—	—	—	—	—
	n,2n	—	—	—	—	—	—	—	—	—	—	—	—	—	—	—	—	—	—	—
²³⁸ Pu	Capture	—	—	—	1.69	0.96	—	—	—	—	—	—	—	—	—	—	—	0.08	0.06	—
	Fission	—	—	—	3.63	0.04	—	—	—	—	—	—	—	—	—	—	—	0.18	0.16	—
	n,2n	—	—	—	0.01	—	—	—	—	—	—	—	—	—	—	—	—	—	—	—
²³⁹ Pu	Capture	—	—	—	—	7.23	210.73	0.18	—	—	—	—	—	—	—	—	—	0.02	0.10	—
	Fission	—	—	—	—	1.53	2.16	—	—	—	—	—	—	—	—	—	—	—	0.02	—
	n,2n	—	—	—	—	0.01	0.01	—	—	—	—	—	—	—	—	—	—	—	—	—
²⁴⁰ Pu	Capture	—	—	—	—	—	147.26	7.02	36.37	0.08	—	—	—	—	—	—	—	0.15	0.02	—
	Fission	—	—	—	—	—	71.93	0.06	0.21	—	—	—	—	—	—	—	—	0.01	—	—
	n,2n	—	—	—	—	—	0.95	—	—	—	—	—	—	—	—	—	—	—	—	—
²⁴¹ Pu	Capture	—	—	—	—	—	—	1.70	573.54	0.02	—	—	—	—	—	—	—	0.04	0.01	—
	Fission	—	—	—	—	—	—	10.04	52.77	0.12	0.01	—	0.01	—	—	—	—	0.23	0.03	—
	n,2n	—	—	—	—	—	—	0.05	0.26	—	—	—	—	—	—	—	—	—	—	—
²⁴² Pu	Capture	—	—	—	—	—	—	—	2668.10	—	—	34.79	—	—	1.30	—	—	—	0.04	0.21
	Fission	—	—	—	—	—	—	—	1042.53	—	—	0.23	—	—	0.01	—	—	—	0.03	—
	n,2n	—	—	—	—	—	—	—	10.34	—	—	—	—	—	—	—	—	—	—	—
²⁴¹ Am	Capture	—	—	0.02	4.28	—	—	—	426.19	4.45	4.60	0.19	4.28	6.55	—	—	—	0.27	0.39	0.20
	Fission	—	—	—	0.06	—	—	—	7.56	1.20	0.08	—	0.10	0.09	—	—	—	0.07	0.01	0.01
	n,2n	—	—	—	—	—	—	—	—	—	—	—	—	—	—	—	—	—	—	—
^{242m} Am	Capture	—	—	—	—	—	—	—	—	—	0.30	0.40	—	—	—	—	—	0.01	—	—
	Fission	—	—	—	—	—	—	—	—	—	1.41	0.02	—	—	—	—	—	0.03	0.02	—
	n,2n	—	—	—	—	—	—	—	—	—	—	—	—	—	—	—	—	—	—	—
²⁴³ Am	Capture	—	—	—	—	—	—	—	—	—	—	10.15	—	—	6.50	3.35	0.04	0.03	0.03	1.07
	Fission	—	—	—	—	—	—	—	—	—	—	1.98	—	—	0.07	0.02	—	—	0.01	0.01
	n,2n	—	—	—	—	—	—	—	—	—	—	—	—	—	—	—	—	—	—	—

^(a) Multiply by the ratio between the total uncertainty on the n_f and the total uncertainty on the Δn of each isotope to get the uncertainty breakdown on n_f (see Table 17 for total uncertainty on the n_f of the isotopes of each system). Multiply by the ratio between the total uncertainty on the burn-up component due to the Δn and the total uncertainty on the Δn of each isotope to get the uncertainty breakdown on the burn-up component due to the Δn (see Table 18 for total uncertainty on the burn-up component due to the Δn of the isotopes of each system).

Table 8. GFR: $\Delta n^{(a)}$, decay, dose, neutron source BOLNA full uncertainty (%) (*cont.*)

		²³⁵ U	²³⁸ U	²³⁷ Np	²³⁸ Pu	²³⁹ Pu	²⁴⁰ Pu	²⁴¹ Pu	²⁴² Pu	²⁴¹ Am	^{242m} Am	²⁴³ Am	²⁴² Cm	²⁴³ Cm	²⁴⁴ Cm	²⁴⁵ Cm	²⁴⁶ Cm	Decay	Dose	N. Sr
	Capture	—	—	—	0.09	—	—	—	—	—	—	—	0.14	16.62	—	—	—	—	—	—
²⁴² Cm	Fission	—	—	—	0.26	—	—	—	—	—	—	—	0.39	0.40	—	—	—	0.03	0.03	0.02
	n,2n	—	—	—	—	—	—	—	—	—	—	—	—	—	—	—	—	—	—	—
	Capture	—	—	—	—	—	—	—	—	—	—	—	—	0.71	—	—	—	—	—	—
²⁴³ Cm	Fission	—	—	—	—	—	—	—	—	—	—	—	—	9.50	—	—	—	—	—	—
	n,2n	—	—	—	—	—	—	—	—	—	—	—	—	—	—	—	—	—	—	—
	Capture	—	—	—	—	—	0.25	—	—	—	—	—	—	—	1.81	50.77	0.97	0.01	—	0.29
²⁴⁴ Cm	Fission	—	—	—	—	—	0.73	—	—	—	—	—	—	—	5.33	2.59	0.03	0.03	—	0.87
	n,2n	—	—	—	—	—	—	—	—	—	—	—	—	0.24	0.01	—	—	—	—	—
	Capture	—	—	—	—	—	—	—	—	—	—	—	—	—	—	6.89	12.68	—	—	0.03
²⁴⁵ Cm	Fission	—	—	—	—	—	—	—	—	—	—	—	—	—	—	106.13	2.09	—	—	0.01
	n,2n	—	—	—	—	—	—	—	—	—	—	—	—	—	—	0.11	—	—	—	—
	Capture	—	—	—	—	—	—	—	—	—	—	—	—	—	—	—	4.45	—	—	—
²⁴⁶ Cm	Fission	—	—	—	—	—	—	—	—	—	—	—	—	—	—	—	3.44	—	—	—
	n,2n	—	—	—	—	—	—	—	—	—	—	—	—	—	—	—	—	—	—	—
Total		4.81	1.88	3.82	6.22	14.64	267.05	12.37	2953.04	4.61	4.82	36.30	4.30	20.26	8.69	117.92	14.06	0.45	0.48	1.44

^(a) Multiply by the ratio between the total uncertainty on the n_f and the total uncertainty on the Δn of each isotope to get the uncertainty breakdown on n_f (see Table 17 for total uncertainty on the n_f of the isotopes of each system). Multiply by the ratio between the total uncertainty on the burn-up component due to the Δn and the total uncertainty on the Δn of each isotope to get the uncertainty breakdown on the burn-up component due to the Δn (see Table 18 for total uncertainty on the burn-up component due to the Δn of the isotopes of each system).

Table 9. LFR: $\Delta n^{(a)}$, decay, dose, neutron source BOLNA diagonal uncertainty (%)

		²³⁵ U	²³⁸ U	²³⁷ Np	²³⁸ Pu	²³⁹ Pu	²⁴⁰ Pu	²⁴¹ Pu	²⁴² Pu	²⁴¹ Am	^{242m} Am	²⁴³ Am	²⁴² Cm	²⁴³ Cm	²⁴⁴ Cm	²⁴⁵ Cm	²⁴⁶ Cm	Decay	Dose	N. Sr
²³⁴ U	Capture	2.69	–	–	–	–	–	–	–	–	–	–	–	–	–	–	–	–	0.01	–
	Fission	0.10	–	–	–	–	–	–	–	–	–	–	–	–	–	–	–	–	0.02	–
	n,2n	–	–	–	–	–	–	–	–	–	–	–	–	–	–	–	–	–	–	–
²³⁵ U	Capture	3.54	–	–	–	–	–	–	–	–	–	–	–	–	–	–	–	–	–	–
	Fission	0.34	–	–	–	–	–	–	–	–	–	–	–	–	–	–	–	–	–	–
	n,2n	0.01	–	–	–	–	–	–	–	–	–	–	–	–	–	–	–	–	–	–
²³⁶ U	Capture	–	–	1.01	–	–	–	–	–	–	–	–	–	–	–	–	–	–	–	–
	Fission	–	–	0.01	–	–	–	–	–	–	–	–	–	–	–	–	–	–	–	–
	n,2n	–	–	–	–	–	–	–	–	–	–	–	–	–	–	–	–	–	–	–
²³⁸ U	Capture	–	1.89	–	–	7.50	–	–	–	–	–	–	–	–	–	–	–	0.01	0.10	–
	Fission	–	0.06	–	–	–	–	–	–	–	–	–	–	–	–	–	–	–	–	–
	n,2n	–	0.03	0.87	–	–	–	–	–	–	–	–	–	–	–	–	–	–	–	–
²³⁷ Np	Capture	–	–	2.47	8.36	–	–	–	–	–	–	–	–	–	–	–	–	0.04	0.02	–
	Fission	–	–	1.43	0.15	–	–	–	–	–	–	–	–	–	–	–	–	–	–	–
	n,2n	–	–	–	–	–	–	–	–	–	–	–	–	–	–	–	–	–	–	–
²³⁸ Pu	Capture	–	–	–	14.98	0.51	–	–	–	–	–	–	–	–	–	–	–	0.06	0.03	–
	Fission	–	–	–	53.64	0.02	–	–	–	–	–	–	–	–	–	–	–	0.23	0.13	–
	n,2n	–	–	–	0.10	–	–	–	–	–	–	–	–	–	–	–	–	–	–	–
²³⁹ Pu	Capture	–	–	–	–	2.74	4.70	0.84	–	–	–	–	–	–	–	–	–	0.01	0.04	–
	Fission	–	–	–	–	1.32	0.02	–	–	–	–	–	–	–	–	–	–	–	0.02	–
	n,2n	–	–	–	–	0.01	–	–	–	–	–	–	–	–	–	–	–	–	–	–
²⁴⁰ Pu	Capture	–	–	–	–	–	5.51	98.21	0.33	0.29	–	–	0.03	–	–	–	–	0.14	0.01	–
	Fission	–	–	–	–	–	3.76	0.67	–	–	–	–	–	–	–	–	–	0.01	–	–
	n,2n	–	–	–	–	–	0.04	0.01	–	–	–	–	–	–	–	–	–	–	–	–
²⁴¹ Pu	Capture	–	–	–	–	–	–	12.99	4.72	0.04	0.67	–	–	–	–	–	–	0.02	–	–
	Fission	–	–	–	–	–	–	86.16	0.29	0.25	4.45	–	0.02	0.01	–	–	–	0.13	0.01	–
	n,2n	–	–	–	–	–	–	0.29	–	–	0.02	–	–	–	–	–	–	–	–	–
²⁴² Pu	Capture	–	–	–	–	–	–	–	17.20	–	–	51.54	–	–	2.34	–	–	–	0.01	0.04
	Fission	–	–	–	–	–	–	–	13.26	–	–	0.34	–	–	0.01	–	–	–	0.01	–
	n,2n	–	–	–	–	–	–	–	0.11	–	–	–	–	–	–	–	–	–	–	–
²⁴¹ Am	Capture	–	–	–	7.93	–	–	–	1.33	4.27	2573.54	–	11.10	8.15	–	–	–	0.05	–	0.03
	Fission	–	–	–	0.08	–	–	–	0.02	1.32	34.28	–	0.18	0.08	–	–	–	0.01	0.01	–
	n,2n	–	–	–	–	–	–	–	–	–	–	–	–	–	–	–	–	–	–	–

^(a) Multiply by the ratio between the total uncertainty on the n_f and the total uncertainty on the Δn of each isotope to get the uncertainty breakdown on n_f (see Table 17 for total uncertainty on the n_f of the isotopes of each system). Multiply by the ratio between the total uncertainty on the burn-up component due to the Δn and the total uncertainty on the Δn of each isotope to get the uncertainty breakdown on the burn-up component due to the Δn (see Table 18 for total uncertainty on the burn-up component due to the Δn of the isotopes of each system).

Table 9. LFR: $\Delta n^{(a)}$, decay, dose, neutron source BOLNA diagonal uncertainty (%) (*cont.*)

		²³⁵ U	²³⁸ U	²³⁷ Np	²³⁸ Pu	²³⁹ Pu	²⁴⁰ Pu	²⁴¹ Pu	²⁴² Pu	²⁴¹ Am	^{242m} Am	²⁴³ Am	²⁴² Cm	²⁴³ Cm	²⁴⁴ Cm	²⁴⁵ Cm	²⁴⁶ Cm	Decay	Dose	N. Sr
	Capture	–	–	–	–	–	–	–	–	–	1262.74	2.15	–	–	–	–	–	0.01	0.17	0.12
^{242m} Am	Fission	–	–	–	–	–	–	–	–	–	5203.84	0.10	0.01	–	–	–	–	0.04	–	–
	n,2n	–	–	–	–	–	–	–	–	–	–	–	–	–	–	–	–	–	–	–
	Capture	–	–	–	–	–	–	–	–	–	–	12.12	–	–	16.28	0.20	–	0.01	–	0.25
²⁴³ Am	Fission	–	–	–	–	–	–	–	–	–	–	3.60	–	–	0.16	–	–	–	0.01	–
	n,2n	–	–	–	–	–	–	–	–	–	–	–	–	–	–	–	–	–	–	–
	Capture	–	–	–	0.24	–	–	–	–	–	–	–	0.36	47.20	–	–	–	–	–	–
²⁴² Cm	Fission	–	–	–	1.17	–	–	–	–	–	–	–	1.79	1.20	–	–	–	–	–	0.01
	n,2n	–	–	–	–	–	–	–	–	–	–	–	–	–	–	–	–	–	–	–
	Capture	–	–	–	–	–	–	–	–	–	–	–	–	1.70	–	–	–	–	–	–
²⁴³ Cm	Fission	–	–	–	–	–	–	–	–	–	–	–	–	60.39	–	–	–	–	–	–
	n,2n	–	–	–	–	–	–	–	–	–	–	–	–	0.02	–	–	–	–	–	–
	Capture	–	–	–	–	–	0.01	–	–	–	–	–	–	0.01	11.41	11.81	0.96	0.01	–	0.18
²⁴⁴ Cm	Fission	–	–	–	–	–	0.02	–	–	–	–	–	–	0.02	43.75	0.53	0.03	0.03	–	0.68
	n,2n	–	–	–	–	–	–	–	–	–	–	–	–	2.36	0.05	–	–	–	–	–
	Capture	–	–	–	–	–	–	–	–	–	–	–	–	–	–	1.93	21.06	–	–	0.03
²⁴⁵ Cm	Fission	–	–	–	–	–	–	–	–	–	–	–	–	–	–	35.80	2.94	–	–	–
	n,2n	–	–	–	–	–	–	–	–	–	–	–	–	–	–	0.03	–	–	–	–
	Capture	–	–	–	–	–	–	–	–	–	–	–	–	–	–	–	34.51	–	–	0.04
²⁴⁶ Cm	Fission	–	–	–	–	–	–	–	–	–	–	–	–	–	–	–	41.93	–	–	0.05
	n,2n	–	–	–	–	–	–	–	–	–	–	–	–	–	–	–	–	–	–	–
Total		4.46	1.90	3.15	56.88	8.11	8.16	131.30	22.27	4.49	5941.28	53.11	11.26	77.14	48.11	37.75	58.33	0.32	0.24	0.76

^(a) Multiply by the ratio between the total uncertainty on the n_f and the total uncertainty on the Δn of each isotope to get the uncertainty breakdown on n_f (see Table 17 for total uncertainty on the n_f of the isotopes of each system). Multiply by the ratio between the total uncertainty on the burn-up component due to the Δn and the total uncertainty on the Δn of each isotope to get the uncertainty breakdown on the burn-up component due to the Δn (see Table 18 for total uncertainty on the burn-up component due to the Δn of the isotopes of each system).

Table 10. LFR: $\Delta n^{(a)}$, decay, dose, neutron source BOLNA full uncertainty (%)

		²³⁵ U	²³⁸ U	²³⁷ Np	²³⁸ Pu	²³⁹ Pu	²⁴⁰ Pu	²⁴¹ Pu	²⁴² Pu	²⁴¹ Am	^{242m} Am	²⁴³ Am	²⁴² Cm	²⁴³ Cm	²⁴⁴ Cm	²⁴⁵ Cm	²⁴⁶ Cm	Decay	Dose	N. Sr
²³⁴ U	Capture	4.70	—	—	—	—	—	—	—	—	—	—	—	—	—	—	—	—	0.01	—
	Fission	0.15	—	—	—	—	—	—	—	—	—	—	—	—	—	—	—	—	0.04	—
	n,2n	—	—	—	—	—	—	—	—	—	—	—	—	—	—	—	—	—	—	—
²³⁵ U	Capture	7.68	—	—	—	—	—	—	—	—	—	—	—	—	—	—	—	—	—	—
	Fission	0.57	—	—	—	—	—	—	—	—	—	—	—	—	—	—	—	—	—	—
	n,2n	0.01	—	—	—	—	—	—	—	—	—	—	—	—	—	—	—	—	—	—
²³⁶ U	Capture	—	—	1.71	—	—	—	—	—	—	—	—	—	—	—	—	—	—	—	—
	Fission	—	—	0.02	—	—	—	—	—	—	—	—	—	—	—	—	—	—	—	—
	n,2n	—	—	—	—	—	—	—	—	—	—	—	—	—	—	—	—	—	—	—
²³⁸ U	Capture	—	2.06	—	—	8.16	—	—	—	—	—	—	—	—	—	—	—	0.01	0.11	—
	Fission	—	0.09	—	—	0.01	—	—	—	—	—	—	—	—	—	—	—	—	—	—
	n,2n	—	0.03	0.87	—	—	—	—	—	—	—	—	—	—	—	—	—	—	—	—
²³⁷ Np	Capture	—	—	4.90	16.62	—	—	—	—	—	—	—	—	—	—	—	—	0.07	0.04	—
	Fission	—	—	2.38	0.24	—	—	—	—	—	—	—	—	—	—	—	—	—	—	—
	n,2n	—	—	—	—	—	—	—	—	—	—	—	—	—	—	—	—	—	—	—
²³⁸ Pu	Capture	—	—	—	26.72	0.91	—	—	—	—	—	—	—	—	—	—	—	0.11	0.05	—
	Fission	—	—	—	91.27	0.03	—	—	—	—	—	—	—	—	—	—	—	0.39	0.23	—
	n,2n	—	—	—	0.10	—	—	—	—	—	—	—	—	—	—	—	—	—	—	—
²³⁹ Pu	Capture	—	—	—	—	4.50	7.73	1.38	—	—	—	—	—	—	—	—	—	0.01	0.06	—
	Fission	—	—	—	—	1.84	0.03	—	—	—	—	—	—	—	—	—	—	—	0.02	—
	n,2n	—	—	—	—	0.01	—	—	—	—	—	—	—	—	—	—	—	—	—	—
²⁴⁰ Pu	Capture	—	—	—	—	—	12.13	216.03	0.73	0.64	—	—	0.06	—	—	—	—	0.31	0.03	—
	Fission	—	—	—	—	—	6.20	1.11	—	—	—	—	—	—	—	—	—	0.01	—	—
	n,2n	—	—	—	—	—	0.04	0.01	—	—	—	—	—	—	—	—	—	—	—	—
²⁴¹ Pu	Capture	—	—	—	—	—	—	23.72	8.62	0.07	1.22	—	0.01	—	—	—	—	0.04	0.01	—
	Fission	—	—	—	—	—	—	159.14	0.54	0.47	8.21	—	0.05	0.01	—	—	—	0.24	0.02	—
	n,2n	—	—	—	—	—	—	0.35	—	—	0.02	—	—	—	—	—	—	—	—	—
²⁴² Pu	Capture	—	—	—	—	—	—	—	27.75	—	—	83.13	—	—	3.77	—	—	—	0.02	0.06
	Fission	—	—	—	—	—	—	—	19.26	—	—	0.50	—	—	0.01	—	—	—	0.02	—
	n,2n	—	—	—	—	—	—	—	0.11	—	—	—	—	—	—	—	—	—	—	—
²⁴¹ Am	Capture	—	—	0.01	13.07	—	—	—	2.20	7.03	4238.15	—	18.29	13.43	—	—	—	0.09	—	0.05
	Fission	—	—	—	0.12	—	—	—	0.03	2.13	55.26	—	0.29	0.13	—	—	—	0.02	0.01	—
	n,2n	—	—	—	—	—	—	—	—	—	—	—	—	—	—	—	—	—	—	—

^(a) Multiply by the ratio between the total uncertainty on the n_f and the total uncertainty on the Δn of each isotope to get the uncertainty breakdown on n_f (see Table 17 for total uncertainty on the n_f of the isotopes of each system). Multiply by the ratio between the total uncertainty on the burn-up component due to the Δn and the total uncertainty on the Δn of each isotope to get the uncertainty breakdown on the burn-up component due to the Δn (see Table 18 for total uncertainty on the burn-up component due to the Δn of the isotopes of each system).

Table 10. LFR: $\Delta n^{(a)}$, decay, dose, neutron source BOLNA full uncertainty (%) (cont.)

		²³⁵ U	²³⁸ U	²³⁷ Np	²³⁸ Pu	²³⁹ Pu	²⁴⁰ Pu	²⁴¹ Pu	²⁴² Pu	²⁴¹ Am	^{242m} Am	²⁴³ Am	²⁴² Cm	²⁴³ Cm	²⁴⁴ Cm	²⁴⁵ Cm	²⁴⁶ Cm	Decay	Dose	N. Sr
	Capture	—	—	—	—	—	—	—	—	—	2210.05	3.77	—	—	—	—	—	0.02	0.29	0.20
^{242m} Am	Fission	—	—	—	—	—	—	—	—	—	10184.80	0.20	0.02	—	—	—	—	0.07	0.01	—
	n,2n	—	—	—	—	—	—	—	—	—	—	—	—	—	—	—	—	—	—	—
	Capture	—	—	—	—	—	—	—	—	—	—	18.75	—	—	25.18	0.31	—	0.02	—	0.39
²⁴³ Am	Fission	—	—	—	—	—	—	—	—	—	—	4.85	—	—	0.22	—	—	—	0.02	—
	n,2n	—	—	—	—	—	—	—	—	—	—	—	—	—	—	—	—	—	—	—
	Capture	—	—	—	0.45	—	—	—	—	—	—	—	0.70	89.98	—	—	—	—	—	—
²⁴² Cm	Fission	—	—	—	2.08	—	—	—	—	—	—	—	3.17	2.14	—	—	—	—	—	0.01
	n,2n	—	—	—	—	—	—	—	—	—	—	—	—	—	—	—	—	—	—	—
	Capture	—	—	—	—	—	—	—	—	—	—	—	—	2.95	—	—	—	—	—	—
²⁴³ Cm	Fission	—	—	—	—	—	—	—	—	—	—	—	—	118.55	—	—	—	—	—	—
	n,2n	—	—	—	—	—	—	—	—	—	—	—	—	0.02	—	—	—	—	—	—
	Capture	—	—	—	—	—	0.01	—	—	—	—	—	—	0.01	19.97	20.67	1.68	0.01	—	0.31
²⁴⁴ Cm	Fission	—	—	—	—	—	0.04	—	—	—	—	—	—	0.03	62.53	0.76	0.04	0.05	—	0.97
	n,2n	—	—	—	—	—	—	—	—	—	—	—	—	2.36	0.05	—	—	—	—	—
	Capture	—	—	—	—	—	—	—	—	—	—	—	—	—	—	3.34	36.44	—	—	0.04
²⁴⁵ Cm	Fission	—	—	—	—	—	—	—	—	—	—	—	—	—	—	70.02	5.74	—	—	0.01
	n,2n	—	—	—	—	—	—	—	—	—	—	—	—	—	—	0.03	—	—	—	—
	Capture	—	—	—	—	—	—	—	—	—	—	—	—	—	—	—	53.34	—	—	0.06
²⁴⁶ Cm	Fission	—	—	—	—	—	—	—	—	—	—	—	—	—	—	—	64.37	—	—	0.08
	n,2n	—	—	—	—	—	—	—	—	—	—	—	—	—	—	—	—	—	—	—
Total		9.02	2.06	5.78	97.44	9.54	15.66	269.37	34.94	7.39	11250.75	85.45	18.58	149.50	70.41	73.09	91.39	0.58	0.40	1.12

^(a) Multiply by the ratio between the total uncertainty on the n_f and the total uncertainty on the Δn of each isotope to get the uncertainty breakdown on n_f (see Table 17 for total uncertainty on the n_f of the isotopes of each system). Multiply by the ratio between the total uncertainty on the burn-up component due to the Δn and the total uncertainty on the Δn of each isotope to get the uncertainty breakdown on the burn-up component due to the Δn (see Table 18 for total uncertainty on the burn-up component due to the Δn of the isotopes of each system).

Table 11. ADMAB: $\Delta n^{(a)}$, decay, dose, neutron source BOLNA diagonal uncertainty (%)

		²³⁷ Np	²³⁸ Pu	²³⁹ Pu	²⁴⁰ Pu	²⁴¹ Pu	²⁴² Pu	²⁴¹ Am	^{242m} Am	²⁴³ Am	²⁴² Cm	²⁴³ Cm	²⁴⁴ Cm	²⁴⁵ Cm	²⁴⁶ Cm	Decay	Dose	N. Sr
²³⁷ Np	Capture	1.71	1.28	—	—	—	—	—	—	—	—	—	—	—	—	0.17	0.20	—
	Fission	0.99	0.03	—	—	—	—	—	—	—	—	—	—	—	—	0.01	0.02	—
	n,2n	—	—	—	—	—	—	—	—	—	—	—	—	—	—	—	—	—
²³⁸ Pu	Capture	—	0.22	0.19	—	—	—	—	—	—	—	—	—	—	—	0.05	0.05	—
	Fission	—	0.74	0.01	—	—	—	—	—	—	—	—	—	—	—	0.16	0.20	—
	n,2n	—	—	—	—	—	—	—	—	—	—	—	—	—	—	—	—	—
²³⁹ Pu	Capture	—	—	0.85	6.72	0.04	—	—	—	—	—	—	—	—	—	—	0.03	—
	Fission	—	—	0.25	0.02	—	—	—	—	—	—	—	—	—	—	—	0.01	—
	n,2n	—	—	—	—	—	—	—	—	—	—	—	—	—	—	—	—	—
²⁴⁰ Pu	Capture	—	—	—	3.54	1.39	—	—	—	—	—	—	—	—	—	—	—	—
	Fission	—	—	—	2.82	0.02	—	—	—	—	—	—	—	—	—	—	—	—
	n,2n	—	—	—	0.04	—	—	—	—	—	—	—	—	—	—	—	—	—
²⁴¹ Pu	Capture	—	—	—	—	1.14	2.31	0.01	—	—	—	—	—	—	—	0.02	—	—
	Fission	—	—	—	—	4.86	0.14	0.02	—	—	—	—	—	—	—	0.09	—	—
	n,2n	—	—	—	—	0.03	—	—	—	—	—	—	—	—	—	—	—	—
²⁴² Pu	Capture	—	—	—	—	—	3.43	—	—	0.61	—	—	—	—	—	—	—	—
	Fission	—	—	—	—	—	2.52	—	—	0.01	—	—	—	—	—	—	—	—
	n,2n	—	—	—	—	—	0.02	—	—	—	—	—	—	—	—	—	—	—
²⁴¹ Am	Capture	—	1.39	—	—	—	2.96	2.45	3.47	—	2.77	5.83	—	—	—	0.25	0.51	0.03
	Fission	—	0.02	—	—	—	0.06	0.95	0.07	—	0.07	0.09	—	—	—	0.10	0.04	—
	n,2n	—	—	—	—	—	—	—	—	—	—	—	—	—	—	—	—	—
^{242m} Am	Capture	—	—	—	—	—	—	—	0.45	—	—	—	—	—	—	0.02	—	—
	Fission	—	—	—	—	—	—	—	1.89	—	—	—	—	—	—	0.07	—	—
	n,2n	—	—	—	—	—	—	—	—	—	—	—	—	—	—	—	—	—
²⁴³ Am	Capture	—	—	—	0.31	—	—	—	—	2.49	—	0.11	5.49	1.13	0.02	0.08	0.12	0.69
	Fission	—	—	—	—	—	—	—	—	0.87	—	—	0.08	0.01	—	0.01	0.04	0.02
	n,2n	—	—	—	—	—	—	—	—	—	—	—	—	—	—	—	—	—
²⁴² Cm	Capture	—	0.03	—	—	—	—	—	—	—	0.08	17.93	—	—	—	0.01	—	—
	Fission	—	0.10	—	—	—	—	—	—	—	0.30	0.42	—	—	—	0.05	—	0.01
	n,2n	—	—	—	—	—	—	—	—	—	—	—	—	—	—	—	—	—
²⁴³ Cm	Capture	—	—	—	—	—	—	—	—	—	—	1.37	—	—	—	—	—	—
	Fission	—	—	—	—	—	—	—	—	—	—	44.02	—	—	—	—	—	—
	n,2n	—	—	—	—	—	—	—	—	—	—	0.02	—	—	—	—	—	—

^(a) Multiply by the ratio between the total uncertainty on the n_f and the total uncertainty on the Δn of each isotope to get the uncertainty breakdown on n_f (see Table 17 for total uncertainty on the n_f of the isotopes of each system). Multiply by the ratio between the total uncertainty on the burn-up component due to the Δn and the total uncertainty on the Δn of each isotope to get the uncertainty breakdown on the burn-up component due to the Δn (see Table 18 for total uncertainty on the burn-up component due to the Δn of the isotopes of each system).

Table 11. ADMAB: $\Delta n^{(a)}$, decay, dose, neutron source BOLNA diagonal uncertainty (%) (*cont.*)

		²³⁷ Np	²³⁸ Pu	²³⁹ Pu	²⁴⁰ Pu	²⁴¹ Pu	²⁴² Pu	²⁴¹ Am	^{242m} Am	²⁴³ Am	²⁴² Cm	²⁴³ Cm	²⁴⁴ Cm	²⁴⁵ Cm	²⁴⁶ Cm	Decay	Dose	N. Sr
²⁴⁴ Cm	Capture	—	—	—	—	—	—	—	—	—	—	0.04	2.24	32.57	0.79	0.04	—	0.32
	Fission	—	—	—	—	—	—	—	—	—	—	0.20	10.64	2.08	0.03	0.19	—	1.54
	n,2n	—	—	—	—	—	—	—	—	—	—	18.70	0.16	0.03	—	—	—	0.02
²⁴⁵ Cm	Capture	—	—	—	—	—	—	—	—	—	—	—	—	1.97	6.28	—	—	—
	Fission	—	—	—	—	—	—	—	—	—	—	—	—	44.13	1.07	—	—	—
	n,2n	—	—	—	—	—	—	—	—	—	—	—	—	0.01	—	—	—	—
²⁴⁶ Cm	Capture	—	—	—	—	—	—	—	—	—	—	—	—	—	0.29	—	—	—
	Fission	—	—	—	—	—	—	—	—	—	—	—	—	—	0.85	—	—	—
	n,2n	—	—	—	—	—	—	—	—	—	—	—	—	—	—	—	—	—
Total		1.98	2.05	0.91	8.11	5.18	5.67	2.63	3.97	2.71	2.79	51.43	12.18	54.94	6.48	0.43	0.60	1.72

^(a) Multiply by the ratio between the total uncertainty on the n_f and the total uncertainty on the Δn of each isotope to get the uncertainty breakdown on n_f (see Table 17 for total uncertainty on the n_f of the isotopes of each system). Multiply by the ratio between the total uncertainty on the burn-up component due to the Δn and the total uncertainty on the Δn of each isotope to get the uncertainty breakdown on the burn-up component due to the Δn (see Table 18 for total uncertainty on the burn-up component due to the Δn of the isotopes of each system).

Table 12. ADMAB: $\Delta n^{(a)}$, decay, dose, neutron source BOLNA full uncertainty (%)

		²³⁷ Np	²³⁸ Pu	²³⁹ Pu	²⁴⁰ Pu	²⁴¹ Pu	²⁴² Pu	²⁴¹ Am	^{242m} Am	²⁴³ Am	²⁴² Cm	²⁴³ Cm	²⁴⁴ Cm	²⁴⁵ Cm	²⁴⁶ Cm	Decay	Dose	N. Sr
²³⁷ Np	Capture	3.44	2.58	—	—	—	—	—	—	—	—	—	—	—	—	0.34	0.40	—
	Fission	1.66	0.05	—	—	—	—	—	—	—	—	—	—	—	—	0.01	0.03	—
	n,2n	—	—	—	—	—	—	—	—	—	—	—	—	—	—	—	—	—
²³⁸ Pu	Capture	—	0.44	0.37	—	—	—	—	—	—	—	—	—	—	—	0.09	0.09	—
	Fission	—	1.26	0.01	—	—	—	—	—	—	—	—	—	—	—	0.27	0.34	—
	n,2n	—	—	—	—	—	—	—	—	—	—	—	—	—	—	—	—	—
²³⁹ Pu	Capture	—	—	1.24	9.78	0.06	—	—	—	—	—	—	—	—	—	—	0.05	—
	Fission	—	—	0.37	0.06	—	—	—	—	—	—	—	—	—	—	—	0.01	—
	n,2n	—	—	0.01	0.01	—	—	—	—	—	—	—	—	—	—	—	—	—
²⁴⁰ Pu	Capture	—	—	—	8.21	3.23	—	—	—	—	—	—	—	—	—	—	—	—
	Fission	—	—	—	4.59	0.03	—	—	—	—	—	—	—	—	—	—	—	—
	n,2n	—	—	—	0.04	—	—	—	—	—	—	—	—	—	—	—	—	—
²⁴¹ Pu	Capture	—	—	—	—	2.18	4.42	0.01	—	—	—	—	—	—	—	0.04	—	—
	Fission	—	—	—	—	9.18	0.27	0.05	—	—	—	—	—	—	—	0.17	—	—
	n,2n	—	—	—	—	0.05	—	—	—	—	—	—	—	—	—	—	—	—
²⁴² Pu	Capture	—	—	—	—	—	5.80	—	—	1.03	—	—	—	—	—	—	—	—
	Fission	—	—	—	—	—	3.72	—	—	0.01	—	—	—	—	—	—	—	—
	n,2n	—	—	—	—	—	0.02	—	—	—	—	—	—	—	—	—	—	—
²⁴¹ Am	Capture	0.01	2.38	—	—	—	5.05	4.18	5.92	—	4.73	9.95	—	—	—	0.42	0.88	0.05
	Fission	—	0.03	—	—	—	0.09	1.51	0.11	—	0.11	0.14	—	—	—	0.16	0.06	—
	n,2n	—	—	—	—	—	—	—	—	—	—	—	—	—	—	—	—	—
^{242m} Am	Capture	—	—	—	—	—	—	—	0.80	—	—	—	—	—	—	0.03	—	—
	Fission	—	—	—	—	—	—	—	3.81	—	—	—	—	—	—	0.14	—	—
	n,2n	—	—	—	—	—	—	—	—	—	—	—	—	—	—	—	—	—
²⁴³ Am	Capture	—	—	—	0.53	—	—	—	—	4.27	—	0.19	9.40	1.93	0.03	0.14	0.20	1.19
	Fission	—	—	—	—	—	—	—	—	1.17	—	—	0.11	0.02	—	0.01	0.06	0.03
	n,2n	—	—	—	—	—	—	—	—	—	—	—	—	—	—	—	—	—
²⁴² Cm	Capture	—	0.05	—	—	—	—	—	—	—	0.14	31.20	—	—	—	0.01	—	—
	Fission	—	0.18	—	—	—	—	—	—	—	0.54	0.77	—	—	—	0.09	—	0.01
	n,2n	—	—	—	—	—	—	—	—	—	—	—	—	—	—	—	—	—
²⁴³ Cm	Capture	—	—	—	—	—	—	—	—	—	—	2.55	—	—	—	—	—	—
	Fission	—	—	—	—	—	—	—	—	—	—	89.27	—	—	—	—	—	—
	n,2n	—	—	—	—	—	—	—	—	—	—	0.02	—	—	—	—	—	—

^(a) Multiply by the ratio between the total uncertainty on the n_f and the total uncertainty on the Δn of each isotope to get the uncertainty breakdown on n_f (see Table 17 for total uncertainty on the n_f of the isotopes of each system). Multiply by the ratio between the total uncertainty on the burn-up component due to the Δn and the total uncertainty on the Δn of each isotope to get the uncertainty breakdown on the burn-up component due to the Δn (see Table 18 for total uncertainty on the burn-up component due to the Δn of the isotopes of each system).

Table 12. ADMAB: $\Delta n^{(a)}$, decay, dose, neutron source BOLNA full uncertainty (%) (*cont.*)

		²³⁷ Np	²³⁸ Pu	²³⁹ Pu	²⁴⁰ Pu	²⁴¹ Pu	²⁴² Pu	²⁴¹ Am	^{242m} Am	²⁴³ Am	²⁴² Cm	²⁴³ Cm	²⁴⁴ Cm	²⁴⁵ Cm	²⁴⁶ Cm	Decay	Dose	N. Sr
²⁴⁴ Cm	Capture	—	—	—	—	—	—	—	—	—	—	0.08	3.93	57.10	1.38	0.07	—	0.56
	Fission	—	—	—	—	—	—	—	—	—	—	0.29	15.13	2.96	0.05	0.27	—	2.18
	n,2n	—	—	—	—	—	—	—	—	—	—	18.70	0.16	0.03	—	—	—	0.02
²⁴⁵ Cm	Capture	—	—	—	—	—	—	—	—	—	—	—	—	3.78	12.08	—	—	—
	Fission	—	—	—	—	—	—	—	—	—	—	—	—	90.97	2.21	—	—	—
	n,2n	—	—	—	—	—	—	—	—	—	—	—	—	0.01	—	—	—	—
²⁴⁶ Cm	Capture	—	—	—	—	—	—	—	—	—	—	—	—	—	0.46	—	—	—
	Fission	—	—	—	—	—	—	—	—	—	—	—	—	—	1.39	—	—	—
	n,2n	—	—	—	—	—	—	—	—	—	—	—	—	—	—	—	—	—
Total		3.82	3.76	1.35	13.58	9.97	9.62	4.45	7.09	4.54	4.76	96.95	18.24	107.52	12.44	0.75	1.05	2.55

^(a) Multiply by the ratio between the total uncertainty on the n_f and the total uncertainty on the Δn of each isotope to get the uncertainty breakdown on n_f (see Table 17 for total uncertainty on the n_f of the isotopes of each system). Multiply by the ratio between the total uncertainty on the burn-up component due to the Δn and the total uncertainty on the Δn of each isotope to get the uncertainty breakdown on the burn-up component due to the Δn (see Table 18 for total uncertainty on the burn-up component due to the Δn of the isotopes of each system).

Table 13. VHTR: $\Delta n^{(a)}$, decay, dose, neutron source BOLNA diagonal uncertainty (%)

		²³⁵ U	²³⁸ U	²³⁷ Np	²³⁸ Pu	²³⁹ Pu	²⁴⁰ Pu	²⁴¹ Pu	²⁴² Pu	²⁴¹ Am	^{242m} Am	²⁴³ Am	²⁴² Cm	²⁴³ Cm	²⁴⁴ Cm	²⁴⁵ Cm	Decay	Dose	N. Sr
²³⁵ U	Capture	0.14	–	0.81	0.73	–	–	–	–	–	–	–	–	–	–	–	0.12	0.12	0.01
	Fission	0.13	–	0.05	0.03	–	–	–	–	–	–	–	–	–	–	–	0.01	0.01	–
	n,2n	–	–	–	–	–	–	–	–	–	–	–	–	–	–	–	–	–	–
²³⁶ U	Capture	–	–	0.40	0.36	–	–	–	–	–	–	–	–	–	–	–	0.06	0.06	–
	Fission	–	–	0.01	–	–	–	–	–	–	–	–	–	–	–	–	–	–	–
	n,2n	–	–	–	–	–	–	–	–	–	–	–	–	–	–	–	–	–	–
²³⁸ U	Capture	–	0.75	–	0.08	0.73	0.74	0.75	0.76	0.76	0.76	0.76	0.76	0.77	0.77	0.77	0.64	0.62	0.76
	Fission	–	–	–	–	–	–	–	–	–	–	–	–	–	–	–	–	–	–
	n,2n	–	–	0.04	0.04	–	–	–	–	–	–	–	–	–	–	–	0.01	0.01	–
²³⁷ Np	Capture	–	–	0.49	0.96	–	–	–	–	–	–	–	–	–	–	–	0.16	0.12	0.01
	Fission	–	–	–	–	–	–	–	–	–	–	–	–	–	–	–	–	–	–
	n,2n	–	–	–	–	–	–	–	–	–	–	–	–	–	–	–	–	–	–
²³⁸ Pu	Capture	–	–	–	0.13	–	–	–	–	–	–	–	–	–	–	–	0.02	0.02	–
	Fission	–	–	–	0.03	–	–	–	–	–	–	–	–	–	–	–	–	–	–
	n,2n	–	–	–	–	–	–	–	–	–	–	–	–	–	–	–	–	–	–
²³⁹ Pu	Capture	–	–	–	0.10	0.44	0.79	0.82	0.88	0.86	0.86	0.92	0.89	0.92	0.95	0.97	0.66	0.06	0.93
	Fission	–	–	–	0.03	0.45	0.43	0.39	0.34	0.36	0.35	0.30	0.33	0.30	0.27	0.25	0.33	0.35	0.27
	n,2n	–	–	–	–	–	–	–	–	–	–	–	–	–	–	–	–	–	–
²⁴⁰ Pu	Capture	–	–	–	0.02	–	0.44	0.07	0.14	0.11	0.12	0.18	0.14	0.18	0.21	0.23	0.04	0.03	0.20
	Fission	–	–	–	–	–	–	–	–	–	–	–	–	–	–	–	–	–	–
	n,2n	–	–	–	–	–	–	–	–	–	–	–	–	–	–	–	–	–	–
²⁴¹ Pu	Capture	–	–	–	0.08	–	–	1.06	4.42	0.95	0.91	4.50	0.84	0.73	4.60	4.66	0.43	0.44	4.22
	Fission	–	–	–	0.09	–	–	1.27	1.03	1.14	1.10	0.89	1.00	0.87	0.78	0.71	0.25	0.25	0.78
	n,2n	–	–	–	–	–	–	–	–	–	–	–	–	–	–	–	–	–	–
²⁴² Pu	Capture	–	–	–	–	–	–	–	0.70	–	–	2.83	–	–	2.95	3.01	0.04	0.02	2.72
	Fission	–	–	–	–	–	–	–	0.01	–	–	0.01	–	–	0.01	–	–	–	0.01
	n,2n	–	–	–	–	–	–	–	–	–	–	–	–	–	–	–	–	–	–
²⁴¹ Am	Capture	–	–	–	0.07	–	–	–	0.01	0.95	0.47	0.01	0.55	0.67	0.01	0.01	0.01	0.02	0.04
	Fission	–	–	–	–	–	–	–	–	0.03	0.03	–	0.03	0.03	–	–	–	–	–
	n,2n	–	–	–	–	–	–	–	–	–	–	–	–	–	–	–	–	–	–
^{242m} Am	Capture	–	–	–	–	–	–	–	–	–	2.39	0.09	–	–	0.10	0.10	–	–	0.09
	Fission	–	–	–	–	–	–	–	–	–	4.71	0.03	–	–	0.03	0.03	0.01	–	0.03
	n,2n	–	–	–	–	–	–	–	–	–	–	–	–	–	–	–	–	–	–

^(a) Multiply by the ratio between the total uncertainty on the n_f and the total uncertainty on the Δn of each isotope to get the uncertainty breakdown on n_f (see Table 17 for total uncertainty on the n_f of the isotopes of each system). Multiply by the ratio between the total uncertainty on the burn-up component due to the Δn and the total uncertainty on the Δn of each isotope to get the uncertainty breakdown on the burn-up component due to the Δn (see Table 18 for total uncertainty on the burn-up component due to the Δn of the isotopes of each system).

Table 13. VHTR: $\Delta n^{(a)}$, decay, dose, neutron source BOLNA diagonal uncertainty (%) (*cont.*)

		²³⁵ U	²³⁸ U	²³⁷ Np	²³⁸ Pu	²³⁹ Pu	²⁴⁰ Pu	²⁴¹ Pu	²⁴² Pu	²⁴¹ Am	^{242m} Am	²⁴³ Am	²⁴² Cm	²⁴³ Cm	²⁴⁴ Cm	²⁴⁵ Cm	Decay	Dose	N. Sr
	Capture	—	—	—	—	—	—	—	—	—	—	0.67	—	—	1.97	2.04	0.02	0.02	1.82
²⁴³ Am	Fission	—	—	—	—	—	—	—	—	—	—	—	—	—	—	—	—	—	—
	n,2n	—	—	—	—	—	—	—	—	—	—	—	—	—	—	—	—	—	—
	Capture	—	—	—	0.01	—	—	—	—	—	—	—	0.13	7.91	—	—	—	—	—
²⁴² Cm	Fission	—	—	—	—	—	—	—	—	—	—	—	0.05	0.04	—	—	—	—	—
	n,2n	—	—	—	—	—	—	—	—	—	—	—	—	—	—	—	—	—	—
	Capture	—	—	—	—	—	—	—	—	—	—	—	—	0.32	—	—	—	—	—
²⁴³ Cm	Fission	—	—	—	—	—	—	—	—	—	—	—	—	1.99	—	—	—	—	—
	n,2n	—	—	—	—	—	—	—	—	—	—	—	—	—	—	—	—	—	—
	Capture	—	—	—	—	—	—	—	—	—	—	—	—	—	0.38	5.17	—	—	0.34
²⁴⁴ Cm	Fission	—	—	—	—	—	—	—	—	—	—	—	—	—	0.03	0.02	—	—	0.02
	n,2n	—	—	—	—	—	—	—	—	—	—	—	—	—	—	—	—	—	—
	Capture	—	—	—	—	—	—	—	—	—	—	—	—	—	—	0.19	—	—	0.01
²⁴⁵ Cm	Fission	—	—	—	—	—	—	—	—	—	—	—	—	—	—	0.77	—	—	—
	n,2n	—	—	—	—	—	—	—	—	—	—	—	—	—	—	—	—	—	—
Total		0.19	0.75	1.03	1.28	0.96	1.25	2.04	4.75	2.13	5.63	5.58	1.88	8.37	6.01	8.02	1.12	0.90	5.55

^(a) Multiply by the ratio between the total uncertainty on the n_f and the total uncertainty on the Δn of each isotope to get the uncertainty breakdown on n_f (see Table 17 for total uncertainty on the n_f of the isotopes of each system). Multiply by the ratio between the total uncertainty on the burn-up component due to the Δn and the total uncertainty on the Δn of each isotope to get the uncertainty breakdown on the burn-up component due to the Δn (see Table 18 for total uncertainty on the burn-up component due to the Δn of the isotopes of each system).

Table 14. VHTR: $\Delta n^{(a)}$, decay, dose, neutron source BOLNA full uncertainty (%)

		²³⁵ U	²³⁸ U	²³⁷ Np	²³⁸ Pu	²³⁹ Pu	²⁴⁰ Pu	²⁴¹ Pu	²⁴² Pu	²⁴¹ Am	^{242m} Am	²⁴³ Am	²⁴² Cm	²⁴³ Cm	²⁴⁴ Cm	²⁴⁵ Cm	Decay	Dose	N. Sr
²³⁵ U	Capture	0.25	–	1.18	1.06	–	–	–	–	–	–	–	–	–	–	–	0.18	0.17	0.01
	Fission	0.24	–	0.22	0.17	–	–	–	–	–	–	–	–	–	–	–	0.03	0.03	–
	n,2n	–	–	–	–	–	–	–	–	–	–	–	–	–	–	–	–	–	–
²³⁶ U	Capture	–	–	0.47	0.42	–	–	–	–	–	–	–	–	–	–	–	0.07	0.07	0.01
	Fission	–	–	0.01	0.01	–	–	–	–	–	–	–	–	–	–	–	–	–	–
	n,2n	–	–	–	–	–	–	–	–	–	–	–	–	–	–	–	–	–	–
²³⁸ U	Capture	–	0.91	–	0.10	0.89	0.90	0.91	0.92	0.92	0.92	0.93	0.92	0.93	0.93	0.93	0.77	0.75	0.92
	Fission	–	0.01	–	–	–	–	–	–	–	–	–	–	–	–	–	–	–	–
	n,2n	–	–	0.04	0.04	–	–	–	–	–	–	–	–	–	–	–	0.01	0.01	–
²³⁷ Np	Capture	–	–	0.51	0.99	–	–	–	–	–	–	–	–	–	–	–	0.17	0.13	0.01
	Fission	–	–	0.01	–	–	–	–	–	–	–	–	–	–	–	–	–	–	–
	n,2n	–	–	–	–	–	–	–	–	–	–	–	–	–	–	–	–	–	–
²³⁸ Pu	Capture	–	–	–	0.18	–	–	–	–	–	–	–	–	–	–	–	0.03	0.02	–
	Fission	–	–	–	0.04	–	–	–	–	–	–	–	–	–	–	–	0.01	0.01	–
	n,2n	–	–	–	–	–	–	–	–	–	–	–	–	–	–	–	–	–	–
²³⁹ Pu	Capture	–	–	–	0.11	0.59	0.96	0.98	1.03	1.01	1.01	1.05	1.03	1.06	1.08	1.09	0.80	0.14	1.06
	Fission	–	–	–	0.06	0.60	0.66	0.63	0.58	0.60	0.59	0.54	0.57	0.53	0.51	0.49	0.53	0.40	0.51
	n,2n	–	–	–	–	–	–	–	–	–	–	–	–	–	–	–	–	–	–
²⁴⁰ Pu	Capture	–	–	–	0.02	–	0.51	0.08	0.16	0.12	0.13	0.20	0.16	0.21	0.24	0.27	0.05	0.03	0.23
	Fission	–	–	–	–	–	–	–	–	–	–	–	–	–	–	–	–	–	–
	n,2n	–	–	–	–	–	–	–	–	–	–	–	–	–	–	–	–	–	–
²⁴¹ Pu	Capture	–	–	–	0.08	–	–	1.10	4.60	0.98	0.95	4.69	0.87	0.76	4.79	4.85	0.45	0.45	4.39
	Fission	–	–	–	0.10	–	–	1.41	1.14	1.26	1.21	0.99	1.11	0.97	0.86	0.79	0.28	0.28	0.86
	n,2n	–	–	–	–	–	–	–	–	–	–	–	–	–	–	–	–	–	–
²⁴² Pu	Capture	–	–	–	–	–	–	–	0.75	–	–	3.05	–	–	3.17	3.23	0.05	0.02	2.93
	Fission	–	–	–	–	–	–	–	0.01	–	–	0.01	–	–	0.01	0.01	–	–	0.01
	n,2n	–	–	–	–	–	–	–	–	–	–	–	–	–	–	–	–	–	–
²⁴¹ Am	Capture	–	–	–	0.08	–	–	–	0.01	0.99	0.49	0.01	0.57	0.69	0.01	0.01	0.01	0.02	0.04
	Fission	–	–	–	–	–	–	–	–	0.03	0.03	–	0.03	0.03	–	–	–	–	–
	n,2n	–	–	–	–	–	–	–	–	–	–	–	–	–	–	–	–	–	–
^{242m} Am	Capture	–	–	–	–	–	–	–	–	–	–	3.18	0.12	–	–	0.13	0.13	–	0.12
	Fission	–	–	–	–	–	–	–	–	–	–	6.08	0.04	–	–	0.04	0.04	0.01	0.04
	n,2n	–	–	–	–	–	–	–	–	–	–	–	–	–	–	–	–	–	–

^(a) Multiply by the ratio between the total uncertainty on the n_f and the total uncertainty on the Δn of each isotope to get the uncertainty breakdown on n_f (see Table 17 for total uncertainty on the n_f of the isotopes of each system). Multiply by the ratio between the total uncertainty on the burn-up component due to the Δn and the total uncertainty on the Δn of each isotope to get the uncertainty breakdown on the burn-up component due to the Δn (see Table 18 for total uncertainty on the burn-up component due to the Δn of the isotopes of each system).

Table 14. VHTR: $\Delta n^{(a)}$, decay, dose, neutron source BOLNA full uncertainty (%) (*cont.*)

		²³⁵ U	²³⁸ U	²³⁷ Np	²³⁸ Pu	²³⁹ Pu	²⁴⁰ Pu	²⁴¹ Pu	²⁴² Pu	²⁴¹ Am	^{242m} Am	²⁴³ Am	²⁴² Cm	²⁴³ Cm	²⁴⁴ Cm	²⁴⁵ Cm	Decay	Dose	N. Sr
	Capture	—	—	—	—	—	—	—	—	—	—	0.76	—	—	2.23	2.31	0.02	0.02	2.06
²⁴³ Am	Fission	—	—	—	—	—	—	—	—	—	—	—	—	—	—	—	—	—	—
	n,2n	—	—	—	—	—	—	—	—	—	—	—	—	—	—	—	—	—	—
	Capture	—	—	—	0.02	—	—	—	—	—	—	—	0.18	11.35	—	—	—	—	—
²⁴² Cm	Fission	—	—	—	0.01	—	—	—	—	—	—	—	0.07	0.06	—	—	—	—	—
	n,2n	—	—	—	—	—	—	—	—	—	—	—	—	—	—	—	—	—	—
	Capture	—	—	—	—	—	—	—	—	—	—	—	—	0.41	—	—	—	—	—
²⁴³ Cm	Fission	—	—	—	—	—	—	—	—	—	—	—	—	2.45	—	—	—	—	—
	n,2n	—	—	—	—	—	—	—	—	—	—	—	—	—	—	—	—	—	—
	Capture	—	—	—	—	—	—	—	—	—	—	—	—	—	0.43	5.76	—	—	0.38
²⁴⁴ Cm	Fission	—	—	—	—	—	—	—	—	—	—	—	—	—	0.03	0.03	—	—	0.03
	n,2n	—	—	—	—	—	—	—	—	—	—	—	—	—	—	—	—	—	—
	Capture	—	—	—	—	—	—	—	—	—	—	—	—	—	—	0.27	—	—	0.02
²⁴⁵ Cm	Fission	—	—	—	—	—	—	—	—	—	—	—	—	—	—	1.04	—	—	—
	n,2n	—	—	—	—	—	—	—	—	—	—	—	—	—	—	—	—	—	—
Total		0.34	0.91	1.38	1.55	1.22	1.56	2.33	5.03	2.40	7.21	5.93	2.15	11.80	6.42	8.76	1.37	1.04	5.94

^(a) Multiply by the ratio between the total uncertainty on the n_f and the total uncertainty on the Δn of each isotope to get the uncertainty breakdown on n_f (see Table 17 for total uncertainty on the n_f of the isotopes of each system). Multiply by the ratio between the total uncertainty on the burn-up component due to the Δn and the total uncertainty on the Δn of each isotope to get the uncertainty breakdown on the burn-up component due to the Δn (see Table 18 for total uncertainty on the burn-up component due to the Δn of the isotopes of each system).

Table 15. PWR: $\Delta n^{(a)}$, decay, dose, neutron source BOLNA diagonal uncertainty (%)

		²³⁵ U	²³⁸ U	²³⁷ Np	²³⁸ Pu	²³⁹ Pu	²⁴⁰ Pu	²⁴¹ Pu	²⁴² Pu	²⁴¹ Am	^{242m} Am	²⁴³ Am	²⁴² Cm	²⁴³ Cm	²⁴⁴ Cm	²⁴⁵ Cm	Decay	Dose	N. Sr
²³⁵ U	Capture	0.05	—	0.71	0.62	0.01	0.01	0.01	—	—	—	—	—	—	—	—	0.27	0.23	0.01
	Fission	0.04	—	0.06	0.04	—	—	—	—	—	—	—	—	—	—	—	0.02	0.02	—
	n,2n	—	—	—	—	—	—	—	—	—	—	—	—	—	—	—	—	0.03	—
²³⁶ U	Capture	—	—	0.34	0.30	0.01	—	—	—	—	—	—	—	—	—	—	0.13	0.11	—
	Fission	—	—	0.08	0.05	—	—	—	—	—	—	—	—	—	—	—	0.02	0.02	—
	n,2n	—	—	—	—	—	—	—	—	—	—	—	—	—	—	—	—	—	—
²³⁸ U	Capture	—	0.62	—	0.09	0.67	0.69	0.69	0.71	0.70	0.70	0.71	0.71	0.71	0.71	0.72	0.44	0.46	0.71
	Fission	—	0.04	—	—	—	—	—	—	—	—	—	—	—	—	—	—	—	—
	n,2n	—	0.02	0.44	0.45	0.01	0.01	—	—	—	—	—	—	—	—	—	0.20	0.17	0.01
²³⁷ Np	Capture	—	—	0.53	0.44	0.01	0.01	0.01	—	—	—	—	—	—	—	—	0.19	0.14	0.01
	Fission	—	—	0.04	0.03	—	—	—	—	—	—	—	—	—	—	—	0.01	0.01	—
	n,2n	—	—	—	—	—	—	—	—	—	—	—	—	—	—	—	—	—	—
²³⁸ Pu	Capture	—	—	—	0.36	0.02	0.01	0.01	—	0.01	—	—	—	—	—	—	0.15	0.11	—
	Fission	—	—	—	0.19	—	—	—	—	—	—	—	—	—	—	—	0.08	0.06	—
	n,2n	—	—	—	—	—	—	—	—	—	—	—	—	—	—	—	—	—	—
²³⁹ Pu	Capture	—	—	—	0.11	0.38	0.67	0.69	0.74	0.72	0.72	0.77	0.73	0.76	0.81	0.82	0.42	—	0.80
	Fission	—	—	—	0.04	0.42	0.40	0.38	0.32	0.35	0.34	0.29	0.33	0.29	0.25	0.23	0.23	0.26	0.25
	n,2n	—	—	—	—	—	—	—	—	—	—	—	—	—	—	—	—	—	—
²⁴⁰ Pu	Capture	—	—	—	0.02	—	0.38	0.07	0.11	0.10	0.10	0.14	0.11	0.13	0.17	0.18	0.03	0.03	0.16
	Fission	—	—	—	—	—	0.02	0.02	0.01	0.01	0.01	0.01	0.01	0.01	0.01	0.01	0.01	—	0.01
	n,2n	—	—	—	—	—	—	—	—	—	—	—	—	—	—	—	—	—	—
²⁴¹ Pu	Capture	—	—	—	0.09	—	0.01	0.92	3.22	0.84	0.83	3.27	0.79	0.71	3.36	3.40	0.31	0.29	3.24
	Fission	—	—	—	0.14	—	—	1.46	1.25	1.34	1.32	1.11	1.26	1.14	0.96	0.89	0.77	0.28	0.95
	n,2n	—	—	—	—	—	—	—	—	—	—	—	—	—	—	—	—	—	—
²⁴² Pu	Capture	—	—	—	—	—	0.01	—	1.37	—	—	2.26	—	0.01	2.45	2.53	0.11	0.01	2.37
	Fission	—	—	—	—	—	—	—	0.08	—	—	0.06	—	—	0.05	0.05	—	0.01	0.05
	n,2n	—	—	—	—	—	—	—	—	—	—	—	—	—	—	—	—	—	—
²⁴¹ Am	Capture	—	—	—	0.08	—	—	—	0.01	1.62	0.21	0.02	0.29	0.46	0.02	0.03	0.01	0.03	0.03
	Fission	—	—	—	—	—	—	—	—	0.05	0.04	—	0.04	0.04	—	—	—	—	—
	n,2n	—	—	—	—	—	—	—	—	—	—	—	—	—	—	—	—	—	—
^{242m} Am	Capture	—	—	—	—	—	—	—	—	—	2.43	0.11	—	—	0.12	0.13	—	—	0.12
	Fission	—	—	—	—	—	—	—	—	—	4.44	0.04	—	—	0.05	0.05	0.01	—	0.05
	n,2n	—	—	—	—	—	—	—	—	—	—	—	—	—	—	—	—	—	—

^(a) Multiply by the ratio between the total uncertainty on the n_f and the total uncertainty on the Δn of each isotope to get the uncertainty breakdown on n_f (see Table 17 for total uncertainty on the n_f of the isotopes of each system). Multiply by the ratio between the total uncertainty on the burn-up component due to the Δn and the total uncertainty on the Δn of each isotope to get the uncertainty breakdown on the burn-up component due to the Δn (see Table 18 for total uncertainty on the burn-up component due to the Δn of the isotopes of each system).

Table 15. PWR: $\Delta n^{(a)}$, decay, dose, neutron source BOLNA diagonal uncertainty (%) (*cont.*)

		²³⁵ U	²³⁸ U	²³⁷ Np	²³⁸ Pu	²³⁹ Pu	²⁴⁰ Pu	²⁴¹ Pu	²⁴² Pu	²⁴¹ Am	^{242m} Am	²⁴³ Am	²⁴² Cm	²⁴³ Cm	²⁴⁴ Cm	²⁴⁵ Cm	Decay	Dose	N. Sr
²⁴³ Am	Capture	—	—	—	—	—	—	—	—	—	—	1.34	—	—	1.45	1.54	0.05	0.05	1.41
	Fission	—	—	—	—	—	—	—	—	—	—	0.03	—	—	0.02	0.02	—	—	0.02
	n,2n	—	—	—	—	—	—	—	—	—	—	—	—	—	—	—	—	—	—
²⁴² Cm	Capture	—	—	—	0.01	—	—	—	—	—	—	—	0.12	4.51	0.01	0.01	0.01	0.01	—
	Fission	—	—	—	0.01	—	—	—	—	—	—	—	0.10	0.09	—	—	0.01	0.01	—
	n,2n	—	—	—	—	—	—	—	—	—	—	—	—	—	—	—	—	—	—
²⁴³ Cm	Capture	—	—	—	—	—	—	—	—	—	—	—	—	0.54	0.01	0.01	—	—	0.01
	Fission	—	—	—	—	—	—	—	—	—	—	—	—	2.52	—	—	—	—	—
	n,2n	—	—	—	—	—	—	—	—	—	—	—	—	—	—	—	—	—	—
²⁴⁴ Cm	Capture	—	—	—	—	—	—	—	—	—	—	—	—	—	1.09	4.73	0.04	—	0.97
	Fission	—	—	—	—	—	—	—	—	—	—	—	—	—	0.20	0.18	0.01	—	0.19
	n,2n	—	—	—	—	—	—	—	—	—	—	—	—	0.08	—	—	—	—	—
²⁴⁵ Cm	Capture	—	—	—	—	—	—	—	—	—	—	—	—	—	—	0.40	—	—	0.07
	Fission	—	—	—	—	—	—	—	—	—	—	—	—	—	—	1.33	—	—	0.02
	n,2n	—	—	—	—	—	—	—	—	—	—	—	—	—	—	—	—	—	—
Total		0.06	0.62	1.05	1.05	0.88	1.11	2.02	3.87	2.50	5.41	4.48	1.87	5.50	4.77	6.84	1.15	0.76	4.61

^(a) Multiply by the ratio between the total uncertainty on the n_f and the total uncertainty on the Δn of each isotope to get the uncertainty breakdown on n_f (see Table 17 for total uncertainty on the n_f of the isotopes of each system). Multiply by the ratio between the total uncertainty on the burn-up component due to the Δn and the total uncertainty on the Δn of each isotope to get the uncertainty breakdown on the burn-up component due to the Δn (see Table 18 for total uncertainty on the burn-up component due to the Δn of the isotopes of each system).

Table 16. PWR: $\Delta n^{(a)}$, decay, dose, neutron source BOLNA full uncertainty (%)

		²³⁵ U	²³⁸ U	²³⁷ Np	²³⁸ Pu	²³⁹ Pu	²⁴⁰ Pu	²⁴¹ Pu	²⁴² Pu	²⁴¹ Am	^{242m} Am	²⁴³ Am	²⁴² Cm	²⁴³ Cm	²⁴⁴ Cm	²⁴⁵ Cm	Decay	Dose	N. Sr
²³⁵ U	Capture	0.09	—	1.21	1.06	0.02	0.02	0.01	0.01	0.01	0.01	—	0.01	—	—	—	0.46	0.40	0.01
	Fission	0.07	—	0.23	0.17	—	—	—	—	—	—	—	—	—	—	—	0.07	0.07	—
	n,2n	—	—	—	—	—	—	—	—	—	—	—	—	—	—	—	—	0.03	—
²³⁶ U	Capture	—	—	0.40	0.35	0.01	0.01	—	—	—	—	—	—	—	—	—	0.15	0.13	—
	Fission	—	—	0.13	0.08	—	—	—	—	—	—	—	—	—	—	—	0.03	0.03	—
	n,2n	—	—	—	—	—	—	—	—	—	—	—	—	—	—	—	—	—	—
²³⁸ U	Capture	—	0.84	—	0.13	0.91	0.93	0.94	0.96	0.95	0.95	0.96	0.96	0.96	0.97	0.97	0.59	0.62	0.96
	Fission	—	0.06	—	—	—	—	—	—	—	—	—	—	—	—	—	—	—	—
	n,2n	—	0.02	0.44	0.45	0.01	0.01	—	—	—	—	—	—	—	—	—	0.20	0.17	0.01
²³⁷ Np	Capture	—	—	0.57	0.48	0.01	0.01	0.01	—	—	—	—	—	—	—	—	0.21	0.15	0.01
	Fission	—	—	0.07	0.05	—	—	—	—	—	—	—	—	—	—	—	0.02	0.02	—
	n,2n	—	—	—	—	—	—	—	—	—	—	—	—	—	—	—	—	—	—
²³⁸ Pu	Capture	—	—	—	0.45	0.02	0.01	0.01	0.01	0.01	0.01	—	0.01	—	—	—	0.19	0.14	—
	Fission	—	—	—	0.30	0.01	—	—	—	—	—	—	—	—	—	—	0.13	0.10	—
	n,2n	—	—	—	—	—	—	—	—	—	—	—	—	—	—	—	—	—	—
²³⁹ Pu	Capture	—	—	—	0.13	0.54	0.87	0.88	0.92	0.91	0.91	0.95	0.92	0.94	0.98	0.99	0.54	0.01	0.97
	Fission	—	—	—	0.07	0.60	0.65	0.63	0.57	0.59	0.59	0.53	0.57	0.53	0.48	0.46	0.38	0.30	0.48
	n,2n	—	—	—	—	—	—	—	—	—	—	—	—	—	—	—	—	—	—
²⁴⁰ Pu	Capture	—	—	—	0.02	—	0.42	0.08	0.12	0.11	0.11	0.15	0.12	0.15	0.18	0.19	0.04	0.03	0.18
	Fission	—	—	—	—	—	0.03	0.03	0.02	0.02	0.02	0.02	0.02	0.02	0.02	0.01	0.02	—	0.02
	n,2n	—	—	—	—	—	—	—	—	—	—	—	—	—	—	—	—	—	—
²⁴¹ Pu	Capture	—	—	—	0.10	—	0.01	1.04	3.65	0.95	0.94	3.71	0.90	0.81	3.81	3.86	0.35	0.33	3.68
	Fission	—	—	—	0.18	—	—	1.84	1.57	1.68	1.65	1.39	1.58	1.43	1.21	1.12	0.97	0.35	1.20
	n,2n	—	—	—	—	—	—	—	—	—	—	—	—	—	—	—	—	—	—
²⁴² Pu	Capture	—	—	—	—	—	0.01	—	1.42	—	—	2.34	—	0.01	2.53	2.62	0.11	0.01	2.46
	Fission	—	—	—	—	—	—	—	0.12	—	—	0.10	—	—	0.08	0.07	—	0.01	0.08
	n,2n	—	—	—	—	—	—	—	—	—	—	—	—	—	—	—	—	—	—
²⁴¹ Am	Capture	—	—	—	0.08	—	—	—	0.01	1.68	0.21	0.02	0.30	0.48	0.03	0.03	0.01	0.03	0.03
	Fission	—	—	—	0.01	—	—	—	—	0.06	0.06	—	0.05	0.05	—	—	0.01	—	—
	n,2n	—	—	—	—	—	—	—	—	—	—	—	—	—	—	—	—	—	—
^{242m} Am	Capture	—	—	—	—	—	—	—	—	—	3.45	0.16	—	—	0.18	0.19	—	—	0.17
	Fission	—	—	—	—	—	—	—	—	—	6.21	0.06	—	—	0.07	0.07	0.01	—	0.07
	n,2n	—	—	—	—	—	—	—	—	—	—	—	—	—	—	—	—	—	—

^(a) Multiply by the ratio between the total uncertainty on the n_f and the total uncertainty on the Δn of each isotope to get the uncertainty breakdown on n_f (see Table 17 for total uncertainty on the n_f of the isotopes of each system). Multiply by the ratio between the total uncertainty on the burn-up component due to the Δn and the total uncertainty on the Δn of each isotope to get the uncertainty breakdown on the burn-up component due to the Δn (see Table 18 for total uncertainty on the burn-up component due to the Δn of the isotopes of each system).

Table 16. PWR: $\Delta n^{(a)}$, decay, dose, neutron source BOLNA full uncertainty (%) (*cont.*)

		²³⁵ U	²³⁸ U	²³⁷ Np	²³⁸ Pu	²³⁹ Pu	²⁴⁰ Pu	²⁴¹ Pu	²⁴² Pu	²⁴¹ Am	^{242m} Am	²⁴³ Am	²⁴² Cm	²⁴³ Cm	²⁴⁴ Cm	²⁴⁵ Cm	Decay	Dose	N. Sr
²⁴³ Am	Capture	—	—	—	—	—	—	—	—	—	—	1.44	—	—	1.55	1.65	0.05	0.05	1.50
	Fission	—	—	—	—	—	—	—	—	—	—	0.03	—	—	0.03	0.03	—	—	0.03
	n,2n	—	—	—	—	—	—	—	—	—	—	—	—	—	—	—	—	—	—
²⁴² Cm	Capture	—	—	—	0.02	—	—	—	—	—	—	—	0.17	6.40	0.01	0.01	0.01	0.01	—
	Fission	—	—	—	0.02	—	—	—	—	—	—	—	0.15	0.14	—	—	0.01	0.01	—
	n,2n	—	—	—	—	—	—	—	—	—	—	—	—	—	—	—	—	—	—
²⁴³ Cm	Capture	—	—	—	—	—	—	—	—	—	—	—	—	0.67	0.01	0.01	—	—	0.01
	Fission	—	—	—	—	—	—	—	—	—	—	—	—	3.27	—	—	—	—	—
	n,2n	—	—	—	—	—	—	—	—	—	—	—	—	—	—	—	—	—	—
²⁴⁴ Cm	Capture	—	—	—	—	—	—	—	—	—	—	—	—	—	1.15	4.98	0.04	—	1.02
	Fission	—	—	—	—	—	—	—	—	—	—	—	—	—	0.31	0.28	0.01	—	0.30
	n,2n	—	—	—	—	—	—	—	—	—	—	—	—	0.08	—	—	—	—	—
²⁴⁵ Cm	Capture	—	—	—	—	—	—	—	—	—	—	—	—	—	—	0.53	—	—	0.09
	Fission	—	—	—	—	—	—	—	—	—	—	—	—	—	—	1.83	—	—	0.02
	n,2n	—	—	—	—	—	—	—	—	—	—	—	—	—	—	—	—	—	—
Total		0.12	0.84	1.49	1.45	1.22	1.49	2.55	4.47	2.94	7.50	5.04	2.36	7.56	5.33	7.51	1.50	0.99	5.16

^(a) Multiply by the ratio between the total uncertainty on the n_f and the total uncertainty on the Δn of each isotope to get the uncertainty breakdown on n_f (see Table 17 for total uncertainty on the n_f of the isotopes of each system). Multiply by the ratio between the total uncertainty on the burn-up component due to the Δn and the total uncertainty on the Δn of each isotope to get the uncertainty breakdown on the burn-up component due to the Δn (see Table 18 for total uncertainty on the burn-up component due to the Δn of the isotopes of each system).

Table 17. η_f BOLNA uncertainties (%) – total by isotope

	ABTR		SFR		EFR		GFR		LFR		ADMAB		VHTR		PWR	
	Diag.	Full	Diag.	Full	Diag.	Full	Diag.	Full	Diag.	Full	Diag.	Full	Diag.	Full	Diag.	Full
²³⁵ U	0.07	0.16	0.31	0.59	2.57	5.14	0.42	0.84	0.36	0.72	–	–	0.25	0.44	0.46	0.87
²³⁸ U	0.01	0.01	0.02	0.02	0.24	0.26	0.04	0.04	0.03	0.03	–	–	0.05	0.06	0.04	0.06
²³⁷ Np	0.25	0.26	0.11	0.22	2.51	3.04	0.25	0.44	0.18	0.33	0.20	0.39	1.03	1.38	1.05	1.49
²³⁸ Pu	0.21	0.36	0.42	0.74	2.71	4.91	0.64	1.15	0.56	0.95	1.13	2.07	1.28	1.55	1.05	1.45
²³⁹ Pu	0.04	0.05	0.06	0.09	1.13	1.33	0.37	0.41	0.20	0.23	0.12	0.18	0.96	1.22	0.88	1.22
²⁴⁰ Pu	0.13	0.22	0.10	0.19	1.25	2.20	0.31	0.44	0.16	0.31	0.26	0.44	1.25	1.56	1.11	1.49
²⁴¹ Pu	0.35	0.72	0.62	1.23	3.99	8.01	0.83	1.55	1.19	2.44	0.90	1.72	2.04	2.33	2.02	2.55
²⁴² Pu	0.13	0.22	0.25	0.40	2.75	4.66	0.51	0.84	0.35	0.55	0.54	0.92	4.75	5.03	3.87	4.47
²⁴¹ Am	0.08	0.13	0.18	0.30	2.12	3.78	0.35	0.60	0.27	0.45	0.31	0.53	2.13	2.40	2.50	2.94
^{242m} Am	0.47	0.86	0.70	1.40	4.26	8.36	2.17	3.85	1.17	2.22	1.72	3.07	5.63	7.21	5.41	7.50
²⁴³ Am	0.35	0.55	0.47	0.76	6.41	10.87	1.07	1.81	0.91	1.46	0.27	0.45	5.58	5.93	4.48	5.04
²⁴² Cm	1.13	1.91	1.38	2.36	1.58	2.87	2.43	4.27	2.49	4.11	2.78	4.75	1.88	2.15	1.87	2.36
²⁴³ Cm	1.30	2.53	1.90	3.77	10.59	20.63	3.91	6.51	3.29	6.37	3.04	5.72	8.37	11.80	5.50	7.56
²⁴⁴ Cm	0.38	0.59	0.73	1.10	4.83	7.67	0.91	1.54	0.88	1.28	1.07	1.60	6.01	6.42	4.77	5.33
²⁴⁵ Cm	0.90	1.69	1.47	2.91	9.37	18.15	1.83	3.60	2.35	4.54	2.48	4.86	8.02	8.76	6.84	7.51
²⁴⁶ Cm	0.51	0.89	0.47	0.77	4.48	7.45	1.35	2.56	0.57	0.89	3.12	5.99	–	–	–	–

Table 18. Burn-up BOLNA uncertainty component [pcm] due to Δn uncertainties (total by isotope)

	ABTR		SFR		EFR		GFR		LFR		ADMAB		VHTR		PWR	
	Diag.	Full	Diag.	Full	Diag.	Full	Diag.	Full	Diag.	Full	Diag.	Full	Diag.	Full	Diag.	Full
²³⁵ U	0.2	0.5	0.4	0.8	2.5	5.0	7.3	14.7	1.3	2.6	–	–	7.0	12.3	2.5	4.7
²³⁸ U	0.5	0.6	0.5	0.5	30.5	32.9	7.3	7.8	3.7	4.0	–	–	7.9	9.6	5.6	7.5
²³⁸ Pu	0.2	0.4	15.5	27.3	23.1	41.9	13.4	24.1	14.0	23.9	40.3	74.0	0.8	1.0	6.1	8.4
²³⁹ Pu	20.7	25.6	15.5	22.3	350.5	411.5	129.4	143.7	86.6	102.0	32.1	47.6	18.7	23.7	189.7	254.9
²⁴⁰ Pu	1.6	2.7	5.4	10.4	28.2	49.7	6.8	9.8	7.1	13.6	6.4	10.8	127.7	159.6	19.6	24.8
²⁴¹ Pu	3.6	7.3	48.6	96.4	178.3	358.1	67.7	127.0	58.4	119.9	75.8	145.9	29.5	33.7	36.8	42.5
²⁴² Pu	0.1	0.1	3.3	5.2	4.1	7.0	2.3	3.8	2.0	3.2	3.7	6.2	15.6	16.5	8.9	12.7
²³⁷ Np	–	0.1	0.2	0.4	1.5	1.8	1.3	2.3	0.2	0.4	–	–	3.5	4.7	3.8	5.2
²⁴¹ Am	–	0.1	0.8	1.3	6.0	10.7	7.4	12.9	1.2	2.0	2.6	4.4	4.3	4.9	6.1	7.2
^{242m} Am	0.1	0.2	35.7	71.1	10.6	20.8	12.6	22.4	6.0	11.3	37.8	67.4	0.4	0.6	0.6	0.9
²⁴³ Am	–	–	2.3	3.7	9.8	16.6	7.0	11.7	2.1	3.4	6.3	10.5	4.9	5.2	21.8	24.5
²⁴² Cm	0.1	0.1	1.7	2.8	0.6	1.2	4.8	8.4	1.6	2.7	16.8	28.6	–	–	–	0.1
²⁴³ Cm	–	–	1.0	1.9	3.6	7.0	2.2	3.7	0.7	1.4	12.5	23.6	–	–	0.1	0.1
²⁴⁴ Cm	–	–	5.2	7.9	5.3	8.5	2.4	4.1	2.4	3.5	45.1	67.5	0.3	0.3	4.5	5.1
²⁴⁵ Cm	–	–	17.9	35.3	18.3	35.5	10.1	19.9	14.6	28.2	101.3	198.4	0.2	0.2	3.2	3.5
²⁴⁶ Cm	–	–	0.3	0.5	0.3	0.5	–	0.1	0.2	0.3	0.4	0.8				
Total	21.1	26.8	67.2	130.7	396.9	552.4	148.6	197.6	107.0	162.9	150.6	281.3	134.0	166.6	196.0	261.6

Appendix O

UNCERTAINTY (%) BREAKDOWN BY ISOTOPE, ENERGY GROUP, CROSS-SECTION

Table 1. ABTR k_{eff} : BOLNA diagonal uncertainty (%) by group

Gr.	[MeV]	σ_{cap}	σ_{fiss}	ν	σ_{el}	σ_{inel}	$\sigma_{\text{n,2n}}$	Total
1	19.6	0.02	0.01	0.01	—	0.05	0.01	0.05
2	6.07	0.01	0.03	0.07	0.03	0.34	—	0.35
3	2.23	0.02	0.04	0.07	0.03	0.33	—	0.34
4	1.35	0.06	0.08	0.05	0.05	0.09	—	0.15
5	4.98e-1	0.08	0.10	0.04	0.05	0.01	—	0.14
6	1.83e-1	0.09	0.11	0.09	0.04	0.04	—	0.18
7	6.74e-2	0.07	0.05	0.05	0.01	—	—	0.10
8	2.48e-2	0.21	0.04	0.03	0.01	—	—	0.22
9	9.12e-3	0.06	0.01	0.01	—	—	—	0.06
10	2.03e-3	0.04	0.02	—	—	—	—	0.04
11	4.54e-4	0.01	0.01	—	0.01	—	—	0.02
12	2.26e-5	—	—	—	—	—	—	0.01
13	4.00e-6	—	—	—	—	—	—	—
14	5.40e-7	—	—	—	—	—	—	—
15	1.00e-7	—	—	—	—	—	—	—
Total		0.27	0.19	0.16	0.09	0.49	0.01	0.62

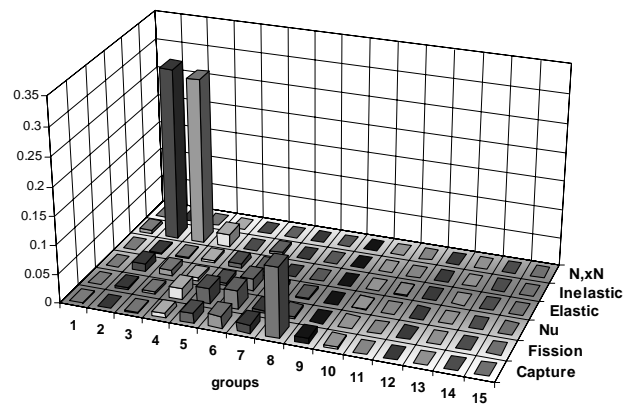


Table 2. ABTR k_{eff} : BOLNA full uncertainty (%) by group

Gr.	[MeV]	σ_{cap}	σ_{fiss}	ν	σ_{el}	σ_{inel}	$\sigma_{\text{n,2n}}$	Total
1	19.6	0.03	0.02	0.03	0.01	0.10	0.01	0.11
2	6.07	0.03	0.06	0.10	0.09	0.49	—	0.51
3	2.23	0.04	0.08	0.09	0.11	0.49	—	0.51
4	1.35	0.09	0.13	0.06	0.15	0.23	—	0.32
5	4.98e-1	0.13	0.14	0.06	0.07	0.02	—	0.22
6	1.83e-1	0.15	0.15	0.10	0.06	0.05	—	0.24
7	6.74e-2	0.12	0.09	0.06	0.02	0.02	—	0.16
8	2.48e-2	0.23	0.06	0.04	0.03	0.01i	—	0.25
9	9.12e-3	0.08	0.02	0.02	0.01	—	—	0.08
10	2.03e-3	0.05	0.02	0.01	0.01	—	—	0.05
11	4.54e-4	0.02	0.01	—	0.02i	—	—	0.02
12	2.26e-5	0.01	—	—	0.01i	—	—	0.01
13	4.00e-6	0.01	—	—	—	—	—	0.01
14	5.40e-7	—	—	—	—	—	—	—
15	1.00e-7	—	—	—	—	—	—	—
Total		0.36	0.29	0.20	0.23	0.73	0.01	0.92

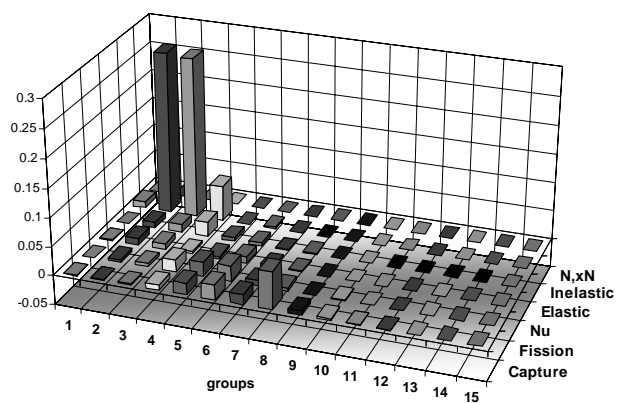


Table 3. ABTR k_{eff} : BOLNA diagonal uncertainty (%) by isotope

Isotope	σ_{cap}	σ_{fiss}	ν	σ_{el}	σ_{inel}	$\sigma_{\text{n,2n}}$	Total
²³⁵ U	—	—	—	—	—	—	0.01
²³⁸ U	0.23	0.03	0.10	0.04	0.45	—	0.52
²³⁸ Pu	—	0.01	—	—	—	—	0.01
²³⁹ Pu	0.13	0.17	0.11	0.01	0.04	—	0.25
²⁴⁰ Pu	0.03	0.05	0.05	—	—	—	0.08
²⁴¹ Pu	—	0.07	—	—	—	—	0.07
²⁴² Pu	—	0.01	—	—	—	—	0.01
²³⁷ Np	—	—	—	—	—	—	—
²⁴¹ Am	—	—	—	—	—	—	0.01
^{242m} Am	—	—	—	—	—	—	—
²⁴³ Am	—	—	—	—	—	—	—
²⁴² Cm	—	—	—	—	—	—	—
²⁴³ Cm	—	—	—	—	—	—	—
²⁴⁴ Cm	—	—	—	—	—	—	—
²⁴⁵ Cm	—	—	—	—	—	—	—
²⁴⁶ Cm	—	—	—	—	—	—	—
⁵⁶ Fe	0.06	—	—	0.06	0.16	—	0.18
⁵² Cr	0.01	—	—	0.04	—	0.01	0.04
⁵⁸ Ni	—	—	—	—	—	—	—
⁹⁰ Zr	—	—	—	0.01	0.03	—	0.03
²³ Na	0.01	—	—	0.04	0.05	—	0.07
¹⁶ O	—	—	—	—	—	—	—
C	—	—	—	—	—	—	—
¹⁰ B	0.02	—	—	—	—	—	0.02
Total	0.27	0.19	0.16	0.09	0.49	0.01	0.62

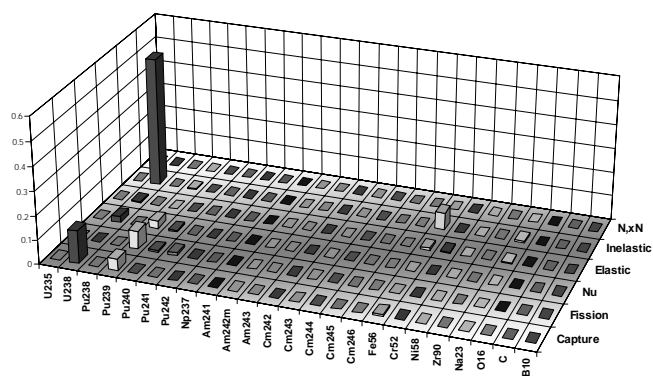


Table 4. ABTR k_{eff} : BOLNA full uncertainty (%) by isotope

Isotope	σ_{cap}	σ_{fiss}	ν	σ_{el}	σ_{inel}	$\sigma_{\text{n,2n}}$	Total
²³⁵ U	0.01	—	—	—	—	—	0.01
²³⁸ U	0.26	0.04	0.14	0.20	0.69	—	0.77
²³⁸ Pu	—	0.01	0.01	—	—	—	0.02
²³⁹ Pu	0.23	0.24	0.13	0.03	0.06	—	0.36
²⁴⁰ Pu	0.06	0.09	0.08	—	0.01	—	0.13
²⁴¹ Pu	0.01	0.12	—	—	—	—	0.12
²⁴² Pu	0.01	0.01	—	—	—	—	0.01
²³⁷ Np	—	—	—	—	—	—	0.01
²⁴¹ Am	0.01	0.01	—	—	—	—	0.01
^{242m} Am	—	—	—	—	—	—	—
²⁴³ Am	—	—	—	—	—	—	—
²⁴² Cm	—	—	—	—	—	—	—
²⁴³ Cm	—	—	—	—	—	—	—
²⁴⁴ Cm	—	—	—	—	—	—	—
²⁴⁵ Cm	—	—	—	—	—	—	—
²⁴⁶ Cm	—	—	—	—	—	—	—
⁵⁶ Fe	0.07	—	—	0.08	0.24	—	0.27
⁵² Cr	0.01	—	—	0.06	—	0.01	0.06
⁵⁸ Ni	—	—	—	—	—	—	—
⁹⁰ Zr	0.01	—	—	0.01	0.03	—	0.04
²³ Na	0.02	—	—	0.05	0.07	—	0.08
¹⁶ O	—	—	—	—	—	—	—
C	—	—	—	—	—	—	—
¹⁰ B	0.04	—	—	—	—	—	0.04
Total	0.36	0.29	0.20	0.23	0.73	0.01	0.92

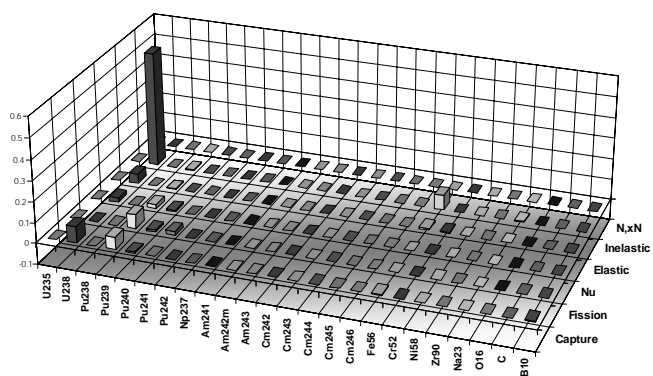


Table 5. ABTR power peak: BOLNA diagonal uncertainty (%) by group

Gr.	[MeV]	σ_{cap}	σ_{fiss}	ν	σ_{el}	σ_{inel}	$\sigma_{\text{n,2n}}$	Total
1	19.6	0.01	—	—	—	—	—	0.01
2	6.07	—	0.01	0.02	0.03	0.04	—	0.05
3	2.23	—	0.01	0.01	0.05	0.06	—	0.08
4	1.35	0.01	0.02	0.01	0.10	0.20	—	0.23
5	4.98e-1	0.04	0.02	0.01	0.09	0.04	—	0.11
6	1.83e-1	0.05	0.03	0.01	0.08	0.01	—	0.10
7	6.74e-2	0.05	0.01	—	0.04	—	—	0.06
8	2.48e-2	0.03	0.01	0.01	0.03	—	—	0.05
9	9.12e-3	0.04	—	—	0.01	—	—	0.04
10	2.03e-3	0.09	0.01	—	—	—	—	0.09
11	4.54e-4	0.04	0.01	—	0.05	—	—	0.06
12	2.26e-5	0.02	—	—	0.02	—	—	0.02
13	4.00e-6	0.01	—	—	—	—	—	0.01
14	5.40e-7	—	—	—	—	—	—	—
15	1.00e-7	—	—	—	—	—	—	—
Total		0.14	0.05	0.02	0.18	0.22	—	0.32

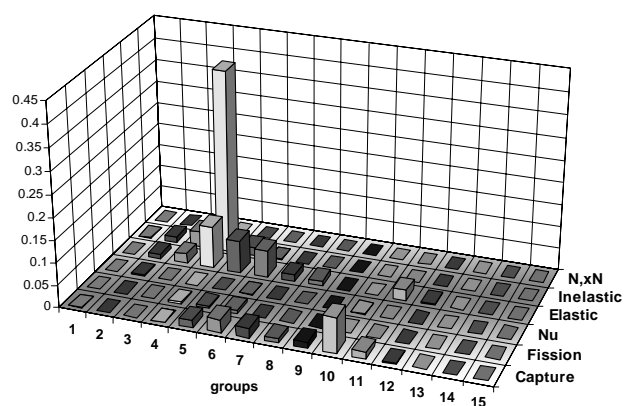


Table 6. ABTR power peak: BOLNA full uncertainty (%) by group

Gr.	[MeV]	σ_{cap}	σ_{fiss}	ν	σ_{el}	σ_{inel}	$\sigma_{\text{n,2n}}$	Total
1	19.6	0.01	—	0.01	—	0.01i	—	—
2	6.07	0.01	0.01	0.02	0.04i	0.06	—	0.05
3	2.23	0.01	0.02	0.02	0.05i	0.08	—	0.07
4	1.35	0.02	0.03	0.01	0.03i	0.16	—	0.16
5	4.98e-1	0.06	0.04	0.01	0.11	0.07	—	0.14
6	1.83e-1	0.07	0.04	0.01	0.10	0.04	—	0.14
7	6.74e-2	0.06	0.02	—	0.05	0.02	—	0.08
8	2.48e-2	0.05	0.01	0.01	0.05	0.02i	—	0.07
9	9.12e-3	0.05	0.01	—	0.01	—	—	0.05
10	2.03e-3	0.12	0.01	—	0.01	—	—	0.12
11	4.54e-4	0.08	0.01	—	0.03	—	—	0.08
12	2.26e-5	0.05	—	—	0.02	—	—	0.05
13	4.00e-6	0.04	—	—	0.01	—	—	0.04
14	5.40e-7	0.01	—	—	—	—	—	0.01
15	1.00e-7	—	—	—	—	—	—	—
Total		0.20	0.08	0.04	0.16	0.20	—	0.34

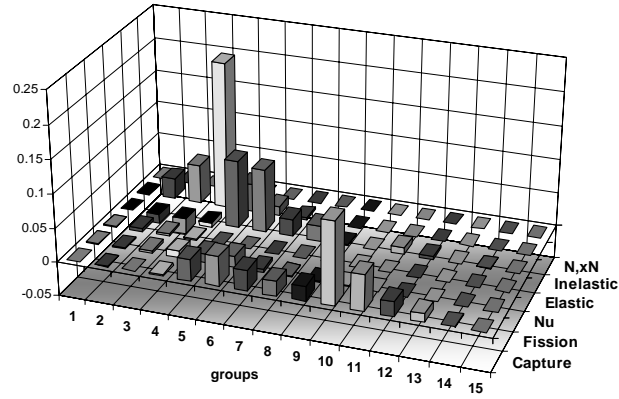


Table 7. ABTR power peak: BOLNA diagonal uncertainty (%) by isotope

Isotope	σ_{cap}	σ_{fiss}	ν	σ_{el}	σ_{inel}	$\sigma_{\text{n,2n}}$	Total
²³⁵ U	—	—	—	—	—	—	—
²³⁸ U	0.03	0.01	0.02	0.13	0.19	—	0.24
²³⁸ Pu	—	0.01	—	—	—	—	0.01
²³⁹ Pu	0.04	0.02	0.01	0.04	0.05	—	0.08
²⁴⁰ Pu	0.01	0.01	0.01	—	—	—	0.01
²⁴¹ Pu	—	0.04	—	—	—	—	0.04
²⁴² Pu	0.01	0.01	—	—	—	—	0.01
²³⁷ Np	—	—	—	—	—	—	—
²⁴¹ Am	—	—	—	—	—	—	0.01
^{242m} Am	—	—	—	—	—	—	—
²⁴³ Am	—	—	—	—	—	—	—
²⁴² Cm	—	—	—	—	—	—	—
²⁴³ Cm	—	—	—	—	—	—	—
²⁴⁴ Cm	—	—	—	—	—	—	—
²⁴⁵ Cm	—	—	—	—	—	—	—
²⁴⁶ Cm	—	—	—	—	—	—	—
⁵⁶ Fe	0.11	—	—	0.07	0.05	—	0.13
⁵² Cr	0.01	—	—	0.06	—	—	0.06
⁵⁸ Ni	—	—	—	0.01	—	—	0.01
⁹⁰ Zr	—	—	—	0.03	—	—	0.03
²³ Na	—	—	—	0.07	0.08	—	0.10
¹⁶ O	—	—	—	—	—	—	—
C	—	—	—	—	—	—	—
¹⁰ B	0.07	—	—	—	—	—	0.07
Total	0.14	0.05	0.02	0.18	0.22	—	0.32

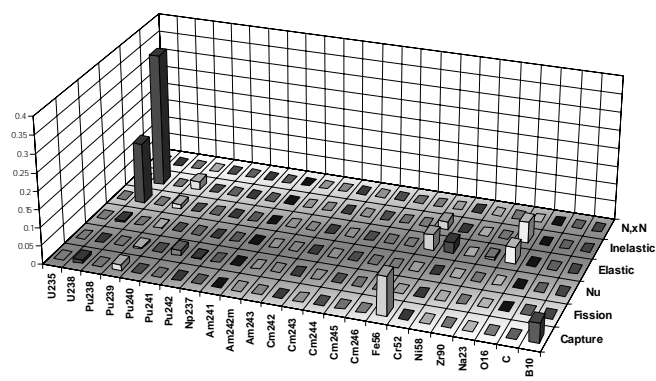


Table 8. ABTR power peak: BOLNA full uncertainty (%) by isotope

Isotope	σ_{cap}	σ_{fiss}	ν	σ_{el}	σ_{inel}	$\sigma_{\text{n,2n}}$	Total
²³⁵ U	—	—	—	—	—	—	—
²³⁸ U	0.04	0.01	0.03	0.04i	0.16	—	0.16
²³⁸ Pu	—	0.01	0.01	—	—	—	0.02
²³⁹ Pu	0.05	0.02	0.01	0.06	0.07	—	0.11
²⁴⁰ Pu	0.02	0.01	0.01	0.01	0.01	—	0.03
²⁴¹ Pu	0.01	0.07	—	—	—	—	0.07
²⁴² Pu	0.01	0.01	—	—	—	—	0.01
²³⁷ Np	—	—	—	—	—	—	0.01
²⁴¹ Am	0.01	0.01	—	—	—	—	0.01
^{242m} Am	—	—	—	—	—	—	—
²⁴³ Am	—	—	—	—	—	—	—
²⁴² Cm	—	—	—	—	—	—	—
²⁴³ Cm	—	—	—	—	—	—	—
²⁴⁴ Cm	—	—	—	—	—	—	—
²⁴⁵ Cm	—	—	—	—	—	—	—
²⁴⁶ Cm	—	—	—	—	—	—	—
⁵⁶ Fe	0.16	—	—	0.06	0.07	—	0.18
⁵² Cr	0.01	—	—	0.08	—	—	0.08
⁵⁸ Ni	—	—	—	0.01	—	—	0.01
⁹⁰ Zr	—	—	—	0.05	—	—	0.05
²³ Na	—	—	—	0.10	0.08	—	0.13
¹⁶ O	—	—	—	—	—	—	—
C	—	—	—	—	—	—	—
¹⁰ B	0.11	—	—	—	—	—	0.11
Total	0.20	0.08	0.04	0.16	0.20	—	0.34

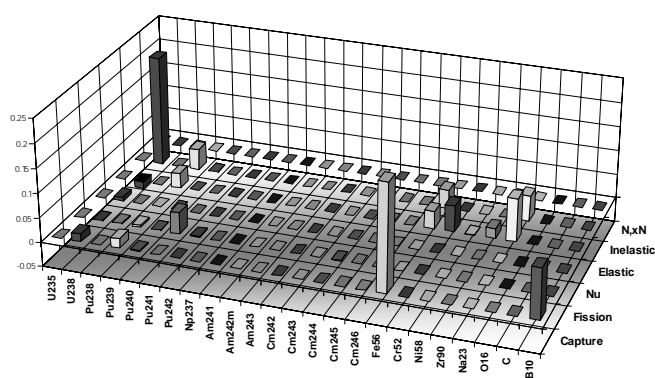


Table 9. ABTR Doppler: BOLNA diagonal uncertainty (%) by group

Gr.	[MeV]	σ_{cap}	σ_{fiss}	ν	σ_{el}	σ_{inel}	$\sigma_{\text{n,2n}}$	Total
1	19.6	0.03	0.01	0.03	—	0.11	0.01	0.12
2	6.07	0.01	0.09	0.16	0.05	1.24	—	1.25
3	2.23	0.02	0.10	0.14	0.04	1.27	—	1.28
4	1.35	0.06	0.22	0.09	0.08	0.99	—	1.02
5	4.98e-1	0.06	0.27	0.08	0.30	0.25	—	0.48
6	1.83e-1	0.13	0.29	0.14	0.56	0.92	—	1.13
7	6.74e-2	0.23	0.14	0.07	0.35	0.18	—	0.49
8	2.48e-2	0.57	0.11	0.01	0.55	0.24	—	0.83
9	9.12e-3	0.82	0.02	0.03	0.22	—	—	0.85
10	2.03e-3	0.74	0.20	0.08	0.13	—	—	0.78
11	4.54e-4	0.13	0.15	0.04	0.29	—	—	0.35
12	2.26e-5	0.02	—	—	—	—	—	0.02
13	4.00e-6	0.01	—	—	—	—	—	0.01
14	5.40e-7	—	—	—	—	—	—	—
15	1.00e-7	—	—	—	—	—	—	—
Total		1.28	0.56	0.31	0.99	2.27	0.01	2.86

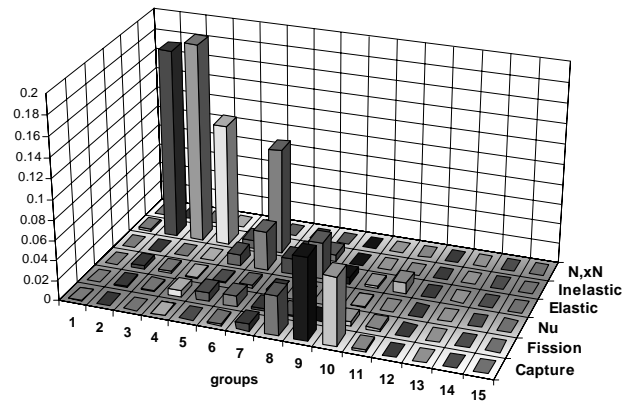


Table 10. ABTR Doppler: BOLNA full uncertainty (%) by group

Gr.	[MeV]	σ_{cap}	σ_{fiss}	ν	σ_{el}	σ_{inel}	$\sigma_{\text{n,2n}}$	Total
1	19.6	0.03	0.05	0.07	0.03	0.33	0.01	0.34
2	6.07	0.02	0.17	0.22	0.28	1.93	—	1.97
3	2.23	0.02i	0.20	0.20	0.33	1.99	—	2.04
4	1.35	0.06i	0.33	0.13	0.43	1.74	—	1.83
5	4.98e-1	0.05	0.37	0.11	0.66	0.64	—	1.00
6	1.83e-1	0.22	0.39	0.16	0.94	1.22	—	1.61
7	6.74e-2	0.35	0.25	0.08	0.71	0.53	—	0.99
8	2.48e-2	0.74	0.17	0.02	0.90	0.47	—	1.27
9	9.12e-3	0.92	0.04	0.02	0.39	0.01	—	0.99
10	2.03e-3	0.81	0.19	0.07	0.37	—	—	0.91
11	4.54e-4	0.33	0.15	0.04	0.40i	—	—	0.17i
12	2.26e-5	0.11	0.02	—	0.05	—	—	0.12
13	4.00e-6	0.10	0.01	—	0.05i	—	—	0.08
14	5.40e-7	0.02	—	—	0.01i	—	—	0.02
15	1.00e-7	—	—	—	—	—	—	—
Total		1.53	0.79	0.40	1.77	3.64	0.01	4.42

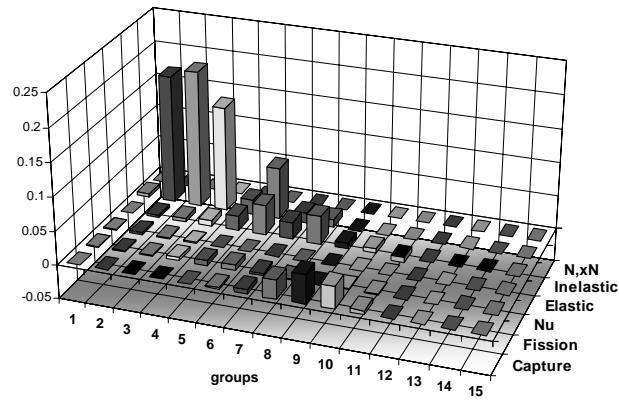


Table 11. ABTR Doppler: BOLNA diagonal uncertainty (%) by isotope

Isotope	σ_{cap}	σ_{fiss}	ν	σ_{el}	σ_{inel}	$\sigma_{\text{n,2n}}$	Total
²³⁵ U	0.02	—	0.01	—	—	—	0.02
²³⁸ U	0.50	0.08	0.21	0.13	2.04	0.01	2.12
²³⁸ Pu	—	0.02	0.01	—	—	—	0.02
²³⁹ Pu	0.91	0.49	0.21	0.03	0.42	—	1.14
²⁴⁰ Pu	0.09	0.13	0.10	0.01	0.07	—	0.20
²⁴¹ Pu	0.02	0.21	0.01	—	—	—	0.21
²⁴² Pu	0.02	0.02	—	—	—	—	0.03
²³⁷ Np	0.02	0.01	—	—	0.01	—	0.03
²⁴¹ Am	0.03	0.01	—	—	—	—	0.03
^{242m} Am	—	—	—	—	—	—	—
²⁴³ Am	0.01	—	—	—	—	—	0.01
²⁴² Cm	—	—	—	—	—	—	—
²⁴³ Cm	—	—	—	—	—	—	—
²⁴⁴ Cm	—	—	—	—	—	—	—
²⁴⁵ Cm	—	—	—	—	—	—	—
²⁴⁶ Cm	—	—	—	—	—	—	—
⁵⁶ Fe	0.71	—	—	0.56	0.73	—	1.17
⁵² Cr	0.03	—	—	0.33	0.01	—	0.34
⁵⁸ Ni	—	—	—	0.11	0.01	—	0.11
⁹⁰ Zr	—	—	—	0.05	0.10	—	0.11
²³ Na	0.02	—	—	0.72	0.49	—	0.87
¹⁶ O	—	—	—	—	—	—	—
C	—	—	—	—	—	—	—
¹⁰ B	0.15	—	—	0.01	—	—	0.15
Total	1.28	0.56	0.31	0.99	2.27	0.01	2.86

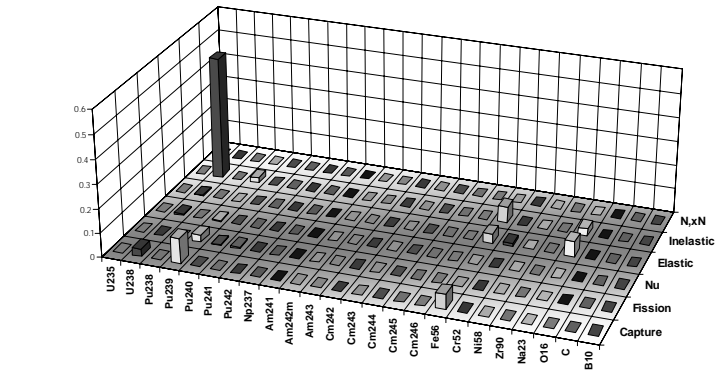


Table 12. ABTR Doppler: BOLNA full uncertainty (%) by isotope

Isotope	σ_{cap}	σ_{fiss}	ν	σ_{el}	σ_{inel}	$\sigma_{\text{n,2n}}$	Total
²³⁵ U	0.04	—	—	—	0.01	—	0.04
²³⁸ U	0.54	0.11	0.30	0.63	3.28	0.01	3.40
²³⁸ Pu	0.01	0.03	0.01	—	—	—	0.03
²³⁹ Pu	1.12	0.67	0.22	0.03	0.94	—	1.62
²⁴⁰ Pu	0.13	0.23	0.14	0.01	0.11	—	0.32
²⁴¹ Pu	0.04	0.34	—	—	0.01	—	0.34
²⁴² Pu	0.04	0.03	—	—	0.01	—	0.05
²³⁷ Np	0.03	0.01	—	—	0.02	—	0.04
²⁴¹ Am	0.05	0.01	—	—	0.01	—	0.05
^{242m} Am	—	0.01	—	—	—	—	0.01
²⁴³ Am	0.01	—	—	—	—	—	0.01
²⁴² Cm	—	—	—	—	—	—	—
²⁴³ Cm	—	—	—	—	—	—	—
²⁴⁴ Cm	—	0.01	—	—	—	—	0.01
²⁴⁵ Cm	—	—	—	—	—	—	—
²⁴⁶ Cm	—	—	—	—	—	—	—
⁵⁶ Fe	0.85	—	—	0.72	1.14	—	1.60
⁵² Cr	0.03	—	—	0.45	0.02	—	0.45
⁵⁸ Ni	—	—	—	0.12	0.01	—	0.12
⁹⁰ Zr	0.01	—	—	0.07	0.11	—	0.13
²³ Na	0.02	—	—	1.41	0.54	—	1.51
¹⁶ O	—	—	—	—	—	—	—
C	—	—	—	—	—	—	—
¹⁰ B	0.23	—	—	0.02	—	—	0.23
Total	1.53	0.79	0.40	1.77	3.64	0.01	4.42

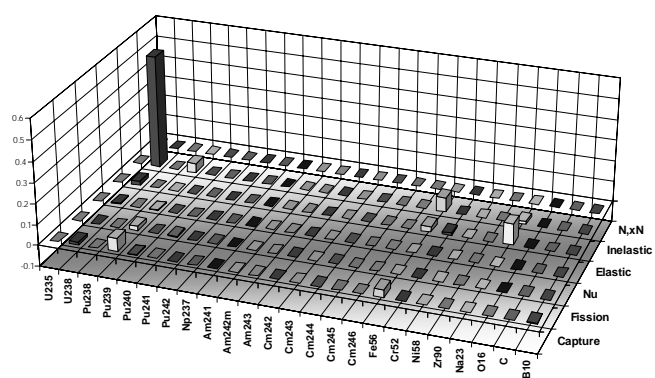


Table 13. ABTR void: BOLNA diagonal uncertainty (%) by group

Gr.	[MeV]	σ_{cap}	σ_{fiss}	ν	σ_{el}	σ_{inel}	$\sigma_{\text{n,2n}}$	Total
1	19.6	0.67	0.01	0.03	0.01	0.53	0.01	0.85
2	6.07	0.07	0.04	0.13	0.21	0.95	—	0.99
3	2.23	0.03	—	0.05	0.36	1.15	—	1.21
4	1.35	0.49	0.62	0.35	0.96	2.38	—	2.71
5	4.98e-1	0.24	0.16	0.08	0.79	0.14	—	0.86
6	1.83e-1	0.27	0.44	0.34	0.76	0.03	—	0.98
7	6.74e-2	0.63	0.38	0.39	0.26	0.06	—	0.87
8	2.48e-2	3.33	0.55	0.43	0.24	0.05	—	3.41
9	9.12e-3	0.88	0.12	0.15	0.16	—	—	0.92
10	2.03e-3	0.62	0.54	0.12	0.11	—	—	0.84
11	4.54e-4	0.04	0.04	0.01	0.02	—	—	0.06
12	2.26e-5	0.01	—	—	0.01	—	—	0.01
13	4.00e-6	—	—	—	—	—	—	—
14	5.40e-7	—	—	—	—	—	—	—
15	1.00e-7	—	—	—	—	—	—	—
Total		3.67	1.17	0.80	1.57	2.87	0.01	5.11

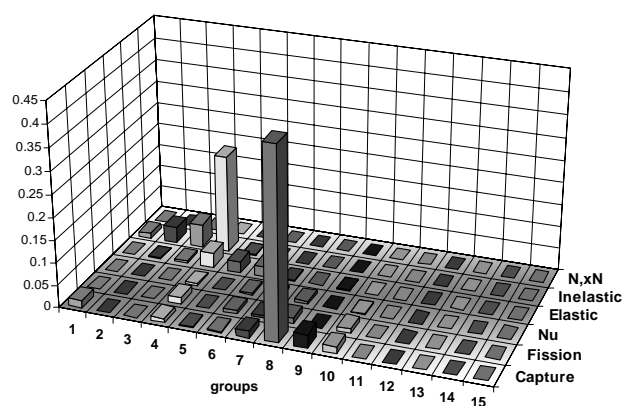


Table 14. ABTR void: BOLNA full uncertainty (%) by group

Gr.	[MeV]	σ_{cap}	σ_{fiss}	ν	σ_{el}	σ_{inel}	$\sigma_{\text{n,2n}}$	Total
1	19.6	0.69	0.02	0.06	0.10	0.86	0.01	1.11
2	6.07	0.17	0.05	0.16	0.54	1.56	—	1.66
3	2.23	0.07	0.02i	0.10	0.71	2.05	—	2.17
4	1.35	0.40	0.51	0.33	1.25	2.64	—	3.01
5	4.98e-1	0.24i	0.11	0.08	1.07	0.23	—	1.07
6	1.83e-1	0.50	0.45	0.35	1.04	0.10i	—	1.29
7	6.74e-2	0.86	0.47	0.47	0.56	0.11i	—	1.22
8	2.48e-2	3.43	0.61	0.50	0.47i	0.08i	—	3.49
9	9.12e-3	1.10	0.23	0.18	0.07	—	—	1.14
10	2.03e-3	0.73	0.53	0.10	0.17i	—	—	0.90
11	4.54e-4	0.13	0.12	0.01	0.06i	—	—	0.16
12	2.26e-5	0.06	0.01	—	0.02i	—	—	0.06
13	4.00e-6	0.04	0.01	—	0.01i	—	—	0.04
14	5.40e-7	0.01	—	—	—	—	—	0.01
15	1.00e-7	—	—	—	—	—	—	—
Total		3.89	1.20	0.89	2.16	3.78	0.01	6.03

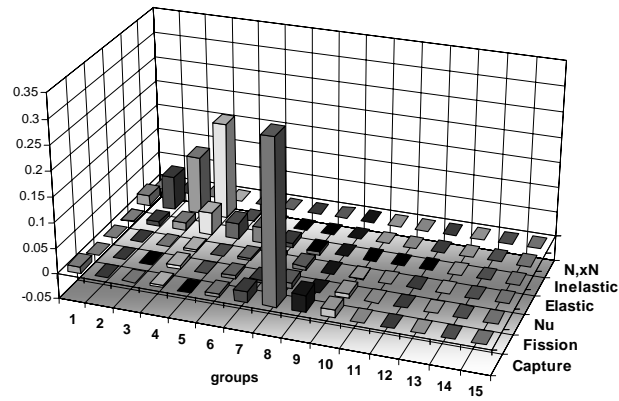


Table 15. ABTR void: BOLNA diagonal uncertainty (%) by isotope

Isotope	σ_{cap}	σ_{fiss}	ν	σ_{el}	σ_{inel}	$\sigma_{\text{n,2n}}$	Total
²³⁵ U	0.04	0.01	0.01	—	—	—	0.04
²³⁸ U	3.36	0.06	0.14	0.82	1.12	—	3.64
²³⁸ Pu	—	0.02	0.02	—	—	—	0.03
²³⁹ Pu	1.23	1.09	0.72	0.23	0.16	—	1.81
²⁴⁰ Pu	0.17	0.33	0.32	0.02	0.01	—	0.49
²⁴¹ Pu	0.02	0.27	0.01	—	—	—	0.27
²⁴² Pu	0.02	0.02	0.01	—	—	—	0.03
²³⁷ Np	0.01	0.01	—	—	—	—	0.01
²⁴¹ Am	0.01	0.01	—	—	—	—	0.01
^{242m} Am	—	—	—	—	—	—	—
²⁴³ Am	—	—	—	—	—	—	—
²⁴² Cm	—	—	—	—	—	—	—
²⁴³ Cm	—	—	—	—	—	—	—
²⁴⁴ Cm	—	—	—	—	—	—	—
²⁴⁵ Cm	—	—	—	—	—	—	—
²⁴⁶ Cm	—	—	—	—	—	—	—
⁵⁶ Fe	0.45	—	—	0.28	0.44	—	0.69
⁵² Cr	0.02	—	—	0.16	0.01	0.01	0.16
⁵⁸ Ni	0.01	—	—	0.03	—	—	0.03
⁹⁰ Zr	0.03	—	—	0.16	0.06	—	0.17
²³ Na	0.68	—	—	1.26	2.60	—	2.97
¹⁶ O	—	—	—	—	—	—	—
C	—	—	—	—	—	—	—
¹⁰ B	0.01	—	—	—	—	—	0.01
Total	3.67	1.17	0.80	1.57	2.87	0.01	5.11

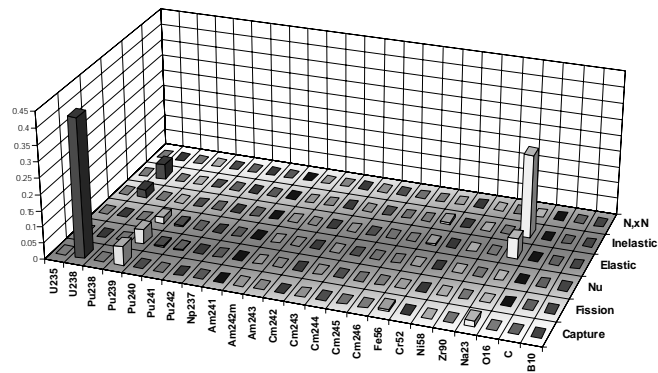


Table 16. ABTR void: BOLNA full uncertainty (%) by isotope

Isotope	σ_{cap}	σ_{fiss}	ν	σ_{el}	σ_{inel}	$\sigma_{\text{n,2n}}$	Total
²³⁵ U	0.06	0.01	0.02	—	—	—	0.06
²³⁸ U	3.44	0.02i	0.20	1.17	0.89	—	3.74
²³⁸ Pu	—	0.03	0.01	—	—	—	0.04
²³⁹ Pu	1.61	1.13	0.82	0.26	0.07i	—	2.14
²⁴⁰ Pu	0.15	0.30	0.28	0.02	0.01	—	0.44
²⁴¹ Pu	0.03	0.27	0.01	—	—	—	0.27
²⁴² Pu	0.02	0.02	0.01	—	—	—	0.03
²³⁷ Np	0.01	0.01	—	—	—	—	0.01
²⁴¹ Am	0.02	0.01	—	—	—	—	0.02
^{242m} Am	—	—	—	—	—	—	—
²⁴³ Am	—	—	—	—	—	—	—
²⁴² Cm	—	—	—	—	—	—	—
²⁴³ Cm	—	—	—	—	—	—	—
²⁴⁴ Cm	—	0.01	—	—	—	—	0.01
²⁴⁵ Cm	—	—	—	—	—	—	—
²⁴⁶ Cm	—	—	—	—	—	—	—
⁵⁶ Fe	0.48	—	—	0.25	0.56	—	0.78
⁵² Cr	0.02	—	—	0.17	0.01	0.01	0.17
⁵⁸ Ni	0.01	—	—	0.03	—	—	0.03
⁹⁰ Zr	0.03	—	—	0.21	0.07	—	0.22
²³ Na	0.71	—	—	1.76	3.63	—	4.10
¹⁶ O	—	—	—	—	—	—	—
C	—	—	—	—	—	—	—
¹⁰ B	0.02	—	—	—	—	—	0.02
Total	3.89	1.20	0.89	2.16	3.78	0.01	6.03

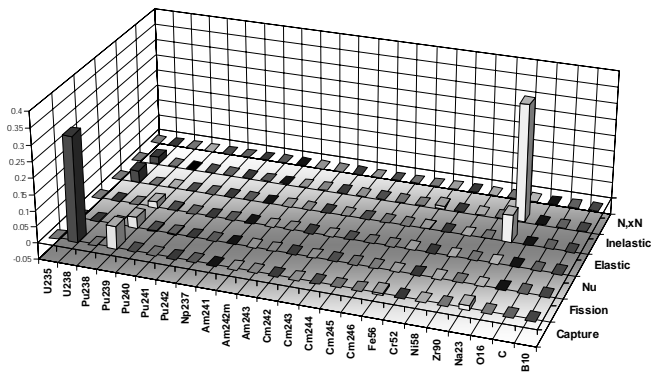


Table 17. ABTR XS burn-up: BOLNA diagonal uncertainty (%) by group

Gr.	[MeV]	σ_{cap}	σ_{fiss}	ν	σ_{el}	σ_{inel}	$\sigma_{\text{n,2n}}$	Total
1	19.6	0.03	0.02	0.02	—	0.06	0.01	0.07
2	6.07	0.01	0.10	0.13	0.04	0.64	—	0.66
3	2.23	0.01	0.12	0.12	0.02	0.76	—	0.78
4	1.35	0.05	0.28	0.22	0.02	0.34	—	0.49
5	4.98e-1	0.08	0.17	0.07	0.04	0.03	—	0.21
6	1.83e-1	0.10	0.23	0.08	0.05	0.05	—	0.27
7	6.74e-2	0.08	0.08	0.05	0.01	—	—	0.13
8	2.48e-2	0.24	0.09	0.04	0.02	—	—	0.26
9	9.12e-3	0.03	0.02	0.02	—	—	—	0.04
10	2.03e-3	0.06	0.05	0.01	0.01	—	—	0.08
11	4.54e-4	0.01	0.02	—	0.03	—	—	0.04
12	2.26e-5	—	—	—	—	—	—	0.01
13	4.00e-6	—	—	—	—	—	—	—
14	5.40e-7	—	—	—	—	—	—	—
15	1.00e-7	—	—	—	—	—	—	—
Total		0.30	0.45	0.31	0.09	1.05	0.01	1.23

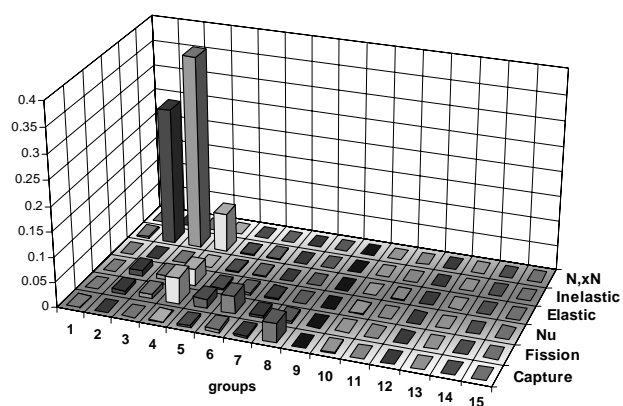


Table 18. ABTR XS burn-up: BOLNA full uncertainty (%) by group

Gr.	[MeV]	σ_{cap}	σ_{fiss}	ν	σ_{el}	σ_{inel}	$\sigma_{\text{n,2n}}$	Total
1	19.6	0.03	0.07	0.05	0.01	0.17	0.01	0.20
2	6.07	0.04	0.21	0.20	0.06	0.96	—	1.00
3	2.23	0.05	0.27	0.20	0.03i	1.07	—	1.12
4	1.35	0.10	0.42	0.30	0.09i	0.68	—	0.85
5	4.98e-1	0.15	0.31	0.16	0.06	0.07	—	0.39
6	1.83e-1	0.17	0.34	0.13	0.07	0.10	—	0.42
7	6.74e-2	0.14	0.20	0.10	0.03	0.03	—	0.27
8	2.48e-2	0.26	0.14	0.08	0.03	0.01	—	0.31
9	9.12e-3	0.06	0.06	0.03	—	—	—	0.09
10	2.03e-3	0.06	0.06	0.04	0.01i	—	—	0.09
11	4.54e-4	0.02	0.03	0.01	0.02i	—	—	0.03
12	2.26e-5	0.02i	0.01	—	0.01i	—	—	0.02i
13	4.00e-6	0.01i	—	—	—	—	—	0.01i
14	5.40e-7	—	—	—	—	—	—	—
15	1.00e-7	—	—	—	—	—	—	—
Total		0.40	0.76	0.48	0.06	1.60	0.01	1.89

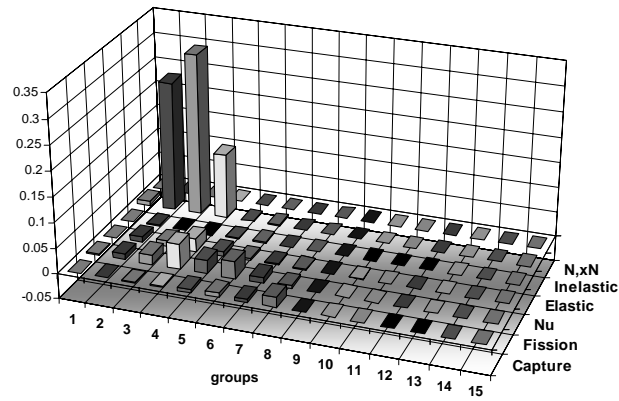


Table 19. ABTR XS burn-up: BOLNA diagonal uncertainty (%) by isotope

Isotope	σ_{cap}	σ_{fiss}	ν	σ_{el}	σ_{inel}	$\sigma_{\text{n,2n}}$	Total
²³⁵ U	0.01	—	—	—	—	—	0.01
²³⁸ U	0.25	0.06	0.15	0.01	0.92	—	0.97
²³⁸ Pu	0.01	0.06	0.03	—	—	—	0.07
²³⁹ Pu	0.06	0.21	0.10	0.01	0.05	—	0.25
²⁴⁰ Pu	0.12	0.30	0.25	0.01	0.02	—	0.41
²⁴¹ Pu	0.01	0.24	0.01	—	—	—	0.24
²⁴² Pu	0.01	0.02	—	—	—	—	0.03
²³⁷ Np	—	0.01	—	—	—	—	0.01
²⁴¹ Am	—	0.01	—	—	—	—	0.01
^{242m} Am	—	0.01	—	—	—	—	0.01
²⁴³ Am	—	—	—	—	—	—	—
²⁴² Cm	—	0.02	—	—	—	—	0.02
²⁴³ Cm	—	—	—	—	—	—	—
²⁴⁴ Cm	—	0.01	—	—	—	—	0.02
²⁴⁵ Cm	—	—	—	—	—	—	—
²⁴⁶ Cm	—	—	—	—	—	—	—
⁵⁶ Fe	0.08	—	—	0.07	0.46	—	0.47
⁵² Cr	0.01	—	—	0.05	0.01	—	0.05
⁵⁸ Ni	—	—	—	—	—	—	0.01
⁹⁰ Zr	—	—	—	—	0.07	—	0.07
²³ Na	0.02	—	—	0.02	0.19	—	0.19
¹⁶ O	—	—	—	—	—	—	—
C	—	—	—	—	—	—	—
¹⁰ B	0.04	—	—	—	—	—	0.04
Total	0.30	0.45	0.31	0.09	1.05	0.01	1.23

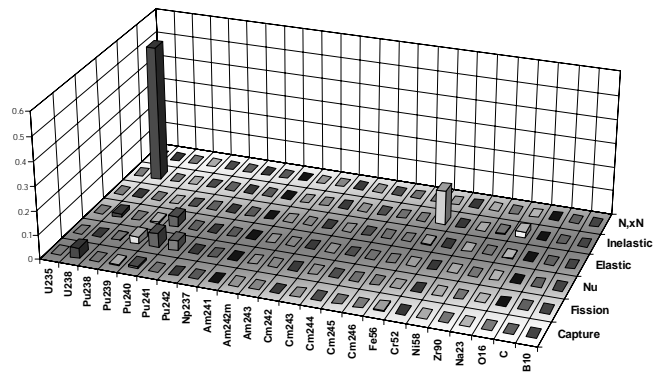


Table 20. ABTR XS burn-up: BOLNA full uncertainty (%) by isotope

Isotope	σ_{cap}	σ_{fiss}	ν	σ_{el}	σ_{inel}	$\sigma_{\text{n,2n}}$	Total
²³⁵ U	0.03	—	—	—	—	—	0.03
²³⁸ U	0.27	0.09	0.21	0.10i	1.43	—	1.47
²³⁸ Pu	0.01	0.11	0.07	—	—	—	0.13
²³⁹ Pu	0.10	0.30	0.12	0.02i	0.07	—	0.34
²⁴⁰ Pu	0.27	0.51	0.41	0.01	0.05	—	0.71
²⁴¹ Pu	0.01	0.45	0.01	—	—	—	0.45
²⁴² Pu	0.01	0.04	0.01	—	—	—	0.04
²³⁷ Np	0.01	0.02	—	—	—	—	0.02
²⁴¹ Am	0.01	0.02	—	—	—	—	0.02
^{242m} Am	—	0.03	—	—	—	—	0.03
²⁴³ Am	—	—	—	—	—	—	—
²⁴² Cm	—	0.04	0.01	—	—	—	0.04
²⁴³ Cm	—	—	—	—	—	—	—
²⁴⁴ Cm	—	0.02	—	—	—	—	0.02
²⁴⁵ Cm	—	0.01	—	—	—	—	0.01
²⁴⁶ Cm	—	—	—	—	—	—	—
⁵⁶ Fe	0.09	—	—	0.08	0.68	—	0.69
⁵² Cr	0.01	—	—	0.07	0.01	—	0.08
⁵⁸ Ni	—	—	—	—	—	—	0.01
⁹⁰ Zr	0.01	—	—	—	0.07	—	0.08
²³ Na	0.02	—	—	0.01	0.23	—	0.23
¹⁶ O	—	—	—	—	—	—	—
C	—	—	—	—	—	—	—
¹⁰ B	0.06	—	—	—	—	—	0.06
Total	0.40	0.76	0.48	0.06	1.60	0.01	1.89

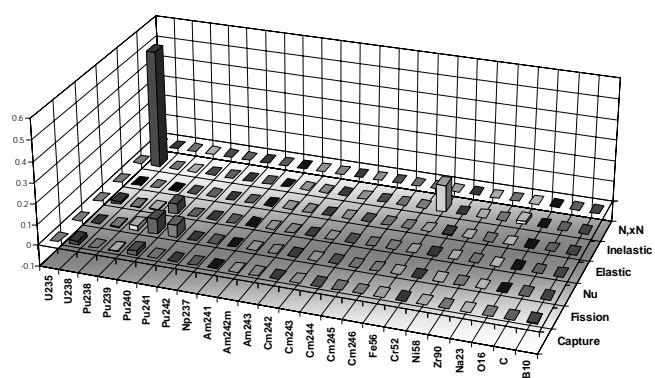


Table 21. SFR k_{eff} : BOLNA diagonal uncertainties (%) by group

Gr.	[MeV]	σ_{cap}	σ_{fiss}	ν	σ_{el}	σ_{inel}	$\sigma_{\text{n,2n}}$	Total
1	19.6	0.03	0.03	0.01	—	0.02	0.01	0.05
2	6.07	0.01	0.16	0.08	0.04	0.11	—	0.21
3	2.23	0.02	0.24	0.09	0.03	0.31	—	0.40
4	1.35	0.06	0.48	0.25	0.02	0.30	—	0.62
5	4.98e-1	0.11	0.39	0.11	0.04	0.01	—	0.42
6	1.83e-1	0.13	0.45	0.07	0.04	0.01	—	0.47
7	6.74e-2	0.11	0.16	0.04	0.01	—	—	0.20
8	2.48e-2	0.12	0.15	0.03	0.01	—	—	0.19
9	9.12e-3	0.06	0.06	0.01	—	—	—	0.08
10	2.03e-3	0.05	0.10	0.02	—	—	—	0.12
11	4.54e-4	0.01	0.04	—	0.01	—	—	0.04
12	2.26e-5	—	—	—	0.01	—	—	0.01
13	4.00e-6	—	—	—	—	—	—	—
14	5.40e-7	—	—	—	—	—	—	—
15	1.00e-7	—	—	—	—	—	—	—
Total		0.26	0.85	0.31	0.08	0.44	0.01	1.04

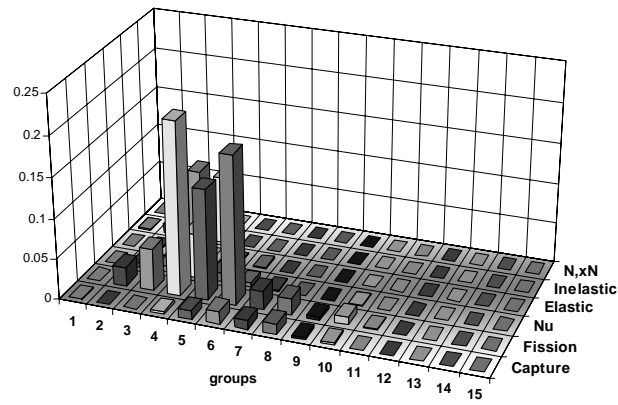


Table 22. SFR k_{eff} : BOLNA full uncertainties (%) by group

Gr.	[MeV]	σ_{cap}	σ_{fiss}	ν	σ_{el}	σ_{inel}	$\sigma_{\text{n,2n}}$	Total
1	19.6	0.04	0.08	0.02	0.01	0.08	0.01	0.12
2	6.07	0.04	0.35	0.15	0.05	0.21	—	0.44
3	2.23	0.06	0.52	0.17	0.05	0.43	—	0.70
4	1.35	0.13	0.79	0.35	0.04	0.41	—	0.97
5	4.98e-1	0.19	0.73	0.23	0.05	0.02	—	0.79
6	1.83e-1	0.22	0.75	0.16	0.06	0.02	—	0.80
7	6.74e-2	0.20	0.44	0.12	0.02	—	—	0.49
8	2.48e-2	0.20	0.22	0.10	0.03	0.01i	—	0.31
9	9.12e-3	0.11	0.13	0.06	0.01i	—	—	0.18
10	2.03e-3	0.07	0.14	0.08	0.01i	—	—	0.18
11	4.54e-4	0.03	0.04	0.03	0.01i	—	—	0.06
12	2.26e-5	0.02	0.01	0.01	0.01i	—	—	0.02
13	4.00e-6	0.01	—	—	—	—	—	0.01
14	5.40e-7	—	—	—	—	—	—	—
15	1.00e-7	—	—	—	—	—	—	—
Total		0.45	1.55	0.54	0.12	0.64	0.01	1.82

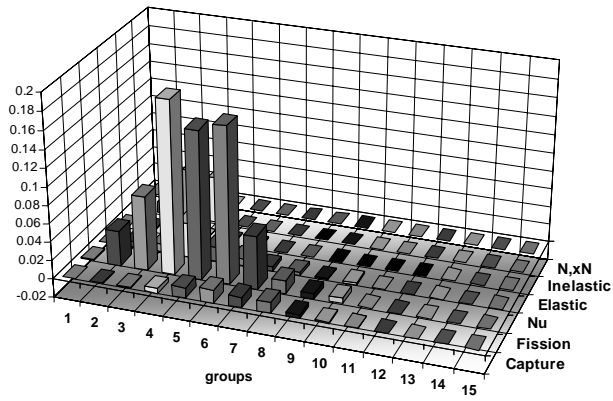


Table 23. SFR k_{eff} : BOLNA diagonal uncertainties (%) by isotope

Isotope	σ_{cap}	σ_{fiss}	ν	σ_{el}	σ_{inel}	$\sigma_{\text{n,2n}}$	Total
²³⁵ U	—	—	—	—	—	—	—
²³⁸ U	0.07	0.01	0.02	0.01	0.14	—	0.16
²³⁸ Pu	0.03	0.30	0.16	—	—	—	0.34
²³⁹ Pu	0.07	0.09	0.06	0.01	0.03	—	0.13
²⁴⁰ Pu	0.14	0.26	0.24	0.01	0.02	—	0.38
²⁴¹ Pu	0.03	0.51	0.01	—	0.01	—	0.52
²⁴² Pu	0.10	0.24	0.05	—	0.02	—	0.26
²³⁷ Np	0.02	0.03	0.01	—	0.01	—	0.03
²⁴¹ Am	0.04	0.05	0.01	—	0.01	—	0.07
^{242m} Am	0.03	0.36	0.02	—	0.01	—	0.37
²⁴³ Am	0.03	0.03	0.01	—	0.01	—	0.05
²⁴² Cm	—	0.02	0.01	—	—	—	0.02
²⁴³ Cm	—	0.01	—	—	—	—	0.01
²⁴⁴ Cm	0.02	0.26	0.06	—	—	—	0.27
²⁴⁵ Cm	—	0.19	0.02	—	—	—	0.19
²⁴⁶ Cm	0.01	0.02	—	—	—	—	0.02
⁵⁶ Fe	0.08	—	—	0.06	0.35	—	0.37
⁵² Cr	0.01	—	—	0.04	0.01	0.01	0.04
⁵⁸ Ni	—	—	—	—	—	—	—
⁹⁰ Zr	—	—	—	—	0.03	—	0.03
²³ Na	0.02	—	—	0.02	0.22	—	0.23
¹⁰ B	0.11	—	—	0.01	—	—	0.12
Total	0.26	0.85	0.31	0.08	0.44	0.01	1.04

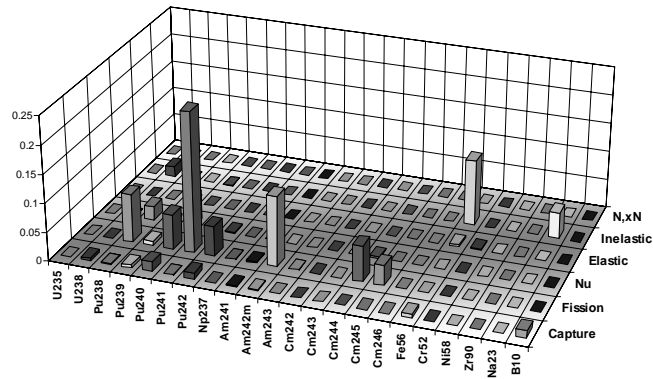


Table 24. SFR k_{eff} : BOLNA full uncertainties (%) by isotope

Isotope	σ_{cap}	σ_{fiss}	ν	σ_{el}	σ_{inel}	$\sigma_{\text{n,2n}}$	Total
²³⁵ U	—	—	—	—	—	—	—
²³⁸ U	0.07	0.01	0.03	0.05	0.23	—	0.24
²³⁸ Pu	0.05	0.53	0.34	—	0.01	—	0.64
²³⁹ Pu	0.12	0.12	0.07	0.02	0.05	—	0.19
²⁴⁰ Pu	0.31	0.44	0.39	0.01	0.04	—	0.66
²⁴¹ Pu	0.06	0.96	0.03	—	0.01	—	0.96
²⁴² Pu	0.17	0.36	0.08	—	0.03	—	0.41
²³⁷ Np	0.04	0.04	0.01	—	0.01	—	0.06
²⁴¹ Am	0.06	0.08	0.02	—	0.01	—	0.11
^{242m} Am	0.05	0.73	0.06	—	0.02	—	0.73
²⁴³ Am	0.05	0.04	0.01	—	0.02	—	0.07
²⁴² Cm	—	0.04	0.01	—	—	—	0.04
²⁴³ Cm	—	0.02	—	—	—	—	0.02
²⁴⁴ Cm	0.04	0.39	0.08	—	0.01	—	0.40
²⁴⁵ Cm	0.01	0.39	0.05	—	—	—	0.39
²⁴⁶ Cm	0.01	0.04	0.01	—	—	—	0.04
⁵⁶ Fe	0.10	—	—	0.09	0.53	—	0.55
⁵² Cr	0.01	—	—	0.06	0.01	0.01	0.06
⁵⁸ Ni	—	—	—	—	—	—	—
⁹⁰ Zr	—	—	—	0.01	0.03	—	0.03
²³ Na	0.02	—	—	0.02	0.25	—	0.25
¹⁰ B	0.17	—	—	0.01	—	—	0.17
Total	0.45	1.55	0.54	0.12	0.64	0.01	1.82

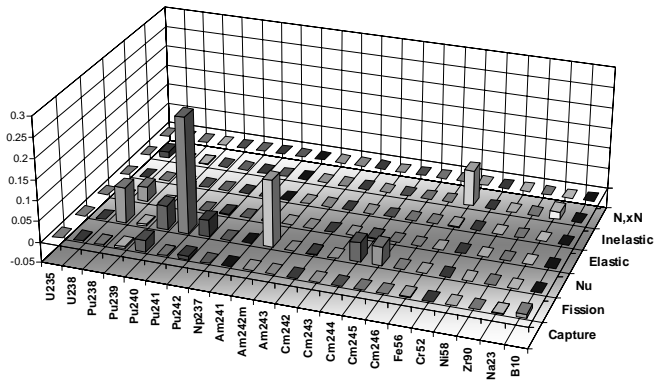


Table 25. SFR power peak: BOLNA diagonal uncertainty (%) by group

Gr.	[MeV]	σ_{cap}	σ_{fiss}	ν	σ_{el}	σ_{inel}	$\sigma_{\text{n,2n}}$	Total
1	19.6	—	—	—	—	0.01	—	0.01
2	6.07	0.01	0.01	—	0.02	0.05	—	0.06
3	2.23	0.01	0.01	—	0.02	0.10	—	0.10
4	1.35	0.04	0.02	0.01	0.04	0.09	—	0.11
5	4.98e-1	0.13	0.01	—	0.05	0.02	—	0.14
6	1.83e-1	0.14	0.01	—	0.03	0.02	—	0.14
7	6.74e-2	0.11	0.01	—	0.01	—	—	0.11
8	2.48e-2	0.08	0.01	—	0.01	—	—	0.08
9	9.12e-3	0.04	0.01	—	—	—	—	0.04
10	2.03e-3	0.05	0.01	—	—	—	—	0.05
11	4.54e-4	0.02	—	—	0.03	—	—	0.04
12	2.26e-5	0.01	—	—	0.01	—	—	0.02
13	4.00e-6	—	—	—	—	—	—	—
14	5.40e-7	—	—	—	—	—	—	—
15	1.00e-7	—	—	—	—	—	—	—
Total		0.25	0.03	0.01	0.09	0.15	—	0.31

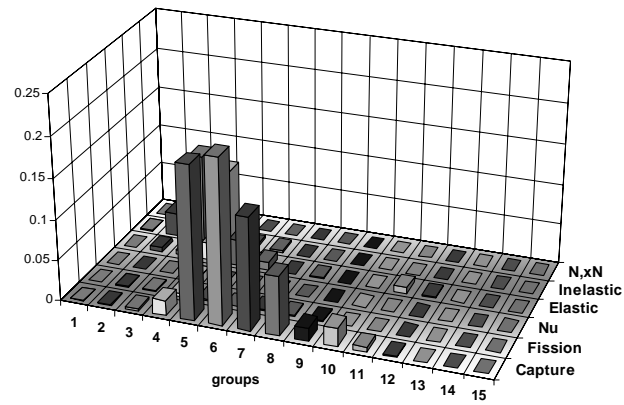


Table 26. SFR power peak: BOLNA full uncertainty (%) by group

Gr.	[MeV]	σ_{cap}	σ_{fiss}	ν	σ_{el}	σ_{inel}	$\sigma_{\text{n,2n}}$	Total
1	19.6	0.01	—	—	—	0.03	—	0.03
2	6.07	0.03	0.02	—	0.03	0.09	—	0.10
3	2.23	0.03	0.02	0.01	0.03	0.14	—	0.15
4	1.35	0.05	0.03	0.01	0.05	0.13	—	0.15
5	4.98e-1	0.19	0.02	0.01	0.07	0.03	—	0.21
6	1.83e-1	0.19	0.01i	—	0.05	0.03	—	0.20
7	6.74e-2	0.16	—	—	0.02	0.01	—	0.16
8	2.48e-2	0.14	0.02	—	0.02i	0.01i	—	0.14
9	9.12e-3	0.09	0.01	—	0.01	—	—	0.10
10	2.03e-3	0.06	0.01	—	0.02i	—	—	0.06
11	4.54e-4	0.04	—	—	0.03	—	—	0.05
12	2.26e-5	0.03	—	—	0.02	—	—	0.04
13	4.00e-6	0.02	—	—	0.01	—	—	0.02
14	5.40e-7	0.01	—	—	—	—	—	0.01
15	1.00e-7	—	—	—	—	—	—	—
Total		0.37	0.05	0.01	0.12	0.22	—	0.45

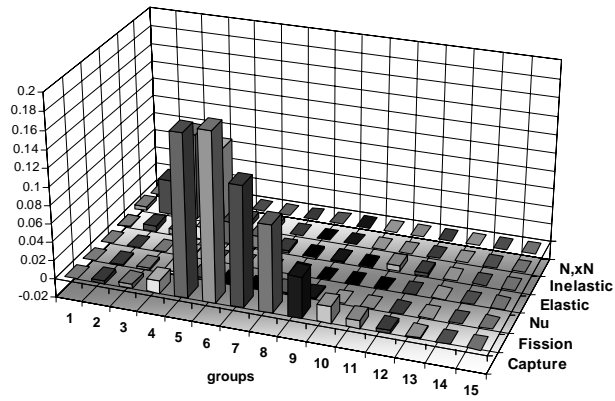


Table 27. SFR power peak: BOLNA diagonal uncertainty (%) by isotope

Isotope	σ_{cap}	σ_{fiss}	ν	σ_{el}	σ_{inel}	$\sigma_{\text{n,2n}}$	Total
²³⁵ U	—	—	—	—	—	—	—
²³⁸ U	—	—	—	0.02	0.05	—	0.05
²³⁸ Pu	—	0.01	0.01	—	—	—	0.01
²³⁹ Pu	0.01	—	—	0.01	0.02	—	0.02
²⁴⁰ Pu	0.01	0.01	0.01	0.02	0.02	—	0.03
²⁴¹ Pu	—	0.02	—	—	—	—	0.02
²⁴² Pu	0.01	0.01	—	—	0.02	—	0.02
²³⁷ Np	—	—	—	—	0.01	—	0.01
²⁴¹ Am	—	—	—	—	—	—	0.01
^{242m} Am	—	0.02	—	—	—	—	0.02
²⁴³ Am	—	—	—	—	0.01	—	0.01
²⁴² Cm	—	—	—	—	—	—	—
²⁴³ Cm	—	—	—	—	—	—	—
²⁴⁴ Cm	—	0.01	—	—	—	—	0.01
²⁴⁵ Cm	—	0.01	—	—	—	—	0.01
²⁴⁶ Cm	—	—	—	—	—	—	—
⁵⁶ Fe	0.05	—	—	0.04	0.11	—	0.13
⁵² Cr	—	—	—	0.01	—	—	0.01
⁵⁸ Ni	—	—	—	—	—	—	—
⁹⁰ Zr	—	—	—	0.01	0.01	—	0.02
²³ Na	—	—	—	0.07	0.07	—	0.10
¹⁰ B	0.24	—	—	0.01	—	—	0.24
Total	0.25	0.03	0.01	0.09	0.15	—	0.31

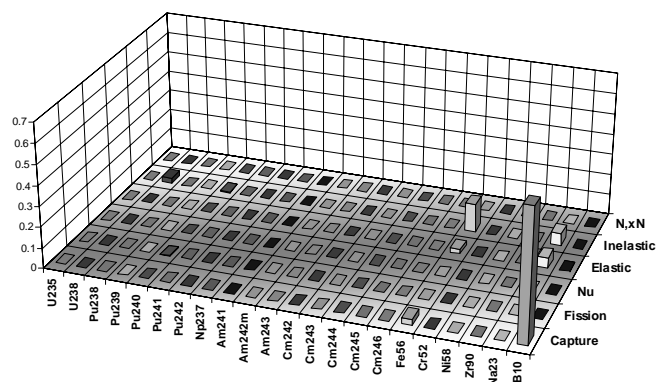


Table 28. SFR power peak: BOLNA full uncertainty (%) by isotope

Isotope	σ_{cap}	σ_{fiss}	ν	σ_{el}	σ_{inel}	$\sigma_{\text{n,2n}}$	Total
²³⁵ U	—	—	—	—	—	—	—
²³⁸ U	0.01	—	—	0.03i	0.07	—	0.07
²³⁸ Pu	—	0.02	—	0.01	—	—	0.02
²³⁹ Pu	0.01	—	—	0.02	0.03	—	0.04
²⁴⁰ Pu	0.02	0.02	0.01	0.03	0.03	—	0.05
²⁴¹ Pu	—	0.02	—	—	—	—	0.02
²⁴² Pu	0.01	0.02	—	—	0.02	—	0.03
²³⁷ Np	—	—	—	—	0.01	—	0.01
²⁴¹ Am	0.01	—	—	—	—	—	0.01
^{242m} Am	—	0.02	—	—	0.01	—	0.02
²⁴³ Am	—	—	—	—	0.01	—	0.01
²⁴² Cm	—	—	—	—	—	—	—
²⁴³ Cm	—	—	—	—	—	—	—
²⁴⁴ Cm	—	0.02	—	—	—	—	0.02
²⁴⁵ Cm	—	0.01	—	—	—	—	0.01
²⁴⁶ Cm	—	—	—	—	—	—	—
⁵⁶ Fe	0.08	—	—	0.06	0.18	—	0.20
⁵² Cr	—	—	—	0.01	—	—	0.01
⁵⁸ Ni	—	—	—	—	—	—	—
⁹⁰ Zr	—	—	—	0.03	0.01	—	0.03
²³ Na	—	—	—	0.10	0.09	—	0.13
¹⁰ B	0.36	—	—	0.02	—	—	0.36
Total	0.37	0.05	0.01	0.12	0.22	—	0.45

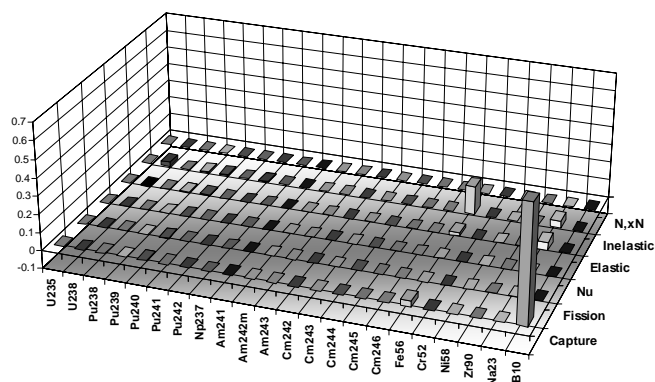


Table 29. SFR Doppler: BOLNA diagonal uncertainty (%) by group

Gr.	[MeV]	σ_{cap}	σ_{fiss}	ν	σ_{el}	σ_{inel}	$\sigma_{\text{n,2n}}$	Total
1	19.6	0.03	0.07	0.01	—	0.06	—	0.10
2	6.07	0.02	0.42	0.18	0.07	0.38	—	0.60
3	2.23	0.02	0.64	0.20	0.04	1.01	—	1.21
4	1.35	0.07	1.24	0.51	0.09	1.47	—	1.99
5	4.98e-1	0.15	0.96	0.21	0.34	0.13	—	1.05
6	1.83e-1	0.62	1.21	0.12	0.46	0.27	—	1.46
7	6.74e-2	0.45	0.45	0.07	0.28	0.08	—	0.70
8	2.48e-2	0.35	0.39	0.05	0.57	0.11	—	0.78
9	9.12e-3	0.41	0.23	0.02	0.41	—	—	0.63
10	2.03e-3	0.92	0.71	0.13	0.30	—	—	1.21
11	4.54e-4	0.28	0.97	0.08	0.28	—	—	1.05
12	2.26e-5	0.06	0.04	0.01	0.04	—	—	0.09
13	4.00e-6	0.02	0.01	—	0.01	—	—	0.03
14	5.40e-7	—	—	—	—	—	—	—
15	1.00e-7	—	—	—	—	—	—	—
Total		1.35	2.52	0.65	1.04	1.85	—	3.62

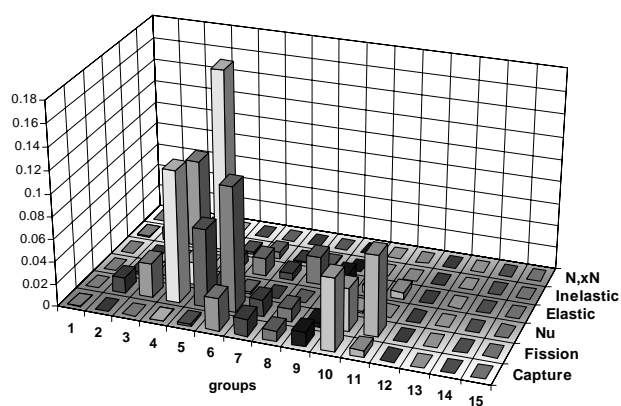


Table 30. SFR Doppler: BOLNA full uncertainty (%) by group

Gr.	[MeV]	σ_{cap}	σ_{fiss}	ν	σ_{el}	σ_{inel}	$\sigma_{\text{n,2n}}$	Total
1	19.6	0.05	0.21	0.04	0.01	0.27	—	0.35
2	6.07	0.02	0.93	0.32	0.10	0.80	—	1.27
3	2.23	0.04i	1.37	0.36	0.10	1.56	—	2.11
4	1.35	0.05i	2.04	0.72	0.13	1.91	—	2.89
5	4.98e-1	0.13	1.85	0.42	0.71	0.29	—	2.05
6	1.83e-1	0.63	1.99	0.28	0.85	0.41	—	2.31
7	6.74e-2	0.56	1.18	0.21	0.64	0.21	—	1.49
8	2.48e-2	0.59	0.49	0.18	0.95	0.21	—	1.25
9	9.12e-3	0.60	0.35	0.13	0.63	0.01	—	0.95
10	2.03e-3	0.88	0.60	0.17	0.61	—	—	1.24
11	4.54e-4	0.14	0.97	0.14i	0.44i	—	—	0.87
12	2.26e-5	0.17i	0.08	0.01	0.16i	—	—	0.22i
13	4.00e-6	0.09i	0.03	0.01i	0.09i	—	—	0.12i
14	5.40e-7	0.03i	—	—	0.02	—	—	0.03i
15	1.00e-7	—	—	—	0.02	—	—	0.02
Total		1.48	4.17	1.05	1.77	2.67	—	5.57

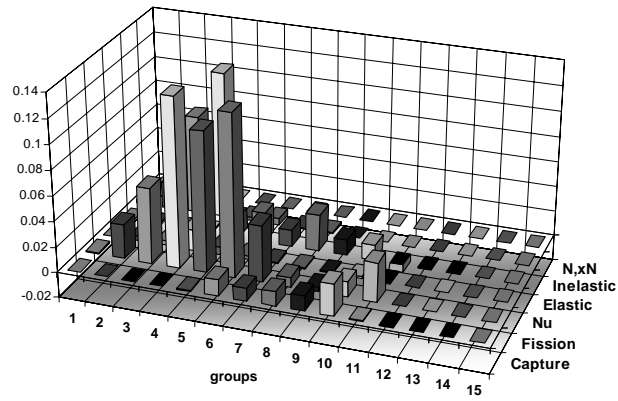


Table 31. SFR Doppler: BOLNA diagonal uncertainty (%) by isotope

Isotope	σ_{cap}	σ_{fiss}	ν	σ_{el}	σ_{inel}	$\sigma_{\text{n,2n}}$	Total
²³⁵ U	0.01	—	—	—	—	—	0.01
²³⁸ U	0.24	0.02	0.05	0.02	0.54	—	0.60
²³⁸ Pu	0.10	0.79	0.33	—	0.03	—	0.86
²³⁹ Pu	0.35	0.26	0.12	0.01	0.20	—	0.49
²⁴⁰ Pu	0.18	0.76	0.50	0.02	0.23	—	0.96
²⁴¹ Pu	0.17	1.69	0.04	—	0.03	—	1.70
²⁴² Pu	0.37	0.62	0.11	—	0.12	—	0.74
²³⁷ Np	0.20	0.07	0.02	—	0.08	—	0.23
²⁴¹ Am	0.31	0.14	0.03	—	0.04	—	0.34
^{242m} Am	0.13	1.07	0.08	0.01	0.05	—	1.08
²⁴³ Am	0.28	0.08	0.02	—	0.10	—	0.31
²⁴² Cm	0.01	0.05	0.01	—	—	—	0.06
²⁴³ Cm	—	0.02	—	—	—	—	0.02
²⁴⁴ Cm	0.07	0.65	0.12	—	0.03	—	0.66
²⁴⁵ Cm	0.02	0.49	0.07	—	0.02	—	0.49
²⁴⁶ Cm	0.07	0.06	0.01	—	0.01	—	0.09
⁵⁶ Fe	1.07	—	—	0.62	1.43	—	1.89
⁵² Cr	0.05	—	—	0.27	0.02	—	0.27
⁵⁸ Ni	—	—	—	0.09	0.01	—	0.09
⁹⁰ Zr	0.01	—	—	0.03	0.10	—	0.10
²³ Na	0.03	—	—	0.79	0.97	—	1.25
¹⁰ B	0.22	—	—	0.04	—	—	0.22
Total	1.35	2.52	0.65	1.04	1.85	—	3.62

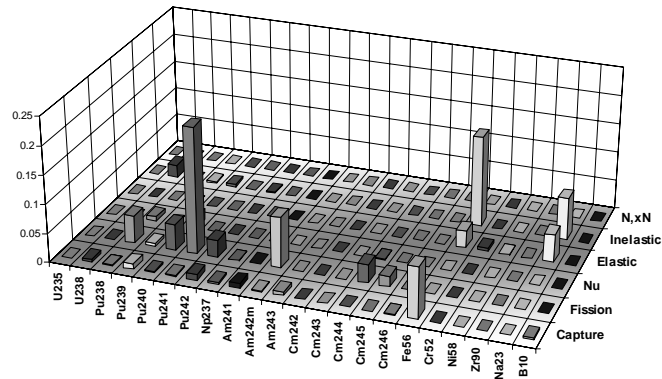


Table 32. SFR Doppler: BOLNA full uncertainty (%) by isotope

Isotope	σ_{cap}	σ_{fiss}	ν	σ_{el}	σ_{inel}	$\sigma_{\text{n,2n}}$	Total
²³⁵ U	0.01	—	—	0.01i	—	—	0.01
²³⁸ U	0.25	0.02	0.06	0.10	0.89	—	0.94
²³⁸ Pu	0.19	1.40	0.52	0.01	0.04	—	1.50
²³⁹ Pu	0.42	0.35	0.13	0.01i	0.44	—	0.71
²⁴⁰ Pu	0.25	1.24	0.88	0.03	0.42	—	1.60
²⁴¹ Pu	0.27	2.75	0.01	0.01	0.06	—	2.77
²⁴² Pu	0.60	0.96	0.16	—	0.19	—	1.15
²³⁷ Np	0.24	0.13	0.02	—	0.15	—	0.31
²⁴¹ Am	0.50	0.22	0.04	0.01	0.04	—	0.55
^{242m} Am	0.18	1.83	0.02	0.01	0.10	—	1.84
²⁴³ Am	0.43	0.12	0.03	—	0.20	—	0.49
²⁴² Cm	0.01	0.10	0.02	—	0.01	—	0.10
²⁴³ Cm	—	0.04	—	—	—	—	0.04
²⁴⁴ Cm	0.11	0.98	0.16	0.01	0.04	—	1.00
²⁴⁵ Cm	0.03	0.94	0.01	—	0.03	—	0.95
²⁴⁶ Cm	0.10	0.09	0.01	—	0.01	—	0.14
⁵⁶ Fe	0.87	—	—	0.81	2.18	—	2.48
⁵² Cr	0.05	—	—	0.38	0.03	—	0.38
⁵⁸ Ni	—	—	—	0.10	0.01	—	0.10
⁹⁰ Zr	0.01	—	—	0.05	0.11	—	0.12
²³ Na	0.03	—	—	1.52	1.05	—	1.85
¹⁰ B	0.35	—	—	0.05	—	—	0.35
Total	1.48	4.17	1.05	1.77	2.67	—	5.57

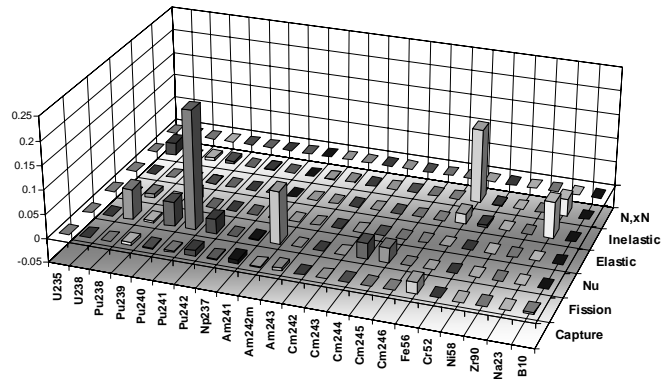


Table 33. SFR void: BOLNA diagonal uncertainties (%) by group

Gr.	[MeV]	σ_{cap}	σ_{fiss}	ν	σ_{el}	σ_{inel}	$\sigma_{\text{n,2n}}$	Total
1	19.6	1.05	0.09	0.02	0.01	0.37	0.05	1.12
2	6.07	0.15	0.50	0.30	0.57	1.01	—	1.31
3	2.23	0.11	0.45	0.22	0.50	1.16	—	1.37
4	1.35	0.80	5.33	2.91	0.67	12.89	—	14.28
5	4.98e-1	0.91	0.62	0.11	0.57	0.07	—	1.25
6	1.83e-1	0.87	2.25	0.36	0.48	0.01	—	2.48
7	6.74e-2	1.16	1.64	0.40	0.27	0.03	—	2.07
8	2.48e-2	1.96	2.10	0.43	0.47	0.01	—	2.94
9	9.12e-3	0.59	0.69	0.12	0.12	—	—	0.92
10	2.03e-3	1.33	3.48	0.54	0.29	—	—	3.78
11	4.54e-4	0.10	0.70	0.07	0.06	—	—	0.71
12	2.26e-5	—	—	—	0.02	—	—	0.03
13	4.00e-6	—	—	—	—	—	—	—
14	5.40e-7	—	—	—	—	—	—	—
15	1.00e-7	—	—	—	—	—	—	—
Total		3.27	7.38	3.07	1.40	12.98	0.05	15.66

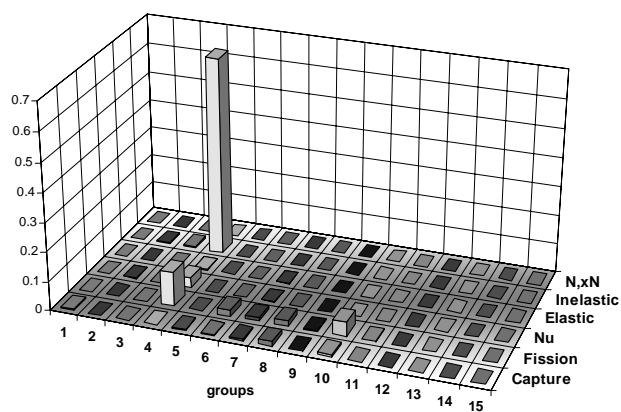


Table 34. SFR void: BOLNA full uncertainties (%) by group

Gr.	[MeV]	σ_{cap}	σ_{fiss}	ν	σ_{el}	σ_{inel}	$\sigma_{\text{n,2n}}$	Total
1	19.6	1.10	0.27	0.05	0.06	1.15	0.05	1.62
2	6.07	0.34	1.23	0.59	0.74	2.37	—	2.85
3	2.23	0.19	1.33	0.58	0.77	3.63	—	3.99
4	1.35	0.50i	4.99	2.45	0.86	13.49	—	14.61
5	4.98e-1	1.09	0.68	0.20	0.80	0.38	—	1.57
6	1.83e-1	1.43	1.16	0.41i	0.74	0.07	—	1.94
7	6.74e-2	1.89	1.82	0.44i	0.12i	0.13	—	2.59
8	2.48e-2	2.56	3.06	0.32i	0.73	0.08i	—	4.04
9	9.12e-3	1.21	1.78	0.08	0.14	—	—	2.15
10	2.03e-3	1.49	3.99	0.53i	0.39	—	—	4.24
11	4.54e-4	0.33	0.80	0.08	0.17i	—	—	0.86
12	2.26e-5	0.02i	0.03	0.01i	0.11i	—	—	0.11i
13	4.00e-6	0.04i	0.02	0.01	0.02i	—	—	0.04i
14	5.40e-7	—	—	—	0.02i	—	—	0.02i
15	1.00e-7	—	—	—	—	—	—	0.01i
Total		4.27	7.90	2.46	1.93	14.22	0.05	17.11

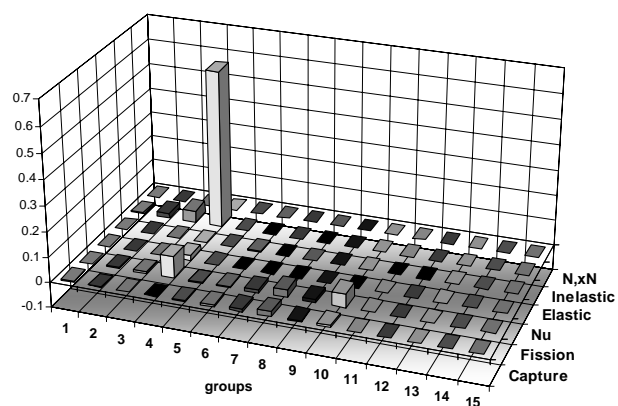


Table 35. SFR void: BOLNA diagonal uncertainties (%) by isotope

Isotope	σ_{cap}	σ_{fiss}	ν	σ_{el}	σ_{inel}	$\sigma_{\text{n,2n}}$	Total
²³⁵ U	0.02	0.01	0.01	—	—	—	0.03
²³⁸ U	1.19	0.02	0.07	0.22	1.13	—	1.65
²³⁸ Pu	0.35	2.25	1.49	0.03	0.07	—	2.72
²³⁹ Pu	0.84	0.84	0.46	0.16	0.53	—	1.39
²⁴⁰ Pu	1.36	2.53	2.52	0.12	0.20	—	3.83
²⁴¹ Pu	0.33	4.33	0.13	0.02	0.09	—	4.34
²⁴² Pu	1.42	2.16	0.55	0.03	0.25	—	2.65
²³⁷ Np	0.30	0.23	0.05	0.01	0.14	—	0.40
²⁴¹ Am	0.51	0.34	0.07	0.01	0.11	—	0.62
^{242m} Am	0.24	3.04	0.21	0.01	0.20	—	3.06
²⁴³ Am	0.43	0.23	0.05	0.01	0.19	—	0.53
²⁴² Cm	0.02	0.14	0.05	—	0.01	—	0.14
²⁴³ Cm	—	0.05	—	—	—	—	0.05
²⁴⁴ Cm	0.22	2.79	0.46	0.02	0.03	—	2.84
²⁴⁵ Cm	0.03	1.27	0.19	—	0.06	—	1.28
²⁴⁶ Cm	0.09	0.20	0.04	—	0.01	—	0.22
⁵⁶ Fe	1.18	—	—	0.90	4.18	—	4.44
⁵² Cr	0.05	—	—	0.47	0.05	0.05	0.47
⁵⁸ Ni	0.02	—	—	0.02	0.01	—	0.03
⁹⁰ Zr	0.04	—	—	0.16	0.17	—	0.24
²³ Na	1.05	—	—	0.89	12.22	—	12.29
¹⁰ B	1.15	—	—	0.16	—	—	1.16
Total	3.27	7.38	3.07	1.40	12.98	0.05	15.66

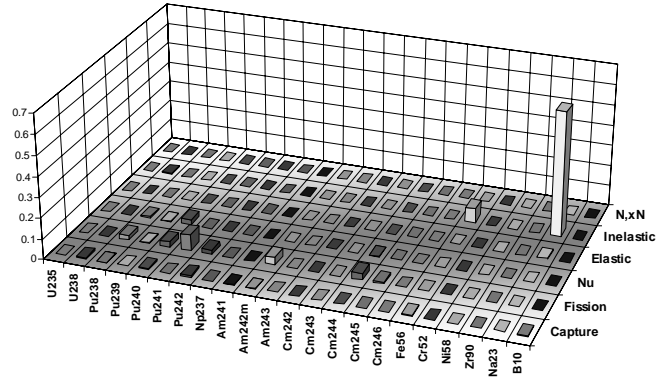


Table 36. SFR void: BOLNA full uncertainties (%) by isotope

Isotope	σ_{cap}	σ_{fiss}	ν	σ_{el}	σ_{inel}	$\sigma_{\text{n,2n}}$	Total
²³⁵ U	0.04	0.01	0.01	—	—	—	0.04
²³⁸ U	1.24	0.01	0.10	0.73	1.96	—	2.43
²³⁸ Pu	0.67	2.90	0.44	0.04	0.09	—	3.00
²³⁹ Pu	1.16	0.87	0.53	0.40	0.71	—	1.75
²⁴⁰ Pu	1.80	2.60	2.18	0.10	0.32	—	3.86
²⁴¹ Pu	0.41	4.09	0.20	0.03	0.13	—	4.12
²⁴² Pu	2.21	2.46	0.57	0.03	0.33	—	3.37
²³⁷ Np	0.40	0.27	0.05	0.01	0.17	—	0.51
²⁴¹ Am	0.79	0.43	0.08	0.01	0.14	—	0.91
^{242m} Am	0.32	3.70	0.33	0.02	0.25	—	3.73
²⁴³ Am	0.70	0.25	0.06	0.02	0.25	—	0.78
²⁴² Cm	0.03	0.12	0.04	—	0.01	—	0.13
²⁴³ Cm	—	0.03	—	—	—	—	0.03
²⁴⁴ Cm	0.29	2.95	0.49	0.02	0.05	—	3.01
²⁴⁵ Cm	0.05	0.95	0.29	—	0.07	—	1.00
²⁴⁶ Cm	0.12	0.25	0.05	—	0.01	—	0.28
⁵⁶ Fe	1.25	—	—	1.12	4.14	—	4.47
⁵² Cr	0.05	—	—	0.51	0.05	0.05	0.51
⁵⁸ Ni	0.02	—	—	0.03	0.01	—	0.04
⁹⁰ Zr	0.04	—	—	0.21	0.20	—	0.29
²³ Na	1.11	—	—	1.19	13.43	—	13.53
¹⁰ B	1.52	—	—	0.17	—	—	1.53
Total	4.27	7.90	2.46	1.93	14.22	0.05	17.11

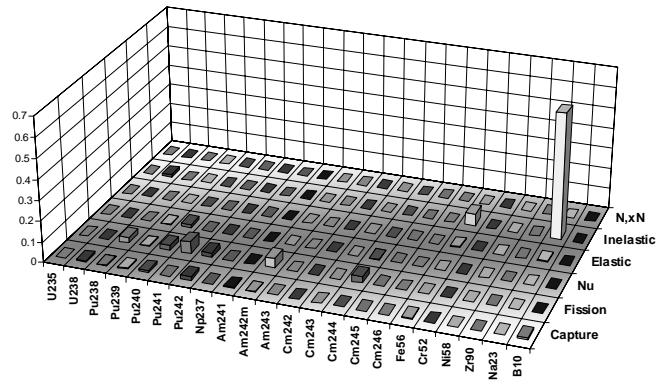


Table 37. SFR XS burn-up: BOLNA diagonal uncertainty (%) by group

Gr.	[MeV]	σ_{cap}	σ_{fiss}	ν	σ_{el}	σ_{inel}	$\sigma_{\text{n,2n}}$	Total
1	19.6	0.04	0.06	0.01	—	0.04	0.01	0.08
2	6.07	0.02	0.35	0.14	0.04	0.19	—	0.43
3	2.23	0.02	0.54	0.16	0.03	0.67	—	0.87
4	1.35	0.05	1.20	0.41	0.06	0.64	—	1.43
5	4.98e-1	0.14	0.68	0.20	0.04	0.01	—	0.73
6	1.83e-1	0.16	0.82	0.11	0.05	0.01	—	0.84
7	6.74e-2	0.13	0.27	0.07	0.01	—	—	0.31
8	2.48e-2	0.14	0.31	0.06	0.03	—	—	0.35
9	9.12e-3	0.06	0.13	0.03	—	—	—	0.14
10	2.03e-3	0.11	0.27	0.05	—	—	—	0.30
11	4.54e-4	0.02	0.11	0.01	0.02	—	—	0.12
12	2.26e-5	—	—	—	0.01	—	—	0.01
13	4.00e-6	—	—	—	—	—	—	—
14	5.40e-7	—	—	—	—	—	—	—
15	1.00e-7	—	—	—	—	—	—	—
Total		0.32	1.81	0.53	0.11	0.95	0.01	2.13

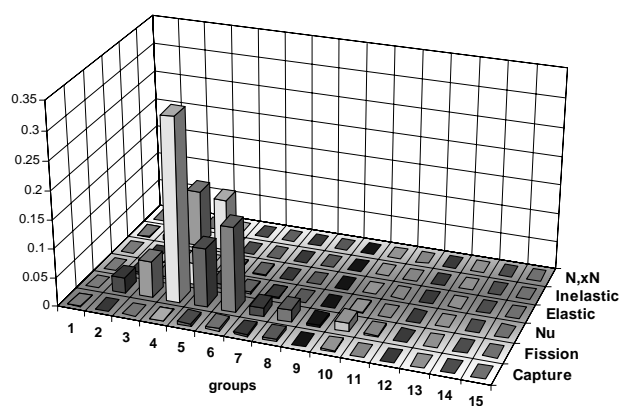


Table 38. SFR XS burn-up: BOLNA full uncertainty (%) by group

Gr.	[MeV]	σ_{cap}	σ_{fiss}	ν	σ_{el}	σ_{inel}	$\sigma_{\text{n,2n}}$	Total
1	19.6	0.04	0.16	0.03	0.01	0.16	0.01	0.23
2	6.07	0.04	0.79	0.26	0.05	0.42	—	0.94
3	2.23	0.05	1.12	0.29	0.05	0.91	—	1.47
4	1.35	0.10	1.77	0.62	0.06	0.88	—	2.07
5	4.98e-1	0.21	1.33	0.42	0.05	0.03	—	1.41
6	1.83e-1	0.23	1.34	0.31	0.07	0.02	—	1.39
7	6.74e-2	0.21	0.76	0.24	0.03	0.01	—	0.82
8	2.48e-2	0.21	0.46	0.22	0.04	—	—	0.56
9	9.12e-3	0.13	0.28	0.14	0.01i	—	—	0.34
10	2.03e-3	0.12	0.30	0.20	—	—	—	0.38
11	4.54e-4	0.05	0.12	0.08	0.02i	—	—	0.15
12	2.26e-5	0.02	0.02	0.01	0.01i	—	—	0.03
13	4.00e-6	0.01	0.01	—	—	—	—	0.02
14	5.40e-7	—	—	—	—	—	—	—
15	1.00e-7	—	—	—	—	—	—	—
Total		0.49	3.09	0.99	0.13	1.34	0.01	3.55

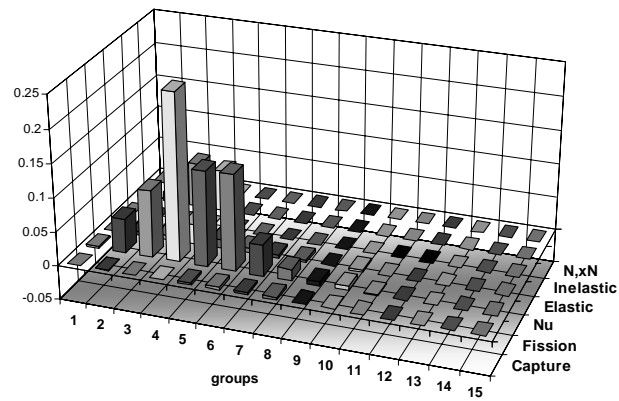


Table 39. SFR XS burn-up: BOLNA diagonal uncertainty (%) by isotope

Isotope	σ_{cap}	σ_{fiss}	ν	σ_{el}	σ_{inel}	$\sigma_{\text{n,2n}}$	Total
²³⁵ U	—	—	—	—	—	—	—
²³⁸ U	0.09	0.02	0.04	—	0.23	—	0.25
²³⁸ Pu	0.03	0.69	0.30	—	0.01	—	0.76
²³⁹ Pu	0.03	0.11	0.05	—	0.01	—	0.13
²⁴⁰ Pu	0.09	0.55	0.38	—	0.03	—	0.67
²⁴¹ Pu	0.01	1.03	0.02	—	0.01	—	1.03
²⁴² Pu	0.10	0.51	0.09	—	0.04	—	0.53
²³⁷ Np	0.01	0.02	—	—	—	—	0.02
²⁴¹ Am	0.01	0.06	0.01	—	—	—	0.07
^{242m} Am	0.07	0.36	0.03	—	0.02	—	0.37
²⁴³ Am	0.04	0.08	0.02	—	0.02	—	0.09
²⁴² Cm	0.01	0.17	0.04	—	—	—	0.18
²⁴³ Cm	—	0.03	—	—	—	—	0.03
²⁴⁴ Cm	0.04	0.92	0.17	—	0.01	—	0.94
²⁴⁵ Cm	—	0.34	0.03	—	—	—	0.34
²⁴⁶ Cm	0.01	0.05	0.01	—	—	—	0.05
⁵⁶ Fe	0.13	—	—	0.07	0.77	—	0.79
⁵² Cr	0.01	—	—	0.05	0.01	0.01	0.06
⁵⁸ Ni	—	—	—	—	—	—	0.01
⁹⁰ Zr	—	—	—	—	0.06	—	0.06
²³ Na	0.02	—	—	0.06	0.49	—	0.49
¹⁰ B	0.22	—	—	0.02	—	—	0.22
Total	0.32	1.81	0.53	0.11	0.95	0.01	2.13

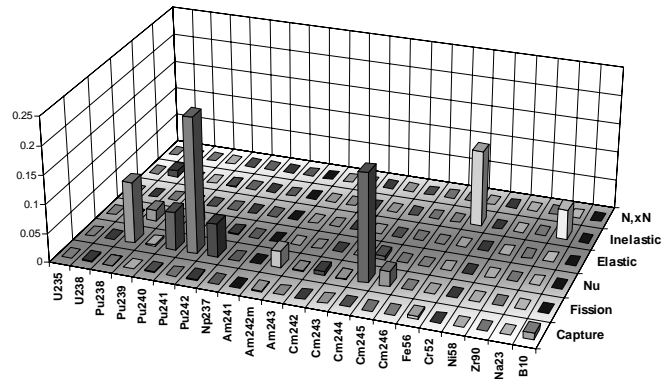


Table 40. SFR XS burn-up: BOLNA full uncertainty (%) by isotope

Isotope	σ_{cap}	σ_{fiss}	ν	σ_{el}	σ_{inel}	$\sigma_{\text{n,2n}}$	Total
²³⁵ U	—	—	—	—	—	—	—
²³⁸ U	0.09	0.02	0.06	0.03	0.37	—	0.39
²³⁸ Pu	0.05	1.23	0.68	—	0.01	—	1.40
²³⁹ Pu	0.05	0.16	0.06	—	0.02	—	0.18
²⁴⁰ Pu	0.21	0.95	0.65	—	0.06	—	1.17
²⁴¹ Pu	0.02	1.85	0.06	—	0.01	—	1.85
²⁴² Pu	0.17	0.78	0.13	—	0.06	—	0.81
²³⁷ Np	0.02	0.04	—	—	—	—	0.04
²⁴¹ Am	0.02	0.10	0.01	—	0.01	—	0.11
^{242m} Am	0.12	0.73	0.07	—	0.03	—	0.74
²⁴³ Am	0.06	0.10	0.02	—	0.03	—	0.13
²⁴² Cm	0.02	0.31	0.07	—	—	—	0.32
²⁴³ Cm	—	0.07	—	—	—	—	0.07
²⁴⁴ Cm	0.08	1.40	0.24	—	0.01	—	1.42
²⁴⁵ Cm	—	0.67	0.08	—	—	—	0.68
²⁴⁶ Cm	0.01	0.09	0.01	—	—	—	0.09
⁵⁶ Fe	0.15	—	—	0.09	1.17	—	1.18
⁵² Cr	0.01	—	—	0.07	0.01	0.01	0.07
⁵⁸ Ni	—	—	—	—	—	—	0.01
⁹⁰ Zr	0.01	—	—	—	0.06	—	0.06
²³ Na	0.02	—	—	0.06	0.54	—	0.54
¹⁰ B	0.32	—	—	0.02	—	—	0.32
Total	0.49	3.09	0.99	0.13	1.34	0.01	3.55

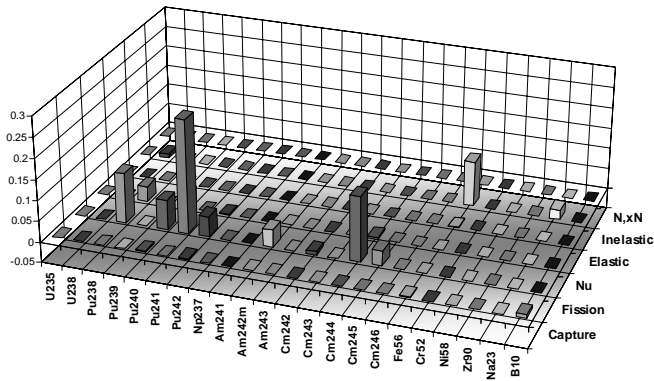


Table 41. EFR k_{eff} : BOLNA diagonal uncertainties (%) by group

Gr.	[MeV]	σ_{cap}	σ_{fiss}	ν	σ_{el}	σ_{inel}	$\sigma_{\text{n,2n}}$	Total
1	19.6	0.13	0.01	0.01	0.01	0.04	0.01	0.14
2	6.07	0.22	0.07	0.08	0.06	0.37	—	0.45
3	2.23	0.02	0.08	0.07	0.04	0.35	—	0.37
4	1.35	0.05	0.16	0.12	0.02	0.17	—	0.27
5	4.98e-1	0.06	0.09	0.04	0.02	0.01	—	0.12
6	1.83e-1	0.09	0.16	0.06	0.03	0.04	—	0.20
7	6.74e-2	0.10	0.07	0.05	0.01	—	—	0.13
8	2.48e-2	0.29	0.07	0.03	—	—	—	0.30
9	9.12e-3	0.14	0.05	0.03	0.01	—	—	0.15
10	2.03e-3	0.07	0.08	0.02	0.01	—	—	0.11
11	4.54e-4	0.01	0.02	—	—	—	—	0.02
12	2.26e-5	—	—	—	—	—	—	—
13	4.00e-6	—	—	—	—	—	—	—
14	5.40e-7	—	—	—	—	—	—	—
15	1.00e-7	—	—	—	—	—	—	—
Total		0.45	0.30	0.19	0.09	0.55	0.01	0.79

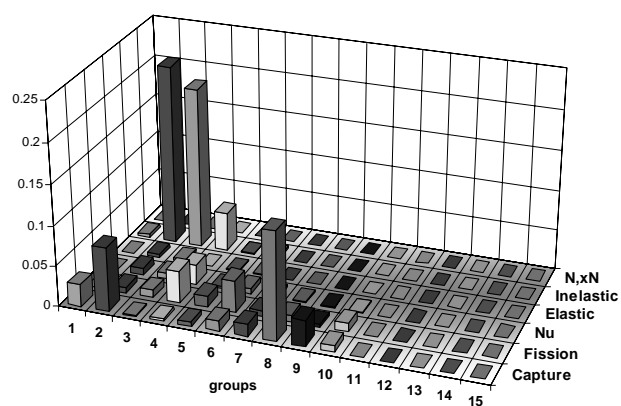


Table 42. EFR k_{eff} : BOLNA full uncertainties (%) by group

Gr.	[MeV]	σ_{cap}	σ_{fiss}	ν	σ_{el}	σ_{inel}	$\sigma_{\text{n,2n}}$	Total
1	19.6	0.14	0.04	0.03	0.03	0.09	0.01	0.18
2	6.07	0.23	0.13	0.12	0.06	0.55	—	0.62
3	2.23	0.05	0.17	0.11	0.10	0.53	—	0.58
4	1.35	0.10	0.25	0.18	0.10	0.34	—	0.48
5	4.98e-1	0.12	0.19	0.09	0.04	0.04	—	0.25
6	1.83e-1	0.17	0.24	0.09	0.04	0.07	—	0.32
7	6.74e-2	0.17	0.16	0.08	0.03	0.02	—	0.25
8	2.48e-2	0.32	0.11	0.06	0.01i	0.01i	—	0.35
9	9.12e-3	0.18	0.08	0.04	0.01i	—	—	0.20
10	2.03e-3	0.09	0.09	0.05	0.01i	—	—	0.13
11	4.54e-4	0.02	0.02	0.01	—	—	—	0.04
12	2.26e-5	—	—	—	—	—	—	—
13	4.00e-6	—	—	—	—	—	—	—
14	5.40e-7	—	—	—	—	—	—	—
15	1.00e-7	—	—	—	—	—	—	—
Total		0.55	0.51	0.30	0.17	0.84	0.01	1.18

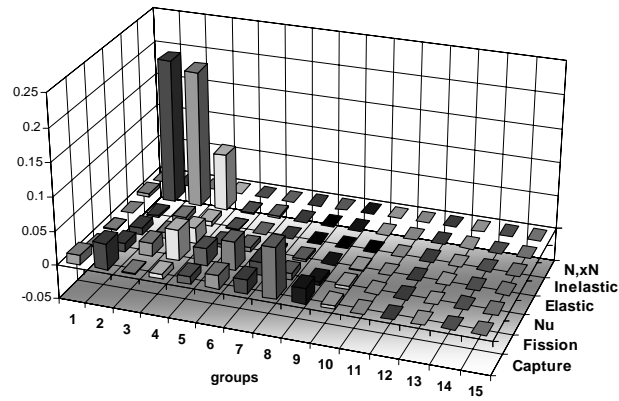


Table 43. EFR k_{eff} : BOLNA diagonal uncertainties (%) by isotope

Isotope	σ_{cap}	σ_{fiss}	ν	σ_{el}	σ_{inel}	$\sigma_{\text{n,2n}}$	Total
²³⁵ U	—	—	—	—	—	—	—
²³⁸ U	0.30	0.02	0.08	0.02	0.50	—	0.59
²³⁸ Pu	0.01	0.06	0.04	—	—	—	0.07
²³⁹ Pu	0.16	0.13	0.09	—	0.04	—	0.23
²⁴⁰ Pu	0.10	0.15	0.14	—	0.02	—	0.23
²⁴¹ Pu	0.01	0.20	0.01	—	—	—	0.20
²⁴² Pu	0.03	0.05	0.01	—	—	—	0.06
²³⁷ Np	—	—	—	—	—	—	—
²⁴¹ Am	0.02	0.02	0.01	—	—	—	0.04
^{242m} Am	—	0.01	—	—	—	—	0.01
²⁴³ Am	0.01	—	—	—	—	—	0.01
²⁴² Cm	—	—	—	—	—	—	—
²⁴³ Cm	—	—	—	—	—	—	—
²⁴⁴ Cm	—	0.04	0.01	—	—	—	0.04
²⁴⁵ Cm	—	0.03	—	—	—	—	0.03
²⁴⁶ Cm	—	—	—	—	—	—	—
⁵⁶ Fe	0.05	—	—	0.01	0.17	—	0.17
⁵² Cr	—	—	—	—	0.01	0.01	0.01
⁵⁸ Ni	0.06	—	—	—	0.03	—	0.06
²³ Na	0.01	—	—	0.02	0.11	—	0.12
¹⁶ O	0.25	—	—	0.08	0.03	—	0.27
Total	0.45	0.30	0.19	0.09	0.55	0.01	0.79

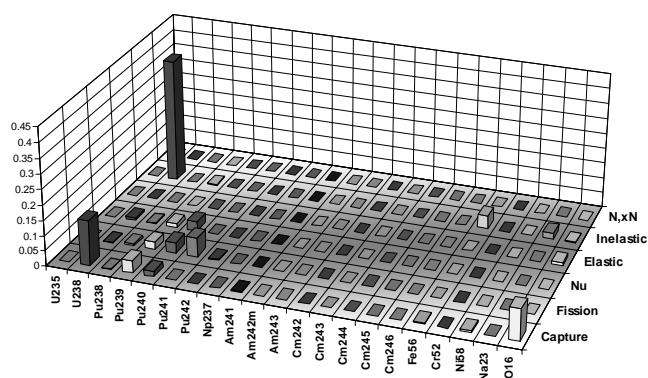


Table 44. EFR k_{eff} : BOLNA full uncertainties (%) by isotope

Isotope	σ_{cap}	σ_{fiss}	ν	σ_{el}	σ_{inel}	$\sigma_{\text{n,2n}}$	Total
²³⁵ U	0.01	—	—	—	—	—	0.01
²³⁸ U	0.33	0.03	0.11	0.16	0.79	—	0.88
²³⁸ Pu	0.02	0.12	0.09	—	—	—	0.15
²³⁹ Pu	0.23	0.18	0.11	0.01	0.07	—	0.32
²⁴⁰ Pu	0.24	0.26	0.24	—	0.04	—	0.43
²⁴¹ Pu	0.02	0.35	0.02	—	—	—	0.36
²⁴² Pu	0.06	0.07	0.02	—	0.01	—	0.09
²³⁷ Np	—	—	—	—	—	—	0.01
²⁴¹ Am	0.04	0.04	0.01	—	—	—	0.06
^{242m} Am	—	0.03	—	—	—	—	0.03
²⁴³ Am	0.01	0.01	—	—	—	—	0.01
²⁴² Cm	—	—	—	—	—	—	—
²⁴³ Cm	—	0.01	—	—	—	—	0.01
²⁴⁴ Cm	0.01	0.06	0.01	—	—	—	0.06
²⁴⁵ Cm	—	0.05	0.01	—	—	—	0.06
²⁴⁶ Cm	—	0.01	—	—	—	—	0.01
⁵⁶ Fe	0.06	—	—	0.01	0.25	—	0.26
⁵² Cr	0.01	—	—	0.01	0.01	0.01	0.01
⁵⁸ Ni	0.07	—	—	—	0.03	—	0.08
²³ Na	0.01	—	—	0.02	0.13	—	0.14
¹⁶ O	0.26	—	—	0.06	0.03	—	0.27
Total	0.55	0.51	0.30	0.17	0.84	0.01	1.18

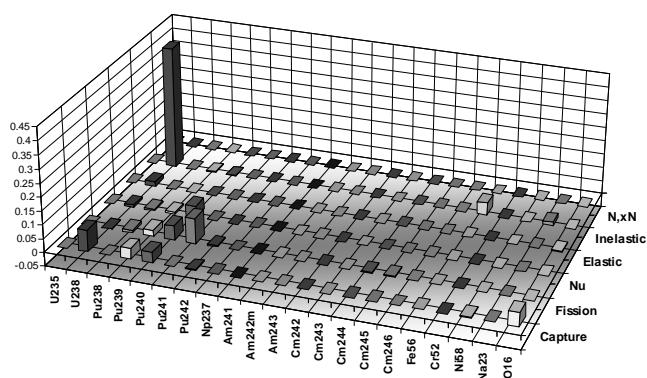


Table 45. EFR power peak: BOLNA diagonal uncertainty (%) by group

Gr.	[MeV]	σ_{cap}	σ_{fiss}	ν	σ_{el}	σ_{inel}	$\sigma_{\text{n,2n}}$	Total
1	19.6	0.04	0.01	—	0.04	0.05	—	0.07
2	6.07	0.06	0.03	0.03	0.35	0.45	—	0.58
3	2.23	0.01	0.04	0.03	0.13	0.38	—	0.41
4	1.35	0.02	0.06	0.05	0.08	0.21	—	0.24
5	4.98e-1	0.02	0.02	0.01	0.09	0.02	—	0.09
6	1.83e-1	0.03	0.02	—	0.09	0.06	—	0.12
7	6.74e-2	0.04	0.02	—	0.05	—	—	0.06
8	2.48e-2	0.23	0.02	0.01	0.03	—	—	0.24
9	9.12e-3	0.07	0.02	0.01	—	—	—	0.08
10	2.03e-3	0.07	0.06	0.01	0.03	—	—	0.09
11	4.54e-4	0.02	0.02	—	0.01	—	—	0.03
12	2.26e-5	—	—	—	—	—	—	—
13	4.00e-6	—	—	—	—	—	—	—
14	5.40e-7	—	—	—	—	—	—	—
15	1.00e-7	—	—	—	—	—	—	—
Total		0.27	0.10	0.06	0.41	0.64	—	0.81

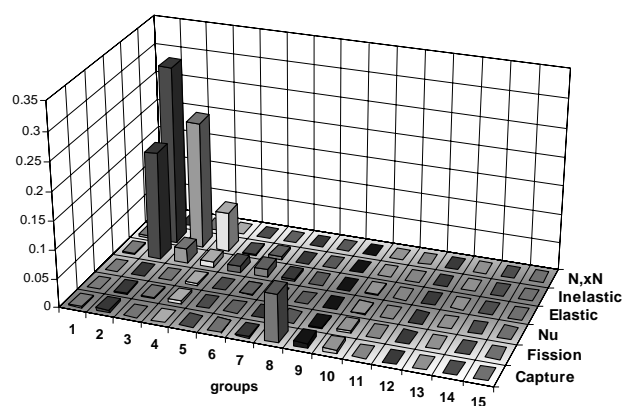


Table 46. EFR power peak: BOLNA full uncertainty (%) by group

Gr.	[MeV]	σ_{cap}	σ_{fiss}	ν	σ_{el}	σ_{inel}	$\sigma_{\text{n,2n}}$	Total
1	19.6	0.04	0.02	0.01	0.15	0.10	—	0.18
2	6.07	0.06	0.05	0.04	0.46	0.62	—	0.78
3	2.23	0.02	0.06	0.04	0.23	0.56	—	0.61
4	1.35	0.03	0.08	0.05	0.04i	0.40	—	0.41
5	4.98e-1	0.04	0.03	0.02	0.20	0.06	—	0.22
6	1.83e-1	0.06	0.02	0.01	0.21	0.10	—	0.24
7	6.74e-2	0.06	0.02	0.01i	0.14	0.02	—	0.15
8	2.48e-2	0.24	0.03	—	0.08	0.01i	—	0.25
9	9.12e-3	0.09	0.03	0.01	0.04i	—	—	0.09
10	2.03e-3	0.09	0.06	0.01i	0.08	—	—	0.13
11	4.54e-4	0.03	0.03	—	0.04	—	—	0.06
12	2.26e-5	—	—	—	0.01	—	—	0.01
13	4.00e-6	—	—	—	—	—	—	0.01
14	5.40e-7	—	—	—	—	—	—	—
15	1.00e-7	—	—	—	—	—	—	—
Total		0.30	0.14	0.08	0.63	0.94	—	1.18

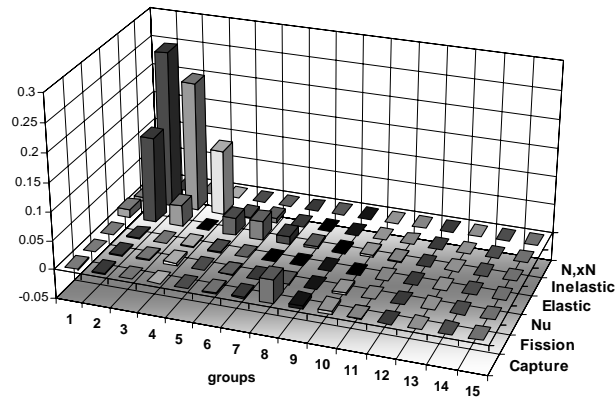


Table 47. EFR power peak: BOLNA diagonal uncertainty (%) by isotope

Isotope	σ_{cap}	σ_{fiss}	ν	σ_{el}	σ_{inel}	$\sigma_{\text{n,2n}}$	Total
²³⁵ U	—	—	—	—	—	—	—
²³⁸ U	0.26	0.01	0.02	0.07	0.60	—	0.66
²³⁸ Pu	—	0.02	0.01	—	—	—	0.03
²³⁹ Pu	0.03	0.04	0.02	0.02	0.03	—	0.07
²⁴⁰ Pu	0.03	0.06	0.05	0.01	0.02	—	0.09
²⁴¹ Pu	—	0.06	—	—	—	—	0.06
²⁴² Pu	0.01	0.02	—	—	—	—	0.02
²³⁷ Np	—	—	—	—	—	—	—
²⁴¹ Am	0.02	0.01	—	—	—	—	0.02
^{242m} Am	—	0.01	—	—	—	—	0.01
²⁴³ Am	—	—	—	—	—	—	0.01
²⁴² Cm	—	—	—	—	—	—	—
²⁴³ Cm	—	—	—	—	—	—	—
²⁴⁴ Cm	—	0.01	—	—	—	—	0.01
²⁴⁵ Cm	—	0.02	—	—	—	—	0.02
²⁴⁶ Cm	—	—	—	—	—	—	—
⁵⁶ Fe	0.03	—	—	0.06	0.16	—	0.17
⁵² Cr	—	—	—	0.04	0.01	—	0.04
⁵⁸ Ni	0.01	—	—	0.03	0.02	—	0.04
²³ Na	—	—	—	0.11	0.12	—	0.17
¹⁶ O	0.07	—	—	0.38	0.03	—	0.39
Total	0.27	0.10	0.06	0.41	0.64	—	0.81

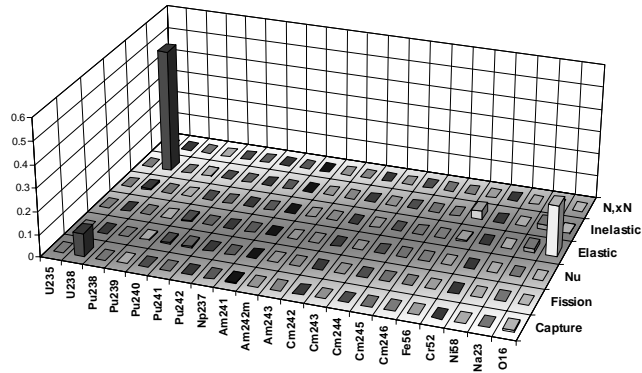


Table 48. EFR power peak: BOLNA full uncertainty (%) by isotope

Isotope	σ_{cap}	σ_{fiss}	ν	σ_{el}	σ_{inel}	$\sigma_{\text{n,2n}}$	Total
²³⁵ U	—	—	—	—	—	—	—
²³⁸ U	0.28	0.01	0.03	0.26i	0.89	—	0.90
²³⁸ Pu	—	0.04	0.01	—	—	—	0.04
²³⁹ Pu	0.04	0.05	0.02	0.03	0.06	—	0.09
²⁴⁰ Pu	0.05	0.09	0.07	0.03	0.03	—	0.13
²⁴¹ Pu	0.01	0.07	—	—	—	—	0.07
²⁴² Pu	0.01	0.03	0.01	—	0.01	—	0.03
²³⁷ Np	—	—	—	—	—	—	—
²⁴¹ Am	0.03	0.01	—	—	0.01	—	0.03
^{242m} Am	—	0.02	—	—	—	—	0.02
²⁴³ Am	0.01	—	—	—	—	—	0.01
²⁴² Cm	—	—	—	—	—	—	—
²⁴³ Cm	—	0.01	—	—	—	—	0.01
²⁴⁴ Cm	—	0.02	—	—	—	—	0.02
²⁴⁵ Cm	—	0.04	0.01	—	—	—	0.04
²⁴⁶ Cm	—	—	—	—	—	—	—
⁵⁶ Fe	0.03	—	—	0.10	0.25	—	0.27
⁵² Cr	—	—	—	0.06	0.01	—	0.06
⁵⁸ Ni	0.02	—	—	0.04	0.02	—	0.05
²³ Na	—	—	—	0.20	0.15	—	0.25
¹⁶ O	0.07	—	—	0.64	0.03	—	0.65
Total	0.30	0.14	0.08	0.63	0.94	—	1.18

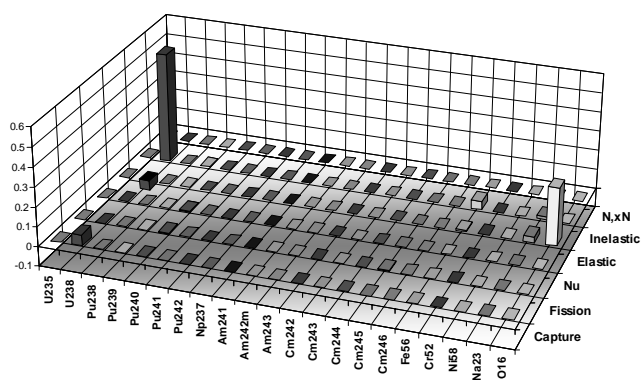


Table 49. EFR Doppler: BOLNA diagonal uncertainty (%) by group

Gr.	[MeV]	σ_{cap}	σ_{fiss}	ν	σ_{el}	σ_{inel}	$\sigma_{\text{n,2n}}$	Total
1	19.6	0.18	0.04	0.02	0.02	0.11	—	0.21
2	6.07	0.28	0.20	0.17	0.17	1.18	—	1.25
3	2.23	0.02	0.23	0.15	0.12	1.14	—	1.18
4	1.35	0.04	0.47	0.29	0.07	0.74	—	0.93
5	4.98e-1	0.03	0.27	0.09	0.17	0.09	—	0.35
6	1.83e-1	0.09	0.46	0.14	0.25	0.36	—	0.65
7	6.74e-2	0.12	0.21	0.09	0.32	0.08	—	0.42
8	2.48e-2	0.38	0.21	0.06	0.46	0.10	—	0.64
9	9.12e-3	0.67	0.14	0.03	0.35	—	—	0.77
10	2.03e-3	0.38	0.22	0.07	0.16	—	—	0.48
11	4.54e-4	0.17	0.48	0.07	0.02	—	—	0.51
12	2.26e-5	—	—	—	—	—	—	—
13	4.00e-6	—	—	—	—	—	—	—
14	5.40e-7	—	—	—	—	—	—	—
15	1.00e-7	—	—	—	—	—	—	—
Total		0.95	0.99	0.43	0.78	1.85	—	2.46

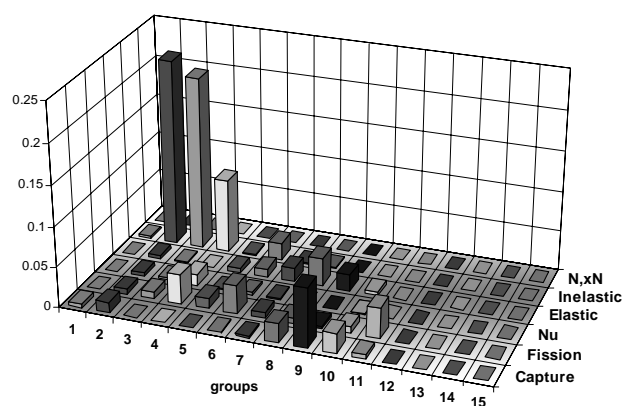


Table 50. EFR Doppler: BOLNA full uncertainty (%) by group

Gr.	[MeV]	σ_{cap}	σ_{fiss}	ν	σ_{el}	σ_{inel}	$\sigma_{\text{n,2n}}$	Total
1	19.6	0.19	0.12	0.05	0.12	0.26	—	0.36
2	6.07	0.29	0.39	0.26	0.27i	1.78	—	1.84
3	2.23	0.03i	0.50	0.25	0.39	1.75	—	1.88
4	1.35	0.08i	0.75	0.40	0.35	1.35	—	1.63
5	4.98e-1	0.07i	0.56	0.20	0.41	0.26	—	0.76
6	1.83e-1	0.11	0.70	0.20	0.53	0.52	—	1.04
7	6.74e-2	0.20	0.47	0.16	0.60	0.24	—	0.85
8	2.48e-2	0.48	0.33	0.11	0.70	0.20	—	0.94
9	9.12e-3	0.72	0.23	0.07	0.56	0.01	—	0.94
10	2.03e-3	0.39	0.23	0.05	0.43	—	—	0.63
11	4.54e-4	0.21	0.46	0.03	0.08i	—	—	0.50
12	2.26e-5	0.01i	0.01	—	0.03i	—	—	0.03i
13	4.00e-6	0.01i	0.01	—	0.01	—	—	—
14	5.40e-7	0.01i	—	—	0.01	—	—	0.01
15	1.00e-7	—	—	—	0.01	—	—	—
Total		1.05	1.56	0.64	1.41	2.92	—	3.80

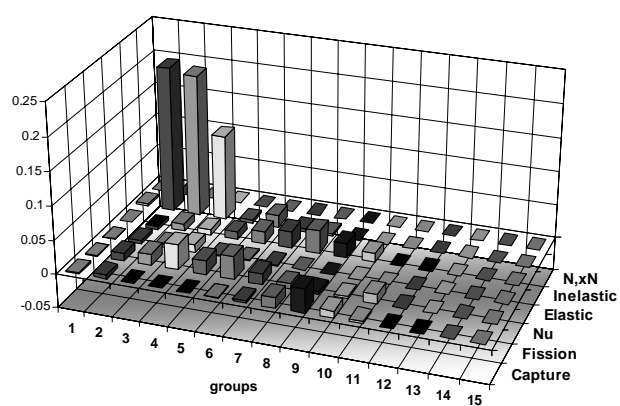


Table 51. EFR Doppler: BOLNA diagonal uncertainty (%) by isotope

Isotope	σ_{cap}	σ_{fiss}	ν	σ_{el}	σ_{inel}	$\sigma_{\text{n,2n}}$	Total
²³⁵ U	0.01	—	—	—	—	—	0.01
²³⁸ U	0.41	0.06	0.16	0.07	1.69	—	1.75
²³⁸ Pu	0.04	0.19	0.09	—	0.01	—	0.22
²³⁹ Pu	0.71	0.42	0.20	0.01	0.21	—	0.88
²⁴⁰ Pu	0.17	0.46	0.33	0.01	0.12	—	0.61
²⁴¹ Pu	0.07	0.71	0.02	—	0.01	—	0.72
²⁴² Pu	0.11	0.14	0.03	—	0.02	—	0.18
²³⁷ Np	0.02	0.01	—	—	0.01	—	0.02
²⁴¹ Am	0.18	0.06	0.01	—	0.01	—	0.19
^{242m} Am	0.01	0.04	—	—	—	—	0.04
²⁴³ Am	0.05	0.01	—	—	0.01	—	0.05
²⁴² Cm	—	—	—	—	—	—	—
²⁴³ Cm	—	0.01	—	—	—	—	0.01
²⁴⁴ Cm	0.01	0.09	0.02	—	—	—	0.09
²⁴⁵ Cm	—	0.07	0.01	—	—	—	0.07
²⁴⁶ Cm	0.01	0.01	—	—	—	—	0.02
⁵⁶ Fe	0.18	—	—	0.15	0.51	—	0.56
⁵² Cr	0.01	—	—	0.07	0.02	—	0.07
⁵⁸ Ni	0.07	—	—	0.38	0.09	—	0.40
²³ Na	0.02	—	—	0.42	0.46	—	0.62
¹⁶ O	0.32	—	—	0.50	0.07	—	0.60
Total	0.95	0.99	0.43	0.78	1.85	—	2.46

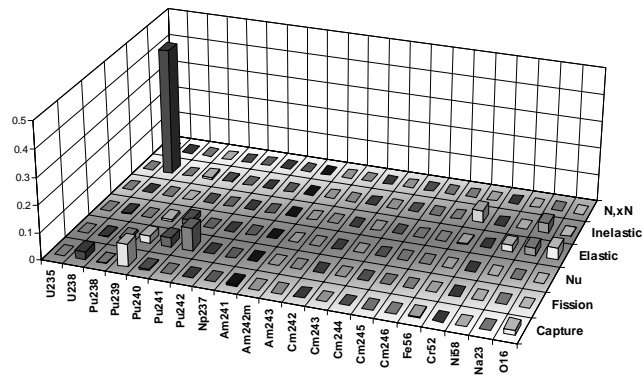


Table 52. EFR Doppler: BOLNA full uncertainty (%) by isotope

Isotope	σ_{cap}	σ_{fiss}	ν	σ_{el}	σ_{inel}	$\sigma_{\text{n,2n}}$	Total
²³⁵ U	0.02	—	—	—	—	—	0.02
²³⁸ U	0.38	0.08	0.22	0.46	2.71	—	2.79
²³⁸ Pu	0.06	0.34	0.11	—	0.01	—	0.36
²³⁹ Pu	0.79	0.54	0.22	0.02i	0.45	—	1.08
²⁴⁰ Pu	0.22	0.81	0.55	0.01	0.23	—	1.02
²⁴¹ Pu	0.11	1.12	—	—	0.02	—	1.13
²⁴² Pu	0.17	0.22	0.04	—	0.03	—	0.28
²³⁷ Np	0.03	0.01	—	—	0.01	—	0.03
²⁴¹ Am	0.30	0.10	0.02	—	0.02	—	0.31
^{242m} Am	0.01	0.06	—	—	—	—	0.06
²⁴³ Am	0.08	0.02	—	—	0.02	—	0.08
²⁴² Cm	—	—	—	—	—	—	—
²⁴³ Cm	—	0.02	—	—	—	—	0.02
²⁴⁴ Cm	0.02	0.14	0.02	—	0.01	—	0.14
²⁴⁵ Cm	—	0.13	—	—	—	—	0.13
²⁴⁶ Cm	0.02	0.01	—	—	—	—	0.02
⁵⁶ Fe	0.14	—	—	0.28	0.80	—	0.86
⁵² Cr	0.02	—	—	0.11	0.02	—	0.12
⁵⁸ Ni	0.09	—	—	0.46	0.10	—	0.48
²³ Na	0.02	—	—	0.71	0.52	—	0.88
¹⁶ O	0.33	—	—	0.99	0.07	—	1.05
Total	1.05	1.56	0.64	1.41	2.92	—	3.80

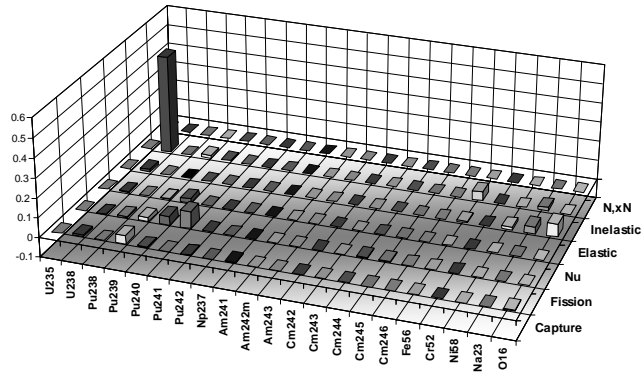


Table 53. EFR void: BOLNA diagonal uncertainties (%) by group

Gr.	[MeV]	σ_{cap}	σ_{fiss}	ν	σ_{el}	σ_{inel}	$\sigma_{\text{n,2n}}$	Total
1	19.6	0.80	—	0.02	0.12	0.36	0.01	0.89
2	6.07	0.52	0.03	0.12	0.75	1.27	—	1.56
3	2.23	0.02	0.10	0.04	0.23	0.89	—	0.92
4	1.35	0.32	0.66	0.59	0.36	5.58	—	5.67
5	4.98e-1	0.10	0.04	0.01	0.60	0.09	—	0.61
6	1.83e-1	0.08	0.14	0.05	0.59	0.20	—	0.65
7	6.74e-2	0.13	0.08	0.06	0.18	0.02	—	0.24
8	2.48e-2	0.99	0.30	0.15	0.08	0.01	—	1.05
9	9.12e-3	0.85	0.30	0.22	0.22	—	—	0.95
10	2.03e-3	1.46	1.72	0.32	0.21	—	—	2.28
11	4.54e-4	0.21	0.49	0.06	0.02	—	—	0.53
12	2.26e-5	—	—	—	—	—	—	—
13	4.00e-6	—	—	—	—	—	—	—
14	5.40e-7	—	—	—	—	—	—	—
15	1.00e-7	—	—	—	—	—	—	—
Total		2.22	1.96	0.73	1.26	5.81	0.01	6.68

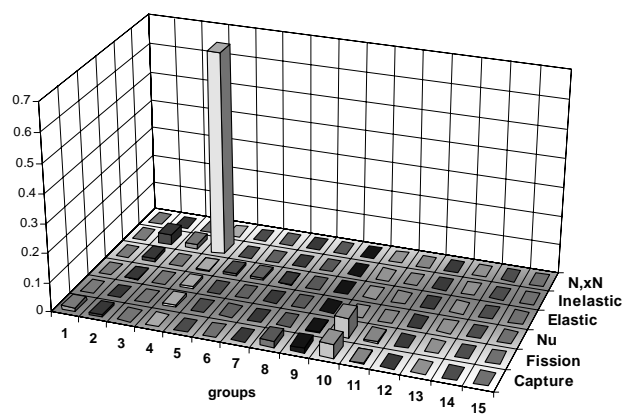


Table 54. EFR void: BOLNA full uncertainties (%) by group

Gr.	[MeV]	σ_{cap}	σ_{fiss}	ν	σ_{el}	σ_{inel}	$\sigma_{\text{n,2n}}$	Total
1	19.6	0.83	0.01	0.04	0.19i	0.76	0.01	1.11
2	6.07	0.56	0.08	0.16	0.75	2.21	—	2.41
3	2.23	0.06	0.20i	0.08i	0.58	2.43	—	2.49
4	1.35	0.32	0.57	0.49	0.93	6.17	—	6.29
5	4.98e-1	0.10	0.05	0.03	0.80	0.31	—	0.86
6	1.83e-1	0.10	0.07i	0.05i	0.79	0.32	—	0.85
7	6.74e-2	0.15	0.04i	0.06i	0.40	0.10	—	0.43
8	2.48e-2	0.94	0.18	0.10	0.28i	0.04i	—	0.92
9	9.12e-3	0.64	0.18i	0.25	0.20	—	—	0.70
10	2.03e-3	1.41	1.75	0.07	0.25i	—	—	2.23
11	4.54e-4	0.34	0.64	0.06	0.04	—	—	0.72
12	2.26e-5	0.03i	—	—	0.03	—	—	0.01i
13	4.00e-6	0.03i	0.01i	—	0.01	—	—	0.03i
14	5.40e-7	0.01i	—	—	0.01	—	—	—
15	1.00e-7	—	—	—	—	—	—	—
Total		2.14	1.94	0.58	1.74	7.04	0.01	7.83

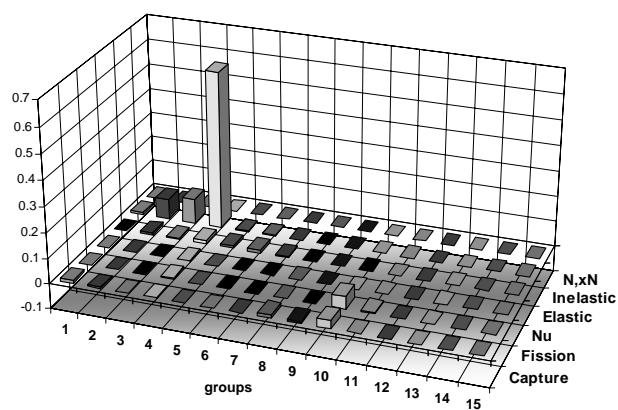


Table 55. EFR void: BOLNA diagonal uncertainty (%) by isotope

Isotope	σ_{cap}	σ_{fiss}	ν	σ_{el}	σ_{inel}	$\sigma_{\text{n,2n}}$	Total
²³⁵ U	0.01	0.01	0.01	—	—	—	0.02
²³⁸ U	1.55	0.03	0.12	0.36	1.39	—	2.12
²³⁸ Pu	0.04	0.22	0.19	—	0.01	—	0.29
²³⁹ Pu	0.85	1.12	0.36	0.05	0.23	—	1.47
²⁴⁰ Pu	0.32	0.71	0.59	0.02	0.06	—	0.98
²⁴¹ Pu	0.09	1.40	0.04	—	0.01	—	1.40
²⁴² Pu	0.14	0.14	0.04	—	0.02	—	0.20
²³⁷ Np	0.03	0.01	—	—	0.01	—	0.03
²⁴¹ Am	0.22	0.05	0.01	—	0.02	—	0.23
^{242m} Am	0.01	0.09	0.01	—	—	—	0.09
²⁴³ Am	0.06	0.01	—	—	0.01	—	0.06
²⁴² Cm	—	—	—	—	—	—	—
²⁴³ Cm	—	0.02	—	—	—	—	0.02
²⁴⁴ Cm	0.01	0.17	0.03	—	—	—	0.18
²⁴⁵ Cm	—	0.10	0.02	—	—	—	0.10
²⁴⁶ Cm	0.01	0.01	—	—	—	—	0.02
⁵⁶ Fe	0.82	—	—	0.16	0.38	—	0.92
⁵² Cr	0.03	—	—	0.06	0.01	0.01	0.07
⁵⁸ Ni	0.16	—	—	0.04	0.05	—	0.17
²³ Na	0.68	—	—	0.90	5.62	—	5.73
¹⁶ O	0.65	—	—	0.79	0.15	—	1.03
Total	2.22	1.96	0.73	1.26	5.81	0.01	6.68

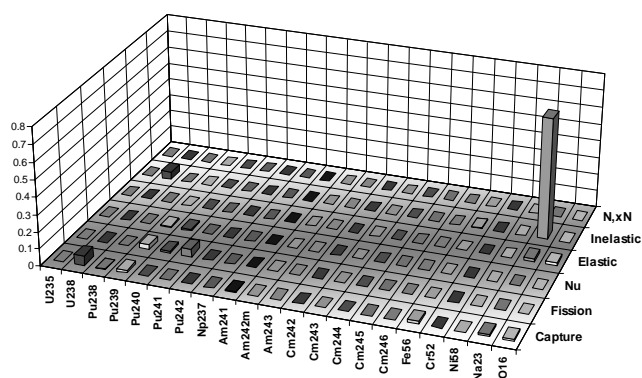


Table 56. EFR void: BOLNA full uncertainty (%) by isotope

Isotope	σ_{cap}	σ_{fiss}	ν	σ_{el}	σ_{inel}	$\sigma_{\text{n,2n}}$	Total
²³⁵ U	0.01	0.01	—	—	—	—	0.01
²³⁸ U	1.49	0.02i	0.14	1.14	2.47	—	3.10
²³⁸ Pu	0.05	0.21	0.05	—	0.01	—	0.22
²³⁹ Pu	0.72	1.21	0.36	0.12	0.32	—	1.49
²⁴⁰ Pu	0.19	0.63	0.42	0.02	0.11	—	0.79
²⁴¹ Pu	0.11	1.33	0.04	—	0.01	—	1.34
²⁴² Pu	0.03	0.11	0.04	—	0.02	—	0.13
²³⁷ Np	0.02	0.01	—	—	0.01	—	0.03
²⁴¹ Am	0.23	0.05	0.01	—	0.02	—	0.24
^{242m} Am	0.01	0.08	0.01	—	—	—	0.08
²⁴³ Am	0.06	0.01	—	—	0.02	—	0.07
²⁴² Cm	—	—	—	—	—	—	—
²⁴³ Cm	—	0.02	—	—	—	—	0.02
²⁴⁴ Cm	0.02	0.18	0.03	—	—	—	0.18
²⁴⁵ Cm	—	0.10	0.02	—	—	—	0.10
²⁴⁶ Cm	0.02	0.01	—	—	—	—	0.02
⁵⁶ Fe	0.84	—	—	0.20	0.41	—	0.95
⁵² Cr	0.03	—	—	0.06	0.01	0.01	0.07
⁵⁸ Ni	0.21	—	—	0.06	0.05	—	0.22
²³ Na	0.72	—	—	1.18	6.57	—	6.72
¹⁶ O	0.67	—	—	0.55	0.15	—	0.88
Total	2.14	1.94	0.58	1.74	7.04	0.01	7.83

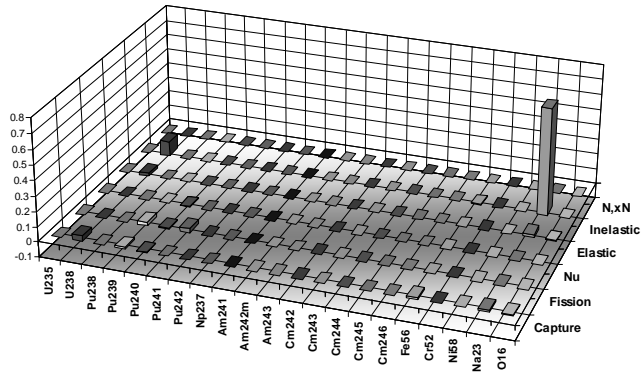


Table 57. EFR XS burn-up: BOLNA diagonal uncertainty (%) by group

Gr.	[MeV]	σ_{cap}	σ_{fiss}	ν	σ_{el}	σ_{inel}	$\sigma_{\text{n,2n}}$	Total
1	19.6	0.16	0.02	0.01	0.05	0.06	0.01	0.18
2	6.07	0.28	0.18	0.07	0.42	0.27	—	0.60
3	2.23	0.01	0.25	0.08	0.23	0.50	—	0.61
4	1.35	0.05	0.59	0.17	0.12	0.39	—	0.74
5	4.98e-1	0.06	0.57	0.05	0.13	0.02	—	0.59
6	1.83e-1	0.09	1.19	0.06	0.13	0.05	—	1.20
7	6.74e-2	0.09	0.47	0.05	0.08	0.01	—	0.49
8	2.48e-2	0.12	0.54	0.05	0.05	0.01	—	0.56
9	9.12e-3	0.09	0.41	0.04	0.01	—	—	0.42
10	2.03e-3	0.12	0.61	0.04	0.01	—	—	0.62
11	4.54e-4	0.02	0.15	0.01	0.01	—	—	0.15
12	2.26e-5	0.01	—	—	0.01	—	—	0.01
13	4.00e-6	—	—	—	—	—	—	—
14	5.40e-7	—	—	—	—	—	—	—
15	1.00e-7	—	—	—	—	—	—	—
Total		0.41	1.80	0.24	0.54	0.69	0.01	2.06

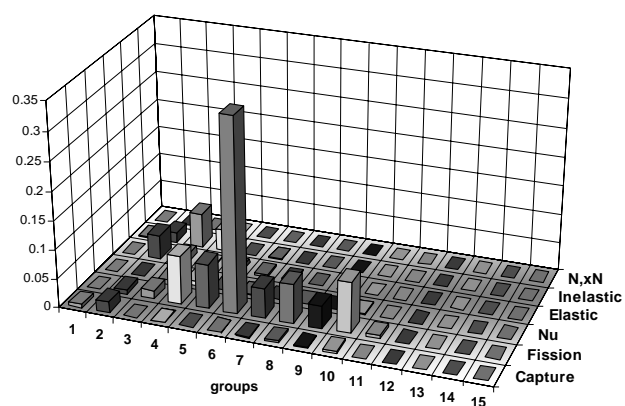


Table 58. EFR XS burn-up: BOLNA full uncertainty (%) by group

Gr.	[MeV]	σ_{cap}	σ_{fiss}	ν	σ_{el}	σ_{inel}	$\sigma_{\text{n,2n}}$	Total
1	19.6	0.17	0.10	0.02	0.20	0.12	0.01	0.31
2	6.07	0.29	0.40	0.12	0.62	0.44	—	0.92
3	2.23	0.05	0.77	0.14	0.43	0.66	—	1.11
4	1.35	0.09	1.19	0.26	0.24	0.56	—	1.37
5	4.98e-1	0.11	1.25	0.15	0.31	0.05	—	1.30
6	1.83e-1	0.14	1.80	0.14	0.32	0.09	—	1.84
7	6.74e-2	0.14	1.16	0.13	0.23	0.03	—	1.20
8	2.48e-2	0.16	0.81	0.11	0.13	0.02	—	0.84
9	9.12e-3	0.12	0.69	0.09	0.05	—	—	0.71
10	2.03e-3	0.15	0.62	0.11	0.05i	—	—	0.64
11	4.54e-4	0.06	0.17	0.03	0.08i	—	—	0.17
12	2.26e-5	0.03	0.01	—	0.03	—	—	0.04
13	4.00e-6	0.01	—	—	0.01i	—	—	0.01i
14	5.40e-7	—	—	—	—	—	—	—
15	1.00e-7	—	—	—	—	—	—	—
Total		0.50	3.14	0.44	0.97	0.98	0.01	3.49

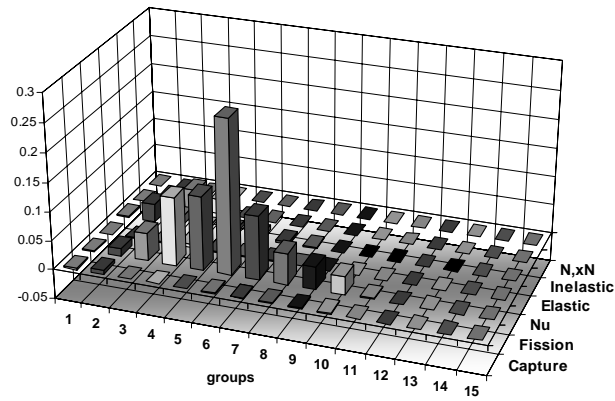


Table 59. EFR XS burn-up: BOLNA diagonal uncertainty (%) by isotope

Isotope	σ_{cap}	σ_{fiss}	ν	σ_{el}	σ_{inel}	$\sigma_{\text{n,2n}}$	Total
²³⁵ U	0.01	—	—	—	—	—	0.01
²³⁸ U	0.11	0.03	0.06	0.09	0.40	—	0.43
²³⁸ Pu	0.01	0.13	0.06	—	—	—	0.14
²³⁹ Pu	0.11	0.18	0.07	0.01	0.02	—	0.22
²⁴⁰ Pu	0.06	0.30	0.19	0.01	0.03	—	0.36
²⁴¹ Pu	0.06	1.73	0.04	—	0.02	—	1.73
²⁴² Pu	—	0.06	0.01	—	0.01	—	0.06
²³⁷ Np	—	—	—	—	—	—	—
²⁴¹ Am	0.10	0.08	0.02	—	0.01	—	0.13
^{242m} Am	—	0.06	—	—	—	—	0.06
²⁴³ Am	0.01	0.01	—	—	0.01	—	0.02
²⁴² Cm	0.01	0.12	0.03	—	—	—	0.13
²⁴³ Cm	—	0.03	—	—	—	—	0.03
²⁴⁴ Cm	0.02	0.30	0.06	—	—	—	0.31
²⁴⁵ Cm	—	0.09	0.01	—	—	—	0.09
²⁴⁶ Cm	—	—	—	—	—	—	—
⁵⁶ Fe	0.13	—	—	0.05	0.45	—	0.47
⁵² Cr	0.01	—	—	0.04	0.01	0.01	0.04
⁵⁸ Ni	0.07	—	—	0.05	0.07	—	0.11
²³ Na	0.02	—	—	0.12	0.33	—	0.35
¹⁶ O	0.31	—	—	0.51	0.05	—	0.60
Total	0.41	1.80	0.24	0.54	0.69	0.01	2.06

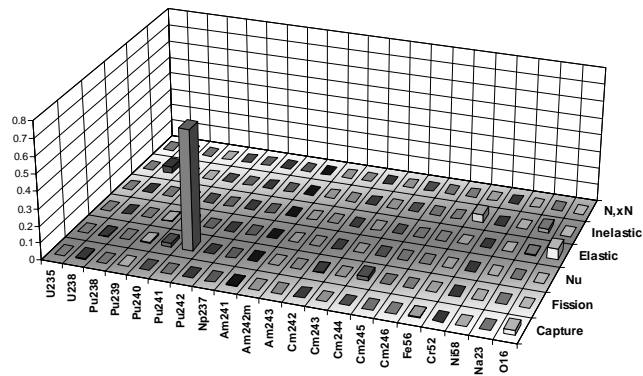


Table 60. EFR XS burn-up: BOLNA full uncertainty (%) by isotope

Isotope	σ_{cap}	σ_{fiss}	ν	σ_{el}	σ_{inel}	$\sigma_{\text{n,2n}}$	Total
²³⁵ U	0.03	—	0.01	—	—	—	0.03
²³⁸ U	0.12	0.04	0.08	0.24i	0.58	—	0.55
²³⁸ Pu	0.01	0.24	0.15	—	—	—	0.29
²³⁹ Pu	0.17	0.24	0.08	0.04	0.04	—	0.31
²⁴⁰ Pu	0.12	0.53	0.36	0.02	0.07	—	0.66
²⁴¹ Pu	0.12	3.02	0.12	—	0.03	—	3.02
²⁴² Pu	—	0.10	0.01	—	0.01	—	0.10
²³⁷ Np	—	—	—	—	—	—	—
²⁴¹ Am	0.18	0.13	0.03	—	0.02	—	0.22
^{242m} Am	—	0.11	0.01	—	—	—	0.11
²⁴³ Am	0.01	0.02	—	—	0.01	—	0.03
²⁴² Cm	0.02	0.23	0.06	—	—	—	0.24
²⁴³ Cm	—	0.05	—	—	—	—	0.05
²⁴⁴ Cm	0.04	0.46	0.09	—	0.01	—	0.47
²⁴⁵ Cm	—	0.18	0.03	—	—	—	0.19
²⁴⁶ Cm	—	0.01	—	—	—	—	0.01
⁵⁶ Fe	0.16	—	—	0.08	0.68	—	0.70
⁵² Cr	0.01	—	—	0.05	0.02	0.01	0.05
⁵⁸ Ni	0.10	—	—	0.06	0.07	—	0.13
²³ Na	0.02	—	—	0.20	0.39	—	0.44
¹⁶ O	0.32	—	—	0.97	0.05	—	1.02
Total	0.50	3.14	0.44	0.97	0.98	0.01	3.49

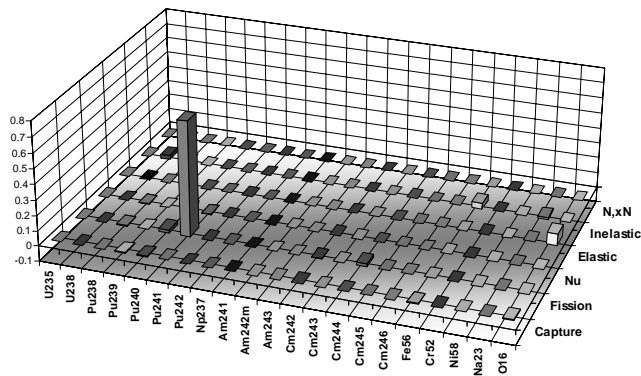


Table 61. GFR k_{eff} : BOLNA diagonal uncertainties (%) by group

Gr.	[MeV]	σ_{cap}	σ_{fiss}	ν	σ_{el}	σ_{inel}	$\sigma_{\text{n,2n}}$	Total
1	19.6	0.15	0.02	0.01	—	0.06	—	0.17
2	6.07	0.01	0.14	0.09	0.04	0.70	—	0.72
3	2.23	0.02	0.15	0.08	0.08	0.62	—	0.65
4	1.35	0.04	0.24	0.11	0.15	0.18	—	0.35
5	4.98e-1	0.04	0.14	0.03	0.09	0.01	—	0.18
6	1.83e-1	0.08	0.28	0.05	0.06	0.02	—	0.31
7	6.74e-2	0.11	0.13	0.04	0.02	—	—	0.18
8	2.48e-2	0.35	0.16	0.03	0.02	—	—	0.39
9	9.12e-3	0.25	0.20	0.05	0.03	—	—	0.32
10	2.03e-3	0.08	0.16	0.02	0.01	—	—	0.18
11	4.54e-4	0.02	0.08	—	—	—	—	0.08
12	2.26e-5	—	—	—	—	—	—	—
13	4.00e-6	—	—	—	—	—	—	—
14	5.40e-7	—	—	—	—	—	—	—
15	1.00e-7	—	—	—	—	—	—	—
Total		0.49	0.56	0.19	0.21	0.95	—	1.24

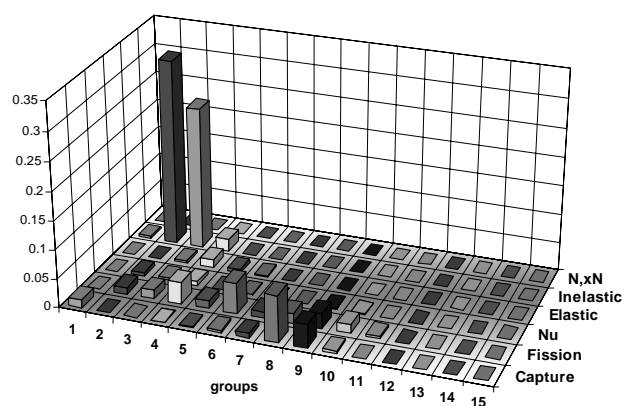


Table 62. GFR k_{eff} : BOLNA full uncertainties (%) by group

Gr.	[MeV]	σ_{cap}	σ_{fiss}	ν	σ_{el}	σ_{inel}	$\sigma_{\text{n,2n}}$	Total
1	19.6	0.15	0.05	0.03	0.03	0.14	—	0.22
2	6.07	0.04	0.23	0.14	0.13	0.99	—	1.03
3	2.23	0.04	0.32	0.13	0.16	0.91	—	0.99
4	1.35	0.08	0.41	0.16	0.21	0.48	—	0.69
5	4.98e-1	0.10	0.32	0.09	0.12	0.04	—	0.37
6	1.83e-1	0.14	0.45	0.08	0.10	0.05	—	0.49
7	6.74e-2	0.19	0.32	0.08	0.02i	0.01	—	0.38
8	2.48e-2	0.39	0.26	0.07	0.02	0.01i	—	0.48
9	9.12e-3	0.31	0.29	0.08	0.03	—	—	0.43
10	2.03e-3	0.14	0.16	0.06	0.01	—	—	0.22
11	4.54e-4	0.06	0.08	0.02	0.01	—	—	0.10
12	2.26e-5	—	0.01	—	—	—	—	0.01
13	4.00e-6	—	0.01	—	—	—	—	0.01
14	5.40e-7	—	—	—	—	—	—	—
15	1.00e-7	—	—	—	—	—	—	—
Total		0.61	0.96	0.31	0.34	1.43	—	1.88

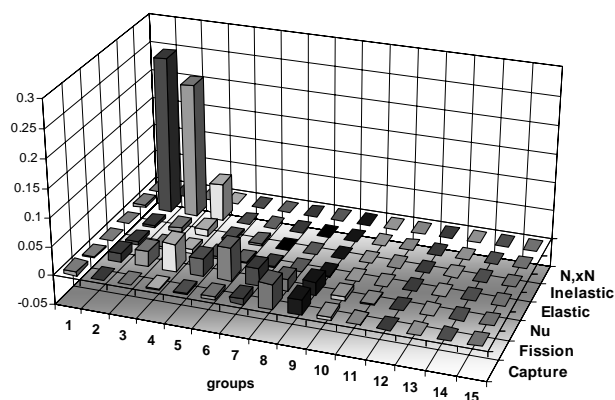


Table 63. GFR k_{eff} : BOLNA diagonal uncertainties (%) by isotope

Isotope	σ_{cap}	σ_{fiss}	ν	σ_{el}	σ_{inel}	$\sigma_{\text{n,2n}}$	Total
²³⁵ U	0.03	0.02	0.01	—	—	—	0.03
²³⁸ U	0.38	0.03	0.10	0.01	0.93	—	1.01
²³⁸ Pu	0.01	0.11	0.06	—	—	—	0.13
²³⁹ Pu	0.19	0.10	0.08	—	0.04	—	0.23
²⁴⁰ Pu	0.07	0.13	0.11	—	0.02	—	0.19
²⁴¹ Pu	0.02	0.47	0.01	—	0.01	—	0.47
²⁴² Pu	0.10	0.13	0.03	—	0.02	—	0.17
²³⁷ Np	0.02	0.02	0.01	—	0.01	—	0.04
²⁴¹ Am	0.14	0.15	0.04	—	0.02	—	0.21
^{242m} Am	—	0.01	—	—	—	—	0.01
²⁴³ Am	0.03	0.03	0.01	—	0.01	—	0.04
²⁴² Cm	—	—	—	—	—	—	—
²⁴³ Cm	—	—	—	—	—	—	—
²⁴⁴ Cm	0.01	0.09	0.02	—	—	—	0.09
²⁴⁵ Cm	—	0.06	0.01	—	—	—	0.06
²⁴⁶ Cm	—	—	—	—	—	—	—
C	0.01	—	—	0.21	0.04	—	0.21
⁴ He	—	—	—	0.01	—	—	0.01
²⁸ Si	0.15	—	—	0.02	0.19	—	0.24
⁹⁰ Zr	0.01	—	—	0.01	—	—	0.01
Total	0.49	0.56	0.19	0.21	0.95	—	1.24

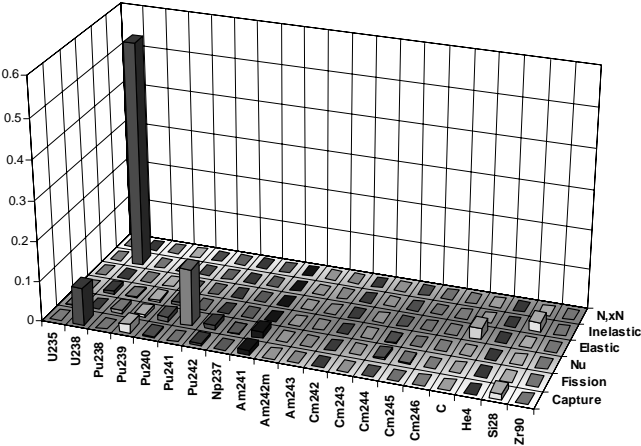


Table 64. GFR k_{eff} : BOLNA full uncertainties (%) by isotope

Isotope	σ_{cap}	σ_{fiss}	ν	σ_{el}	σ_{inel}	$\sigma_{\text{n,2n}}$	Total
²³⁵ U	0.06	0.02	0.02	—	—	—	0.07
²³⁸ U	0.41	0.04	0.15	0.13	1.41	—	1.48
²³⁸ Pu	0.03	0.20	0.15	—	—	—	0.25
²³⁹ Pu	0.23	0.15	0.09	—	0.07	—	0.30
²⁴⁰ Pu	0.17	0.23	0.20	—	0.03	—	0.35
²⁴¹ Pu	0.04	0.82	0.04	—	0.01	—	0.82
²⁴² Pu	0.17	0.21	0.04	—	0.02	—	0.27
²³⁷ Np	0.05	0.04	0.01	—	0.01	—	0.06
²⁴¹ Am	0.24	0.24	0.05	—	0.03	—	0.34
²⁴² Am	—	0.01	—	—	—	—	0.01
²⁴³ Am	0.05	0.04	0.01	—	0.02	—	0.07
²⁴² Cm	—	—	—	—	—	—	—
²⁴³ Cm	—	0.01	—	—	—	—	0.01
²⁴⁴ Cm	0.01	0.13	0.03	—	—	—	0.13
²⁴⁵ Cm	—	0.12	0.02	—	—	—	0.12
²⁴⁶ Cm	—	—	—	—	—	—	—
C	0.01	—	—	0.31	0.06	—	0.31
⁴ He	—	—	—	0.02	—	—	0.02
²⁸ Si	0.16	—	—	0.02	0.22	—	0.27
⁹⁰ Zr	0.01	—	—	0.02	—	—	0.02
Total	0.61	0.96	0.31	0.34	1.43	—	1.88

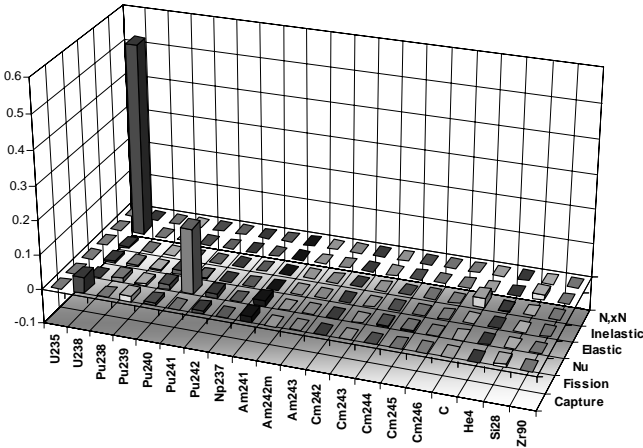


Table 65. GFR power peak: BOLNA diagonal uncertainty (%) by group

Gr.	[MeV]	σ_{cap}	σ_{fiss}	ν	σ_{el}	σ_{inel}	$\sigma_{\text{n,2n}}$	Total
1	19.6	0.07	0.01	0.01	—	0.10	—	0.12
2	6.07	0.01	0.07	0.05	0.10	0.91	—	0.92
3	2.23	0.01	0.07	0.05	0.10	0.61	—	0.62
4	1.35	0.02	0.10	0.04	0.10	0.11	—	0.19
5	4.98e-1	0.02	0.04	0.01	0.04	—	—	0.06
6	1.83e-1	0.04	0.06	0.01	0.04	0.01	—	0.08
7	6.74e-2	0.06	0.02	0.01	0.04	—	—	0.08
8	2.48e-2	0.26	0.01	—	0.04	—	—	0.26
9	9.12e-3	0.14	0.03	0.01	0.07	—	—	0.16
10	2.03e-3	0.06	0.04	—	0.02	—	—	0.08
11	4.54e-4	0.01	0.01	—	0.01	—	—	0.01
12	2.26e-5	—	—	—	0.01	—	—	0.01
13	4.00e-6	—	0.01	—	—	—	—	0.01
14	5.40e-7	—	—	—	0.01	—	—	0.01
15	1.00e-7	—	—	—	—	—	—	—
Total		0.32	0.17	0.08	0.20	1.10	—	1.18

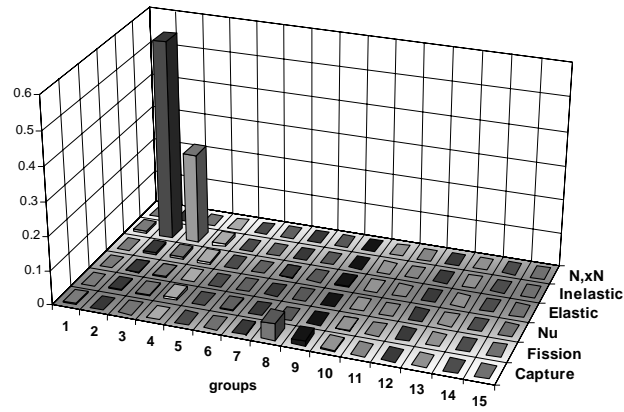


Table 66. GFR power peak: BOLNA full uncertainty (%) by group

Gr.	[MeV]	σ_{cap}	σ_{fiss}	ν	σ_{el}	σ_{inel}	$\sigma_{\text{n,2n}}$	Total
1	19.6	0.07	0.02	0.02	0.03	0.19	—	0.21
2	6.07	0.02	0.11	0.07	0.13	1.17	—	1.19
3	2.23	0.02	0.13	0.07	0.16	0.94	—	0.96
4	1.35	0.04	0.16	0.06	0.20	0.40	—	0.48
5	4.98e-1	0.05	0.09	0.02	0.08	0.02	—	0.13
6	1.83e-1	0.08	0.10	0.02	0.08	0.03	—	0.16
7	6.74e-2	0.10	0.06	0.02	0.07	—	—	0.13
8	2.48e-2	0.28	0.02	0.01	0.07	—	—	0.29
9	9.12e-3	0.17	0.04	0.01	0.09	—	—	0.20
10	2.03e-3	0.11	0.04	—	0.04	—	—	0.12
11	4.54e-4	0.03	0.01	0.01	0.02	—	—	0.04
12	2.26e-5	—	—	—	0.03i	—	—	0.03i
13	4.00e-6	—	—	—	0.01i	—	—	0.01i
14	5.40e-7	—	—	—	0.02i	—	—	0.02i
15	1.00e-7	—	—	—	0.01i	—	—	0.01i
Total		0.38	0.28	0.12	0.34	1.57	—	1.68

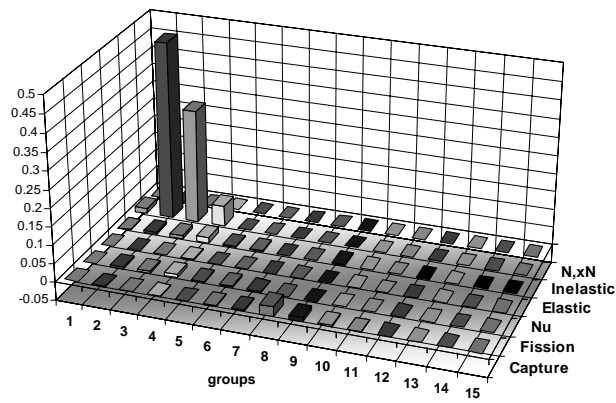


Table 67. GFR power peak: BOLNA diagonal uncertainty (%) by isotope

Isotope	σ_{cap}	σ_{fiss}	ν	σ_{el}	σ_{inel}	$\sigma_{\text{n,2n}}$	Total
²³⁵ U	0.02	0.02	0.01	—	—	—	0.03
²³⁸ U	0.29	0.02	0.06	0.03	1.08	—	1.12
²³⁸ Pu	—	0.04	0.02	—	—	—	0.04
²³⁹ Pu	0.04	0.02	0.01	—	0.01	—	0.05
²⁴⁰ Pu	0.03	0.05	0.04	—	0.01	—	0.07
²⁴¹ Pu	0.01	0.09	—	—	—	—	0.09
²⁴² Pu	0.03	0.05	0.01	—	—	—	0.06
²³⁷ Np	0.02	0.01	—	—	0.01	—	0.03
²⁴¹ Am	0.10	0.08	0.02	—	0.02	—	0.13
^{242m} Am	—	0.01	—	—	—	—	0.01
²⁴³ Am	0.02	0.02	—	—	0.01	—	0.03
²⁴² Cm	—	—	—	—	—	—	—
²⁴³ Cm	—	—	—	—	—	—	—
²⁴⁴ Cm	—	0.05	0.01	—	—	—	0.06
²⁴⁵ Cm	—	0.05	0.01	—	—	—	0.05
²⁴⁶ Cm	—	—	—	—	—	—	—
C	0.01	—	—	0.16	0.06	—	0.17
⁴ He	—	—	—	0.01	—	—	0.01
²⁸ Si	0.07	—	—	0.04	0.21	—	0.23
⁹⁰ Zr	0.05	—	—	0.11	0.02	—	0.12
Total	0.32	0.17	0.08	0.20	1.10	—	1.18

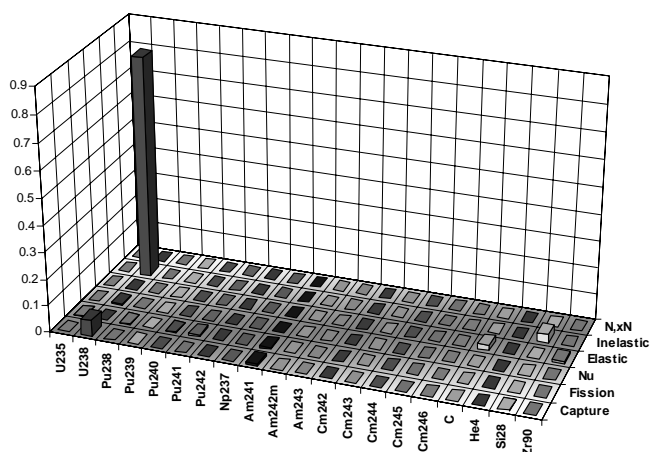


Table 68. GFR power peak: BOLNA full uncertainty (%) by isotope

Isotope	σ_{cap}	σ_{fiss}	ν	σ_{el}	σ_{inel}	$\sigma_{\text{n,2n}}$	Total
²³⁵ U	0.30	0.02	0.09	0.08i	1.54	—	1.57
²³⁸ U	0.01	0.06	0.03	—	—	—	0.07
²³⁸ Pu	0.06	0.03	0.01	0.01	0.01	—	0.07
²³⁹ Pu	0.06	0.08	0.06	—	—	—	0.12
²⁴⁰ Pu	0.02	0.16	0.01	—	—	—	0.16
²⁴¹ Pu	0.05	0.08	0.02	—	—	—	0.09
²⁴² Pu	0.03	0.03	0.01	—	0.01	—	0.04
²³⁷ Np	0.17	0.13	0.03	0.01	0.03	—	0.22
²⁴¹ Am	—	0.01	—	—	—	—	0.01
^{242m} Am	0.04	0.02	0.01	—	0.01	—	0.05
²⁴³ Am	—	—	—	—	—	—	—
²⁴² Cm	—	0.01	—	—	—	—	0.01
²⁴³ Cm	0.01	0.08	0.02	—	—	—	0.09
²⁴⁴ Cm	—	0.10	0.02	—	—	—	0.10
²⁴⁵ Cm	—	—	—	—	—	—	—
²⁴⁶ Cm	0.01	—	—	0.28	0.08	—	0.29
C	—	—	—	0.01	—	—	0.01
⁴ He	0.07	—	—	0.07	0.25	—	0.27
²⁸ Si	0.05	—	—	0.20	0.01	—	0.20
⁹⁰ Zr	0.38	0.28	0.12	0.34	1.57	—	1.68
Total	0.50	0.40	0.19	1.08	1.25	0.02	1.78

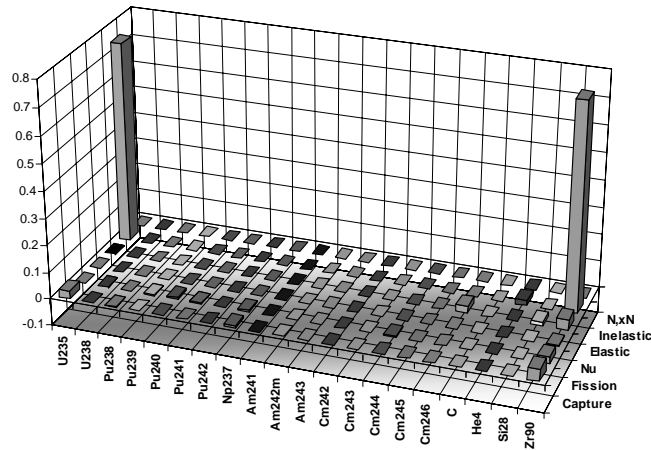


Table 69. GFR Doppler: BOLNA diagonal uncertainty (%) by group

Gr.	[MeV]	σ_{cap}	σ_{fiss}	ν	σ_{el}	σ_{inel}	$\sigma_{\text{n,2n}}$	Total
1	19.6	0.21	0.05	0.03	0.01	0.16	0.01	0.27
2	6.07	0.02	0.32	0.19	0.10	1.92	—	1.96
3	2.23	0.02	0.37	0.17	0.21	1.76	—	1.82
4	1.35	0.03	0.59	0.22	0.49	0.62	—	1.02
5	4.98e-1	0.01	0.37	0.07	0.44	0.05	—	0.58
6	1.83e-1	0.03	0.72	0.09	0.45	0.20	—	0.88
7	6.74e-2	0.08	0.34	0.08	0.51	0.04	—	0.62
8	2.48e-2	0.27	0.38	0.06	0.50	0.04	—	0.68
9	9.12e-3	0.92	0.34	0.03	0.49	—	—	1.10
10	2.03e-3	0.69	0.34	0.06	0.10	—	—	0.78
11	4.54e-4	0.29	1.00	0.06	0.03	—	—	1.05
12	2.26e-5	—	—	—	—	—	—	—
13	4.00e-6	—	—	—	—	—	—	—
14	5.40e-7	—	—	—	—	—	—	—
15	1.00e-7	—	—	—	—	—	—	—
Total		1.24	1.66	0.38	1.20	2.69	0.01	3.62

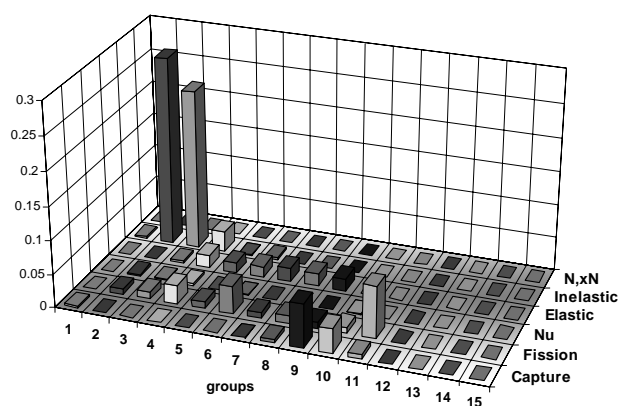


Table 70. GFR Doppler: BOLNA full uncertainty (%) by group

Gr.	[MeV]	σ_{cap}	σ_{fiss}	ν	σ_{el}	σ_{inel}	$\sigma_{\text{n,2n}}$	Total
1	19.6	0.21	0.13	0.07	0.07	0.37	0.01	0.45
2	6.07	0.03	0.55	0.27	0.34	2.74	—	2.83
3	2.23	0.02i	0.78	0.26	0.44	2.60	—	2.76
4	1.35	0.04i	1.03	0.31	0.64	1.53	—	1.97
5	4.98e-1	0.03i	0.83	0.15	0.63	0.16	—	1.06
6	1.83e-1	0.06	1.14	0.14	0.64	0.33	—	1.36
7	6.74e-2	0.20	0.80	0.13	0.87	0.14	—	1.21
8	2.48e-2	0.52	0.58	0.11	0.87	0.10	—	1.18
9	9.12e-3	1.14	0.54	0.09	0.86	—	—	1.53
10	2.03e-3	0.98	0.35	0.06i	0.13	—	—	1.05
11	4.54e-4	0.60	1.00	0.06i	0.07	—	—	1.17
12	2.26e-5	0.01i	0.03	—	0.02i	—	—	0.01
13	4.00e-6	—	0.01	—	0.01i	—	—	0.01i
14	5.40e-7	—	—	—	0.01	—	—	0.01
15	1.00e-7	—	—	—	—	—	—	—
Total		1.72	2.52	0.56	1.95	4.11	0.01	5.51

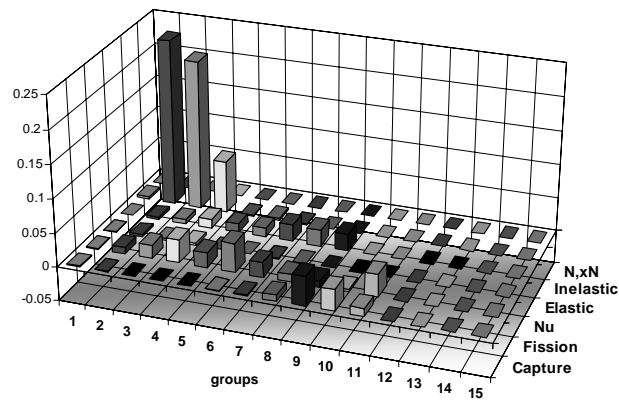


Table 71. GFR Doppler: BOLNA diagonal uncertainty (%) by isotope

Isotope	σ_{cap}	σ_{fiss}	ν	σ_{el}	σ_{inel}	$\sigma_{\text{n,2n}}$	Total
²³⁵ U	0.10	0.03	0.02	—	0.01	—	0.11
²³⁸ U	0.60	0.08	0.21	0.03	2.63	0.01	2.70
²³⁸ Pu	0.05	0.28	0.12	—	0.01	—	0.31
²³⁹ Pu	0.67	0.29	0.13	—	0.14	—	0.76
²⁴⁰ Pu	0.10	0.33	0.23	—	0.06	—	0.42
²⁴¹ Pu	0.11	1.47	0.04	—	0.02	—	1.47
²⁴² Pu	0.32	0.34	0.06	—	0.05	—	0.47
²³⁷ Np	0.15	0.06	0.01	—	0.03	—	0.16
²⁴¹ Am	0.70	0.36	0.07	0.01	0.07	—	0.79
^{242m} Am	—	0.02	—	—	—	—	0.02
²⁴³ Am	0.16	0.06	0.01	—	0.03	—	0.18
²⁴² Cm	—	—	—	—	—	—	—
²⁴³ Cm	—	0.01	—	—	—	—	0.01
²⁴⁴ Cm	0.02	0.20	0.04	—	0.01	—	0.21
²⁴⁵ Cm	—	0.14	0.02	—	—	—	0.14
²⁴⁶ Cm	—	—	—	—	—	—	—
C	0.02	—	—	1.19	0.10	—	1.20
⁴ He	—	—	—	0.03	—	—	0.03
²⁸ Si	0.21	—	—	0.16	0.55	—	0.61
⁹⁰ Zr	0.02	—	—	0.04	0.01	—	0.05
Total	1.24	1.66	0.38	1.20	2.69	0.01	3.62

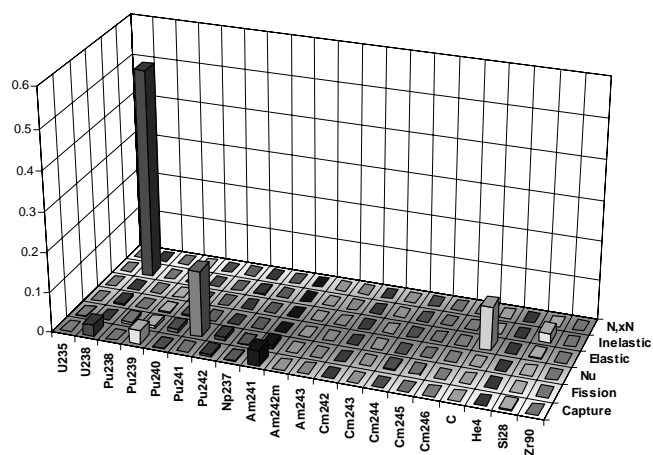


Table 72. GFR Doppler: BOLNA full uncertainty (%) by isotope

Isotope	σ_{cap}	σ_{fiss}	ν	σ_{el}	σ_{inel}	$\sigma_{\text{n,2n}}$	Total
²³⁵ U	0.13	0.04	—	0.01i	0.01	—	0.14
²³⁸ U	0.70	0.10	0.29	0.26	4.05	0.01	4.13
²³⁸ Pu	0.07	0.49	0.17	—	0.01	—	0.53
²³⁹ Pu	0.71	0.37	0.15	0.04i	0.27	—	0.86
²⁴⁰ Pu	0.14	0.59	0.39	0.01	0.13	—	0.73
²⁴¹ Pu	0.20	2.20	0.01	—	0.04	—	2.21
²⁴² Pu	0.43	0.52	0.08	—	0.08	—	0.68
²³⁷ Np	0.20	0.10	0.02	—	0.06	—	0.24
²⁴¹ Am	1.24	0.56	0.10	0.01	0.08	—	1.37
^{242m} Am	—	0.03	—	—	—	—	0.03
²⁴³ Am	0.28	0.08	0.02	—	0.07	—	0.30
²⁴² Cm	—	—	—	—	—	—	—
²⁴³ Cm	—	0.02	—	—	—	—	0.02
²⁴⁴ Cm	0.03	0.31	0.05	—	0.01	—	0.32
²⁴⁵ Cm	0.01	0.28	—	—	0.01	—	0.28
²⁴⁶ Cm	—	—	—	—	—	—	0.01
C	0.02	—	—	1.90	0.15	—	1.91
⁴ He	—	—	—	0.05	—	—	0.05
²⁸ Si	0.21	—	—	0.33	0.64	—	0.75
⁹⁰ Zr	0.02	—	—	0.07	0.02	—	0.07
Total	1.72	2.52	0.56	1.95	4.11	0.01	5.51

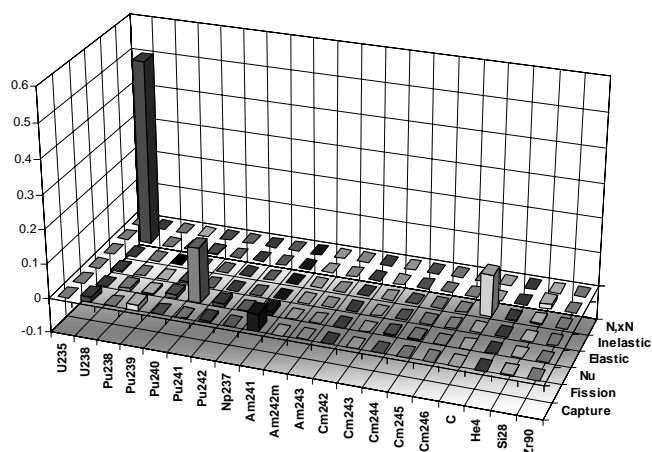


Table 73. GFR void: BOLNA diagonal uncertainties (%) by group

Gr.	[MeV]	σ_{cap}	σ_{fiss}	ν	σ_{el}	σ_{inel}	$\sigma_{\text{n,2n}}$	Total
1	19.6	0.02	0.02	0.01	0.03	0.08	—	0.09
2	6.07	0.01	0.10	0.02	0.49	0.76	—	0.91
3	2.23	0.06	0.11	0.11	1.47	3.14	—	3.48
4	1.35	0.18	0.81	0.42	2.88	1.84	—	3.55
5	4.98e-1	0.04	0.18	0.03	0.38	0.01	—	0.42
6	1.83e-1	0.17	0.62	0.10	0.14	0.01	—	0.66
7	6.74e-2	0.26	0.31	0.10	0.04	—	—	0.42
8	2.48e-2	1.00	0.43	0.09	0.06	—	—	1.09
9	9.12e-3	0.89	0.67	0.16	0.11	—	—	1.13
10	2.03e-3	0.39	0.73	0.08	0.05	—	—	0.83
11	4.54e-4	0.13	0.59	0.04	0.02	—	—	0.60
12	2.26e-5	—	0.01	—	0.01	—	—	0.01
13	4.00e-6	—	0.01	—	—	—	—	0.01
14	5.40e-7	—	—	—	0.01	—	—	0.01
15	1.00e-7	—	—	—	—	—	—	—
Total		1.44	1.64	0.50	3.30	3.72	—	5.46

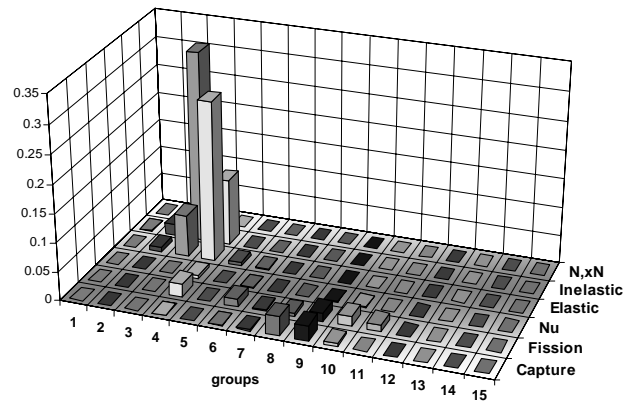


Table 74. GFR void: BOLNA full uncertainties (%) by group

Gr.	[MeV]	σ_{cap}	σ_{fiss}	ν	σ_{el}	σ_{inel}	$\sigma_{\text{n,2n}}$	Total
1	19.6	0.02	0.02	0.01i	0.33	0.14i	—	0.30
2	6.07	0.02i	0.13i	0.05i	1.32	1.94	—	2.34
3	2.23	0.01	0.19	0.14	2.62	4.08	—	4.86
4	1.35	0.05i	0.54	0.31	3.63	3.06	—	4.79
5	4.98e-1	0.12	0.29	0.01	0.43	0.09	—	0.54
6	1.83e-1	0.30	0.63	0.09	0.24	0.09i	—	0.74
7	6.74e-2	0.45	0.61	0.10	0.08i	0.02	—	0.76
8	2.48e-2	1.13	0.72	0.11	0.11	0.04	—	1.35
9	9.12e-3	1.07	0.91	0.17	0.14	—	—	1.42
10	2.03e-3	0.61	0.75	0.06	0.07	—	—	0.97
11	4.54e-4	0.32	0.60	0.06	0.04	—	—	0.68
12	2.26e-5	0.02	0.04	0.01	0.03i	—	—	0.04
13	4.00e-6	—	0.04	—	0.01i	—	—	0.04
14	5.40e-7	—	0.01	—	0.03i	—	—	0.02i
15	1.00e-7	—	0.01	—	0.01i	—	—	—
Total		1.78	1.86	0.43	4.71	5.46	—	7.67

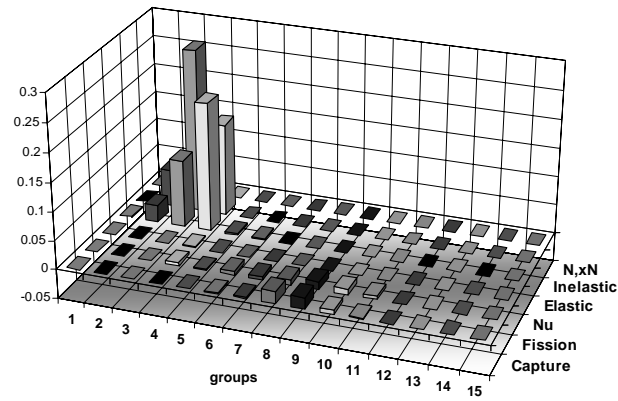


Table 75. GFR void: BOLNA diagonal uncertainties (%) by isotope

Isotope	σ_{cap}	σ_{fiss}	ν	σ_{el}	σ_{inel}	$\sigma_{\text{n,2n}}$	Total
²³⁵ U	0.09	0.05	0.02	—	0.01	—	0.11
²³⁸ U	1.13	0.04	0.09	0.04	3.66	—	3.83
²³⁸ Pu	0.04	0.26	0.18	—	0.01	—	0.31
²³⁹ Pu	0.66	0.32	0.22	—	0.23	—	0.80
²⁴⁰ Pu	0.19	0.38	0.38	—	0.07	—	0.57
²⁴¹ Pu	0.08	1.42	0.04	—	0.03	—	1.43
²⁴² Pu	0.33	0.38	0.10	—	0.12	—	0.53
²³⁷ Np	0.09	0.06	0.01	—	0.05	—	0.12
²⁴¹ Am	0.45	0.32	0.06	—	0.12	—	0.57
²⁴² Am	—	0.02	—	—	—	—	0.02
²⁴³ Am	0.10	0.06	0.01	—	0.05	—	0.13
²⁴² Cm	—	—	—	—	—	—	—
²⁴³ Cm	—	0.01	—	—	—	—	0.01
²⁴⁴ Cm	0.02	0.28	0.05	—	0.01	—	0.28
²⁴⁵ Cm	—	0.14	0.02	—	0.01	—	0.15
²⁴⁶ Cm	—	—	—	—	—	—	—
C	—	—	—	1.59	0.06	—	1.59
⁴ He	—	—	—	2.89	—	—	2.89
²⁸ Si	0.02	—	—	0.16	0.61	—	0.63
⁹⁰ Zr	0.02	—	—	0.06	0.01	—	0.06
Total	1.44	1.64	0.50	3.30	3.72	—	5.46

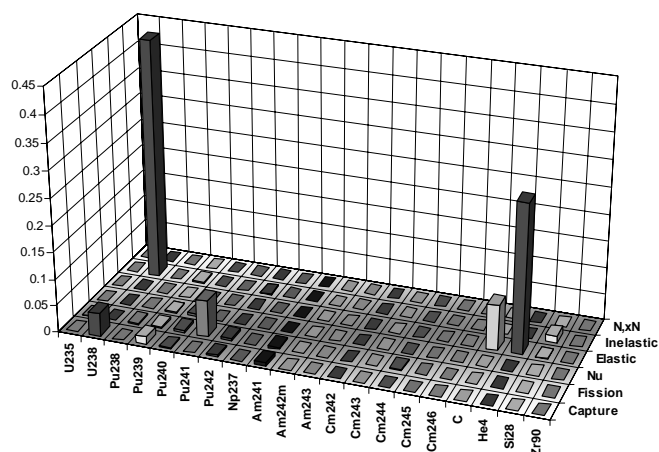


Table 76. GFR void: BOLNA full uncertainties (%) by isotope

Isotope	σ_{cap}	σ_{fiss}	ν	σ_{el}	σ_{inel}	$\sigma_{\text{n,2n}}$	Total
²³⁵ U	0.16	0.05	0.05	0.01i	0.01	—	0.17
²³⁸ U	1.23	0.03	0.08	0.46	5.40	—	5.56
²³⁸ Pu	0.09	0.29	0.12	—	0.02	—	0.32
²³⁹ Pu	0.73	0.39	0.24	0.03i	0.31	—	0.92
²⁴⁰ Pu	0.30	0.33	0.27	—	0.10	—	0.53
²⁴¹ Pu	0.12	1.65	0.09	—	0.04	—	1.66
²⁴² Pu	0.52	0.40	0.10	—	0.16	—	0.68
²³⁷ Np	0.14	0.05	0.01	—	0.06	—	0.16
²⁴¹ Am	0.82	0.34	0.07	—	0.17	—	0.90
^{242m} Am	—	0.03	—	—	—	—	0.03
²⁴³ Am	0.19	0.06	0.02	—	0.08	—	0.21
²⁴² Cm	—	—	—	—	—	—	—
²⁴³ Cm	—	0.01	—	—	—	—	0.01
²⁴⁴ Cm	0.03	0.27	0.05	—	0.01	—	0.27
²⁴⁵ Cm	0.01	0.17	0.05	—	0.01	—	0.17
²⁴⁶ Cm	—	—	—	—	—	—	—
C	—	—	—	1.65	0.05	—	1.65
⁴ He	—	—	—	4.38	—	—	4.38
²⁸ Si	0.02	—	—	0.22	0.61	—	0.65
⁹⁰ Zr	0.02	—	—	0.06	0.02	—	0.07
Total	1.78	1.86	0.43	4.71	5.46	—	7.67

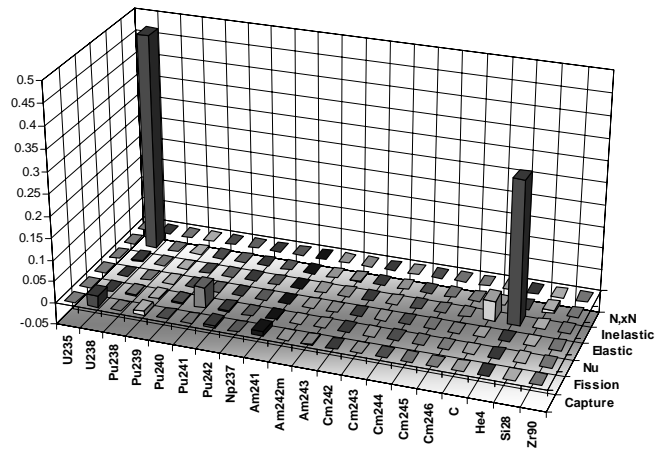


Table 77. GFR XS burn-up: BOLNA diagonal uncertainty (%) by group

Gr.	[MeV]	σ_{cap}	σ_{fiss}	ν	σ_{el}	σ_{inel}	$\sigma_{\text{n,2n}}$	Total
1	19.6	0.24	0.22	0.08	0.01	0.33	0.01	0.47
2	6.07	0.04	2.63	0.84	0.13	3.29	—	4.30
3	2.23	0.07	2.11	0.78	0.29	2.56	—	3.42
4	1.35	0.23	3.64	1.14	0.08	0.41	—	3.84
5	4.98e-1	0.31	2.85	0.58	0.21	0.05	—	2.93
6	1.83e-1	0.63	3.90	0.40	0.14	0.04	—	3.98
7	6.74e-2	0.83	1.98	0.37	0.16	0.01	—	2.19
8	2.48e-2	1.17	2.13	0.33	0.15	0.01	—	2.46
9	9.12e-3	1.17	2.73	0.44	0.15	—	—	3.01
10	2.03e-3	0.74	2.01	0.28	0.11	—	—	2.16
11	4.54e-4	0.20	1.14	0.07	0.01	—	—	1.16
12	2.26e-5	0.01	0.01	—	0.01	—	—	0.02
13	4.00e-6	—	0.01	—	—	—	—	0.01
14	5.40e-7	—	—	—	0.01	—	—	0.01
15	1.00e-7	—	—	—	—	—	—	—
Total		2.16	8.32	1.91	0.50	4.20	0.01	9.77

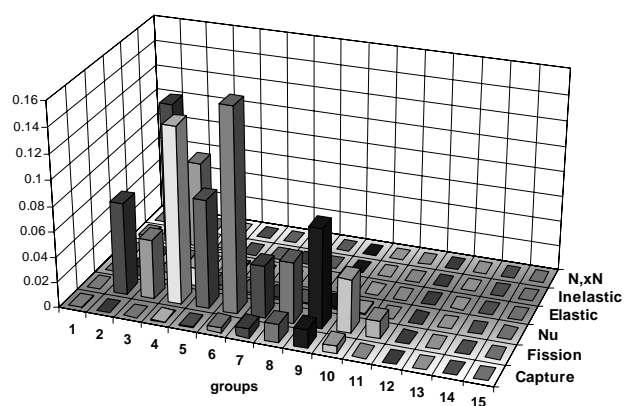


Table 78. GFR XS burn-up: BOLNA full uncertainty (%) by group

Gr.	[MeV]	σ_{cap}	σ_{fiss}	ν	σ_{el}	σ_{inel}	$\sigma_{\text{n,2n}}$	Total
1	19.6	0.24	0.82	0.18	0.09	0.66	0.01	1.10
2	6.07	0.14	4.32	1.25	0.42	4.38	—	6.30
3	2.23	0.18	4.63	1.29	0.39	3.80	—	6.15
4	1.35	0.44	6.51	2.07	0.21	1.46	—	7.00
5	4.98e-1	0.71	5.81	1.45	0.28	0.09	—	6.04
6	1.83e-1	1.11	6.51	1.20	0.22	0.02i	—	6.72
7	6.74e-2	1.39	4.84	1.15	0.27	0.02i	—	5.17
8	2.48e-2	1.73	3.78	1.08	0.25	0.03	—	4.30
9	9.12e-3	1.80	4.07	1.25	0.25	—	—	4.63
10	2.03e-3	1.37	2.44	1.01	0.11	—	—	2.98
11	4.54e-4	0.68	1.17	0.47	0.02i	—	—	1.43
12	2.26e-5	0.02	0.08	0.03	0.03i	—	—	0.08
13	4.00e-6	—	0.08	0.02	—	—	—	0.09
14	5.40e-7	—	0.02	0.01	0.02i	—	—	0.01i
15	1.00e-7	—	0.02	0.01	0.01i	—	—	0.02
Total		3.54	14.86	4.05	0.84	6.02	0.01	16.94

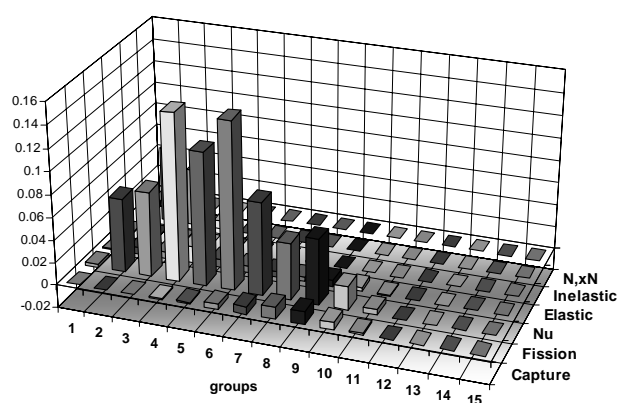


Table 79. GFR XS burn-up: BOLNA diagonal uncertainty (%) by isotope

Isotope	σ_{cap}	σ_{fiss}	ν	σ_{el}	σ_{inel}	$\sigma_{\text{n,2n}}$	Total
²³⁵ U	0.48	0.25	0.13	—	0.03	—	0.56
²³⁸ U	1.02	0.13	0.38	0.02	4.17	0.01	4.31
²³⁸ Pu	0.35	2.49	1.35	—	0.05	—	2.86
²³⁹ Pu	0.46	0.14	0.14	—	0.08	—	0.51
²⁴⁰ Pu	0.04	0.29	0.19	—	0.04	—	0.35
²⁴¹ Pu	0.26	5.97	0.16	—	0.10	—	5.97
²⁴² Pu	0.41	0.73	0.14	—	0.07	—	0.85
²³⁷ Np	0.29	0.30	0.08	—	0.08	—	0.43
²⁴¹ Am	1.55	1.92	0.43	0.01	0.26	—	2.52
^{242m} Am	0.15	2.50	0.16	—	0.06	—	2.52
²⁴³ Am	0.18	0.19	0.05	—	0.05	—	0.27
²⁴² Cm	0.40	3.62	1.07	—	0.06	—	3.79
²⁴³ Cm	0.01	0.26	0.01	—	—	—	0.26
²⁴⁴ Cm	0.17	1.85	0.43	—	0.04	—	1.90
²⁴⁵ Cm	—	0.24	0.03	—	—	—	0.24
²⁴⁶ Cm	0.01	0.02	—	—	—	—	0.02
C	0.02	—	—	0.49	0.14	—	0.51
⁴ He	—	—	—	0.02	—	—	0.02
²⁸ Si	0.24	—	—	0.06	0.44	—	0.51
⁹⁰ Zr	0.04	—	—	0.09	0.01	—	0.09
Total	2.16	8.32	1.91	0.50	4.20	0.01	9.77

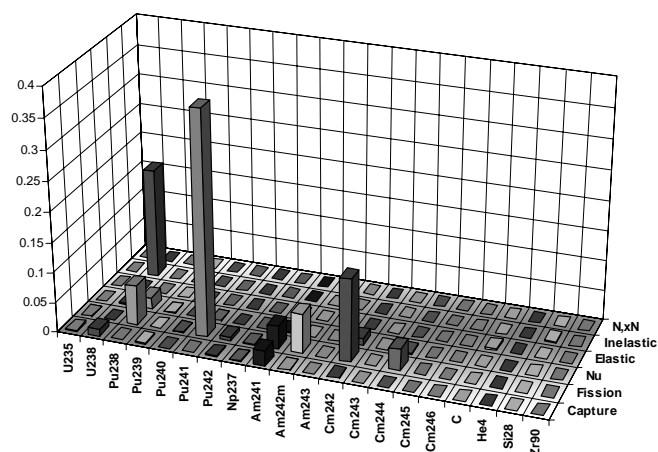


Table 80. GFR XS burn-up: BOLNA full uncertainty (%) by isotope

Isotope	σ_{cap}	σ_{fiss}	ν	σ_{el}	σ_{inel}	$\sigma_{\text{n,2n}}$	Total
²³⁵ U	0.96	0.26	0.35	0.03i	0.05	—	1.06
²³⁸ U	1.12	0.17	0.54	0.35	5.97	0.01	6.11
²³⁸ Pu	0.71	4.53	3.36	—	0.08	—	5.69
²³⁹ Pu	0.59	0.19	0.16	0.02i	0.14	—	0.65
²⁴⁰ Pu	0.09	0.50	0.33	—	0.04	—	0.60
²⁴¹ Pu	0.53	10.48	0.47	—	0.15	—	10.51
²⁴² Pu	0.68	1.13	0.21	—	0.10	—	1.34
²³⁷ Np	0.53	0.52	0.11	—	0.14	—	0.77
²⁴¹ Am	2.79	2.99	0.60	0.01	0.39	—	4.15
^{242m} Am	0.28	4.88	0.45	—	0.10	—	4.91
²⁴³ Am	0.33	0.25	0.06	—	0.09	—	0.43
²⁴² Cm	0.63	6.87	1.83	—	0.09	—	7.13
²⁴³ Cm	0.01	0.54	0.04	—	—	—	0.54
²⁴⁴ Cm	0.29	2.84	0.62	—	0.06	—	2.93
²⁴⁵ Cm	0.01	0.49	0.08	—	—	—	0.50
²⁴⁶ Cm	0.01	0.04	0.01	—	—	—	0.04
C	0.02	—	—	0.75	0.19	—	0.77
⁴ He	—	—	—	0.03	—	—	0.03
²⁸ Si	0.25	—	—	0.10	0.52	—	0.59
⁹⁰ Zr	0.04	—	—	0.15	0.01	—	0.15
Total	3.54	14.86	4.05	0.84	6.02	0.01	16.94

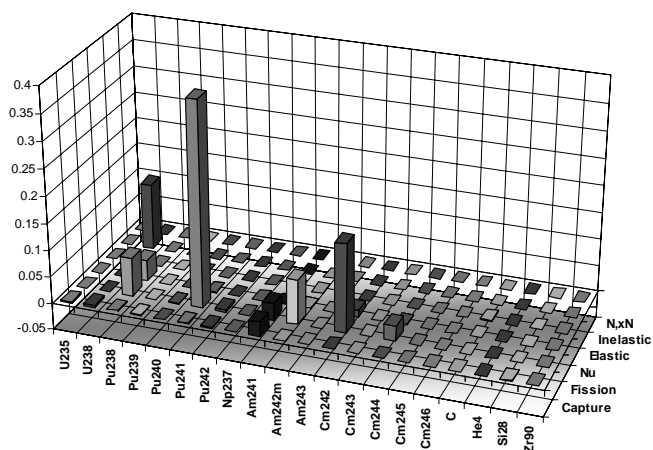


Table 81. LFR k_{eff} : BOLNA diagonal uncertainties (%) by group

Gr.	[MeV]	σ_{cap}	σ_{fiss}	ν	σ_{el}	σ_{inel}	$\sigma_{\text{n,2n}}$	Total
1	19.6	0.01	0.01	0.01	—	0.04	—	0.04
2	6.07	0.01	0.07	0.06	0.01	0.22	—	0.24
3	2.23	0.02	0.11	0.07	0.02	0.36	—	0.39
4	1.35	0.09	0.30	0.20	0.09	0.27	—	0.47
5	4.98e-1	0.24	0.24	0.10	0.04	0.04	—	0.36
6	1.83e-1	0.20	0.27	0.09	0.01	0.08	—	0.36
7	6.74e-2	0.15	0.10	0.05	0.01	0.01	—	0.19
8	2.48e-2	0.22	0.09	0.03	0.01	—	—	0.24
9	9.12e-3	0.06	0.03	0.01	—	—	—	0.07
10	2.03e-3	0.02	0.01	—	—	—	—	0.02
11	4.54e-4	—	0.01	—	0.01	—	—	0.01
12	2.26e-5	—	—	—	—	—	—	—
13	4.00e-6	—	—	—	—	—	—	—
14	5.40e-7	—	—	—	—	—	—	—
15	1.00e-7	—	—	—	—	—	—	—
Total		0.42	0.51	0.26	0.10	0.51	—	0.88

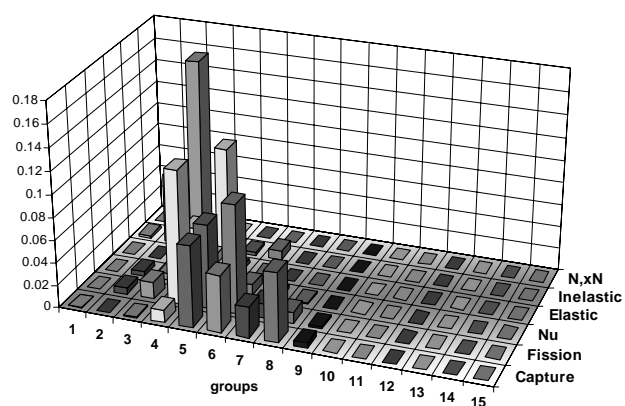


Table 82. LFR k_{eff} : BOLNA full uncertainties (%) by group

Gr.	[MeV]	σ_{cap}	σ_{fiss}	ν	σ_{el}	σ_{inel}	$\sigma_{\text{n,2n}}$	Total
1	19.6	0.01	0.04	0.02	—	0.07	—	0.09
2	6.07	0.04	0.17	0.11	0.04	0.39	—	0.44
3	2.23	0.06	0.26	0.12	0.06	0.52	—	0.60
4	1.35	0.15	0.47	0.28	0.12	0.45	—	0.73
5	4.98e-1	0.34	0.43	0.19	0.07	0.10	—	0.59
6	1.83e-1	0.32	0.43	0.15	0.02	0.13	—	0.57
7	6.74e-2	0.23	0.25	0.11	0.01i	0.04	—	0.36
8	2.48e-2	0.27	0.14	0.08	0.02	0.01	—	0.31
9	9.12e-3	0.11	0.08	0.05	—	—	—	0.14
10	2.03e-3	0.02	0.02	0.03	0.01i	—	—	0.04
11	4.54e-4	0.01	0.01	0.01	0.01i	—	—	0.01
12	2.26e-5	0.01	—	—	—	—	—	0.01
13	4.00e-6	—	—	—	—	—	—	—
14	5.40e-7	—	—	—	—	—	—	—
15	1.00e-7	—	—	—	—	—	—	—
Total		0.62	0.88	0.43	0.16	0.81	—	1.43

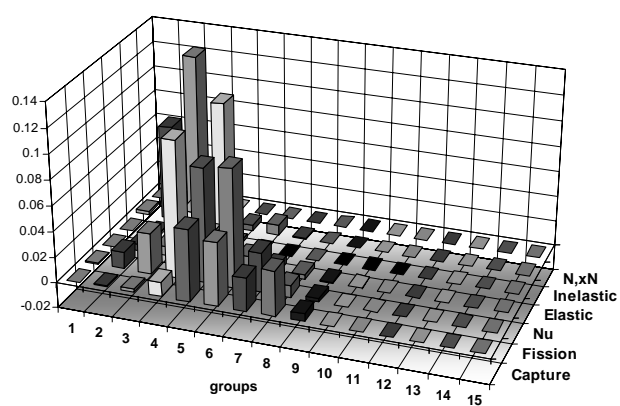


Table 83. LFR k_{eff} : BOLNA diagonal uncertainties (%) by isotope

Isotope	σ_{cap}	σ_{fiss}	ν	σ_{el}	σ_{inel}	$\sigma_{\text{n,2n}}$	Total
²³⁵ U	—	—	—	—	—	—	0.01
²³⁸ U	0.22	0.02	0.07	0.01	0.44	—	0.50
²³⁸ Pu	0.02	0.20	0.11	—	—	—	0.23
²³⁹ Pu	0.10	0.15	0.10	—	0.05	—	0.21
²⁴⁰ Pu	0.12	0.21	0.20	—	0.03	—	0.32
²⁴¹ Pu	0.02	0.33	0.01	—	—	—	0.33
²⁴² Pu	0.05	0.12	0.03	—	0.01	—	0.13
²³⁷ Np	0.01	0.02	—	—	0.01	—	0.02
²⁴¹ Am	0.03	0.04	0.01	—	0.01	—	0.05
^{242m} Am	—	0.04	—	—	—	—	0.04
²⁴³ Am	0.01	0.01	—	—	0.01	—	0.02
²⁴² Cm	—	0.01	—	—	—	—	0.01
²⁴³ Cm	—	—	—	—	—	—	—
²⁴⁴ Cm	0.01	0.11	0.02	—	—	—	0.11
²⁴⁵ Cm	—	0.11	0.01	—	—	—	0.11
²⁴⁶ Cm	—	0.01	—	—	—	—	0.01
⁵⁶ Fe	0.04	—	—	0.01	0.16	—	0.17
⁵² Cr	—	—	—	0.01	—	—	0.01
⁵⁸ Ni	—	—	—	—	—	—	—
⁹⁰ Zr	0.01	—	—	0.01	0.04	—	0.04
²⁰⁴ Pb	0.01	—	—	—	0.01	—	0.01
²⁰⁶ Pb	0.04	—	—	0.02	0.13	—	0.14
²⁰⁷ Pb	0.02	—	—	0.02	0.12	—	0.12
²⁰⁸ Pb	0.01	—	—	0.09	0.05	—	0.10
¹⁰ B	0.31	—	—	0.02	—	—	0.31
Total	0.42	0.51	0.26	0.10	0.51	—	0.88

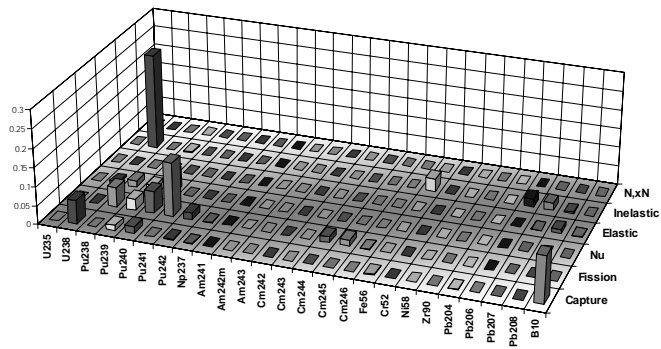


Table 84. LFR k_{eff} : BOLNA full uncertainties (%) by isotope

Isotope	σ_{cap}	σ_{fiss}	ν	σ_{el}	σ_{inel}	$\sigma_{\text{n,2n}}$	Total
²³⁵ U	0.01	—	—	—	—	—	0.01
²³⁸ U	0.25	0.03	0.09	0.07	0.73	—	0.78
²³⁸ Pu	0.03	0.34	0.23	—	0.01	—	0.42
²³⁹ Pu	0.17	0.21	0.12	0.01	0.10	—	0.31
²⁴⁰ Pu	0.27	0.35	0.33	—	0.06	—	0.56
²⁴¹ Pu	0.03	0.61	0.02	—	0.01	—	0.61
²⁴² Pu	0.08	0.17	0.04	—	0.02	—	0.19
²³⁷ Np	0.02	0.03	—	—	0.02	—	0.04
²⁴¹ Am	0.05	0.06	0.01	—	0.01	—	0.08
^{242m} Am	—	0.07	—	—	—	—	0.07
²⁴³ Am	0.02	0.02	—	—	0.02	—	0.03
²⁴² Cm	—	0.02	—	—	—	—	0.02
²⁴³ Cm	—	0.01	—	—	—	—	0.01
²⁴⁴ Cm	0.02	0.16	0.03	—	—	—	0.16
²⁴⁵ Cm	—	0.22	0.03	—	—	—	0.22
²⁴⁶ Cm	—	0.02	—	—	—	—	0.02
⁵⁶ Fe	0.05	—	—	0.02	0.24	—	0.25
⁵² Cr	—	—	—	0.01	—	—	0.01
⁵⁸ Ni	—	—	—	—	—	—	—
⁹⁰ Zr	0.01	—	—	0.01	0.04	—	0.04
²⁰⁴ Pb	0.03	—	—	—	0.01	—	0.03
²⁰⁶ Pb	0.09	—	—	0.03	0.18	—	0.20
²⁰⁷ Pb	0.05	—	—	0.02	0.16	—	0.17
²⁰⁸ Pb	0.02	—	—	0.13	0.05	—	0.14
¹⁰ B	0.44	—	—	0.03	—	—	0.44
Total	0.62	0.88	0.43	0.16	0.81	—	1.43

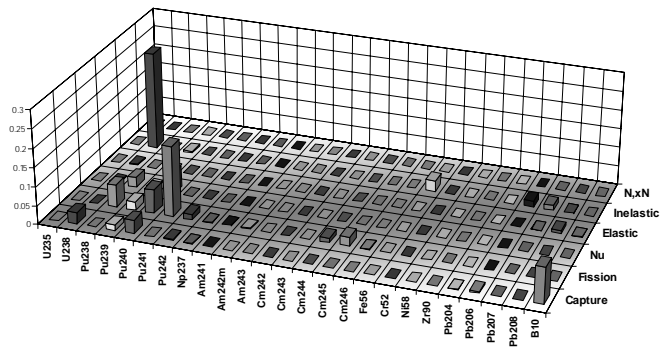


Table 85. LFR power peak: BOLNA diagonal uncertainty (%) by group

Gr.	[MeV]	σ_{cap}	σ_{fiss}	ν	σ_{el}	σ_{inel}	$\sigma_{\text{n,2n}}$	Total
1	19.6	—	—	—	—	—	—	—
2	6.07	0.01	0.01	0.01	0.01	0.01	—	0.02
3	2.23	0.02	0.01	0.01	0.03	0.03	—	0.04
4	1.35	0.08	0.02	0.01	0.13	0.12	—	0.19
5	4.98e-1	0.27	—	—	0.09	0.03	—	0.29
6	1.83e-1	0.22	0.02	—	0.03	0.02	—	0.22
7	6.74e-2	0.15	0.01	—	0.01	—	—	0.15
8	2.48e-2	0.09	0.01	—	0.02	—	—	0.09
9	9.12e-3	0.04	—	—	0.01	—	—	0.04
10	2.03e-3	0.04	0.01	—	0.01	—	—	0.04
11	4.54e-4	0.01	—	—	0.01	—	—	0.02
12	2.26e-5	—	—	—	0.01	—	—	0.01
13	4.00e-6	—	—	—	—	—	—	—
14	5.40e-7	—	—	—	—	—	—	—
15	1.00e-7	—	—	—	—	—	—	—
Total		0.40	0.03	0.01	0.17	0.12	—	0.45

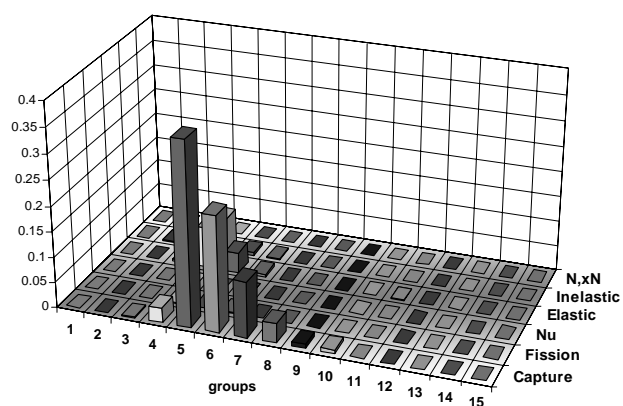


Table 86. LFR power peak: BOLNA full uncertainty (%) by group

Gr.	[MeV]	σ_{cap}	σ_{fiss}	ν	σ_{el}	σ_{inel}	$\sigma_{\text{n,2n}}$	Total
1	19.6	0.01	—	—	—	—	—	0.01
2	6.07	0.03	0.01	0.01	0.02	0.01	—	0.04
3	2.23	0.04	0.02	0.01	0.07	0.04	—	0.09
4	1.35	0.09	0.02	0.01	0.17	0.10	—	0.22
5	4.98e-1	0.36	0.01	—	0.14	0.05	—	0.39
6	1.83e-1	0.32	0.01	—	0.07	0.04	—	0.33
7	6.74e-2	0.20	0.01	—	0.03	0.01	—	0.21
8	2.48e-2	0.16	0.01	—	0.03i	—	—	0.15
9	9.12e-3	0.10	0.01	—	0.02i	—	—	0.10
10	2.03e-3	0.05	0.01	—	0.03i	—	—	0.04
11	4.54e-4	0.03	—	—	0.03	—	—	0.04
12	2.26e-5	0.02	—	—	0.01	—	—	0.02
13	4.00e-6	0.01	—	—	—	—	—	0.01
14	5.40e-7	0.01	—	—	—	—	—	0.01
15	1.00e-7	—	—	—	—	—	—	—
Total		0.57	0.04	0.02	0.24	0.13	—	0.64

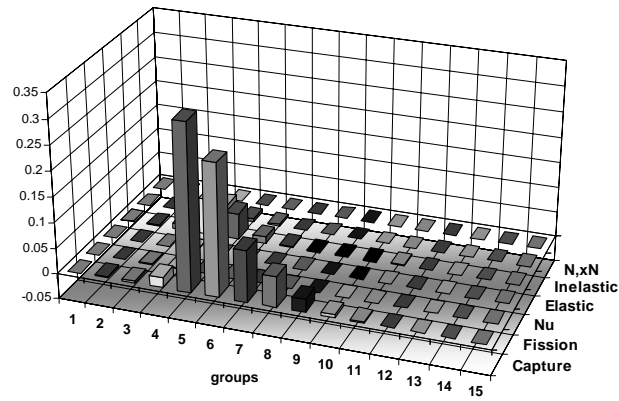


Table 87. LFR power peak: BOLNA diagonal uncertainty (%) by isotope

Isotope	σ_{cap}	σ_{fiss}	ν	σ_{el}	σ_{inel}	$\sigma_{\text{n,2n}}$	Total
²³⁵ U	—	—	—	—	—	—	—
²³⁸ U	0.02	—	0.01	0.05	0.10	—	0.11
²³⁸ Pu	—	0.01	0.01	—	—	—	0.01
²³⁹ Pu	0.01	0.01	0.01	0.01	0.03	—	0.03
²⁴⁰ Pu	—	0.02	0.01	0.01	0.01	—	0.02
²⁴¹ Pu	—	0.02	—	—	—	—	0.02
²⁴² Pu	—	0.01	—	—	0.01	—	0.01
²³⁷ Np	—	—	—	—	—	—	—
²⁴¹ Am	—	—	—	—	—	—	0.01
^{242m} Am	—	—	—	—	—	—	—
²⁴³ Am	—	—	—	—	—	—	—
²⁴² Cm	—	—	—	—	—	—	—
²⁴³ Cm	—	—	—	—	—	—	—
²⁴⁴ Cm	—	0.01	—	—	—	—	0.01
²⁴⁵ Cm	—	0.01	—	—	—	—	0.01
²⁴⁶ Cm	—	—	—	—	—	—	—
⁵⁶ Fe	0.04	—	—	0.02	0.04	—	0.06
⁵² Cr	—	—	—	0.01	—	—	0.01
⁵⁸ Ni	—	—	—	—	—	—	—
⁹⁰ Zr	—	—	—	0.02	—	—	0.02
²⁰⁴ Pb	0.01	—	—	—	—	—	0.01
²⁰⁶ Pb	0.02	—	—	0.04	0.03	—	0.05
²⁰⁷ Pb	0.01	—	—	0.04	0.04	—	0.06
²⁰⁸ Pb	—	—	—	0.14	—	—	0.14
¹⁰ B	0.40	—	—	0.03	—	—	0.40
Total	0.40	0.03	0.01	0.17	0.12	—	0.45

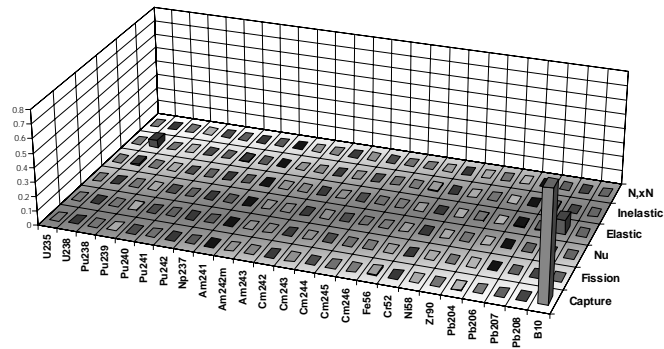


Table 88. LFR power peak: BOLNA full uncertainty (%) by isotope

Isotope	σ_{cap}	σ_{fiss}	ν	σ_{el}	σ_{inel}	$\sigma_{\text{n,2n}}$	Total
²³⁵ U	—	—	—	—	—	—	—
²³⁸ U	0.02	—	0.01	0.04i	0.09	—	0.08
²³⁸ Pu	—	0.02	—	—	—	—	0.02
²³⁹ Pu	0.01	0.01	0.01	0.02	0.04	—	0.05
²⁴⁰ Pu	—	0.02	0.01	0.01	0.02	—	0.03
²⁴¹ Pu	—	0.02	—	—	—	—	0.02
²⁴² Pu	—	0.01	—	—	0.01	—	0.02
²³⁷ Np	—	—	—	—	0.01	—	0.01
²⁴¹ Am	—	0.01	—	—	—	—	0.01
^{242m} Am	—	—	—	—	—	—	—
²⁴³ Am	—	—	—	—	0.01	—	0.01
²⁴² Cm	—	—	—	—	—	—	—
²⁴³ Cm	—	—	—	—	—	—	—
²⁴⁴ Cm	—	0.01	—	—	—	—	0.01
²⁴⁵ Cm	—	0.01	—	—	—	—	0.01
²⁴⁶ Cm	—	—	—	—	—	—	—
⁵⁶ Fe	0.06	—	—	0.02	0.05	—	0.08
⁵² Cr	—	—	—	0.01	—	—	0.01
⁵⁸ Ni	—	—	—	—	—	—	—
⁹⁰ Zr	—	—	—	0.04	—	—	0.04
²⁰⁴ Pb	0.02	—	—	—	—	—	0.02
²⁰⁶ Pb	0.04	—	—	0.06	0.04	—	0.08
²⁰⁷ Pb	0.03	—	—	0.05	0.05	—	0.08
²⁰⁸ Pb	0.01	—	—	0.22	—	—	0.22
¹⁰ B	0.57	—	—	0.04	—	—	0.57
Total	0.57	0.04	0.02	0.24	0.13	—	0.64

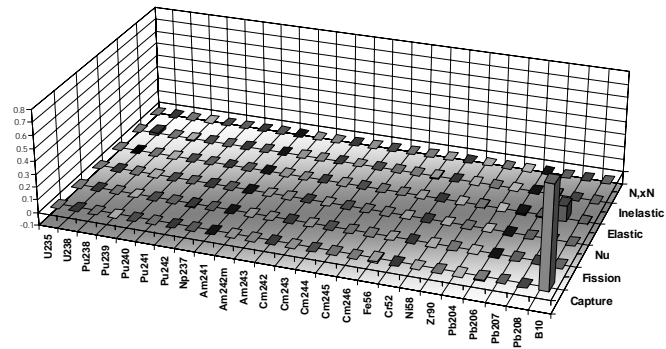


Table 89. LFR Doppler: BOLNA diagonal uncertainty (%) by group

Gr.	[MeV]	σ_{cap}	σ_{fiss}	ν	σ_{el}	σ_{inel}	$\sigma_{\text{n,2n}}$	Total
1	19.6	0.01	0.03	0.01	—	0.09	—	0.09
2	6.07	0.03	0.16	0.12	0.02	0.64	—	0.67
3	2.23	0.04	0.27	0.14	0.02	1.09	—	1.13
4	1.35	0.15	0.74	0.39	0.07	1.08	—	1.38
5	4.98e-1	0.35	0.57	0.18	0.28	0.26	—	0.79
6	1.83e-1	0.31	0.63	0.13	0.30	0.64	—	1.00
7	6.74e-2	0.29	0.22	0.07	0.46	0.16	—	0.62
8	2.48e-2	0.52	0.05	0.01	0.68	0.16	—	0.87
9	9.12e-3	1.07	0.16	0.10	0.38	0.01	—	1.15
10	2.03e-3	0.39	0.34	0.08	0.07	—	—	0.53
11	4.54e-4	0.08	0.21	0.03	0.27	—	—	0.36
12	2.26e-5	0.02	0.01	—	—	—	—	0.02
13	4.00e-6	0.01	—	—	—	—	—	0.01
14	5.40e-7	—	—	—	—	—	—	—
15	1.00e-7	—	—	—	—	—	—	—
Total		1.38	1.26	0.51	1.04	1.82	—	2.85

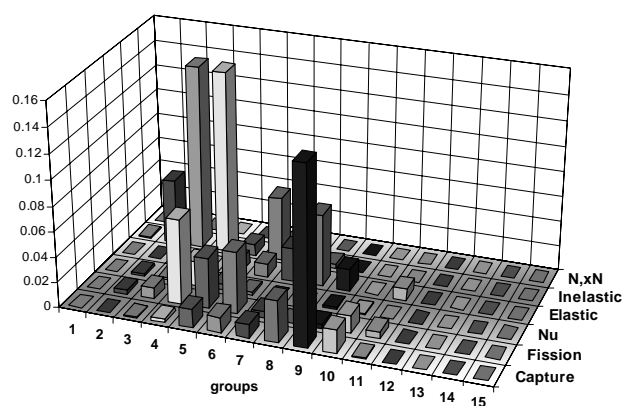


Table 90. LFR Doppler: BOLNA full uncertainty (%) by group

Gr.	[MeV]	σ_{cap}	σ_{fiss}	ν	σ_{el}	σ_{inel}	$\sigma_{\text{n,2n}}$	Total
1	19.6	0.02	0.10	0.04	0.01	0.18	—	0.21
2	6.07	0.07	0.40	0.21	0.05i	1.21	—	1.29
3	2.23	0.07	0.62	0.24	0.09	1.64	—	1.77
4	1.35	0.12	1.13	0.50	0.11	1.70	—	2.10
5	4.98e-1	0.38	1.01	0.31	0.44	0.59	—	1.34
6	1.83e-1	0.43	1.00	0.21	0.63	0.93	—	1.57
7	6.74e-2	0.54	0.52	0.14	0.81	0.44	—	1.20
8	2.48e-2	0.86	0.13	0.03i	1.00	0.31	—	1.36
9	9.12e-3	1.27	0.10	0.08i	0.73	0.01	—	1.47
10	2.03e-3	0.47	0.33	0.15i	0.30i	—	—	0.47
11	4.54e-4	0.20	0.22	0.06i	0.59i	—	—	0.51i
12	2.26e-5	0.09	0.03	0.01i	0.02	—	—	0.09
13	4.00e-6	0.06	0.02	0.01i	0.03i	—	—	0.06
14	5.40e-7	0.02	—	—	0.01	—	—	0.02
15	1.00e-7	—	—	—	0.01	—	—	—
Total		1.81	2.07	0.69	1.54	2.92	—	4.35

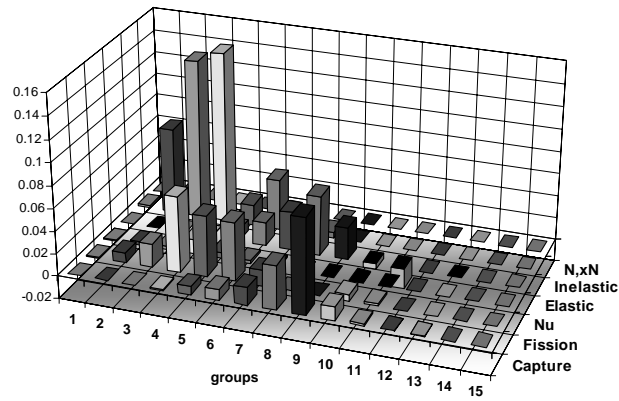


Table 91. LFR Doppler: BOLNA diagonal uncertainty (%) by isotope

Isotope	σ_{cap}	σ_{fiss}	ν	σ_{el}	σ_{inel}	$\sigma_{\text{n,2n}}$	Total
²³⁵ U	0.03	—	—	—	—	—	0.03
²³⁸ U	0.23	0.05	0.13	0.07	1.55	—	1.58
²³⁸ Pu	0.07	0.48	0.22	—	0.02	—	0.53
²³⁹ Pu	0.94	0.38	0.18	0.01	0.29	—	1.07
²⁴⁰ Pu	0.28	0.52	0.40	0.01	0.20	—	0.74
²⁴¹ Pu	0.05	0.85	0.02	—	0.01	—	0.85
²⁴² Pu	0.33	0.29	0.05	—	0.06	—	0.45
²³⁷ Np	0.07	0.04	0.01	—	0.06	—	0.10
²⁴¹ Am	0.15	0.08	0.02	—	0.04	—	0.18
^{242m} Am	0.01	0.09	—	—	—	—	0.09
²⁴³ Am	0.07	0.03	0.01	—	0.05	—	0.09
²⁴² Cm	—	0.02	—	—	—	—	0.03
²⁴³ Cm	—	0.01	—	—	—	—	0.01
²⁴⁴ Cm	0.03	0.26	0.04	—	0.01	—	0.26
²⁴⁵ Cm	—	0.25	0.02	—	0.01	—	0.25
²⁴⁶ Cm	0.02	0.02	—	—	—	—	0.03
⁵⁶ Fe	0.45	—	—	0.34	0.57	—	0.81
⁵² Cr	0.02	—	—	0.14	0.01	—	0.14
⁵⁸ Ni	—	—	—	0.05	—	—	0.05
⁹⁰ Zr	0.02	—	—	0.08	0.10	—	0.13
²⁰⁴ Pb	0.16	—	—	0.02	0.03	—	0.16
²⁰⁶ Pb	0.13	—	—	0.37	0.41	—	0.56
²⁰⁷ Pb	0.06	—	—	0.38	0.48	—	0.62
²⁰⁸ Pb	0.05	—	—	0.80	0.12	—	0.81
¹⁰ B	0.70	—	—	0.11	—	—	0.71
Total	1.38	1.26	0.51	1.04	1.82	—	2.85

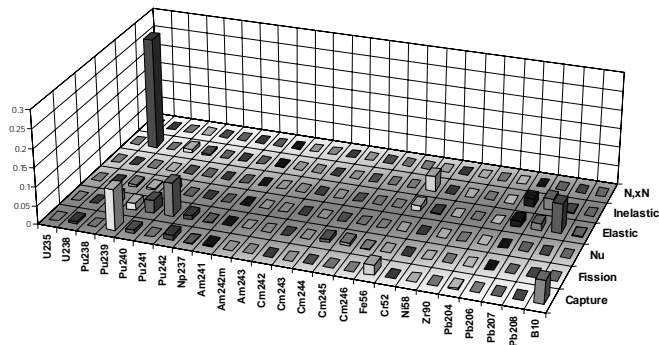


Table 92. LFR Doppler: BOLNA full uncertainty (%) by isotope

Isotope	σ_{cap}	σ_{fiss}	ν	σ_{el}	σ_{inel}	$\sigma_{\text{n,2n}}$	Total
²³⁵ U	0.04	—	—	—	0.01	—	0.04
²³⁸ U	0.25	0.07	0.19	0.21	2.56	—	2.59
²³⁸ Pu	0.14	0.80	0.25	—	0.03	—	0.85
²³⁹ Pu	1.07	0.49	0.19	0.04i	0.62	—	1.35
²⁴⁰ Pu	0.44	0.86	0.58	0.02	0.34	—	1.18
²⁴¹ Pu	0.09	1.44	—	—	0.03	—	1.44
²⁴² Pu	0.53	0.42	0.07	—	0.09	—	0.68
²³⁷ Np	0.11	0.06	0.01	—	0.11	—	0.17
²⁴¹ Am	0.28	0.13	0.02	—	0.04	—	0.31
^{242m} Am	0.01	0.16	—	—	0.01	—	0.16
²⁴³ Am	0.13	0.04	0.01	—	0.10	—	0.17
²⁴² Cm	—	0.04	0.01	—	—	—	0.04
²⁴³ Cm	—	0.02	—	—	—	—	0.02
²⁴⁴ Cm	0.04	0.37	0.05	—	0.02	—	0.38
²⁴⁵ Cm	0.01	0.49	—	—	0.01	—	0.49
²⁴⁶ Cm	0.02	0.04	0.01	—	—	—	0.05
⁵⁶ Fe	0.52	—	—	0.47	0.83	—	1.09
⁵² Cr	0.02	—	—	0.20	0.01	—	0.20
⁵⁸ Ni	—	—	—	0.05	—	—	0.05
⁹⁰ Zr	0.02	—	—	0.11	0.12	—	0.16
²⁰⁴ Pb	0.25	—	—	0.04	0.04	—	0.26
²⁰⁶ Pb	0.27	—	—	0.59	0.59	—	0.88
²⁰⁷ Pb	0.08	—	—	0.60	0.61	—	0.86
²⁰⁸ Pb	0.06	—	—	1.15	0.13	—	1.15
¹⁰ B	1.01	—	—	0.14	—	—	1.02
Total	1.81	2.07	0.69	1.54	2.92	—	4.35

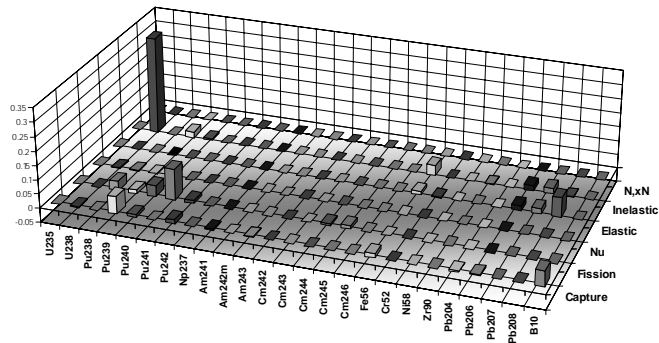


Table 93. LFR void: BOLNA diagonal uncertainties (%) by group

Gr.	[MeV]	σ_{cap}	σ_{fiss}	ν	σ_{el}	σ_{inel}	$\sigma_{\text{n,2n}}$	Total
1	19.6	0.10	0.08	0.06	0.01	0.68	0.03	0.69
2	6.07	0.11	0.32	0.34	0.22	2.90	—	2.95
3	2.23	0.11	0.15	0.13	0.28	2.49	—	2.51
4	1.35	0.35	0.06	0.04	1.30	1.86	—	2.30
5	4.98e-1	0.46	0.52	0.20	0.56	0.15	—	0.93
6	1.83e-1	0.55	0.64	0.19	0.05	0.13	—	0.87
7	6.74e-2	0.62	0.42	0.22	0.06	0.02	—	0.79
8	2.48e-2	1.11	0.43	0.16	0.13	0.01	—	1.21
9	9.12e-3	0.37	0.21	0.09	0.01	—	—	0.43
10	2.03e-3	0.07	0.04	0.01	0.04	—	—	0.09
11	4.54e-4	0.01	0.01	—	0.09	—	—	0.09
12	2.26e-5	—	—	—	—	—	—	0.01
13	4.00e-6	—	—	—	—	—	—	—
14	5.40e-7	—	—	—	—	—	—	—
15	1.00e-7	—	—	—	—	—	—	—
Total		1.56	1.11	0.54	1.47	4.31	0.03	4.97

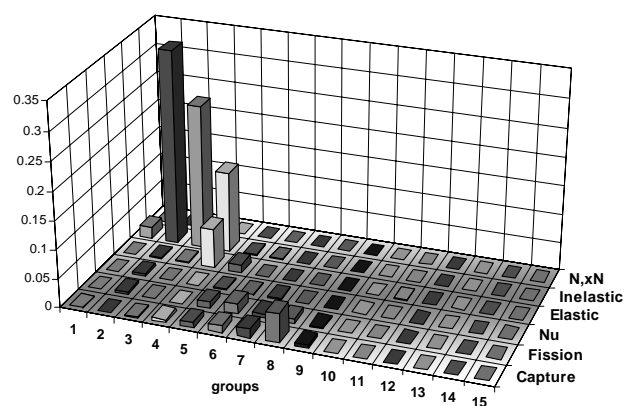


Table 94. LFR void: BOLNA full uncertainties (%) by group

Gr.	[MeV]	σ_{cap}	σ_{fiss}	ν	σ_{el}	σ_{inel}	$\sigma_{\text{n,2n}}$	Total
1	19.6	0.13	0.11	0.13	0.09	0.98	0.03	1.01
2	6.07	0.25	0.20	0.37	0.64	3.87	—	3.95
3	2.23	0.33	0.17i	0.21	0.91	3.68	—	3.81
4	1.35	0.72	0.24	0.06i	1.78	2.72	—	3.34
5	4.98e-1	0.85	0.76	0.29	1.07	0.08i	—	1.59
6	1.83e-1	1.00	0.91	0.26	0.22	0.11	—	1.40
7	6.74e-2	1.06	0.78	0.30	0.06i	0.03	—	1.35
8	2.48e-2	1.36	0.61	0.25	0.29	0.01i	—	1.54
9	9.12e-3	0.69	0.41	0.16	0.08i	—	—	0.81
10	2.03e-3	0.18	0.06	0.05	0.15i	—	—	0.12
11	4.54e-4	0.06	0.01	0.01i	0.23i	—	—	0.22i
12	2.26e-5	0.01	—	0.01i	0.01i	—	—	0.01i
13	4.00e-6	—	—	—	—	—	—	—
14	5.40e-7	—	—	—	—	—	—	—
15	1.00e-7	—	—	—	—	—	—	—
Total		2.43	1.62	0.72	2.37	6.07	0.03	7.18

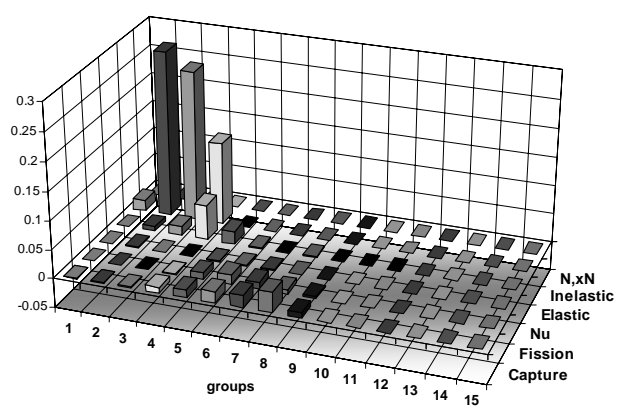


Table 95. LFR void: BOLNA diagonal uncertainties (%) by isotope

Isotope	σ_{cap}	σ_{fiss}	ν	σ_{el}	σ_{inel}	$\sigma_{\text{n,2n}}$	Total
²³⁵ U	0.02	0.01	—	—	—	—	0.02
²³⁸ U	1.04	0.06	0.28	0.16	3.11	0.01	3.29
²³⁸ Pu	0.06	0.37	0.21	—	0.01	—	0.43
²³⁹ Pu	0.35	0.40	0.31	0.03	0.20	—	0.65
²⁴⁰ Pu	0.31	0.26	0.27	0.01	0.09	—	0.50
²⁴¹ Pu	0.03	0.85	0.02	—	0.02	—	0.86
²⁴² Pu	0.19	0.14	0.03	—	0.04	—	0.24
²³⁷ Np	0.04	0.02	0.01	—	0.02	—	0.05
²⁴¹ Am	0.09	0.09	0.02	—	0.02	—	0.13
^{242m} Am	0.01	0.10	0.01	—	—	—	0.10
²⁴³ Am	0.03	0.03	0.01	—	0.02	—	0.05
²⁴² Cm	—	0.02	0.01	—	—	—	0.02
²⁴³ Cm	—	0.01	—	—	—	—	0.01
²⁴⁴ Cm	0.02	0.10	0.05	—	0.01	—	0.11
²⁴⁵ Cm	—	0.26	0.03	—	—	—	0.26
²⁴⁶ Cm	0.01	0.02	—	—	—	—	0.02
⁵⁶ Fe	0.13	—	—	0.15	0.90	—	0.93
⁵² Cr	—	—	—	0.04	0.02	0.02	0.05
⁵⁸ Ni	0.01	—	—	—	—	—	0.01
⁹⁰ Zr	0.02	—	—	0.06	0.57	—	0.58
²⁰⁴ Pb	0.17	—	—	0.02	0.13	—	0.21
²⁰⁶ Pb	0.58	—	—	0.34	1.95	—	2.07
²⁰⁷ Pb	0.34	—	—	0.28	1.84	0.01	1.89
²⁰⁸ Pb	0.20	—	—	1.38	0.71	0.02	1.57
¹⁰ B	0.73	—	—	0.05	0.01	—	0.73
Total	1.56	1.11	0.54	1.47	4.31	0.03	4.97

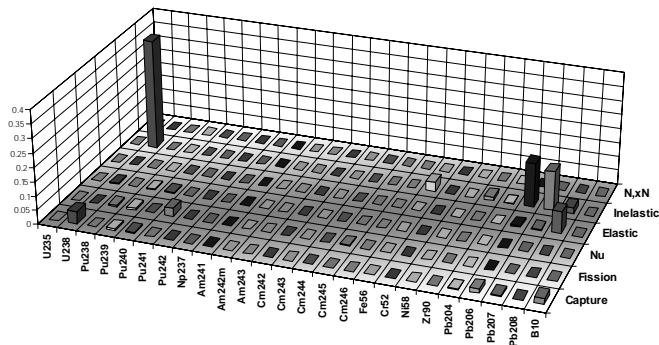


Table 96. LFR void: BOLNA full uncertainties (%) by isotope

Isotope	σ_{cap}	σ_{fiss}	ν	σ_{el}	σ_{inel}	$\sigma_{\text{n,2n}}$	Total
²³⁵ U	0.03	0.01	0.01	—	—	—	0.03
²³⁸ U	1.09	0.08	0.37	1.06	4.46	0.01	4.73
²³⁸ Pu	0.10	0.45	0.39	—	0.02	—	0.60
²³⁹ Pu	0.53	0.52	0.36	0.13	0.25	—	0.87
²⁴⁰ Pu	0.62	0.11	0.30	0.03	0.06	—	0.70
²⁴¹ Pu	0.04	1.37	0.05	—	0.02	—	1.37
²⁴² Pu	0.32	0.18	0.04	—	0.04	—	0.37
²³⁷ Np	0.06	0.02	0.01	—	0.02	—	0.07
²⁴¹ Am	0.14	0.11	0.03	—	0.03	—	0.18
^{242m} Am	0.01	0.16	0.01	—	—	—	0.16
²⁴³ Am	0.05	0.04	0.01	—	0.01	—	0.06
²⁴² Cm	—	0.03	0.01	—	—	—	0.03
²⁴³ Cm	—	0.01	—	—	—	—	0.01
²⁴⁴ Cm	0.04	0.10	0.06	—	0.01	—	0.12
²⁴⁵ Cm	0.01	0.43	0.06	—	—	—	0.44
²⁴⁶ Cm	0.01	0.02	—	—	—	—	0.03
⁵⁶ Fe	0.16	—	—	0.20	1.49	—	1.51
⁵² Cr	—	—	—	0.06	0.03	0.02	0.07
⁵⁸ Ni	0.01	—	—	—	—	—	0.01
⁹⁰ Zr	0.02	—	—	0.11	0.61	—	0.62
²⁰⁴ Pb	0.42	—	—	0.03	0.17	—	0.46
²⁰⁶ Pb	1.31	—	—	0.49	2.77	—	3.10
²⁰⁷ Pb	0.77	—	—	0.35	2.47	0.01	2.61
²⁰⁸ Pb	0.37	—	—	2.01	0.73	0.02	2.17
¹⁰ B	1.14	—	—	0.06	0.01	—	1.14
Total	2.43	1.62	0.72	2.37	6.07	0.03	7.18

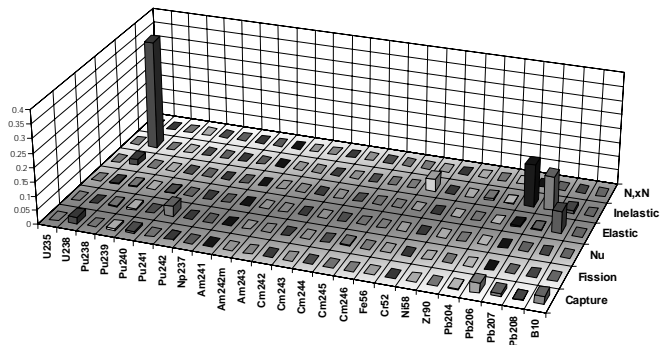


Table 97. LFR XS burn-up: BOLNA diagonal uncertainty (%) by group

Gr.	[MeV]	σ_{cap}	σ_{fiss}	ν	σ_{el}	σ_{inel}	$\sigma_{\text{n,2n}}$	Total
1	19.6	0.01	0.02	0.01	—	0.04	—	0.04
2	6.07	0.01	0.14	0.06	0.02	0.11	—	0.19
3	2.23	0.01	0.22	0.08	0.02	0.31	—	0.39
4	1.35	0.06	0.69	0.21	0.09	0.22	—	0.77
5	4.98e-1	0.19	0.61	0.14	0.05	0.03	—	0.66
6	1.83e-1	0.19	0.73	0.10	0.02	0.04	—	0.77
7	6.74e-2	0.15	0.26	0.07	0.01	0.01	—	0.31
8	2.48e-2	0.17	0.25	0.05	0.01	—	—	0.31
9	9.12e-3	0.05	0.11	0.03	0.01	—	—	0.12
10	2.03e-3	0.03	0.04	0.01	0.01	—	—	0.05
11	4.54e-4	—	0.02	—	0.01	—	—	0.02
12	2.26e-5	—	—	—	—	—	—	—
13	4.00e-6	—	—	—	—	—	—	—
14	5.40e-7	—	—	—	—	—	—	—
15	1.00e-7	—	—	—	—	—	—	—
Total		0.37	1.27	0.31	0.11	0.40	—	1.42

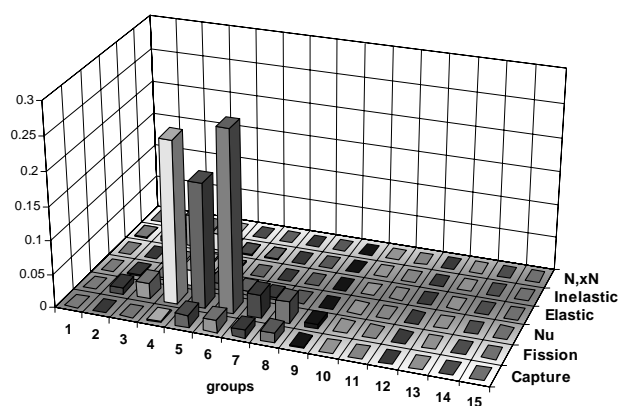


Table 98. LFR XS burn-up: BOLNA full uncertainty (%) by group

Gr.	[MeV]	σ_{cap}	σ_{fiss}	ν	σ_{el}	σ_{inel}	$\sigma_{\text{n,2n}}$	Total
1	19.6	0.01	0.07	0.02	—	0.06	—	0.09
2	6.07	0.03	0.37	0.12	0.02	0.19	—	0.43
3	2.23	0.04	0.57	0.15	0.05	0.40	—	0.72
4	1.35	0.09	1.10	0.33	0.11	0.34	—	1.21
5	4.98e-1	0.28	1.10	0.27	0.09	0.05	—	1.17
6	1.83e-1	0.28	1.16	0.21	0.03	0.06	—	1.21
7	6.74e-2	0.23	0.67	0.18	0.01	0.02	—	0.73
8	2.48e-2	0.22	0.38	0.14	0.03	0.01i	—	0.46
9	9.12e-3	0.12	0.23	0.09	0.01i	—	—	0.28
10	2.03e-3	0.03	0.05	0.05	0.01i	—	—	0.08
11	4.54e-4	0.01	0.02	0.02	0.01i	—	—	0.03
12	2.26e-5	—	—	—	0.01	—	—	0.01
13	4.00e-6	—	—	—	—	—	—	0.01
14	5.40e-7	—	—	—	—	—	—	—
15	1.00e-7	—	—	—	—	—	—	—
Total		0.53	2.21	0.58	0.16	0.57	—	2.42

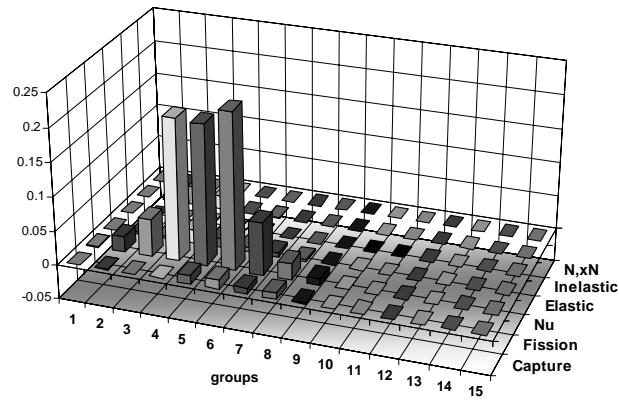


Table 99. LFR XS burn-up: BOLNA diagonal uncertainty (%) by isotope

Isotope	σ_{cap}	σ_{fiss}	ν	σ_{el}	σ_{inel}	$\sigma_{\text{n,2n}}$	Total
²³⁵ U	0.02	—	—	—	—	—	0.02
²³⁸ U	0.14	0.03	0.07	0.01	0.17	—	0.23
²³⁸ Pu	0.02	0.43	0.20	—	—	—	0.47
²³⁹ Pu	0.03	0.18	0.10	—	0.02	—	0.21
²⁴⁰ Pu	0.03	0.28	0.17	—	0.01	—	0.33
²⁴¹ Pu	0.02	0.94	0.02	—	—	—	0.94
²⁴² Pu	0.01	0.11	0.01	—	—	—	0.11
²³⁷ Np	0.03	0.03	0.01	—	0.03	—	0.05
²⁴¹ Am	0.08	0.05	0.01	—	0.02	—	0.09
^{242m} Am	—	0.11	0.01	—	—	—	0.11
²⁴³ Am	—	0.02	—	—	—	—	0.02
²⁴² Cm	0.02	0.32	0.07	—	0.01	—	0.33
²⁴³ Cm	—	0.03	—	—	—	—	0.03
²⁴⁴ Cm	0.03	0.50	0.08	—	0.01	—	0.51
²⁴⁵ Cm	—	0.18	0.02	—	0.01	—	0.19
²⁴⁶ Cm	—	0.02	—	—	—	—	0.02
⁵⁶ Fe	0.06	—	—	0.02	0.25	—	0.25
⁵² Cr	0.01	—	—	0.01	—	—	0.01
⁵⁸ Ni	—	—	—	—	—	—	—
⁹⁰ Zr	0.01	—	—	0.01	0.05	—	0.05
²⁰⁴ Pb	0.02	—	—	—	0.01	—	0.02
²⁰⁶ Pb	0.05	—	—	0.02	0.19	—	0.20
²⁰⁷ Pb	0.03	—	—	0.02	0.16	—	0.17
²⁰⁸ Pb	0.02	—	—	0.10	0.05	—	0.11
¹⁰ B	0.31	—	—	0.03	—	—	0.31
Total	0.37	1.27	0.31	0.11	0.40	—	1.42

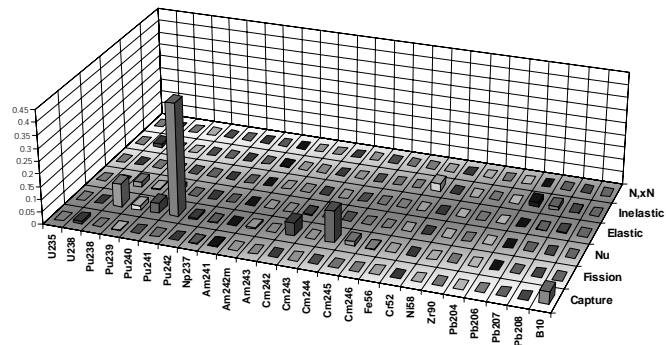


Table 100. LFR XS burn-up: BOLNA full uncertainty (%) by isotope

Isotope	σ_{cap}	σ_{fiss}	ν	σ_{el}	σ_{inel}	$\sigma_{\text{n,2n}}$	Total
²³⁵ U	0.04	—	0.01	—	—	—	0.04
²³⁸ U	0.15	0.05	0.10	0.04i	0.25	—	0.31
²³⁸ Pu	0.03	0.74	0.43	—	0.01	—	0.85
²³⁹ Pu	0.04	0.26	0.12	0.01	0.02	—	0.28
²⁴⁰ Pu	0.03	0.48	0.30	—	0.01	—	0.57
²⁴¹ Pu	0.04	1.72	0.05	—	0.01	—	1.72
²⁴² Pu	0.01	0.16	0.02	—	—	—	0.16
²³⁷ Np	0.06	0.04	0.01	—	0.05	—	0.09
²⁴¹ Am	0.13	0.08	0.02	—	0.02	—	0.15
^{242m} Am	0.01	0.21	0.01	—	—	—	0.21
²⁴³ Am	0.01	0.02	—	—	—	—	0.02
²⁴² Cm	0.03	0.58	0.12	—	0.01	—	0.59
²⁴³ Cm	—	0.06	—	—	—	—	0.06
²⁴⁴ Cm	0.05	0.72	0.12	—	0.01	—	0.73
²⁴⁵ Cm	0.01	0.36	0.05	—	0.01	—	0.36
²⁴⁶ Cm	—	0.03	—	—	—	—	0.03
⁵⁶ Fe	0.07	—	—	0.04	0.36	—	0.37
⁵² Cr	0.01	—	—	0.01	—	—	0.01
⁵⁸ Ni	—	—	—	—	—	—	—
⁹⁰ Zr	0.01	—	—	0.02	0.05	—	0.06
²⁰⁴ Pb	0.04	—	—	—	0.02	—	0.04
²⁰⁶ Pb	0.12	—	—	0.03	0.26	—	0.29
²⁰⁷ Pb	0.07	—	—	0.02	0.22	—	0.24
²⁰⁸ Pb	0.03	—	—	0.15	0.06	—	0.16
¹⁰ B	0.45	—	—	0.03	—	—	0.45
Total	0.53	2.21	0.58	0.16	0.57	—	2.42

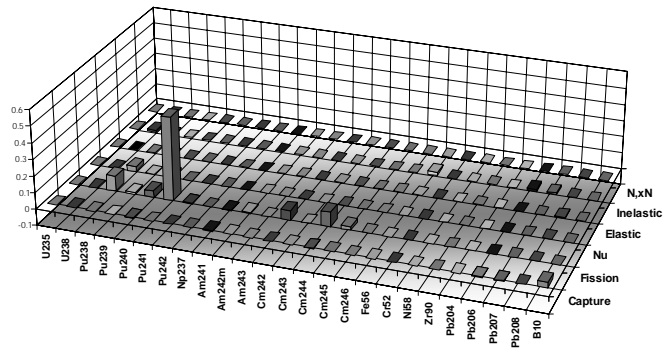


Table 101. ADMAB k_{eff} : BOLNA diagonal uncertainty (%) by group

Gr.	[MeV]	σ_{cap}	σ_{fiss}	ν	σ_{el}	σ_{inel}	$\sigma_{\text{n,2n}}$	Total
1	19.6	0.02	0.03	0.01	—	0.02	—	0.04
2	6.07	0.01	0.35	0.12	0.01	0.12	—	0.39
3	2.23	0.02	0.52	0.17	0.03	0.57	—	0.79
4	1.35	0.12	1.36	0.22	0.18	0.60	—	1.51
5	4.98e-1	0.14	0.38	0.05	0.06	0.15	—	0.44
6	1.83e-1	0.18	0.50	0.05	0.04	0.31	—	0.61
7	6.74e-2	0.16	0.19	0.03	0.01	0.03	—	0.25
8	2.48e-2	0.13	0.16	0.03	0.01	—	—	0.21
9	9.12e-3	0.12	0.12	0.02	—	—	—	0.17
10	2.03e-3	0.07	0.09	0.01	—	—	—	0.11
11	4.54e-4	0.01	0.02	—	—	—	—	0.02
12	2.26e-5	—	—	—	—	—	—	—
13	4.00e-6	—	—	—	—	—	—	—
14	5.40e-7	—	—	—	—	—	—	—
15	1.00e-7	—	—	—	—	—	—	—
Total		0.35	1.65	0.31	0.20	0.91	—	1.95

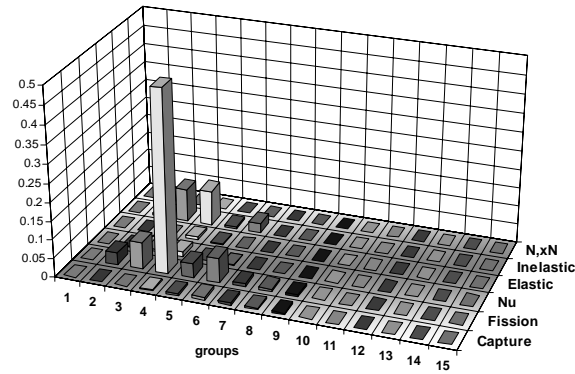


Table 102. ADMAB k_{eff} : BOLNA full uncertainty (%) by group

Gr.	[MeV]	σ_{cap}	σ_{fiss}	ν	σ_{el}	σ_{inel}	$\sigma_{\text{n,2n}}$	Total
1	19.6	0.02	0.11	0.02	0.01	0.09	—	0.14
2	6.07	0.04	0.74	0.18	0.01	0.27	—	0.81
3	2.23	0.07	1.04	0.25	0.08	0.78	—	1.32
4	1.35	0.19	1.78	0.30	0.19	0.76	—	1.98
5	4.98e-1	0.25	0.89	0.13	0.09	0.24	—	0.97
6	1.83e-1	0.27	0.89	0.10	0.07	0.31i	—	0.89
7	6.74e-2	0.28	0.55	0.08	0.02	0.08i	—	0.62
8	2.48e-2	0.22	0.24	0.07	0.01	0.01	—	0.34
9	9.12e-3	0.20	0.21	0.06	0.01	—	—	0.30
10	2.03e-3	0.15	0.12	0.05	—	—	—	0.19
11	4.54e-4	0.04	0.03	0.02	—	—	—	0.06
12	2.26e-5	—	—	—	—	—	—	0.01
13	4.00e-6	—	—	—	—	—	—	—
14	5.40e-7	—	—	—	—	—	—	—
15	1.00e-7	—	—	—	—	—	—	—
Total		0.61	2.61	0.47	0.23	1.10	—	2.94

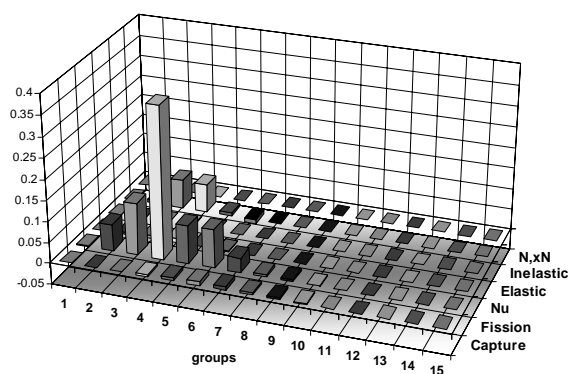


Table 103. ADMAB k_{eff} : BOLNA diagonal uncertainty (%) by isotope

Isotope	σ_{cap}	σ_{fiss}	ν	σ_{el}	σ_{inel}	$\sigma_{\text{n,2n}}$	Total
²³⁸ Pu	0.01	0.12	0.06	—	0.01	—	0.14
²³⁹ Pu	0.07	0.09	0.05	—	0.07	—	0.14
²⁴⁰ Pu	0.03	0.10	0.09	—	0.01	—	0.14
²⁴¹ Pu	0.04	0.55	0.01	—	0.01	—	0.56
²⁴² Pu	0.03	0.10	0.02	—	0.01	—	0.11
²³⁷ Np	0.09	0.17	0.04	—	0.07	—	0.21
²⁴¹ Am	0.27	0.52	0.11	—	0.11	—	0.61
^{242m} Am	—	0.07	—	—	—	—	0.07
²⁴³ Am	0.17	0.26	0.06	—	0.56	—	0.64
²⁴² Cm	—	—	—	—	—	—	—
²⁴³ Cm	—	0.06	—	—	—	—	0.06
²⁴⁴ Cm	0.06	1.32	0.25	—	0.02	—	1.35
²⁴⁵ Cm	—	0.50	0.05	—	0.01	—	0.50
²⁴⁶ Cm	—	—	—	—	—	—	—
⁵⁶ Fe	0.04	—	—	0.02	0.63	—	0.63
⁵⁷ Fe	0.01	—	—	—	0.02	—	0.02
⁵² Cr	—	—	—	—	0.01	—	0.01
⁵⁸ Ni	—	—	—	—	—	—	—
⁹⁰ Zr	0.01	—	—	0.01	0.09	—	0.09
¹⁵ N	—	—	—	0.19	0.01	—	0.19
Pb	0.04	—	—	0.03	0.04	—	0.06
²⁰⁹ Bi	0.01	—	—	0.02	0.28	—	0.28
Total	0.35	1.65	0.31	0.20	0.91	—	1.95

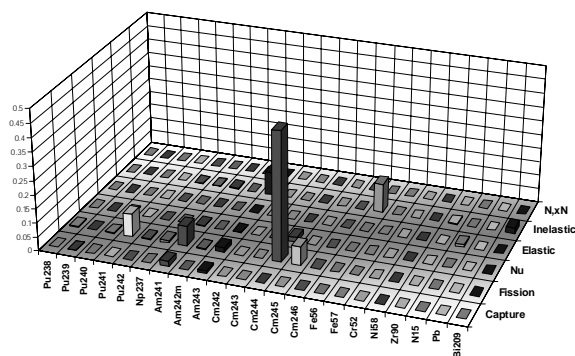


Table 104. ADMAB k_{eff} : BOLNA full uncertainty (%) by isotope

Isotope	σ_{cap}	σ_{fiss}	ν	σ_{el}	σ_{inel}	$\sigma_{\text{n,2n}}$	Total
²³⁸ Pu	0.02	0.21	0.13	—	0.01	—	0.25
²³⁹ Pu	0.10	0.12	0.06	0.01	0.11	—	0.20
²⁴⁰ Pu	0.08	0.16	0.14	—	0.03	—	0.23
²⁴¹ Pu	0.07	1.04	0.04	—	0.02	—	1.05
²⁴² Pu	0.06	0.15	0.03	—	0.02	—	0.17
²³⁷ Np	0.18	0.29	0.06	—	0.13	—	0.37
²⁴¹ Am	0.46	0.83	0.16	—	0.16	—	0.97
^{242m} Am	0.01	0.14	0.01	—	—	—	0.14
²⁴³ Am	0.29	0.35	0.09	—	0.43	—	0.63
²⁴² Cm	—	—	—	—	—	—	—
²⁴³ Cm	—	0.12	0.01	—	—	—	0.12
²⁴⁴ Cm	0.11	1.90	0.36	—	0.04	—	1.94
²⁴⁵ Cm	0.01	1.04	0.13	—	0.01	—	1.05
²⁴⁶ Cm	—	—	—	—	—	—	—
⁵⁶ Fe	0.05	—	—	0.02	0.93	—	0.93
⁵⁷ Fe	0.01	—	—	—	0.03	—	0.03
⁵² Cr	—	—	—	—	0.01	—	0.01
⁵⁸ Ni	—	—	—	—	—	—	—
⁹⁰ Zr	0.02	—	—	0.01	0.10	—	0.10
¹⁵ N	—	—	—	0.22	0.01	—	0.22
Pb	0.07	—	—	0.05	0.04	—	0.09
²⁰⁹ Bi	0.02	—	—	0.03	0.31	—	0.31
Total	0.61	2.61	0.47	0.23	1.10	—	2.94

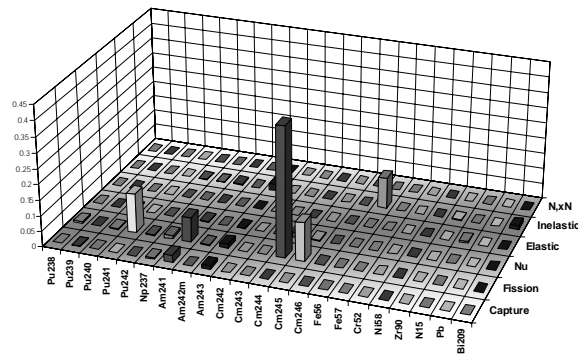


Table 105. ADMAB power peak: BOLNA diagonal uncertainty (%) by group

Gr.	[MeV]	σ_{cap}	σ_{fiss}	ν	σ_{el}	σ_{inel}	$\sigma_{\text{n,2n}}$	Total
1	19.6	0.12	0.23	0.08	0.01	0.18	0.01	0.32
2	6.07	0.07	2.41	0.88	0.08	0.94	—	2.74
3	2.23	0.15	3.63	1.19	0.22	4.35	—	5.79
4	1.35	0.89	9.64	1.57	1.44	4.66	—	10.95
5	4.98e-1	1.10	2.80	0.40	0.58	1.28	—	3.34
6	1.83e-1	1.38	3.67	0.35	0.40	2.38	—	4.61
7	6.74e-2	1.21	1.43	0.25	0.13	0.22	—	1.91
8	2.48e-2	1.04	1.18	0.20	0.04	—	—	1.59
9	9.12e-3	0.92	0.94	0.17	0.04	—	—	1.32
10	2.03e-3	0.55	0.68	0.08	0.04	—	—	0.88
11	4.54e-4	0.05	0.17	0.01	0.05	—	—	0.18
12	2.26e-5	0.01	—	—	0.01	—	—	0.01
13	4.00e-6	—	—	—	—	—	—	—
14	5.40e-7	—	—	—	—	—	—	—
15	1.00e-7	—	—	—	—	—	—	—
Total		2.76	11.75	2.25	1.63	6.99	0.01	14.22

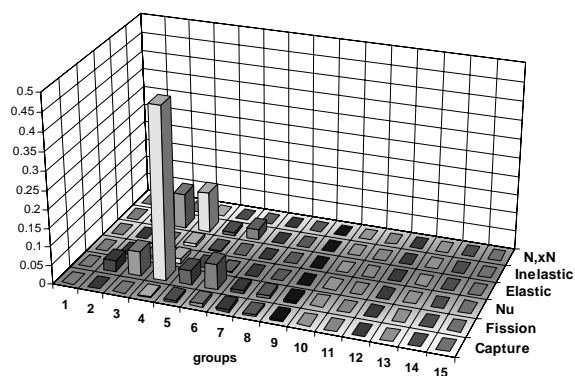


Table 106. ADMAB power peak: BOLNA full uncertainty (%) by group

Gr.	[MeV]	σ_{cap}	σ_{fiss}	ν	σ_{el}	σ_{inel}	$\sigma_{\text{n,2n}}$	Total
1	19.6	0.16	0.76	0.14	0.09	0.71	0.01	1.06
2	6.07	0.30	5.14	1.28	0.14	2.04	—	5.69
3	2.23	0.53	7.28	1.76	0.61	5.95	—	9.60
4	1.35	1.46	12.63	2.15	1.56	5.99	—	14.30
5	4.98e-1	1.97	6.44	0.93	0.75	2.02	—	7.13
6	1.83e-1	2.14	6.54	0.72	0.62	2.44i	—	6.51
7	6.74e-2	2.16	4.06	0.59	0.15	0.68i	—	4.59
8	2.48e-2	1.74	1.82	0.53	0.09	0.04	—	2.58
9	9.12e-3	1.56	1.62	0.44	0.08	—	—	2.29
10	2.03e-3	1.17	0.88	0.36	0.08	—	—	1.50
11	4.54e-4	0.34	0.26	0.13	0.09	—	—	0.45
12	2.26e-5	0.03	0.02	0.03	0.03	—	—	0.05
13	4.00e-6	0.02	0.01	0.01	0.01	—	—	0.02
14	5.40e-7	—	—	—	—	—	—	0.01
15	1.00e-7	—	—	—	—	—	—	—
Total		4.75	18.62	3.42	1.96	8.58	0.01	21.42

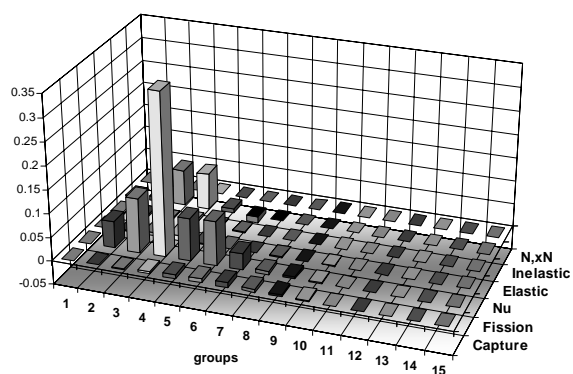


Table 107. AMAB power peak: BOLNA diagonal uncertainty (%) by isotope

Isotope	σ_{cap}	σ_{fiss}	ν	σ_{el}	σ_{inel}	$\sigma_{\text{n,2n}}$	Total
²³⁸ Pu	0.07	0.88	0.46	—	0.05	—	1.00
²³⁹ Pu	0.51	0.63	0.40	—	0.58	—	1.07
²⁴⁰ Pu	0.26	0.70	0.64	—	0.10	—	0.99
²⁴¹ Pu	0.30	4.07	0.10	—	0.08	—	4.08
²⁴² Pu	0.27	0.73	0.16	—	0.12	—	0.80
²³⁷ Np	0.67	1.22	0.29	—	0.59	—	1.54
²⁴¹ Am	2.10	3.64	0.82	—	0.87	—	4.37
^{242m} Am	0.03	0.52	0.03	—	0.02	—	0.53
²⁴³ Am	1.35	1.80	0.46	0.01	4.37	—	4.93
²⁴² Cm	—	—	—	—	—	—	—
²⁴³ Cm	—	0.43	0.02	—	—	—	0.43
²⁴⁴ Cm	0.47	9.35	1.78	0.01	0.18	0.01	9.53
²⁴⁵ Cm	0.03	3.67	0.36	—	0.07	—	3.69
²⁴⁶ Cm	—	0.01	—	—	—	—	0.01
⁵⁶ Fe	0.35	—	—	0.11	4.87	—	4.88
⁵⁷ Fe	0.09	—	—	—	0.15	—	0.17
⁵² Cr	0.03	—	—	0.03	0.07	—	0.09
⁵⁸ Ni	0.01	—	—	0.01	0.02	—	0.03
⁹⁰ Zr	0.07	—	—	0.13	0.67	—	0.69
¹⁵ N	0.01	—	—	1.62	0.05	—	1.62
Pb	0.26	—	—	0.07	0.27	—	0.39
²⁰⁹ Bi	0.10	—	—	0.04	2.01	—	2.02
Total	2.76	11.75	2.25	1.63	6.99	0.01	14.22

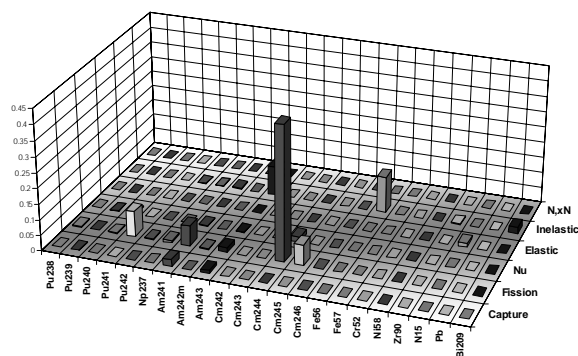


Table 108. ADMAB power peak: BOLNA full uncertainty (%) by isotope

Isotope	σ_{cap}	σ_{fiss}	ν	σ_{el}	σ_{inel}	$\sigma_{\text{n,2n}}$	Total
²³⁸ Pu	0.13	1.52	0.94	—	0.07	—	1.79
²³⁹ Pu	0.77	0.90	0.47	0.05i	0.86	—	1.54
²⁴⁰ Pu	0.63	1.15	1.02	—	0.20	—	1.68
²⁴¹ Pu	0.57	7.61	0.27	—	0.15	—	7.63
²⁴² Pu	0.45	1.08	0.23	—	0.17	—	1.20
²³⁷ Np	1.40	2.05	0.41	—	1.04	—	2.73
²⁴¹ Am	3.58	5.81	1.14	0.01	1.22	—	7.03
^{242m} Am	0.05	1.05	0.08	—	0.04	—	1.05
²⁴³ Am	2.25	2.43	0.64	0.01	3.52	—	4.88
²⁴² Cm	—	—	—	—	—	—	—
²⁴³ Cm	—	0.87	0.05	—	—	—	0.87
²⁴⁴ Cm	0.86	13.43	2.56	0.01	0.29	0.01	13.71
²⁴⁵ Cm	0.06	7.56	0.99	—	0.10	—	7.63
²⁴⁶ Cm	—	0.02	—	—	—	—	0.02
⁵⁶ Fe	0.40	—	—	0.18	7.22	—	7.23
⁵⁷ Fe	0.09	—	—	—	0.20	—	0.22
⁵² Cr	0.04	—	—	0.03	0.08	—	0.10
⁵⁸ Ni	0.02	—	—	0.01	0.02	—	0.03
⁹⁰ Zr	0.13	—	—	0.19	0.75	—	0.79
¹⁵ N	0.01	—	—	1.94	0.06	—	1.94
Pb	0.46	—	—	0.09	0.28	—	0.54
²⁰⁹ Bi	0.16	—	—	0.05	2.23	—	2.23
Total	4.75	18.62	3.42	1.96	8.58	0.01	21.42

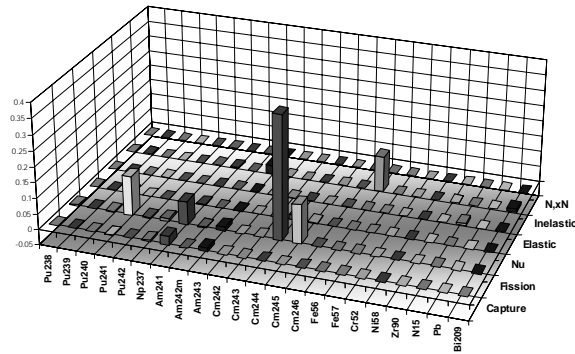


Table 109. ADMAB void: BOLNA diagonal uncertainty (%) by group

Gr.	[MeV]	σ_{cap}	σ_{fiss}	ν	σ_{el}	σ_{inel}	$\sigma_{\text{n,2n}}$	Total
1	19.6	0.25	0.51	0.17	0.02	0.89	0.23	1.09
2	6.07	0.27	3.65	1.32	0.86	3.22	0.01	5.12
3	2.23	0.22	1.80	0.55	1.03	10.59	—	10.80
4	1.35	0.48	0.31	0.11	1.41	4.10	—	4.38
5	4.98e-1	0.60	0.54	0.09	0.77	0.83	—	1.40
6	1.83e-1	0.72	1.00	0.11	0.49	0.80	—	1.55
7	6.74e-2	0.85	0.73	0.13	0.16	0.13	—	1.15
8	2.48e-2	0.80	0.69	0.12	0.16	0.01	—	1.07
9	9.12e-3	0.94	0.78	0.14	0.03	—	—	1.23
10	2.03e-3	0.36	0.40	0.05	0.09	—	—	0.55
11	4.54e-4	0.02	0.01	—	0.06	—	—	0.07
12	2.26e-5	0.01	—	—	0.01	—	—	0.01
13	4.00e-6	—	—	—	—	—	—	—
14	5.40e-7	—	—	—	—	—	—	—
15	1.00e-7	—	—	—	—	—	—	—
Total		1.91	4.47	1.47	2.17	11.89	0.23	13.11

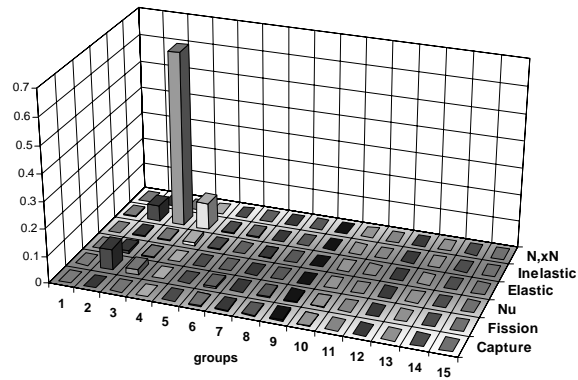


Table 110. ADMAB void: BOLNA full uncertainty (%) by group

Gr.	[MeV]	σ_{cap}	σ_{fiss}	ν	σ_{el}	σ_{inel}	$\sigma_{\text{n,2n}}$	Total
1	19.6	0.29	1.05	0.25	0.15	1.71	0.23	2.06
2	6.07	0.46	4.17	1.44	1.22	4.38	0.01	6.36
3	2.23	0.48	2.66	0.79	1.81	11.47	—	11.95
4	1.35	0.93	0.64i	0.16i	2.05	5.35	—	5.77
5	4.98e-1	1.13	0.69	0.18	1.51	0.58i	—	1.94
6	1.83e-1	1.24	1.23	0.19	0.92	0.65	—	2.08
7	6.74e-2	1.41	1.22	0.22	0.43	0.26	—	1.95
8	2.48e-2	1.34	1.11	0.21	0.39	0.03i	—	1.79
9	9.12e-3	1.39	1.18	0.22	0.12i	—	—	1.83
10	2.03e-3	0.82	0.53	0.13	0.30i	—	—	0.94
11	4.54e-4	0.13	0.03	0.02	0.20i	—	—	0.15i
12	2.26e-5	0.03	0.01i	0.02i	0.01i	—	—	0.02
13	4.00e-6	0.02	0.01i	0.01i	—	—	—	0.01
14	5.40e-7	—	—	—	—	—	—	—
15	1.00e-7	—	—	—	—	—	—	—
Total		3.26	5.62	1.73	3.51	13.51	0.23	15.49

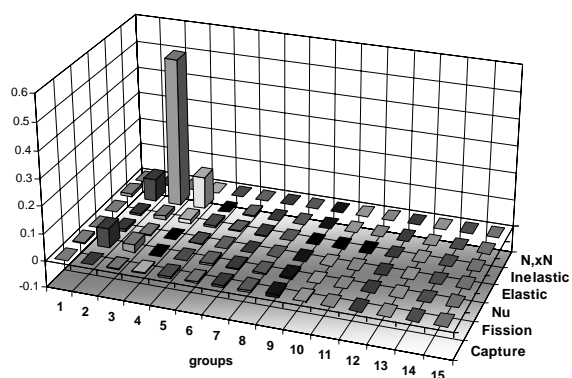


Table 111. ADMAB void: BOLNA diagonal uncertainty (%) by isotope

Isotope	σ_{cap}	σ_{fiss}	ν	σ_{el}	σ_{inel}	$\sigma_{\text{n,2n}}$	Total
²³⁸ Pu	0.04	0.33	0.14	—	0.02	—	0.36
²³⁹ Pu	0.38	0.23	0.19	0.03	0.33	—	0.59
²⁴⁰ Pu	0.15	0.26	0.21	0.01	0.08	—	0.38
²⁴¹ Pu	0.11	1.44	0.04	0.01	0.08	—	1.45
²⁴² Pu	0.20	0.28	0.05	—	0.04	—	0.35
²³⁷ Np	0.44	0.63	0.26	0.02	0.24	—	0.85
²⁴¹ Am	1.28	2.73	0.66	0.03	0.48	—	3.13
^{242m} Am	0.01	0.21	0.01	—	0.01	0.01	0.21
²⁴³ Am	0.76	1.38	0.38	0.04	1.39	—	2.14
²⁴² Cm	—	—	—	—	—	—	—
²⁴³ Cm	—	0.12	0.01	—	—	—	0.12
²⁴⁴ Cm	0.27	2.55	1.18	0.02	0.18	0.04	2.83
²⁴⁵ Cm	0.02	1.12	0.17	—	0.02	—	1.13
²⁴⁶ Cm	—	0.01	—	—	—	—	0.01
⁵⁶ Fe	0.30	—	—	0.71	3.81	0.01	3.89
⁵⁷ Fe	0.01	—	—	0.01	0.09	—	0.09
⁵² Cr	0.03	—	—	0.21	0.08	—	0.23
⁵⁸ Ni	0.02	—	—	0.01	0.02	—	0.03
⁹⁰ Zr	0.04	—	—	0.16	1.48	—	1.49
¹⁵ N	0.02	—	—	0.55	0.09	0.02	0.56
Pb	0.82	—	—	1.69	2.24	0.07	2.92
²⁰⁹ Bi	0.42	—	—	0.98	10.83	0.21	10.88
Total	1.91	4.47	1.47	2.17	11.89	0.23	13.11

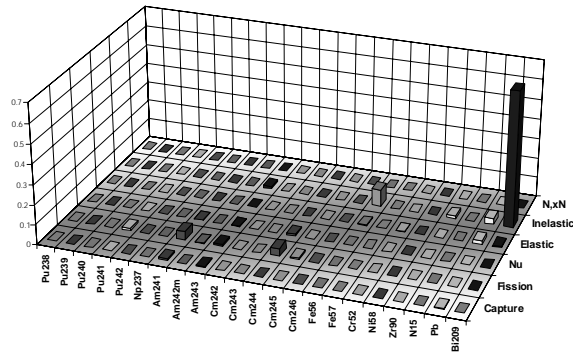


Table 112. ADMAB void: BOLNA full uncertainty (%) by isotope

Isotope	σ_{cap}	σ_{fiss}	ν	σ_{el}	σ_{inel}	$\sigma_{\text{n,2n}}$	Total
²³⁸ Pu	0.09	0.40	0.22	—	0.02	—	0.47
²³⁹ Pu	0.50	0.27	0.22	0.16	0.41	—	0.76
²⁴⁰ Pu	0.32	0.25	0.24	0.03	0.06	—	0.48
²⁴¹ Pu	0.13	2.04	0.09	0.01	0.09	—	2.04
²⁴² Pu	0.33	0.35	0.06	—	0.05	—	0.49
²³⁷ Np	0.81	0.77	0.29	0.03	0.21	—	1.18
²⁴¹ Am	2.14	3.32	0.78	0.05	0.71	—	4.08
^{242m} Am	0.02	0.32	0.03	—	0.01	0.01	0.32
²⁴³ Am	1.30	1.62	0.44	0.07	0.65	—	2.22
²⁴² Cm	—	—	—	—	—	—	—
²⁴³ Cm	—	0.18	0.02	—	—	—	0.18
²⁴⁴ Cm	0.45	3.20	1.35	0.04	0.24	0.04	3.51
²⁴⁵ Cm	0.03	1.55	0.31	0.01	0.02	—	1.58
²⁴⁶ Cm	—	0.01	—	—	—	—	0.01
⁵⁶ Fe	0.37	—	—	0.99	5.43	0.01	5.53
⁵⁷ Fe	0.02	—	—	0.02	0.12	—	0.13
⁵² Cr	0.04	—	—	0.29	0.10	—	0.31
⁵⁸ Ni	0.03	—	—	0.01	0.02	—	0.03
⁹⁰ Zr	0.04	—	—	0.31	1.54	—	1.57
¹⁵ N	0.02	—	—	0.76	0.11	0.02	0.77
Pb	1.53	—	—	2.84	2.28	0.07	3.96
²⁰⁹ Bi	0.73	—	—	1.56	12.01	0.21	12.13
Total	3.26	5.62	1.73	3.51	13.51	0.23	15.49

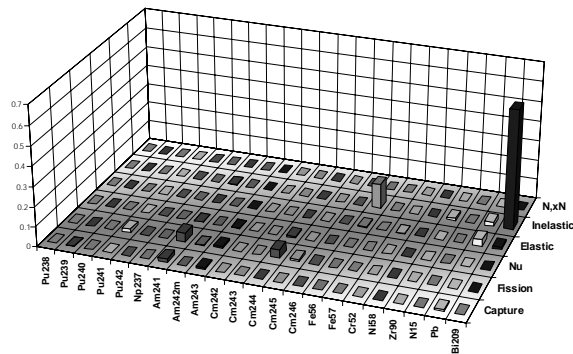


Table 113. ADMAB XS burn-up: BOLNA diagonal uncertainty (%) by group

Gr.	[MeV]	σ_{cap}	σ_{fiss}	ν	σ_{el}	σ_{inel}	$\sigma_{\text{n,2n}}$	Total
1	19.6	0.01	0.51	0.17	—	0.07	0.01	0.54
2	6.07	0.08	6.40	2.23	0.01	0.65	0.01	6.81
3	2.23	0.21	10.23	3.25	0.13	2.38	—	11.00
4	1.35	1.04	23.88	7.59	0.34	3.52	—	25.33
5	4.98e-1	1.28	13.52	4.75	0.42	0.95	—	14.42
6	1.83e-1	1.47	7.58	2.39	0.04	1.77	—	8.28
7	6.74e-2	1.34	4.16	1.50	0.05	0.16	—	4.63
8	2.48e-2	1.22	2.94	1.13	0.06	—	—	3.38
9	9.12e-3	0.77	2.24	0.79	0.04	—	—	2.49
10	2.03e-3	0.25	1.28	0.37	0.01	—	—	1.35
11	4.54e-4	0.04	0.18	0.07	—	—	—	0.20
12	2.26e-5	—	—	—	—	—	—	0.01
13	4.00e-6	—	—	—	—	—	—	—
14	5.40e-7	—	—	—	—	—	—	—
15	1.00e-7	—	—	—	—	—	—	—
Total		2.98	31.45	10.28	0.57	4.75	0.01	33.56

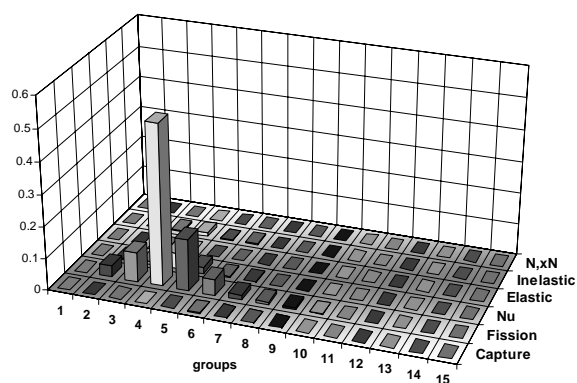


Table 114. ADMAB XS burn-up: BOLNA full uncertainty (%) by group

Gr.	[MeV]	σ_{cap}	σ_{fiss}	ν	σ_{el}	σ_{inel}	$\sigma_{\text{n,2n}}$	Total
1	19.6	0.04	2.05	0.36	0.02i	0.24	0.01	2.10
2	6.07	0.35	14.58	4.14	0.02i	1.43	0.01	15.23
3	2.23	0.64	19.84	5.71	0.15i	3.22	—	20.91
4	1.35	1.68	33.49	12.16	0.27	3.97	—	35.89
5	4.98e-1	2.21	24.36	9.41	0.42	1.89	—	26.28
6	1.83e-1	2.50	15.98	6.65	0.06	2.32i	—	17.33
7	6.74e-2	2.48	10.45	5.27	0.09	0.65i	—	11.95
8	2.48e-2	2.00	5.86	4.56	0.09	0.04i	—	7.69
9	9.12e-3	1.42	4.38	3.73	0.08	—	—	5.93
10	2.03e-3	0.59	2.96	2.50	0.02	—	—	3.92
11	4.54e-4	0.04i	0.56	1.07	0.01i	—	—	1.21
12	2.26e-5	0.01	0.01	0.08	—	—	—	0.08
13	4.00e-6	—	—	0.02	—	—	—	0.02
14	5.40e-7	—	—	0.01	—	—	—	0.01
15	1.00e-7	0.01	0.01i	0.04	—	—	—	0.04
Total		5.20	52.47	20.01	0.51	5.11	0.01	56.63

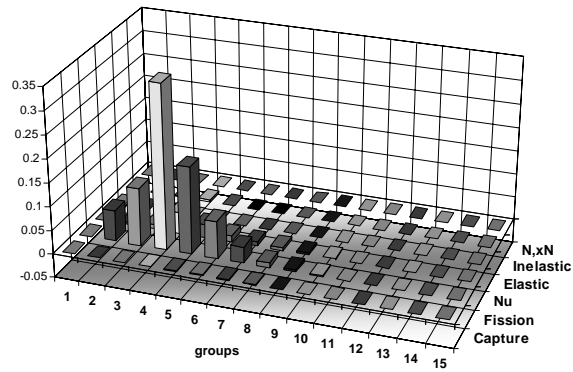


Table 115. ADMAB XS burn-up: BOLNA diagonal uncertainty (%) by isotope

Isotope	σ_{cap}	σ_{fiss}	ν	σ_{el}	σ_{inel}	$\sigma_{\text{n,2n}}$	Total
²³⁸ Pu	1.32	17.43	8.91	0.01	0.81	—	19.64
²³⁹ Pu	0.40	0.71	0.39	—	0.87	—	1.25
²⁴⁰ Pu	0.32	0.57	0.48	—	0.04	—	0.81
²⁴¹ Pu	0.46	5.45	0.13	—	0.15	—	5.47
²⁴² Pu	0.75	1.51	0.33	—	0.19	—	1.72
²³⁷ Np	0.39	1.37	0.35	—	0.68	—	1.62
²⁴¹ Am	1.71	5.03	1.16	—	1.26	—	5.58
^{242m} Am	0.31	6.41	0.36	—	0.25	0.01	6.43
²⁴³ Am	0.91	1.96	0.53	—	3.98	—	4.56
²⁴² Cm	0.72	12.51	3.29	—	0.36	—	12.96
²⁴³ Cm	—	0.45	0.02	—	—	—	0.45
²⁴⁴ Cm	1.17	19.73	3.56	0.01	0.27	—	20.09
²⁴⁵ Cm	0.05	5.86	0.65	—	0.07	—	5.89
²⁴⁶ Cm	0.01	0.20	0.03	—	0.01	—	0.20
⁵⁶ Fe	0.24	—	—	0.05	1.59	—	1.61
⁵⁷ Fe	0.08	—	—	—	0.04	—	0.09
⁵² Cr	0.02	—	—	0.03	0.01	—	0.03
⁵⁸ Ni	—	—	—	—	—	—	—
⁹⁰ Zr	0.06	—	—	0.04	0.19	—	0.20
¹⁵ N	—	—	—	0.56	0.02	—	0.56
Pb	0.32	—	—	0.05	0.09	—	0.33
²⁰⁹ Bi	0.06	—	—	0.03	0.56	0.01	0.56
Total	2.98	31.45	10.28	0.57	4.75	0.01	33.56

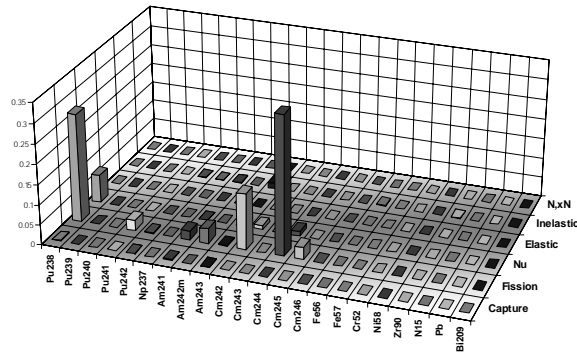


Table 116. ADMAB XS burn-up: BOLNA full uncertainty (%) by isotope

Isotope	σ_{cap}	σ_{fiss}	ν	σ_{el}	σ_{inel}	$\sigma_{\text{n,2n}}$	Total
²³⁸ Pu	2.57	30.16	18.35	0.01	1.17	—	35.42
²³⁹ Pu	0.66	1.01	0.45	0.08	1.32	—	1.85
²⁴⁰ Pu	0.73	0.98	0.87	0.01	0.08	—	1.50
²⁴¹ Pu	0.87	10.57	0.31	—	0.26	—	10.61
²⁴² Pu	1.26	2.24	0.46	—	0.27	—	2.62
²³⁷ Np	0.78	2.30	0.49	—	1.17	—	2.73
²⁴¹ Am	2.84	7.96	1.60	—	1.82	—	8.79
^{242m} Am	0.57	12.80	0.97	—	0.38	0.01	12.86
²⁴³ Am	1.38	2.65	0.73	—	3.98	—	5.03
²⁴² Cm	1.30	23.00	5.29	—	0.53	—	23.64
²⁴³ Cm	0.01	0.89	0.06	—	—	—	0.89
²⁴⁴ Cm	2.06	28.52	5.20	0.01	0.45	—	29.06
²⁴⁵ Cm	0.10	11.91	1.80	—	0.10	—	12.05
²⁴⁶ Cm	0.02	0.33	0.06	—	0.02	—	0.34
⁵⁶ Fe	0.25	—	—	0.05	1.15	—	1.17
⁵⁷ Fe	0.08	—	—	—	0.02	—	0.08
⁵² Cr	0.02	—	—	0.02	0.02	—	0.04
⁵⁸ Ni	—	—	—	—	—	—	—
⁹⁰ Zr	0.06	—	—	0.03	0.19	—	0.21
¹⁵ N	—	—	—	0.49	0.02	—	0.49
Pb	0.39	—	—	0.08	0.09	—	0.41
²⁰⁹ Bi	0.06	—	—	0.04	0.55	0.01	0.55
Total	5.20	52.47	20.01	0.51	5.11	0.01	56.63

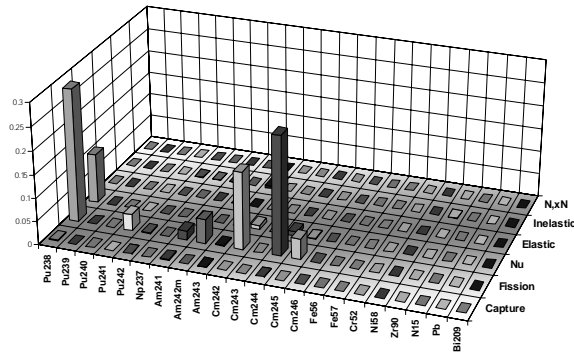


Table 117. VHTR k_{eff} BOC: BOLNA diagonal uncertainty (%) by group

Gr.	[MeV]	σ_{cap}	σ_{fiss}	ν	σ_{el}	σ_{inel}	$\sigma_{\text{n,2n}}$	Total
1	19.6	0.03	—	—	—	0.04	—	0.05
2	6.07	—	—	—	0.01	0.03	—	0.03
3	2.23	—	—	—	0.01	—	—	0.01
4	1.35	—	—	—	0.01	—	—	0.01
5	4.98e-1	—	—	—	0.01	—	—	0.01
6	1.83e-1	—	—	—	—	—	—	—
7	6.74e-2	0.01	—	—	—	—	—	0.01
8	2.48e-2	0.01	—	—	—	—	—	0.01
9	9.12e-3	0.02	—	—	—	—	—	0.03
10	2.03e-3	0.02	—	—	—	—	—	0.02
11	4.54e-4	0.08	0.01	0.02	0.01	—	—	0.09
12	2.26e-5	0.09	0.01	0.02	—	—	—	0.09
13	4.00e-6	0.05	—	0.03	0.01	—	—	0.06
14	5.40e-7	0.10	0.03	0.28	—	—	—	0.29
15	1.00e-7	0.05	0.01	0.15	—	—	—	0.16
Total		0.18	0.03	0.32	0.02	0.05	—	0.37

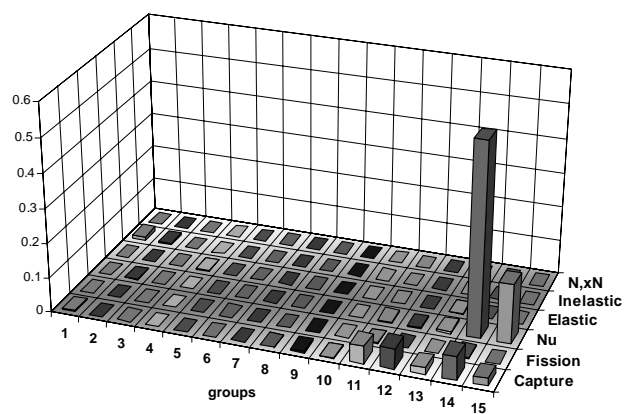


Table 118. VHTR k_{eff} BOC: BOLNA full uncertainty (%) by group

Gr.	[MeV]	σ_{cap}	σ_{fiss}	ν	σ_{el}	σ_{inel}	$\sigma_{\text{n,2n}}$	Total
1	19.6	0.03	—	—	—	0.05	—	0.06
2	6.07	—	—	0.01	0.01	0.04	—	0.05
3	2.23	—	—	0.01	0.01	—	—	0.02
4	1.35	0.01	—	0.01	0.02	—	—	0.02
5	4.98e-1	0.01	—	0.01	0.01	—	—	0.02
6	1.83e-1	0.01	—	0.01	—	—	—	0.02
7	6.74e-2	0.02	—	0.01	—	—	—	0.02
8	2.48e-2	0.02	—	0.02	—	—	—	0.03
9	9.12e-3	0.04	—	0.02	0.01	—	—	0.05
10	2.03e-3	0.03	—	0.04	0.01	—	—	0.05
11	4.54e-4	0.10	0.01i	0.08	0.01	—	—	0.13
12	2.26e-5	0.10	0.01i	0.07	0.01	—	—	0.13
13	4.00e-6	0.06	—	0.09	0.01	—	—	0.11
14	5.40e-7	0.12	0.03i	0.36	—	—	—	0.38
15	1.00e-7	0.09	0.02i	0.27	—	—	—	0.28
Total		0.22	0.04i	0.47	0.04	0.07	—	0.53

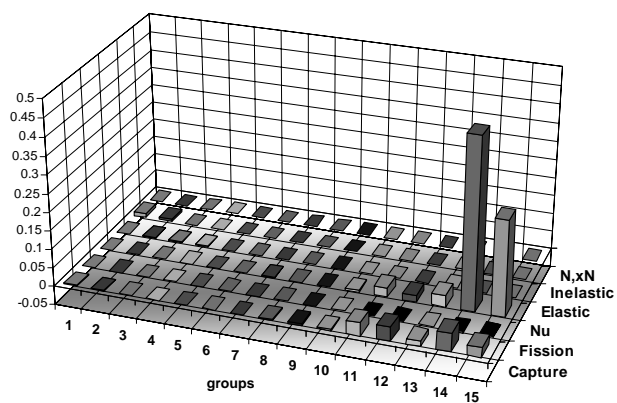


Table 119. VHTR k_{eff} BOC: BOLNA diagonal uncertainty (%) by isotope

Isotope	σ_{cap}	σ_{fiss}	ν	σ_{el}	σ_{inel}	$\sigma_{\text{n,2n}}$	Total
^{235}U	0.10	0.03	0.32	—	—	—	0.34
^{238}U	0.12	—	—	—	—	—	0.12
O	—	—	—	—	—	—	—
Si	0.01	—	—	—	—	—	0.01
C	0.07	—	—	0.02	0.05	—	0.09
Total	0.18	0.03	0.32	0.02	0.05	—	0.37

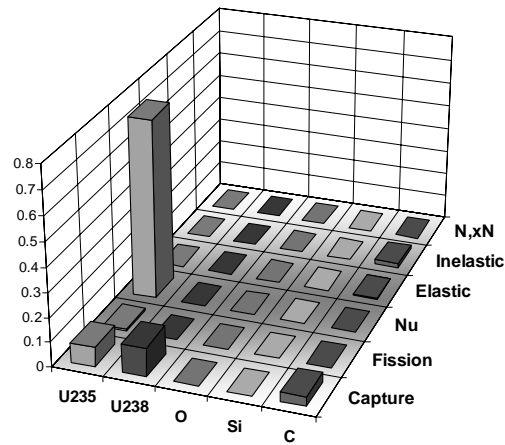


Table 120. VHTR k_{eff} BOC: BOLNA full uncertainty (%) by isotope

Isotope	σ_{cap}	σ_{fiss}	ν	σ_{el}	σ_{inel}	$\sigma_{\text{n,2n}}$	Total
^{235}U	0.13	0.04i	0.47	—	—	—	0.49
^{238}U	0.15	—	—	—	—	—	0.15
O	—	—	—	—	—	—	—
Si	0.01	—	—	—	—	—	0.01
C	0.09	—	—	0.04	0.07	—	0.12
Total	0.22	0.04i	0.47	0.04	0.07	—	0.53

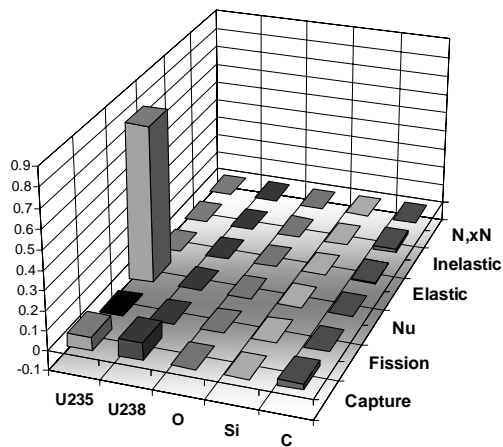


Table 121. VHTR k_{eff} EOC: BOLNA diagonal uncertainty (%) by group

Gr.	[MeV]	σ_{cap}	σ_{fiss}	ν	σ_{el}	σ_{inel}	$\sigma_{\text{n,2n}}$	Total
1	19.6	0.04	—	—	—	0.05	—	0.06
2	6.07	0.01	—	—	0.01	—	—	0.01
3	2.23	—	—	—	0.01	—	—	0.01
4	1.35	—	—	—	0.01	—	—	0.01
5	4.98e-1	—	—	—	—	—	—	—
6	1.83e-1	—	—	—	—	—	—	—
7	6.74e-2	—	—	—	—	—	—	—
8	2.48e-2	0.01	—	—	—	—	—	0.01
9	9.12e-3	0.02	0.01	—	—	—	—	0.02
10	2.03e-3	0.02	0.01	—	—	—	—	0.02
11	4.54e-4	0.11	0.05	0.02	0.01	—	—	0.12
12	2.26e-5	0.12	0.02	0.01	0.01	—	—	0.12
13	4.00e-6	0.09	0.03	0.02	0.01	—	—	0.10
14	5.40e-7	0.21	0.20	0.16	—	—	—	0.34
15	1.00e-7	0.04	0.05	0.09	—	—	—	0.11
Total		0.29	0.22	0.19	0.02	0.05	—	0.41

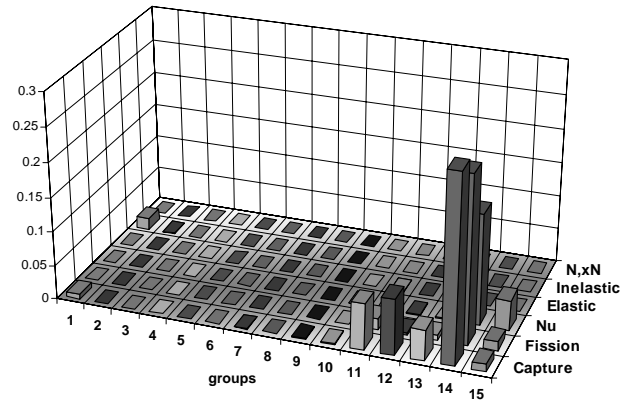


Table 122. VHTR k_{eff} EOC: BOLNA full uncertainty (%) by group

Gr.	[MeV]	σ_{cap}	σ_{fiss}	ν	σ_{el}	σ_{inel}	$\sigma_{\text{n,2n}}$	Total
1	19.6	0.04	—	—	—	0.05	—	0.06
2	6.07	0.01	—	0.01	0.01	0.01i	—	0.01
3	2.23	—	—	0.01	0.01	—	—	0.01
4	1.35	—	—	0.01	0.01	—	—	0.02
5	4.98e-1	0.01	—	0.01	—	—	—	0.01
6	1.83e-1	0.01	—	0.01	—	—	—	0.01
7	6.74e-2	0.01	—	0.01	—	—	—	0.01
8	2.48e-2	0.02	—	0.01	—	—	—	0.02
9	9.12e-3	0.03	0.01	0.02	—	—	—	0.04
10	2.03e-3	0.04	0.02	0.03	0.01	—	—	0.05
11	4.54e-4	0.12	0.06	0.06	0.01	—	—	0.15
12	2.26e-5	0.13	0.04	0.05	0.01	—	—	0.15
13	4.00e-6	0.10	0.06	0.06	0.02	—	—	0.13
14	5.40e-7	0.18	0.17	0.21	—	—	—	0.33
15	1.00e-7	0.07	0.06	0.15	—	—	—	0.18
Total		0.29	0.20	0.28	0.04	0.05	—	0.46

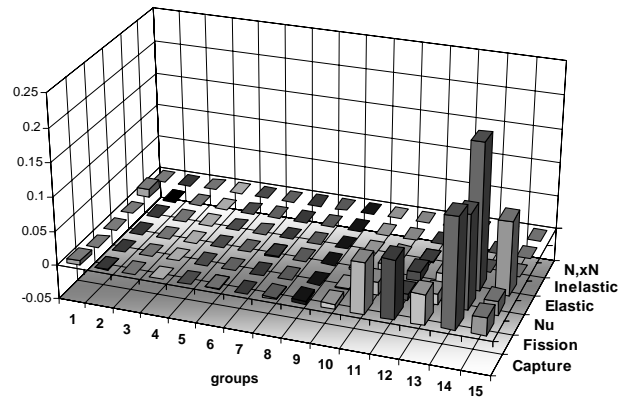


Table 123. VHTR k_{eff} EOC: BOLNA diagonal uncertainty (%) by isotope

Isotope	σ_{cap}	σ_{fiss}	ν	σ_{el}	σ_{inel}	$\sigma_{\text{n,2n}}$	Total
²³⁵ U	0.05	0.03	0.17	—	—	—	0.18
²³⁸ U	0.16	—	—	—	—	—	0.16
²³⁷ Np	0.01	—	—	—	—	—	0.01
²³⁸ Pu	—	—	—	—	—	—	—
²³⁹ Pu	0.16	0.15	0.07	—	—	—	0.24
²⁴⁰ Pu	0.05	—	—	—	—	—	0.05
²⁴¹ Pu	0.12	0.15	0.03	—	—	—	0.19
²⁴² Pu	0.01	—	—	—	—	—	0.01
²⁴¹ Am	—	—	—	—	—	—	—
^{242m} Am	—	—	—	—	—	—	—
²⁴³ Am	—	—	—	—	—	—	—
²⁴² Cm	—	—	—	—	—	—	—
²⁴³ Cm	—	—	—	—	—	—	—
²⁴⁴ Cm	—	—	—	—	—	—	—
²⁴⁵ Cm	—	—	—	—	—	—	—
O	0.01	—	—	—	—	—	0.01
Si	0.01	—	—	—	—	—	0.01
C	0.10	—	—	0.02	0.05	—	0.11
Total	0.29	0.22	0.19	0.02	0.05	—	0.41

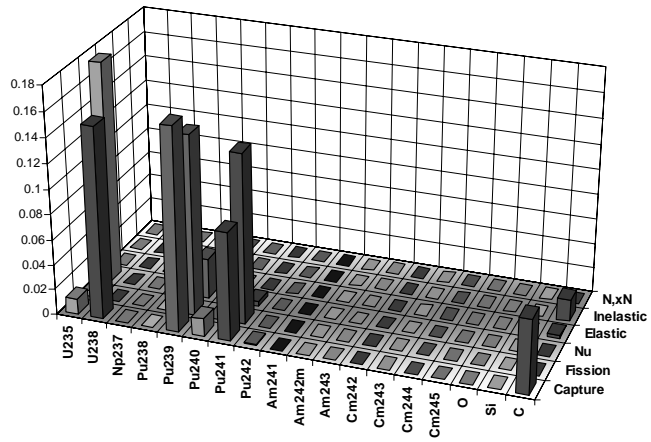


Table 124. VHTR k_{eff} EOC: BOLNA full uncertainty (%) by isotope

Isotope	σ_{cap}	σ_{fiss}	ν	σ_{el}	σ_{inel}	$\sigma_{\text{n,2n}}$	Total
²³⁵ U	0.05	0.03	0.27	—	—	—	0.27
²³⁸ U	0.19	—	—	—	—	—	0.19
²³⁷ Np	0.01	—	—	—	—	—	0.01
²³⁸ Pu	—	—	—	—	—	—	—
²³⁹ Pu	0.11	0.10	0.07	—	—	—	0.17
²⁴⁰ Pu	0.06	—	—	—	—	—	0.06
²⁴¹ Pu	0.13	0.18	0.04	—	—	—	0.22
²⁴² Pu	0.02	—	—	—	—	—	0.02
²⁴¹ Am	—	—	—	—	—	—	—
²⁴² Am	—	—	—	—	—	—	—
²⁴³ Am	—	—	—	—	—	—	—
²⁴² Cm	—	—	—	—	—	—	—
²⁴³ Cm	—	—	—	—	—	—	—
²⁴⁴ Cm	—	—	—	—	—	—	—
²⁴⁵ Cm	—	—	—	—	—	—	—
O	0.01	—	—	—	—	—	0.01
Si	0.01	—	—	—	—	—	0.01
C	0.12	—	—	0.04	0.05	—	0.13
Total	0.29	0.20	0.28	0.04	0.05	—	0.46

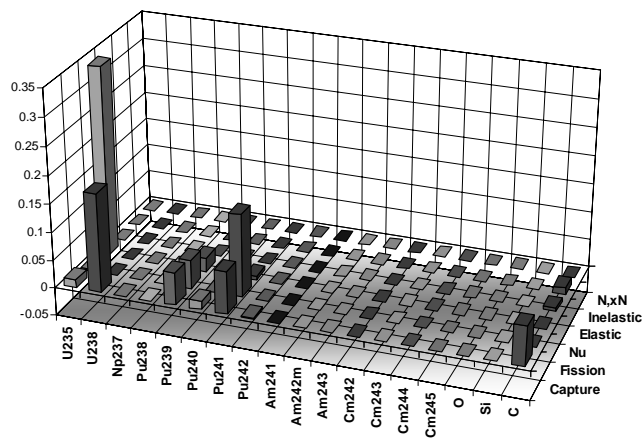


Table 125. VHTR power peak BOC: BOLNA diagonal uncertainty (%) by group

Gr.	[MeV]	σ_{cap}	σ_{fiss}	ν	σ_{el}	σ_{inel}	$\sigma_{\text{n,2n}}$	Total
1	19.6	0.02	—	—	0.01	0.04	—	0.04
2	6.07	—	—	—	0.12	0.75	—	0.75
3	2.23	—	—	—	0.13	0.01	—	0.13
4	1.35	—	—	—	0.21	—	—	0.21
5	4.98e-1	—	—	—	0.13	—	—	0.13
6	1.83e-1	—	—	—	0.06	—	—	0.06
7	6.74e-2	—	—	—	0.06	—	—	0.06
8	2.48e-2	—	—	—	0.05	—	—	0.05
9	9.12e-3	—	—	—	0.08	—	—	0.08
10	2.03e-3	—	—	—	0.07	—	—	0.07
11	4.54e-4	0.01	0.01	0.01	0.12	—	—	0.12
12	2.26e-5	—	0.01	0.01	0.03	—	—	0.03
13	4.00e-6	0.04	0.01	0.01	0.03	—	—	0.05
14	5.40e-7	0.05	0.05	0.05	0.12	—	—	0.15
15	1.00e-7	0.03	0.02	0.02	0.04	—	—	0.06
Total		0.07	0.06	0.06	0.38	0.75	—	0.85

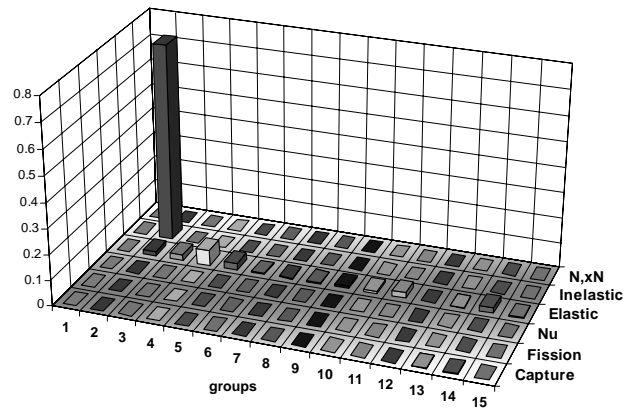


Table 126. VHTR power peak BOC: BOLNA full uncertainty (%) by group

Gr.	[MeV]	σ_{cap}	σ_{fiss}	ν	σ_{el}	σ_{inel}	$\sigma_{\text{n,2n}}$	Total
1	19.6	0.02	—	—	0.07	0.17	—	0.19
2	6.07	—	—	—	0.23	0.76	—	0.80
3	2.23	—	—	—	0.25	0.02	—	0.25
4	1.35	—	—	—	0.31	0.01	—	0.31
5	4.98e-1	—	—	—	0.16	—	—	0.16
6	1.83e-1	—	—	—	0.11	—	—	0.11
7	6.74e-2	—	—	—	0.10	—	—	0.10
8	2.48e-2	—	—	0.01	0.10	—	—	0.10
9	9.12e-3	0.01	—	0.01	0.12	—	—	0.12
10	2.03e-3	—	0.01	0.01	0.12	—	—	0.12
11	4.54e-4	0.01	0.02	0.03	0.15	—	—	0.16
12	2.26e-5	0.01	0.02	0.03	0.07	—	—	0.08
13	4.00e-6	0.04	0.03	0.03	0.08i	—	—	0.05i
14	5.40e-7	0.07	0.08	0.07	0.14	—	—	0.19
15	1.00e-7	0.06	0.05	0.05	0.08	—	—	0.12
Total		0.10	0.10	0.10	0.59	0.78	—	1.00

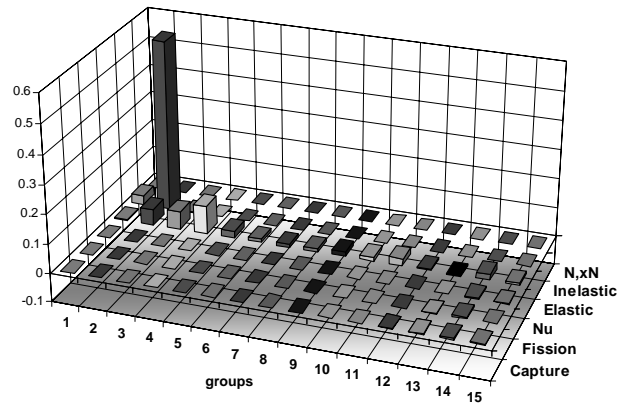


Table 127. VHTR power peak BOC: BOLNA diagonal uncertainty (%) by isotope

Isotope	σ_{cap}	σ_{fiss}	ν	σ_{el}	σ_{inel}	$\sigma_{\text{n,2n}}$	Total
²³⁵ U	0.03	0.06	0.06	—	—	—	0.09
²³⁸ U	0.01	—	—	—	0.01	—	0.02
O	—	—	—	—	—	—	—
Si	—	—	—	—	0.01	—	0.01
C	0.06	—	—	0.38	0.75	—	0.84
Total	0.07	0.06	0.06	0.38	0.75	—	0.85

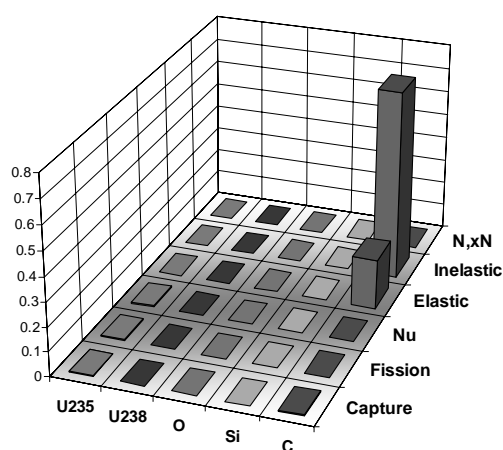


Table 128. VHTR power peak BOC: BOLNA full uncertainty (%) by isotope

Isotope	σ_{cap}	σ_{fiss}	ν	σ_{el}	σ_{inel}	$\sigma_{\text{n,2n}}$	Total
²³⁵ U	0.07	0.10	0.10	0.01	—	—	0.15
²³⁸ U	0.01	—	—	—	0.02	—	0.02
O	—	—	—	—	—	—	—
Si	—	—	—	—	0.01	—	0.01
C	0.08	—	—	0.59	0.78	—	0.99
Total	0.10	0.10	0.10	0.59	0.78	—	1.00

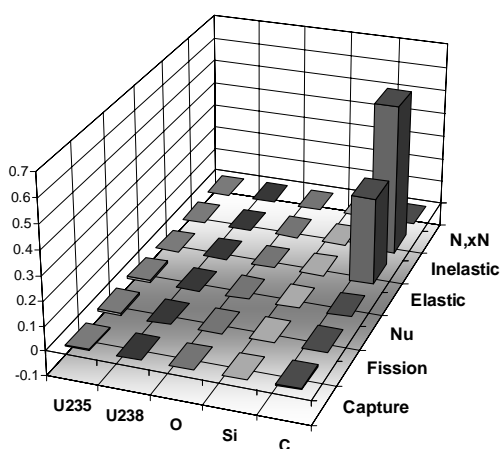


Table 129. VHTR power peak EOC: BOLNA diagonal uncertainty (%) by group

Gr.	[MeV]	σ_{cap}	σ_{fiss}	ν	σ_{el}	σ_{inel}	$\sigma_{\text{n,2n}}$	Total
1	19.6	0.02	—	—	0.01	0.04	—	0.05
2	6.07	—	—	—	0.12	0.79	—	0.80
3	2.23	—	—	—	0.14	0.01	—	0.14
4	1.35	—	—	—	0.22	—	—	0.22
5	4.98e-1	—	—	—	0.14	—	—	0.14
6	1.83e-1	—	—	—	0.06	—	—	0.06
7	6.74e-2	—	—	—	0.06	—	—	0.06
8	2.48e-2	—	—	—	0.06	—	—	0.06
9	9.12e-3	—	—	—	0.08	—	—	0.08
10	2.03e-3	—	—	—	0.08	—	—	0.08
11	4.54e-4	0.01	0.03	0.01	0.13	—	—	0.14
12	2.26e-5	—	0.02	0.01	0.03	—	—	0.04
13	4.00e-6	0.05	0.02	—	0.05	—	—	0.08
14	5.40e-7	0.07	0.11	0.01	0.15	—	—	0.19
15	1.00e-7	0.02	0.02	0.01	0.04	—	—	0.05
Total		0.09	0.12	0.02	0.41	0.79	—	0.90

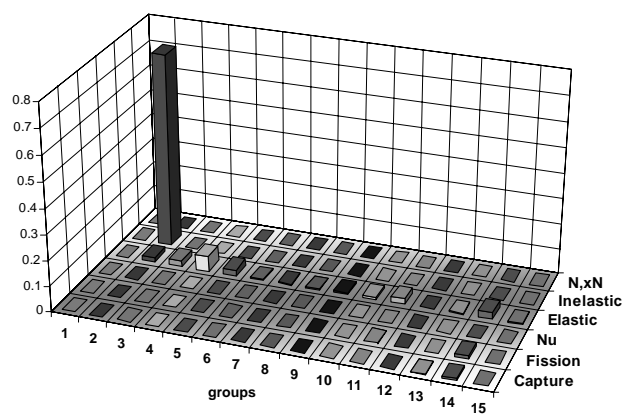


Table 130. VHTR power peak EOC: BOLNA full uncertainty (%) by group

Gr.	[MeV]	σ_{cap}	σ_{fiss}	ν	σ_{el}	σ_{inel}	$\sigma_{\text{n,2n}}$	Total
1	19.6	0.02	—	—	0.07	0.19	—	0.20
2	6.07	—	—	—	0.25	0.81	—	0.85
3	2.23	—	—	—	0.26	0.02	—	0.26
4	1.35	—	—	—	0.33	0.01	—	0.33
5	4.98e-1	—	—	—	0.17	—	—	0.17
6	1.83e-1	—	—	—	0.11	—	—	0.11
7	6.74e-2	—	—	—	0.11	—	—	0.11
8	2.48e-2	—	—	—	0.10	—	—	0.10
9	9.12e-3	—	—	—	0.12	—	—	0.12
10	2.03e-3	—	0.01	0.01	0.12	—	—	0.12
11	4.54e-4	0.01	0.04	0.02	0.16	—	—	0.16
12	2.26e-5	0.01	0.03	0.01	0.08	—	—	0.08
13	4.00e-6	0.05	0.04	0.01	0.10i	—	—	0.08i
14	5.40e-7	0.10	0.12	0.02	0.16	—	—	0.23
15	1.00e-7	0.04	0.04	0.01	0.09	—	—	0.11
Total		0.12	0.15	0.04	0.62	0.83	—	1.06

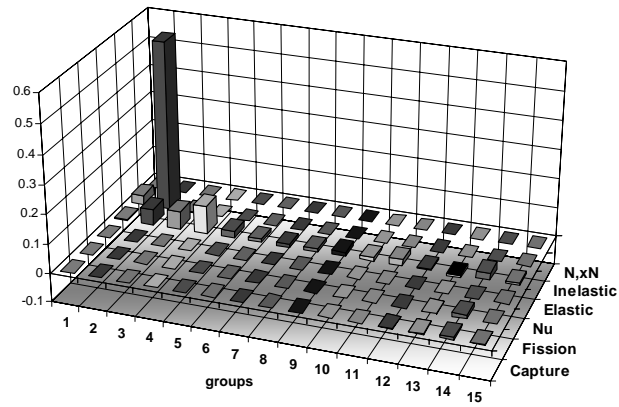


Table 131. VHTR power peak EOC: BOLNA diagonal uncertainty (%) by isotope

Isotope	σ_{cap}	σ_{fiss}	ν	σ_{el}	σ_{inel}	$\sigma_{\text{n,2n}}$	Total
²³⁵ U	0.01	0.02	0.02	—	—	—	0.03
²³⁸ U	0.01	—	—	—	0.01	—	0.02
²³⁷ Np	—	—	—	—	—	—	—
²³⁸ Pu	—	—	—	—	—	—	—
²³⁹ Pu	0.05	0.08	0.01	—	—	—	0.10
²⁴⁰ Pu	0.01	—	—	—	—	—	0.01
²⁴¹ Pu	0.04	0.08	—	—	—	—	0.09
²⁴² Pu	—	—	—	—	—	—	—
²⁴¹ Am	—	—	—	—	—	—	—
^{242m} Am	—	—	—	—	—	—	—
²⁴³ Am	—	—	—	—	—	—	—
²⁴² Cm	—	—	—	—	—	—	—
²⁴³ Cm	—	—	—	—	—	—	—
²⁴⁴ Cm	—	—	—	—	—	—	—
²⁴⁵ Cm	—	—	—	—	—	—	—
O	—	—	—	—	—	—	—
Si	—	—	—	—	0.01	—	0.01
C	0.06	—	—	0.41	0.79	—	0.89
Total	0.09	0.12	0.02	0.41	0.79	—	0.90

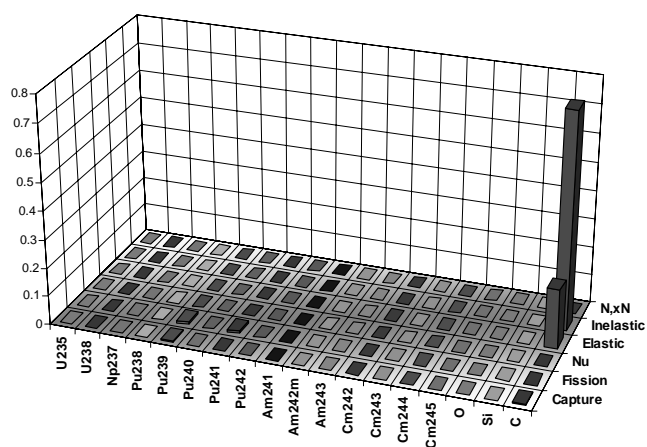


Table 132. VHTR power peak EOC: BOLNA full uncertainty (%) by isotope

Isotope	σ_{cap}	σ_{fiss}	ν	σ_{el}	σ_{inel}	$\sigma_{\text{n,2n}}$	Total
²³⁵ U	0.03	0.04	0.04	—	—	—	0.06
²³⁸ U	0.01	—	—	—	0.02	—	0.02
²³⁷ Np	—	—	—	—	—	—	—
²³⁸ Pu	—	—	—	—	—	—	—
²³⁹ Pu	0.08	0.10	0.01	—	—	—	0.13
²⁴⁰ Pu	0.01	—	—	—	—	—	0.01
²⁴¹ Pu	0.04	0.10	—	—	—	—	0.10
²⁴² Pu	—	—	—	—	—	—	—
²⁴¹ Am	—	—	—	—	—	—	—
^{242m} Am	—	—	—	—	—	—	—
²⁴³ Am	—	—	—	—	—	—	—
²⁴² Cm	—	—	—	—	—	—	—
²⁴³ Cm	—	—	—	—	—	—	—
²⁴⁴ Cm	—	—	—	—	—	—	—
²⁴⁵ Cm	—	—	—	—	—	—	—
O	—	—	—	—	—	—	—
Si	—	—	—	—	0.01	—	0.01
C	0.08	—	—	0.62	0.83	—	1.04
Total	0.12	0.15	0.04	0.62	0.83	—	1.06

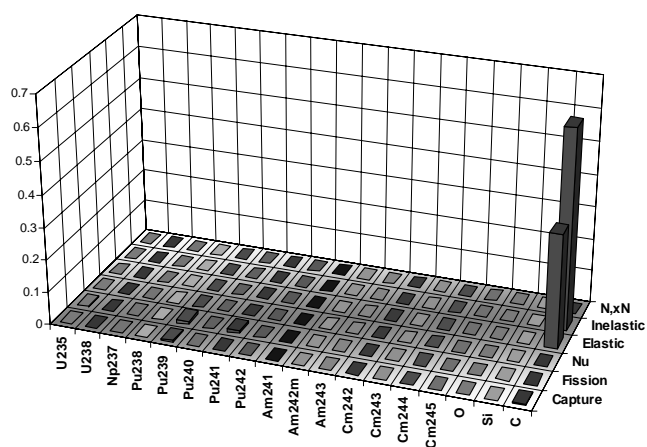


Table 133. VHTR Doppler BOC: BOLNA diagonal uncertainty (%) by group

Gr.	[MeV]	σ_{cap}	σ_{fiss}	ν	σ_{el}	σ_{inel}	$\sigma_{\text{n,2n}}$	Total
1	19.6	0.04	—	—	—	0.02	—	0.05
2	6.07	0.01	—	—	0.06	0.52	—	0.52
3	2.23	—	—	—	0.07	0.01	—	0.07
4	1.35	—	—	—	0.12	—	—	0.12
5	4.98e-1	—	—	—	0.08	—	—	0.08
6	1.83e-1	0.01	—	—	0.04	—	—	0.04
7	6.74e-2	0.01	—	—	0.03	—	—	0.04
8	2.48e-2	0.02	—	—	0.03	—	—	0.04
9	9.12e-3	0.03	0.02	0.01	0.05	—	—	0.06
10	2.03e-3	0.03	0.01	0.01	0.05	—	—	0.06
11	4.54e-4	0.52	0.03	0.06	0.07	—	—	0.53
12	2.26e-5	0.57	0.03	0.03	0.01	—	—	0.57
13	4.00e-6	1.07	0.06	0.38	0.02	—	—	1.14
14	5.40e-7	0.91	0.31	2.74	0.09	—	—	2.90
15	1.00e-7	0.99	0.17	2.56	0.07	—	—	2.75
Total		1.89	0.36	3.76	0.24	0.52	—	4.27

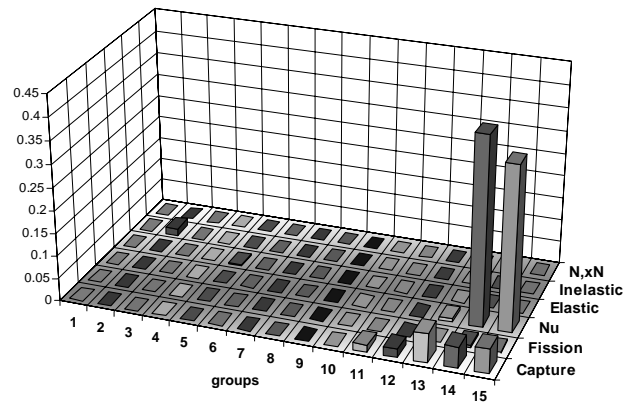


Table 134. VHTR Doppler BOC: BOLNA full uncertainty (%) by group

Gr.	[MeV]	σ_{cap}	σ_{fiss}	ν	σ_{el}	σ_{inel}	$\sigma_{\text{n,2n}}$	Total
1	19.6	0.04	—	0.01	0.04	0.10i	—	0.08i
2	6.07	0.01	—	0.02	0.13	0.51	—	0.52
3	2.23	—	—	0.02	0.14	0.01	—	0.14
4	1.35	0.01	—	0.03	0.18	—	—	0.18
5	4.98e-1	0.01	—	0.03	0.10	—	—	0.10
6	1.83e-1	0.02	—	0.03	0.07	—	—	0.07
7	6.74e-2	0.02	—	0.03	0.06	—	—	0.07
8	2.48e-2	0.03	—	0.04	0.06	—	—	0.08
9	9.12e-3	0.06	0.02	0.06	0.07	—	—	0.11
10	2.03e-3	0.10	0.02	0.09	0.08	—	—	0.15
11	4.54e-4	0.58	0.05	0.19	0.10	—	—	0.62
12	2.26e-5	0.63	0.05	0.14	0.03	—	—	0.65
13	4.00e-6	1.08	0.11	0.48	0.06	—	—	1.19
14	5.40e-7	0.07	0.27	1.09	0.12	—	—	1.13
15	1.00e-7	0.38	0.21i	1.05i	0.11	—	—	1.00i
Total		1.44	0.21	0.61	0.38	0.50	—	1.70

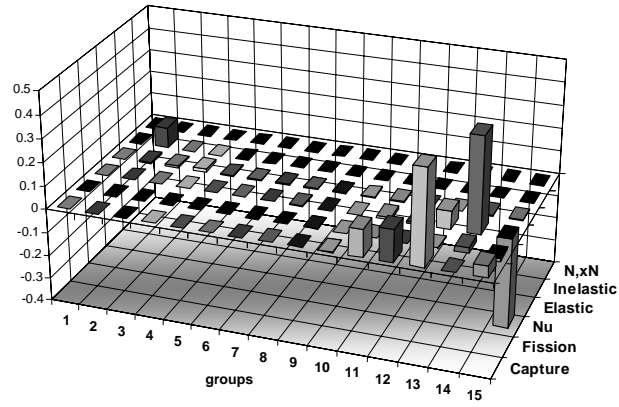


Table 135. VHTR Doppler BOC: BOLNA diagonal uncertainty (%) by isotope

Isotope	σ_{cap}	σ_{fiss}	ν	σ_{el}	σ_{inel}	$\sigma_{\text{n,2n}}$	Total
²³⁵ U	1.19	0.36	3.76	—	—	—	3.96
²³⁸ U	0.81	—	0.01	—	0.01	—	0.81
²³⁷ Np	—	—	—	—	—	—	—
²³⁸ Pu	—	—	—	—	—	—	—
²³⁹ Pu	—	—	—	—	—	—	—
²⁴⁰ Pu	—	—	—	—	—	—	—
²⁴¹ Pu	—	—	—	—	—	—	—
²⁴² Pu	—	—	—	—	—	—	—
²⁴¹ Am	—	—	—	—	—	—	—
^{242m} Am	—	—	—	—	—	—	—
²⁴³ Am	—	—	—	—	—	—	—
²⁴² Cm	—	—	—	—	—	—	—
²⁴³ Cm	—	—	—	—	—	—	—
²⁴⁴ Cm	—	—	—	—	—	—	—
²⁴⁵ Cm	—	—	—	—	—	—	—
O	0.01	—	—	—	—	—	0.01
Si	0.09	—	—	—	0.01	—	0.09
C	1.22	—	—	0.24	0.52	—	1.35
Total	1.89	0.36	3.76	0.24	0.52	—	4.27

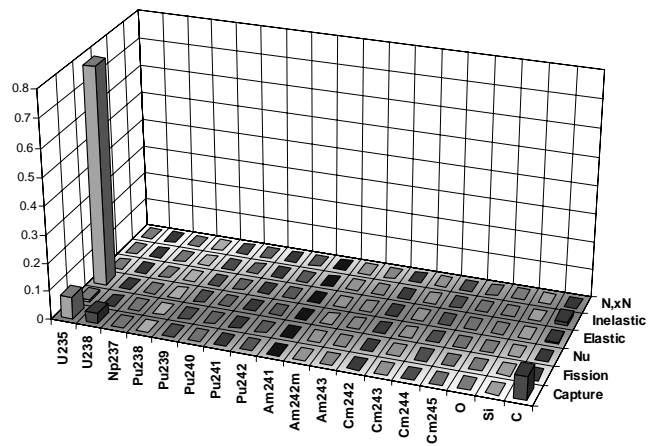


Table 136. VHTR Doppler BOC: BOLNA full uncertainty (%) by isotope

Isotope	σ_{cap}	σ_{fiss}	ν	σ_{el}	σ_{inel}	$\sigma_{\text{n,2n}}$	Total
²³⁵ U	0.36	0.21	0.61	0.01	—	—	0.74
²³⁸ U	0.87	—	0.01	0.01	0.01	—	0.87
²³⁷ Np	—	—	—	—	—	—	—
²³⁸ Pu	—	—	—	—	—	—	—
²³⁹ Pu	—	—	—	—	—	—	—
²⁴⁰ Pu	—	—	—	—	—	—	—
²⁴¹ Pu	—	—	—	—	—	—	—
²⁴² Pu	—	—	—	—	—	—	—
²⁴¹ Am	—	—	—	—	—	—	—
^{242m} Am	—	—	—	—	—	—	—
²⁴³ Am	—	—	—	—	—	—	—
²⁴² Cm	—	—	—	—	—	—	—
²⁴³ Cm	—	—	—	—	—	—	—
²⁴⁴ Cm	—	—	—	—	—	—	—
²⁴⁵ Cm	—	—	—	—	—	—	—
O	0.01	—	—	—	—	—	0.01
Si	0.02	—	—	—	0.01	—	0.02
C	1.09	—	—	0.38	0.50	—	1.26
Total	1.44	0.21	0.61	0.38	0.50	—	1.70

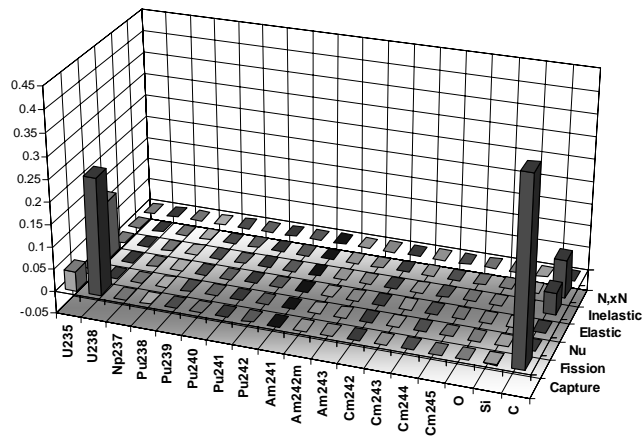


Table 137. VHTR Doppler EOC: BOLNA diagonal uncertainty (%) by group

Gr.	[MeV]	σ_{cap}	σ_{fiss}	ν	σ_{el}	σ_{inel}	$\sigma_{\text{n,2n}}$	Total
1	19.6	0.04	—	—	—	0.03	—	0.05
2	6.07	0.01	—	—	0.03	0.36	—	0.36
3	2.23	—	—	—	0.04	0.01	—	0.04
4	1.35	—	—	—	0.07	—	—	0.07
5	4.98e-1	—	—	—	0.05	—	—	0.05
6	1.83e-1	—	—	—	0.02	—	—	0.02
7	6.74e-2	—	—	—	0.02	—	—	0.02
8	2.48e-2	0.01	—	—	0.02	—	—	0.02
9	9.12e-3	0.01	0.01	—	0.03	—	—	0.03
10	2.03e-3	0.02	0.02	0.01	0.03	—	—	0.04
11	4.54e-4	0.42	0.12	0.04	0.04	—	—	0.44
12	2.26e-5	0.48	0.05	0.02	—	—	—	0.48
13	4.00e-6	0.98	0.23	0.14	0.03	—	—	1.02
14	5.40e-7	1.10	1.28	0.72	0.02	—	—	1.84
15	1.00e-7	0.74	0.64	1.31	0.05	—	—	1.64
Total		1.77	1.46	1.50	0.13	0.36	—	2.77

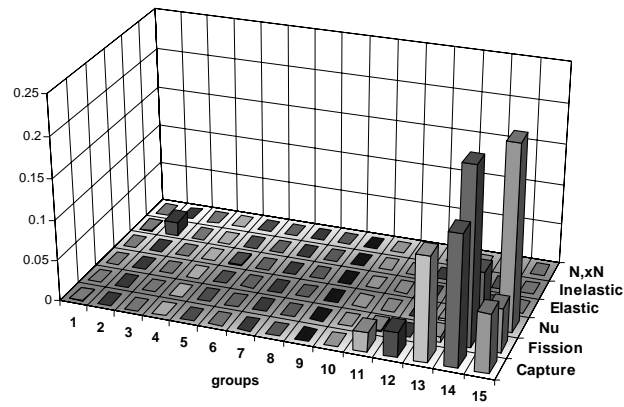


Table 138. VHTR Doppler EOC: BOLNA full uncertainty (%) by group

Gr.	[MeV]	σ_{cap}	σ_{fiss}	ν	σ_{el}	σ_{inel}	$\sigma_{\text{n,2n}}$	Total
1	19.6	0.04	—	—	0.02	0.10i	—	0.09i
2	6.07	0.01	—	—	0.07	0.35	—	0.36
3	2.23	—	0.01	—	0.08	0.01	—	0.08
4	1.35	—	0.01	0.01i	0.10	—	—	0.10
5	4.98e-1	—	—	0.01i	0.05	—	—	0.05
6	1.83e-1	0.01	0.01	0.01i	0.04	—	—	0.04
7	6.74e-2	0.01	—	0.01i	0.04	—	—	0.04
8	2.48e-2	0.02	—	0.01i	0.04	—	—	0.04
9	9.12e-3	0.04	0.02	0.02i	0.04	—	—	0.06
10	2.03e-3	0.08	—	0.03i	0.03	—	—	0.08
11	4.54e-4	0.46	0.12	0.07i	0.03	—	—	0.47
12	2.26e-5	0.52	0.11	0.06i	0.01i	—	—	0.53
13	4.00e-6	0.99	0.14i	0.16i	0.03i	—	—	0.97
14	5.40e-7	0.63	0.96	0.37i	0.04	—	—	1.09
15	1.00e-7	0.50	0.38	0.94	0.06	—	—	1.13
Total		1.46	1.04	0.84	0.19	0.33	—	2.01

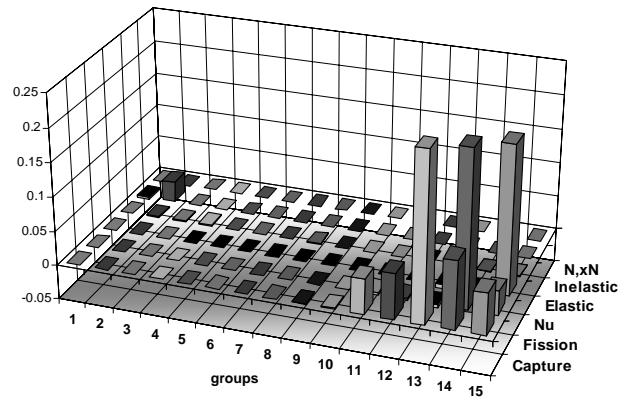


Table 139. VHTR Doppler EOC: BOLNA diagonal uncertainty (%) by isotope

Isotope	σ_{cap}	σ_{fiss}	ν	σ_{el}	σ_{inel}	$\sigma_{\text{n,2n}}$	Total
²³⁵ U	0.37	0.20	1.42	—	—	—	1.48
²³⁸ U	0.66	—	0.01	—	0.01	—	0.66
²³⁷ Np	0.04	—	—	—	—	—	0.04
²³⁸ Pu	0.01	—	—	—	—	—	0.01
²³⁹ Pu	0.99	1.16	0.49	—	—	—	1.60
²⁴⁰ Pu	0.35	—	—	—	—	—	0.35
²⁴¹ Pu	0.54	0.86	0.15	—	—	—	1.02
²⁴² Pu	0.05	—	—	—	—	—	0.05
²⁴¹ Am	0.02	—	—	—	—	—	0.02
^{242m} Am	—	0.01	—	—	—	—	0.01
²⁴³ Am	0.01	—	—	—	—	—	0.01
²⁴² Cm	—	—	—	—	—	—	—
²⁴³ Cm	—	—	—	—	—	—	—
²⁴⁴ Cm	—	—	—	—	—	—	—
²⁴⁵ Cm	—	—	—	—	—	—	—
O	0.01	—	—	—	—	—	0.01
Si	0.06	—	—	—	—	—	0.06
C	1.08	—	—	0.13	0.36	—	1.15
Total	1.77	1.46	1.50	0.13	0.36	—	2.77

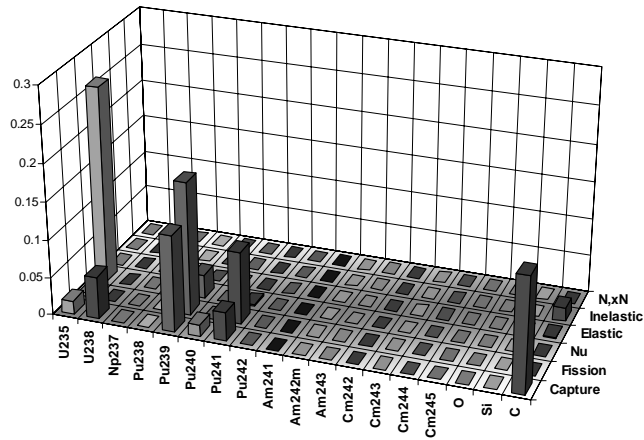


Table 140. VHTR Doppler EOC: BOLNA full uncertainty (%) by isotope

Isotope	σ_{cap}	σ_{fiss}	ν	σ_{el}	σ_{inel}	$\sigma_{\text{n,2n}}$	Total
²³⁵ U	0.25	0.03	0.68	—	—	—	0.73
²³⁸ U	0.67	—	0.01	—	0.01	—	0.67
²³⁷ Np	0.04	—	—	—	—	—	0.04
²³⁸ Pu	0.01	—	—	—	—	—	0.01
²³⁹ Pu	0.46	0.72	0.49	—	—	—	0.98
²⁴⁰ Pu	0.26	—	—	—	—	—	0.26
²⁴¹ Pu	0.54	0.75	0.01	—	—	—	0.93
²⁴² Pu	0.05	—	—	—	—	—	0.05
²⁴¹ Am	0.02	—	—	—	—	—	0.02
^{242m} Am	—	—	—	—	—	—	—
²⁴³ Am	0.01	—	—	—	—	—	0.01
²⁴² Cm	—	—	—	—	—	—	—
²⁴³ Cm	—	—	—	—	—	—	—
²⁴⁴ Cm	—	—	—	—	—	—	—
²⁴⁵ Cm	—	—	—	—	—	—	—
O	0.01	—	—	—	—	—	0.01
Si	0.03	—	—	—	—	—	0.03
C	1.01	—	—	0.19	0.33	—	1.09
Total	1.46	1.04	0.84	0.19	0.33	—	2.01

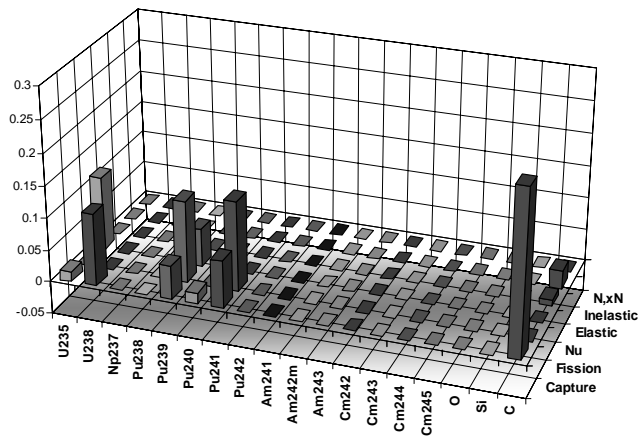


Table 141. VHTR XS burn-up: BOLNA diagonal uncertainty (%) by group

Gr.	[MeV]	σ_{cap}	σ_{fiss}	ν	σ_{el}	σ_{inel}	$\sigma_{\text{n,2n}}$	Total
1	19.6	0.04	—	—	—	0.05	—	0.06
2	6.07	0.01	—	—	—	0.12	—	0.12
3	2.23	—	—	—	—	—	—	0.01
4	1.35	—	—	—	0.01	—	—	0.01
5	4.98e-1	—	—	—	0.01	—	—	0.01
6	1.83e-1	0.01	—	—	—	—	—	0.01
7	6.74e-2	0.01	—	—	—	—	—	0.01
8	2.48e-2	0.02	—	—	—	—	—	0.02
9	9.12e-3	0.04	0.01	—	—	—	—	0.04
10	2.03e-3	0.02	0.02	—	—	—	—	0.03
11	4.54e-4	0.09	0.20	0.02	—	—	—	0.22
12	2.26e-5	0.11	0.09	0.02	0.01	—	—	0.14
13	4.00e-6	0.19	0.13	0.04	0.02	—	—	0.23
14	5.40e-7	0.81	0.77	0.58	0.02	—	—	1.26
15	1.00e-7	0.15	0.18	0.27	—	—	—	0.35
Total		0.86	0.83	0.64	0.03	0.13	—	1.37

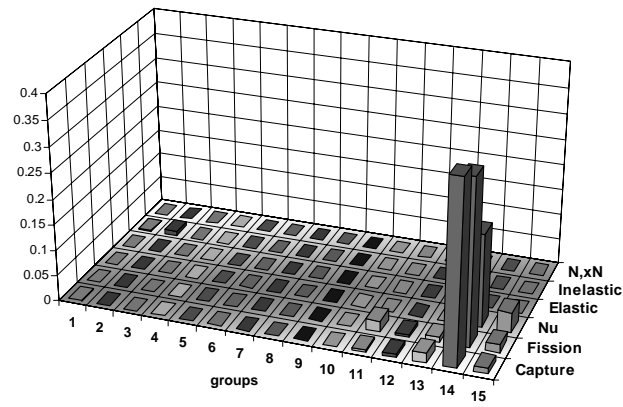


Table 142. VHTR XS burn-up: BOLNA full uncertainty (%) by group

Gr.	[MeV]	σ_{cap}	σ_{fiss}	ν	σ_{el}	σ_{inel}	$\sigma_{\text{n,2n}}$	Total
1	19.6	0.04	—	—	—	0.06i	—	0.04i
2	6.07	0.01	—	0.01	0.01	0.09	—	0.09
3	2.23	—	0.01	0.01	0.01	—	—	0.02
4	1.35	0.01	0.01	0.01	0.01	—	—	0.02
5	4.98e-1	0.01	0.01	0.01	0.01	—	—	0.02
6	1.83e-1	0.02	0.01	0.02	0.01	—	—	0.03
7	6.74e-2	0.03	0.01	0.02	0.01	—	—	0.03
8	2.48e-2	0.03	0.01	0.02	0.01	—	—	0.04
9	9.12e-3	0.06	0.01	0.03	0.01	—	—	0.06
10	2.03e-3	0.04	0.07	0.04	0.01	—	—	0.09
11	4.54e-4	0.11	0.24	0.09	0.01i	—	—	0.28
12	2.26e-5	0.15	0.16	0.08	0.01	—	—	0.24
13	4.00e-6	0.21	0.22	0.13	0.02	—	—	0.33
14	5.40e-7	0.68	0.65	0.70	0.02	—	—	1.17
15	1.00e-7	0.24	0.24	0.47	0.01	—	—	0.58
Total		0.78	0.79	0.87	0.04	0.07	—	1.41

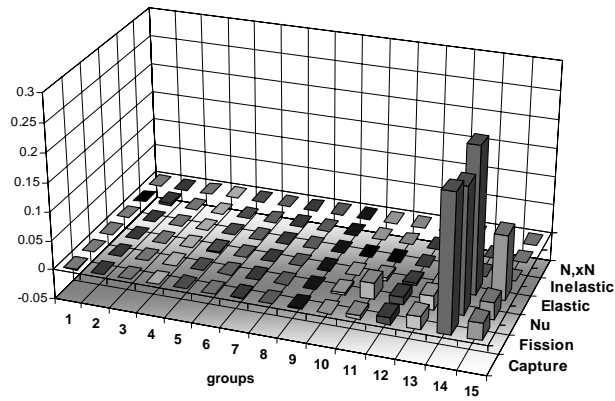


Table 143. VHTR XS burn-up: BOLNA diagonal uncertainty (%) by isotope

Isotope	σ_{cap}	σ_{fiss}	ν	σ_{el}	σ_{inel}	$\sigma_{\text{n,2n}}$	Total
²³⁵ U	0.23	0.01	0.57	—	—	—	0.61
²³⁸ U	0.14	—	0.01	—	—	—	0.14
²³⁷ Np	0.02	—	—	—	—	—	0.02
²³⁸ Pu	—	—	—	—	—	—	—
²³⁹ Pu	0.64	0.60	0.28	—	—	—	0.92
²⁴⁰ Pu	0.19	—	—	—	—	—	0.19
²⁴¹ Pu	0.46	0.58	0.10	—	—	—	0.75
²⁴² Pu	0.06	—	—	—	—	—	0.06
²⁴¹ Am	0.01	—	—	—	—	—	0.01
^{242m} Am	—	—	—	—	—	—	—
²⁴³ Am	0.01	—	—	—	—	—	0.01
²⁴² Cm	—	—	—	—	—	—	—
²⁴³ Cm	—	—	—	—	—	—	—
²⁴⁴ Cm	—	—	—	—	—	—	—
²⁴⁵ Cm	—	—	—	—	—	—	—
O	0.01	—	—	—	—	—	0.01
Si	—	—	—	—	—	—	—
C	0.11	—	—	0.03	0.13	—	0.17
Total	0.86	0.83	0.64	0.03	0.13	—	1.37

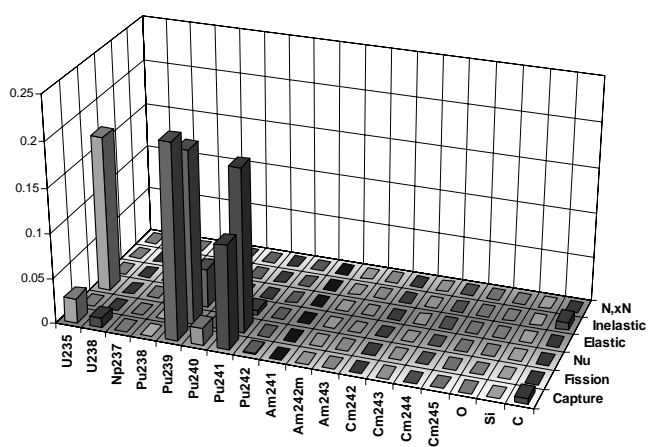


Table 144. VHTR XS burn-up: BOLNA full uncertainty (%) by isotope

Isotope	σ_{cap}	σ_{fiss}	ν	σ_{el}	σ_{inel}	$\sigma_{\text{n,2n}}$	Total
²³⁵ U	0.31	0.04i	0.81	—	—	—	0.86
²³⁸ U	0.15	—	0.01	—	—	—	0.15
²³⁷ Np	0.02	—	—	—	—	—	0.02
²³⁸ Pu	—	—	—	—	—	—	—
²³⁹ Pu	0.43	0.40	0.28	—	—	—	0.65
²⁴⁰ Pu	0.22	—	—	—	—	—	0.22
²⁴¹ Pu	0.49	0.68	0.15	—	—	—	0.85
²⁴² Pu	0.06	—	—	—	—	—	0.06
²⁴¹ Am	0.01	—	—	—	—	—	0.01
^{242m} Am	—	0.01	—	—	—	—	0.01
²⁴³ Am	0.01	—	—	—	—	—	0.01
²⁴² Cm	—	—	—	—	—	—	—
²⁴³ Cm	—	—	—	—	—	—	—
²⁴⁴ Cm	—	—	—	—	—	—	—
²⁴⁵ Cm	—	—	—	—	—	—	—
O	0.01	—	—	—	—	—	0.01
Si	—	—	—	—	—	—	0.01
C	0.12	—	—	0.04	0.07	—	0.15
Total	0.78	0.79	0.87	0.04	0.07	—	1.41

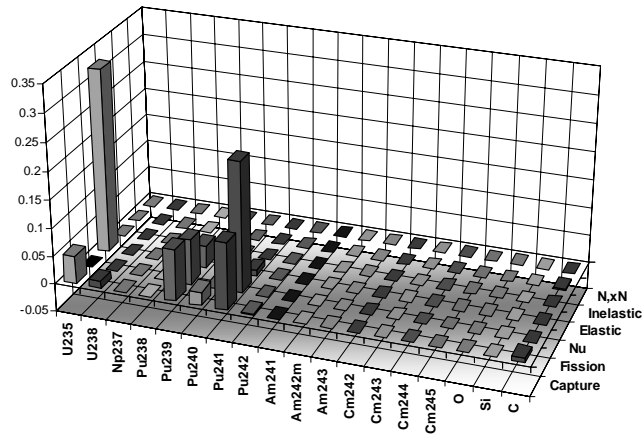


Table 145. PWR k_{eff} BOC: BOLNA diagonal uncertainty (%) by group

Gr.	[MeV]	σ_{cap}	σ_{fiss}	ν	σ_{el}	σ_{inel}	$\sigma_{\text{n,2n}}$	Total
1	19.6	0.12	—	—	—	0.01	—	0.12
2	6.07	0.20	—	0.02	—	0.03	—	0.21
3	2.23	0.01	—	0.01	—	0.02	—	0.02
4	1.35	0.01	—	—	—	—	—	0.01
5	4.98e-1	0.01	—	—	—	—	—	0.01
6	1.83e-1	0.01	—	—	—	—	—	0.01
7	6.74e-2	0.02	—	—	—	—	—	0.02
8	2.48e-2	0.04	—	—	—	—	—	0.04
9	9.12e-3	0.05	0.01	—	—	—	—	0.05
10	2.03e-3	0.03	—	0.01	—	—	—	0.03
11	4.54e-4	0.07	0.01	0.04	—	—	—	0.08
12	2.26e-5	0.05	0.01	0.02	—	0.01	—	0.06
13	4.00e-6	0.02	—	0.03	—	—	—	0.04
14	5.40e-7	0.05	0.01	0.15	—	—	—	0.16
15	1.00e-7	0.06	0.01	0.17	—	—	—	0.18
Total		0.27	0.03	0.24	—	0.04	—	0.36

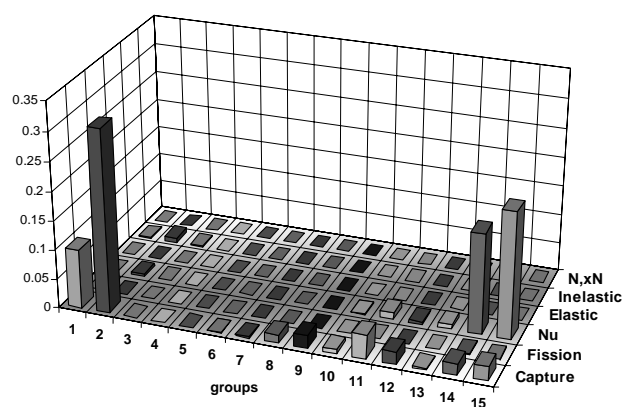


Table 146. PWR k_{eff} BOC: BOLNA full uncertainty (%) by group

Gr.	[MeV]	σ_{cap}	σ_{fiss}	ν	σ_{el}	σ_{inel}	$\sigma_{\text{n,2n}}$	Total
1	19.6	0.12	—	0.01	—	0.02	—	0.13
2	6.07	0.21	0.01	0.04	—	0.04	—	0.22
3	2.23	0.01	—	0.03	—	0.03	—	0.04
4	1.35	0.02	—	0.03	—	—	—	0.03
5	4.98e-1	0.03	—	0.02	—	—	—	0.04
6	1.83e-1	0.04	—	0.02	—	—	—	0.04
7	6.74e-2	0.04	—	0.02	—	—	—	0.05
8	2.48e-2	0.06	—	0.02	—	—	—	0.07
9	9.12e-3	0.08	—	0.03	—	0.01	—	0.09
10	2.03e-3	0.05	—	0.05	—	0.01	—	0.07
11	4.54e-4	0.09	0.01i	0.10	—	0.01	—	0.14
12	2.26e-5	0.07	0.01i	0.08	—	—	—	0.10
13	4.00e-6	0.04	—	0.10	—	—	—	0.10
14	5.40e-7	0.08	0.02i	0.24	—	—	—	0.25
15	1.00e-7	0.08	0.02i	0.25	—	—	—	0.26
Total		0.32	0.03i	0.40	—	0.05	—	0.51

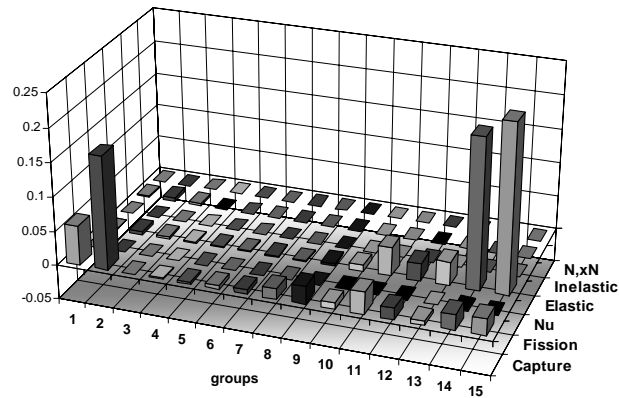


Table 147. PWR k_{eff} BOC: BOLNA diagonal uncertainty (%) by isotope

Isotope	σ_{cap}	σ_{fiss}	ν	σ_{el}	σ_{inel}	$\sigma_{\text{n,2n}}$	Total
²³⁵ U	0.09	0.02	0.23	—	—	—	0.25
²³⁸ U	0.11	0.01	0.03	—	0.03	—	0.12
²³⁷ Np	—	—	—	—	—	—	—
²³⁸ Pu	—	—	—	—	—	—	—
²³⁹ Pu	—	—	—	—	—	—	—
²⁴⁰ Pu	—	—	—	—	—	—	—
²⁴¹ Pu	—	—	—	—	—	—	—
²⁴² Pu	—	—	—	—	—	—	—
²⁴¹ Am	—	—	—	—	—	—	—
^{242m} Am	—	—	—	—	—	—	—
²⁴³ Am	—	—	—	—	—	—	—
²⁴² Cm	—	—	—	—	—	—	—
²⁴³ Cm	—	—	—	—	—	—	—
²⁴⁴ Cm	—	—	—	—	—	—	—
²⁴⁵ Cm	—	—	—	—	—	—	—
O	0.23	—	—	—	0.02	—	0.24
H	0.01	—	—	—	0.01	—	0.01
Zr	0.01	—	—	—	—	—	0.01
Total	0.27	0.03	0.24	—	0.04	—	0.36

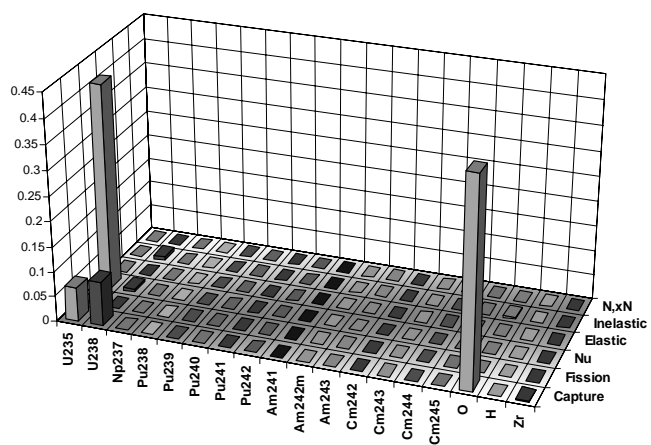


Table 148. PWR k_{eff} BOC: BOLNA full uncertainty (%) by isotope

Isotope	σ_{cap}	σ_{fiss}	ν	σ_{el}	σ_{inel}	$\sigma_{\text{n,2n}}$	Total
²³⁵ U	0.15	0.03i	0.39	—	—	—	0.42
²³⁸ U	0.15	0.01	0.04	—	0.04	—	0.16
²³⁷ Np	—	—	—	—	—	—	—
²³⁸ Pu	—	—	—	—	—	—	—
²³⁹ Pu	—	—	—	—	—	—	—
²⁴⁰ Pu	—	—	—	—	—	—	—
²⁴¹ Pu	—	—	—	—	—	—	—
²⁴² Pu	—	—	—	—	—	—	—
²⁴¹ Am	—	—	—	—	—	—	—
^{242m} Am	—	—	—	—	—	—	—
²⁴³ Am	—	—	—	—	—	—	—
²⁴² Cm	—	—	—	—	—	—	—
²⁴³ Cm	—	—	—	—	—	—	—
²⁴⁴ Cm	—	—	—	—	—	—	—
²⁴⁵ Cm	—	—	—	—	—	—	—
O	0.24	—	—	—	0.03	—	0.24
H	0.01	—	—	—	0.02	—	0.02
Zr	0.02	—	—	—	—	—	0.02
Total	0.32	0.03i	0.40	—	0.05	—	0.51

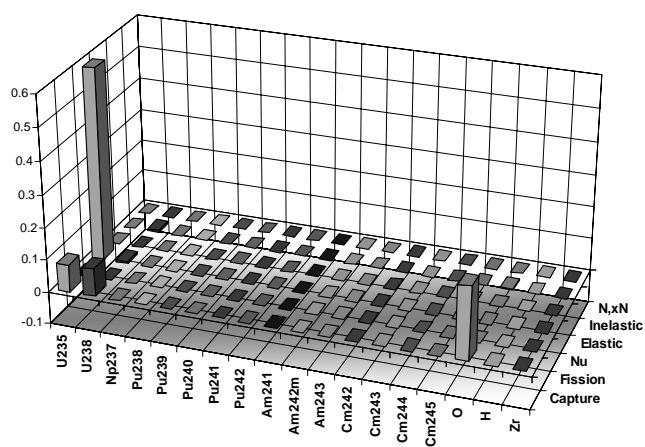


Table 149. PWR k_{eff} EOC: BOLNA diagonal uncertainty (%) by group

Gr.	[MeV]	σ_{cap}	σ_{fiss}	ν	σ_{el}	σ_{inel}	$\sigma_{\text{n,2n}}$	Total
1	19.6	0.22	—	0.01	—	0.07	0.01	0.23
2	6.07	0.36	0.02	0.06	—	0.13	—	0.39
3	2.23	0.01	0.02	0.04	—	0.07	—	0.08
4	1.35	0.01	0.01	—	—	—	—	0.02
5	4.98e-1	—	0.01	—	—	—	—	0.01
6	1.83e-1	0.01	0.01	—	—	—	—	0.01
7	6.74e-2	0.01	—	—	—	—	—	0.01
8	2.48e-2	0.06	—	—	—	—	—	0.06
9	9.12e-3	0.04	0.01	—	—	0.01	—	0.04
10	2.03e-3	0.04	0.02	—	—	0.01	—	0.05
11	4.54e-4	0.12	0.14	0.02	—	0.01	—	0.18
12	2.26e-5	0.09	0.06	0.01	—	0.01	—	0.11
13	4.00e-6	0.06	0.07	0.01	—	0.02	—	0.10
14	5.40e-7	0.18	0.22	0.09	—	0.01	—	0.30
15	1.00e-7	0.11	0.18	0.10	—	—	—	0.23
Total		0.51	0.33	0.15	—	0.17	0.01	0.64

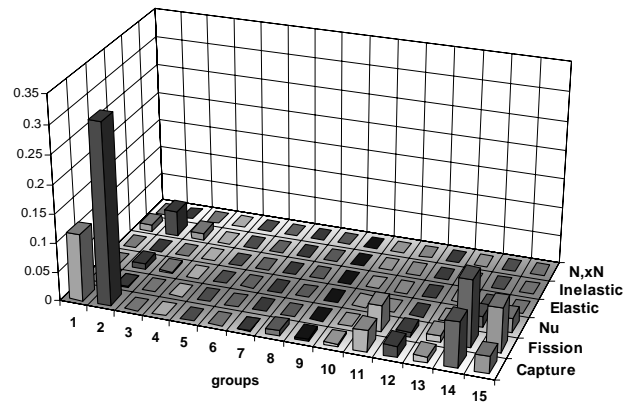


Table 150. PWR k_{eff} EOC: BOLNA full uncertainty (%) by group

Gr.	[MeV]	σ_{cap}	σ_{fiss}	ν	σ_{el}	σ_{inel}	$\sigma_{\text{n,2n}}$	Total
1	19.6	0.23	0.01	0.03	—	0.10	0.01	0.25
2	6.07	0.37	0.03	0.08	—	0.17	—	0.41
3	2.23	0.01	0.03	0.06	—	0.12	—	0.14
4	1.35	0.01	0.02	0.02	—	0.01	—	0.03
5	4.98e-1	0.01	0.01	0.01	—	—	—	0.02
6	1.83e-1	0.01	0.01	0.01	—	—	—	0.02
7	6.74e-2	0.02	0.01	0.01	—	0.01	—	0.02
8	2.48e-2	0.07	0.01	0.01	—	0.01	—	0.07
9	9.12e-3	0.07	0.01	0.01	—	0.01	—	0.07
10	2.03e-3	0.08	0.05	0.02	—	0.01	—	0.10
11	4.54e-4	0.16	0.16	0.04	—	0.01	—	0.23
12	2.26e-5	0.12	0.09	0.04	—	0.01i	—	0.15
13	4.00e-6	0.08	0.13	0.03	—	0.02i	—	0.15
14	5.40e-7	0.17	0.22	0.12	—	0.02	—	0.30
15	1.00e-7	0.15	0.21	0.13	—	0.01i	—	0.29
Total		0.55	0.38	0.22	—	0.23	0.01	0.74

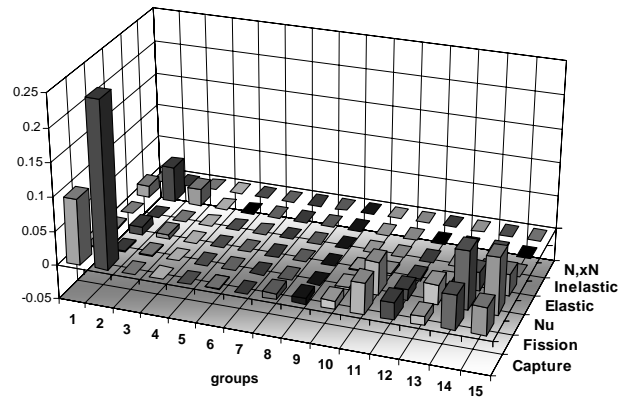


Table 151. PWR k_{eff} EOC: BOLNA diagonal uncertainty (%) by isotope

Isotope	σ_{cap}	σ_{fiss}	ν	σ_{el}	σ_{inel}	$\sigma_{\text{n,2n}}$	Total
²³⁵ U	0.03	0.02	0.10	—	—	—	0.11
²³⁸ U	0.18	0.02	0.07	—	0.13	0.01	0.24
²³⁷ Np	0.02	—	—	—	—	—	0.02
²³⁸ Pu	0.01	0.01	—	—	—	—	0.01
²³⁹ Pu	0.14	0.19	0.07	—	—	—	0.25
²⁴⁰ Pu	0.09	0.01	—	—	—	—	0.09
²⁴¹ Pu	0.11	0.26	0.04	—	—	—	0.29
²⁴² Pu	0.04	0.01	—	—	—	—	0.04
²⁴¹ Am	0.01	—	—	—	—	—	0.01
^{242m} Am	—	—	—	—	—	—	—
²⁴³ Am	0.02	—	—	—	—	—	0.02
²⁴² Cm	—	—	—	—	—	—	—
²⁴³ Cm	—	—	—	—	—	—	—
²⁴⁴ Cm	0.01	0.01	—	—	—	—	0.01
²⁴⁵ Cm	—	0.01	0.01	—	—	—	0.01
O	0.42	—	—	—	0.10	—	0.43
H	0.01	—	—	—	0.03	—	0.04
Zr	0.02	—	—	—	—	—	0.02
Total	0.51	0.33	0.15	—	0.17	0.01	0.64

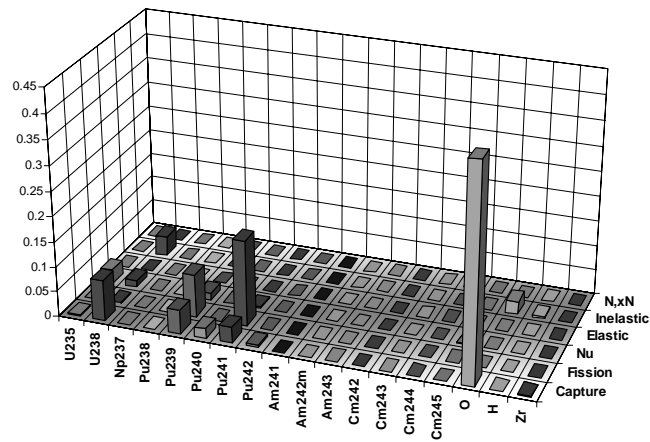


Table 152. PWR k_{eff} EOC: BOLNA full uncertainty (%) by isotope

Isotope	σ_{cap}	σ_{fiss}	ν	σ_{el}	σ_{inel}	$\sigma_{\text{n,2n}}$	Total
²³⁵ U	0.03	0.02	0.17	—	—	—	0.17
²³⁸ U	0.26	0.03	0.10	—	0.17	0.01	0.33
²³⁷ Np	0.02	—	—	—	—	—	0.02
²³⁸ Pu	0.01	0.01	0.01	—	—	—	0.02
²³⁹ Pu	0.07	0.18	0.07	—	—	—	0.21
²⁴⁰ Pu	0.12	0.01	0.01	—	—	—	0.12
²⁴¹ Pu	0.13	0.34	0.06	—	—	—	0.37
²⁴² Pu	0.05	0.01	—	—	—	—	0.05
²⁴¹ Am	0.01	—	—	—	—	—	0.01
^{242m} Am	—	—	—	—	—	—	—
²⁴³ Am	0.02	—	—	—	—	—	0.02
²⁴² Cm	—	—	—	—	—	—	—
²⁴³ Cm	—	—	—	—	—	—	—
²⁴⁴ Cm	0.01	0.01	—	—	—	—	0.01
²⁴⁵ Cm	—	0.01	0.01	—	—	—	0.02
O	0.43	—	—	—	0.15	—	0.46
H	0.02	—	—	—	0.05	—	0.06
Zr	0.03	—	—	—	0.01	—	0.04
Total	0.55	0.38	0.22	—	0.23	0.01	0.74

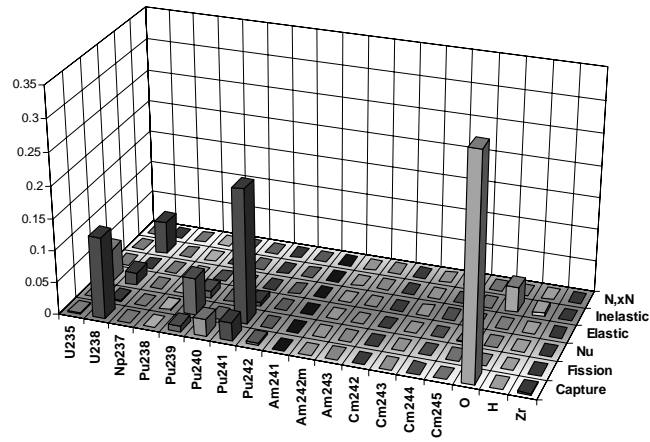


Table 153. PWR Doppler BOC: BOLNA diagonal uncertainty (%) by group

Gr.	[MeV]	σ_{cap}	σ_{fiss}	ν	σ_{el}	σ_{inel}	$\sigma_{\text{n,2n}}$	Total
1	19.6	0.21	—	0.01	—	0.09	0.01	0.23
2	6.07	0.32	0.02	0.07	—	0.18	—	0.38
3	2.23	0.01	0.01	0.04	—	0.09	—	0.10
4	1.35	0.01	0.01	0.01	—	—	—	0.02
5	4.98e-1	0.01	—	0.01	—	—	—	0.01
6	1.83e-1	0.02	—	0.01	—	—	—	0.02
7	6.74e-2	0.02	—	—	—	—	—	0.02
8	2.48e-2	0.06	—	0.01	—	—	—	0.06
9	9.12e-3	0.17	0.04	0.01	—	0.02	—	0.18
10	2.03e-3	0.32	0.02	0.02	—	0.04	—	0.33
11	4.54e-4	0.79	0.05	0.12	—	0.04	—	0.80
12	2.26e-5	0.32	0.04	0.08	—	0.04	—	0.33
13	4.00e-6	0.03	0.01	0.05	—	—	—	0.06
14	5.40e-7	0.29	0.08	0.87	—	—	—	0.92
15	1.00e-7	0.20	0.04	0.59	—	—	—	0.62
Total		1.06	0.13	1.06	—	0.23	0.01	1.53

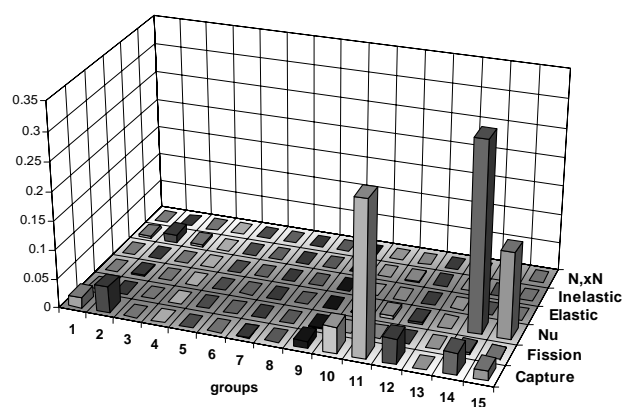


Table 154. PWR Doppler BOC: BOLNA full uncertainty. (%) by group

Gr.	[MeV]	σ_{cap}	σ_{fiss}	ν	σ_{el}	σ_{inel}	$\sigma_{\text{n,2n}}$	Total
1	19.6	0.22	0.01	0.03	—	0.13	0.01	0.26
2	6.07	0.33	0.03	0.10	—	0.23	—	0.41
3	2.23	0.01	0.02	0.08	—	0.16	—	0.18
4	1.35	0.03	0.01	0.06	—	0.02	—	0.07
5	4.98e-1	0.04	0.01	0.05	—	0.01	—	0.07
6	1.83e-1	0.05	0.01	0.05	—	—	—	0.07
7	6.74e-2	0.06	0.01	0.05	—	—	—	0.07
8	2.48e-2	0.10	0.01	0.05	—	0.01	—	0.11
9	9.12e-3	0.29	0.04	0.08	—	0.04	—	0.31
10	2.03e-3	0.48	0.02	0.10	—	0.05	—	0.50
11	4.54e-4	0.88	0.05	0.23	—	0.04	—	0.91
12	2.26e-5	0.41	0.03	0.20	—	0.02i	—	0.45
13	4.00e-6	0.09	0.02	0.16	—	0.01	—	0.18
14	5.40e-7	0.28	0.04	0.62	—	0.02	—	0.68
15	1.00e-7	0.20i	0.04i	0.51i	—	0.02	—	0.55i
Total		1.22	0.09	0.54	—	0.31	0.01	1.37

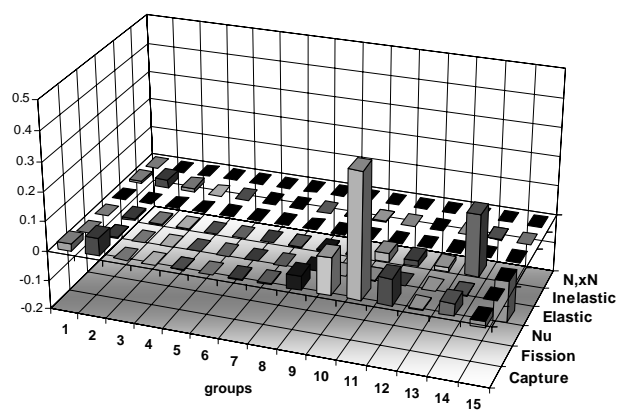


Table 155. PWR Doppler BOC: BOLNA diagonal uncertainty (%) by isotope

Isotope	σ_{cap}	σ_{fiss}	ν	σ_{el}	σ_{inel}	$\sigma_{\text{n,2n}}$	Total
²³⁵ U	0.35	0.12	1.06	—	—	—	1.12
²³⁸ U	0.93	0.03	0.08	—	0.17	0.01	0.95
²³⁷ Np	—	—	—	—	—	—	—
²³⁸ Pu	—	—	—	—	—	—	—
²³⁹ Pu	—	—	—	—	—	—	—
²⁴⁰ Pu	—	—	—	—	—	—	—
²⁴¹ Pu	—	—	—	—	—	—	—
²⁴² Pu	—	—	—	—	—	—	—
²⁴¹ Am	—	—	—	—	—	—	—
^{242m} Am	—	—	—	—	—	—	—
²⁴³ Am	—	—	—	—	—	—	—
²⁴² Cm	—	—	—	—	—	—	—
²⁴³ Cm	—	—	—	—	—	—	—
²⁴⁴ Cm	—	—	—	—	—	—	—
²⁴⁵ Cm	—	—	—	—	—	—	—
O	0.38	—	—	—	0.13	—	0.41
H	0.02	—	—	—	0.07	—	0.08
Zr	0.02	—	—	—	0.01	—	0.02
Total	1.06	0.13	1.06	—	0.23	0.01	1.53

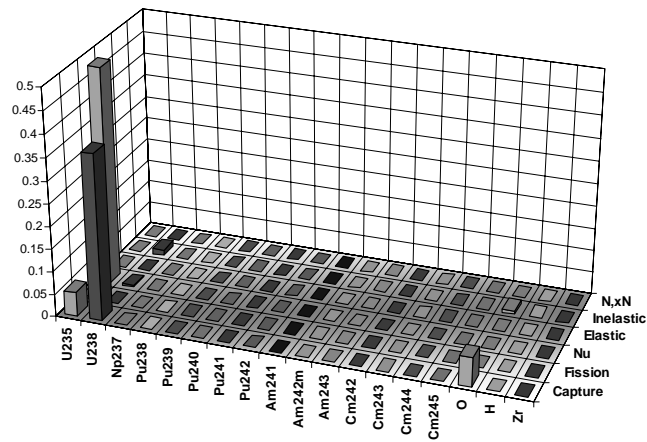


Table 156. PWR Doppler BOC: BOLNA full uncertainty (%) by isotope

Isotope	σ_{cap}	σ_{fiss}	ν	σ_{el}	σ_{inel}	$\sigma_{\text{n,2n}}$	Total
²³⁵ U	0.20	0.08	0.53	—	0.01	—	0.57
²³⁸ U	1.13	0.04	0.11	—	0.23	0.01	1.16
²³⁷ Np	—	—	—	—	—	—	—
²³⁸ Pu	—	—	—	—	—	—	—
²³⁹ Pu	—	—	—	—	—	—	—
²⁴⁰ Pu	—	—	—	—	—	—	—
²⁴¹ Pu	—	—	—	—	—	—	—
²⁴² Pu	—	—	—	—	—	—	—
²⁴¹ Am	—	—	—	—	—	—	—
^{242m} Am	—	—	—	—	—	—	—
²⁴³ Am	—	—	—	—	—	—	—
²⁴² Cm	—	—	—	—	—	—	—
²⁴³ Cm	—	—	—	—	—	—	—
²⁴⁴ Cm	—	—	—	—	—	—	—
²⁴⁵ Cm	—	—	—	—	—	—	—
O	0.40	—	—	—	0.18	—	0.44
H	—	—	—	—	0.12	—	0.12
Zr	0.02	—	—	—	0.01	—	0.02
Total	1.22	0.09	0.54	—	0.31	0.01	1.37

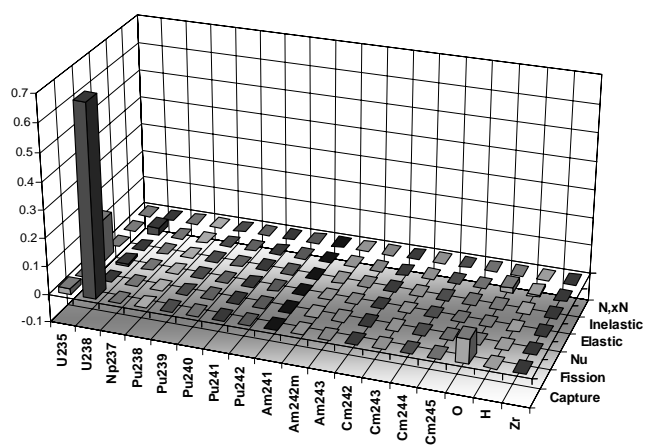


Table 157. PWR Doppler EOC: BOLNA diagonal uncertainty (%) by group

Gr.	[MeV]	σ_{cap}	σ_{fiss}	ν	σ_{el}	σ_{inel}	$\sigma_{\text{n,2n}}$	Total
1	19.6	0.24	0.01	0.02	—	0.16	0.01	0.29
2	6.07	0.34	0.05	0.11	—	0.30	—	0.47
3	2.23	0.01	0.03	0.07	—	0.15	—	0.17
4	1.35	0.01	0.02	0.01	—	0.01	—	0.03
5	4.98e-1	—	0.01	—	—	—	—	0.01
6	1.83e-1	—	0.01	—	—	—	—	0.01
7	6.74e-2	0.01	—	—	—	—	—	0.01
8	2.48e-2	0.05	0.01	—	—	—	—	0.05
9	9.12e-3	0.16	0.02	—	—	0.02	—	0.16
10	2.03e-3	0.34	0.03	—	—	0.05	—	0.34
11	4.54e-4	0.86	0.18	0.02	—	0.05	—	0.88
12	2.26e-5	0.38	0.03	0.03	—	0.04	—	0.39
13	4.00e-6	0.15	0.04	—	—	0.05	—	0.16
14	5.40e-7	0.85	0.90	0.37	—	0.07	—	1.30
15	1.00e-7	0.40	0.77	0.42	—	0.05	—	0.96
Total		1.45	1.20	0.57	—	0.40	0.01	2.01

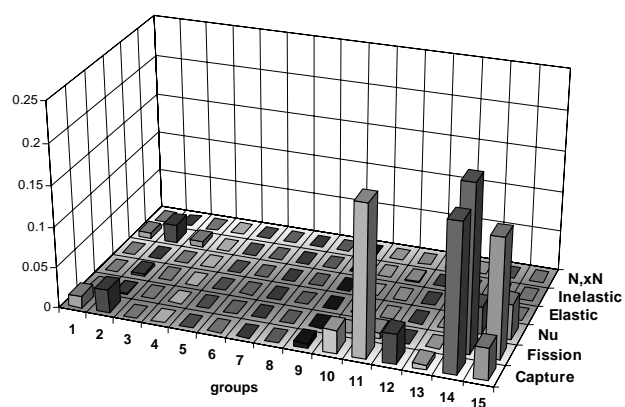


Table 158. PWR Doppler EOC: BOLNA full uncertainty (%) by group

Gr.	[MeV]	σ_{cap}	σ_{fiss}	ν	σ_{el}	σ_{inel}	$\sigma_{\text{n,2n}}$	Total
1	19.6	0.25	0.02	0.05	—	0.23	0.01	0.34
2	6.07	0.35	0.06	0.14	—	0.38	—	0.54
3	2.23	0.01	0.05	0.11	—	0.27	—	0.29
4	1.35	0.01	0.04	0.02	—	0.03	—	0.06
5	4.98e-1	0.01	0.03	—	—	0.01	—	0.03
6	1.83e-1	0.01	0.03	—	—	—	—	0.03
7	6.74e-2	0.01	0.02	—	—	0.01	—	0.02
8	2.48e-2	0.07	0.01	—	—	0.02	—	0.07
9	9.12e-3	0.28	0.02	0.01i	—	0.05	—	0.28
10	2.03e-3	0.50	0.06i	0.01i	—	0.06	—	0.50
11	4.54e-4	0.95	0.14	0.02i	—	0.04	—	0.96
12	2.26e-5	0.47	0.07	0.03i	—	0.01i	—	0.48
13	4.00e-6	0.16	0.12i	0.01i	—	0.05i	—	0.08
14	5.40e-7	0.71	0.68	0.25	—	0.12	—	1.03
15	1.00e-7	0.30i	0.67	0.28	—	0.10i	—	0.65
Total		1.44	0.96	0.41	—	0.53	0.01	1.86

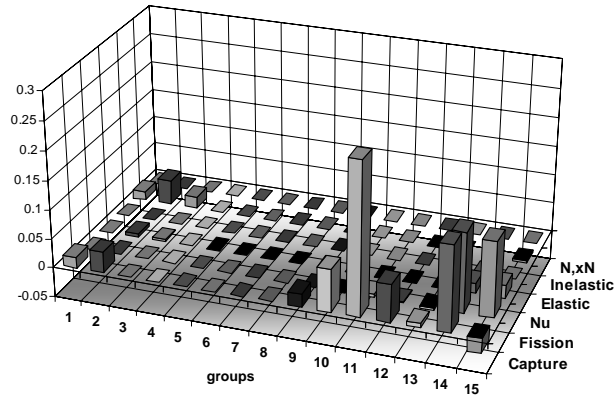


Table 159. PWR Doppler EOC: BOLNA diagonal uncertainty (%) by isotope

Isotope	σ_{cap}	σ_{fiss}	ν	σ_{el}	σ_{inel}	$\sigma_{\text{n,2n}}$	Total
²³⁵ U	0.09	0.08	0.42	—	—	—	0.44
²³⁸ U	1.04	0.05	0.13	—	0.29	0.01	1.09
²³⁷ Np	0.04	—	—	—	—	—	0.04
²³⁸ Pu	0.04	0.02	0.01	—	—	—	0.04
²³⁹ Pu	0.67	0.79	0.32	—	—	—	1.08
²⁴⁰ Pu	0.34	0.01	0.01	—	—	—	0.34
²⁴¹ Pu	0.53	0.90	0.15	—	—	—	1.06
²⁴² Pu	0.03	0.01	—	—	—	—	0.03
²⁴¹ Am	0.01	—	—	—	—	—	0.01
^{242m} Am	—	0.01	—	—	—	—	0.01
²⁴³ Am	0.01	—	—	—	—	—	0.01
²⁴² Cm	—	—	—	—	—	—	—
²⁴³ Cm	—	—	—	—	—	—	—
²⁴⁴ Cm	—	0.01	—	—	—	—	0.01
²⁴⁵ Cm	—	0.03	0.03	—	—	—	0.05
O	0.42	—	—	—	0.25	—	0.49
H	0.05	—	—	—	0.10	—	0.11
Zr	0.02	—	—	—	0.01	—	0.03
Total	1.45	1.20	0.57	—	0.40	0.01	2.01

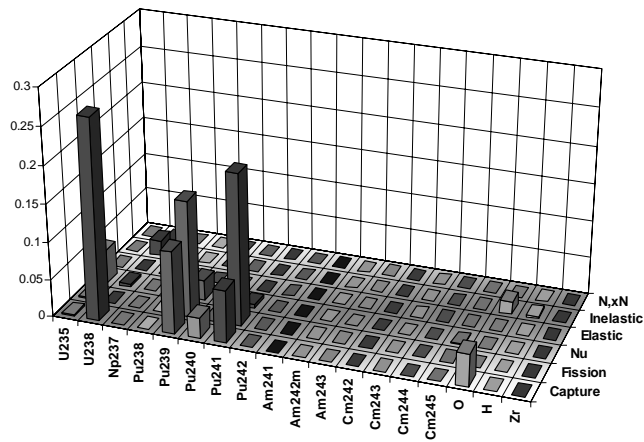


Table 160. PWR Doppler EOC: BOLNA full uncertainty (%) by isotope

Isotope	σ_{cap}	σ_{fiss}	ν	σ_{el}	σ_{inel}	$\sigma_{\text{n,2n}}$	Total
²³⁵ U	0.03	0.03	0.17	—	—	—	0.18
²³⁸ U	1.19	0.07	0.18	—	0.38	0.01	1.27
²³⁷ Np	0.04	0.01	—	—	—	—	0.04
²³⁸ Pu	0.02	0.03	0.01	—	—	—	0.04
²³⁹ Pu	0.40	0.47	0.32	—	—	—	0.69
²⁴⁰ Pu	0.17	0.02	0.01	—	—	—	0.17
²⁴¹ Pu	0.53	0.84	0.04	—	—	—	0.99
²⁴² Pu	0.03	0.02	—	—	—	—	0.03
²⁴¹ Am	0.01	—	—	—	—	—	0.01
^{242m} Am	—	—	—	—	—	—	—
²⁴³ Am	0.01	—	—	—	—	—	0.01
²⁴² Cm	—	—	—	—	—	—	—
²⁴³ Cm	—	—	—	—	—	—	—
²⁴⁴ Cm	—	0.02	—	—	—	—	0.02
²⁴⁵ Cm	—	0.02	0.02	—	—	—	0.03
O	0.43	—	—	—	0.33	—	0.54
H	0.01	—	—	—	0.17	—	0.17
Zr	0.01	—	—	—	0.01	—	0.02
Total	1.44	0.96	0.41	—	0.53	0.01	1.86

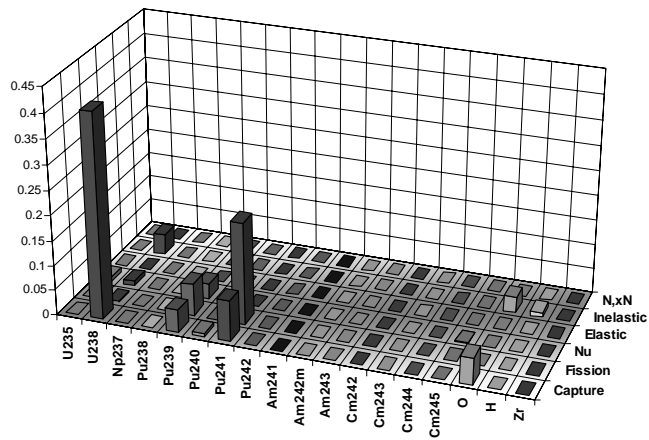


Table 161. PWR XS burn-up: BOLNA diagonal uncertainty (%) by group

Gr.	[MeV]	σ_{cap}	σ_{fiss}	ν	σ_{el}	σ_{inel}	$\sigma_{\text{n,2n}}$	Total
1	19.6	0.21	0.01	0.01	—	0.11	0.01	0.24
2	6.07	0.32	0.04	0.08	—	0.21	—	0.40
3	2.23	0.01	0.03	0.05	—	0.11	—	0.12
4	1.35	0.01	0.02	0.01	—	—	—	0.03
5	4.98e-1	0.01	0.01	—	—	—	—	0.02
6	1.83e-1	0.02	0.01	—	—	—	—	0.02
7	6.74e-2	0.03	—	—	—	—	—	0.03
8	2.48e-2	0.06	0.01	—	—	—	—	0.06
9	9.12e-3	0.09	0.02	0.01	—	0.01	—	0.09
10	2.03e-3	0.04	0.03	0.01	—	0.01	—	0.06
11	4.54e-4	0.11	0.28	0.05	—	0.01	—	0.31
12	2.26e-5	0.09	0.12	0.03	—	0.02	—	0.15
13	4.00e-6	0.13	0.14	0.05	—	0.03	—	0.20
14	5.40e-7	0.38	0.45	0.26	—	0.01	—	0.64
15	1.00e-7	0.22	0.37	0.19	—	0.01	—	0.47
Total		0.63	0.68	0.34	—	0.27	0.01	1.02

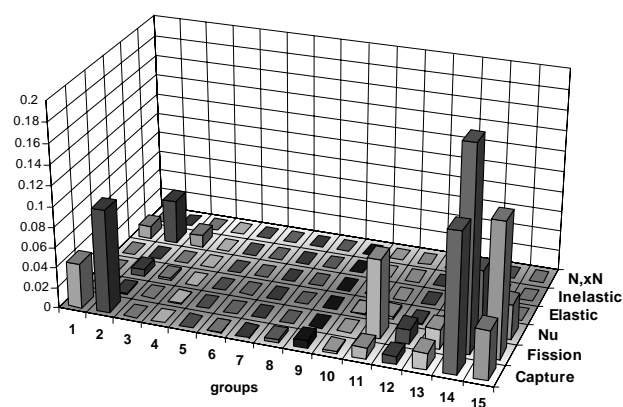


Table 162. PWR XS burn-up: BOLNA full uncertainty (%) by group

Gr.	[MeV]	σ_{cap}	σ_{fiss}	ν	σ_{el}	σ_{inel}	$\sigma_{\text{n,2n}}$	Total
1	19.6	0.23	0.02	0.04	—	0.16	0.01	0.28
2	6.07	0.33	0.05	0.11	—	0.27	—	0.45
3	2.23	0.02	0.05	0.08	—	0.19	—	0.21
4	1.35	0.03	0.04	0.04	—	0.02	—	0.07
5	4.98e-1	0.05	0.03	0.03	—	—	—	0.06
6	1.83e-1	0.06	0.03	0.03	—	—	—	0.07
7	6.74e-2	0.07	0.02	0.03	—	0.01	—	0.08
8	2.48e-2	0.09	0.01	0.03	—	0.01	—	0.10
9	9.12e-3	0.13	0.02	0.05	—	0.01	—	0.14
10	2.03e-3	0.07	0.10	0.06	—	0.01	—	0.14
11	4.54e-4	0.15	0.34	0.14	—	0.01i	—	0.39
12	2.26e-5	0.13	0.19	0.11	—	0.02i	—	0.26
13	4.00e-6	0.15	0.26	0.13	—	0.04i	—	0.33
14	5.40e-7	0.33	0.45	0.35	—	0.04	—	0.66
15	1.00e-7	0.28	0.45	0.30	—	0.03i	—	0.60
Total		0.67	0.80	0.54	—	0.37	0.01	1.23

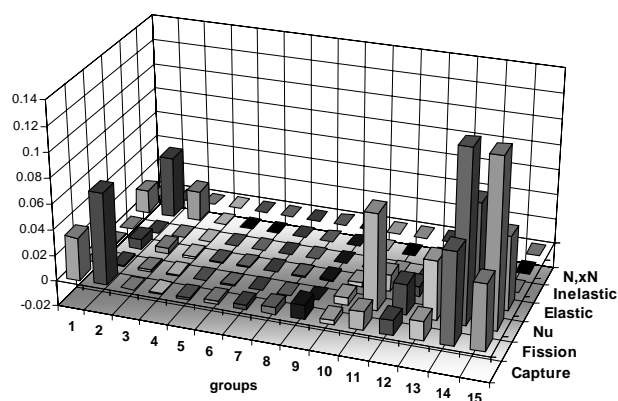


Table 163. PWR XS burn-up: BOLNA diagonal uncertainty (%) by isotope

Isotope	σ_{cap}	σ_{fiss}	ν	σ_{el}	σ_{inel}	$\sigma_{\text{n,2n}}$	Total
²³⁵ U	0.15	0.01	0.28	—	—	—	0.31
²³⁸ U	0.16	0.04	0.10	—	0.20	0.01	0.28
²³⁷ Np	0.04	—	—	—	—	—	0.04
²³⁸ Pu	0.02	0.02	0.01	—	—	—	0.03
²³⁹ Pu	0.29	0.39	0.16	—	—	—	0.51
²⁴⁰ Pu	0.19	0.01	0.01	—	—	—	0.19
²⁴¹ Pu	0.24	0.55	0.08	—	—	—	0.61
²⁴² Pu	0.09	0.01	—	—	—	—	0.09
²⁴¹ Am	0.02	—	—	—	—	—	0.02
^{242m} Am	—	0.01	—	—	—	—	0.01
²⁴³ Am	0.04	—	—	—	—	—	0.04
²⁴² Cm	—	—	—	—	—	—	—
²⁴³ Cm	—	—	—	—	—	—	—
²⁴⁴ Cm	0.02	0.01	—	—	—	—	0.02
²⁴⁵ Cm	—	0.02	0.02	—	—	—	0.02
O	0.39	—	—	—	0.17	—	0.42
H	0.02	—	—	—	0.05	—	0.05
Zr	0.02	—	—	—	0.01	—	0.02
Total	0.63	0.68	0.34	—	0.27	0.01	1.02

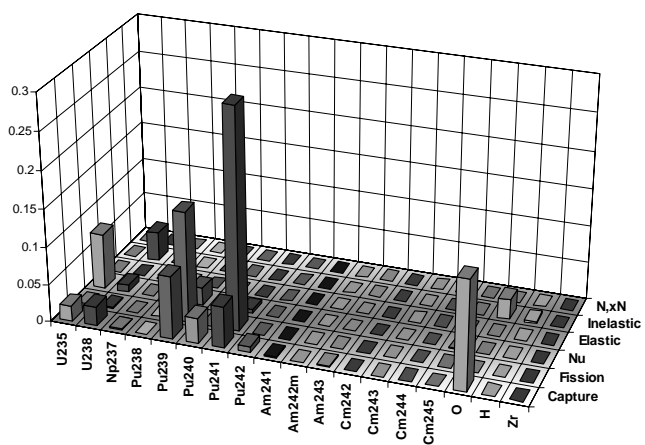
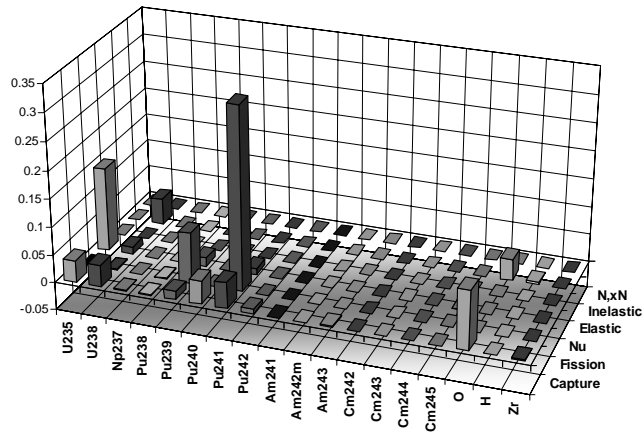


Table 164. PWR XS burn-up: BOLNA full uncertainty (%) by isotope

Isotope	σ_{cap}	σ_{fiss}	ν	σ_{el}	σ_{inel}	$\sigma_{\text{n,2n}}$	Total
²³⁵ U	0.24	0.03i	0.48	—	—	—	0.53
²³⁸ U	0.24	0.05	0.14	—	0.27	0.01	0.39
²³⁷ Np	0.04	0.01	—	—	—	—	0.04
²³⁸ Pu	0.03	0.03	0.02	—	—	—	0.05
²³⁹ Pu	0.15	0.37	0.16	—	—	—	0.43
²⁴⁰ Pu	0.25	0.02	0.01	—	—	—	0.25
²⁴¹ Pu	0.27	0.71	0.13	—	—	—	0.77
²⁴² Pu	0.10	0.02	—	—	—	—	0.10
²⁴¹ Am	0.02	—	—	—	—	—	0.02
^{242m} Am	—	0.01	—	—	—	—	0.01
²⁴³ Am	0.05	—	—	—	—	—	0.05
²⁴² Cm	—	—	—	—	—	—	—
²⁴³ Cm	—	—	—	—	—	—	—
²⁴⁴ Cm	0.02	0.02	—	—	—	—	0.03
²⁴⁵ Cm	—	0.02	0.03	—	—	—	0.03
O	0.40	—	—	—	0.24	—	0.47
H	0.02	—	—	—	0.08	—	0.08
Zr	0.03	—	—	—	0.01	—	0.03
Total	0.67	0.80	0.54	—	0.37	0.01	1.23



Appendix P

COMPLETE LISTS OF TARGET ACCURACY RESULTS

Table 1. ABTR target accuracy results

Isotope	Cross-section	Energy range	Uncertainty (%)			
			Initial	Required		
				$\lambda=1$	$\lambda \neq 1^{(a)}$	$\lambda \neq 1^{(b)}$
^{238}U	σ_{capt}	6.07-2.23 MeV	13.5	13.5	11.7	8.4
		2.23-1.35 MeV	6.1	6.1	6.0	4.6
		1.35-0.498 MeV	2.3	2.3	2.3	1.8
		183-67.4 keV	1.7	1.7	1.7	1.4
		67.4-24.8 keV	1.6	1.6	1.6	1.5
		24.8-9.12 keV	9.4	2.9	2.1	1.6
		9.12-2.03 keV	3.1	3.1	3.1	2.7
	ν	6.07-2.23 MeV	1.2	1.2	1.2	1.0
		2.23-1.35 MeV	1.3	1.3	1.3	1.1
	σ_{el}	6.07-2.23 MeV	14.6	14.6	11.8	8.2
		2.23-1.35 MeV	18.8	14.6	10.8	7.9
		1.35-0.498 MeV	5.4	5.4	4.1	3.2
	σ_{inel}	19.6-6.07 MeV	29.3	11.8	15.0	20.8
		6.07-2.23 MeV	19.8	3.3	4.2	5.8
		2.23-1.35 MeV	20.6	3.6	4.5	6.3
		1.35-0.498 MeV	11.6	6.5	8.2	11.4
		183-67.4 keV	11.0	7.1	8.9	11.0
^{239}Pu	σ_{capt}	1.35-0.498 MeV	18.2	9.5	6.9	5.2
		498-183 keV	11.6	5.7	4.1	3.2
		183-67.4 keV	9.0	5.0	3.7	2.8
		67.4-24.8 keV	10.1	5.8	4.2	3.2
		24.8-9.12 keV	7.4	5.6	4.1	3.1
		9.12-2.03 keV	15.5	7.4	5.3	4.1
	σ_{fiss}	498-183 keV	0.7	0.7	0.7	0.6
		183-67.4 keV	0.9	0.9	0.9	0.7
	σ_{el}	1.35-0.498 MeV	10.3	10.3	10.3	8.1
	σ_{inel}	6.07-2.23 MeV	22.2	12.2	14.5	21.1
		2.23-1.35 MeV	19.0	14.8	18.9	19.0
		1.35-0.498 MeV	29.0	18.8	23.8	29.0
^{240}Pu	σ_{capt}	498-183 keV	14.3	13.1	13.7	10.9
		183-67.4 keV	13.8	11.5	12.0	9.3
		67.4-24.8 keV	11.3	11.3	11.3	10.4
	σ_{fiss}	1.35-0.498 MeV	5.8	4.9	5.1	3.9
	ν	1.35-0.498 MeV	3.7	3.7	3.7	3.2
^{241}Pu	σ_{fiss}	2.23-1.35 MeV	21.3	21.3	21.0	17.4
		1.35-0.498 MeV	16.6	11.7	11.8	8.9
		498-183 keV	13.5	8.8	9.1	6.9
		183-67.4 keV	19.9	8.8	9.1	7.0
		24.8-9.12 keV	11.3	11.3	11.3	10.0

* See Table 23 in the main text for the details of the λ_i set $\lambda \neq 1^{(a)}$ and $\lambda \neq 1^{(b)}$

Table 1. ABTR target accuracy results (*cont.*)

Isotope	Cross-section	Energy range	Uncertainty (%)			
			Initial	Required		
				$\lambda=1$	$\lambda \neq 1$ ^(a)	$\lambda \neq 1$ ^(b)
⁵⁶ Fe	σ_{capt}	19.6-6.07 MeV	46.2	23.7	15.2	12.0
		1.35-0.498 MeV	7.4	7.4	7.4	7.3
		183-67.4 keV	10.8	8.1	5.9	4.5
		67.4-24.8 keV	13.2	10.2	7.4	5.7
		2.03-0.454 keV	11.2	8.2	5.9	4.5
		454-22.6 eV	11.3	11.3	10.9	8.3
	σ_{el}	6.07-2.23 MeV	8.1	6.9	5.0	3.8
		2.23-1.35 MeV	5.9	5.9	5.1	3.9
	σ_{inel}	19.6-6.07 MeV	13.0	10.2	12.8	13.0
		6.07-2.23 MeV	7.2	6.1	7.2	7.2
		2.23-1.35 MeV	25.4	5.6	7.1	9.9
		1.35-0.498 MeV	16.1	7.5	9.4	13.1
⁵² Cr	σ_{el}	1.35-0.498 MeV	4.2	4.2	4.2	4.2
		498-183 keV	5.2	5.2	5.1	3.9
		183-67.4 keV	11.4	8.0	5.8	4.4
⁹⁰ Zr	σ_{inel}	6.07-2.23 MeV	18.0	10.7	13.4	18.0
²³ Na	σ_{capt}	19.6-6.07 MeV	46.4	26.7	27.0	18.3
	σ_{el}	1.35-0.498 MeV	3.0	3.0	3.0	2.5
		498-183 keV	3.3	3.3	3.3	2.9
	σ_{inel}	1.35-0.498 MeV	28.0	10.1	12.4	17.7
¹⁰ B	σ_{capt}	498-183 keV	15.0	13.5	10.8	8.6
		183-67.4 keV	10.0	10.0	8.3	6.0
		67.4-24.8 keV	10.0	10.0	9.4	7.7

* See Table 23 in the main text for the details of the λ_i set $\lambda \neq 1$ ^(a) and $\lambda \neq 1$ ^(b)

Table 2. SFR target accuracy results

Isotope	Cross-Section	Energy range	Uncertainty (%)			
			Initial	Required		
				$\lambda=1$	$\lambda \neq 1^{(a)}$	$\lambda \neq 1^{(b)}$
^{238}U	σ_{capt}	24.8-9.12 keV	9.4	4.3	3.0	2.7
		6.07-2.23 MeV	19.8	5.4	6.6	10.7
	σ_{inel}	2.23-1.35 MeV	20.6	5.0	6.2	10.0
		1.35-0.498 MeV	11.6	5.5	6.8	11.0
^{237}Np	σ_{fiss}	1.35-0.498 MeV	5.8	5.8	5.8	5.5
^{238}Pu	σ_{capt}	183-67.4 keV	16.6	11.5	11.5	10.2
		67.4-24.8 keV	22.1	13.0	13.0	11.5
	σ_{fiss}	6.07-2.23 MeV	20.5	5.9	5.9	5.2
		2.23-1.35 MeV	33.8	5.6	5.6	5.0
		1.35-0.498 MeV	17.1	3.3	3.3	3.0
		498-183 keV	17.1	3.6	3.7	3.2
		183-67.4 keV	8.8	5.0	5.0	4.4
		67.4-24.8 keV	11.9	6.4	6.5	5.7
		24.8-9.12 keV	11.2	6.8	6.8	6.0
	ν	6.07-2.23 MeV	5.3	4.8	4.8	4.3
		2.23-1.35 MeV	5.4	4.5	4.5	4.0
		1.35-0.498 MeV	7.0	2.7	2.7	2.4
		498-183 keV	7.0	3.1	3.1	2.8
		183-67.4 keV	6.5	4.3	4.3	3.8
		67.4-24.8 keV	6.0	5.5	5.6	4.9
		24.8-9.12 keV	5.5	5.5	5.5	5.2
^{239}Pu	σ_{capt}	1.35-0.498 MeV	18.2	10.9	7.6	6.9
		498-183 keV	11.6	6.9	4.9	4.3
		183-67.4 keV	9.0	6.0	4.2	3.8
		67.4-24.8 keV	10.1	6.6	4.7	4.1
		24.8-9.12 keV	7.4	5.7	4.0	3.6
		9.12-2.03 keV	15.5	6.9	4.9	4.3
	σ_{inel}	6.07-2.23 MeV	22.2	13.1	15.9	22.2
		1.35-0.498 MeV	29.0	12.2	15.1	24.5
^{240}Pu	σ_{capt}	1.35-0.498 MeV	16.3	7.4	7.4	6.6
		498-183 keV	14.3	5.4	5.4	4.8
		183-67.4 keV	13.8	4.5	4.6	4.1
		67.4-24.8 keV	11.3	4.9	4.9	4.4
		24.8-9.12 keV	10.2	4.9	4.9	4.4
	σ_{fiss}	19.6-6.07 MeV	9.6	8.5	8.5	7.6
		6.07-2.23 MeV	4.8	2.8	2.8	2.5
		2.23-1.35 MeV	5.7	2.6	2.6	2.3
		1.35-0.498 MeV	5.8	1.8	1.8	1.6
		498-183 keV	3.9	3.9	3.9	3.4
		183-67.4 keV	5.7	5.7	5.7	5.3
		2.03-0.454 keV	21.6	12.5	12.5	11.1
	ν	6.07-2.23 MeV	2.7	2.2	2.2	2.0
		2.23-1.35 MeV	2.7	2.1	2.1	1.9
		1.35-0.498 MeV	3.7	1.5	1.5	1.3
		498-183 keV	4.8	3.2	3.3	2.9
		183-67.4 keV	4.8	4.8	4.8	4.5

* See Table 23 in the main text for the details of the λ_i set $\lambda \neq 1^{(a)}$ and $\lambda \neq 1^{(b)}$

Table 2. SFR target accuracy results (*cont.*)

Isotope	Cross-Section	Energy range	Uncertainty (%)			
			Initial	Required		
				$\lambda=1$	$\lambda \neq 1^{(a)}$	$\lambda \neq 1^{(b)}$
^{241}Pu	σ_{capt}	1.35-0.498 MeV	31.7	14.4	14.5	12.7
		498-183 keV	20.5	11.2	11.2	9.9
	σ_{fiss}	6.07-2.23 MeV	14.2	6.5	6.5	5.8
		2.23-1.35 MeV	21.3	5.8	5.8	5.1
		1.35-0.498 MeV	16.6	3.4	3.4	3.0
		498-183 keV	13.5	2.6	2.6	2.3
		183-67.4 keV	19.9	2.6	2.6	2.3
		67.4-24.8 keV	8.7	3.3	3.4	3.0
		24.8-9.12 keV	11.3	3.5	3.5	3.1
		9.12-2.03 keV	10.4	5.4	5.4	4.8
		2.03-0.454 keV	12.7	4.4	4.4	3.9
		454 eV-22.6 eV	19.4	8.6	8.6	7.6
^{242}Pu	σ_{capt}	498-183 keV	24.1	11.4	11.4	10.0
		183-67.4 keV	32.3	9.6	9.8	8.6
		67.4-24.8 keV	37.3	9.2	9.5	8.1
		24.8-9.12 keV	38.6	8.4	8.3	7.6
		9.12-2.03 keV	38.5	12.1	13.1	10.6
	σ_{fiss}	19.6-6.07 MeV	37.2	15.1	15.6	13.8
		6.07-2.23 MeV	15.1	5.3	5.3	4.7
		2.23-1.35 MeV	21.4	4.9	4.9	4.4
		1.35-0.498 MeV	19.0	3.5	3.5	3.1
		498-183 keV	18.6	8.8	8.8	7.8
	ν	1.35-0.498 MeV	3.1	2.9	2.9	2.6
	σ_{inel}	1.35-0.498 MeV	59.8	26.2	26.9	37.8
^{241}Am	σ_{capt}	183-67.4 keV	6.8	6.1	6.1	5.4
		67.4-24.8 keV	8.0	7.5	7.5	6.6
	σ_{fiss}	6.07-2.23 MeV	11.7	6.8	6.8	6.0
		2.23-1.35 MeV	9.8	6.4	6.5	5.7
		1.35-0.498 MeV	8.3	5.8	5.8	5.2
$^{242\text{m}}\text{Am}$	σ_{capt}	498-183 keV	29.0	14.5	14.5	12.8
		183-67.4 keV	19.4	11.9	12.0	10.6
	σ_{fiss}	6.07-2.23 MeV	23.4	8.0	8.0	7.1
		2.23-1.35 MeV	19.7	8.1	8.2	7.2
		1.35-0.498 MeV	16.5	4.2	4.2	3.8
		498-183 keV	16.6	3.1	3.1	2.7
		183-67.4 keV	16.6	3.1	3.1	2.8
		67.4-24.8 keV	14.4	4.0	4.1	3.6
		24.8-9.12 keV	11.8	4.2	4.2	3.7
		9.12-2.03 keV	12.4	6.5	6.5	5.8
		2.03-0.454 keV	12.2	5.1	5.2	4.6
^{243}Am	σ_{capt}	183-67.4 keV	6.6	6.6	6.6	6.3
	σ_{fiss}	6.07-2.23 MeV	11.0	8.2	8.1	7.3
		1.35-0.498 MeV	9.2	7.2	7.2	6.3
^{244}Cm	σ_{fiss}	6.07-2.23 MeV	31.3	8.1	8.2	7.2
		2.23-1.35 MeV	43.8	8.1	8.2	7.3
		1.35-0.498 MeV	50.0	5.1	5.1	4.6
		498-183 keV	36.5	12.1	13.0	10.5
	ν	6.07-2.23 MeV	11.1	6.8	6.9	6.0
		2.23-1.35 MeV	10.7	6.8	6.8	6.0
		1.35-0.498 MeV	5.5	4.3	4.4	3.9

* See Table 23 in the main text for the details of the λ_i set $\lambda \neq 1^{(a)}$ and $\lambda \neq 1^{(b)}$

Table 2. SFR target accuracy results (*cont.*)

Isotope	Cross-Section	Energy range	Uncertainty (%)			
			Initial	Required		
				$\lambda=1$	$\lambda \neq 1^{(a)}$	$\lambda \neq 1^{(b)}$
^{245}Cm	σ_{fiss}	2.23-1.35 MeV	44.2	14.3	15.2	13.6
		1.35-0.498 MeV	49.4	8.8	8.8	8.0
		498-183 keV	37.2	6.6	6.6	5.9
		183-67.4 keV	47.5	6.7	6.8	6.0
		67.4-24.8 keV	26.5	8.8	8.8	7.8
		24.8-9.12 keV	13.5	9.1	9.1	8.1
^{246}Cm	σ_{fiss}	1.35-0.498 MeV	40.0	16.3	17.0	15.0
^{56}Fe	σ_{capt}	19.6-6.07 MeV	46.2	14.4	11.0	11.4
		183-67.4 keV	10.8	5.8	4.1	3.6
		67.4-24.8 keV	13.2	7.1	5.0	4.4
		2.03-0.454 keV	11.2	5.3	3.8	3.4
	σ_{el}	6.07-2.23 MeV	8.1	5.2	3.7	3.3
		2.23-1.35 MeV	5.9	5.0	3.6	3.2
	σ_{inel}	19.6-6.07 MeV	13.0	9.1	11.2	13.0
		6.07-2.23 MeV	7.2	4.1	5.1	7.2
		2.23-1.35 MeV	25.4	3.3	4.1	6.6
		1.35-0.498 MeV	16.1	3.2	3.9	6.4
^{52}Cr	σ_{el}	498-183 keV	5.2	5.2	4.3	3.8
		183-67.4 keV	11.4	6.3	4.5	4.0
^{90}Zr	σ_{inel}	6.07-2.23 MeV	18.0	8.9	10.9	17.7
^{23}Na	σ_{capt}	19.6-6.07 MeV	46.4	17.9	15.5	14.3
	σ_{inel}	2.23-1.35 MeV	12.6	9.4	11.5	12.6
		1.35-0.498 MeV	28.0	4.0	4.9	7.9
^{10}B	σ_{capt}	1.35-0.498 MeV	15.0	9.3	6.6	5.9
		498-183 keV	15.0	5.2	3.7	3.3
		183-67.4 keV	10.0	4.3	3.1	2.8
		67.4-24.8 keV	10.0	5.1	3.6	3.2
		24.8-9.12 keV	8.0	5.6	4.0	3.6

* See Table 23 in the main text for the details of the λ_i set $\lambda \neq 1^{(a)}$ and $\lambda \neq 1^{(b)}$

Table 3. EFR target accuracy results

Isotope	Cross-section	Energy range	Uncertainty (%)		
			Initial	Required	
				$\lambda=1$	$\lambda \neq 1$ ^(a)
²³⁴ U	σ_{capt}	67.4-24.8 keV	22.7	18.0	21.5
		24.8-9.12 keV	19.2	17.0	19.2
	σ_{fiss}	1.35-0.498 MeV	38.0	29.6	31.8
²³⁵ U	σ_{capt}	183-67.4 keV	30.6	22.6	18.9
		67.4-24.8 keV	32.9	23.1	18.7
		24.8-9.12 keV	34.0	22.9	19.4
		9.12-2.03 keV	33.9	24.6	21.1
²³⁸ U	σ_{capt}	24.8-9.12 keV	9.4	2.9	1.7
		9.12-2.03 keV	3.1	3.1	2.0
		2.03-0.454 keV	2.1	2.1	1.9
	σ_{inel}	6.07-2.23 MeV	19.8	3.7	3.8
		2.23-1.35 MeV	20.6	4.0	4.1
		1.35-0.498 MeV	11.6	5.0	5.2
		183-67.4 keV	11.0	8.5	8.7
²³⁸ Pu	σ_{fiss}	2.23-1.35 MeV	33.8	24.4	29.7
		1.35-0.498 MeV	17.1	9.7	8.6
		498-183 keV	17.1	11.5	10.2
²³⁹ Pu	σ_{capt}	2.23-1.35 MeV	26.6	26.6	25.5
		498-183 keV	11.6	9.0	5.3
		183-67.4 keV	9.0	7.0	4.1
		67.4-24.8 keV	10.1	6.7	4.0
		24.8-9.12 keV	7.4	6.1	3.7
		9.12-2.03 keV	15.5	5.6	3.3
	σ_{inel}	6.07-2.23 MeV	22.2	13.8	14.4
²⁴⁰ Pu	σ_{capt}	1.35-0.498 MeV	16.3	16.0	16.3
		498-183 keV	14.3	8.9	8.5
		183-67.4 keV	13.8	6.7	6.4
		67.4-24.8 keV	11.3	6.1	6.0
		24.8-9.12 keV	10.2	6.5	6.5
	σ_{fiss}	6.07-2.23 MeV	4.8	4.8	4.0
		2.23-1.35 MeV	5.7	5.0	4.2
		1.35-0.498 MeV	5.8	3.5	2.9
	ν	1.35-0.498 MeV	3.7	2.8	2.4
²⁴¹ Pu	σ_{fiss}	1.35-0.498 MeV	16.6	8.0	7.1
		498-183 keV	13.5	6.7	5.9
		183-67.4 keV	19.9	5.7	5.1
		67.4-24.8 keV	8.7	6.2	5.5
		24.8-9.12 keV	11.3	6.8	5.9
		9.12-2.03 keV	10.4	7.6	6.7
		2.03-0.454 keV	12.7	6.9	6.1
²⁴² Pu	σ_{capt}	183-67.4 keV	32.3	32.3	31.1
		67.4-24.8 keV	37.3	26.4	27.4
		24.8-9.12 keV	38.6	25.2	26.0
		9.12-2.03 keV	38.5	28.1	29.0
	σ_{fiss}	1.35-0.498 MeV	19.0	10.9	9.3
²⁴² Cm	σ_{fiss}	6.07-2.23 MeV	52.6	44.3	42.4
		498-183 keV	66.0	50.9	50.3
		183-67.4 keV	62.7	49.1	48.2

* See Table 23 in the main text for the details of the λ_i set $\lambda \neq 1$ ^(a)

Table 3. EFR target accuracy results (*cont.*)

Isotope	Cross-section	Energy range	Uncertainty (%)		
			Initial	Required	
				$\lambda=1$	$\lambda \neq 1$ ^(a)
²⁴³ Cm	σ_{fiss}	1.35-0.498 MeV	49.6	43.1	40.9
		498-183 keV	37.3	37.3	35.8
		183-67.4 keV	47.4	41.8	39.1
²⁴⁴ Cm	σ_{fiss}	2.23-1.35 MeV	43.8	41.1	38.2
		1.35-0.498 MeV	50.0	20.2	16.6
		498-183 keV	36.5	36.5	35.6
²⁴⁵ Cm	σ_{fiss}	1.35-0.498 MeV	49.4	43.0	40.8
		498-183 keV	37.2	37.2	35.8
		183-67.4 keV	47.5	42.3	39.8
⁵⁶ Fe	σ_{capt}	2.03-0.454 keV	11.2	8.4	5.0
	σ_{inel}	6.07-2.23 MeV	7.2	6.2	6.4
		2.23-1.35 MeV	25.4	6.6	6.8
		1.35-0.498 MeV	16.1	8.4	8.6
⁵⁸ Ni	σ_{capt}	19.6-6.07 MeV	47.8	19.9	11.6
		6.07-2.23 MeV	14.5	9.0	5.4
²³ Na	σ_{inel}	1.35-0.498 MeV	28.0	7.9	8.2
¹⁶ O	σ_{capt}	19.6-6.07 MeV	100.0	14.2	8.4
		6.07-2.23 MeV	100.0	10.9	6.4
	σ_{el}	6.07-2.23 MeV	54.9	16.1	16.5
		2.23-1.35 MeV	12.2	8.5	8.7
	σ_{inel}	19.6-6.07 MeV	100.0	28.2	28.7

* See Table 23 in the main text for the details of the λ_i set $\lambda \neq 1$ ^(a)

Table 4. GFR target accuracy results

Isotope	Cross-section	Energy range	Uncertainty (%)		
			Initial	Required	
				$\lambda=1$	$\lambda \neq 1$ ^(a)
²³⁵ U	σ_{capt}	9.12-2.03 keV	33.9	13.2	10.5
²³⁸ U	σ_{capt}	1.35-0.498 MeV	2.3	2.3	2.1
		67.4-24.8 keV	1.6	1.6	1.3
		24.8-9.12 keV	9.4	1.6	1.2
		9.12-2.03 keV	3.1	1.4	1.1
		2.03-0.454 keV	2.1	1.9	1.5
	ν	6.07-2.23 MeV	1.2	1.2	0.9
		2.23-1.35 MeV	1.3	1.3	1.0
	σ_{inel}	19.6-6.07 MeV	29.3	7.1	9.6
		6.07-2.23 MeV	19.8	1.6	2.2
		2.23-1.35 MeV	20.6	1.8	2.4
		1.35-0.498 MeV	11.6	2.4	3.3
		183-67.4 keV	11.0	6.6	8.9
²³⁸ Pu	σ_{fiss}	6.07-2.23 MeV	20.5	7.4	8.2
		2.23-1.35 MeV	33.8	7.5	8.2
		1.35-0.498 MeV	17.1	4.7	5.2
		498-183 keV	17.1	6.0	6.6
		67.4-24.8 keV	11.9	6.9	7.6
		24.8-9.12 keV	11.2	7.2	7.9
		9.12-2.03 keV	7.5	6.0	6.6
	ν	1.35-0.498 MeV	7.0	4.0	4.4
		498-183 keV	7.0	5.2	5.7
²³⁹ Pu	σ_{capt}	183-67.4 keV	9.0	5.6	4.4
		67.4-24.8 keV	10.1	4.9	3.8
		24.8-9.12 keV	7.4	4.1	3.2
		9.12-2.03 keV	15.5	2.8	2.2
	σ_{inel}	6.07-2.23 MeV	22.2	7.6	10.4
		1.35-0.498 MeV	29.0	11.8	15.3
²⁴⁰ Pu	σ_{capt}	183-67.4 keV	13.8	6.0	6.6
		67.4-24.8 keV	11.3	5.1	5.6
		24.8-9.12 keV	10.2	5.0	5.5
	σ_{fiss}	6.07-2.23 MeV	4.8	3.0	3.4
		2.23-1.35 MeV	5.7	3.1	3.4
		1.35-0.498 MeV	5.8	2.2	2.5
		2.03-0.454 keV	21.6	9.0	9.9
	ν	6.07-2.23 MeV	2.7	2.5	2.7
		2.23-1.35 MeV	2.7	2.5	2.7
		1.35-0.498 MeV	3.7	1.9	2.1
		498-183 keV	4.8	4.7	4.8
²⁴¹ Pu	σ_{fiss}	6.07-2.23 MeV	14.2	5.8	6.4
		2.23-1.35 MeV	21.3	5.5	6.0
		1.35-0.498 MeV	16.6	3.5	3.8
		498-183 keV	13.5	3.1	3.4
		183-67.4 keV	19.9	2.5	2.8
		67.4-24.8 keV	8.7	2.5	2.8
		24.8-9.12 keV	11.3	2.6	2.9
		9.12-2.03 keV	10.4	2.2	2.4
		2.03-0.454 keV	12.7	2.8	3.1
		454-22.6 eV	19.4	4.7	5.2

* See Table 23 in the main text for the details of the λ_i set $\lambda \neq 1$ ^(a)

Table 4. GFR target accuracy results (*cont.*)

Isotope	Cross-section	Energy range	Uncertainty (%)		
			Initial	Required	
				$\lambda=1$	$\lambda \neq 1$ ^(a)
²⁴² Pu	σ_{capt}	183-67.4 keV	32.3	12.9	13.6
		67.4-24.8 keV	37.3	8.8	9.7
		24.8-9.12 keV	38.6	8.0	8.9
		9.12-2.03 keV	38.5	6.8	7.5
	σ_{fiss}	6.07-2.23 MeV	15.1	5.5	6.0
		2.23-1.35 MeV	21.4	5.4	5.9
		1.35-0.498 MeV	19.0	4.0	4.4
²⁴¹ Am	σ_{capt}	498-183 keV	5.3	4.6	5.1
		183-67.4 keV	6.8	3.5	3.8
		67.4-24.8 keV	8.0	3.4	3.7
		24.8-9.12 keV	6.9	3.4	3.8
		9.12-2.03 keV	6.7	2.9	3.2
		2.03-0.454 keV	6.6	3.3	3.6
	σ_{fiss}	6.07-2.23 MeV	11.7	3.3	3.6
		2.23-1.35 MeV	9.8	3.3	3.6
		1.35-0.498 MeV	8.3	3.0	3.3
²⁴⁴ Cm	σ_{fiss}	6.07-2.23 MeV	31.3	11.5	12.2
		2.23-1.35 MeV	43.8	12.8	13.4
		1.35-0.498 MeV	50.0	7.7	8.5
²⁴⁵ Cm	σ_{fiss}	1.35-0.498 MeV	49.4	16.3	16.7
		498-183 keV	37.2	13.3	13.9
		183-67.4 keV	47.5	10.7	11.4
		67.4-24.8 keV	26.5	10.8	11.6
C	σ_{el}	6.07-2.23 MeV	5.0	3.5	2.7
		2.23-1.35 MeV	5.0	2.4	1.8
		1.35-0.498 MeV	5.0	1.7	1.4
		498-183 keV	5.0	2.2	1.7
		183-67.4 keV	3.0	2.1	1.7
		9.12-2.03 keV	3.0	3.0	2.5
	σ_{inel}	19.6-6.07 MeV	30.0	9.4	12.6
		6.07-2.23 MeV	35.0	11.1	14.4
²⁸ Si	σ_{capt}	19.6-6.07 MeV	52.9	5.6	4.4
	σ_{inel}	6.07-2.23 MeV	13.5	3.0	4.1
		2.23-1.35 MeV	50.0	5.8	7.9

* See Table 23 in the main text for the details of the λ_i set $\lambda \neq 1$ ^(a)

Table 5. LFR target accuracy results

Isotope	Cross-section	Energy range	Uncertainty (%)		
			Initial	Required	
				$\lambda=1$	$\lambda \neq 1$ ^(a)
²³⁸ U	σ_{capt}	1.35-0.498 MeV	2.3	2.1	1.6
		498-183 keV	1.4	1.4	1.3
		183-67.4 keV	1.7	1.7	1.4
		24.8-9.12 keV	9.4	2.0	1.5
		9.12-2.03 keV	3.1	3.1	2.4
	ν	6.07-2.23 MeV	1.2	1.2	1.1
		2.23-1.35 MeV	1.3	1.3	1.2
	σ_{inel}	6.07-2.23 MeV	19.8	2.8	3.7
		2.23-1.35 MeV	20.6	2.3	3.1
		1.35-0.498 MeV	11.6	2.1	2.8
		498-183 keV	4.2	3.1	4.2
		183-67.4 keV	11.0	3.6	4.7
²³⁸ Pu	σ_{fiss}	6.07-2.23 MeV	20.5	7.5	8.0
		2.23-1.35 MeV	33.8	6.8	7.4
		1.35-0.498 MeV	17.1	3.3	3.6
		498-183 keV	17.1	3.4	3.6
		183-67.4 keV	8.8	4.6	5.0
		67.4-24.8 keV	11.9	5.5	5.9
		24.8-9.12 keV	11.2	6.5	7.1
	ν	1.35-0.498 MeV	7.0	2.7	3.0
		498-183 keV	7.0	2.9	3.1
		183-67.4 keV	6.5	4.0	4.3
²³⁹ Pu	σ_{capt}	1.35-0.498 MeV	18.2	7.0	5.3
		498-183 keV	11.6	4.2	3.2
		183-67.4 keV	9.0	4.0	3.0
		67.4-24.8 keV	10.1	4.5	3.4
		24.8-9.12 keV	7.4	4.5	3.4
		9.12-2.03 keV	15.5	5.5	4.2
	σ_{fiss}	498-183 keV	0.7	0.7	0.6
		183-67.4 keV	0.9	0.9	0.7
	σ_{inel}	1.35-0.498 MeV	29.0	7.3	9.6
		498-183 keV	34.0	12.3	15.3
²⁴⁰ Pu	σ_{capt}	1.35-0.498 MeV	16.3	6.3	6.9
		498-183 keV	14.3	4.3	4.6
		183-67.4 keV	13.8	4.0	4.3
		67.4-24.8 keV	11.3	4.3	4.6
		24.8-9.12 keV	10.2	5.1	5.5
	σ_{fiss}	6.07-2.23 MeV	4.8	3.1	3.3
		2.23-1.35 MeV	5.7	2.8	3.0
		1.35-0.498 MeV	5.8	1.6	1.7
		498-183 keV	3.9	3.1	3.3
		183-67.4 keV	5.7	4.7	5.1
	ν	6.07-2.23 MeV	2.7	2.5	2.7
		2.23-1.35 MeV	2.7	2.2	2.4
		1.35-0.498 MeV	3.7	1.3	1.4
		498-183 keV	4.8	2.6	2.8
		183-67.4 keV	4.8	4.1	4.4
	σ_{inel}	183-67.4 keV	42.6	13.0	15.8

* See Table 23 in the main text for the details of the λ_i set $\lambda \neq 1$ ^(a) and $\lambda \neq 1$ ^(b)

Table 5. LFR target accuracy results (*cont.*)

Isotope	Cross-section	Energy range	Uncertainty (%)		
			Initial	Required	
				$\lambda=1$	$\lambda \neq 1$ ^(a)
²⁴¹ Pu	σ_{fiss}	2.23-1.35 MeV	21.3	7.6	8.1
		1.35-0.498 MeV	16.6	3.7	3.9
		498-183 keV	13.5	2.6	2.8
		183-67.4 keV	19.9	2.6	2.8
		67.4-24.8 keV	8.7	3.1	3.3
		24.8-9.12 keV	11.3	3.6	3.9
		9.12-2.03 keV	10.4	5.4	5.8
²⁴² Pu	σ_{capt}	183-67.4 keV	32.3	11.4	11.9
		67.4-24.8 keV	37.3	11.1	11.7
		24.8-9.12 keV	38.6	12.1	12.7
	σ_{fiss}	6.07-2.23 MeV	15.1	7.3	7.8
		2.23-1.35 MeV	21.4	6.5	7.1
		1.35-0.498 MeV	19.0	3.9	4.2
²⁴¹ Am	σ_{fiss}	1.35-0.498 MeV	8.3	5.2	5.6
^{242m} Am	σ_{fiss}	498-183 keV	16.6	7.9	8.4
²⁴⁴ Cm	σ_{fiss}	2.23-1.35 MeV	43.8	13.5	14.3
		1.35-0.498 MeV	50.0	6.4	7.0
²⁴⁵ Cm	σ_{fiss}	1.35-0.498 MeV	49.4	11.1	11.9
		498-183 keV	37.2	7.0	7.5
		183-67.4 keV	47.5	7.2	7.8
		67.4-24.8 keV	26.5	8.9	9.4
⁵⁶ Fe	σ_{capt}	183-67.4 keV	10.8	5.8	4.4
		67.4-24.8 keV	13.2	7.0	5.3
	σ_{inel}	2.23-1.35 MeV	25.4	4.2	5.5
		1.35-0.498 MeV	16.1	3.6	4.7
⁹⁰ Zr	σ_{inel}	6.07-2.23 MeV	18.0	6.4	8.6
²⁰⁶ Pb	σ_{capt}	183-67.4 keV	15.1	7.1	5.4
		6.07-2.23 MeV	5.5	3.4	4.5
		2.23-1.35 MeV	14.2	3.3	4.3
		1.35-0.498 MeV	9.2	3.9	5.1
²⁰⁷ Pb	σ_{inel}	6.07-2.23 MeV	5.0	4.1	5.0
		2.23-1.35 MeV	13.8	5.0	6.5
		1.35-0.498 MeV	11.3	3.0	3.9
²⁰⁸ Pb	σ_{el}	1.35-0.498 MeV	7.2	2.7	2.1
		498-183 keV	4.9	3.4	2.6
	σ_{inel}	19.6-6.07 MeV	17.8	6.9	9.1
		6.07-2.23 MeV	5.4	3.6	4.7
¹⁰ B	σ_{capt}	1.35-0.498 MeV	15.0	4.5	3.4
		498-183 keV	15.0	2.4	1.8
		183-67.4 keV	10.0	2.3	1.7
		67.4-24.8 keV	10.0	2.7	2.1
		24.8-9.12 keV	8.0	3.2	2.4
		9.12-2.03 keV	8.0	5.0	3.8

* See Table 23 in the main text for the details of the λ_i set $\lambda \neq 1$ ^(a)

Table 6. ADMAB target accuracy results

Isotope	Cross-section	Energy range	Uncertainty (%)		
			Initial	Required	
				$\lambda=1$	$\lambda \neq 1$ ^(a)
^{238}Pu	σ_{fiss}	6.07-2.23 MeV	20.5	7.4	7.3
		2.23-1.35 MeV	33.8	6.0	6.0
		1.35-0.498 MeV	17.1	3.4	3.4
		498-183 keV	17.1	3.9	3.9
	ν	1.35-0.498 MeV	7.0	2.8	2.8
		498-183 keV	7.0	3.4	3.4
^{239}Pu	σ_{capt}	1.35-0.498 MeV	18.2	7.1	5.0
		498-183 keV	11.6	5.1	3.6
		183-67.4 keV	9.0	4.8	3.4
		67.4-24.8 keV	10.1	5.1	3.6
		24.8-9.12 keV	7.4	4.5	3.2
		9.12-2.03 keV	15.5	4.1	2.9
	σ_{fiss}	498-183 keV	0.7	0.7	0.7
		183-67.4 keV	0.9	0.9	0.7
	σ_{inel}	6.07-2.23 MeV	22.2	7.8	9.6
		2.23-1.35 MeV	19.0	6.1	7.5
		1.35-0.498 MeV	29.0	4.7	5.8
^{240}Pu	σ_{capt}	183-67.4 keV	13.8	6.2	6.2
	σ_{fiss}	6.07-2.23 MeV	4.8	3.7	3.7
		2.23-1.35 MeV	5.7	3.0	3.0
		1.35-0.498 MeV	5.8	1.9	1.9
	ν	2.23-1.35 MeV	2.7	2.4	2.4
		1.35-0.498 MeV	3.7	1.6	1.6
^{241}Pu	σ_{capt}	1.35-0.498 MeV	31.7	7.5	7.5
		498-183 keV	20.5	7.2	7.2
	σ_{fiss}	6.07-2.23 MeV	14.2	5.1	5.1
		2.23-1.35 MeV	21.3	3.9	3.9
		1.35-0.498 MeV	16.6	2.1	2.1
		498-183 keV	13.5	1.7	1.7
		183-67.4 keV	19.9	1.7	1.7
		67.4-24.8 keV	8.7	2.0	2.0
		24.8-9.12 keV	11.3	2.1	2.1
		9.12-2.03 keV	10.4	2.2	2.2
		2.03-0.454 keV	12.7	2.9	2.9
		454-22.6 eV	19.4	6.9	6.9
^{242}Pu	σ_{capt}	24.8-9.12 keV	38.6	10.2	10.1
	σ_{fiss}	6.07-2.23 MeV	15.1	6.5	6.5
		2.23-1.35 MeV	21.4	5.2	5.2
		1.35-0.498 MeV	19.0	3.5	3.5
	ν	1.35-0.498 MeV	3.1	2.9	2.9
^{237}Np	σ_{capt}	1.35-0.498 MeV	10.3	4.6	4.6
		498-183 keV	5.8	2.8	2.8
		67.4-24.8 keV	6.7	2.7	2.7
		24.8-9.12 keV	5.3	2.7	2.7
		9.12-2.03 keV	5.3	2.9	2.9
		2.03-0.454 keV	5.5	3.5	3.5

* See Table 23 in the main text for the details of the λ_i set $\lambda \neq 1$ ^(a)

Table 6. ADMAB target accuracy results (*cont.*)

Isotope	Cross-section	Energy range	Uncertainty (%)		
			Initial	Required	
				$\lambda=1$	$\lambda \neq 1$ ^(a)
²³⁷ Np	σ_{fiss}	6.07-2.23 MeV	7.9	2.9	2.9
		2.23-1.35 MeV	7.6	2.4	2.4
		1.35-0.498 MeV	5.8	1.5	1.5
		498-183 keV	5.8	3.8	3.8
	σ_{inel}	2.23-1.35 MeV	22.4	5.6	6.8
		1.35-0.498 MeV	28.6	5.0	6.1
		498-183 keV	45.0	9.7	11.9
²⁴¹ Am	σ_{capt}	1.35-0.498 MeV	6.9	2.2	2.2
		498-183 keV	5.3	1.7	1.7
		183-67.4 keV	6.8	1.5	1.5
		67.4-24.8 keV	8.0	1.8	1.8
		24.8-9.12 keV	6.9	1.9	1.9
		9.12-2.03 keV	6.7	2.1	2.1
		2.03-0.454 keV	6.6	2.6	2.6
	σ_{fiss}	19.6-6.07 MeV	12.7	5.6	5.6
		6.07-2.23 MeV	11.7	1.7	1.7
		2.23-1.35 MeV	9.8	1.4	1.4
		1.35-0.498 MeV	8.3	1.2	1.2
		498-183 keV	8.3	3.9	3.9
	ν	6.07-2.23 MeV	2.0	1.4	1.4
		2.23-1.35 MeV	1.9	1.1	1.1
	σ_{inel}	6.07-2.23 MeV	15.2	6.4	7.9
		2.23-1.35 MeV	29.6	4.6	5.7
		1.35-0.498 MeV	24.5	3.9	4.8
		498-183 keV	23.0	7.6	9.3
^{242m} Am	σ_{fiss}	1.35-0.498 MeV	16.5	6.3	6.3
		498-183 keV	16.6	4.8	4.8
		183-67.4 keV	16.6	4.8	4.8
		67.4-24.8 keV	14.4	5.6	5.6
		24.8-9.12 keV	11.8	5.9	5.9
²⁴³ Am	σ_{capt}	1.35-0.498 MeV	14.2	3.1	3.1
		498-183 keV	8.9	2.4	2.4
		183-67.4 keV	6.6	2.0	2.0
		67.4-24.8 keV	4.6	2.2	2.2
		24.8-9.12 keV	6.8	2.3	2.3
		9.12-2.03 keV	6.6	2.5	2.5
		2.03-0.454 keV	6.6	3.1	3.1
	σ_{fiss}	6.07-2.23 MeV	11.0	2.3	2.3
		2.23-1.35 MeV	6.0	1.9	1.9
		1.35-0.498 MeV	9.2	1.6	1.6
	ν	6.07-2.23 MeV	2.0	1.9	1.9
		2.23-1.35 MeV	1.9	1.5	1.5
	σ_{inel}	6.07-2.23 MeV	17.9	4.8	5.8
		2.23-1.35 MeV	35.3	3.8	4.6
		1.35-0.498 MeV	42.2	2.3	2.8
		498-183 keV	41.0	3.6	4.4
		183-67.4 keV	79.5	3.7	4.5
		67.4-24.8 keV	80.8	12.1	14.8

* See Table 23 in the main text for the details of the λ_i set $\lambda \neq 1$ ^(a)

Table 6. ADMAB target accuracy results (*cont.*)

Isotope	Cross-section	Energy range	Uncertainty (%)		
			Initial	Required	
				$\lambda=1$	$\lambda \neq 1$ ^(a)
²⁴² Cm	σ_{fiss}	6.07-2.23 MeV	52.6	26.0	26.1
		498-183 keV	66.0	28.4	28.1
		183-67.4 keV	62.7	27.8	27.5
		67.4-24.8 keV	28.2	24.1	24.9
²⁴³ Cm	σ_{fiss}	1.35-0.498 MeV	49.6	10.0	10.0
		498-183 keV	37.3	8.3	8.3
		183-67.4 keV	47.4	8.2	8.3
²⁴⁴ Cm	σ_{capt}	498-183 keV	22.5	6.0	6.0
		183-67.4 keV	17.7	5.9	5.9
		67.4-24.8 keV	17.4	5.8	5.8
		24.8-9.12 keV	19.3	5.7	5.7
	σ_{fiss}	6.07-2.23 MeV	31.3	3.0	3.0
		2.23-1.35 MeV	43.8	2.6	2.6
		1.35-0.498 MeV	50.0	1.5	1.5
		498-183 keV	36.5	3.9	3.9
		183-67.4 keV	47.6	7.2	7.2
	ν	6.07-2.23 MeV	11.1	2.5	2.5
		2.23-1.35 MeV	10.7	2.1	2.1
		1.35-0.498 MeV	5.5	1.3	1.3
		498-183 keV	5.6	3.5	3.5
²⁴⁵ Cm	σ_{fiss}	6.07-2.23 MeV	31.0	7.1	7.1
		2.23-1.35 MeV	44.2	5.8	5.8
		1.35-0.498 MeV	49.4	3.3	3.3
		498-183 keV	37.2	2.9	2.9
		183-67.4 keV	47.5	2.9	2.9
		67.4-24.8 keV	26.5	3.2	3.2
		24.8-9.12 keV	13.5	3.3	3.4
		9.12-2.03 keV	13.2	3.6	3.6
		2.03-0.454 keV	13.0	4.7	4.7
	ν	1.35-0.498 MeV	3.0	2.9	2.9
		498-183 keV	3.0	2.7	2.7
		183-67.4 keV	3.0	2.7	2.7
⁵⁶ Fe	σ_{capt}	183-67.4 keV	10.8	4.7	3.4
		67.4-24.8 keV	13.2	5.5	3.9
		2.03-0.454 keV	11.2	5.1	3.6
	σ_{inel}	6.07-2.23 MeV	7.2	2.5	3.1
		2.23-1.35 MeV	25.4	1.6	2.0
⁹⁰ Zr	σ_{inel}	1.35-0.498 MeV	16.1	1.5	1.8
		6.07-2.23 MeV	18.0	3.3	4.0
¹⁵ N	σ_{el}	2.23-1.35 MeV	5.0	3.0	2.1
		1.35-0.498 MeV	5.0	1.2	0.8
		498-183 keV	5.0	1.9	1.3
		183-67.4 keV	5.0	2.2	1.6
Pb	σ_{capt}	9.12-2.03 keV	182.3	19.8	14.4
	σ_{inel}	6.07-2.23 MeV	5.4	2.9	3.6
²⁰⁹ Bi	σ_{inel}	6.07-2.23 MeV	2.4	2.4	2.4
		2.23-1.35 MeV	34.1	2.8	3.4
		1.35-0.498 MeV	41.8	4.2	5.1

* See Table 23 in the main text for the details of the λ_i set $\lambda \neq 1$ ^(a)

Table 7. VHTR target accuracy results

Isotope	Cross-section	Energy range	Uncertainty (%)		
			Initial	Required	
				$\lambda=1$	$\lambda \neq 1$ ^(a)
²³⁵ U	σ_{capt}	24.8-9.12 keV	34.0	14.9	18.4
		9.12-2.03 keV	33.9	14.0	17.0
		0.54-0.10 eV	1.6	1.5	1.6
	ν	0.54-0.10 eV	0.7	0.6	0.6
²³⁸ U	σ_{capt}	454-22.6 eV	1.7	1.2	1.2
		22.6-4.00 eV	1.0	0.9	0.9
²³⁹ Pu	σ_{capt}	0.54-0.10 eV	1.4	0.9	0.9
	σ_{fiss}	0.54-0.10 eV	0.9	0.8	0.7
²⁴¹ Pu	σ_{capt}	0.54-0.10 eV	6.8	2.4	3.2
	σ_{fiss}	454-22.6 eV	19.4	6.4	8.3
		4.00-0.54 eV	26.8	9.4	11.6
		0.54-0.10 eV	2.9	1.5	2.0
		0.10 eV-thermal	3.3	3.0	3.3
C	σ_{capt}	19.6-6.07 MeV	20.0	7.1	7.1
		4.00-0.54 eV	20.0	5.0	4.9
		0.54-0.10 eV	2.0	2.0	1.9
	σ_{inel}	19.6-6.07 MeV	30.0	7.1	11.9
		6.07-2.23 MeV	35.0	13.7	24.6

* See Table 23 in the main text for the details of the λ_i set $\lambda \neq 1$ ^(a)

Table 8. PWR target accuracy results

Isotope	Cross-section	Energy range	Uncertainty (%)		
			Initial	Required	
				$\lambda=1$	$\lambda \neq 1$ ^(a)
²³⁵ U	σ_{capt}	67.4-24.8 keV	32.9	19.9	18.5
		24.8-9.12 keV	34.0	17.8	16.2
		9.12-2.03 keV	33.9	11.5	10.3
²³⁸ U	σ_{capt}	24.8-9.12 keV	9.4	4.6	4.0
		9.12-2.03 keV	3.1	3.1	2.9
		454-22.6 eV	1.7	1.4	1.3
	σ_{scatt}	19.6-6.07 MeV	13.3	13.1	11.6
		6.07-2.23 MeV	14.6	5.1	4.6
		2.23-1.35 MeV	18.8	8.0	7.1
²³⁹ Pu	σ_{capt}	0.54-0.10 eV	1.4	1.0	0.9
	σ_{fiss}	0.54-0.10 eV	0.9	0.9	0.8
²⁴⁰ Pu	σ_{capt}	0.54-0.10 eV	3.2	3.1	3.2
		0.10 eV-thermal	4.8	3.1	4.0
²⁴¹ Pu	σ_{capt}	22.6-4.00 eV	8.4	7.3	8.4
		0.54-0.10 eV	6.8	3.0	3.8
	σ_{fiss}	2.03-0.454 keV	12.7	11.2	12.7
		454-22.6 eV	19.4	4.7	5.9
		22.6-4.00 eV	4.2	3.3	4.2
		4.00-0.54 eV	26.8	7.7	9.8
		0.54-0.10 eV	2.9	1.7	2.2
		0.10 eV-thermal	3.3	1.9	2.4
²⁴² Pu	σ_{capt}	4.00-0.54 eV	3.8	3.4	3.8
O	σ_{capt}	19.6-6.07 MeV	100.0	12.1	10.9
		6.07-2.23 MeV	100.0	9.9	8.9
	σ_{scatt}	19.6-6.07 MeV	84.6	15.6	13.9
		6.07-2.23 MeV	54.9	12.6	11.3
		2.23-1.35 MeV	12.2	8.3	7.5

* See Table 23 in the main text for the details of the λ_i set $\lambda \neq 1$ ^(a)

Table 9. ABTR, SFR, EFR target accuracy results

Isotope	Cross-section	Energy range	Uncertainty (%)	
			Initial	Required $\lambda=1$
^{234}U	σ_{capt}	67.4-24.8 keV	22.7	18.1
		24.8-9.12 keV	19.2	17.1
	σ_{fiss}	1.35-0.498 MeV	38.0	28.7
^{235}U	σ_{capt}	183-67.4 keV	30.6	22.7
		67.4-24.8 keV	32.9	22.7
		24.8-9.12 keV	34.0	23.5
		9.12-2.03 keV	33.9	24.7
^{238}U	σ_{capt}	24.8-9.12 keV	9.4	3.8
	σ_{inel}	19.6-6.07 MeV	29.3	20.1
		6.07-2.23 MeV	19.8	4.6
		2.23-1.35 MeV	20.6	4.5
		1.35-0.498 MeV	11.6	5.5
^{238}Pu	σ_{capt}	183-67.4 keV	16.6	11.6
		67.4-24.8 keV	22.1	12.9
	σ_{fiss}	6.07-2.23 MeV	20.5	5.9
		2.23-1.35 MeV	33.8	5.6
		1.35-0.498 MeV	17.1	3.3
		498-183 keV	17.1	3.7
		183-67.4 keV	8.8	5.0
		67.4-24.8 keV	11.9	6.5
		24.8-9.12 keV	11.2	6.8
	ν	6.07-2.23 MeV	5.3	4.8
		2.23-1.35 MeV	5.4	4.5
		1.35-0.498 MeV	7.0	2.8
		498-183 keV	7.0	3.1
		183-67.4 keV	6.5	4.3
		67.4-24.8 keV	6.0	5.6
^{239}Pu	σ_{capt}	1.35-0.498 MeV	18.2	10.1
		498-183 keV	11.6	6.5
		183-67.4 keV	9.0	5.6
		67.4-24.8 keV	10.1	6.3
		24.8-9.12 keV	7.4	5.5
		9.12-2.03 keV	15.5	6.7
	σ_{inel}	6.07-2.23 MeV	22.2	12.4
		1.35-0.498 MeV	29.0	12.1
^{240}Pu	σ_{capt}	6.07-2.23 MeV	32.5	28.7
		1.35-0.498 MeV	16.3	7.4
		498-183 keV	14.3	5.4
		183-67.4 keV	13.8	4.6
		67.4-24.8 keV	11.3	4.9
		24.8-9.12 keV	10.2	5.0
	σ_{fiss}	19.6-6.07 MeV	9.6	8.6
		6.07-2.23 MeV	4.8	2.8
		2.23-1.35 MeV	5.7	2.6
		1.35-0.498 MeV	5.8	1.8
		498-183 keV	3.9	3.9
		2.03-0.454 keV	21.6	12.4
	ν	6.07-2.23 MeV	2.7	2.2
		2.23-1.35 MeV	2.7	2.1
		1.35-0.498 MeV	3.7	1.5
		498-183 keV	4.8	3.3

Table 9. ABTR, SFR, EFR target accuracy results (cont.)

Isotope	Cross-section	Energy range	Uncertainty (%)	
			Initial	Required $\lambda=1$
^{241}Pu	σ_{capt}	1.35-0.498 MeV	31.7	14.5
		498-183 keV	20.5	11.2
	σ_{fiss}	6.07-2.23 MeV	14.2	6.5
		2.23-1.35 MeV	21.3	5.8
		1.35-0.498 MeV	16.6	3.4
		498-183 keV	13.5	2.6
		183-67.4 keV	19.9	2.6
		67.4-24.8 keV	8.7	3.3
		24.8-9.12 keV	11.3	3.5
		9.12-2.03 keV	10.4	5.4
		2.03-0.454 keV	12.7	4.4
		454-22.6 eV	19.4	8.6
^{242}Pu	σ_{capt}	498-183 keV	24.1	11.3
		183-67.4 keV	32.3	9.5
		67.4-24.8 keV	37.3	9.5
		24.8-9.12 keV	38.6	8.4
		9.12-2.03 keV	38.5	12.1
	σ_{fiss}	19.6-6.07 MeV	37.2	15.2
		6.07-2.23 MeV	15.1	5.3
		2.23-1.35 MeV	21.4	4.9
		1.35-0.498 MeV	19.0	3.5
		498-183 keV	18.6	8.8
^{241}Am	σ_{capt}	183-67.4 keV	6.8	6.1
		67.4-24.8 keV	8.0	7.4
	σ_{fiss}	6.07-2.23 MeV	11.7	6.9
		2.23-1.35 MeV	9.8	6.5
		1.35-0.498 MeV	8.3	5.8
$^{242\text{m}}\text{Am}$	σ_{capt}	498-183 keV	29.0	14.6
		183-67.4 keV	19.4	12.0
	σ_{fiss}	6.07-2.23 MeV	23.4	8.0
		2.23-1.35 MeV	19.7	8.2
		1.35-0.498 MeV	16.5	4.3
		498-183 keV	16.6	3.1
		183-67.4 keV	16.6	3.1
		67.4-24.8 keV	14.4	4.1
		24.8-9.12 keV	11.8	4.3
		9.12-2.03 keV	12.4	6.5
		2.03-0.454 keV	12.2	5.2
^{243}Am	σ_{fiss}	6.07-2.23 MeV	11.0	8.2
		1.35-0.498 MeV	9.2	7.2
^{242}Cm	σ_{fiss}	6.07-2.23 MeV	52.6	39.9
		498-183 keV	66.0	48.7
		183-67.4 keV	62.7	46.5
^{243}Cm	σ_{fiss}	1.35-0.498 MeV	49.6	38.0
		498-183 keV	37.3	30.9
		183-67.4 keV	47.4	35.7

Table 9. ABTR, SFR, EFR target accuracy results (*cont.*)

Isotope	Cross-section	Energy range	Uncertainty (%)	
			Initial	Required $\lambda=1$
^{244}Cm	σ_{fiss}	6.07-2.23 MeV	31.3	8.2
		2.23-1.35 MeV	43.8	8.2
		1.35-0.498 MeV	50.0	5.1
		498-183 keV	36.5	12.1
	ν	6.07-2.23 MeV	11.1	6.9
		2.23-1.35 MeV	10.7	6.8
		1.35-0.498 MeV	5.5	4.4
^{245}Cm	σ_{fiss}	2.23-1.35 MeV	44.2	14.8
		1.35-0.498 MeV	49.4	9.0
		498-183 keV	37.2	6.6
		183-67.4 keV	47.5	6.8
		67.4-24.8 keV	26.5	8.8
		24.8-9.12 keV	13.5	9.2
^{246}Cm	σ_{fiss}	1.35-0.498 MeV	40.0	16.2
^{10}B	σ_{capt}	1.35-0.498 MeV	15.0	9.3
		498-183 keV	15.0	5.2
		183-67.4 keV	10.0	4.4
		67.4-24.8 keV	10.0	5.1
		24.8-9.12 keV	8.0	5.7
^{52}Cr	σ_{el}	183-67.4 keV	11.4	6.3
^{56}Fe	σ_{capt}	19.6-6.07 MeV	46.2	14.9
		183-67.4 keV	10.8	5.8
		67.4-24.8 keV	13.2	7.0
		2.03-0.454 keV	11.2	5.3
	σ_{el}	6.07-2.23 MeV	8.1	5.2
		2.23-1.35 MeV	5.9	5.0
	σ_{inel}	19.6-6.07 MeV	13.0	8.9
		6.07-2.23 MeV	7.2	4.1
		2.23-1.35 MeV	25.4	3.3
		1.35-0.498 MeV	16.1	3.2
^{23}Na	σ_{capt}	19.6-6.07 MeV	46.4	17.4
	σ_{inel}	2.23-1.35 MeV	12.6	9.3
		1.35-0.498 MeV	28.0	4.0
^{58}Ni	σ_{capt}	19.6-6.07 MeV	47.8	35.7
^{16}O	σ_{capt}	19.6-6.07 MeV	100.0	62.3
		6.07-2.23 MeV	100.0	39.5
	σ_{el}	6.07-2.23 MeV	54.9	38.2
	σ_{inel}	19.6-6.07 MeV	100.0	71.6
^{90}Zr	σ_{inel}	6.07-2.23 MeV	18.0	8.8

Table 10. ABTR, SFR, EFR, GFR, EFR, ADMAB target accuracy results

Isotope	Cross-section	Energy range	Uncertainty (%)	
			Initial	Required $\lambda=1$
^{234}U	σ_{capt}	67.4-24.8 keV	22.7	19.2
		24.8-9.12 keV	19.2	18.0
	σ_{fiss}	1.35-0.498 MeV	38.0	28.2
^{235}U	σ_{capt}	183-67.4 keV	30.6	23.8
		67.4-24.8 keV	32.9	23.4
		24.8-9.12 keV	34.0	23.9
		9.12-2.03 keV	33.9	14.8
^{238}U	σ_{capt}	24.8-9.12 keV	9.4	1.8
		9.12-2.03 keV	3.1	1.8
	σ_{inel}	19.6-6.07 MeV	29.3	9.0
		6.07-2.23 MeV	19.8	2.0
		2.23-1.35 MeV	20.6	2.1
		1.35-0.498 MeV	11.6	2.3
		498-183 keV	4.2	3.8
		183-67.4 keV	11.0	4.2
^{237}Np	σ_{capt}	1.35-0.498 MeV	10.3	4.7
		498-183 keV	5.8	2.9
		67.4-24.8 keV	6.7	2.7
		24.8-9.12 keV	5.3	2.8
		9.12-2.03 keV	5.3	2.9
		2.03-0.454 keV	5.5	3.6
	σ_{fiss}	6.07-2.23 MeV	7.9	3.0
		2.23-1.35 MeV	7.6	2.4
		1.35-0.498 MeV	5.8	1.5
		498-183 keV	5.8	3.9
	σ_{inel}	2.23-1.35 MeV	22.4	5.7
		1.35-0.498 MeV	28.6	5.1
		498-183 keV	45.0	9.9
^{238}Pu	σ_{fiss}	6.07-2.23 MeV	20.5	6.4
		2.23-1.35 MeV	33.8	5.5
		1.35-0.498 MeV	17.1	3.0
		498-183 keV	17.1	3.3
		183-67.4 keV	8.8	5.5
		67.4-24.8 keV	11.9	6.2
		24.8-9.12 keV	11.2	7.0
	ν	1.35-0.498 MeV	7.0	2.5
		498-183 keV	7.0	2.9
		183-67.4 keV	6.5	4.9
^{239}Pu	σ_{capt}	1.35-0.498 MeV	18.2	6.6
		498-183 keV	11.6	4.4
		183-67.4 keV	9.0	4.0
		67.4-24.8 keV	10.1	4.2
		24.8-9.12 keV	7.4	3.8
		9.12-2.03 keV	15.5	3.2
	σ_{inel}	6.07-2.23 MeV	22.2	7.3
		2.23-1.35 MeV	19.0	6.3
		1.35-0.498 MeV	29.0	4.7
		498-183 keV	34.0	14.1

Table 10. ABTR, SFR, EFR, GFR, EFR, ADMAB target accuracy results (*cont.*)

Isotope	Cross-section	Energy range	Uncertainty (%)	
			Initial	Required
				$\lambda=1$
²⁴⁰ Pu	σ_{capt}	6.07-2.23 MeV	32.5	31.3
		1.35-0.498 MeV	16.3	7.6
		498-183 keV	14.3	5.2
		183-67.4 keV	13.8	4.3
		67.4-24.8 keV	11.3	4.7
		24.8-9.12 keV	10.2	5.2
	σ_{fiss}	6.07-2.23 MeV	4.8	2.9
		2.23-1.35 MeV	5.7	2.6
		1.35-0.498 MeV	5.8	1.6
		498-183 keV	3.9	3.7
		2.03-0.454 keV	21.6	11.8
	ν	6.07-2.23 MeV	2.7	2.6
		2.23-1.35 MeV	2.7	2.1
		1.35-0.498 MeV	3.7	1.3
		498-183 keV	4.8	2.8
	σ_{inel}	183-67.4 keV	42.6	14.5
²⁴¹ Pu	σ_{capt}	1.35-0.498 MeV	31.7	7.7
		498-183 keV	20.5	7.4
	σ_{fiss}	6.07-2.23 MeV	14.2	5.0
		2.23-1.35 MeV	21.3	3.9
		1.35-0.498 MeV	16.6	2.1
		498-183 keV	13.5	1.7
		183-67.4 keV	19.9	1.7
		67.4-24.8 keV	8.7	1.9
		24.8-9.12 keV	11.3	2.0
		9.12-2.03 keV	10.4	2.1
		2.03-0.454 keV	12.7	2.7
		454-22.6 eV	19.4	5.4
²⁴² Pu	σ_{capt}	183-67.4 keV	32.3	11.5
		67.4-24.8 keV	37.3	9.9
		24.8-9.12 keV	38.6	8.4
		9.12-2.03 keV	38.5	8.6
	σ_{fiss}	19.6-6.07 MeV	37.2	30.2
		6.07-2.23 MeV	15.1	5.5
		2.23-1.35 MeV	21.4	4.7
		1.35-0.498 MeV	19.0	3.2
	ν	1.35-0.498 MeV	3.1	2.6
	σ_{inel}	1.35-0.498 MeV	59.8	31.6

Table 10. ABTR, SFR, EFR, GFR, EFR, ADMAB target accuracy results (*cont.*)

Isotope	Cross-section	Energy range	Uncertainty (%)	
			Initial	Required $\lambda=1$
^{241}Am	σ_{capt}	1.35-0.498 MeV	6.9	2.3
		498-183 keV	5.3	1.7
		183-67.4 keV	6.8	1.6
		67.4-24.8 keV	8.0	1.8
		24.8-9.12 keV	6.9	1.9
		9.12-2.03 keV	6.7	2.1
		2.03-0.454 keV	6.6	2.6
	σ_{fiss}	19.6-6.07 MeV	12.7	5.7
		6.07-2.23 MeV	11.7	1.7
		2.23-1.35 MeV	9.8	1.4
		1.35-0.498 MeV	8.3	1.2
		498-183 keV	8.3	4.0
	ν	6.07-2.23 MeV	2.0	1.4
		2.23-1.35 MeV	1.9	1.2
	σ_{inel}	6.07-2.23 MeV	15.2	6.6
		2.23-1.35 MeV	29.6	4.7
		1.35-0.498 MeV	24.5	4.0
		498-183 keV	23.0	7.7
$^{242\text{m}}\text{Am}$	σ_{fiss}	6.07-2.23 MeV	23.4	21.4
		1.35-0.498 MeV	16.5	6.3
		498-183 keV	16.6	4.7
		183-67.4 keV	16.6	4.8
		67.4-24.8 keV	14.4	5.6
		24.8-9.12 keV	11.8	5.9
^{243}Am	σ_{capt}	1.35-0.498 MeV	14.2	3.2
		498-183 keV	8.9	2.4
		183-67.4 keV	6.6	2.1
		67.4-24.8 keV	4.6	2.3
		24.8-9.12 keV	6.8	2.4
		9.12-2.03 keV	6.6	2.5
		2.03-0.454 keV	6.6	3.1
	σ_{fiss}	6.07-2.23 MeV	11.0	2.3
		2.23-1.35 MeV	6.0	1.9
		1.35-0.498 MeV	9.2	1.7
	ν	6.07-2.23 MeV	2.0	1.9
		2.23-1.35 MeV	1.9	1.6
	σ_{inel}	6.07-2.23 MeV	17.9	4.9
		2.23-1.35 MeV	35.3	3.9
		1.35-0.498 MeV	42.2	2.3
		498-183 keV	41.0	3.7
		183-67.4 keV	79.5	3.7
		67.4-24.8 keV	80.8	12.4
^{242}Cm	σ_{fiss}	6.07-2.23 MeV	52.6	31.7
		498-183 keV	66.0	32.6
		183-67.4 keV	62.7	32.3
^{243}Cm	σ_{fiss}	1.35-0.498 MeV	49.6	10.2
		498-183 keV	37.3	8.5
		183-67.4 keV	47.4	8.4

Table 10. ABTR, SFR, EFR, GFR, EFR, ADMAB target accuracy results (*cont.*)

Isotope	Cross-section	Energy range	Uncertainty (%)	
			Initial	Required $\lambda=1$
^{244}Cm	σ_{capt}	498-183 keV	22.5	6.2
		183-67.4 keV	17.7	6.1
		67.4-24.8 keV	17.4	5.9
		24.8-9.12 keV	19.3	5.9
	σ_{fiss}	6.07-2.23 MeV	31.3	3.0
		2.23-1.35 MeV	43.8	2.6
		1.35-0.498 MeV	50.0	1.5
		498-183 keV	36.5	4.0
		183-67.4 keV	47.6	7.3
	ν	6.07-2.23 MeV	11.1	2.5
		2.23-1.35 MeV	10.7	2.2
		1.35-0.498 MeV	5.5	1.3
		498-183 keV	5.6	3.6
^{245}Cm	σ_{fiss}	6.07-2.23 MeV	31.0	7.3
		2.23-1.35 MeV	44.2	5.9
		1.35-0.498 MeV	49.4	3.4
		498-183 keV	37.2	3.0
		183-67.4 keV	47.5	2.9
		67.4-24.8 keV	26.5	3.3
		24.8-9.12 keV	13.5	3.4
		9.12-2.03 keV	13.2	3.7
		2.03-0.454 keV	13.0	4.8
	ν	498-183 keV	3.0	2.7
		183-67.4 keV	3.0	2.7
^{246}Cm	σ_{fiss}	1.35-0.498 MeV	40.0	30.5
^{10}B	σ_{capt}	1.35-0.498 MeV	15.0	5.4
		498-183 keV	15.0	2.9
		183-67.4 keV	10.0	2.7
		67.4-24.8 keV	10.0	3.3
		24.8-9.12 keV	8.0	3.9
		9.12-2.03 keV	8.0	6.0
^{209}Bi	σ_{inel}	2.23-1.35 MeV	34.1	2.8
		1.35-0.498 MeV	41.8	4.3
C	σ_{el}	6.07-2.23 MeV	5.0	4.5
		2.23-1.35 MeV	5.0	3.0
		1.35-0.498 MeV	5.0	2.2
		498-183 keV	5.0	2.9
		183-67.4 keV	3.0	2.7
	σ_{inel}	19.6-6.07 MeV	30.0	12.0
^{56}Fe	σ_{capt}	6.07-2.23 MeV	35.0	13.7
		19.6-6.07 MeV	46.2	30.3
		183-67.4 keV	10.8	4.6
		67.4-24.8 keV	13.2	5.4
	σ_{inel}	2.03-0.454 keV	11.2	5.2
		6.07-2.23 MeV	7.2	2.6
		2.23-1.35 MeV	25.4	1.7
		1.35-0.498 MeV	16.1	1.5

Table 10. ABTR, SFR, EFR, GFR, EFR, ADMAB target accuracy results (*cont.*)

Isotope	Cross-section	Energy range	Uncertainty (%)	
			Initial	Required $\lambda=1$
¹⁵ N	σ_{el}	2.23-1.35 MeV	5.0	3.1
		1.35-0.498 MeV	5.0	1.2
		498-183 keV	5.0	1.9
		183-67.4 keV	5.0	2.3
²³ Na	σ_{capt}	19.6-6.07 MeV	46.4	30.7
	σ_{inel}	1.35-0.498 MeV	28.0	10.5
⁵⁸ Ni	σ_{capt}	19.6-6.07 MeV	47.8	31.5
¹⁶ O	σ_{capt}	19.6-6.07 MeV	100.0	37.9
		6.07-2.23 MeV	100.0	37.9
	σ_{el}	6.07-2.23 MeV	54.9	31.8
	σ_{inel}	19.6-6.07 MeV	100.0	37.9
Pb	σ_{capt}	9.12-2.03 keV	182.3	20.3
	σ_{inel}	6.07-2.23 MeV	5.4	3.0
²⁰⁶ Pb	σ_{capt}	183-67.4 keV	15.1	8.6
	σ_{inel}	6.07-2.23 MeV	5.5	4.2
		2.23-1.35 MeV	14.2	4.0
		1.35-0.498 MeV	9.2	4.7
²⁰⁷ Pb	σ_{inel}	6.07-2.23 MeV	5.0	4.9
		2.23-1.35 MeV	13.8	6.0
		1.35-0.498 MeV	11.3	3.6
²⁰⁸ Pb	σ_{el}	1.35-0.498 MeV	7.2	3.3
		498-183 keV	4.9	4.2
	σ_{inel}	19.6-6.07 MeV	17.8	8.4
		6.07-2.23 MeV	5.4	4.4
²⁸ Si	σ_{capt}	19.6-6.07 MeV	52.9	7.2
	σ_{inel}	6.07-2.23 MeV	13.5	3.9
		2.23-1.35 MeV	50.0	7.4
⁹⁰ Zr	σ_{inel}	6.07-2.23 MeV	18.0	3.3

Appendix Q
ANL DIAGONAL MATRIX

Table 1. ANL variance matrix (fissile isotopes) – values in %

Gr	E [MeV]	²³² Th						²³³ U						²³⁴ U						²³⁵ U					
		v	σ _f	σ _{inel}	σ _{el}	σ _{capt}	σ _{n,2n}	v	σ _f	σ _{inel}	σ _{el}	σ _{capt}	σ _{n,2n}	v	σ _f	σ _{inel}	σ _{el}	σ _{capt}	σ _{n,2n}	v	σ _f	σ _{inel}	σ _{el}	σ _{capt}	σ _{n,2n}
1	19.6	2	5	15	10	20	100	2	20	20	10	10	100	3	20	15	10	20	100	1	5	10	5	15	50
2	6.07	2	5	15	10	20	100	2	20	20	10	10	100	3	20	15	10	20	100	1	5	10	5	15	50
3	2.23	2	5	15	10	20	0	2	10	20	10	10	0	3	20	15	10	20	0	1	5	10	5	15	0
4	1.35	2	5	15	10	20	0	2	10	20	10	10	0	3	20	15	10	20	0	1	5	15	5	15	0
5	4.98e-1	2	5	20	10	15	0	2	10	30	10	10	0	3	20	20	10	20	0	1	5	15	5	15	0
6	1.83e-1	2	5	0	10	15	0	2	10	0	10	10	0	3	20	20	10	20	0	1	5	15	5	15	0
7	6.74e-2	2	5	0	10	15	0	2	10	0	10	10	0	3	20	25	10	20	0	1	5	20	5	10	0
8	2.48e-2	2	5	0	10	10	0	2	10	0	10	20	0	3	20	0	10	20	0	1	5	25	5	10	0
9	9.12e-3	2	10	0	10	10	0	2	10	0	10	20	0	3	20	0	10	20	0	1	5	25	5	5	0
10	2.03e-3	2	10	0	10	10	0	2	10	0	10	20	0	3	20	0	10	20	0	0.5	3	30	5	5	0
11	4.54e-4	2	10	0	10	10	0	2	10	0	10	10	0	3	20	0	10	10	0	0.5	3	0	5	5	0
12	2.26e-5	2	10	0	10	5	0	2	10	0	10	5	0	3	20	0	10	10	0	0.5	3	0	5	5	0
13	4.00e-6	2	10	0	10	5	0	2	5	0	10	5	0	3	20	0	10	10	0	0.5	3	0	5	3	0
14	5.40e-7	2	50	0	5	1	0	2	2	0	10	3	0	3	20	0	2	10	0	0.5	1	0	5	1	0
15	1.00e-7	2	50	0	5	1	0	2	2	0	10	3	0	3	20	0	2	5	0	0.3	1	0	5	1	0

Table 1. ANL variance matrix (fissile isotopes) – values in % (*cont.*)

		²³⁶ U						²³⁸ U						²³⁷ Np						²³⁸ Pu					
Gr	E [MeV]	v	σ _f	σ _{inel}	σ _{el}	σ _{capt}	σ _{n,2n}	v	σ _f	σ _{inel}	σ _{el}	σ _{capt}	σ _{n,2n}	v	σ _f	σ _{inel}	σ _{el}	σ _{capt}	σ _{n,2n}	v	σ _f	σ _{inel}	σ _{el}	σ _{capt}	σ _{n,2n}
1	19.6	3	20	15	10	20	100	3	5	20	5	30	30	3	10	50	5	10	100	3	10	15	10	10	100
2	6.07	2	20	15	10	20	0	2	5	15	5	10	0	2	10	50	5	10	0	2	10	15	10	10	0
3	2.23	2	20	15	10	20	0	2	5	10	5	5	0	2	10	50	5	10	0	2	10	15	10	10	0
4	1.35	2	20	15	10	20	0	2	5	10	5	5	0	2	10	50	5	10	0	2	10	15	10	10	0
5	4.98e-1	2	20	20	10	20	0	2	5	10	5	5	0	2	10	50	5	10	0	2	10	20	10	10	0
6	1.83e-1	2	20	20	10	20	0	2	20	10	5	5	0	2	10	50	5	10	0	2	10	20	10	10	0
7	6.74e-2	2	20	25	10	20	0	2	20	15	5	5	0	2	10	60	5	10	0	2	30	25	10	10	0
8	2.48e-2	2	20	0	10	20	0	2	20	0	5	5	0	2	10	0	5	10	0	2	30	0	10	20	0
9	9.12e-3	2	20	0	10	20	0	2	20	0	5	3	0	2	10	0	5	10	0	2	30	0	10	20	0
10	2.03e-3	2	20	0	10	8	0	2	20	0	5	3	0	2	20	0	5	10	0	2	30	0	10	20	0
11	4.54e-4	2	20	0	10	8	0	2	20	0	5	3	0	2	20	0	5	10	0	2	30	0	10	20	0
12	2.26e-5	2	20	0	10	8	0	2	20	0	5	3	0	2	20	0	5	10	0	2	20	0	10	10	0
13	4.00e-6	2	20	0	10	8	0	2	20	0	5	3	0	2	20	0	5	10	0	2	20	0	10	10	0
14	5.40e-7	2	20	0	7	4	0	2	20	0	1	1	0	2	20	0	5	4	0	2	20	0	7	10	0
15	1.00e-7	2	20	0	7	4	0	2	20	0	1	1	0	2	20	0	5	4	0	2	20	0	7	10	0

		²³⁹ Pu						²⁴⁰ Pu						²⁴¹ Pu						²⁴² Pu					
Gr	E [MeV]	v	σ _f	σ _{inel}	σ _{el}	σ _{capt}	σ _{n,2n}	v	σ _f	σ _{inel}	σ _{el}	σ _{capt}	σ _{n,2n}	v	σ _f	σ _{inel}	σ _{el}	σ _{capt}	σ _{n,2n}	v	σ _f	σ _{inel}	σ _{el}	σ _{capt}	σ _{n,2n}
1	19.6	1	5	10	5	15	50	3	5	15	10	20	100	1	20	15	10	10	100	3	10	15	10	20	100
2	6.07	1	5	10	5	15	50	2	5	15	10	20	0	1	20	15	10	10	100	2	10	15	10	20	0
3	2.23	1	5	10	5	15	0	2	5	15	10	20	0	1	10	15	10	10	0	2	10	15	10	20	0
4	1.35	1	5	15	5	15	0	2	5	15	10	20	0	1	10	15	10	10	0	2	10	15	10	20	0
5	4.98e-1	1	5	15	5	15	0	2	5	20	10	20	0	1	10	20	10	10	0	2	20	20	10	20	0
6	1.83e-1	1	5	15	5	15	0	2	5	20	10	20	0	1	10	20	10	10	0	2	20	20	10	15	0
7	6.74e-2	1	5	20	5	10	0	2	5	25	10	20	0	1	10	25	10	10	0	2	20	25	10	10	0
8	2.48e-2	1	5	25	5	10	0	2	5	0	10	10	0	1	10	0	10	20	0	2	20	0	10	10	0
9	9.12e-3	1	5	30	5	5	0	2	10	0	10	10	0	1	10	0	10	20	0	2	20	0	10	10	0
10	2.03e-3	0.5	3	0	5	5	0	2	10	0	10	10	0	1	10	0	10	20	0	2	20	0	10	10	0
11	4.54e-4	0.5	3	0	5	5	0	2	10	0	10	10	0	1	10	0	10	10	0	2	20	0	10	10	0
12	2.26e-5	0.5	3	0	5	5	0	2	10	0	10	10	0	1	10	0	10	5	0	2	20	0	10	5	0
13	4.00e-6	0.5	3	0	5	4	0	2	10	0	10	7	0	1	5	0	10	5	0	2	20	0	10	5	0
14	5.40e-7	0.5	2	0	5	3	0	2	50	0	5	3	0	0.5	2	0	7	3	0	2	50	0	7	4	0
15	1.00e-7	0.3	1	0	5	2	0	2	50	0	5	2	0	0.5	2	0	7	3	0	2	50	0	7	3	0

Table 1. ANL variance matrix (fissile isotopes) – values in % (cont.)

		²⁴¹ Am						^{242m} Am						²⁴³ Am						^{242,243,244} Cm					
Gr	E [MeV]	v	σ _f	σ _{inel}	σ _{el}	σ _{capt}	σ _{n,2n}	v	σ _f	σ _{inel}	σ _{el}	σ _{capt}	σ _{n,2n}	v	σ _f	σ _{inel}	σ _{el}	σ _{capt}	σ _{n,2n}	v	σ _f	σ _{inel}	σ _{el}	σ _{capt}	σ _{n,2n}
1	19.6	3	10	50	10	10	100	5	20	50	10	40	100	5	10	50	10	10	100	5	40	50	10	40	100
2	6.07	2	10	50	10	10	0	3	20	50	10	40	100	3	10	50	10	10	0	5	40	50	10	40	0
3	2.23	2	10	50	10	10	0	3	20	50	10	40	0	3	10	50	10	10	0	5	40	50	10	40	0
4	1.35	2	10	50	10	10	0	3	20	50	10	40	0	3	10	50	10	10	0	5	40	50	10	40	0
5	4.98e-1	2	10	50	10	10	0	3	20	50	10	40	0	3	10	50	10	10	0	5	40	50	10	40	0
6	1.83e-1	2	10	50	10	10	0	3	20	50	10	40	0	3	10	50	10	10	0	5	40	50	10	40	0
7	6.74e-2	2	10	55	10	10	0	3	20	55	10	40	0	3	10	55	10	10	0	5	40	55	10	40	0
8	2.48e-2	2	20	0	10	10	0	3	10	0	10	40	0	3	10	0	10	10	0	5	40	0	10	40	0
9	9.12e-3	2	20	0	10	10	0	3	10	0	10	40	0	3	10	0	10	10	0	5	40	0	10	40	0
10	2.03e-3	2	20	0	10	10	0	3	10	0	10	40	0	3	10	0	10	10	0	5	40	0	10	40	0
11	4.54e-4	2	20	0	10	10	0	3	10	0	10	40	0	3	20	0	10	20	0	5	40	0	10	40	0
12	2.26e-5	2	20	0	10	10	0	3	10	0	10	40	0	3	40	0	10	20	0	5	40	0	10	40	0
13	4.00e-6	2	20	0	10	10	0	3	5	0	10	40	0	3	40	0	10	20	0	5	40	0	10	40	0
14	5.40e-7	2	20	0	10	10	0	3	5	0	10	40	0	3	40	0	10	20	0	5	40	0	10	40	0
15	1.00e-7	2	20	0	10	10	0	3	5	0	10	40	0	3	40	0	10	20	0	5	40	0	10	40	0
		²⁴⁵ Cm																							
Gr	E [MeV]	v	σ _f	σ _{inel}	σ _{el}	σ _{capt}	σ _{n,2n}																		
1	19.6	5	40	50	10	40	100																		
2	6.07	5	40	50	10	40	100																		
3	2.23	5	40	50	10	40	0																		
4	1.35	5	40	50	10	40	0																		
5	4.98e-1	5	40	50	10	40	0																		
6	1.83e-1	5	40	50	10	40	0																		
7	6.74e-2	5	40	55	10	40	0																		
8	2.48e-2	5	40	0	10	40	0																		
9	9.12e-3	5	40	0	10	40	0																		
10	2.03e-3	5	40	0	10	40	0																		
11	4.54e-4	5	40	0	10	40	0																		
12	2.26e-5	5	40	0	10	40	0																		
13	4.00e-6	5	40	0	10	40	0																		
14	5.40e-7	5	40	0	10	40	0																		
15	1.00e-7	5	40	0	10	40	0																		

Table 2. ANL variance matrix (structural isotopes) – values in %

		Pb				Bi				⁵⁶ Fe				⁵⁷ Fe				⁵⁸ Ni				⁵² Cr			
Gr	E [MeV]	σ _{inel}	σ _{el}	σ _{capt}	σ _{n,2n}	σ _{inel}	σ _{el}	σ _{capt}	σ _{n,2n}	σ _{inel}	σ _{el}	σ _{capt}	σ _{n,2n}	σ _{inel}	σ _{el}	σ _{capt}	σ _{n,2n}	σ _{inel}	σ _{el}	σ _{capt}	σ _{n,2n}	σ _{inel}	σ _{el}	σ _{capt}	σ _{n,2n}
1	19.6	40	20	20	100	40	20	20	100	20	30	45	100	20	30	45	100	20	20	15	100	40	10	20	100
2	6.07	40	20	20	0	40	20	20	0	15	20	30	0	15	20	30	0	20	20	10	0	10	10	20	0
3	2.23	40	20	20	0	40	20	20	0	10	10	15	0	10	10	15	0	20	20	10	0	10	10	20	0
4	1.35	45	20	20	0	45	20	20	0	20	10	10	0	10	10	10	0	25	10	10	0	15	10	15	0
5	4.98e-1	0	20	20	0	0	20	20	0	0	10	8	0	10	10	8	0	0	10	10	0	0	10	10	0
6	1.83e-1	0	20	20	0	0	20	20	0	0	10	8	0	20	10	8	0	0	10	10	0	0	10	10	0
7	6.74e-2	0	20	20	0	0	20	20	0	0	8	8	0	20	8	8	0	0	10	10	0	0	10	10	0
8	2.48e-2	0	20	20	0	0	20	20	0	0	6	8	0	25	6	8	0	0	10	10	0	0	10	10	0
9	9.12e-3	0	20	20	0	0	20	20	0	0	4	8	0	0	4	8	0	0	10	10	0	0	10	10	0
10	2.03e-3	0	20	20	0	0	20	20	0	0	4	8	0	0	4	8	0	0	4	10	0	0	10	10	0
11	4.54e-4	0	20	20	0	0	20	20	0	0	4	8	0	0	4	8	0	0	4	10	0	0	10	10	0
12	2.26e-5	0	20	20	0	0	20	20	0	0	4	8	0	0	4	8	0	0	4	10	0	0	10	10	0
13	4.00e-6	0	20	20	0	0	20	20	0	0	4	8	0	0	4	8	0	0	4	10	0	0	10	10	0
14	5.40e-7	0	20	20	0	0	20	20	0	0	4	8	0	0	4	8	0	0	4	5	0	0	4	8	0
15	1.00e-7	0	20	20	0	0	20	20	0	0	4	8	0	0	4	8	0	0	4	5	0	0	4	8	0
		Zr				¹⁵ N				Si				C				O				Na			
Gr	E [MeV]	σ _{inel}	σ _{el}	σ _{capt}	σ _{n,2n}	σ _{inel}	σ _{el}	σ _{capt}	σ _{n,2n}	σ _{inel}	σ _{el}	σ _{capt}	σ _{n,2n}	σ _{inel}	σ _{el}	σ _{capt}	σ _{n,2n}	σ _{inel}	σ _{el}	σ _{capt}	σ _{n,2n}	σ _{inel}	σ _{el}	σ _{capt}	σ _{n,2n}
1	19.6	20	20	20	100	30	5	30	100	30	5	20	100	30	5	20	0	35	5	20	0	30	5	10	100
2	6.07	20	20	20	0	35	5	30	0	30	5	20	0	35	5	20	0	0	5	20	0	30	5	10	0
3	2.23	20	20	20	0	0	5	30	0	35	5	20	0	0	5	20	0	0	5	20	0	30	5	10	0
4	1.35	25	20	20	0	0	5	30	0	0	5	20	0	0	5	20	0	0	5	20	0	30	5	10	0
5	4.98e-1	0	20	20	0	0	5	30	0	0	5	20	0	0	5	20	0	0	5	20	0	35	5	10	0
6	1.83e-1	0	20	20	0	0	5	30	0	0	5	20	0	0	3	20	0	0	3	20	0	0	5	8	0
7	6.74e-2	0	20	20	0	0	5	30	0	0	5	20	0	0	3	20	0	0	3	20	0	0	5	8	0
8	2.48e-2	0	20	20	0	0	5	30	0	0	5	20	0	0	3	20	0	0	3	20	0	0	5	8	0
9	9.12e-3	0	20	20	0	0	5	30	0	0	5	20	0	0	3	20	0	0	3	20	0	0	5	8	0
10	2.03e-3	0	20	20	0	0	5	30	0	0	5	20	0	0	3	20	0	0	3	20	0	0	5	7	0
11	4.54e-4	0	20	20	0	0	5	30	0	0	5	20	0	0	3	20	0	0	3	20	0	0	5	7	0
12	2.26e-5	0	20	20	0	0	5	30	0	0	5	20	0	0	2	20	0	0	2	20	0	0	3	7	0
13	4.00e-6	0	20	20	0	0	5	30	0	0	5	20	0	0	2	20	0	0	2	20	0	0	3	7	0
14	5.40e-7	0	20	20	0	0	5	30	0	0	5	20	0	0	1	2	0	0	1	2	0	0	2	5	0
15	1.00e-7	0	20	20	0	0	5	30	0	0	5	20	0	0	1	2	0	0	1	2	0	0	2	5	0

Table 2. ANL variance matrix (structural isotopes) – values in % (*cont.*)

Gr	E [MeV]	¹⁰ B				H (bonded)				Al				Gd				Er				⁹ Be			
		σ _{inel}	σ _{el}	σ _{capt}	σ _{n,2n}	σ _{inel}	σ _{el}	σ _{capt}	σ _{n,2n}	σ _{inel}	σ _{el}	σ _{capt}	σ _{n,2n}	σ _{inel}	σ _{el}	σ _{capt}	σ _{n,2n}	σ _{inel}	σ _{el}	σ _{capt}	σ _{n,2n}	σ _{inel}	σ _{el}	σ _{capt}	σ _{n,2n}
1	19.6	30	10	15	0	0	2	20	0	15	8	10	100	30	5	15	0	30	5	15	0	30	5	10	0
2	6.07	30	10	15	0	0	2	20	0	15	8	10	0	30	5	10	0	30	5	10	0	35	5	10	0
3	2.23	30	10	15	0	0	2	20	0	15	8	10	0	30	5	8	0	30	5	8	0	0	5	10	0
4	1.35	35	10	15	0	0	2	20	0	20	6	7	0	30	5	8	0	30	5	8	0	0	5	10	0
5	4.98e-1	0	10	15	0	0	2	20	0	0	6	7	0	30	5	8	0	30	5	8	0	0	5	10	0
6	1.83e-1	0	10	10	0	0	1	20	0	0	6	7	0	30	5	8	0	30	5	8	0	0	5	8	0
7	6.74e-2	0	10	10	0	0	1	20	0	0	5	7	0	35	5	8	0	35	5	8	0	0	5	8	0
8	2.48e-2	0	5	8	0	0	1	20	0	0	5	6	0	0	5	8	0	0	5	8	0	0	5	8	0
9	9.12e-3	0	5	8	0	0	1	20	0	0	5	6	0	0	5	8	0	0	5	8	0	0	5	8	0
10	2.03e-3	0	5	5	0	0	1	20	0	0	5	6	0	0	4	8	0	0	4	8	0	0	5	7	0
11	4.54e-4	0	5	5	0	0	1	10	0	0	4	5	0	0	4	8	0	0	4	8	0	0	5	7	0
12	2.26e-5	0	3	5	0	0	1	10	0	0	4	5	0	0	4	8	0	0	4	8	0	0	3	7	0
13	4.00e-6	0	3	3	0	0	1	10	0	0	4	5	0	0	3	8	0	0	3	8	0	0	3	7	0
14	5.40e-7	0	2	1	0	0	0.5	2	0	0	3	5	0	0	1	8	0	0	1	8	0	0	2	5	0
15	1.00e-7	0	2	1	0	0	0.5	2	0	0	3	5	0	0	1	8	0	0	1	8	0	0	2	5	0
Gr	E [MeV]	⁶ Li				⁷ Li				¹⁹ F				⁴ He											
		σ _{inel}	σ _{el}	σ _{capt}	σ _{n,2n}	σ _{inel}	σ _{el}	σ _{capt}	σ _{n,2n}	σ _{inel}	σ _{el}	σ _{capt}	σ _{n,2n}	σ _{inel}	σ _{el}	σ _{capt}	σ _{n,2n}								
1	19.6	30	5	10	0	30	5	10	100	30	5	10	100	0	5	20	0								
2	6.07	30	5	10	0	30	5	10	0	30	5	10	0	0	5	20	0								
3	2.23	35	5	10	0	30	5	10	0	30	5	10	0	0	5	20	0								
4	1.35	0	5	10	0	35	5	10	0	30	5	10	0	0	5	20	0								
5	4.98e-1	0	5	10	0	0	5	10	0	30	5	10	0	0	5	20	0								
6	1.83e-1	0	5	8	0	0	5	8	0	35	5	8	0	0	3	20	0								
7	6.74e-2	0	5	8	0	0	5	8	0	0	5	8	0	0	3	20	0								
8	2.48e-2	0	5	8	0	0	5	8	0	0	5	8	0	0	3	20	0								
9	9.12e-3	0	5	8	0	0	5	8	0	0	5	8	0	0	3	20	0								
10	2.03e-3	0	5	7	0	0	5	7	0	0	5	7	0	0	3	20	0								
11	4.54e-4	0	5	7	0	0	5	7	0	0	5	7	0	0	3	20	0								
12	2.26e-5	0	3	7	0	0	3	7	0	0	3	7	0	0	2	20	0								
13	4.00e-6	0	3	7	0	0	3	7	0	0	3	7	0	0	2	20	0								
14	5.40e-7	0	2	5	0	0	2	5	0	0	2	5	0	0	1	2	0								
15	1.00e-7	0	2	5	0	0	2	5	0	0	2	5	0	0	1	2	0								

Appendix R
BOLNA DIAGONAL MATRIX

Table 1. BOLNA variance matrix (fissile isotopes)

^{235}U , ^{238}U and ^{239}Pu (with nu-bar corrected) from ORNL; ^{246}Cm from ANL – values in %

Gr	E [MeV]	^{232}Th						^{233}U						^{234}U						^{235}U					
		v	σ_f	σ_{inel}	σ_{el}	σ_{capt}	$\sigma_{n,2n}$	v	σ_f	σ_{inel}	σ_{el}	σ_{capt}	$\sigma_{n,2n}$	v	σ_f	σ_{inel}	σ_{el}	σ_{capt}	$\sigma_{n,2n}$	v	σ_f	σ_{inel}	σ_{el}	σ_{capt}	$\sigma_{n,2n}$
1	19.6		2.11	4.85	1.39	17.4	10	0.84	3.98	10.79	2.51	57.01	18.44		12.9	32.41	1.6	56.74	34.85	0.89	0.5	21.73	9.6	61.13	20.35
2	6.07		2.1	3.77	1.22	25.67	0	0.25	6.44	4.48	4.02	61.4	0		23.52	29.45	2.06	26.11	0	0.69	0.47	6.79	4.15	36.99	8.86
3	2.23		2.1	3.94	4	3.41	0	0.22	7.26	31.58	3	38.88	0		13.83	21.15	4.88	15.91	0	0.56	0.48	6.41	4.54	19.14	0
4	1.35		2.15	4.41	1.8	1.89	0	0.18	7.26	40.46	1.88	30.35	0		37.97	14.61	2	11.99	0	0.55	0.46	7.55	3.56	16.1	0
5	4.98e-1		95.17	12.58	1.65	1.24	0	0.18	7.26	14.29	2.49	10.62	0		37.97	25.97	2.75	13.98	0	0.61	0.5	11.32	2.87	22.13	0
6	1.83e-1		46.92	23.6	1.18	1.14	0	0.19	7.26	0	3.16	8.94	0		31.61	31.49	1.6	12.92	0	0.66	0.53	15.01	2.38	30.64	0
7	6.74e-2		0	0	0.48	1.4	0	0.18	7.26	0	4.06	13.29	0		22.84	0	5.3	22.72	0	0.66	0.5	14.72	2.63	32.89	0
8	2.48e-2		0	0	0.31	1.46	0	0.21	7.26	0	4.19	13.52	0		19.41	0	4.86	19.16	0	0.66	0.58	50	3.24	34.03	0
9	9.12e-3		0	0	0.48	2.8	0	0.18	7.26	0	9.04	14.19	0		13.69	0	3.58	11.53	0	0.66	3.18	48.48	5.16	33.92	0
10	2.03e-3		0	0	1.53	3.35	0	0.3	10.35	0	6.17	7.92	0		14.97	0	6.94	1.86	0	0.66	0.77	0	2.07	4.56	0
11	4.54e-4		0	0	3.82	2.21	0	0.25	4.49	0	6	4.28	0		5.11	0	23.16	2.42	0	0.66	0.44	0	1.33	0.63	0
12	2.26e-5		0	0	1.53	3.28	0	0.14	2.23	0	5.61	3.02	0		17.49	0	17.12	1.38	0	0.69	0.62	0	1.52	0.65	0
13	4.00e-6		0	0	0.86	1.9	0	0.13	5.03	0	4.16	9.06	0		21.85	0	2.32	9.34	0	0.69	0.4	0	1.78	1.36	0
14	5.40e-7		0	0	0.81	1.31	0	0.13	1.46	0	2.14	2.59	0		24.67	0	2.02	3.08	0	0.71	0.3	0	3.42	1.55	0
15	1.00e-7		0	0	0.79	1.25	0	0.13	1.03	0	5.34	4.23	0		24.81	0	1.98	2.93	0	0.71	0.25	0	4.9	1.73	0

Table 1. BOLNA variance matrix (fissile isotopes) (cont.)*²³⁵U, ²³⁸U and ²³⁹Pu (with nu-bar corrected) from ORNL; ²⁴⁶Cm from ANL – values in %*

		²³⁶ U						²³⁸ U						²³⁷ Np						²³⁸ Pu					
Gr	E [MeV]	v	σ _f	σ _{inel}	σ _{el}	σ _{capt}	σ _{n,2n}	v	σ _f	σ _{inel}	σ _{el}	σ _{capt}	σ _{n,2n}	v	σ _f	σ _{inel}	σ _{el}	σ _{capt}	σ _{n,2n}	v	σ _f	σ _{inel}	σ _{el}	σ _{capt}	σ _{n,2n}
1	19.6		14.64	32.82	1.01	48.32	18.49	1.26	0.57	29.28	13.34	21.41	5.32	1.94	5.58	42.85	2.39	41.47	9.51	2.17	25.2	24.56	0.92	50.91	58.36
2	6.07		26.9	7.07	0.89	47.92	0	1.17	0.55	19.75	14.57	13.5	0	2.19	7.9	6.54	3.7	36.48	0	5.3	20.53	5.69	0.82	28.81	0
3	2.23		28.88	15.45	3.84	36	0	1.34	0.6	20.58	18.78	6.05	0	1.47	7.63	22.35	4.12	17.62	0	5.39	33.82	28.65	6.24	21.55	0
4	1.35		31.97	37.2	0.65	15.1	0	1.3	2.91	11.56	5.35	2.27	0	0.66	5.82	28.6	3.62	10.34	0	7	17.11	44.92	6	9.74	0
5	4.98e-1		31.97	38.02	3.34	14.25	0	2	5.26	4.19	1.92	1.41	0	0.6	5.79	44.99	3.47	5.79	0	7	17.11	43.09	9.52	12.31	0
6	1.83e-1		16.47	34.14	1.43	10.53	0	2	5.14	10.96	2.12	1.67	0	0.6	5.79	54.97	4.07	2.08	0	6.5	8.78	20.81	4.1	16.62	0
7	6.74e-2		7.62	0	0.76	7.84	0	2	5.14	11.12	3.76	1.64	0	0.6	5.79	36.27	4.37	6.66	0	6	11.91	0	5.26	22.14	0
8	2.48e-2		6.68	0	0.46	7.04	0	2	50.31	0	1.52	9.43	0	0.6	5.79	0	4.48	5.25	0	5.5	11.2	0	4.85	18.03	0
9	9.12e-3		3.5	0	0.46	3.89	0	2	214.62	0	0.67	3.11	0	0.6	5.79	0	3.93	5.25	0	5	7.47	0	4.43	9.6	0
10	2.03e-3		3.3	0	2.26	1.24	0	2	9.69	0	0.72	2.1	0	0.6	5.77	0	2.44	5.54	0	4.5	4.26	0	4.35	3.69	0
11	4.54e-4		1.37	0	5.96	1.2	0	2	2.38	0	2.39	1.71	0	0.6	7.54	0	2.41	1.7	0	4	8.09	0	20.01	4.66	0
12	2.26e-5		2.57	0	2.35	0.44	0	2	5.82	0	5.97	1.03	0	0.6	4.64	0	2.31	0.55	0	3.5	18.98	0	10.11	9.12	0
13	4.00e-6		15.79	0	4.77	3.47	0	2	51.89	0	0.82	2.45	0	0.6	5.58	0	2.23	0.7	0	3	4.57	0	5.79	3.71	0
14	5.40e-7		19.58	0	4.91	3.44	0	2	55.19	0	0.92	1.66	0	0.6	14.74	0	2.18	2.41	0	2.4	4.63	0	5.1	1.39	0
15	1.00e-7		19.86	0	4.89	3.58	0	2	55.42	0	0.94	1.64	0	0.6	4.55	0	2.03	1.55	0	2.4	4.87	0	4.69	1.41	0
		²³⁹ Pu						²⁴⁰ Pu						²⁴¹ Pu						²⁴² Pu					
Gr	E [MeV]	v	σ _f	σ _{inel}	σ _{el}	σ _{capt}	σ _{n,2n}	v	σ _f	σ _{inel}	σ _{el}	σ _{capt}	σ _{n,2n}	v	σ _f	σ _{inel}	σ _{el}	σ _{capt}	σ _{n,2n}	v	σ _f	σ _{inel}	σ _{el}	σ _{capt}	σ _{n,2n}
1	19.6	0.5	0.63	23.06	6.94	37.08	8.53	1.09	9.56	37.11	2.34	52.16	54.09	0.45	24.09	25.15	4.45	55.39	39.68	0.9	37.24	26.25	0.8	78.47	51.7
2	6.07	0.17	0.69	22.18	9.36	37.8	4.34	2.65	4.8	9.65	5.19	32.47	0	0.27	14.16	19.47	3.74	54.1	33.43	2.21	15.1	3.27	0.51	22.72	0
3	2.23	0.17	0.89	19	10.3	26.56	0	2.69	5.65	10.09	5.42	19.74	0	0.27	21.26	18.38	4.39	38.41	0	2.24	21.42	29.28	3.34	16.12	0
4	1.35	0.12	0.64	29.01	10.29	18.18	0	3.74	5.82	7.79	4.76	16.28	0	0.28	16.62	19.78	5.38	31.66	0	3.11	18.98	59.78	3.68	12.48	0
5	4.98e-1	0.19	0.68	34.01	5.66	11.55	0	4.81	3.91	9.78	5.53	14.29	0	0.29	13.54	20.92	5.16	20.51	0	4.01	18.63	37.99	1.73	24.05	0
6	1.83e-1	0.54	0.85	46.06	3.98	9.04	0	4.81	5.7	42.55	5.76	13.79	0	0.29	19.87	30.09	4.69	11.29	0	4.01	32.07	19	1.78	32.28	0
7	6.74e-2	0.58	0.72	40.04	2.37	10.12	0	4.81	7.45	48.58	5.8	11.31	0	0.29	8.74	37.51	3.92	4.43	0	4.01	33.06	0	1.59	37.26	0
8	2.48e-2	0.58	0.96	28.52	2.16	7.39	0	4.81	7.45	0	5.05	10.21	0	0.29	11.29	0	9.14	7.79	0	4.01	33.19	0	1.42	38.63	0
9	9.12e-3	0.65	0.62	8.64	4.04	15.46	0	4.81	8.01	0	2.08	4.35	0	0.29	10.44	0	9.29	7.73	0	4.01	13.23	0	1.59	38.45	0
10	2.03e-3	0.2	1.2	0	0.74	1.39	0	4.81	21.62	0	1.26	1.47	0	0.29	12.68	0	10.96	7.74	0	4.01	5.89	0	3.76	1.7	0
11	4.54e-4	0.2	1.24	0	1.2	1.25	0	4.81	4.72	0	1.64	1.63	0	0.29	19.38	0	10.87	7.43	0	4.01	1.96	0	2.29	2.23	0
12	2.26e-5	0.2	0.47	0	0.24	0.61	0	4.81	8.91	0	3.25	5.5	0	0.29	4.21	0	10.66	8.38	0	4.01	6.46	0	5.94	7.4	0
13	4.00e-6	0.2	1.43	0	0.3	1.22	0	4.81	1.22	0	0.48	0.44	0	0.29	26.83	0	11.49	6.37	0	4.01	7.6	0	4.68	3.78	0
14	5.40e-7	0.2	0.88	0	0.44	1.36	0	4.81	29.76	0	4.58	3.23	0	0.29	2.94	0	9.91	6.84	0	4.01	5.24	0	7.19	7.1	0
15	1.00e-7	0.2	1.11	0	0.68	1.6	0	4.81	48.46	0	5.64	4.79	0	0.29	3.27	0	11.32	3.59	0	4.01	5.09	0	6.99	6.89	0

Table 1. BOLNA variance matrix (fissile isotopes) (*cont.*)*²³⁵U, ²³⁸U and ²³⁹Pu (with nu-bar corrected) from ORNL; ²⁴⁶Cm from ANL – values in %*

Gr	E [MeV]	²⁴¹ Am						^{242m} Am						²⁴³ Am						²⁴² Cm					
		v	σ _f	σ _{inel}	σ _{el}	σ _{capt}	σ _{n,2n}	v	σ _f	σ _{inel}	σ _{el}	σ _{capt}	σ _{n,2n}	v	σ _f	σ _{inel}	σ _{el}	σ _{capt}	σ _{n,2n}	v	σ _f	σ _{inel}	σ _{el}	σ _{capt}	σ _{n,2n}
1	19.6	1.88	12.74	55.29	3.51	28.83	10.03	10.43	21.37	55.82	8.36	84.91	31.77	1.88	14.44	61.97	7.51	60.42	26.63	10.55	31.49	34.35	3.01	52.78	53.54
2	6.07	1.98	11.67	15.2	3.77	15.38	0	0.91	23.36	17.32	12.05	63.01	37.23	1.98	11.03	17.87	4.64	41.5	0	11.08	52.59	11.03	5.27	37.41	0
3	2.23	1.91	9.81	29.63	5.12	9.16	0	0.66	19.7	23.84	11.15	43.35	0	1.91	5.97	35.3	7.49	21.66	0	10.68	19.02	11.42	2.85	23.61	0
4	1.35	0.98	8.25	24.45	4.52	6.9	0	0.68	16.51	26.47	12.06	39.41	0	1.09	9.18	42.15	4.11	14.18	0	5.5	23.39	18	1.66	19.02	0
5	4.98e-1	1	8.29	23.03	5.5	5.29	0	0.7	16.57	27.1	13.66	29	0	1.2	9.62	40.98	5.9	8.92	0	5.6	66	27.19	1.71	18.18	0
6	1.83e-1	1	8.29	48.53	5.2	6.79	0	0.7	16.57	33.65	13.91	19.39	0	1.2	9.62	79.53	7.84	6.6	0	5.6	62.67	53.15	2.04	20.32	0
7	6.74e-2	1	7.39	51.78	4.81	7.96	0	0.7	14.43	31.15	12.76	18.01	0	1.2	7.12	80.77	4.41	4.57	0	5.6	28.15	31.73	2.34	22.36	0
8	2.48e-2	1	13.71	0	11.54	6.85	0	0.7	11.8	50	18.89	19.17	0	1.2	13.79	0	9.13	6.77	0	5.6	16.2	0	2.11	21.25	0
9	9.12e-3	1	13.51	0	12.35	6.66	0	0.7	12.36	0	19.36	20.23	0	1.2	13.54	0	9.6	6.64	0	5.6	20.95	0	28.28	18.67	0
10	2.03e-3	1	13.41	0	9.7	6.59	0	0.7	12.2	0	19.42	20.08	0	1.2	13.41	0	7.68	6.58	0	5.6	11.68	0	23.54	6.75	0
11	4.54e-4	1	8.08	0	14.53	3.67	0	0.7	10.39	0	16.68	11.39	0	1.2	9.64	0	8.96	2.31	0	5.6	9.32	0	12.64	4.55	0
12	2.26e-5	1	5.15	0	14.03	1.82	0	0.7	10.38	0	19.95	13.25	0	1.2	5.95	0	8.22	1.74	0	5.6	24.01	0	18.18	3.7	0
13	4.00e-6	1	6.72	0	14.2	5.54	0	0.7	7	0	20.61	13.57	0	1.2	4.81	0	7	3.43	0	5.6	35.58	0	19.87	32.51	0
14	5.40e-7	1	8.93	0	13.81	1.26	0	0.7	8.83	0	17.64	19.87	0	1.2	2.25	0	12.41	3.75	0	5.6	41.17	0	19.67	39.23	0
15	1.00e-7	1	3.02	0	13.03	1.8	0	0.7	8.06	0	21.78	19.6	0	1.2	2.12	0	11.44	3.58	0	5.6	42.55	0	19.68	40.77	0
Gr	E [MeV]	²⁴³ Cm						²⁴⁴ Cm						²⁴⁵ Cm						²⁴⁶ Cm					
		v	σ _f	σ _{inel}	σ _{el}	σ _{capt}	σ _{n,2n}	v	σ _f	σ _{inel}	σ _{el}	σ _{capt}	σ _{n,2n}	v	σ _f	σ _{inel}	σ _{el}	σ _{capt}	σ _{n,2n}	v	σ _f	σ _{inel}	σ _{el}	σ _{capt}	σ _{n,2n}
1	19.6	9.64	18.4	50.75	5.65	77.57	52.75	10.55	17.86	38.26	10.58	89.19	40.91	9.64	18.11	85.1	4.81	71.21	22.43	5	40	50	10	40	100
2	6.07	1.41	31.38	2.52	9.12	44.12	36.53	11.08	31.25	22.67	10.23	53.78	0	2.91	30.96	13.01	7.25	36.17	93.53	5	40	50	10	40	100
3	2.23	1.24	44.06	7.42	6.47	17.74	0	10.68	43.8	15.1	5.56	36.49	0	2.85	44.17	40.92	7.45	29.12	0	5	40	50	10	40	0
4	1.35	1.28	49.6	9.45	4.85	31.19	0	5.5	50.01	18.18	10.77	20.8	0	2.95	49.43	54.47	4.75	24.82	0	5	40	50	10	40	0
5	4.98e-1	1.31	37.25	11.78	10.71	29.72	0	5.6	36.53	29.09	9.33	22.54	0	3.01	37.22	81.84	9.94	19.32	0	5	40	50	10	40	0
6	1.83e-1	1.31	47.35	20.24	12.77	23.36	0	5.6	47.56	63.31	8.38	17.71	0	3.01	47.45	94.96	15	17.56	0	5	40	50	10	40	0
7	6.74e-2	1.31	26.48	27.75	11.6	18.18	0	5.6	26.26	59.72	9.21	17.43	0	3.01	26.53	94.77	13.67	10.5	0	5	40	55	10	40	0
8	2.48e-2	1.31	12.39	0	17.71	17.97	0	5.6	19.03	0	14.93	19.32	0	3.01	13.47	0	18.14	12.89	0	5	40	0	10	40	0
9	9.12e-3	1.31	12.21	0	18.04	18.38	0	5.6	11.92	0	14.04	12.14	0	3.01	13.18	0	18.23	12.49	0	5	40	0	10	40	0
10	2.03e-3	1.31	12.19	0	18.02	18.7	0	5.6	5.27	0	7.72	4.47	0	3.01	13.03	0	18.11	12.32	0	5	40	0	10	40	0
11	4.54e-4	1.31	8.04	0	15.54	14.52	0	5.6	5.7	0	3.61	4.6	0	3.01	8.66	0	15.1	9.6	0	5	40	0	10	40	0
12	2.26e-5	1.31	3.34	0	18.81	5.12	0	5.6	17.09	0	7.75	6.64	0	3.01	3.89	0	20.25	7.87	0	5	40	0	10	40	0
13	4.00e-6	1.31	6.44	0	19.53	7.99	0	5.6	21.99	0	6.62	11.79	0	3.01	6.21	0	21.78	11.79	0	5	40	0	10	40	0
14	5.40e-7	1.31	19.52	0	24.91	15.5	0	5.6	26.4	0	6.16	12.16	0	3.01	5.12	0	20.78	7.46	0	5	40	0	10	40	0
15	1.00e-7	1.31	10.53	0	23.41	16.38	0	5.6	27.18	0	6.12	12.51	0	3.01	3.82	0	19.44	8.39	0	5	40	0	10	40	0

Table 2. BOLNA variance matrix (structural isotopes)*Only ^{204}Pb , ^{206}Pb , ^{207}Pb , ^{208}Pb from NRG; C, ^{10}B and ^4He from ANL – values in %*

Gr	E [MeV]	^{204}Pb				^{206}Pb				^{207}Pb				^{208}Pb				Bi				^{56}Fe			
		σ_{inel}	σ_{el}	σ_{capt}	$\sigma_{\text{n,2n}}$	σ_{inel}	σ_{el}	σ_{capt}	$\sigma_{\text{n,2n}}$	σ_{inel}	σ_{el}	σ_{capt}	$\sigma_{\text{n,2n}}$	σ_{inel}	σ_{el}	σ_{capt}	$\sigma_{\text{n,2n}}$	σ_{inel}	σ_{el}	σ_{capt}	$\sigma_{\text{n,2n}}$	σ_{inel}	σ_{el}	σ_{capt}	$\sigma_{\text{n,2n}}$
1	19.6	19.78	3.81	56.24	4.58	19.82	3.74	63.4	4.38	17.01	4	61.28	5.69	17.84	3.55	63.34	5.22	5.25	0.83	47.58	9.39	12.97	4.61	46.24	7.05
2	6.07	5.56	6.08	31.43	0	5.45	5.88	30.43	0	4.98	5.81	24.25	0	5.38	4.99	28.98	0	2.44	1.02	27.74	0	7.23	8.14	31.69	0
3	2.23	14.2	5.12	27.61	0	14.17	4.7	24.54	0	13.77	4.43	21.56	0	0	6.3	22.56	0	34.07	2.06	17.56	0	25.4	5.89	23.48	0
4	1.35	7.74	5.26	17.89	0	9.15	5.14	19.37	0	11.31	4.78	19.46	0	0	7.15	22.4	0	41.77	4.59	11.35	0	16.12	0.64	7.43	0
5	4.98e-1	0	2.81	14.07	0	0	2.74	15.94	0	0	2.44	16.41	0	0	4.88	21.28	0	0	2.22	8.32	0	0	1.71	4.02	0
6	1.83e-1	0	3.95	13.37	0	0	3.84	15.05	0	0	3.73	15.94	0	0	3.2	21.79	0	0	1.8	8.79	0	0	2.08	10.77	0
7	6.74e-2	0	6.63	13.38	0	0	6.51	14.65	0	0	6.35	15.96	0	0	5.57	21.98	0	0	1.88	6.05	0	0	2.05	13.19	0
8	2.48e-2	0	9.29	12.03	0	0	9.1	13.94	0	0	8.85	15.05	0	0	8.11	60.4	0	0	2.41	3.85	0	0	4.6	8.81	0
9	9.12e-3	0	12.71	12.47	0	0	12.41	12.8	0	0	12	14.27	0	0	11.05	182.3	0	0	1.82	0.71	0	0	3.98	8.56	0
10	2.03e-3	0	17.71	13.57	0	0	17.23	276.57	0	0	16.6	20.01	0	0	15.02	317.06	0	0	1.93	0.43	0	0	4.16	11.23	0
11	4.54e-4	0	11.41	8.31	0	0	11.09	8.66	0	0	10.69	8.6	0	0	9.61	13.94	0	0	1.85	1.47	0	0	4.28	11.25	0
12	2.26e-5	0	0	0	0	0	0	0	0	0	0	0	0	0	0	0	0	0	1.82	1.82	0	0	4.31	11.25	0
13	4.00e-6	0	0	0	0	0	0	0	0	0	0	0	0	0	0	0	0	0	1.8	1.86	0	0	4.31	11.25	0
14	5.40e-7	0	0	0	0	0	0	0	0	0	0	0	0	0	0	0	0	0	1.8	1.87	0	0	4.31	11.25	0
15	1.00e-7	0	0	0	0	0	0	0	0	0	0	0	0	0	0	0	0	0	1.78	1.87	0	0	4.21	9.4	0
Gr	E [MeV]	^{57}Fe				^{58}Ni				^{52}Cr				^{90}Zr				^{91}Zr				^{92}Zr			
		σ_{inel}	σ_{el}	σ_{capt}	$\sigma_{\text{n,2n}}$	σ_{inel}	σ_{el}	σ_{capt}	$\sigma_{\text{n,2n}}$	σ_{inel}	σ_{el}	σ_{capt}	$\sigma_{\text{n,2n}}$	σ_{inel}	σ_{el}	σ_{capt}	$\sigma_{\text{n,2n}}$	σ_{inel}	σ_{el}	σ_{capt}	$\sigma_{\text{n,2n}}$	σ_{inel}	σ_{el}	σ_{capt}	$\sigma_{\text{n,2n}}$
1	19.6	15.15	2.59	85.38	19.2	12.28	3.52	47.76	8.3	8.56	3.55	49.2	10.53	11.32	0.44	46.36	6.74	7.16	1.93	66.62	14.94	9.83	0.84	52.99	25.39
2	6.07	11.08	3.24	53.46	0	10.08	4.64	14.54	0	2.24	2.4	23.27	0	17.96	0.92	18.59	0	19.75	1.7	45.69	0	14.87	1.07	40.32	0
3	2.23	34.21	2.71	18.33	0	31.07	0.93	9.68	0	3.12	2.92	19.31	0	18.52	3.96	9.14	0	5.18	4.15	22.89	0	15.07	4.1	21.53	0
4	1.35	10.29	1.28	11.99	0	0	1.54	7.71	0	0	4.19	4.36	0	50	3.39	6.26	0	50	4.11	16.83	0	40.85	2.41	11.31	0
5	4.98e-1	8.54	2.39	11.14	0	0	2.68	2.65	0	0	5.21	5.51	0	0	2.77	5.16	0	0	4.54	13.03	0	0	2.16	7.55	0
6	1.83e-1	12.1	1.65	6.51	0	0	3.21	1.21	0	0	11.43	10.56	0	0	2.02	3.13	0	0	4.03	8.96	0	0	2.01	5.15	0
7	6.74e-2	0	2.81	6.6	0	0	3.05	3.44	0	0	12.63	5.45	0	0	3.09	5.2	0	0	5.47	12.21	0	0	3.02	3.42	0
8	2.48e-2	0	5.1	8.27	0	0	8.05	0.83	0	0	13.28	13.42	0	0	4.43	7.89	0	0	3.11	3.42	0	0	3.65	3.11	0
9	9.12e-3	0	2.5	4.64	0	0	3.61	2.82	0	0	10.28	12.97	0	0	5.93	6.96	0	0	2.92	2.66	0	0	1.94	4.13	0
10	2.03e-3	0	16.11	29.24	0	0	2.96	2.41	0	0	7.79	2.75	0	0	6.83	10.55	0	0	5.75	5.62	0	0	5.44	4.96	0
11	4.54e-4	0	8.48	10.69	0	0	2.77	2.4	0	0	7.37	2.7	0	0	6.73	5.95	0	0	5.89	5.58	0	0	5.38	27.61	0
12	2.26e-5	0	7.69	11.67	0	0	2.74	2.4	0	0	7.21	2.69	0	0	6.7	2.75	0	0	5.91	10.2	0	0	5.37	30.75	0
13	4.00e-6	0	7.65	11.73	0	0	2.73	2.4	0	0	7.22	2.68	0	0	6.7	2.56	0	0	5.92	10.42	0	0	5.37	30.93	0
14	5.40e-7	0	7.65	11.74	0	0	2.73	2.4	0	0	7.21	2.68	0	0	6.7	2.53	0	0	5.93	10.46	0	0	5.37	30.96	0
15	1.00e-7	0	7.48	10.79	0	0	2.67	2.21	0	0	7.05	2.24	0	0	6.7	2.52	0	0	5.91	10.47	0	0	5.29	30.96	0

Table 2. BOLNA variance matrix (structural isotopes) (cont.)*Only ^{204}Pb , ^{206}Pb , ^{207}Pb , ^{208}Pb from NRG; C, ^{10}B and ^4He from ANL – values in %*

Gr	E [MeV]	^{94}Zr				Si				O				Na				H				Al			
		σ_{inel}	σ_{el}	σ_{capt}	$\sigma_{\text{n,2n}}$	σ_{inel}	σ_{el}	σ_{capt}	$\sigma_{\text{n,2n}}$	σ_{inel}	σ_{el}	σ_{capt}	$\sigma_{\text{n,2n}}$	σ_{inel}	σ_{el}	σ_{capt}	$\sigma_{\text{n,2n}}$	σ_{inel}	σ_{el}	σ_{capt}	$\sigma_{\text{n,2n}}$	σ_{inel}	σ_{el}	σ_{capt}	$\sigma_{\text{n,2n}}$
1	19.6	6.85	0.79	63.78	26.24	21.38	0.69	52.87	50	100	84.61	100	100	18.79	1.8	46.44	11.07		0.76	1.96		11.46	1.04	50.11	20
2	6.07	20.75	0.37	43.1	0	13.54	2.77	11.12	0	0	54.92	100	0	8.87	4.62	24.33	0		0.87	1.7		17.05	2.19	23.93	0
3	2.23	10.43	2.63	25.76	0	50	1.66	10.07	0	0	12.18	100	0	12.56	3.72	1.7	0		0.87	1.6		26.23	1.78	10.42	0
4	1.35	41.27	1.1	14.22	0	0	1.43	6.77	0	0	1.43	100	0	28	3.01	7.44	0		0.62	1.39		17.71	1.55	5.68	0
5	4.98e-1	0	1.08	10.11	0	0	1.08	3.86	0	0	1.68	81.81	0	50	3.31	6.81	0		0.7	1.25		0	1.98	10.24	0
6	1.83e-1	0	1.05	6.71	0	0	2.97	5.65	0	0	1.68	69.63	0	0	3.25	23.59	0		0.55	1.15		0	1.76	5.33	0
7	6.74e-2	0	2.63	4.62	0	0	4.3	11.19	0	0	2.36	47.27	0	0	2.38	6.79	0		0.5	1		0	2.49	5.48	0
8	2.48e-2	0	3.02	3.31	0	0	4.18	8.93	0	0	2.35	28.21	0	0	2.87	6.63	0		0.5	0.85		0	2.51	5.97	0
9	9.12e-3	0	2.9	5.54	0	0	3.62	8.71	0	0	2.24	12.1	0	0	3.23	1.18	0		0.5	0.71		0	0.98	5.25	0
10	2.03e-3	0	4.99	14.24	0	0	3.23	5.12	0	0	2.23	9.36	0	0	4.93	2.28	0		0.34	0.56		0	0.74	1.32	0
11	4.54e-4	0	4.78	3.5	0	0	3.03	3.57	0	0	2.22	10.42	0	0	4.76	2.3	0		0.1	0.5		0	0.63	1.3	0
12	2.26e-5	0	4.73	3.51	0	0	2.97	3.25	0	0	2.22	11.29	0	0	4.73	2.29	0		0.1	0.5		0	0.61	1.3	0
13	4.00e-6	0	4.73	3.51	0	0	2.97	3.23	0	0	2.23	10.62	0	0	4.71	2.29	0		0.1	0.5		0	0.61	1.3	0
14	5.40e-7	0	4.73	3.51	0	0	2.97	3.22	0	0	2.23	11.03	0	0	4.7	2.29	0		0.1	0.5		0	0.61	1.3	0
15	1.00e-7	0	4.73	3.51	0	0	2.9	2.96	0	0	2	8	0	0	4.59	2.07	0		0.1	0.5		0	0.6	1.2	0
Gr	E [MeV]	^{155}Gd				^{156}Gd				^{157}Gd				^{158}Gd				^{160}Gd				^{166}Er			
		σ_{inel}	σ_{el}	σ_{capt}	$\sigma_{\text{n,2n}}$	σ_{inel}	σ_{el}	σ_{capt}	$\sigma_{\text{n,2n}}$	σ_{inel}	σ_{el}	σ_{capt}	$\sigma_{\text{n,2n}}$	σ_{inel}	σ_{el}	σ_{capt}	$\sigma_{\text{n,2n}}$	σ_{inel}	σ_{el}	σ_{capt}	$\sigma_{\text{n,2n}}$	σ_{inel}	σ_{el}	σ_{capt}	$\sigma_{\text{n,2n}}$
1	19.6	21.4	1.89	69.29	6.99	19.27	1.15	59.28	8.45	12.52	2.2	69.27	8.92	35.34	1.51	57.37	8.07	42.58	1.15	78.62	18.01	15.73	0.91	41	7.16
2	6.07	11.68	3.58	38.94	0	7.37	1.97	18.81	0	10.26	3.55	16.18	0	7.39	1.32	18.37	0	25.24	1.77	30.38	0	16.82	1.55	32	0
3	2.23	14.2	3.71	19.61	0	8.51	2	9.17	0	16.28	3.73	8.67	0	18.98	1.57	13.6	0	18.96	1.08	22.68	0	49.08	2.35	15.82	0
4	1.35	16.37	5.93	11.04	0	12.64	5.6	6.48	0	22.82	6.12	6.13	0	22.9	3.71	5.31	0	18.88	2.44	10.96	0	35.11	0.57	9.53	0
5	4.98e-1	24.81	4.49	7.4	0	22.89	6.12	5.44	0	28.53	5.23	5.2	0	36.88	4.19	4.94	0	69.41	3.26	10.99	0	3.54	6.33	11.59	0
6	1.83e-1	35.74	2.66	4.03	0	31.24	4.26	3.48	0	30.01	3.7	3.97	0	60.91	2.93	3.82	0	91.34	2.74	9.18	0	50	5.47	13.43	0
7	6.74e-2	0	3.1	3.99	0	0	2.92	3.7	0	21.25	2.47	3.12	0	0	2.98	3.71	0	0	2.77	6.91	0	0	3.9	3.24	0
8	2.48e-2	0	3.95	6.02	0	0	3.21	4.92	0	0	3.29	3.11	0	0	3.88	6.24	0	0	3.51	9.15	0	0	2.6	6.26	0
9	9.12e-3	0	4.65	7.35	0	0	3.94	6.97	0	0	4.1	5.27	0	0	0.1	0.73	0	0	1.83	9.09	0	0	3.32	3.15	0
10	2.03e-3	0	5.35	8.21	0	0	13.87	62.96	0	0	5.58	6.18	0	0	0.33	0.77	0	0	3.26	9.17	0	0	4.74	3.13	0
11	4.54e-4	0	3.97	4.51	0	0	14.61	22.6	0	0	2.27	1.49	0	0	1.18	0.85	0	0	8.6	7.76	0	0	7.71	3.97	0
12	2.26e-5	0	20.19	4.83	0	0	4.89	48.84	0	0	7.66	2.29	0	0	4.76	3.36	0	0	11.06	17.51	0	0	4.39	6.59	0
13	4.00e-6	0	14.06	6.4	0	0	3.71	41.96	0	0	1.15	2.96	0	0	1.86	7.46	0	0	11.64	17.1	0	0	3.85	9.14	0
14	5.40e-7	0	2.29	4.07	0	0	3.6	41.46	0	0	0.87	1.49	0	0	1.91	8.49	0	0	11.75	17.05	0	0	3.78	9.36	0
15	1.00e-7	0	0.72	0.59	0	0	3.58	41.39	0	0	1.15	0.2	0	0	1.91	8.64	0	0	11.72	17.05	0	0	3.69	8.63	0

Table 2. BOLNA variance matrix (structural isotopes) (cont.)*Only ^{204}Pb , ^{206}Pb , ^{207}Pb , ^{208}Pb from NRG; C, ^{10}B and ^4He from ANL – values in %*

Gr	E [MeV]	^{167}Er				^{168}Er				^{170}Er				^{19}F				C				^{10}B			
		σ_{inel}	σ_{el}	σ_{capt}	$\sigma_{\text{n,2n}}$	σ_{inel}	σ_{el}	σ_{capt}	$\sigma_{\text{n,2n}}$	σ_{inel}	σ_{el}	σ_{capt}	$\sigma_{\text{n,2n}}$	σ_{inel}	σ_{el}	σ_{capt}	$\sigma_{\text{n,2n}}$	σ_{inel}	σ_{el}	σ_{capt}	$\sigma_{\text{n,2n}}$	σ_{inel}	σ_{el}	σ_{capt}	$\sigma_{\text{n,2n}}$
1	19.6	9.17	0.9	67.61	30.27	19.36	0.93	31.96	9.13	26.88	0.92	25.17	15.84	4.54	8.71	15.86	7.2	30	5	20	0	30	10	15	0
2	6.07	12.29	1.54	49.14	0	13.43	1.36	49.67	0	14.56	1.3	26	0	9.12	8.12	15.42	0	35	5	20	0	30	10	15	0
3	2.23	10.2	2.45	30.21	0	44.37	2.43	21.89	0	53.41	2.58	11.08	0	7.3	2.12	8.5	0	0	5	20	0	30	10	15	0
4	1.35	5.97	0.78	12.93	0	37.67	0.54	12.98	0	51.08	0.68	8.9	0	22.03	1.65	5.14	0	0	5	20	0	35	10	15	0
5	4.98e-1	4.22	6.65	9.33	0	7.28	5.96	14.97	0	19.18	5.62	7.47	0	15.88	1.02	6.13	0	0	5	20	0	0	10	15	0
6	1.83e-1	6.61	5.57	8.23	0	50	4.82	19.44	0	41.37	4.07	4.99	0	0	1.08	2	0	0	3	20	0	0	10	10	0
7	6.74e-2	0	3.82	3.92	0	0	3.09	9.74	0	0	7.65	6.22	0	0	0.97	2.89	0	0	3	20	0	0	10	10	0
8	2.48e-2	0	2.92	4.01	0	0	2.32	3.1	0	0	5.7	4.7	0	0	1.68	2.55	0	0	3	20	0	0	5	8	0
9	9.12e-3	0	2.92	4.47	0	0	3.8	3.21	0	0	4.17	2.26	0	0	2.05	4.39	0	0	3	20	0	0	5	8	0
10	2.03e-3	0	5.12	2.81	0	0	5.34	6.15	0	0	4.82	3.38	0	0	2.05	6.05	0	0	3	20	0	0	5	5	0
11	4.54e-4	0	6.69	1.88	0	0	8.6	5.05	0	0	7.7	7.21	0	0	2.05	6.09	0	0	3	20	0	0	5	5	0
12	2.26e-5	0	5.88	1.13	0	0	8.67	3.22	0	0	17.92	4.91	0	0	2.05	6.1	0	0	2	20	0	0	3	5	0
13	4.00e-6	0	29.75	1.04	0	0	8.8	3.07	0	0	17.87	3.92	0	0	2.05	6.11	0	0	2	20	0	0	3	3	0
14	5.40e-7	0	9.57	1.02	0	0	8.83	3.05	0	0	17.89	3.7	0	0	2.05	6.11	0	0	1	2	0	0	2	1	0
15	1.00e-7	0	57.65	1.2	0	0	8.65	2.8	0	0	17.52	3.41	0	0	2	5.55	0	0	1	2	0	0	2	1	0

		^4He			
Gr	E [MeV]	σ_{inel}	σ_{el}	σ_{capt}	$\sigma_{\text{n,2n}}$
1	19.6	0	5	20	0
2	6.07	0	5	20	0
3	2.23	0	5	20	0
4	1.35	0	5	20	0
5	4.98e-1	0	5	20	0
6	1.83e-1	0	3	20	0
7	6.74e-2	0	3	20	0
8	2.48e-2	0	3	20	0
9	9.12e-3	0	3	20	0
10	2.03e-3	0	3	20	0
11	4.54e-4	0	3	20	0
12	2.26e-5	0	2	20	0
13	4.00e-6	0	2	20	0
14	5.40e-7	0	1	2	0
15	1.00e-7	0	1	2	0